National Research
Council Canada

Conseil national
de recherches Canada

NRC · CNRC

Canadian Journal of Fisheries and Aquatic Sciences

Journal canadien des sciences halieutiques et aquatiques

100th Anniversary

100e anniversaire

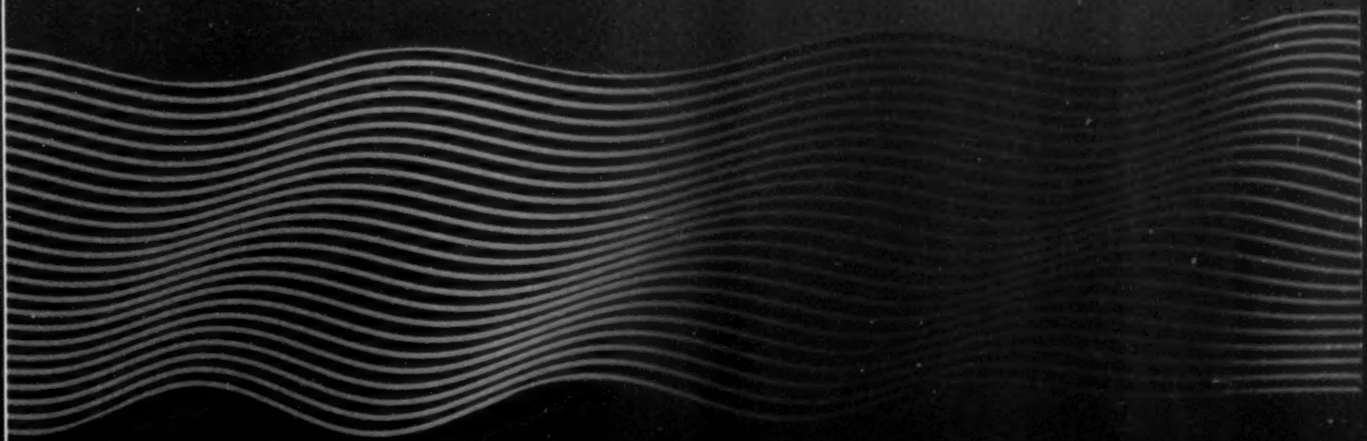

http://www.nrc.ca/cisti/journals

ISSN 0706-652X / CJFSDX 58(5) 841–1042 (2001)

The *Canadian Journal of Fisheries and Aquatic Sciences*, previously published as *Contributions to Canadian Biology* 1901–1925, *Contributions to Canadian Biology and Fisheries* 1926–1934, *Journal of the Biological Board of Canada* 1934–1937, and *Journal of the Fisheries Research Board of Canada* 1938–1979, is issued monthly to form annual volumes of 12 numbers plus supplements.

Editorial policy: The Journal publishes original research articles, perspectives (syntheses, critiques, re-evaluations), discussions (comment and reply), and rapid communications. Manuscripts may concern cells, organisms, populations, communities, ecosystems, or processes that affect aquatic systems. They may cover a range of disciplines including biology and ecology of marine and freshwater organisms, limnology, oceanography, physiology, toxicology, genetics, economics, disease, and management. Preference will be given to manuscripts that emphasize understanding of observed phenomena and interpretation of experimental results. The Journal encourages papers that lead from clearly stated purpose or rationale and from testable hypotheses, concepts, or questions to identifiable conclusions or syntheses. Such papers may amplify, modify, question, or redirect accumulated knowledge embodied in contemporary perceptions of a particular state of aquatic sciences. The Journal discourages papers that are essentially descriptive, except in emerging disciplines; have only site-specific or local applications (a certain year, place, taxon, chemical compound, etc.); only confirm previously established principles; or apply standard techniques without breaking new methodological ground.

Manuscripts for publication should be submitted to the Editors, *Canadian Journal of Fisheries and Aquatic Sciences*, Department of Zoology, University of Guelph, Guelph, ON N1G 2W1, Canada (519-824-4120 ext. 2646; fax: 519-767-9798; e-mail: cjfas@uoguelph.ca).

Submissions in either English or French are acceptable. The information must be original, that is, not copyrighted, published, or submitted elsewhere except in abstract form or unless by written consent of the Editor. NRC accepts no responsibility for statements or opinions expressed by a contributor. Acceptance of an advertisement, announcement, or other material does not imply endorsement by either the Journal's Editors or NRC. The use of proprietary names does not imply endorsement of the product or company.

Correspondence concerning accepted manuscripts and corrected proofs should be sent to NRC Research Press, National Research Council of Canada, Ottawa, ON K1A 0R6, Canada.

Instructions to Authors are published once a year in the first issue of each volume. Copies are available from NRC Research Press or from our web site. The **Publication Policy** of NRC Research Press is also available at our web site: <http://www.nrc.ca/cisti/journals/>.

Microfilm: Issues from 1934 through the current volume can be purchased on 16- or 35-mm microfilm. Photocopies of individual articles or issues can be purchased from University Microfilms International, 330 North Zeeb Road, Ann Arbor, MI 48106, U.S.A.

U.S. periodical postage paid at Champlain, N.Y., and at additional mailing offices. Attention U.S. POSTMASTER: Send address changes to **Canadian Journal of Fisheries and Aquatic Sciences**, c/o USACAN Media Distribution Center, P.O. Box 2888, Plattsburg, NY 12901, U.S.A.

Publié sans interruption depuis 1901, le *Journal canadien des sciences halieutiques et aquatiques* a paru sous plusieurs titres : *Contributions to Canadian Biology* 1901–1925, *Contributions to Canadian Biology and Fisheries* 1926–1934, *Journal of the Biological Board of Canada* 1934–1937, et *Journal of the Fisheries Research Board of Canada* 1938–1979. Le Journal paraît tous les mois, formant ainsi un volume de 12 numéros, et offre en plus jusqu'à deux suppléments par année.

Politique éditoriale : On publie, dans le Journal, des articles rendant compte de recherche originale, des perspectives (synthèses, critiques et réévaluations), des discussions (commentaires et réponses) et des communications rapides. Les documents peuvent porter sur les cellules, organismes, populations, communautés, écosystèmes ou processus qui affectent les systèmes aquatiques. Ils peuvent relever de divers domaines y compris la biologie et l'écologie des organismes marins et d'eau douce, la limnologie, l'océanographie, la physiologie, la toxicologie, la génétique, l'économie, la pathologie et la gestion. On accorde la préséance aux articles qui contribuent à la compréhension de phénomènes observés et à l'interprétation de résultats expérimentaux. On invite les auteurs à soumettre des articles ayant des objectifs précis ou relevant d'hypothèses, de concepts ou de questions vérifiables et se terminant par de solides conclusions ou d'utiles synthèses. Ces articles enrichissent, changent, mettent en question ou réorientent les connaissances acquises sur divers aspects des sciences aquatiques. On décourage toutefois la soumission d'articles simplement descriptifs (à moins qu'il ne s'agisse de nouvelles disciplines), d'application très limitée (applicables à une seule année, une seule région ou un seul taxon, portant sur un unique composé chimique, etc.); d'articles qui ne font que reprendre les principes énoncés dans des articles précédents; et d'articles rendant compte de l'application de normes sans gain de méthodologie.

Les auteurs voudront adresser leurs **manuscrits** aux directeurs scientifiques, *Journal canadien des sciences halieutiques et aquatiques*, Department of Zoology, University of Guelph, Guelph, ON N1G 2W1, Canada (519-824-4120 poste 2646; télécopieur : 519-767-9798; courriel : cjfas@uoguelph.ca).

Les contributions peuvent être en anglais ou en français. Elles doivent être originales, c.-à.-d. qu'elles ne doivent pas avoir fait l'objet d'un copyright, avoir été publiées ou soumises ailleurs, sauf sous forme abrégée ou avec le consentement du rédacteur. Le CNRC ne se tient en aucune façon responsable des opinions exprimées par un collaborateur ou des déclarations qui pourrait faire ce dernier. La publication d'annonces publicitaires, d'avis et autres n'implique pas l'endossement de leur contenu par les directeurs du Journal ou du CNRC. L'utilisation des noms de marques de commerce ne signifie aucunement une sanction du produit en question ou de la compagnie qui le fabrique.

La correspondance ayant trait aux manuscrits acceptés et les **épreuves corrigés** doivent être envoyées aux Presses scientifiques du CNRC, Conseil national de recherches du Canada, Ottawa, ON K1A 0R6, Canada.

Recommandations aux auteurs sont publiés une fois par année dans le premier numéro de chaque volume. Des copies, ainsi que la **Politique de publication**, sont disponibles auprès des Presses scientifiques du CNRC ou au site web : <http://www.nrc.ca/cisti/journals/>.

Microfilms : On peut acheter sur microfilms de 16 ou 35 mm tous les numéros depuis 1934. Des photocopies d'articles ou de numéros individuels sont aussi en vente auprès de University Microfilms International, 330 North Zeeb Road, Ann Arbor, MI 48106, É.-U.

This journal is indexed or abstracted in / Ce journal est signalé ou résumé dans
ABSEARCH, Aquatic Sciences and Fisheries Abstracts, Biological Abstracts, Biological & Agricultural Index, CAB Abstracts, Chemical Abstracts, Current Contents, Elsevier BIOBASE, Environmental Abstracts, Environmental Periodicals Bibliography, GEOBASE, GeoRef, Life Sciences Collection, Meteorological and Geoastrophysical Abstracts, Oceanic Abstracts, PASCAL Database, and Science Citation Index.

Volume 58, Number 5, May 2001

Canadian Journal of Fisheries and Aquatic Sciences

Published by the National Research Council of Canada

Volume 58, numéro 5, mai 2001

Journal canadien des sciences halieutiques et aquatiques

Publié par le Conseil national de recherches du Canada

Editors / directeurs scientifiques John C. Roff and Moira M. Ferguson

Assistant to the Editors / adjointe aux directeurs scientifiques **Holly Foster**

Associate Editors / directeurs scientifiques associés

M.T. Arts, *Environment Canada, Burlington*
D. Boisclair, *Université de Montréal*
U. Borgmann, *Environment Canada, Burlington*
S.E. Campana, *DFO/MPO, Dartmouth*
R. Carignan, *Université de Montréal*
D.G. Dixon, *University of Waterloo*
A.E. Dizon, *National Marine Fisheries Service, La Jolla, Calif.*
J.J. Dodson, *Université Laval*
J.A. Downing, *Iowa State University*
K.T. Frank, *DFO/MPO, Dartmouth*
D.F. Houlihan, *University of Aberdeen, Aberdeen, Scotland*
F.A. Huntingford, *University of Glasgow*
J.A. Hutchings, *Dalhousie University*
G.S. Jamieson, *DFO/MPO, Nanaimo*
B. Jonsson, *Norwegian Institute for Nature Research, Oslo, Norway*
D.M. Mason, *NOAA-Great Lakes Environmental Research Laboratory, Ann Arbor, Mich.*
A. Mazumder, *University of Victoria*
D.L. Parrish, *Vermont Cooperative Fish and Wildlife Research Unit (USGS/BRD), University of Vermont*
P. Pepin, *DFO/MPO, St. John's*
E.E. Prepas, *University of Alberta*
T.M. Powell, *University of California, Berkeley, Calif.*
T.J. Quinn II, *University of Alaska–Fairbanks, Juneau, Alaska*
T.P. Quinn, *University of Washington*
R.D. Robarts, *Environment Canada, Saskatoon*
B. Sainte-Marie, *DFO/MPO, Mont-Joli*
D.W. Schindler, *University of Alberta*
S.J. Smith, *DFO/MPO, Dartmouth*
W.G. Sprules, *University of Toronto*
R.J. Thompson, *Memorial University of Newfoundland*
C.J. Walters, *University of British Columbia*
R.D. Ward, *CSIRO Division of Fisheries, Australia*
C.M. Wood, *McMaster University*
B. de Young, *Memorial University of Newfoundland*

NRC Research Press / Presses scientifiques du CNRC

Editor-in-chief / directeur général **Bruce P. Dancik**
Assistant Editor-in-chief / directeur général adjoint **Iain E.P. Taylor**

Journals Program / Programme des revues

(Fax / télécopieur : 613-952-7656; e-mail / courriel : research.journals@nrc.ca;
URL: http://www.nrc.ca/cisti/journals/)

Director / directrice **Aldyth Holmes**
Business Manager / gestionnaire des affaires **Paul McClymont**
Managing Editor / rédactrice administrative **Cecily M. Pearson (613-993-9099)**
Publication Officer / agente de publication **Jennifer McColl**
Advertising / annonces publicitaires **Judy Heyman (613-993-0151)**
Reprints / tirés à part **Roxanne Landriault (613-990-2254)**
Subscriptions / abonnements **Helen Goulet (613-993-9084)**

© National Research Council of Canada 2001. World rights reserved. No part of this publication may be reproduced, stored, or transmitted in any form or by any means, without the written permission of the publisher, except as stated below.

The National Research Council of Canada grants **permission*** to individuals to make single copies of articles for personal use. Any person may reproduce short excerpts from articles in the journal for any purpose that respects the moral rights of authors, provided that the source is fully acknowledged. As a courtesy, the consent of authors of such material should be obtained directly from the author.

Authorization to reproduce items for other than personal use, as stated above, is granted by the National Research Council of Canada provided that the copyright fee of $7.00 per copy is paid directly to CANCOPY, One Yonge Street, Suite 1900, Toronto, ON M5E 1E5, Canada.

*The above permission does not extend to other kinds of copying, such as copying for general distribution, for advertising, or promotional purposes, for creating new collective works, or for resale. For such copying, arrangements must be made with the publisher, National Research Council of Canada, Ottawa, ON K1A 0R6, Canada.

© Conseil national de recherches du Canada 2001. Tous droits réservés. Il est interdit de reproduire, de sauvegarder ou de transmettre quelque partie de la présente publication dans quelque format ou de quelque façon sans le consentement écrit de l'éditeur, à l'exception des conditions suivantes.

Le Conseil national de recherches du Canada accorde aux particuliers le droit de faire des copies individuelles pour leur usage personnel. Toute personne peut reproduire de courts extraits des articles de la Revue pour autant que les droits moraux de l'auteur soient respectés et que la mention de provenance soit clairement indiquée. Il est de convenance de demander le consentement de l'auteur avant de faire mention de son travail.

On obtiendra l'autorisation de reproduire des articles à d'autres fins que l'usage personnel (tel qu'on l'a décrit ci-dessus) auprès du Conseil national de recherches du Canada pour autant que des redevances de droits d'auteurs de 7,00 $/copie soient versées au CANCOPY, 1, rue Yonge, bureau 1900, Toronto, ON M5E 1E5, Canada.

*La permission ci-dessus ne s'applique pas à la reproduction à grande échelle, telle que la reproduction aux fins de distribution générale, publicitaire ou promotionnelle, de compilation de nouveaux ouvrages collectifs ou de revente. Dans de tels cas, il faudra ratifier une entente particulière avec l'éditeur, le Conseil national de recherches du Canada, Ottawa, ON K1A 0R6, Canada.

Subscription information

The *Canadian Journal of Fisheries and Aquatic Sciences* (ISSN 0706-652X) is published monthly by the National Research Council of Canada. 2001 annual subscription rates (second class postage) for Canada are $687CAN institutional and $208CAN personal, for US & foreign $687US institutional and $208US personal. For air mail add $150US to foreign rate. Canadian customers please include 7% GST (business no. 12149 1807 RT 0275). Subscriptions are entered for the calendar year. Remittances should be made payable to the Receiver General for Canada credit NRC. Price for regular single issues: institutional, $80.00; personal, $30.00. Supplements will be priced separately. Special rates apply to members of Canadian scientific and engineering societies if they subscribe through their respective societies.

There are no refunds on cancelled subscriptions once delivery has begun. Claims for missing issues should be made within four months (N. America) or six months (outside N. America) following the date of publication. The publisher expects to supply missing issues only when losses have occurred in transit and when the reserve stock will permit. For change of address and subscription enquiries: Subscription Office, NRC Research Press, National Research Council of Canada, Ottawa, ON K1A 0R6, Canada; tel.: 613-993-9084; fax: 613-952-7656; e-mail: research.journals@nrc.ca.

Microform backfiles are available from UMI, P.O. Box 1346, Ann Arbor, MI 48106-1346, U.S.A., and Micromedia Ltd., 20 Victoria St., Toronto, ON M5C 2N8, Canada.

All issues of the *Canadian Journal of Fisheries and Aquatic Sciences* since 1996 are available on the Web. Pricing information can be found at <http://www.nrc.ca/cisti/journals/>.

Renseignements sur l'abonnement

Journal canadien des sciences halieutiques et aquatiques (ISSN 0706-652X) est une publication mensuelle du Conseil national de recherches du Canada. Le prix de l'abonnement annuel au Canada (courrier de deuxième classe) est de 687 $CAN pour les organismes et de 208 $CAN pour les particuliers. À l'étranger (y compris les É.-U.), le prix de l'abonnement est de 687 $US pour les organismes et de 208 $US pour les particuliers. L'expédition par avion exige des frais de 150 $US en sus du prix d'abonnement à l'étranger. Les clients du Canada doivent ajouter la TPS de 7% (numéro d'entreprise 12149 1807 RT 0275). Les abonnements sont pour l'année civile. Tout paiement doit être adressé au Receveur général du Canada, crédit du CNRC. Le prix par numéro est de 80 $ pour les organismes et de 30 $ pour les particuliers. Le prix des hors-série varie. Les membres des sociétés canadiennes de sciences et de génie bénéficient de taux préférentiels en s'abonnant via leurs sociétés respectives.

Aucun remboursement ne sera accordé ni aucune annulation acceptée une fois que les livraisons auront commencé. Les réclamations de numéros manquants devront être soumises dans les quatre mois (Amérique du Nord) ou dans les six mois (à l'extérieur de l'Amérique du Nord) suivant la date de publication. L'éditeur ne fournira de numéros manquants que si le document a été perdu pendant l'expédition et que si le stock le permet. Adressez tout changement d'adresse ou toute question quant à l'abonnement au : Bureau des abonnements, Presses scientifiques du CNRC, Conseil national de recherches Canada, Ottawa, ON K1A 0R6, Canada; téléphone : 613-993-9084; télécopieur : 613-952-7656; courriel : research. journals@nrc.ca.

On peut obtenir les fichiers rétrospectifs sur **microforme** auprès de UMI, P.O. Box 1346, Ann Arbor, MI 48106-1346, É.-U., et auprès de Micromedia Ltée, 20 rue Victoria, Toronto, ON M5C 2N8, Canada.

À partir de 1996, tous les numéros de *Journal canadien des sciences halieutiques et aquatiques* sont accessibles sur le Web. On trouvera des renseignements sur les tarifs à <http://www.nrc.ca/cisti/journals>.

RAPID COMMUNICATION/COMMUNICATION RAPIDE

Invasion of transgenes from salmon or other genetically modified organisms into natural populations

Philip W. Hedrick

Abstract: In recent years, there has been widespread concern about the ecological and genetic effects of genetically modified organisms. In salmon and other fishes, transgenic growth hormone genes have been shown to have large effects on size and various traits related to fitness. In this paper, I have shown by using a deterministic model that if such a transgene has a male-mating advantage and a general viability disadvantage, then the conditions for its invasion in a natural population are very broad. More specifically, for 66.7% of the possible combinations of the possible mating and viability parameters, the transgene increases in frequency, and for 50% of the combinations, it goes to fixation. In addition, by this increase in the frequency of the transgene, the viability of the natural population is reduced, increasing the probability of extinction of the natural population. These findings provide independent confirmation of previous concerns about the inherent risks of transgenic organisms, especially for native salmon populations potentially affected by commercial salmon production using transgenic stocks.

Résumé : Depuis quelques années, les effets écologiques et génétiques des organismes génétiquement modifiés sont devenus l'objet de préoccupations universelles. Chez le saumon et d'autres poissons, les gènes transgéniques de l'hormone de croissance ont des effets importants sur la taille et sur d'autres caractéristiques reliées au fitness. L'utilisation d'un modèle déterministe a permis de démontrer que si un tel transgène procure un avantage aux mâles lors de l'accouplement et un désavantage pour la viabilité générale, les conditions qui permettent son insertion dans la population sont très larges. En particulier, dans 66,7% des combinaisons des valeurs possibles des variables reliées à l'accouplement et à la viabilité, la fréquence du transgène augmente et, dans 50% des combinaisons, il y a fixation du transgène. De plus, l'augmentation de la fréquence du transgène entraîne une réduction de la viabilité de la population naturelle et augmente la probabilité de son extinction. Ces résultats confirment de façon indépendante la pertinence des préoccupations concernant les risques inhérents aux organismes transgéniques, particulièrement pour les populations de saumons indigènes qui risquent d'être affectées par une production commerciale qui utilise des stocks transgéniques.

[Traduit par la Rédaction]

Many genetically modified (GM) animals and plants utilize genes from other organisms, transgenes, to increase yield or change other economically important traits. Recently, Losey et al. (1999) showed that corn transformed with the bacterium *Bacillus thuringiensis* has detrimental effects on nontarget monarch butterflies (however, see Wraight et al. 2000), a report that raised great concern about the risks associated with GM organisms. In addition, if transgenes can spread by gene flow and selective advantage from GM organisms into natural populations of the same or related species, then issues about GM organisms are further amplified.

Fish of several species transgenic for growth hormone genes are much larger than non-transgenic fish, and the muscular and molecular bases of this size increase has been documented in coho salmon, *Oncorhynchus kisutch* (Hill et al. 2000). Because larger males have increased mating success (Howard et al. 1998), these transgenes, once introduced by gene flow, may invade (increase in frequency) in a natural population because of this selective mating advantage. Transgenes may also potentially increase male mating success by changing factors such as mating behavior, color, etc. (W. Muir, personal communication). However, if the transgene also reduces viability, it may result in the extinction of the natural population because of reduced population fitness (Muir and Howard 1999). In this paper, I show that the conditions for invasion of transgenes and a consequent reduction in fitness are broad, raising great concerns about the

Received February 23, 2001. Accepted March 29, 2001. Published on the NRC Research Press Web site on April 12, 2001.
J16235

P.W. Hedrick. Department of Biology, Arizona State University, Tempe, AZ 85287, U.S.A. (e-mail: philip.hedrick@asu.edu).

DOI: 10.1139/cjfas-58-5-841

Table 1. Proportions of the three types of progeny produced from the nine possible mating types.

Mating		Progeny		
Male	Female	A_tA_t	A_tA	AA
A_tA_t	A_tA_t	$P^2/\overline{m}$	—	—
	A_tA	$PH/2\overline{m}$	$PH/2\overline{m}$	—
	AA	—	$PQ/2\overline{m}$	—
A_tA	A_tA_t	$PH/2\overline{m}$	$PH/2\overline{m}$	—
	A_tA	$P^2/4\overline{m}$	$P^2/2\overline{m}$	$P^2/4\overline{m}$
	AA	—	$HQ/2\overline{m}$	$HQ/2\overline{m}$
AA	A_tA_t	—	$PQ(1-m)/\overline{m}$	—
	A_tA	—	$HQ(1-m)/2\overline{m}$	$HQ(1-m)/2\overline{m}$
	AA	—	—	$Q^2(1-m)/\overline{m}$
		$P' = \dfrac{p^2}{\overline{m}}$	$H' = \dfrac{2pq - mQp}{\overline{m}}$	$Q' = \dfrac{q^2 - mQp}{\overline{m}}$

Note: m is the mating disadvantage for wildtype homozygotes.

Fig. 1. The conditions for invasion of a transgene (shaded region), fixation of the transgene (to the right of broken line), and a stable equilibrium (between the solid and broken lines) as a function of the mating disadvantage (m) of the wildtype genotype lacking the transgene and the viability disadvantage (s) of the transgene genotypes. The mean fitness for the populations is reduced from 1 before the transgene is introduced to $1 - s$ after the transgene is fixed.

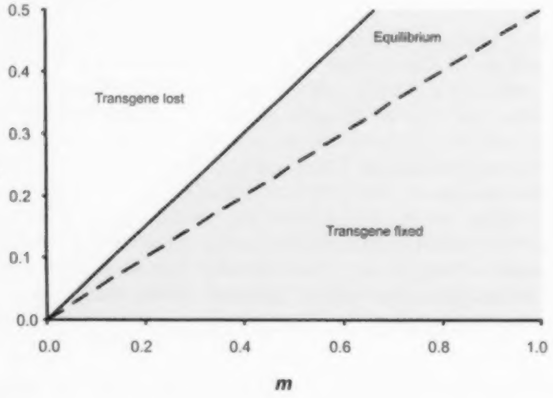

widespread use of GM organisms, particularly in production of salmon and other fishes.

Let us assume that A_t and A indicate the presence and absence of the transgene, with frequencies of p and q, respectively, and that genotypes A_tA_t, A_tA, and AA indicate homozygosity, hemizygosity, and the absence of the transgene (wildtype), respectively. Also assume that the relative male-mating successes of these genotypes are 1, 1, and $1 - m$, i.e., there is a mating disadvantage of m for the wildtype males, which do not have the transgene. For individuals of both sexes, assume that the relative viabilities of genotypes A_tA_t, A_tA, and AA are $1 - s$, $1 - s$, and 1, i.e., the two genotypes having the transgene have a viability disadvantage of s. Also assume that the frequencies of genotypes A_tA_t, A_tA, and AA are P, H, and Q, that all females are mated, and that the sum of the mating types is standardized to unity. Therefore, the proportion of progeny genotypes from each of the nine possible mating types is as given in Table 1. The frequencies of the three genotypes in the progeny after mating and reproduction are (by summing the columns in Table 1)

$$P' = p^2/\overline{m}$$

$$H' = (2pq - mQp)/\overline{m}$$

$$Q' = (q^2 - mQp)/\overline{m}$$

where $\overline{m} = 1 - mQ$. After differential viability, the genotypic frequencies become

$$P'' = P'(1 - s)/\overline{w}$$

$$H'' = H'(1 - s)/\overline{w}$$

$$Q'' = Q'/\overline{w}$$

where $\overline{w} = 1 - s(P' + H')$.

The conditions for invasion of the transgene can be determined by either iterating these equations or by assuming that $p'' = P'' + H''/2$ and by substitution from the expressions above to obtain

$$\frac{p''}{p} = \frac{1 - mQ(1-s)/2}{1 - mQ - sp(1 + q - mQ)}$$

An increase in the frequency of the transgene occurs when $m > 2s/(1 + s)$, and if $m > 2s$, then the transgene invades and goes to fixation (Fig. 1). Overall, for 66.7% of the possible combinations of m and s, the transgene increases in frequency, and for 50% of the combinations, it goes to fixation. These straightforward relationships between the relative mating success and viability of organisms with and without the transgene simplify the design of future experiments to evaluate the potential invasion of a transgene and its impact on natural populations.

The fundamental theorem of Fisher (1958) predicts that the mean fitness of the population, $\overline{w}$, is expected to increase over time because of selection. However, in this situation, as the transgene invades as the result of selection for mating success favoring its increase, the mean fitness is reduced, not increased. This occurs here because it is assumed that all females are mated, with or without the presence of the transgene, so that there is no influence of differences in mating success on mean fitness. In other words, the increase in the transgene does not increase the mean fitness through a mating advantage of the transgenic genotypes of the population. As the transgene increases in frequency, the mean fitness is reduced because the viability of individuals with the transgene is less than that of wildtype individuals. If the transgene becomes fixed, then $\overline{w} = 1 - s$ so that the relative fitness is reduced by an amount s. If this increased mortality results in a negative population growth rate, then the population will become extinct.

If $2s/(1 + s) < m < 2s$, then there is a stable equilibrium, as is also found for a similar antagonistic pleiotropy model (Hedrick 1999) with selection for female fecundity and viability. For the stable equilibrium for the transgene, the mean fitness is also reduced as a function of the equilibrium genotypic frequencies, i.e., $\overline{w} = 1 - s(P'_e + H'_e)$.

Several assumptions are inherent in these predictions. First, I have assumed that there is a negative pleiotropic effect of the transgene increasing mating success and reducing viability. This scenario is based on the emphasis of increasing body size in many transgenic experiments and the positive correlation of large body size and mating success (Muir and Howard 1999). Similar conclusions about the invasion of the transgene would occur if the associations are the opposite, i.e., the transgene reduces mating success and increases viability. On the other hand, if the transgene reduces both mating success and viability, then it would not invade, and if the transgene increases both mating success and viability, then it would always be predicted to invade. Second, for the population fitness to be reduced by the invasion of the transgene, it was assumed that all reproductive females are mated, regardless of the presence or absence of the transgene (also assumed by Muir and Howard 1999). In many fish populations of normal density, this assumption is probably nearly realized, but if the population size declines to low numbers, then this assumption may not be true.

The present model distills the parameters of mating advantage and viability disadvantage for transgenic organisms into two parameters. Muir and Howard (1999) examined the effect of these parameters on the time to extinction when the transgene invaded, but they did not provide the exact conditions for transgenic invasion. Muir and Howard (1999) used a deterministic, individual-explicit model to investigate the impact of a transgene invasion, which gave a detailed examination of the dynamical effects of the invasion on the transgene frequency and the population number. On the other hand, the simpler approach given here provides, in a traditional population genetic framework, a clearer understanding of the factors causing these initially counterintuitive results and the generality of the conclusions.

The description presented here simplifies the variation observed in life history, mating behavior, and other factors influencing the evolution and ecology of fishes. For example, details concerning the life history, population structure, and mating behavior of Pacific salmon (Groot and Margolis 1991) could be incorporated into a more realistic model. More specifically, the time spent in both freshwater and marine environments may be influenced by growth rate. Differences in time spent in these stages by transgenic and non-transgenic fish could potentially influence the dynamics and invasion of the transgene.

At this point, it is not clear whether fish transgenic for growth hormone genes will either have a mating advantage or a viability disadvantage. For example, Farrell et al. (1997) found that transgenic coho salmon are slower swimmers, possibly resulting in a viability disadvantage under natural conditions. On the other hand, Stevens et al. (1998) found that transgenic Atlantic salmon were more active than non-transgenic fish. Fitness differences between transgenic and non-transgenic fish will potentially depend on a number of factors, such as what species is receiving the transgene, what is the source species of the transgene, and the ecological context (Kapuscinski and Hallerman 1991; Reichhardt 2000).

However, as I have shown above, there are very broad conditions in which a transgene with a large mating advantage and a pleiotropic viability disadvantage may invade natural populations, reduce their fitness, and potentially cause their extinction. These findings should serve to alert researchers of the inherent risks of accidental releases of GM organisms into natural populations. In particular, consideration of the potentially very detrimental effects of accidental releases of transgenic fish and shellfish on natural populations should be of paramount concern in the commercial production of these transgenic organisms. For example, native salmon populations already under threat could potentially be further impacted by commercial salmon production using transgenic stocks.

Acknowledgements

The author thanks anonymous reviewers and S. Kumar for comments on an earlier version of the manuscript and the Ullman Professorship for support.

References

Farrell, A.P., Bennet, W., and, Devlin, R.H. 1997. Growth-enhanced transgenic salmon can be inferior swimmers. Can. J. Zool. **75**: 335–337.

Fisher, R.A. 1958. The genetical theory of natural selection. Dover, New York.

Groot, C., and Marcolis, L. (*Editors*). 1991. Pacific salmon life histories. The University of British Columbia Press, Vancouver, B.C.

Hedrick, P.W. 1999. Antagonistic pleiotropy and genetic polymorphism: a perspective. Heredity, **82**: 126–133.

Hill, J.A., Kiessling, A., and Devlin, R.H. 2000. Coho salmon (*Oncorhynchus kisutch*) transgenic for a growth hormone gene construct exhibit increased rates of muscle hyperplasia and detectable levels of differential gene expression. Can. J. Fish. Aquat. Sci. **57**: 939–950.

Howard, R.D., Martens, R.S., Innes, S.A., Drnevich, J.M., and Hale, J. 1998. Mate choice and mate competition influence male body size in Japanese medaka. Anim. Behav. **55**: 1151–1163.

Kapuscinski, A.R., and Hallerman, E.M. 1991. Implications of introduction of transgenic fish into natural ecosystems. Can. J. Fish. Aquat. Sci. **48**(Suppl. 1): 99–107.

Losey, J.E., Rayor, L.S., and Carter, M.E. 1999. Transgenic pollen harms monarch larvae. Nature (London), **399**: 214.

Muir, W.M., and Howard, R.D. 1999. Possible ecological risks of transgenic organism release when transgenes affect mating success: sexual selection and the Trojan gene hypothesis. Proc. Natl. Acad. Sci. U.S.A. **96**: 13853–13856.

Reichhardt, A. 2000. Will souped up salmon sink or swim? Nature (London), **406**: 10–12.

Stevens, E.D., Sutterlin, A., and Cook, T. 1998. Respiratory metabolism and swimming performance in growth hormone transgenic Atlantic salmon. Can. J. Fish. Aquat. Sci. **55**: 2028–2035.

Wraight, C.L., Zangerl, A.R., Carroll, M.J., and Berenbaum, M.R. 2000. Absence of toxicity of *Bacillus thuringiensis* pollen to black swallowtails under field conditions. Proc. Natl. Acad. Sci. U.S.A. **97**: 7700–7703.

Laboratory testing of a growth hypothesis for juvenile squid *Loligo pealeii* (Cephalopoda: Loliginidae)

Emma M.C. Hatfield, Roger T. Hanlon, John W. Forsythe, and Eric P.M. Grist

Abstract: Growth modeling in squid has been hampered by a paucity of raw growth data on live individuals. We reared wild juvenile squid *Loligo pealeii*, for up to 97 days post capture, to determine the form of growth and to test the hypothesis that a 5°C difference in temperature would significantly affect growth rates. Precapture growth rates (the instantaneous relative growth rate or percent increase in body mass per day (IRGR)) of 8–11% were estimated using statolith age data. Laboratory growth rates over a maximum of 97 experimental days fell into two phases in which most *L. pealeii* grew exponentially, albeit at a slower rate in phase 2. In both phases, the values of IRGR were significantly higher for *L. pealeii* reared at 20°C than for those reared at 15°C, being respectively, 4.36 and 2.69 in phase 1 and 2.57 and 1.63 in phase 2. This study provides strong evidence of phase-specific temperature sensitivity in squid growth. The IRGR values obtained were used to simulate the growth of squid hatched in nature from May to September in a simple predictive model. The growth simulations indicated that, by the end of phase-1 growth, squid hatched in June and July were two and three times the weight, respectively, at the same age, as squid hatched in May, owing to their exposure to warmer temperatures.

Résumé : La modélisation de la croissance chez le calmar est entravée par l'absence de données brutes sur la croissance d'individus vivants. Nous avons donc gardé en élevage des jeunes calmars sauvages *Loligo pealeii*, jusqu'à 97 jours après leur capture pour déterminer l'allure de leur courbe de croissance et pour vérifier l'hypothèse voulant qu'une différence de température de 5°C affecte de façon significative leurs taux de croissance. Les taux de croissance avant la capture (le taux instantané de croissance relative ou le pourcentage d'accroissement journalier de la masse corporelle (IRGR)) ont été estimés à 8–11% à partir des âges déterminés sur les statolithes. Les taux de croissance en laboratoire au cours d'une expérience d'une durée maximale de 97 jours se répartissaient en deux phases durant lesquelles la plupart des calmars affichaient une croissance exponentielle, bien qu'à un taux plus lent dans la phase 2. Dans les deux phases, les valeurs d'IRGR étaient significativement plus élevées chez les calmars élevés à 20°C que chez ceux gardés à 15°C, soit respectivement 4,36 et 2,69 dans la phase 1, et 2,57 et 1,63 dans la phase 2. Notre étude confirme donc fortement que la croissance des calmars est affectée par la température de façon différente selon la phase. L'insertion des valeurs d'IRGR dans un modèle prédictif simple a permis de simuler la croissance de calmars éclos en nature de mai à septembre. Ces simulations indiquent qu'à la fin de la phase 1 de la croissance, les calmars éclos en juin et en juillet avaient atteint au même âge, respectivement deux ou trois fois la masse de calmars éclos en mai, à cause de leur exposition à des températures plus chaudes.

[Traduit par la Rédaction]

Introduction

The squid resources of the Northeast United States have become a major contributor to the region's fishery economy (Cadrin and Hatfield 1999). In 1998, the first-sale values of *Loligo pealeii*, the inshore longfin squid, and *Illex illecebrosus*, the northern shortfin squid, were US$32 million and US$9 million, respectively (National Marine Fisheries Service 1999). Squid landings, and fishing effort directed toward them, have increased steadily, as worldwide demand has grown, and the region's fisheries have diversified because of over-exploitation of traditional finfish species. Recent stock assessments (Northeast Fisheries Science Center 1999) have concluded that both squid species are at least fully utilized, and there is concern that the limited knowledge of the biology and dynamics of the species available results in considerable uncertainty in projecting stock responses to intensive harvest.

Received March 28, 2000. Accepted January 25, 2001. Published on the NRC Research Press Web site on April 12, 2001.
J15687

E.M.C. Hatfield.[1] National Marine Fisheries Service, Northeast Fisheries Science Center, Woods Hole, MA 02543, U.S.A.
R.T. Hanlon. Marine Biological Laboratory, Woods Hole, MA 02543, U.S.A.
J.W. Forsythe. National Resource Center for Cephalopods, Marine Biomedical Institute, Galveston, TX 77555, U.S.A.
E.P.M. Grist. School of Biological Sciences, Royal Holloway, University of London, Egham TW20 0EX, U.K.

[1] Author to whom all correspondence should be sent at the following address: Fisheries Research Services Marine Laboratory Aberdeen, P.O. Box 101, Victoria Road, Aberdeen AB11 9DB, Scotland, U.K. (e-mail: e.hatfield@marlab.ac.uk).

DOI: 10.1139/cjfas-58-5-845

Working hypotheses of the life cycles of both species have changed dramatically in recent years, particularly since statolith aging has indicated considerably shorter life-spans than previously assumed (Macy 1995; Dawe and Beck 1997). With life cycles of less than a year, factors that influence the rates of growth, spawning, distribution, and availability to the fishery become critical research gaps for both squid species. The use of statoliths as a tool for age determination has promoted an increase in our understanding of the growth and development of many squid species (see recent review by Jackson 1994). Recent age-determination studies on *L. pealeii* (Macy 1995; Brodziak and Macy 1996) have demonstrated that this species, in common with other loliginid squid, has a life-span of 1 year or less, and that the population may comprise a number of different cohorts. Prior to these studies, it was presumed that *L. pealeii* had a spawning period restricted to spring to late autumn and a life-span of up to 30 months. The considerable variability in size seen within these populations was explained by the presence of two hypothetical cohorts—comprising a "short" generation living about 1 year and a "long" generation with a life-span of up to 30 months (Summers 1983)— with the possibility that crossed generations accounted for the changes seen in length–frequency distributions (Mesnil 1977). Recent statolith-based age data (Macy 1995; Brodziak and Macy 1996) suggest that the population spawns throughout the year, although the relative contributions to the population from different times of the year have yet to be ascertained.

Recent modeling studies on the growth of squid have suggested that temperature in early life should have an enormous influence on growth rate (Forsythe 1993; Grist and des Clers 1998). Certainly, back-calculations from age at capture imply that the warmer the ambient temperature experienced post hatching, the higher the growth rate (Dawe and Beck 1997; Jackson et al. 1997; Hatfield 2000). Recent age data for *L. pealeii* lend support to this hypothesis (Brodziak and Macy 1996). A laboratory investigation of growth in *Loligo forbesi* reared at temperatures differing by an average of 1°C, found a 2% body weight per day increase in *L. forbesi* reared at the higher temperature over the initial growth phase (Forsythe and Hanlon 1989). This temperature effect on growth ensures that the potential exists for squid of the same size to be very different in age. Within a given season, this may lead to a confusing picture of size and maturity, if the ages of individual squid are unknown. This in turn could lead to inaccurate growth and maturation rates being calculated and to data on yield per recruit being over- or underestimated.

Laboratory culture (sensu strictu: egg to egg full life-cycle culture; Boletzky and Hanlon 1983) of *L. pealeii* has been attempted a number of times, with little or no success (reviewed in Summers 1983). To date, it has not proven possible to rear (i.e., grow animals through part of the life cycle) more than a few individual *L. pealeii* beyond the early hatchling stage (Yang et al. 1980; Hanlon et al. 1987). Long-term survival has been most successful with adult *L. pealeii*. Despite these and other logistical challenges (Summers and McMahon 1974; Hanlon et al. 1983), wild-caught *L. pealeii* were maintained and reared in the present study. The aim of this investigation was to capture and rear juvenile *L. pealeii* under two different regimes of temperature, to test if a 5°C difference in temperature would produce a significant difference in growth rate. Mean weekly temperatures in Great Harbor, Woods Hole, for 1998 (D. Mountain, National Marine Fisheries Service (NMFS), 166 Water Street, Woods Hole, MA 02543, U.S.A., unpublished data) ranged from 14.4 (±0.85 SE) to 22.3 (±0.81 SE)°C from late May to mid-October. Since this period encompasses the study dates, the temperatures are probably indicative of those experienced in Vineyard Sound, where the *L. pealeii* were caught and (most likely) hatched. Thus, using a 5°C difference in temperature, this study permits a preliminary evaluation of size variability in the exploited *L. pealeii* population, based on early growth at the different temperatures.

Materials and methods

Capture

Multiple field-collection trips were made using a 16-ft (1ft = 0.3048 m) dive-boat from mid-June to mid-August 1998. *Loligo pealeii* were collected successfully by night-lighting in Vineyard Sound, Mass., on only two nights, 13 and 19 August 1998. The boat was allowed to drift, and a 500-W halogen lamp attached to a small generator was deployed amidships in an attempt to attract small squid.

Great emphasis was placed on obtaining squid by methods that imparted as little skin damage as possible, particularly to the fins (Hulet et al. 1979; Hanlon et al. 1983). *Loligo pealeii* were caught with a fine-meshed shallow dip net approx. 50 cm in diameter. Upon net-capture, every effort was made to handle the animals briefly while transferring them to a covered shipboard seawater transport tank (152 × 92 × 30 cm deep), so that the air-to-water transfer would last only a few seconds.

Loligo pealeii were transferred to the laboratory by slowly filling a large thick clear plastic bag with water and herding a small number (4–5) of individuals into the bag. *Loligo pealeii* were released into the experimental tanks from the water-filled bags as carefully as possible; they were allowed to swim slowly from the bag into the tank. Tank water temperatures were set to the required experimental temperatures prior to the introduction of *L. pealeii* and, thus, individuals in each tank had to acclimate from ambient conditions to the tank temperature over a period of some 12 h.

Experimental design

Four experimental tanks located in the Marine Resources Center of the Marine Biological Laboratory were used (Fig. 1); two were maintained at 20°C and two at 15°C, for the duration of the experiment. *Loligo pealeii* caught on 13 August were placed in the two tanks at the front of the group; those caught on 19 August were placed in the two tanks at the rear. In each tank, the grouped *L. pealeii* were differentiated on the basis of size and (or) distinguishing marks, so the growth of individuals could be followed.

Lighting was provided by two double fluorescent tubes on the ceiling; lights were generally on between 07:30 and 16:30 Monday–Friday and between ca. 08:00 and 17:00 Saturday–Sunday. Two 25-W red lights were erected over the tank area, and these were timed to be on between 19:00 and 06:00 every night.

The polyethylene tanks were round, deep marine blue in colour, and approx. 950 L in capacity, with gravel on the bottom. To keep *L. pealeii* away from the tank walls, a substrate-free border of some 20 cm between the edge of the gravel and the edge of the tank wall was maintained. Circular covers of polystyrene enhanced the gravel border effect (i.e., the sides of the tanks were illuminated).

Fig. 1. Design of the experiment in which *Loligo pealeii* were reared at two temperatures, 15 and 20°C, showing the four tanks used, the numbers stocked in each tank at the start of the experiment, and the individual *L. pealeii* (IDs) used in the data analyses, with their survival times.

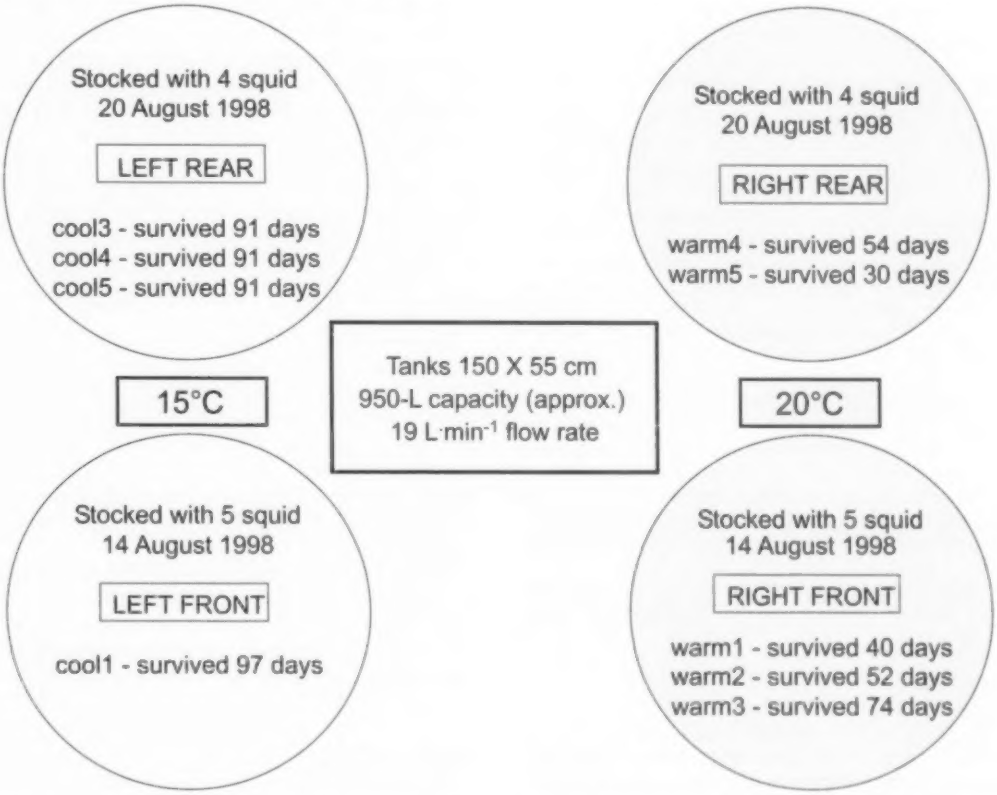
Stocked with 4 squid
20 August 1998
LEFT REAR
cool3 - survived 91 days
cool4 - survived 91 days
cool5 - survived 91 days
Stocked with 4 squid
20 August 1998
RIGHT REAR
warm4 - survived 54 days
warm5 - survived 30 days
15°C
Tanks 150 X 55 cm
950-L capacity (approx.)
19 L·min⁻¹ flow rate
20°C
Stocked with 5 squid
14 August 1998
LEFT FRONT
cool1 - survived 97 days
Stocked with 5 squid
14 August 1998
RIGHT FRONT
warm1 - survived 40 days
warm2 - survived 52 days
warm3 - survived 74 days

The entire tank area was cordoned off, using black plastic sheeting, in an area some 5 m^2, to isolate *L. pealeii* from disturbance.

There was a fairly slow water flow into the tanks (approx. 19 $L \cdot min^{-1}$) through a 1 in. (1 in. = 25.4 mm) polyvinyl chloride pipe spray-bar set across the radius of the tank. The spray-bar was angled upwards slightly to create a slow circular water movement in the tank.

All tanks received water drawn from the cut at Woods Hole, which is connected directly to Vineyard Sound where *L. pealeii* were collected. Two of the tanks (cool water at 15°C) were supplied from a flow-through system in the Marine Resources Center, while the other two (warm water at 20°C) were supplied from a semiclosed loop that was operated in a largely open flow-through manner. The latter system contained about 34 500 L of water, of which a high percentage (9.7%) was exchanged in the loop every hour. This water was either heated or chilled to maintain a temperature of approximately 20°C. Biological filters were in the loop, but the rapid water turnover and the low biomass of *L. pealeii* assured high water quality.

Food items were introduced into the tank with minimal disturbance. The feeding regime was changed several times throughout the duration of the experiment. Initially *L. pealeii* were fed small amounts five times per day, at a rate of 75% of the grouped body weight per tank per day. This frequency was reduced to two times per day, equivalent to 25% of the grouped body weight per day, as the experiment progressed. Feeding was always ad libitum. Daily feeding consisted of small live fishes (initially killifish, *Fundulus grandis*) and the grass shrimp (*Paleomonetes vulgaris*). The fish diet was then changed to feeder guppies (family Poecilidae), because a consistent source of the right-sized killifish could not be found. Neither fish species would be part of the natural diet of *L. pealeii*, but they were readily eaten by them. *Loligo pealeii* were observed feeding on *P. vulgaris* in the natural environment during dive observations in the summer months in Narragansett Bay, Rhode Island (W.K. Macy, Graduate School of Oceanography, University of Rhode Island, R.I., U.S.A., personal communication).

Once a week, *L. pealeii* were removed from each tank and weighed; *L. pealeii* were herded into a submerged water-filled plastic bag for removal from the tank. Individuals were removed carefully from the plastic bag by hand and held head down, to allow excess water to drain from the mantle cavity. Water was then removed from the weigher's hand and fingers, and the animal placed into a tared beaker of water. Once weighed, each *L. pealeii* was placed in a second bag of water, taken from the same tank from which the individual had been removed. Any lesions or features distinguishing individual *L. pealeii* were noted at this time. *Loligo pealeii* were returned to their tank by submerging the water-filled bag and letting them swim slowly from the bag into the tank. For consistency, all measurements were taken by the senior author; however, for this reason, it was not possible to take measurements on 17 September and 29 October 1998.

Growth

The instantaneous relative growth rate (IRGR; percent increase in body mass per day) was calculated to facilitate the comparison of growth at the two different temperatures and between tanks. The instantaneous growth rate of cephalopods is typically calculated using the equation

$$(1) \qquad \mathrm{IRGR} = b \times 100 = \left(\frac{\ln \mathrm{BM}_2 - \ln \mathrm{BM}_1}{t_2 - t_1} \right) \times 100$$

where ln BM_2 is the natural log of body mass at time t_2, ln BM_1 is the natural log of body mass at time t_1, t_2 is the experimental-day number at the second measurement, and t_1 is the experimental-day number at the first measurement (Forsythe and Van Heukelem 1987).

To determine if growth across the entire duration of the experiment was consistent, the values of IRGR from week to week were calculated for each *L. pealeii* using eq. 1. By comparing each weekly IRGR value to the running mean of previous values, it was possible to identify, with some clarity, the point at which IRGR values begin to decline. The point at which the values of IRGR begin to decrease noticeably and consistently is indicative of a change in growth rate. This enabled different phases of growth to be identified.

To describe growth in each identified phase of the experiment, linear ($Y = a + bX$), exponential ($Y = ae^{bX}$), and logarithmic or power ($Y = aX^b$) functions were fitted to the data sets. The best fits were chosen on the basis of the highest adjusted r^2 values (DeRusha et al. 1987; Forsythe and Hanlon 1989). Data were analysed and graphed and curve fits examined using the program Kaleidagraph® v3.0.4 (Synergy Software, 2457 Perkiomen Ave., Reading, PA 19606-2049, U.S.A.) for Macintosh® computers.

Values of IRGR for each phase of growth were calculated from the exponential function (Forsythe and Van Heukelem 1987) with the formula:

$$(2) \qquad \mathrm{BM(g)} = ae^{b(t_2 - t_1)}$$

where BM is the body mass in grams, a is the y-intercept, e is the natural logarithm, and b (× 100) equals IRGR for the time period $t_2 - t_1$. Growth rates for each phase of growth were compared. First, a general linear model (GLM) was used to test for within-treatment effects for each growth phase to see if growth differed between the front and rear tanks at the same temperature, using the statistical package MINITAB v.11 (Minitab Inc. 1996). Time was the covariate, ln BM the dependent variable, and tank identification (ID; front left or right and rear left or right) the factor. The data for front and rear tanks were then combined and a F test performed, to determine if the variance of the values of IRGR within each treatment was similar. Finally, a one-tailed t test was performed, to detect any significance of difference in the mean values of IRGR at the different temperatures over the different phases of growth. A one-tailed test was used, as there was an a priori assumption that the higher temperature would produce a faster growth rate.

Age determination

Most *L. pealeii* were retained after death, weighed, dissected, sexed, and assigned a maturity rating (indeterminate, immature, maturing, mature); statoliths were removed to enable putative age determinations. Statoliths were cleaned in ethyl alcohol, allowed to air-dry, and then mounted in "Crystalbond" resin; statoliths were ground and counted according to the method of Macy (1995).

These statolith age data were then used to derive an age for each individual at the start date of each tank experiment and to show growth rates during the different growth phases as a function of age rather than time from day 1 of the experiment. These growth equations, coupled with interpolated growth data derived for each temperature, enabled simulations of growth to be performed across the range of temperatures likely to be encountered inshore in the summer.

Results

Water quality

In the flow-through water system (cool-water tanks), the major water-quality parameters over the time period of the experiment were temperature 15.3 (±0.4)°C, pH 8.0, salinity 32 ppt, conductivity 46.1 mS, dissolved oxygen ~8.5 ppm (cephalopods have high respiration rates and require highly aerated water), NH_3 <<0.075 $mg \cdot L^{-1}$, NO_2 <<0.01 $mg \cdot L^{-1}$, and NO_3 0.6 $mg \cdot L^{-1}$. The major water-quality parameters in the semiclosed water system (warm-water tanks) were nearly identical to those in the flow-through system, except that dissolved oxygen concentrations were slightly lower (7.9–8.3 ppm); temperature was 20.1 (±0.2)°C.

Survival

Eighteen *L. pealeii* were caught: 10 on the night of 13 August and 8 on the night of 19 August 1998. Ambient temperature at capture was around 20°C. Mean survival time was 38 (±12.1) days. Nine *L. pealeii* survived beyond 21 days, up to a maximum of 97 days. Figure 1 shows the numbers, placement, and identities of each *L. pealeii* used in the growth-rate calculations. This is the first study in which so many *L. pealeii*, at this small size, have been reared successfully over such a long period.

Growth measurements were collected from all nine surviving *L. pealeii*. Age, sex, and maturity data (shown in Table 1) were available for only seven of the nine *L. pealeii*; the other two (warm1 and warm5) were discarded accidentally before measurements could be taken. Age data were also available for the first *L. pealeii* to die, 6 days after capture.

Age determination

The original statolith increment counts for each individual are shown in Table 1 and estimate the age of each *L. pealeii* at day 1 of the experiment, assuming one increment is laid down per day. Under incident light, the statoliths of individuals that had been put into the warm-water tanks were milky white and translucent from the area of the natal check to the edge of the statolith in both the dome and rostral areas. This is apparent in Fig. 2*a*. However, the statoliths of four of the five *L. pealeii* that were placed in the cool-water tanks were translucent to about two-thirds of the way out to the edge of the statolith. Then a very obvious transparent zone was discernable, with the remainder of the statolith to the edge being more transparent than translucent (this is apparent in Fig. 2*b*). The one cool-water treatment *L. pealeii* in which the transparent zone was not particularly obvious died on the sixth day of the experiment. This suggested that the transparent zone was correlated with the experimental period in the laboratory and was possibly a response to thermal decrease upon coming into the laboratory. The inner edge of the transparent zone was also associated with a check mark, which was not obvious in the warm-water *L. pealeii*.

Increment counts were made from the inner edge of the transparent zone to the outer edge of the statolith in the four cool-water *L. pealeii* statoliths with this zone. Unexpectedly, only about half as many increments were counted for each individual as there were number of days in the experiment (Table 1). For the cool-water *L. pealeii*, a new estimate for age at day 1 of the experiment was derived that was calculated as esti-

Table 1. Sex, maturity, and statolith-derived age data for eight of the nine *Loligo pealeii* reared for a maximum of 97 days between 14 August and 19 November 1998.

ID	Sex	Maturity rating	Original no. of increments	Date of death (1998)	No. of days in tank	Estimated age at day 1 (days)	Mean no. of increments in transparent zone	Mean no. of increments/ tank day	Revised age at day 1 (days)	Age at death (days)	Estimated hatch date (1998)
Cool1	Female	Immature	106	19 November	97	9	42	0.43	64	161	11 June
Cool2		Juvenile	88	19 August	6	82	3[a]	0.50[a]	85[a]	91[a]	20 May
Cool3	Male	Mature	128	19 November	91	37	47	0.51	81	172	31 May
Cool4	Female	Mature mated	127	19 November	91	36	45	0.49	82	173	30 May
Cool5	Female	Maturing	135	19 November	91	44	56	0.61	79	170	2 June
Warm2	Male	Mature	88	5 October	52	36	26[a]	0.50[a]	62[a]	114[a]	13 June
Warm3	Female	Mature	111	27 October	74	37	37[a]	0.50[a]	74[a]	148[a]	1 June
Warm4	Male	Mature	124	7 October	54	70	27[a]	0.50[a]	97[a]	151[a]	9 May

[a] Value is an estimate because no transparent zones were apparent in the statoliths.

Table 2. Values of the instantaneous relative growth rate (IRGR) modeled for growth of *Loligo pealeii* from hatching to the date of capture, derived from original count values and revised count values of the number of increments in the statolith.

	IRGR derived from	
ID	original counts	revised counts
Cool1	78.3	11.1
Cool3	21.6	9.9
Cool4	22.6	9.9
Warm2	18.9	11
Warm3	19.5	9.8
Warm4	11.3	8.2
Average	28.7	9.9

mated age plus half the number of experimental days for each individual (Table 1). This same correction was applied to the increment counts from the warm water *L. pealeii* statoliths.

Precapture growth rates

By estimating precapture growth rates, it is possible to assess how realistic the initial estimated and revised ages reported in the previous section (Table 1) were; comparisons can also be made with the growth rates obtained in the laboratory. Growth rates were calculated using both the initial estimated age at capture and the revised age at experimental day 1 (Table 1). For these six *L. pealeii*, a hatching size of 1.5 mg was plotted along with the weight and estimated ages at experimental day 1 (hatching body weight was estimated from the length–weight relationship of Macy (1980) for juvenile *L. pealeii*). An exponential curve fit equation was used to connect the two points, and the slope exponent of the resulting function was used to estimate the IRGR.

Unquestionably, the growth rates derived using the initial age estimates were unrealistically high (see Table 2). Mean group growth rates of 28.76% body mass per day are unheard of in the genus *Loligo* at any temperature or life stage. This indicates that the initial age estimates were not indicative of *L. pealeii* true age. The growth rates of 8–11% body mass per day, using the revised age estimates, are much more realistic for this species and have been reported by several authors that have cultured *Loligo* spp. These estimates suggest that *L. pealeii* collected in Vineyard Sound had been growing at a mean IRGR of 9.9% from hatching until capture.

Laboratory growth

Growth measurements for the nine longest surviving squid are given in Table 3. The raw data are given to facilitate their accurate use by others in future modeling efforts. The mean size at day 1 of the experiment in the 15°C tanks was 4.13 (±1.64) g. The mean size at day 1 in the 20°C tanks was 2.81 (±1.89) g.

The literature demonstrates overwhelmingly that growth in weight of young post-hatching cephalopods is initially exponential in form and then changes to a slower form of growth. By definition, if growth is exponential in form, IRGR values calculated from measurement to measurement will remain at a consistent value, although as in any biologi-

Fig. 2. Images of *Loligo pealeii* statoliths from warm-water (*a*) and cold-water (*b*) rearing conditions viewed under incident light. An obvious transparent band is seen in the cold water reared *L. pealeii* statolith (*b*) that is lacking in the warm-water reared *L. pealeii* statolith (*a*). Scale bars = 0.26 mm (*a*) and 0.23 mm (*b*).

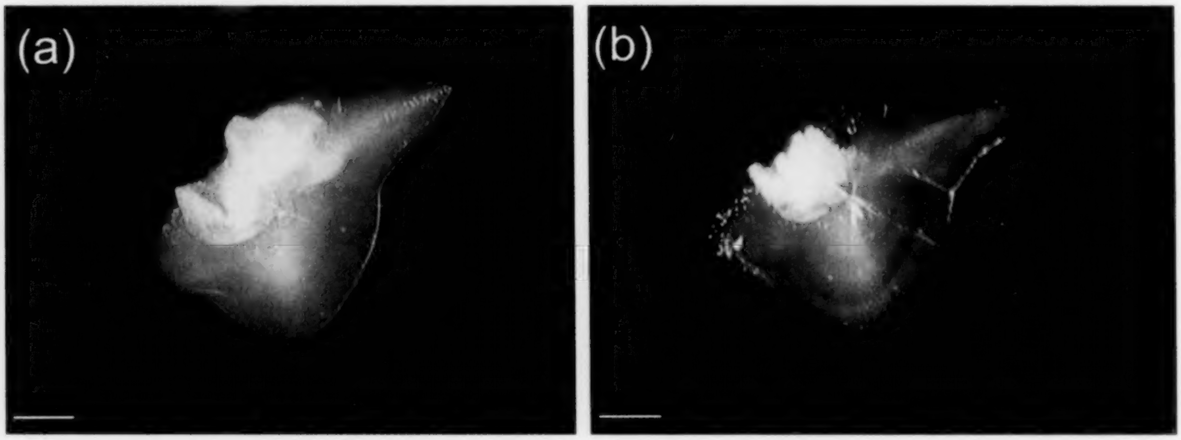

cal system, there will be some fluctuation. The point at which IRGR values begin to decline steadily marks the end of the initial exponential growth phase. To determine if growth occurred in more than one phase, values of IRGR were calculated for each *L. pealeii* from week to week (shown in Table 4). By comparing each weekly IRGR to the running mean of previous values, it was possible to identify, with some clarity, the point at which the IRGR values were declining. Rates remained constant throughout the first 21 days in individuals warm3, warm4, and warm5; throughout 27 days in individuals cool1 and warm2; throughout 35 days in individuals cool3 and cool4; and throughout 42 days in individual cool5. Growth up to this time (indicated by "**" in Table 4) is denoted as "phase-1 growth." Growth beyond this time is denoted as "phase-2 growth."

For most *L. pealeii* in growth phases 1 and 2, the exponential model provided the best fit to the individual growth trajectories, explaining the growth pattern for six of nine squid in phase 1 and five of six squid in phase 2. The ranges of the adjusted r^2 values for exponential fits were 0.98–1.0 for phase 1 and 0.91–0.99 for phase 2. The values of IRGR were derived from the exponential model ($b \times 100$).

Results of the GLM determined that there were no within-treatment effects between the front and rear tanks that were held at the same temperature for squid in each growth phase separately, thus within-treatment growth data were combined to test for any differences between treatments. The mean values of IRGR derived from the exponential-model results were 4.36 for phase-1 warm-water tanks, 2.69 for phase-1 cool-water tanks, 2.57 for phase-2 warm-water tanks, and 1.63 for phase-2 cool-water tanks. An F test to test if the samples had been drawn from populations with equal or similar variances and were thus comparable statistically showed no significant difference between the variances of the combined treatment data for both growth phases separately (15°C tanks vs. 20°C tanks). The one-tailed t test showed that the mean value of IRGR for both growth phases was significantly higher ($p < 0.01$) for *L. pealeii* reared at 20.1 (±0.2)°C than for those reared at 15. 3 (±0.4)°C. However, it is clear that post-capture phase-1 growth rates were not a continuation of the estimated precapture growth rates. For the period of phase-1 growth, a 5°C difference in temperature altered IRGR by 1.7%. In phase 2, the difference was 0.97%. More sophisticated statistics were not possible, owing to the combination of a small number of individuals and the staggered start date of the experiment between the front and rear tanks.

The mean size of *L. pealeii* at day 1 in the 15°C tanks was 4.13 g and, in the 20°C tanks, was 2.81 g. However, to achieve a meaningful comparison of calculated growth trajectories, it is necessary to account for the initial size of each individual at the start of each growth phase. We calculated such pooled average growth trajectories at 15 and 20°C for *L. pealeii* in phase 1, assuming a hatchling size of 1.5 mg (Fig. 3*a*) and a conservative phase-2 entry size of 5 g (Fig. 3*b*). The equations in each phase, with b calculated as the mean of the exponential-model values ($\text{IRGR} \equiv b \times 100$), are thus:

Phase 1	15°C	$\text{BM} = 0.0015\ e^{(0.0269 \cdot \text{age})}$
	20°C	$\text{BM} = 0.0015\ e^{(0.0436 \cdot \text{age})}$
Phase 2	15°C	$\text{BM} = 5.0\ e^{(0.0163 \cdot \text{age})}$
	20°C	$\text{BM} = 5.0\ e^{(0.0257 \cdot \text{age})}$

Thus, in each phase of growth, with the same assumed initial size, it is clear from Fig. 3 that squid grow faster at the higher temperature.

Modeling field growth of juvenile *L. pealeii*

The real value of the information provided above about the relationship between temperature and growth rate in *L. pealeii* lies in using it to make simple hypotheses about field growth that can be tested with future collections of field data. Values of IRGR can be estimated for different temperatures, through linear interpolation of the values for phase-1 and phase-2 growth at 15 and 20°C. The resultant equations for each growth phase are

Phase 1	$\text{IRGR} = (0.00334 \cdot T - 0.0232) \times 100$
Phase 2	$\text{IRGR} = (0.00188 \cdot T - 0.0119) \times 100$

where T is temperature. These equations can be used to estimate the mean monthly growth rate of *L. pealeii* during any month for which mean daily water temperature is known.

Table 3. Raw data for nine *Loligo pealeii* reared for a maximum of 97 days between 14 August and 20 November 1998.

	Front tanks					Rear tanks					
		Wet body mass (g)					Wet body mass (g)				
		15°C	20°C				15°C			20°C	
Date (1998)	Expt. day	Cool1	Warm1	Warm2	Warm3	Expt. day	Cool3	Cool4	Cool5	Warm4	Warm5
14 August	1	1.72	1.08	1.34	2.06	—	—	—	—	—	—
20 August	6	1.93	1.47	1.73	2.63	1	4.47	5.09	5.24	4.17	5.49
27 August	13	2.31	2.02	2.37	3.6	7	5.12	5.39	5.96	5.53	7.74
3 September	20	2.94	2.57	2.79	5.01	14	6.29	6.45	7.31	7.32	10.53
10 September	27	3.57	3.34	3.91	6.4	21	7.5	7.99	8.95	9.28	14.2
17 September	34	na	na	na	na	28	na	na	na	na	na
24 September	41	4.66	—	4.14	7.06	35	11.41	11.87	12.27	12.73	—
1 October	48	5.25	—	4.02	10.97	42	12.54	13.64	14.73	14.2	—
8 October	55	5.82	—	—	13.42	49	14.41	14.87	15.98	—	—
15 October	62	6.59	—	—	18.93	56	15.76	16.73	17.3	—	—
22 October	69	7.7	—	—	22.13	63	16.48	18.59	21.91	—	—
29 October	76	na	—	—	na	70	na	na	na	—	—
5 November	83	9.78	—	—	—	77	22	23.91	25.92	—	—
12 November	90	10.94	—	—	—	84	24.98	27.96	27.81	—	—
19 November	97	11.42	—	—	—	91	27.68	31.18	29.34	—	—

Note: Each squid was weighed individually in a tared beaker of seawater. Tanks were held at either 15 or 20°C for the duration of the experiment. Experiments in the front tanks were initiated on 14 August 1998 and in the rear tanks on 20 August 1998. Squid were not weighed on 17 September or 29 October 1998 (denoted with "na"). A dash (—) denotes a measurement missing, owing to death of the individual.

Table 4. Values of the instantaneous relative growth rate (IRGR) calculated[a] from week to week for individual *Loligo pealeii*, to discern the point at which exponential growth started to decay (indicated by "**") in rearing experiments.

Front tanks					Rear tanks					
Experimental days	Cool1	Warm1	Warm2	Warm3	Experimental days	Cool3	Cool4	Cool5	Warm4	Warm5
1–6	1.92	5.14	4.26	4.07	1–7	1.94	0.82	1.84	4.03	4.91
6–13	2.57	4.54	4.5	4.6	7–14	2.94	2.54	2.92	4.01	4.4
13–20	3.45	3.44	2.33	4.72**	14–21	2.51	3.06	2.89	3.34**	4.27**
20–27	2.77**	3.74**	4.82**	3.5	21–28	na	na	na	na	na
27–34	na	na	na	na	21–35	3.00**	2.83**	2.25	2.26	—
27–41	1.9	—	0.41	0.7	35–42	1.35	1.99	2.61**	1.56	—
41–48	1.7	—	–0.42	1.42	42–49	1.99	1.23	1.16	—	—
48–55	1.47	—	—	2.88	49–56	1.28	1.68	1.13	—	—
55–62	1.78	—	—	4.91	56–63	0.64	1.51	3.37	—	—
62–69	2.22	—	—	2.23	63–70	na	na	na	—	—
69–76	na	—	—	—	63–77	2.06	1.8	1.2	—	—
69–83	1.71	—	—	—	77–84	1.81	2.23	1.01	—	—
83–90	1.6	—	—	—	84–91	1.45	1.56	0.77	—	—
90–97	0.61	—	—	—	—	—	—	—	—	—

Note: A dash (—) denotes a measurement missing; na, not available.

[a] Calculated using the equation $(\ln BM_2 - \ln BM_1/t_2 - t_1) \times 100$, where BM is wet body mass in grams and t is the number of days in a front or rear experimental tank.

The mean monthly temperatures from May to October 1998 at the NMFS aquarium water intake for water pumped in from Great Harbor, Woods Hole, are shown in Fig. 4. It is obvious that the temperatures vary to a large extent through spring, summer, and autumn. To use constant-temperature growth data to predict size at age for wild *L. pealeii* would therefore be unrealistic.

Using the temperature data in Fig. 4, a separate simulation was performed to project, hypothetically, the growth of juvenile *L. pealeii* with an average initial live weight of 1.0 g (as they enter coastal waters near Woods Hole) starting in the month of May through to September. In this simple model, growth was assumed to be exponential in form, from the first to the last day of each month, at the mean daily growth rate for that month as determined from that month's mean daily water temperature. For example, the animals starting in May with a weight of 1.0 g grew for 30 days at a growth rate of 1.89%/day based on a mean daily water temperature of 12.6°C. On 1 June, the growth rate became 3.29%/day for the next 30 days, based on a mean daily water temperature in June of 16.8°C, and so on, month by month. Each group was assumed to grow at phase-1 growth rates for 60 days and at phase-2 growth rates thereafter. Since *L. pealeii* generally remain inshore only until October, the May cohort

Fig. 3. Mean growth curves for *Loligo pealeii* in (*a*) phase-1 and (*b*) phase-2 growth at 15°C (■) and 20°C (▲), derived from the growth of nine *L. pealeii*. Curves in *a* are plotted from an approximate hatching size of 0.0015 g; curves in *b* are plotted from a theoretical starting size of 5 g.

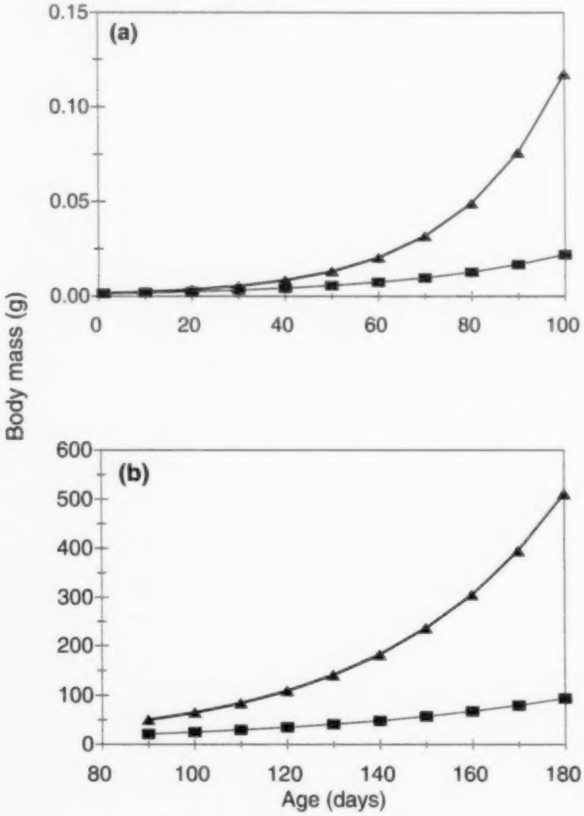

simulation was run for 6 months, while the September cohort simulation was run for only 2 months. Figure 4 presents the results of this simulation over time, from 1 May to 31 October. As expected, the May cohort (being the oldest) is the largest at each monthly interval. However, *L. pealeii* in the June cohort almost equal those in the May cohort in size after just 30 days of growth and remains close to the May cohort throughout. This is caused by the low temperatures encountered by the May cohort, which significantly retard growth. In contrast, the July and August cohorts continually diverge from one another, as elevated temperatures ensure higher growth for both cohorts.

Perhaps the most significant potential outcome of monthly temperature change can be seen in Fig. 5, where the growth of cohorts is compared from the same starting point on the *x*-axis. Only the May, June, and July cohorts are shown for clarity. By the end of phase-1 growth at 60 days, the May cohort is nearly 5 g in weight, while the June and July cohorts are two and three times that weight, respectively, at the same age. The May cohort is never able to make up the discrepancy caused by the lower water temperatures in May.

Figure 5 also demonstrates that, for early summer cohorts emerging in May–July, increasing water temperature ensures that later cohorts grow faster for at least the first 120 days after hatching. Although (as we see from Fig. 5) younger cohorts do not actually surpass older ones in size in the simplified climatic scenario here, the potential for them to do so is self-evident.

Maturation

Two of the four females were fully mature at the conclusion of the experiment. Warm3 (dorsal mantle length (ML) at death, 69 mm) laid an egg mop of 41 fingers just before she died, with a mean of 79.6 (±38.2) eggs per finger (measured from a subsample of 10 egg fingers). Cool4 (ML at death, 84 mm) had an oviduct packed with mature oocytes and there were spermatophores in the seminal receptacle. Cool5 (ML at death, 86 mm) had many mature oocytes in the ovary but none in the oviduct. The three identified males were all fully mature, with spermatophores in the spermatophoric sac (MLs at death of ~34, 58, and 84 mm).

Discussion

Growth was fast and exponential in both phases. Temperature alone caused a significant change in growth rate during both growth phases of *L. pealeii*. This effect diminished during the second growth phase. Growth in both phases, however, was best described by an exponential model for the majority of the individual *L. pealeii*.

To attain the sizes and ages at capture, the growth of the *L. pealeii* in this study would have to have been sustained at around 9.9% body mass per day prior to capture (actual range 8.2–11.0%). This rate is achievable by the loliginids *Loligo vulgaris* (Turk et al. 1986) and *Loligo opalescens* (Yang et al. 1986); both grew at rates of about 8% body mass per day at 17.4°C and 15°C, respectively, during their early life stage from hatching to the end of phase-1 growth. In *Sepioteuthis lessoniana*, rates of 6–13% body mass per day were achieved at temperatures of 20°C and higher (Lee et al. 1994; Forsythe et al. 2001).

The fact that post-capture IRGR values in *L. pealeii* were lower than the estimated precapture IRGR of 9.9% of body mass per day may be due to some laboratory artefact that depressed growth. Most of the squid were damaged at capture (even if only slightly), which may have depressed growth, owing to the healing process. Three squid (cool3, cool4, and cool5) sustained damage to the tips of their mantle and fins but still managed to grow throughout the course of the experiment, and even to reach maturity, albeit at a much smaller size than is possible for the species. At death, a significant portion of the mantle tissue below the fin tip was missing, even though there seemed to be no infection present; these can clearly be quite resilient beasts. It is also likely that, although food was not limited in supply, the food itself was not optimal for growth. It is thus likely that the findings in this study are conservative estimates of growth potential at temperature. Finally, the relatively small sample size of this study must be considered and, for that reason, the extrapolations made from this data set have been very conservative and in no way should be considered as defini-

Fig. 4. Simulation of the growth of *Loligo pealeii* for individuals hatched on the first day of each month from May to September. Mean monthly temperatures for Great Harbor, Woods Hole, are shown for each month. Instantaneous relative growth rate (IRGR) values for phases 1 and 2 are shown below the temperature values. *Loligo pealeii* were grown from a starting size of 1 g. Growth is simulated at the phase-1 rate for 60 days and at the phase-2 rate thereafter. Symbols: May, ○; June, ◆; July, ⊞; August, ●; September, ◇.

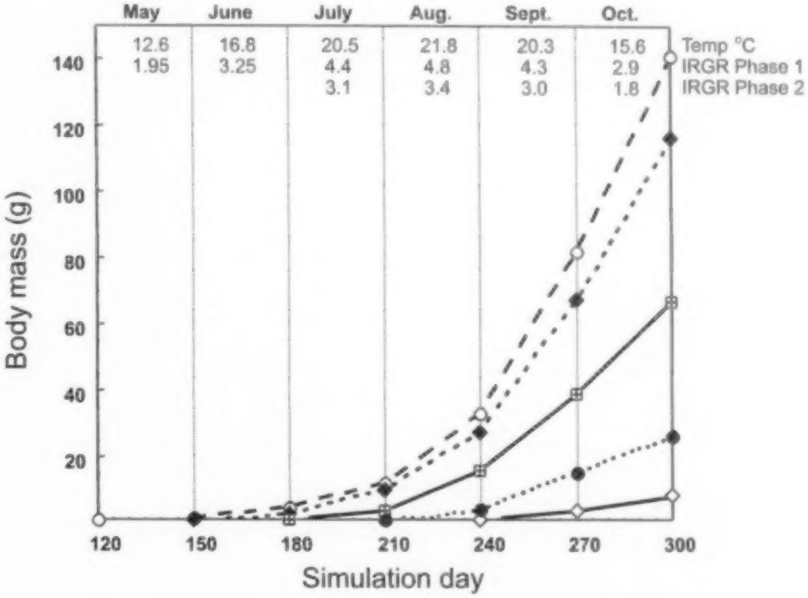

tive for this species. However, every extrapolation presented falls fully within the realm of known parameters of growth capability in the genus *Loligo*.

Growth comparisons for young loliginid squid

In previous laboratory studies of growth in six species of loliginid squid (discussed in Forsythe and Hanlon 1989), growth (measured as length or mass or both) was found to be exponential for at least 2 months post hatching. In *L. forbesi*, Forsythe and Hanlon (1989) demonstrated two phases of growth, an exponential phase lasting 3–4 months post hatching, followed by a slower growth phase best described by either an exponential or a power function in different experiments. The conclusion in the *L. forbesi* study was that the second, slower growth phase was more likely to be explained by a power function, given that various metabolic constraints would seem to preclude true exponential growth in individuals growing from subadult to adult sizes (O'Dor and Wells 1987).

However, the present study was surprising in that small *L. pealeii* continued to grow exponentially for a longer time. Two clear phases of growth were present. Growth patterns in the first phase were more variable. In the first phase, all the cool-water reared *L. pealeii* clearly showed exponential growth. The warm-water reared *L. pealeii* showed more variability: two showed linear growth, two exponential growth, and one logarithmic (power) growth. The growth of one of the two *L. pealeii* showing linear growth was almost as well fitted by the exponential model (warm1), whereas growth of the other was almost as well fitted by the power model (warm5). This higher variability at a higher temperature is hard to explain, as one would still expect squid to follow an exponential growth trajectory at this stage of the life cycle. In a recent analysis of *Loligo gahi*, Hatfield (2000), studying the wild population, demonstrated that there was greater variability in the growth rate of squid that hatched in the summer versus the winter. Perhaps this variability is just a feature of the intrinsic plasticity of growth demonstrated by so many cephalopod species (Boyle and Boletzky 1996).

In the second phase, five of the six *L. pealeii* for which there were data clearly showed exponential growth. The sixth *L. pealeii*, cool5, showed linear growth over this period. This second phase growth period lasted to the end of the experiment, to estimated ages of almost 6 months in four individuals. Sustained exponential growth in the second growth phase was demonstrated in *L. forbesi* in experiment LF86 (Forsythe and Hanlon 1989), where squid grew at this rate to ages of almost 15 months at a temperature of around 14°C.

The inflection point in this study seems to be related to neither size nor age in particular, although in *S. lessoniana*, another loliginid squid, there does seem to be a defined size at which the inflection point occurs (Forsythe et al. 2001). Metabolic constraints generally limit the size to which any animal can grow at an exponential rate (reviewed recently for fish and cephalopods by Pauly (1999)). Beyond this size, growth is slower in form—in cephalopods it is usually described by a power function (see, for example, Forsythe et al. 2001). In our present study, both phases of growth were exponential in form, although phase-2 growth was slower. The captive *L. pealeii* probably grew at a slower rate than they would have in the wild (demonstrated by the age data) and were much smaller at maturity than most wild-caught *L. pealeii*. Because of their small body size, the con-

Fig. 5. Simulation of the growth of *Loligo pealeii* for individuals hatched on the first day of each month from May to July. The simulations are the same as those in Fig. 4 but are plotted on the same start date, to show the effect of ambient temperature in a more easily comparable style. Symbols: May, ○; June, ◆; July, ⊞.

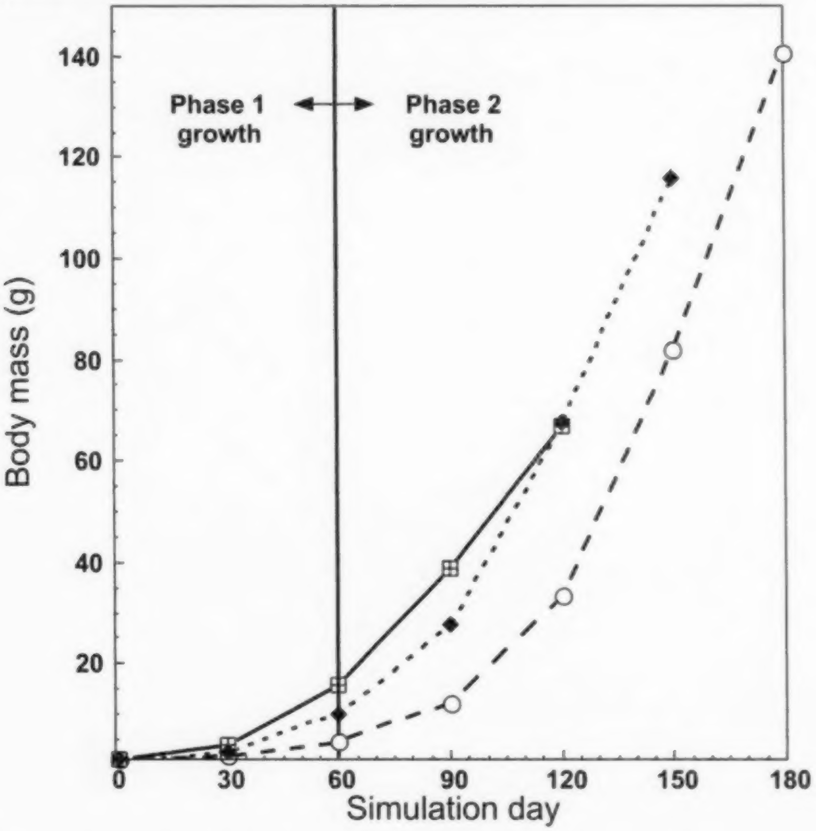

straints on their physiology might have had a less dominant effect on shaping the growth trajectory, enabling growth to continue to be exponential in form into the second phase.

The growth rates seen in this study are comparable with those obtained for other loliginid species in laboratory studies of growth. Table 5 shows comparative values of IRGR over the same size (body mass) range as the *L. pealeii* in this study. For *L. forbesi* (Forsythe and Hanlon 1989) and *L. opalescens* (Yang et al. 1986), IRGR values were calculated from the published growth equations. Both the phase-2 values obtained here for *L. pealeii* are directly comparable with those obtained previously for *L. forbesi* and *L. opalescens*. The growth values for phase-1 growth in *L. forbesi* and *L. opalescens* are not comparable with the phase-1 values derived in the current study, because in this case, growth of *L. pealeii* was only monitored from ages of around 70 days and older, whereas rates for the other two species were calculated from hatching to 2–3 months of age. Data are available for *L. pealeii*, *Loligo plei*, and *Lolliguncula brevis* from Hanlon et al. (1983). The data from Hanlon et al. (1983) are for particular individuals, whereas the data for *L. forbesi* and *L. opalescens* are averages from group rearing studies. However, the IRGRs at similar sizes and temperatures in all previous studies are comparable with the values obtained in the current study.

Neither sex nor maturity appear to have affected the growth rates in the rearing experiment. There were no significant differences in rates between individuals within phase 1 or phase 2 (for each temperature). Size and age for mature *L. pealeii* in the experiment ranged from 22.1 to 31.2 g and from 148 to 173 days, respectively, for females and from 4.0 to 27.7 g and from 114 to 172 days, respectively, for males. In a recent analysis of maturity data from commercial and research samples in 1997 and 1998 for *L. pealeii* taken both inshore and offshore (E.M.C. Hatfield and S.X. Cadrin, unpublished data), the minimum size at maturity was 20.9 g for females and 8.3 g for males. Four percent of females sampled were mature in the 15- to 30-g range, with another 8% mature in the 30- to 45-g range. For sampled males, 2% were mature in the 0- to 15-g range and another 7% were mature in the 15- to 30-g range. Thus the small size of sexually mature squid seen in our rearing experiments is also seen in the wild population, and is not unusual. In another recent analysis of age and maturity data for *L. pealeii* sampled from 1993 to 1997 (W.K. Macy, Graduate School of Oceanography, University of Rhode Island, R.I., U.S.A., personal communication), the minimum age for mature females was 109 days and for mature males was 119 days. The minimum size for a mature female was 45 mm ML (equivalent to a body mass of about 6.5 g, using the length/weight equation of Lange and Johnson 1981) at

Table 5. Comparison of the instantaneous relative growth rate (IRGR) of several loliginid species reared under experimental growth conditions at similar temperatures and size ranges.

Species	IRGR	T (°C)	Size range (g)	Growth phase	Source
Loligo pealeii	2.69	15	1.7–14.7	1	This study
	4.36	20	1.1–9.3	1	This study
	1.63	15	3.6–31.2	2	This study
	2.57	20	3.3–22.1	2	This study
Loligo forbesi	1.55	14	1.4–30.3	2	Forsythe and Hanlon 1989
Loligo opalescens	2.7	15–19	1.2–30.0	2	Yang et al. 1986
L. pealeii	1.9	21–23	27.6–49.1	2	Hanlon et al. 1983
Loligo plei	3.3	20–21	13.0–39.2	2	Hanlon et al. 1983
Lolliguncula brevis	2.6–3.8	19–22	3.3–28.0	1, 2	Hanlon et al. 1983
	2.0	20–22	5.8–18.2	1, 2	Hanlon et al. 1983
	4.6	21–22	5.5–18.8	1, 2	Hanlon et al. 1983

an age of 156 days. For males, the minimum size at maturity was 25 mm ML (equivalent to a body mass of 1.84 g) at an age of 178 days. The minimum-age data are similar to those for males in our rearing experiment and, for females, show an even younger age at maturity than we observed. The minimum-size data show that *L. pealeii* are capable of maturing at an incredibly small size, coupled with very slow growth.

In other experimental research on *L. pealeii*, it has been suggested that captivity accelerates sexual maturation (Hanlon et al. 1983) or, at least, produces mature individuals of smaller size than in the wild population (Yang et al. 1986). The latter observation could be the result of reduced growth rates in captivity. Certainly in the present study, *L. pealeii* grew at a rate lower than that at which they were probably growing prior to capture. If *L. pealeii* had continued to grow at the 9.9% (body mass per day increase) precapture rate estimated earlier, then it is probable that larger sizes at maturity might have been attained. However, the sizes and ages at maturity attained by *L. pealeii* in our study fall within the range seen in the wild population.

In modeling growth of wild-caught *L. pealeii*, Brodziak and Macy (1996) stated that the selected growth curves indicated that growth was dependent on maturity stage, sex, and hatching season. The hatching-season data implied an effect of temperature, which we have shown to affect growth of this species significantly. In the current study, however, neither sex nor maturity seemed to affect the growth rate. Brodziak and Macy (1996) demonstrated values of IRGR, beyond the first 3 months of age, of 1.93 for females and 2.68 for males among individuals hatched from June to October, that is, during the warmer inshore months. The values for wild-caught males are comparable with the values obtained for *L. pealeii* reared at 15°C. However, these values are for *L. pealeii* that ranged in size from approximately 10 to 770 g, considerably beyond the sizes observed in our rearing study.

Modeling of field growth in juvenile squid

The steeper gradient of the phase-1 curve in Fig. 4 implies that phase-1 growth is more sensitive to temperature than phase-2 growth. As far as we are aware, this is the strongest empirical evidence to date that establishes "phase-specific" temperature sensitivity in squid growth. Forsythe and Hanlon (1989) and Forsythe (1993) obtained phase-1 growth (from an amalgamation of data from previous studies) without deriving a phase-2 equivalent.

It is this temperature-differential mechanism that provides later-hatched cohorts with the opportunity to catch up with older squid in terms of size and, in turn, of development, through seasonally increasing water temperature. That this mechanism is strong enough to produce life-cycle synchronization of a population has been postulated further (Grist and des Clers 1998).

The results of the growth simulation in this study more closely mirror the hypothesized effect of temperature on growth in simulation 2 of Forsythe's (1993) model than that in simulation 1. In Forsythe's (1993) simulation 1, growth was only considered to be temperature dependent in the first growth phase. Beyond phase 1, growth was assumed to be independent of temperature. Thus, the weight of younger faster-growing squid surpassed that of older slower-growing squid that had hatched into cooler water. In the current study, phase-2 growth is still clearly temperature dependent and will thus be affected by ambient temperature. The squid that seem to benefit most in terms of a higher rate of increase in body mass, conferring larger size at a given age, are those hatched in June and July. In these 2 months, temperatures are on the increase and continue to rise through August and into early September, when most squid move offshore (Summers 1983) as temperatures inshore begin to cool. Squid that hatch early (May) and late (September) benefit the least from temperature effects: in May, because the early temperatures are low even though later temperatures are higher, and in September, because the temperatures are lower and on the decrease. At day 120, the May cohort is less than half the size of the June–July groups. This is an excellent illustration of why length–frequency analyses, not calibrated with statolith aging data (which would compensate for temperature), can grossly miscalculate cohort age and growth rates.

Loliginid squid, for which increment periodicity has been validated at one ring per day, and for which statolith increments were clearly visible, were all reared in tanks under natural light, so that they experienced a diel light periodicity (Jackson 1990*a*, 1990*b*; Jackson et al. 1997). Where loliginid squid were reared under artificial light conditions, the statolith increments were less clearly visible (Hixon and Villoch 1984; Jackson et al. 1993). This phenomenon has been noted also for an illicinid species (Dawe et al. 1985). It is possible that the unexpected statolith-increment count encountered in the current study, corresponding to half the number of days spent in the tank, results from dim and artificial light conditions throughout the experiment, coupled with the lack of a diurnal rhythm in temperature or migration. The environment in which *L. pealeii* were reared was an attempt to minimize disturbance to individual *L. pealeii*, to maximize life-span in captivity, not to mimic natural conditions to measure increment periodicity.

Temperature checks in fish otoliths, as a response to a rapid decrease in temperature, are well documented, and this phenomenon is used in salmonid hatcheries to "bar code" batches of fry (Volk et al. 1999). Zones of different optical quality, hypothesized to relate to environmental changes, have been noted in both squid and fish species. Jackson (1993) hypothesized that the optically different zones apparent in statoliths of *Moroteuthis ingens* might be related to a shift from an oceanic to a demersal existence. Several authors have described changes in fish otolith zones that are possibly related to habitat shifts, for example, in flounder (Campana 1984) and various myctophid species (Gartner 1991). The very obvious zonation apparent in the statoliths of *L. pealeii* captured in warm water (ca. 20°C) and placed directly into 15°C water does seem to suggest a strong temperature effect.

Future studies to determine the effects of temperature on the growth of juvenile loliginid squid would be even more useful if they were to incorporate the following factors: individuals should be stained with tetracycline prior to the start of the experiment to mark the squid statoliths; individuals should be held under a natural-light regime of the same periodicity and quality as that experienced in the wild; squid should not be anaesthetized when weighed; a more balanced diet of fish and crustaceans should be used, with marine fish of the right size given to provide the right nutrients; and possible further analysis of statolith zonation with different temperatures.

Acknowledgements

We are very grateful to the staff of the MBL Marine Resources Center, especially Ed Enos, Janice Hanley, Bill Mebane, and Geoff Till. Eleonore Hatfield, Chad Keith, and especially Lynette Suslowicz gave much needed assistance with weighing squid and cleaning tanks. Thanks also to Bill Macy for preparing and "reading" statoliths. Joe Cavanaugh, Mike Maxwell, John Rummel, and Nadav Shashar all helped in feeding squid. EMCH especially thanks Steve Murawski for his support at NMFS. Funding for EMCH was provided through the National Research Council Research Associateship program.

References

Boletzky, S.v., and Hanlon, R.T. 1983. A review of the laboratory maintenance, rearing and culture of cephalopod molluscs. Mem. Natl. Mus. Vic. **44**: 147–187.

Boyle, P.R., and Boletzky, S.v. 1996. Cephalopod populations: definitions and dynamics. *In* The role of cephalopods in the world's oceans. *Edited by* M.R. Clarke. Philos. Trans. R. Soc. Ser. B, Biol. Sci. No. 351. pp. 985–1002.

Brodziak, J.K.T., and Macy, W.K. 1996. Growth of the long-finned squid, *Loligo pealei*, in the northwest Atlantic. Fish. Bull. **94**: 212–236.

Cadrin, S.X., and Hatfield, E.M.C. 1999. Stock assessment of longfin inshore squid *Loligo pealeii*. Ref. Doc. 99-12 of the Northeast Fisheries Science Center, 166 Water St., Woods Hole, MA 02543, U.S.A.

Campana, S.E. 1984. Microstructural growth patterns in the otoliths of larval and juvenile starry flounder, *Platichthys stellatus*. Can. J. Zool. **62**: 1507–1512.

Dawe, E.G., and Beck, P.C. 1997. Population structure, growth and sexual maturation of short-finned squid (*Illex illecebrosus*) at Newfoundland. Can. J. Fish. Aquat. Sci. **54**: 137–146.

Dawe, E.G., O'Dor, R.K., Odense, P.H., and Hurley, G.V. 1985. Validation and application of an ageing technique for short-finned squid (*Illex illecebrosus*). J. Northwest Atl. Fish. Sci. **6**: 107–116.

DeRusha, R.H., Forsythe, J.W., and Hanlon, R.T. 1987. Laboratory growth, reproduction and life-span of the Pacific pygmy octopus, *Octopus digueti*. Pac. Sci. **41**: 104–121.

Forsythe, J.W. 1993. A working hypothesis of how seasonal temperature change may impact the field growth of young cephalopods. *In* Recent advances in fisheries biology. *Edited by* T. Okutani, R.K. O'Dor, and T. Kubodera. Tokai University Press, Tokyo. pp. 133–143.

Forsythe, J.W., and Hanlon, R.T. 1989. Growth of the Eastern Atlantic squid, *Loligo forbesi* Steenstrup (Mollusca: Cephalopoda). Aquacult. Fish. Manag. **20**: 1–4.

Forsythe, J.W., and Van Heukelem, W.F. 1987. Growth. *In* Cephalopod life cycles. Vol. II. *Edited by* P.R. Boyle. Academic Press, London. pp. 135–156.

Forsythe, J.W., Walsh, L.S., Turk, P.E., and Lee, P.G. 2001. Impact of temperature on juvenile growth and age at first egg-laying of the Pacific reef squid, *Sepioteuthis lessoniana*, reared in captivity. Mar. Biol. **138**: 103–112.

Gartner, J.V., Jr. 1991. Life histories of three species of lanternfishes (Pisces: Myctophidae) from the eastern Gulf of Mexico. I. Morphological and microstructural analysis of sagittal otoliths. Mar. Biol. (Berlin), **111**: 11–20.

Grist, E.P.M., and des Clers, S. 1998. How seasonal temperature variations may influence the structure of annual squid populations. IMA J. Math. Appl. Med. Biol. **15**: 187–209.

Hanlon, R.T., Hixon, R.F., and Hulet, W.H. 1983. Survival, growth, and behavior of the loliginid squids *Loligo plei*, *Loligo pealei*, and *Lolliguncula brevis* (Mollusca: Cephalopoda) in closed sea water systems. Biol. Bull. (Woods Hole, Mass.), **165**: 637–685.

Hanlon, R.T., Turk, P.E., Lee, P.G., and Yang, W.T. 1987. Laboratory rearing of the squid *Loligo pealei* to the juvenile stage: growth comparisons with fishery data. Fish. Bull. **85**: 163–167.

Hatfield, E.M.C. 2000. Do some like it hot? Temperature as a possible determinant of variability in the growth of the Patagonian squid, *Loligo gahi* (Cephalopoda: Loliginidae). Fish. Res. (Amst.), **47**: 27–40.

Hixon, R.F., and Villoch, M.R. 1984. Growth rings in the statoliths of young laboratory cultured squids (*Loligo opalescens*). Am. Malacol. Bull. **2**: 93.

Hulet, W.H., Villoch, M.R., Hixon, R.F., and Hanlon, R.T. 1979. Fin damage in captured and reared squids. Lab. Anim. Sci. **29**: 528–533.

Jackson, G.D. 1990*a*. Age and growth of the tropical near-shore loliginid squid *Sepioteuthis lessoniana* determined from statolith growth ring analysis. Fish. Bull. **88**: 113–118.

Jackson, G.D. 1990*b*. The use of tetracycline staining techniques to determine statolith growth ring periodicity in the tropical loliginid squids *Loliolus noctiluca* and *Loligo chinensis*. Veliger, **33**: 395–399.

Jackson, G.D. 1993. Growth zones within the statolith microstructure of the deepwater squid *Moroteuthis ingens* (Cephalopoda: Onychoteuthidae): evidence for a habitat shift? Can. J. Fish. Aquat. Sci. **50**: 2366–2374.

Jackson, G.D. 1994. Application and future potential of statolith increment analysis in squids and sepioids. Can. J. Fish. Aquat. Sci. **51**: 2612–2625.

Jackson, G.D., Arkhipkin, A.I., Bizikov, V.A., and Hanlon, R.T. 1993. Laboratory and field corroboration of age and growth from statoliths and gladii of the loliginid squid *Sepioteuthis lessoniana* (Mollusca, Cephalopoda). *In* Recent advances in fisheries biology. *Edited by* T. Okutani, R.K. O'Dor, and T. Kubodera. Tokai University Press, Tokyo. pp. 189–199.

Jackson, G.D., Forsythe, J.W., Hixon, R.F., and Hanlon, R.T. 1997. Age, growth and maturation of *Lolliguncula brevis* (Cephalopoda: Loliginidae) in the Northwestern Gulf of Mexico with a comparison of length–frequency versus statolith age analysis. Can. J. Fish. Aquat. Sci. **54**: 2907–2919.

Lange, A.M.T., and Johnson, K.L. 1981. Dorsal mantle length—total weight relationships of squids *Loligo pealei* and *Illex illecebrosus* from the Atlantic coast of the United States. NOAA (Natl. Ocean Atmos. Adm.) Tech. Rep. NMFS (Natl. Mar. Fish. Serv.) SSRF (Spec. Sci. Rep. Fish.) 745.

Lee, P.G., Turk, P.E., Yang, W.T., and Hanlon, R.T. 1994. Biological characteristics and biomedical applications of the squid *Sepioteuthis lessoniana* cultured through multiple generations. Biol. Bull. (Woods Hole, Mass.), **186**: 328–341.

Macy, W.K. 1980. The ecology of the common squid, *Loligo pealei* LeSueur, 1821, in Rhode Island waters. Ph.D. thesis, University of Rhode Island, Narragansett, R.I.

Macy, W.K. 1995. The application of digital image processing to the aging of long-finned squid, *Loligo pealei*, using the statolith. *In* Recent developments in fish otolith research. *Edited by* D.H. Secor, J.M. Dean, and S.E. Campana. University of South Carolina Press, Columbia. pp. 283–302.

Mesnil, B. 1977. Growth and life cycle of squid, *Loligo pealei* and *Illex illecebrosus*, from the northwest Atlantic. International Commission for the Northwest Atlantic Fisheries (ICNAF) Sel. Pap. No. 2. pp. 55–69.

Minitab Inc. 1996. MINITAB® reference manual. State College, Pennsylvania.

National Marine Fisheries Service (NMFS). 1999. Fisheries of the United States, 1998. Current Fishery Statistics No. 9800. NMFS, FISTI, 1315 East West Highway, Silver Spring, MD 20910-3282, U.S.A.

Northeast Fisheries Science Center (NEFSC). 1999. 29th Northeast Regional Stock Assessment Workshop (29th SAW): Stock Assessment Review Committee (SARC) consensus summary of assessments. Ref. Doc. 99-14 of the Northeast Fisheries Science Center, 166 Water St., Woods Hole, MA 02543, U.S.A..

O'Dor, R.K., and Wells, M.J. 1987. Energy and nutrient flow. *In* Cephalopod life cycles. Vol. II. *Edited by* P.R. Boyle. Academic Press Inc., London. pp. 109–133.

Pauly, D. 1999. Why squids—though not fish—may be better understood by pretending they are. S. Afr. J. Mar. Sci. **20**: 47–58.

Summers, W.C. 1983. *Loligo pealei*. *In* Cephalopod life cycles. Vol. I. Species accounts. *Edited by* P.R. Boyle. Academic Press, London. pp. 115–142.

Summers, W.C., and McMahon, J.J. 1974. Studies on the maintenance of adult squid (*Loligo pealei*). I. Factorial survey. Biol. Bull. (Woods Hole, Mass.), **146**: 279–290.

Turk, P.E., Hanlon, R.T., Bradford, L.A., and Yang, W.T. 1986. Aspects of feeding, growth and survival of the European squid *Loligo vulgaris* Lamarck, 1799, reared through the early growth stages. Vie Milieu, **36**: 9–13.

Volk, E.C., Schroder, S.L., and Grimm, J.J. 1999. Otolith thermal marking. Fish. Res. (Amst.), **43**: 205–219.

Yang, W.T., Hanlon, R.T., Hixon, R.F., and Hulet, W.H. 1980. First success in rearing hatchlings of the squid *Loligo pealei* Lesueur 1821. Malacol. Rev. **13**: 79–80.

Yang, W.T., Hixon, R.F., Turk, P.E., Krejci, M.E., Hulet, W.H., and Hanlon, R.T. 1986. Growth, behavior and sexual maturation of the market squid, *Loligo opalescens*, cultured through the life cycle. Fish. Bull. **84**: 771–798.

Application of a two-dimensional hydrodynamic reservoir model to Lake Erie

L. Boegman, M.R. Loewen, P.F. Hamblin, and D.A. Culver

Abstract: The relative impacts of changes in nutrient loading and zebra mussel establishment on plankton in large lakes are strongly influenced by hydrodynamics, yet adequately modelling the temporal–spatial complexity of physical and biological processes has been difficult. We adapted a two-dimensional public domain model, CE-QUAL-W2, to test whether it could provide a hydrodynamically accurate simulation of the seasonal variation in the vertical–longitudinal thermal structure of Lake Erie. The physical forcing for the model is derived from surface meteorological buoys and measurements of precipitation, inflows, and outflows. To calibrate and validate the model, predictions were compared with an extensive set of field data collected during May through September 1994. The model accurately predicted water-level fluctuations without adjustment. However, significant modifications to the eddy coefficient turbulence algorithm were required to simulate acceptable longitudinal currents. The thermal structure was accurately predicted in all three basins, even though this laterally averaged model cannot simulate Coriolis effects. We are currently extending the model's water-quality module to include the effects of nutrient loading and zebra mussels on the plankton.

Résumé : Les impacts relatifs des changements dans la charge de nutriments et de l'établissement de Moules zébrées sur le plancton dans des lacs de grande taille sont grandement influencés par les facteurs hydrodynamiques; cependant la modélisation de la complexité spatiotemporelle des processus physiques et biologiques s'est avérée difficile. Nous avons adapté le modèle bidimensionnel CE-QUAL-W2 du domaine public pour évaluer s'il pouvait fournir une simulation hydrodynamique fidèle de la variation saisonnière de la structure thermique verticale et horizontale du lac Érié. Le forçage physique du modèle s'est fait à partir de données provenant des bouées météorologiques de surface et des mesures de précipitations, d'entrées et de sorties d'eau. Des comparaisons des prédictions du modèle avec une vaste série d'observations de terrain de mai à septembre 1994 ont permis de calibrer et de valider le modèle. Le modèle prédit précisément, et sans nécessité d'ajustement, les fluctuations des niveaux d'eau. Des modifications importantes de l'algorithme du coefficient de turbulence tourbillonnaire ont cependant été nécessaires pour générer des courants longitudinaux acceptables. Le modèle a prédit correctement la structure thermique dans les trois bassins, bien que ce modèle (basé sur des moyennes latérales) soit incapable de simuler les effets des forces de Coriolis. Nous sommes présentement à élargir le module de qualité des eaux du modèle pour y inclure les effets de la charge de nutriments et de la présence de Moules zébrées sur le plancton.

[Traduit par la Rédaction]

Introduction

The water quality of Lake Erie (Fig. 1*a*) deteriorated dramatically from approximately 1950 to 1980, owing to eutrophication that was particularly strong in the western basin. In the 1970s, joint Canadian and United States legislation mandated tertiary treatment of municipal waste water and implemented programs to reduce agricultural runoff. Lake Erie water quality improved and significant phytoplankton reductions in the western basin were observed (e.g., Nicholls et al. 1977). In 1988, the discovery of filter-feeding zebra mussels (*Dreissena polymorpha*) in the lower Great Lakes and their subsequent proliferation (e.g., Berkman et al. 1998) created a potential for further reductions in phytoplankton biomass and increased water clarity (e.g., Holland 1993; Leach 1993; Nicholls and Hopkins 1993). Numerous mathematical models have been used to examine the hydrodynamics and nutrient – plankton – zebra mussel dynamics of Lake Erie; however, models published to date have been either physically based (e.g., Ivey and Patterson 1984; Kuan

Received April 7, 2000. Accepted January 24, 2001. Published on the NRC Research Press Web site on April 12, 2001.
J15709

L. Boegman[1] **and M.R. Loewen.**[2,3] Environmental Fluid Dynamics Laboratory, Department of Mechanical and Industrial Engineering, University of Toronto, Toronto, ON M5S 3G8, Canada.
P.F. Hamblin. Aquatic Ecosystems Restoration Branch, National Water Research Institute, Burlington, ON L7R 4A6, Canada.
D.A. Culver. Department of Evolution, Ecology, and Organismal Biology, Ohio State University, Columbus, OH 43210, U.S.A.

[1] Present address: Department of Environmental Engineering, Centre for Water Research, University of Western Australia, Nedlands WA 6907, Australia.
[2] Corresponding author (e-mail: mrloewen@civil.ualberta.ca).
[3] Present address: Department of Civil and Environmental Engineering, University of Alberta, Edmonton, AB T6G 2G7, Canada.

DOI: 10.1139/cjfas-58-5-858

Fig. 1. (*a*) Lake Erie bathymetric plan view. Note major geological features and 1994 monitoring buoy locations as marked: W_2, current meter (10 m deep); W_1 and E, meteorological buoy and thermistor chain (10 and 63 m deep, respectively); C, meteorological buoy, thermistor chain, and current meter (25 m deep). (*b*) CE-QUAL-W2 solution plane (longitudinal cross-section), showing width contours (contour interval is 20 km).

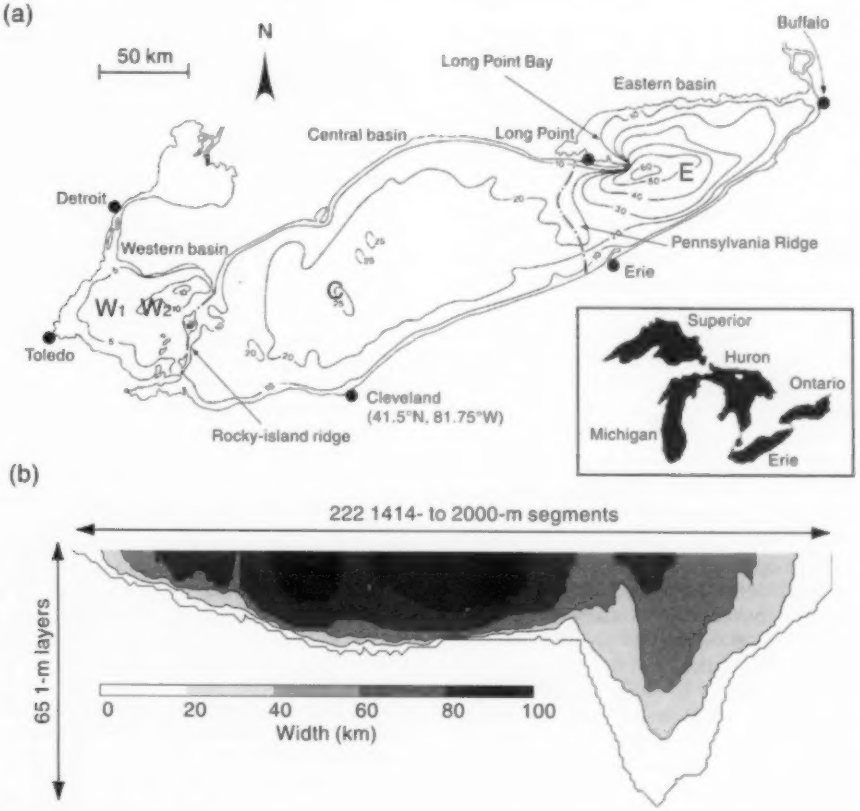

1995) or biological and nutrient based (e.g., Madenjian 1995; Arnott and Vanni 1996). Laboratory (e.g., O'Riordan et al. 1995), field (e.g., Ackerman et al. 2001), and numerical (e.g., Lucas et al. 1998) studies have shown that fully understanding the relative roles of changes in nutrient loading and zebra mussels on large natural lakes, like Lake Erie, requires models that couple hydrodynamics and the dynamics of water quality and biota. The problem involves adequately modelling the complexity of physical and biological processes in time and space, with sufficient computational efficiency that long-term trends in water quality may be economically simulated. To date, the ability of such models is limited by the computationally expensive nature of high resolution hydrodynamic simulation.

A one-dimensional thermodynamic model, DYRESM, was successfully used to simulate the vertical mixing for 1 month in the central basin of Lake Erie (Ivey and Patterson 1984). At their mid-central-basin sampling location, the lake is relatively vast, and has a uniform depth and horizontal isotherms throughout the simulation period. Under such conditions, horizontal advection was found to have a negligible effect upon temperature. However, all field observations were averaged over 48 h, because DYRESM is not dimensionally capable of simulating the strong surface (barotropic) seiches that oscillate along the lake's longitudinal axis. Mixing coefficients, identical to those used in prior simulations of much smaller water bodies, were found to adequately describe the vertical turbulent processes.

A three-dimensional hydrodynamic model, the Princeton Ocean Model, was applied to Lake Erie for a 150-day summer simulation on a Cray super computer (Kuan 1995). Using a σ-system coordinate, Kuan's model had 14 vertical levels varying in thickness from 6 m in the eastern basin to 0.0375 m in the western basin. Barotropic motions were reproduced, leading to accurate water level predictions. Central- and eastern-basin currents were simulated satisfactorily in both phase and magnitude. A strong correlation was found between the accuracy of the predicted currents and the quality of the applied meteorological forcing field. Lake-surface temperatures and fully mixed water columns were reproduced to within an average of 1°C over the entire simulation; however, during stratification, the model under- and over-predicted epilimnetic and hypolimnetic temperatures, respectively. The model failed to reproduce a distinct thermocline structure and central basin hypolimnion throughout the summer period. This was hypothesized to be a result of coarse vertical grid resolution.

The primary goal of this study was to test whether a two-dimensional model could provide a hydrodynamically accurate simulation of the seasonal variation in the vertical–longitudinal thermal structure and hydrodynamics of a large lake such as Lake Erie. For this study, the two-dimensional public domain model CE-QUAL-W2 was chosen, as it contains a fully predictive coupled water quality and hydrodynamic model that runs in a reasonable amount of time (~1 h) using a FORTRAN compiler on a personal computer (Pentium II 450 MHz). Previous applications of CE-QUAL-W2 have been limited to small reservoirs, for example, a thermal and dissolved oxygen application to DeGray Lake, Arkansas (Martin 1988), and modelling combined sewer overflow in Cheatham Lake, Tennessee (Adams et al. 1997). To our knowledge, this is the first application of CE-QUAL-W2 to a large natural lake.

This two-dimensional model resolves the longitudinal and vertical axes and is therefore suited for application to relatively long, narrow water bodies such as Lake Erie with a 6:1 aspect ratio of the main axis to the mean breadth. Lake Erie can be subdivided into three distinct physiographic basins: western, central, and eastern, with average depths of 10, 25, and 50 m, respectively (Figs. 1*a* and 1*b*). The western and central basins are separated by a rocky chain of islands that follow the 10 m depth contour from Point Pelee, Ontario, to Marblehead, Ohio, while the eastern and central basins are separated by the Pennsylvania Ridge, a low, wide, submerged sand and gravel ridge, extending from Long Point, Ontario, to Erie, Pennsylvania. We aligned the model's longitudinal direction with Lake Erie's longitudinal axis, which also corresponds to the direction of hydraulic flow, strongest seiching, and gradients in nutrient concentration and plankton biomass (Charlton 1994). Further, the vertical thermal structure must be accurately modelled, because of its important influence on vertical mixing and, hence, on the vertical distribution of nutrients and algae. This is especially important, because ultimately the model will be used to estimate the algal availability to benthic-feeding zebra mussels. Briefly, Lake Erie's thermal structure is observed to exhibit a decrease in depth-averaged temperature when moving from the shallow well-mixed western basin to the deeper seasonally stratified central and eastern basins (e.g., Schertzer and Hamblin 2001). Increased winds during late summer and early fall result in a deepening of the thermocline and eventual breakdown of the summer thermal stratification. The sharp thermocline found in the central basin has been observed to act as a vertical barrier to exchange between the epilimnion and hypolimnion, thus suppressing vertical mixing and leading to anoxic conditions in the central-basin hypolimnion (Charlton 1980).

We have modified CE-QUAL-W2 to make it applicable to a large wind-driven lake and then hydrodynamically calibrated it for Lake Erie, using water levels, horizontal currents, and temperatures from an extensive 137-day field-data set (May through September 1994). The empirical nature of the turbulence scheme made it necessary to separately calibrate the model to the observed data in each of the three basins.

Methods

Model description

The model bathymetry was specified using a digital 2 km bathymetric grid of Lake Erie obtained from the National Atmospheric and Oceanic Administration (NOAA; www.glerl.noaa.gov/data/bathy.html). To obtain a better fit to the shoreline, the NOAA grid is aligned 27.33° counterclockwise from the central meridian of NOAA bathymetric chart 14820. In this two-dimensional application, the NOAA grid was laterally averaged into 65 vertical layers spaced at 1-m intervals and 222 longitudinal segments in ascending order from west to east (Fig. 1*b*). A unique width is specified for each node, and depths are relative to the Great Lakes Datum (GLD) of 1985. Segments 65–222 (central and eastern basins) are spaced at 2000-m intervals and oriented along the longitudinal axis of the NOAA grid (27.33° counterclockwise from the chart central meridian); to account for the "angled" nature of the western basin to this axis, segments 1–52, spaced at 1414-m intervals, are oriented 162.33° counterclockwise from the chart central meridian; segments 53–64 (triangle from Sandusky, Ohio, to Point Pelee, Ontario, to Lorain, Ohio) are spaced at 1779-m intervals and are transitionally oriented between western- and central-basin segments. Long Point Bay (Fig. 1*a*), which averages 1–8 m in depth, was filled in west of the tip of Long Point, Ontario, to correctly represent the constriction in lake width due to Long Point. This bathymetric modification can be considered negligible, reducing total lake volume by ~0.3%.

CE-QUAL-W2 solves for the hydrodynamic variables by the direct solution of six fundamental equations and six unknowns. The governing equations, laterally and layer averaged, are the horizontal-momentum equation, the constituent – heat transport equation, the free water surface elevation equation, the hydrostatic-pressure equation, the continuity equation, and the equation of state. The six unknowns are water-surface elevation, pressure, horizontal velocity, vertical velocity, constituent concentration – temperature, and density. The governing equations have been derived by simplifying the turbulent time-averaged three-dimensional equations of motion (longitudinal-, lateral-, and vertical-momentum equations), through the use of scaling arguments (see Cole and Buchak 1995; Wells 1997). If the longitudinal-length scale is much greater than the vertical-length scale, vertical velocities may be considered much smaller than longitudinal velocities (a reasonable assumption in a stratified water column forced by horizontal winds); this allows the vertical-momentum equation to be reduced to the hydrostatic-pressure equation, wherein the small terms have been neglected. An unfortunate result of this simplification is that vertical accelerations, such as diurnal penetrative convection, are not accurately modelled. The momentum equations are further simplified through lateral averaging after decomposing all velocities and pressure into a lateral average and deviation from the lateral average. The resultant laterally averaged lateral velocities are identically zero, which results in the removal of the lateral-momentum equation as well as the Coriolis terms in the longitudinal-momentum equation. The validity and effects of these simplifications will be discussed below.

The equations and unknowns are solved using a first-order, upwinded, finite-difference scheme, applied to a fixed grid of variable-node spacing. A z-level vertical coordinate system is used. The explicit temporal formulation of the effects of vertical eddy viscosity (A_z) on horizontal velocities necessitates a time step (Δt) restriction for physically realistic results:

$$(1) \qquad \Delta t < \Delta z^2 \times A_z^{-1}$$

where Δz is the local vertical grid point spacing. For lengthy applications, this restriction can severely limit the feasible A_z range, while maintaining reasonable run times.

Surface heat exchange is calculated using an explicit term-by-term process from incident shortwave radiation, wind speed, air temperature, dew-point temperature, cloud cover, and water-surface temperature. The sediment–water heat flux was set to zero, because in a lake as large as Lake Erie, it is considered to be negligible. When density instabilities occurred, they were eliminated by setting the local vertical eddy diffusivity to 1000 $m^2 \cdot s^{-1}$, resulting in vertical mixing of adjacent layers during the next time step. Water densities are calculated on the basis of water temperature and solids concentration (Gill 1982). Shear production at the lake bed is calculated using modelled velocities and the Chézy coefficient, which is inversely proportional to the bottom roughness (e.g., Stacey et al. 1995).

Input and calibration data

The following meteorological data were supplied by the National Water Research Institute (NWRI), Burlington, Ontario: air temperature, dew-point temperature, wind speed, wind direction, and incident shortwave solar radiation. All these variables (Table 1) were recorded at 10-min intervals by meteorological buoys (MET3 climate buoy) deployed in each of the three basins (Fig. 1*a*). We modified the source code and input files of CE-QUAL-W2 to directly read the shortwave-radiation values rather than calculate shortwave radiation from cloud-cover observations, latitude, and sun angle. Direct cloud-cover observations were not available and, therefore, were estimated by regression from the daily shortwave radiation, for the purpose of calculating the incoming long-wave radiation (Tennessee Valley Authority 1972).

Owing to the size of Lake Erie and, thus, its spatially varying meteorological conditions, the CE-QUAL-W2 source code was further modified to allow unique surface-forcing conditions at each longitudinal segment, as determined by linear interpolation between the three surface meteorological buoys (Boegman 1999). Gaps in data series due to instrument failure or maintenance were overcome by substitution of data from adjacent buoys.

Water-inflow rates and temperatures were specified for the Grand (Ontario), Maumee, Sandusky, and Detroit rivers; while outflows were specified for the Welland Canal and the Niagara River (Table 1). All variables were sampled daily, with the exception of the Grand River water temperatures, which were sampled at a frequency greater than or equal to biweekly.

Observed water level time series were obtained from NOAA gauges that recorded water levels hourly at Toledo and Buffalo. Current-meter data (EG&G and SACM-3 meters with ±1 $\text{cm}\cdot\text{s}^{-1}$ and ±5° error), provided by NWRI for the central- and western-basin sampling locations (Fig. 1*a*), were used to calibrate the modelled longitudinal currents. NWRI also provided temperature time series data for all three basins, which were recorded using Brankner temperature loggers supplemented by temperatures measured with Neil Brown current meters. On the simulation start date (10 May 1994), the model is initialized with a zero-velocity field and a horizontal water surface (174.55 m relative to GLD 1985), determined as the average water level between Toledo and Buffalo. Further, a unique initial temperature is specified at each segment by vertically integrating and longitudinally interpolating five Seabird temperature profiles obtained on 10 and 11 May during an NWRI lakewide cruise.

Original vertical eddy viscosity algorithm

Empirically derived eddy coefficients were used to model turbulence. The horizontal-dispersion coefficients for momentum and temperature–constituents are assumed to be time and space invariant and are set equal to 1 $\text{m}^2\cdot\text{s}^{-1}$. The vertical diffusion coefficients for momentum (A_z) and temperature–constituents (D_z) vary in space and time and are computed locally by the model at each time step.

The vertical eddy viscosity (i.e., A_z) is formulated by analogy to Prandtl's mixing–length model, as (Cole and Buchak 1995; Wells 1997):

$$(2) \qquad A_z = k\left(\frac{l^2}{2}\right)\sqrt{\left(\frac{\partial U}{\partial z}\right)^2 + \left(\frac{\partial V}{\partial z}\right)^2}\, e^{-c\mathrm{Ri}}$$

where k is the von Karman constant, l is a turbulent length scale taken arbitrarily as the vertical grid point spacing, U is the longitudinal velocity, V is the lateral velocity, Ri is the local Richardson number (e.g., Fischer et al. 1979), and c is a constant taken as 1.5. Although now considered incorrect in principle (Tennekes and Lumley 1972), the simplicity of mixing–length or eddy viscosity models for general engineering purposes has supported their evolution and application, albeit in an empirical sense. These models are thus reliant on field data for adjustment and calibration.

Table 1. Variation in meteorological and inflow–outflow data for Lake Erie from 20 May to 13 September 1994.

Input	Maximum	Minimum	Mean
Air temperature (°C)	30.3	4.6	19.4
Wind speed ($\text{m}\cdot\text{s}^{-1}$)	16.2	0	4.5
Detroit River flow ($\text{m}^3\cdot\text{s}^{-1}$)	6051	5302	5709
Detroit River temperature (°C)	24	12	20.6
Niagara River flow ($\text{m}^3\cdot\text{s}^{-1}$)	6824	5720	6284

The longitudinal–vertical nature of this two-dimensional model causes the lateral velocity and its vertical gradient $\partial V/\partial z$ (in eq. 2) to be zero. To account for this, it is assumed that the effect of cross-wind shear ($\tau_{\text{wind-}y}$) on A_z is to generate a lateral-wind wave component, so that (Cole and Buchak 1995):

$$(3) \qquad A_z = k\left(\frac{l^2}{2}\right)\sqrt{\left(\frac{\partial U}{\partial z}\right)^2 + \left(\frac{\tau_{\text{wind-}y}\, e^{-2kz}}{A_z}\right)^2}\, e^{-c\mathrm{Ri}}$$

where the A_z on the right hand side of eq. 3 is the explicit value determined in the previous time step. The resultant vertical eddy viscosities are exponentially damped with depth from the wind-dependent surface value, thus approaching zero at the lake bed. A_z is reduced in stratified regions, based on the local Richardson number. In the original algorithm, A_z was limited numerically, so that:

$$(4) \qquad 1.4\cdot10^{-6}\ \text{m}^2\cdot\text{s}^{-1} < A_z < 10^{-4}\ \text{m}^2\cdot\text{s}^{-1}$$

where the lower limit is the molecular viscosity of water and the upper limit is based on a balance between empirical observations and computational efficiency as determined by eq. 1. In Fig. 2, longitudinal currents modelled using the original A_z algorithm are compared with the observed longitudinal currents at 3, 11, and 24 m at central basin station C. Power spectra of the observed and predicted currents were estimated by dividing the time series into segments 256 points in length, using a 256-point Blackman window and overlapping adjacent segments by 128 points. One observes that the modelled currents have a spectral-energy content 1.5 orders of magnitude greater than the field-observed currents at a frequency of 0.01 cycles per hour (cph) (Fig. 2), and exhibit a large-amplitude low-frequency oscillation, which is characteristic of an undamped internal seiche (Figs. 2*a*–2*c*). As a result, subsurface temperatures were underpredicted by as much as 12°C in the central and western basins (Fig. 3). Given that surface temperatures were correctly simulated (not shown), this suggests that the model incorrectly estimates the interbasin exchange flow of cold hypolimnetic water.

Modified vertical eddy viscosity algorithm

The undamped proliferation of internal seiches in numerical models of large lakes results from the incorrect specification of the nonlinear and turbulent processes governing dissipation of energy imparted to the lake by the surface-wind field (Imberger 1998; Saggio and Imberger 1998). These processes include the dissipation of basin-scale currents through shear production in the benthic boundary layer, nonlinear decay of basin-scale internal waves to higher modes, and the shoaling and breaking of internal waves as they impinge on sloped boundaries at the depth of the meta-

Fig. 2. Hourly time series of observed (thin black line), modelled with the original A_z algorithm (broken line), and modelled with the modified A_z algorithm (thick black line) longitudinal-current velocities at depths of 3 m (*a*), 11 m (*b*), and 24 m (*c*), and their respective energy spectra (*d*, *e*, and *f*) in central Lake Erie at C (see Fig. 1 for position of C).

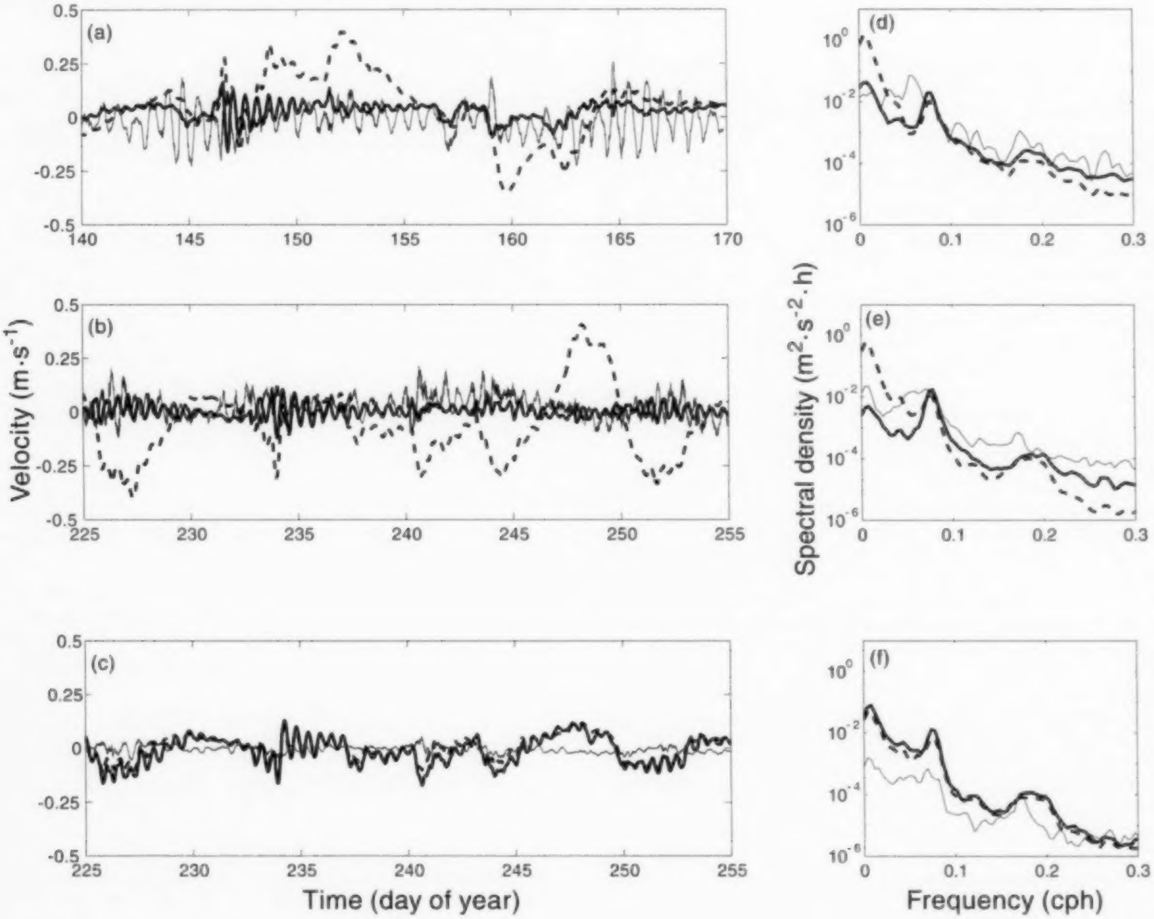

limnion. Poor spatial resolution and the hydrostatic approximation prevent the physical realization of these processes (with the exception of boundary-layer shear) within CE-QUAL-W2's original eddy coefficient model framework. Further, Coriolis forces are significant in Lake Erie, which has a width greater than 100 km, many times the ~5 km internal Rossby radius of deformation (Gill 1982). As a result, momentum transfer from the longitudinal to the transverse direction, which is not possible in our transversely averaged model, could be acting to reduce the strength of the observed longitudinal seiches relative to those modelled.

To compensate for the above energy fluxes, ad hoc adjustments were made to the A_z algorithm until optimal agreement with the 1994 temperature and current data was obtained. The upper A_z bound (eq. 4) was increased from 10^{-4} to $10^{-2}\ \text{m}^2\cdot\text{s}^{-1}$, which reduced the modelled surface currents to the same order of magnitude as those observed (Fig. 2) and to approximately 2–3% of the wind speed, in accordance with Gill (1982). Epilimnetic A_z values have been estimated from temperature microstructure profiles measured in an offshore zone of the central basin (McCune 1998), wherein they were found to range from $3\cdot10^{-4}\ \text{m}^2\cdot\text{s}^{-1}$ in light winds to $4\cdot10^{-2}\ \text{m}^2\cdot\text{s}^{-1}$ during a storm event, and in a high-energy nearshore zone of the western basin, wherein they ranged from 10^{-4} to $10^{-2}\ \text{m}^2\cdot\text{s}^{-1}$ (W. Edwards, Deptartment of Evolution, Ecology, and Organismal Biology, Ohio State University, personal communication); thus these range modifications are reasonable.

A_z was then linearly interpolated from the surface value to a wind-dependent range of 0.05–$0.1\ \text{m}^2\cdot\text{s}^{-1}$ in the benthic boundary layer. This is an increase of five orders of magnitude from the original turbulence scheme, which had predicted benthic A_z values of from $1.4\cdot10^{-6}$ to $10^{-5}\ \text{m}^2\cdot\text{s}^{-1}$. The source code was modified, so that the Richardson number reduction was only applied when vertical-density differences between layers were in excess of $0.01\ \text{kg}\cdot\text{m}^{-3}$. These changes significantly improved the modelled central basin longitudinal current at 11 m (reducing the strength of the 0.01-cph oscillation; Figs. 2*b* and 2*e*) but not at 24 m (Figs. 2*c* and 2*f*). Note that Lake Erie is 25 m deep at this central-basin site. McCune (1998) observed that the maximum value of A_z in the central-basin hypolimnion was approximately $10^{-5}\ \text{m}^2\cdot\text{s}^{-1}$, suggesting that the A_z values calculated for this basin using the original A_z algorithm were reasonable. However, increasing the value of A_z through the metalimnion and hypolimnion (Table 2) can be justified, in that it accounts for the lack of dissipative and rotational processes described above. These modifications to A_z resulted in a reduction of the time step from 600 to 2 s and an increase in run time from 1 h to

Fig. 3. Hourly time series of observed (thin black line), modelled with the original A_z algorithm (broken line), and modelled with the modified A_z algorithm (thick black line) temperature at a depth of 9.4 m in the western basin at W_2 (*a*) and at a depth of 14 m in the central basin at C (*b*) (see Fig. 1 for positions of W_2 and C).

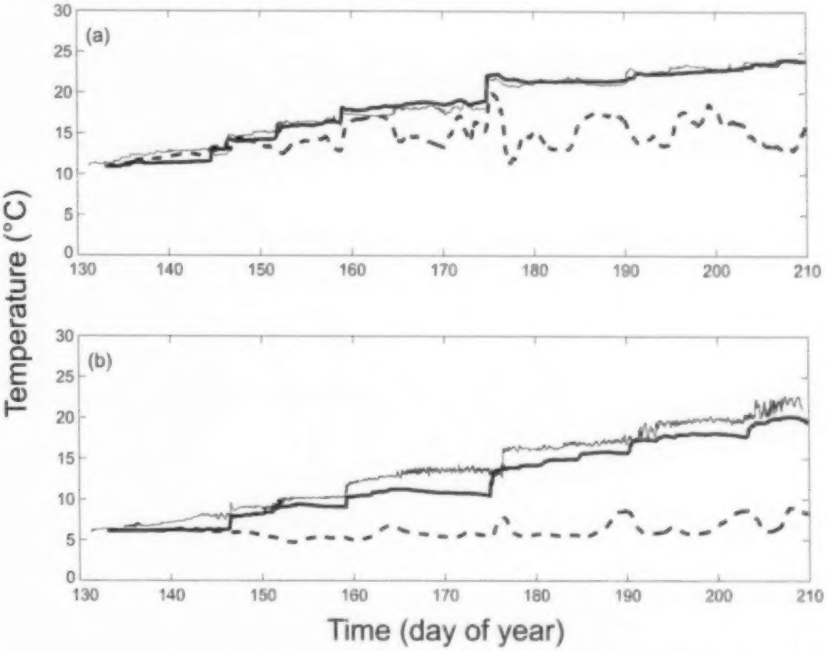

1 week. It was therefore necessary to remove the time-step restriction (eq. 1), which was accomplished by making the effects of A_z on the horizontal velocity implicit (Patankar 1980; Boegman 1999).

As mixing coefficients for mass (D_z) and momentum (A_z) are not assumed to be equal, the augmented values of A_z used herein do not increase vertical mixing of scalar variables (e.g., heat). The vertical eddy diffusivity (D_z) is calculated as a fraction of A_z, by dividing by the turbulent Prandtl number ($\mathrm{Pr_T}$):

$$(5)\qquad D_z = \hat{A}_z \mathrm{Pr}_T^{-1}$$

where $\hat{A}_z$ is the vertical eddy viscosity computed using the original algorithm (eq. 4). Results from a sensitivity analysis (Boegman 1999) showed that the optimal values for $\mathrm{Pr_T}$ were 2.0 in the western and central basins and 7.0 in the eastern basin. Note that the default Prandtl number used in CE-QUAL-W2 is 7.0, the commonly accepted *laminar* value for heat in fresh water (e.g., Fischer et al. 1979). Experimental evidence (cf. Hinze 1959) suggests that $\mathrm{Pr_T}$ is close to unity, thus supporting our empirically determined lower model values. Coupled with the modified A_z algorithm, the D_z changes significantly improved modelled western and central basin temperature time series (Fig. 3).

Results

Water level

Surface gravitational seiches with typical amplitudes of 10–30 cm are ubiquitous on Lake Erie. The periods of the lowest four natural seiche modes are 14.38, 9.14, 5.93, and 4.15 h (Platzman and Rao 1964). At both Toledo and Buffalo, the modelled water levels follow the lowest mode period of 14 h (0.07 cph) very well with respect to wavelength, phase, and amplitude (Fig. 4*c*). Storm surges, up to 1 m in height, associated with strong cyclonic disturbances travelling northeast over the Great Lakes (Hamblin 1987), are well simulated and frequent in the observed and modelled time series (e.g., days = 147, 176; Figs. 4*a* and 4*c*).

Water-level power spectra were estimated by dividing the time series into segments 256 points in length, applying a 256-point Blackman window and overlapping adjacent segments by 128 points. Frequencies of the lowest three natural surface seiche modes (0.07, 0.11, and 0.17 cph) are clearly evident in both the modelled and observed energy spectra from Toledo (Fig. 4*d*). Low-frequency high-energy peaks can also be seen in both the modelled and observed water level spectra at periods of 100 h (0.01 cph) and 24 h (0.042 cph). These same frequencies are evident in the frequency spectrum of the longitudinal-wind component (Fig. 4*b*). Platzman and Rao (1964) concluded that the diurnal (0.042 cph) peak in the water-level spectra was due to the diurnal component in the atmospheric forcing on the lake, while Hamblin (1987) and Boyce and Chiocchio (1987) found the 100-h (0.01 cph) peak to be a direct result of a dominance of storm events with time scales greater than 1 day.

Currents

Comparison of modelled and observed longitudinal current time series at depths of 3.4 and 8 m at the western basin station (W_2) showed reasonable agreement both in phase and amplitude (Figs. 5*a* and 5*c*). Observed and modelled energy spectra for current velocities (Figs. 5*b* and 5*d*) both exhibit Lake Erie's lowest three natural barotropic frequencies (0.07, 0.11, and 0.17 cph). The spectral peaks are more defined in the modelled spectra, as the modelled time series

Table 2. Summary of vertical eddy viscosity (A_z) modifications to the original CE-QUAL-W2 source code.

Zone	Original A_z routine[a]	Modified A_z routine[b]
Epilimnion	Max. $A_z = 10^{-4}$ m^2·s^{-1}; surface currents 3–10% of surface wind speed	Increased max. A_z by 2 orders of magnitude to $A_z = 10^{-2}$ m^2·s^{-1}, to reduce surface currents to 2–3% of surface wind speed
Metalimnion	A_z reduction as a function of local Richardson number prevents mixing across thermocline	Placed limit on Richardson number reduction and increased A_z, to account for metalimnetic boundary dissipation
Hypolimnion	A_z approaches 0 at bed; very strong internal seiche developed affecting interbasin exchange flow	Increased A_z by 4 orders of magnitude to $0.05 < A_z < 0.1$ m^2·s^{-1}, to increase benthic dissipation

[a] Developed for hydraulically driven reservoirs.
[b] Herein developed for wind-driven Lake Erie.

Fig. 4. Hourly time series comparing the central basin longitudinal wind speed (*a*) and the observed (thin black line) and modelled with the modified A_z algorithm (thick black line) Toledo water levels (*c*) and their respective energy spectra (*b* and *d*).

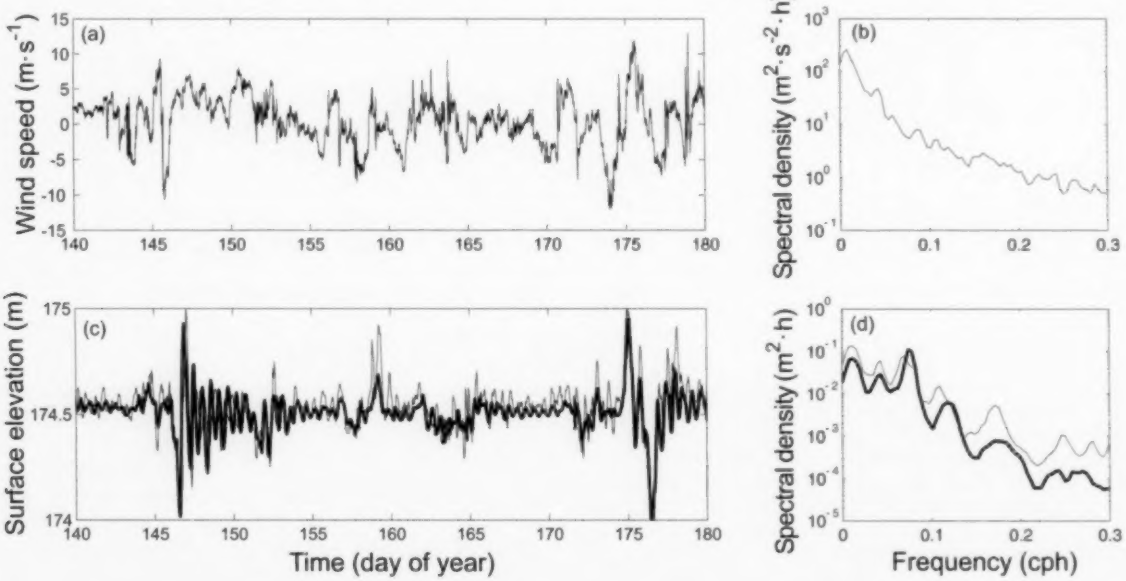

is of significantly greater length. Wind-forced diurnal and 0.01 cph storm frequency peaks may also be seen in both modelled and observed longitudinal current energy spectra.

Direct comparison of central-basin longitudinal-current time series is difficult, because 0.056-cph inertial currents, which result from Coriolis effects on basin-scale Poincaré waves (Gill 1982), are observed to be quite strong in the central-basin epilimnion but are removed through lateral averaging of CE-QUAL-W2's governing equations (Fig. 2*d*). Nevertheless, both the modelled and observed central basin current time series at 3-, 11-, and 24-m depths have spectral peaks at periods of 100 h (0.01 cph), 24 h (0.042 cph), 14 h (0.07 cph), and 6 h (0.17 cph) (Figs. 2*d*–2*f*). The 14- and 6-h currents correspond to the first and third modes of the surface gravitational seiches. The 9-h second mode (0.11 cph) is only simulated at a depth of 24 m. At this depth, where the observed currents (measured 1 m above the bed) are relatively quiescent, the model predicts 1.5 orders of magnitude more spectral energy at 0.01 and 0.07 cph than is observed (Fig. 2*f*). Examination of animations of lakewide vector plots of the predicted velocities showed that the excess energy at low frequencies was caused by hypolimnetic exchange flow between the central and eastern basins. Overall the modelled current velocities agree well with the 1994 field observations and with the observations of Boyce and Chiocchio (1987), who found that, in Lake Erie's central basin, the inertial (0.056 cph) and first mode barotropic (0.07 cph) currents dominated the observed energy spectra. Smaller energy peaks were found at the diurnal (0.042 cph) and 100-h (0.01 cph) periods, while the second and third baroclinic modes contained little energy.

Temperatures

The vertical variations in water temperature predicted by the model for the western basin (station W_1) are very similar to those found in the observed data for this location (Fig. 6). The water column remains fully mixed until late June when stratification occurs near day 173 (23 June). The model lags behind the observations by approximately 3 days (e.g., the model predicts the occurrence of the 15°C isotherm on day 152 (1 June), yet it was observed on day 149).

In both the modelled and observed results for central basin (station C), the degree of stratification increases through June, culminating with a firmly established thermocline at a depth of approximately 20 m by day 196 (15 July; Fig. 7). Previous field measurements have shown that the thermocline is usually

Fig. 5. Hourly time series of observed (thin black line) and modelled with the modified A_z algorithm (thick black line) longitudinal-current velocities in the western basin at 3.4 m (*a*) and 8.0 m (*b*), and their respective energy spectra (*c* and *d*).

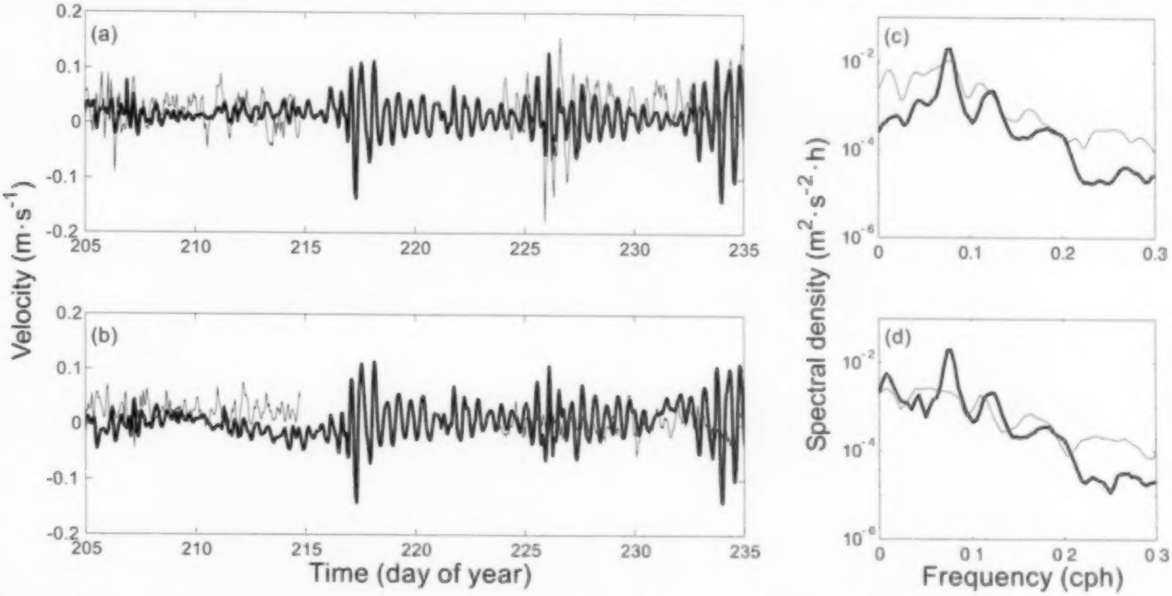

Fig. 6. Depth versus time isotherms comparing temperatures modelled with the modified A_z algorithm (*a*) and the observed vertical temperature distribution (*b*) in western Lake Erie at W_1 (see Fig. 1 for position of W_1). The isotherm contour interval is 2.5°C. Both modelled and observed isotherms are linearly interpolated from hourly temperature time series at depths of 0, 5, and 9.4 m.

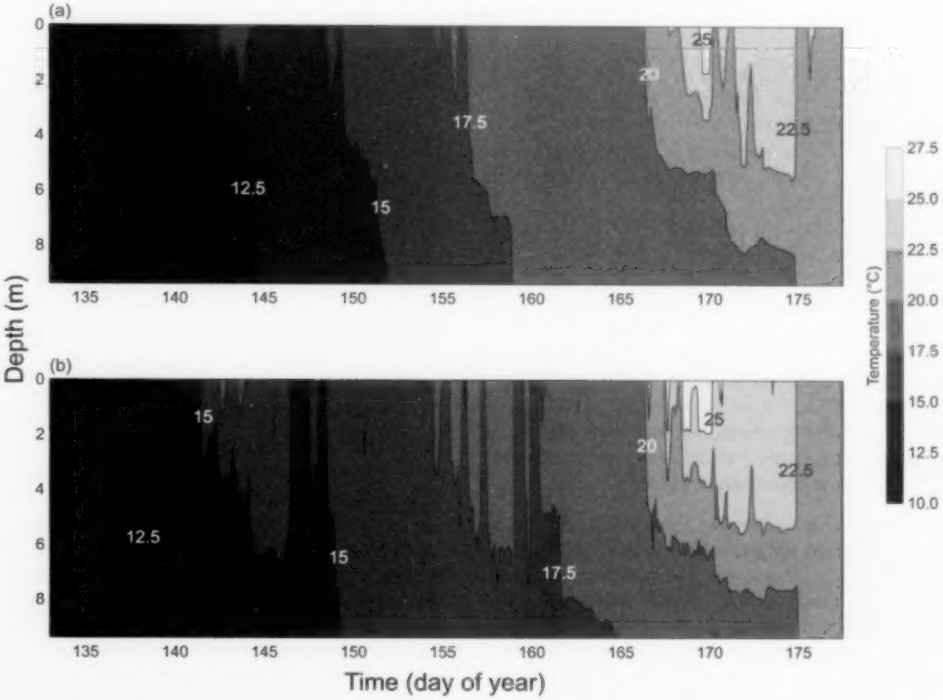

firmly established by the middle of July at a depth of 15 m (Schertzer et al. 1987). This distinct thermocline persists through the end of the simulation (day 269).

The formation and location of the thermocline in the eastern basin (station E) are well simulated by the model (Fig. 8); however, the observed thermocline has a steeper temperature gradient. Thickening of the metalimnion likely results artificially from numerical diffusion (Patankar 1980).

THE PAPER AND INK USED IN
PUBLICATION MAY AFFECT T
THE MICROFORM E

Fig. 7. Depth versus time isotherms comparing temperatures modelled with the modified A_z algorithm (*a*) and the observed vertical temperature distribution (*b*) in western Lake Erie at C (see Fig. 1 for position of C). The isotherm contour interval is 2.5°C. Both modelled and observed isotherms are linearly interpolated from hourly temperature time series at depths of 0, 2, 5, 8, 11, 14, 17, and 24 m.

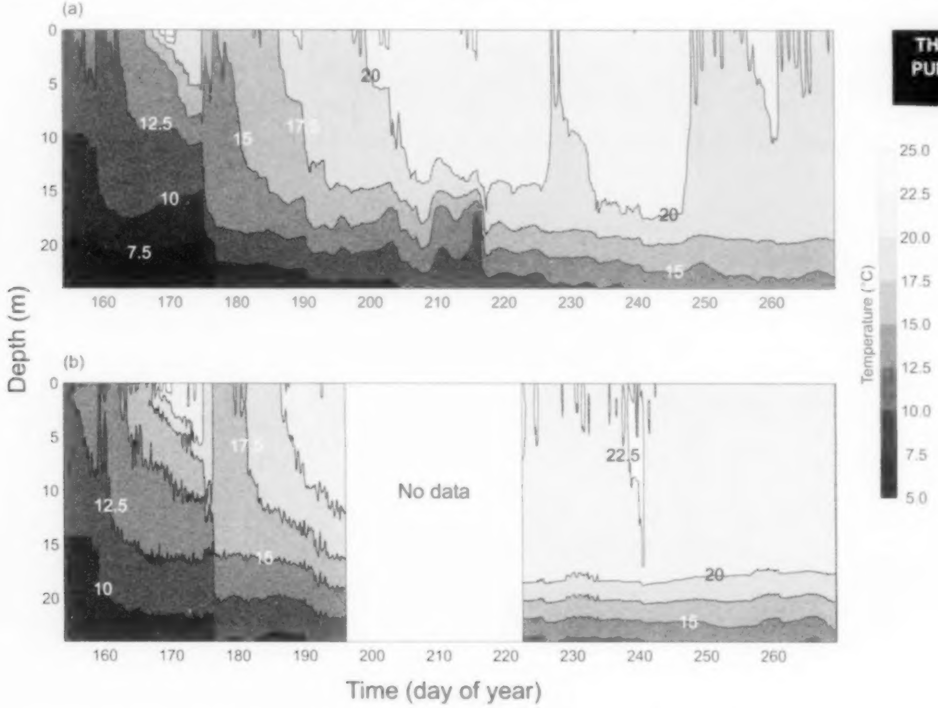

The modelled isotherms exhibit a strong 4- to 5-day (0.01 cph) low-frequency oscillation with amplitude of approximately 5 m, which is not apparent in the observed isotherms. Note once again, that this 0.01-cph frequency is the dominant frequency in both the surface-wind forcing and the excessively strong central basin 24 m current.

In both the central and eastern basins, the model correctly simulates the sharpening and deepening of the thermocline through August and September. However, the model does not reproduce the high-frequency diurnal isotherm oscillations evident in the observed data in the central and eastern basins. These oscillations are likely a result of diurnal wind forcing and penetrative convection in the metalimnion and epilimnion, respectively.

The model's quantitative performance between observed and modelled temperature (temp.) time series was evaluated by calculating the mean absolute error (MAE):

$$(6)\qquad \mathrm{MAE} = \left(\sum_{i=1}^{n} \left| (\text{observed temp.})_i - (\text{modelled temp.})_i \right| \right) \cdot n^{-1}$$

where n is the number of samples. At W_1, the MAE is less than 0.6°C at depths of 0, 2, 5, and 9.4 m. At C, the MAE ranges between 1.4 and 1.8°C at depths of 0, 2, 5, 8, 11, 14, 17, and 24 m. The MAE, as expected, is greater in the central basin than in the well-mixed western basin, because simulating temperatures within a thermally stratified water column is inherently more difficult. At E, in the deep quiescent hypolimnion, the modelled and observed temperature remains near 4°C throughout the season, with a maximum MAE of 0.7°C at depths of 35, 50, and 61 m. Within the epilimnion and metalimnion, the maximum MAE between the modelled and observed temperatures at depths of 0, 2, 10, and 20 m is 1.7°C.

Thermocline deepening events are correctly simulated as steplike temperature increases observed near days 148, 160, and 176 (Fig. 3). These events correspond to strong surface wind forcing (Fig. 4*a*), as indicated by storm surges (Fig. 4*c*), increased vertical mixing in the epilimnion, and a deepening of the modelled and observed mixed layer near days 148, 160, and 175 (Figs. 6–8). This is consistent with the observations of Schertzer et al. (1987) that mixed layer deepening in the central basin was primarily associated with strong-wind events.

Discussion

The discrepancy between modelled and observed hypolimnetic central basin currents may be examined by considering exchange flow between the central and eastern basins. Observational studies have shown a net westward hypolimnetic transport at the junction between the central and eastern basins (Bartish 1987; Saylor and Miller 1987). Eighty to one-hundred percent of this flow is confined by the Pennsylvania Ridge to the Pennsylvania Channel (near Erie, Pennsylvania; Chiocchio 1981) and is thus named the Pennsylvania Current. The observations of Bartish (1987) agree with our predictions that suggest that the Pennsylvania Cur-

NK USED IN THE ORIGINAL
AFFECT THE QUALITY OF
OFORM EDITION.

Fig. 8. Depth versus time isotherms comparing temperatures modelled with the modified A_z algorithm (*a*) and the observed vertical temperature distribution (*b*) in western Lake Erie at E (see Fig. 1 for position of E). The isotherm contour interval is 2.5°C. Both modelled and observed isotherms are linearly interpolated from hourly temperature time series at depths of 0, 2, 10, 20, 35, 50, and 61 m.

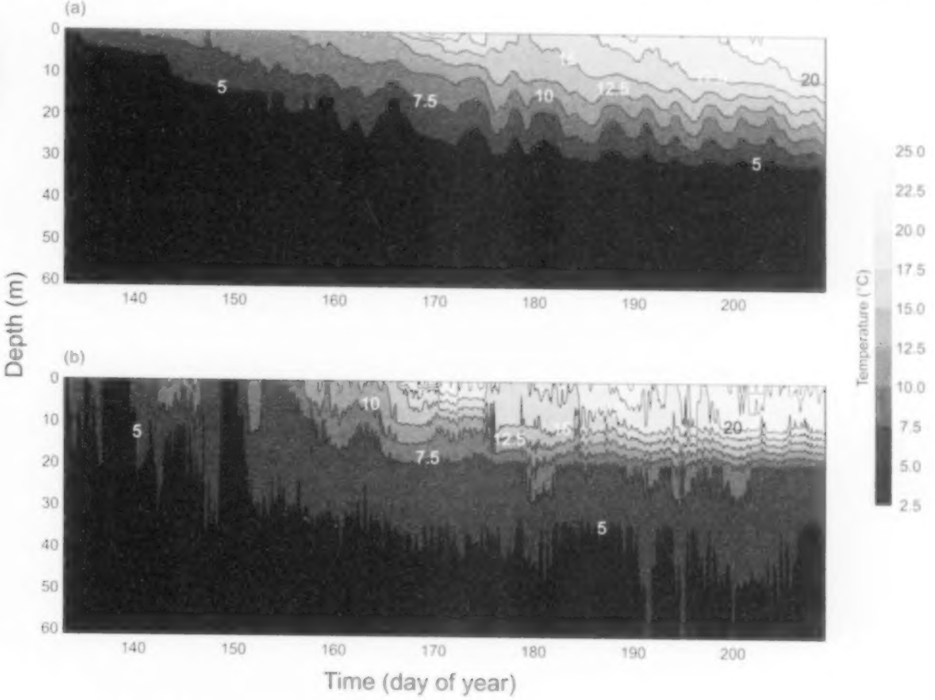

rent is driven by baroclinic flows associated with a basin-scale vertical and horizontal mode one seiche in the eastern basin. The strength of the Pennsylvania Current is proportional to the magnitude of the wind forcing (Bartish 1987), and it is observed to periodically fluctuate at periods of 50–150 h (Chiocchio 1981) and 100 h (0.01 cph; Boyce et al. 1980), in agreement with the period of the typical storm cycle and our modelled central basin hypolimnetic currents.

Further attempts to reduce the strength of the modelled central basin hypolimnetic current had negligible effects. These included: increasing the surface A_z maximum value by approximately two orders of magnitude (to ~1.0 $m^2 \cdot s^{-1}$) and the bed A_z by one order of magnitude (to ~0.5–1.0 $m^2 \cdot s^{-1}$); the addition of sidewall friction (e.g., Stacey et al. 1995); and increasing the height of the Pennsylvania Ridge to account for bathymetric simplifications resulting from discretization and lateral averaging. However, removal of the reduction of A_z in the thermocline region as a function of the Richardson number was found to reduce the modelled central basin hypolimnetic currents. This result is not surprising, as the enhanced vertical mixing prevents stratification, which acts as a wave guide for the baroclinic motions that drive basin-scale benthic currents.

An important aspect of this study is the determination of the effects of lateral averaging for Lake Erie. Although Lake Erie has a 6:1 length-to-width aspect ratio it has a maximum width that is greater than 100 km, many times the internal Rossby radius of deformation (~5 km). That is, at length scales greater than ~5 km in Lake Erie, the effects of the earth's rotation become important. This being the case, momentum transfer by Coriolis forces, from longitudinal to transverse, could be acting to reduce longitudinal basin-scale seiche strength by directing momentum laterally, away from the lake's longitudinal axis. A simple analytical model for the current excited by a sudden increase in wind shear acting on the epilimnion gives the longitudinal-current velocity in the inertial (nonrotating) frame (U_I) as the product of the wind stress (w) times the elapsed time (t) divided by the product of water density (ρ) and epilimnion thickness (h):

$$(7) \qquad U_I = \frac{wt}{\rho h}$$

The longitudinal current in the rotational frame (U_R) is given by

$$(8) \qquad U_R = \frac{w}{\rho h} \frac{\sin(ft)}{f}$$

where f is the Coriolis parameter for Lake Erie: $f = 9.77 \cdot 10^{-5} \cdot s^{-1}$ (Gill 1982). For a short time, the two flows are close in speed and direction, but after one-quarter of an inertial period (~4.5 h for Lake Erie), the longitudinal current in the rotational flow vanishes and, after 9 h, it opposes the wind. This simple analysis suggests that the reduction of longitudinal momentum is compensated for in the case of the 2-dimensional model by augmented values of vertical eddy viscosity.

Although in the present study we only intended to develop a hydrodynamically accurate model for 1994, the model should provide accurate predictions for other ice-free periods without further adjustment of the turbulence scheme. This fol-

Fig. 7. Depth versus time isotherms comparing temperatures modelled with the modified A_z algorithm (*a*) and the observed vertical temperature distribution (*b*) in western Lake Erie at C (see Fig. 1 for position of C). The isotherm contour interval is 2.5°C. Both modelled and observed isotherms are linearly interpolated from hourly temperature time series at depths of 0, 2, 5, 8, 11, 14, 17, and 24 m.

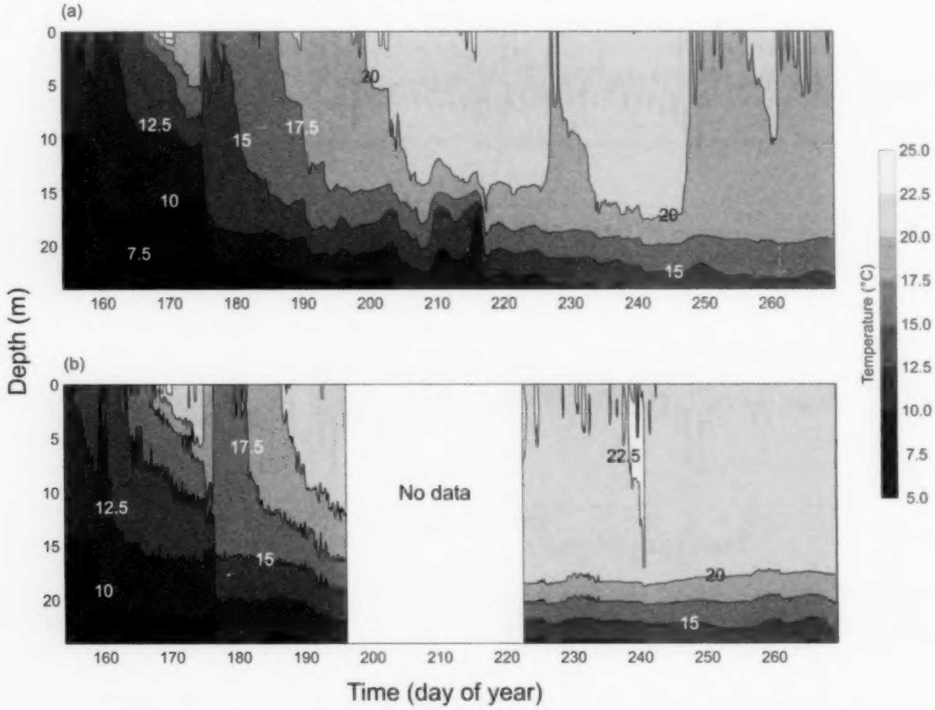

The modelled isotherms exhibit a strong 4- to 5-day (0.01 cph) low-frequency oscillation with amplitude of approximately 5 m, which is not apparent in the observed isotherms. Note once again, that this 0.01-cph frequency is the dominant frequency in both the surface-wind forcing and the excessively strong central basin 24 m current.

In both the central and eastern basins, the model correctly simulates the sharpening and deepening of the thermocline through August and September. However, the model does not reproduce the high-frequency diurnal isotherm oscillations evident in the observed data in the central and eastern basins. These oscillations are likely a result of diurnal wind forcing and penetrative convection in the metalimnion and epilimnion, respectively.

The model's quantitative performance between observed and modelled temperature (temp.) time series was evaluated by calculating the mean absolute error (MAE):

$$\text{(6)}\qquad \text{MAE} = \left(\sum_{i=1}^{n}\left|(\text{observed temp.})_i - (\text{modelled temp.})_i\right|\right)\cdot n^{-1}$$

where n is the number of samples. At W_1, the MAE is less than 0.6°C at depths of 0, 2, 5, and 9.4 m. At C, the MAE ranges between 1.4 and 1.8°C at depths of 0, 2, 5, 8, 11, 14, 17, and 24 m. The MAE, as expected, is greater in the central basin than in the well-mixed western basin, because simulating temperatures within a thermally stratified water column is inherently more difficult. At E, in the deep quiescent hypolimnion, the modelled and observed temperature remains near 4°C throughout the season, with a maximum MAE of 0.7°C at depths of 35, 50, and 61 m. Within the epilimnion and metalimnion, the maximum MAE between the modelled and observed temperatures at depths of 0, 2, 10, and 20 m is 1.7°C.

Thermocline deepening events are correctly simulated as steplike temperature increases observed near days 148, 160, and 176 (Fig. 3). These events correspond to strong surface wind forcing (Fig. 4*a*), as indicated by storm surges (Fig. 4*c*), increased vertical mixing in the epilimnion, and a deepening of the modelled and observed mixed layer near days 148, 160, and 175 (Figs. 6–8). This is consistent with the observations of Schertzer et al. (1987) that mixed layer deepening in the central basin was primarily associated with strong-wind events.

Discussion

The discrepancy between modelled and observed hypolimnetic central basin currents may be examined by considering exchange flow between the central and eastern basins. Observational studies have shown a net westward hypolimnetic transport at the junction between the central and eastern basins (Bartish 1987; Saylor and Miller 1987). Eighty to one-hundred percent of this flow is confined by the Pennsylvania Ridge to the Pennsylvania Channel (near Erie, Pennsylvania; Chiocchio 1981) and is thus named the Pennsylvania Current. The observations of Bartish (1987) agree with our predictions that suggest that the Pennsylvania Cur-

Fig. 8. Depth versus time isotherms comparing temperatures modelled with the modified A_z algorithm (*a*) and the observed vertical temperature distribution (*b*) in western Lake Erie at E (see Fig. 1 for position of E). The isotherm contour interval is 2.5°C. Both modelled and observed isotherms are linearly interpolated from hourly temperature time series at depths of 0, 2, 10, 20, 35, 50, and 61 m.

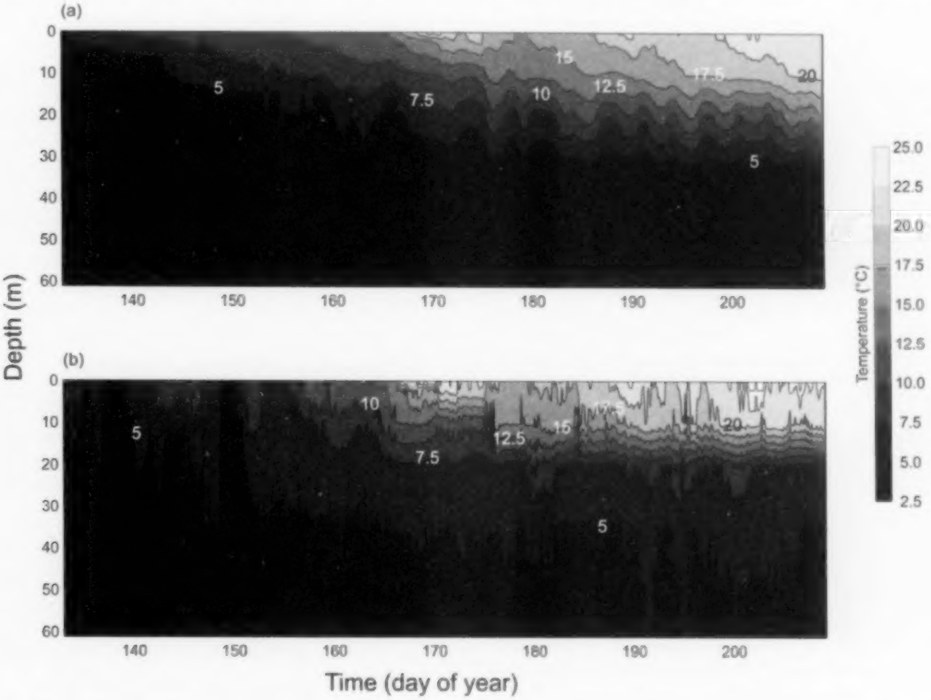

rent is driven by baroclinic flows associated with a basin-scale vertical and horizontal mode one seiche in the eastern basin. The strength of the Pennsylvania Current is proportional to the magnitude of the wind forcing (Bartish 1987), and it is observed to periodically fluctuate at periods of 50–150 h (Chiocchio 1981) and 100 h (0.01 cph; Boyce et al. 1980), in agreement with the period of the typical storm cycle and our modelled central basin hypolimnetic currents.

Further attempts to reduce the strength of the modelled central basin hypolimnetic current had negligible effects. These included: increasing the surface A_z maximum value by approximately two orders of magnitude (to ~1.0 $m^2 \cdot s^{-1}$) and the bed A_z by one order of magnitude (to ~0.5–1.0 $m^2 \cdot s^{-1}$); the addition of sidewall friction (e.g., Stacey et al. 1995); and increasing the height of the Pennsylvania Ridge to account for bathymetric simplifications resulting from discretization and lateral averaging. However, removal of the reduction of A_z in the thermocline region as a function of the Richardson number was found to reduce the modelled central basin hypolimnetic currents. This result is not surprising, as the enhanced vertical mixing prevents stratification, which acts as a wave guide for the baroclinic motions that drive basin-scale benthic currents.

An important aspect of this study is the determination of the effects of lateral averaging for Lake Erie. Although Lake Erie has a 6:1 length-to-width aspect ratio it has a maximum width that is greater than 100 km, many times the internal Rossby radius of deformation (~5 km). That is, at length scales greater than ~5 km in Lake Erie, the effects of the earth's rotation become important. This being the case, momentum transfer by Coriolis forces, from longitudinal to transverse, could be acting to reduce longitudinal basin-scale seiche strength by directing momentum laterally, away from the lake's longitudinal axis. A simple analytical model for the current excited by a sudden increase in wind shear acting on the epilimnion gives the longitudinal-current velocity in the inertial (nonrotating) frame (U_I) as the product of the wind stress (w) times the elapsed time (t) divided by the product of water density (ρ) and epilimnion thickness (h):

$$U_I = \frac{wt}{\rho h} \tag{7}$$

The longitudinal current in the rotational frame (U_R) is given by

$$U_R = \frac{w}{\rho h}\frac{\sin(ft)}{f} \tag{8}$$

where f is the Coriolis parameter for Lake Erie: $f = 9.77 \cdot 10^{-5} \cdot s^{-1}$ (Gill 1982). For a short time, the two flows are close in speed and direction, but after one-quarter of an inertial period (~4.5 h for Lake Erie), the longitudinal current in the rotational flow vanishes and, after 9 h, it opposes the wind. This simple analysis suggests that the reduction of longitudinal momentum is compensated for in the case of the 2-dimensional model by augmented values of vertical eddy viscosity.

Although in the present study we only intended to develop a hydrodynamically accurate model for 1994, the model should provide accurate predictions for other ice-free periods without further adjustment of the turbulence scheme. This follows from the fact that the 1994 meteorological data set was found to be typical for Lake Erie for the time period May–September when compared with historical records (Boyce and Chiocchio 1987; Hamblin 1987). In particular, the mean and standard deviation of the surface-wind field, the predominant forcing mechanism contributing to vertical turbulent mixing, were within the expected range of values. Obviously if other years were to be studied, the predicted time series would vary depending on the exact details of the meteorological forcing. In other words, as the time and intensity of storm events varied from year to year, so would the predicted time of occurrence of phenomena such as thermocline deepening.

CE-QUAL-W2's eddy viscosity turbulence model, developed for narrow hydraulically driven lakes and reservoirs, was found to be problematic for large wind-driven Lake Erie. Modifications to the vertical-mixing algorithm were required, to suppress excessive low frequency wind forced oscillations. Once the vertical-mixing routine was adjusted, longitudinal currents were modelled qualitatively in the western and central basins, with the possible exception of near-bed currents in the central basin. The model accurately predicted water levels and the thermal structure in the longitudinal–vertical plane. These results support the further extension of the model to include the effects of zebra mussels and zooplankton under a regimen of varying nutrient inputs and meteorological forcing. This has allowed us to use the model to: (*i*) investigate the effects of longitudinal and vertical mixing on nutrient availability to zebra mussels and (*ii*) quantify the relative influence of reductions in phosphorus and the introduction and proliferation of zebra mussels on the dramatic changes in Lake Erie's water. These results will be reported elsewhere.

Acknowledgements

The assistance of T. Cole in modifying the CE-QUAL-W2 source code and providing advice is gratefully acknowledged. The authors are grateful to F.M. Boyce, who was responsible for the collection of moored meteorological-, temperature-, and current-meter data in the central and eastern basins. This project was funded by the Ohio Sea Grant College Program grant NA86RG0053 (project R/EM-20) to D.A.C. and by Ohio State University and the University of Toronto. M.N. Charlton is thanked for his encouragement of this study. Numerous agencies and individuals provided input data. The United States Geological Survey provided the Maumee and Sandusky river inflows and the Niagara River outflow. NOAA provided the Detroit River inflow and over-lake precipitation measurements. Environment Canada provided Grand River (Ontario) inflow data. The Ontario Ministry of the Environment provided Detroit and Grand river temperatures. P. Richards at Heidelberg College, Tiffin, Ohio, provided Maumee and Sandusky river temperatures.

References

Ackerman, J.D, Loewen, M.R., and Hamblin, P.F. 2001. Benthic pelagic coupling over a zebra mussel bed in western Lake Erie. Limnol. Oceanogr. In press.

Adams, W.R., Thackston, E.L., and Speece, R.E. 1997. Modeling CSO impacts from Nashville using EPA's demonstration approach. J. Environ. Engineering, **123**: 126–133.

Arnott, D.L., and Vanni, M.J. 1996. Nitrogen and phosphorus recycling by the zebra mussel (*Dreissena polymorpha*) in the western basin of Lake Erie. Can. J. Fish. Aquat. Sci. **53**: 646–659.

Bartish, T. 1987. A review of the exchange processes among the three basins of Lake Erie. J. Gt. Lakes Res. **13**: 607–618.

Berkman, P.A., Haltuch, M.A., Tichich, E., Garton, D.W., Kennedy, G.W., Gannon, J.E., Mackey, S.D., Fuller, J.A., and Liebenthal, D.L. 1998. Invading mussel beds in Lake Erie. Nature (London), **393**: 27–28.

Boegman, L. 1999. Application of a two-dimensional hydrodynamic and water quality model to Lake Erie. M.A.Sc. thesis, Department of Mechanical and Industrial Engineering, University of Toronto, Toronto, Canada.

Boyce, F.M., and Chiocchio, F. 1987. Water movements at a mid-central basin site: time and space scales, relation to wind and internal pressure gradients. J. Gt. Lakes Res. **13**: 530–541.

Boyce, F.M., Chiocchio, F., Eid, B., Penicka, F., and Rosa, F. 1980. Hypolimnion flow between the central and eastern basins of Lake Erie during 1977. J. Gt. Lakes Res. **6**: 290–306.

Charlton, M.N. 1980. Hypolimnion oxygen consumption in lakes: discussion of productivity and morphometry effects. Can. J. Fish. Aquat. Sci. **37**: 1531–1539.

Charlton, M.N. 1994. The case for research on the effects of zebra mussels in Lake Erie: visualization of information from August and September 1993. J. Biol. Syst. **2**: 467–480.

Chiocchio, F. 1981. Lake Erie hypolimnion and mesolimnion flow exchange between central and eastern basins during 1978. Internal Rep. APSD 009 of the National Water Research Institute, Canada Centre for Inland Waters, Burlington, Ont., Canada.

Cole, T.M., and Buchak, E.M. 1995. CE-QUAL-W2: a two-dimensional, laterally averaged, hydrodynamic and water quality model, version 2.0: user manual. Instruction Rep. EL-95-1 of the U.S. Army Engineer Waterways Experiment Station, Vicksburg, Miss., U.S.A.

Fischer, H.B., List, E.J., Koh, R.C.Y., Imberger, J., and Brooks, N.H. 1979. Mixing in inland and coastal waters. Academic Press, New York.

Gill, A.E. 1982. Atmosphere–ocean dynamics. Academic Press, New York.

Hamblin, P.F. 1987. Meteorological forcing and water level fluctuations on Lake Erie. J. Gt. Lakes Res. **13**: 436–453.

Hinze, J.O. 1959. Turbulence. McGraw-Hill, New York.

Holland, R. 1993. Changes in planktonic diatoms and water transparency in Hatchery Bay, Bass Island area, western Lake Erie since the establishment of the zebra mussel. J. Gt. Lakes Res. **19**: 617–624.

Imberger, J. 1998. Flux paths in a stratified lake: a review. *In* Physical process in lakes and oceans. *Edited by* J. Imberger. Coast. Estuar. Stud. **54**: 1–18.

Ivey, G.N., and Patterson, J.C. 1984. A model of the vertical mixing in Lake Erie in summer. Limnol. Oceanogr. **29**: 553–563.

Kuan, C. 1995. Qualitative skill assessment of the Princeton coastal ocean circulation model for Lake Erie. Ph.D. thesis, Department of Civil Engineering, The Ohio State University, Columbus.

Leach, J.H. 1993. Impacts of the zebra mussel on water quality and fish spawning reefs in western Lake Erie. *In* Zebra mussels: biology, impacts and control. *Edited by* T.F. Nalepa and D.W. Schloesser. pp. 381–398.

Lucas, L.V., Cloern, J.E., Koseff, J.R., Monismith, S.G., and Thompson, J.K. 1998. Does the Sverdrup critical depth model explain bloom dynamics in estuaries? J. Mar. Res. **56**: 375–415.

Madenjian, C.P. 1995. Removal of algae by the zebra mussel (*Dreissena polymorpha*) population in western Lake Erie—a bioenergetics approach. Can. J. Fish. Aquat. Sci. **52**: 381–390.

Martin, J.L. 1988. Application of two-dimensional water quality model. J. Environ. Engineering, **114**: 317–336.

McCune, K.C. 1998. Temperature gradient microprofiling in the central basin of Lake Erie: a study of vertical turbulent process. M.Sc. thesis, Department of Civil Engineering, The Ohio State University, Columbus.

Nicholls, K.H., and Hopkins, G.J. 1993. Recent changes in Lake Erie (north shore) phytoplankton: cumulative impacts of phosphorus loading reductions and the zebra mussel introduction. J. Gt. Lakes Res. **19**: 637–647.

Nicholls, K.H., Standen, D.W., Hopkins, G.J., and Carney, E.C. 1977. Declines in near-shore phytoplankton of Lake Erie's western basin since 1971. J. Gt. Lakes Res. **3**: 72–78.

O'Riordan, C.A., Monismith, S.G., and Koseff, J.R. 1995. The effect of bivalve excurrent jet dynamics on mass transfer in a benthic boundary layer. Limnol. Oceanogr. **40**: 330–344.

Patankar, S.V. 1980. Numerical heat transfer and fluid flow. Taylor and Francis, Washington, D.C.

Platzman, G.W., and Rao, D.B. 1964. Spectra of Lake Erie water levels. J. Geophys. Res. **60**: 2525–2535.

Saggio, A., and Imberger, J. 1998. Internal weather in a stratified lake. Limnol. Oceanogr. **43**: 1780–1795.

Saylor, J.H., and Miller, G.S. 1987. Studies of large-scale currents in Lake Erie, 1979–80. J. Gt. Lakes Res. **13**: 487–514.

Schertzer, W.M., and Hamblin, P.F. 2001. Lake Erie thermal structure: variability, trends and potential changes. *In* Lake Erie at the millenium: changes, trends and trajectories. *Edited by* J.J.H. Ciborowski, M.N. Charlton, R.J. Kries, and J.M. Reutter. Canadian Scholars' Press, Toronto, Canada.

Schertzer, W.M., Saylor, J.H., Boyce, F.M., Robertson, D.G., and Rosa, F. 1987. Seasonal thermal cycle of Lake Erie. J. Gt. Lakes Res. **13**: 468–486.

Stacey, M.W., Pond, S., and Nowak, Z.P. 1995. A numerical model of the circulation in Knight Inlet, British Columbia, Canada. J. Phys. Oceanogr. **25**: 1037–1062.

Tennekes, H., and Lumley, J.L. 1972. A first course in turbulence. MIT Press, Cambridge, Mass.

Tennessee Valley Authority. 1972. Heat and mass transfer between a water surface and the atmosphere. Rep. No. 0-6803 of the Tennessee Valley Authority, Knoxville, Tenn., U.S.A.

Wells, S.A. 1997. Theoretical basis for the CE-QUAL-W2 river basin model. Tech. Rep. EWR-6-97 of the Department of Civil Engineering, Portland State University, Portland, Oreg., U.S.A.

Stable nitrogen isotopes as indicators of anthropogenic activities in small freshwater systems

James L. Lake, Richard A. McKinney, Frank A. Osterman, Richard J. Pruell, John Kiddon, Stephan A. Ryba, and Alan D. Libby

Abstract: Stable nitrogen isotope ratios ($\delta^{15}N$) were measured in fish, mussel, and sediment samples taken from 17 small freshwater sites to examine food chain length and trophic position across sites affected by differing levels of anthropogenic activity. Both shoreline development and fish species composition varied greatly among sites, and a range of up to 11.2‰ was found for the $\delta^{15}N$ values of largemouth bass (*Micropterus salmoides*). Fish $\delta^{15}N$ values were baseline corrected using unionid mussel (*Elliptio complanata*) $\delta^{15}N$ values. Predators, such as largemouth bass and chain pickerel (*Esox niger*), exhibited normalized $\delta^{15}N$ values that were less variable than those of benthic-feeding fishes. Relationships between $\delta^{15}N$ and dissolved inorganic nitrogen concentrations indicated that $\delta^{15}N$ was a valid descriptor of eutrophication at sites with low dissolved inorganic nitrogen concentrations. The fraction of residential land in buffer zones surrounding sites was correlated with fish $\delta^{15}N$, indicating that urban development, and presumably human wastewater, resulted in elevated $\delta^{15}N$ values in these small freshwater systems.

Résumé : Des mesures des rapports d'isotopes stables d'azote ($\delta^{15}N$) dans des poissons, des moules et des échantillons de sédiments récoltés à 17 sites d'eau douce ont permis d'étudier la longueur de la chaîne alimentaire et les positions trophiques dans une série de milieux affectés à des degrés divers par l'activité humaine. Le développement de la ligne de berge et la composition spécifique des poissons varient considérablement d'un site à l'autre; les valeurs de $\delta^{15}N$ chez l'Achigan à grande bouche (*Micropterus salmoides*) s'élevent jusqu'à 11,2‰. Les valeurs de $\delta^{15}N$ chez les poissons ont été corrigées en utilisant comme référence les valeurs de $\delta^{15}N$ des moules (*Elliptio complanata*). Les prédateurs, comme les Achigans à grande bouche et les Brochets maillés (*Esox niger*), possèdent des valeurs normalisées de $\delta^{15}N$ moins variables que celles des poissons benthonophages. Les relations entre les valeurs de $\delta^{15}N$ et les concentrations d'azote inorganique dissous indiquent que le $\delta^{15}N$ est un bon descripteur de l'eutrophisation aux sites de basses concentrations d'azote inorganique dissous. La proportion de terres résidentielles dans la zone tampon autour des sites est en corrélation avec le $\delta^{15}N$ des poissons, ce qui laisse croire que le développement urbain, et sans doute les eaux d'égouts d'origine anthropique, amènent une augmentation des valeurs de $\delta^{15}N$ dans ces petits systèmes d'eau douce.

[Traduit par la Rédaction]

Introduction

Measurements of stable isotopes of nitrogen have been used to indicate system-level changes at aquatic and estuarine sites resulting from development in adjacent watersheds (Cabana and Rasmussen 1996; McClelland et al. 1997; McClelland and Valiela 1998) and to estimate trophic structure in aquatic systems (Cabana and Rasmussen 1994; Vander Zanden and Rasmussen 1996). Biogeochemical processes can be selective for one nitrogen isotope over another (Mariotti et al. 1981), which may result in changes in ratios of the nitrogen isotopes in ammonia, nitrates, and nitrites at aquatic sites. Nitrogen isotope fractionation also has been found during uptake and assimilation of nitrogen nutrients by marine phytoplankton (Pennock et al. 1996; Waser et al. 1998), and similar fractionation probably occurs at freshwater sites. Changes in the $\delta^{15}N$ values at sites can also result from the introduction of nitrogen in synthetic fertilizers or in wastewater. Many factors may be involved in establishing the $\delta^{15}N$ value at a site, but studies have related increases in $\delta^{15}N$ values in aquatic and marine systems to the extent of anthropogenic activity in watersheds and the input of wastewater (Cabana and Rasmussen 1996; McClelland et al. 1997; McClelland and Valiela 1998). These increases might be expected because wastewater generally has a higher $\delta^{15}N$ value than those in other inputs to aquatic systems (Heaton 1986; Aravena et al. 1993; McClelland and Valiela 1998).

Quantified trophic positions for fish are calculated at sites by measuring $\delta^{15}N$ values in fish and baseline species (often filter-feeding bivalves) and dividing the difference between them by a constant $\delta^{15}N$ value representing one trophic level. This approach is possible because the heavier nitrogen isotope is preferentially retained in the protein of consumers

Received January 5, 2000. Accepted February 7, 2001. Published on the NRC Research Press Web site on April 12, 2001.
J15513

J.L. Lake,[1] R.A. McKinney, F.A. Osterman, R.J. Pruell, J. Kiddon, and S.A. Ryba. National Health and Environmental Effects Research Laboratory, Atlantic Ecology Division, U.S. Environmental Protection Agency, 27 Tarzwell Drive, Narragansett, RI 02882, U.S.A.
A.D. Libby. Rhode Island Division of Fish and Wildlife, P.O. Box 218, West Kingston, RI 02892, U.S.A.

[1] Corresponding author (e-mail: lake.jim@epa.gov).

DOI: 10.1139/cjfas-58-5-870

Fig. 1. Map showing the locations of the freshwater sites sampled in Rhode Island for this study. Numbers adjacent to sites correspond to the site numbers listed in Table 1.

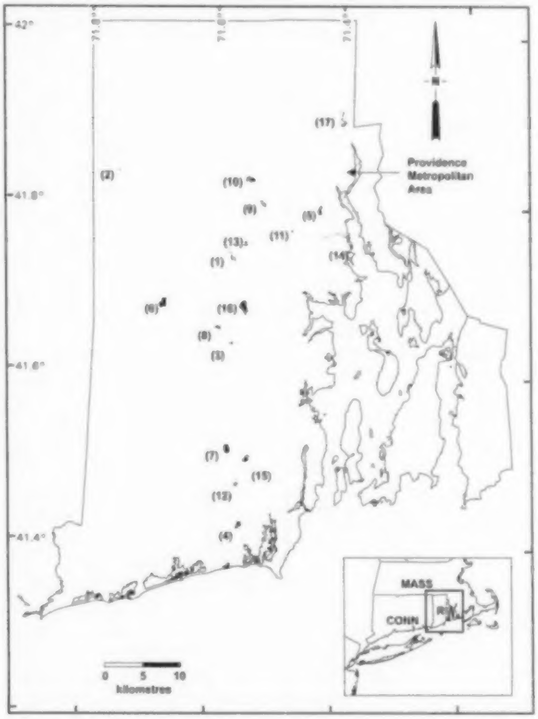

(Schoeninger and DeNiro 1984) and because estimates of the magnitude of increase in $\delta^{15}N$ for one trophic step have been made from laboratory feeding studies (Minigawa and Wada 1984). Differences in biogeochemical processes and inputs may cause overall shifts in $\delta^{15}N$ values at sites, and normalization to appropriate baseline species has been used to facilitate comparison of trophic positions between or among sites (Cabana and Rasmussen 1996; Vander Zanden et al. 1997). Due to their low feeding position, filter-feeding bivalves were initially used to establish the baseline at freshwater sites, but in larger systems with pelagic, profundal, and littoral zones, other methods of establishing "baseline organisms" have been suggested (Vander Zanden and Rasmussen 1999). In aquatic systems, a variety of stressors (acidity, organic pollution, contaminants, etc.) can decrease species richness (Ford 1989) and can shorten food chains (Woodwell 1983; Odum 1985; Weinstein and Birk 1989). Studies also have documented the lengthening of food chains resulting from introductions of foreign species into some aquatic sites (Cabana and Rasmussen 1994). Therefore, ecologists are tempted to compare trophic position values and food chain length among systems and relate changes in these values to the extent of environmental stress. There are several factors that may constrain this use, however, particularly for sites that vary greatly in physical and chemical properties and biological composition. Any trophic structural change found between such sites cannot be ascribed to a particular stress because differences in species composition and omnivority may have caused changes in $\delta^{15}N$ values for the same species at the different sites, and the response to stress, at both the organismal and the system level, may vary among sites. Models used to estimate trophic position use a constant (usually 3.4‰) as an average trophic step; however, this is a mean value for a trophic transfer of one step from laboratory feeding studies (Minigawa and Wada 1984), and the magnitude of change for any specific trophic step in the field may vary substantially from this value. The $\delta^{15}N$ values can give a description of nitrogen movement through food chains, however, and studies in boreal lakes found that 69% of the variability in food chain length calculated using $\delta^{15}N$ values was explained by fish species richness (Vander Zanden et al. 1999). This suggests that species addition or deletion (e.g., by anthropogenic stress) will be reflected in food chain length.

Within the small state of Rhode Island, there are freshwater sites encompassing environmental conditions extending from almost pristine to highly impacted and containing a range of fish communities, many of which contain largemouth bass (*Micropterus salmoides*) as the top aquatic predator. The objectives of the present study were to examine changes in food chain length and trophic position among these sites and to relate these changes to the levels of anthropogenic activity measured here as (*i*) the extent of residential development in land areas surrounding sites and (*ii*) the concentration of dissolved inorganic nitrogen (DIN) at sites.

Materials and methods

Samples were collected at freshwater sites in Rhode Island from spring 1996 through spring 1998. Fourteen of the sites were ponds or small lakes that ranged from 4 to 87 ha in size; average depths ranged from 0.6 to 4.3 m (Fig. 1; Table 1). These water bodies are referred to as "ponds" in this study. The three other sites were sections of rivers that were constrained by dams. These sites ranged from 5.7 to 30 ha in size; depths were estimated to be 2.1–2.4 m. Sizes and depths of sites were obtained from the Rhode Island Geographical Information System, Providence, R.I., and Guthrie and Stolgitis (1994). Nutrient samples were taken in a plastic bucket and immediately poured into glass bottles. Bottles were capped and transported to the laboratory on ice. Samples were analyzed within 24 h of collection. Total ammonia-nitrogen and nitrite/nitrate-nitrogen were analyzed by colorimetric techniques based on published methods (Verdouw et al. 1978; Hach Company 1997) on a Milton Roy (Rochester, N.Y.) Spectronic 1201 spectrophotometer. The concentrations of these nitrogen nutrients were summed and referred to as "DIN concentrations" in this paper.

Fish were collected by electrofishing using a Smith Root model SR-16 electrofishing workboat. At smaller sites (<12 ha), electrofishing was done along the whole shoreline; at larger sites (>12 ha), the shoreline was divided into 12 equal-length sections and sampling was done at stations within each section. Each station consisted of 6 min of electrofishing. When possible, fish samples representing small, medium, and large fish of each species were selected for stable isotope analysis. Samples of bulk sediment were collected from the approximate center of the site by a ponar grab. Samples of unionid mussels (*Elliptio complanata*) were collected with clam rakes or by diving. Mussel samples were usually taken from one sampling location at each site. A study found no significant difference in $\delta^{15}N$ values among mussels taken from several stations at some of these sites (McKinney et al. 1999), which supports the use of one sampling location in our study. Personnel of the Rhode Island Department of Environmental Manage-

Table 1. Site names and numbers, numbers of fish species at sites, most abundant fish species, site areas and depths, type of wastewater treatment of residences onshore, DIN concentrations of water samples, fraction of residential land in buffer zones, food chain length, and additional site information.

Site	Site No.	Total no. of fish species	Most abundant fish species	Area (ha)	Average depth (m)	Wastewater treatment	DIN concentration (μmol·L^{-1})[a]	n[b]	Fraction of residential land in buffer zone[c]	Food chain length (‰)[d]	Additional site information
Upper Pawtuxet River	1	10	Chain pickerel (*Esox niger*)	21.1	2.1	Septic	7.2	2			Minimal development
Shippee Saw Mill Pond	2	8	Yellow perch (*Perca flavescens*)	4.0	0.6	No wastewater	6.0	2	0.01		Minimal development
Tarbox Pond	3	7	Yellow perch	4.9	2.4	No wastewater	4.6	2	0.00		Minimal development
Tucker Pond	4	11	Yellow perch	38.1	3.4	Septic	6.1	1	0.07	5.8	15 lots, low occupancy
Mashapaug Pond	5	7	White perch (*Morone americana*)	27.1	2.1	Sewer	149.4	2	0.23		Industrial site
Quidnick Reservoir	6	10	Yellow perch	72.5	3.7	Septic	6.4	1	0.27	7.1	40 lots, low occupancy
Yawgoo Pond	7	9	Yellow perch	66.0	2.7	Septic	4.1	1	0.05	7.8	3 lots occupied
Mishnock Lake	8	7	Pumpkinseed (*Lepomis gibbosus*)	19.4	2.4	Septic	31.1	1	0.57	5.5	63 lots, old septic systems
Simmons Reservoir	9	8	Yellow perch	18.6	1.5	Septic	154.7	2	0.15		At base of major state landfill
Oak Swamp Reservoir	10	8	Yellow perch	42.9	1.5	Septic	13.0	2	0.49	7.3	92 lots, old septic systems
Meshanticut Pond	11	9	Bluegill (*Lepomis macrochirus*)	4.5	1.5	Sewer	23.0	1	0.54	6.6	65 lots adjacent
Larkin Pond	12	8	Largemouth bass (*Micropterus salmoides*)	17.8	4.3	No wastewater	8.3	1	0.05	7.0	Minimal development[e]
J.L. Curran Upper Reservoir	13	4	Bluegill	11.3	3.0	Septic	44.6	2	0.03	7.7	6 lots, farm drains to pond
Lower Pawtuxet River	14	6	White sucker (*Catostomus commersoni*)	5.7	2.1	Sewage treatment plant input	192.6	2			Sewage treatment plant inputs
Hundred Acre Pond	15	13	Largemouth bass	33.6	5.5	Septic	31.0	1	0.28	7.1	30 houses occupied onshore
Tiogue Lake	16	10	White sucker	86.6	1.8	Septic	55.3	1	0.61	6.8	205 lots, old septic systems
Blackstone River	17	12	White sucker	30.0	2.4	Sewage treatment plant input	118.9	1		5.8	Sewage treatment plant inputs

[a] DIN concentration is the sum of nitrite, nitrate, and ammonia concentrations at sites.

[b] Water samples for nutrient analyses were taken during 1996 and 1997 at selected sites. All sites were sampled in 1998.

[c] Residential land area/total land area in buffer zones for pond sites.

[d] Food chain length calculated as the difference between δ^{15}N values of mussels and largemouth bass at sites. Samples from Mashapaug Pond were not included. Either largemouth bass or mussels were not found at sites without listed values.

[e] Girl Scout camp onshore; total of 900 occupants during the summer months.

ment, Division of Fish and Wildlife, identified the fish and mussel species.

Fish samples were placed on ice and transported to the laboratory. Usually, samples were processed the next day, but some samples were frozen for storage and thawed before processing. Samples were taken from the dorsal muscle of fish and from the foot of mussels. Sediment samples were placed in jars and frozen until processed. Sediment samples were mixed and an aliquot was taken for analysis. All samples were dried, ground, and a small aliquot (~1.5 mg) weighed for isotopic analysis.

The nitrogen isotopic composition of the samples was determined by continuous-flow isotope ratio mass spectrometry employing a Carlo-Erba NA 1500 series II elemental analyzer interfaced to a Micromass Optima mass spectrometer located at our facility (National Health and Environmental Effects Research Laboratory, Atlantic Ecology Division). Sample nitrogen was combusted completely to N_2 at 1200°C in the elemental analyzer, and the $^{15}N/^{14}N$ ratio of N_2 was analyzed immediately in the mass spectrometer. The isotope ratio of the sample tissue was compared with the isotope ratio of a reference material of known isotopic composition. Results are reported using delta notation ($\delta^{15}N = [(R_{sample}/R_{reference}) - 1] \times 1000$, where R is the $^{15}N/^{14}N$ ratio). The isotopic composition of the tissue is expressed as a part per thousand (‰) difference from the composition of a recognized reference material, which by convention is N_2 in air (Mariotti 1983). To reduce the effect of measurement error, all samples were analyzed in duplicate. The typical difference between analytical duplicates was about 0.1‰. The $\delta^{15}N$ values reported in this paper are means of the two analytical duplicates. Sample material analyzed periodically over a several month period exhibited a precision of ±0.30‰, calculated as a standard deviation of all replicate values. This latter estimate of precision is applicable for $\delta^{15}N$ values determined in this study. Samples were taken from three different locations in the dorsal muscle of an individual largemouth bass and an individual yellow perch (*Perca flavescens*) to determine sample variability within the muscle of organisms. Standard deviations of the mean results were low, 0.10 and 0.13‰ for largemouth bass and yellow perch, respectively.

At some sites, only limited numbers of organisms of some species were available for analysis. For sites where only one organism of a species was available, its $\delta^{15}N$ value was used. When two organisms were available, their mean $\delta^{15}N$ value was used. For sites where three or more organisms of the same species were available, the relationship between organism length and $\delta^{15}N$ was evaluated. If no significant relationship was found ($\alpha = 0.05$), the mean of all $\delta^{15}N$ values was used. In six instances, there was a significant linear relationship between fish length and $\delta^{15}N$. When a relationship was found, the mean length of all fish of the species or the mean length of the first 30 fish (all that were measured during sampling) was substituted in the relationship to calculate the $\delta^{15}N$ value. For unionids, the $\delta^{15}N$ value is the mean of measurements of three or more organisms, except for Mashapaug Pond, which only had one organism. No relationships were found between size and $\delta^{15}N$ for mussels.

We used the $\delta^{15}N$ of unionid mussels for normalization of $\delta^{15}N$ values of fish species to allow comparisons of food chain length and trophic position among sites as done in previous studies (Cabana and Rasmussen 1996; Vander Zanden et al. 1997). Unionid mussels are logical choices because they selectively feed on phytoplankton (Tessier et al. 1984); further, these organisms are long lived, and thus, their use as a "baseline" organism avoids problems with temporal variability in $\delta^{15}N$ values that may be encountered with lower-level organisms (e.g., phytoplankton).

For our normalizations, the $\delta^{15}N$ values of mussels were subtracted from the $\delta^{15}N$ values of the fish species. In this paper, these values are referred to as "normalized $\delta^{15}N$ values." It is important to note that these values are $\delta^{15}N$ differences relative to the baseline (mussels), not trophic position values. We did not divide these differences in $\delta^{15}N$ values by the constant 3.4‰ to calculate trophic positions as done in previous work (Cabana and Rasmussen 1996; Vander Zanden et al. 1997).

Food chain length was taken as the difference in $\delta^{15}N$ values between the top-level predator (largemouth bass) and a primary consumer (unionid mussels). This approach is similar to that used in previous studies (Cabana and Rasmussen 1996) and that of later work (Vander Zanden et al. 1999), although a different method of determining baseline organisms was used in the later study.

Sources of possible wastewater inputs to sites were investigated by physical inspection of sites and from review of town records and GIS data (Rhode Island Geographical Information System, Providence, R.I.).

Data were compared using linear regression analyses. Dixon's test for extreme values was used to identify irregular $\delta^{15}N$ differences between fish species and mussels and between fish species and sediments (Snedecor and Cochran 1980). Because the $\delta^{15}N$ values within a site were correlated and multiple analyses done, a specific p value was not assigned to show the degree of difference of the extreme values from "normal" values. Rather, the values identified as extreme by the test were considered descriptive and were used to show trends in the data. The p values for linear regressions are included.

Results

The 17 sites selected for this study ranged from highly developed to rural (Fig. 1; Table 1). There were no direct measures of the input of wastewater at these sites, but some sites had known inputs, from sewage treatment plants, or probable inputs, from old septic systems, while at other sites, inputs were minimal or nonexistent (Table 1).

Variations in the fish communities were found among sites. White sucker (*Catostomus commersoni*) usually was the most abundant species at industrial and highly developed sites, while yellow perch was most abundant at most of the rural sites (Table 1). Some sites had large numbers of one species, while other sites had a more even distribution between several species. The unionid mussel was found at 13 sites.

Largemouth bass had the highest $\delta^{15}N$ values of all fish except at two sites. For largemouth bass, $\delta^{15}N$ values averaged 14.2‰ and ranged from 7.9 to 19.1‰ across sites. The $\delta^{15}N$ values and ranges for all sites are given in the Appendix.

The consistency of trophic positioning was examined by comparing normalized $\delta^{15}N$ values for fish species across sites. Examination of normalized $\delta^{15}N$ values for fish species that were present at >50% of the sampling sites using Dixon's test identified three extreme values at Mashapaug Pond. Normalized $\delta^{15}N$ values for pumpkinseed (*Lepomis gibbosus*) and brown bullhead (*Ameiurus nebulosus*) in Tiogue Lake and brown bullhead in Mishnock Lake also were identified as extreme values by Dixon's test. Only one mussel was found at Mashapaug Pond, and its $\delta^{15}N$ value appears to be abnormal. Consequently, the $\delta^{15}N$ value of the Mashapaug Pond mussel was not used in subsequent comparisons in this study. The removal of the Mashapaug Pond data decreased the coefficients of variation for normalized $\delta^{15}N$ values for fish (Table 2). Even without the Mashapaug Pond data, largemouth bass, chain pickerel (*Esox niger*), and black crappie (*Pomoxis nigromaculatus*) showed lower coefficients of variation of normalized $\delta^{15}N$ values than those of lower-level fish

Table 2. Normalized $\delta^{15}N$ values of fish species and mussels across all sites, standard deviations, coefficients of variation, and number of sites.

Species[a]	Normalized $\delta^{15}N$ values				Normalized $\delta^{15}N$ values[b]			
	Mean (‰)	±SD (‰)	CV	*n*	Mean (‰)	±SD (‰)	CV	*n*
Largemouth bass (*Micropterus salmoides*)	6.4	1.4	21.7	12	6.8	0.8	11.3	11
Chain pickerel (*Esox niger*)	5.5	0.7	12.7	11	5.5	0.7	12.7	11
Black crappie (*Pomoxis nigromaculatus*)	5.7	0.3	5.1	4	5.7	0.3	5.1	4
Yellow perch (*Perca flavescens*)	4.4	1.3	30.2	12	4.4	1.3	30.2	12
Pumpkinseed (*Lepomis gibbosus*)	3.9	1.7	43.0	11	4.3	1.2	28.8	10
Bluegill (*Lepomis macrochirus*)	3.8	1.5	39.4	11	4.2	0.8	18.2	10
White perch (*Morone americana*)	3.6	2.0	54.2	6	4.3	1.2	29.2	5
White sucker (*Catostomus commersoni*)	3.0	1.0	34.3	4	3.0	1.0	34.3	4
Brown bullhead (*Ameiurus nebulosus*)	3.5	1.7	48.5	9	3.5	1.7	48.5	9
American eel (*Anguilla rostrata*)	4.4	0.3	6.1	6	4.4	0.3	6.1	6
Golden shiner (*Notemigonus crysoleucas*)	3.2	1.3	40.3	8	3.2	1.3	40.3	8

[a] Includes fish species found at four or more sites.

[b] Samples from Mashapaug Pond were not included.

Table 3. Linear regression relationships of $\delta^{15}N$ values between mussels and fish species and between sediment and fish species, coefficients of determination, *p* values, and number of sites.

Species	$\delta^{15}N$ mussels to $\delta^{15}N$ fish[a]			$\delta^{15}N$ sediment to $\delta^{15}N$ fish		
	r^2	*p*	*n*	r^2	*p*	*n*
Largemouth bass (*Micropterus salmoides*)	0.92	<0.001	11	0.65	<0.001	16
Chain pickerel (*Esox niger*)	0.91	<0.001	11	0.71	<0.001	13
Yellow perch (*Perca flavescens*)	0.72	<0.001	12	0.59	<0.001	15
Pumpkinseed (*Lepomis gibbosus*)	0.79	<0.001	10	0.69	<0.001	14
Bluegill (*Lepomis macrochirus*)	0.90	<0.001	10	0.51	0.006	13
Brown bullhead (*Ameiurus nebulosus*)	0.42	0.060	9	0.61	0.002	13
Golden shiner (*Notemigonus crysoleucas*)	0.83	0.002	8	0.53	0.010	11

[a] Samples from Mashapaug Pond were not included.

(i.e., yellow perch, pumpkinseed, bluegill (*Lepomis macrochirus*), white sucker, and brown bullhead) (Table 2). This suggests a more consistent trophic position for the top-level predators.

We compared the $\delta^{15}N$ values of mussels and sediment for use for predicting $\delta^{15}N$ values of fish species. The proportions of the variance in the data explained by the linear regression model (r^2) between sediment and fish species were lower than those between mussels and fish (Table 3), indicating that use of mussels was advantageous for the prediction of $\delta^{15}N$ values of fish. However, significant linear regressions between $\delta^{15}N$ values in sediment and most fish species were found (Table 3).

The relationships between DIN concentrations for sites and $\delta^{15}N$ values for species were examined as indications of the impact of enrichment on stable nitrogen isotopes. Increases in DIN concentrations resulted in increases in $\delta^{15}N$ values; these relationships were best modeled by logarithmic curves (Fig. 2).

Land use in watersheds and in buffer zones surrounding our pond sites from GIS data was compared with $\delta^{15}N$ values of samples from sites. Comparisons of relationships between $\delta^{15}N$ values of samples and of fractions of forest land, agricultural land, wetlands, and residential land in these land areas showed useful relationships ($p < 0.05$) only for fraction of residential land. The relationships between $\delta^{15}N$ values of samples and fraction of residential land in the buffer zone were less variable than those utilizing land use in the entire watersheds (Table 4; Fig. 3).

Fig. 2. Relationships between DIN concentrations (μmol·L^{-1}) in water samples from sample sites and $\delta^{15}N$ values of largemouth bass (diamonds), yellow perch (squares), mussels (triangles), and sediment (circles). Best fits for data are logarithmic relationships.

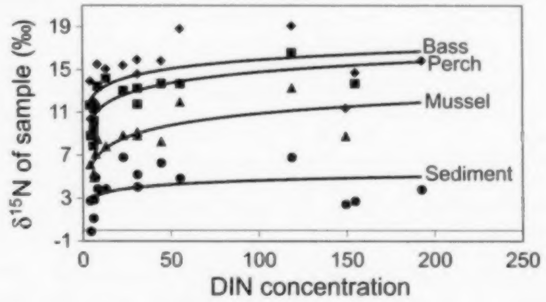

Food chain length was calculated as the difference between $\delta^{15}N$ values of the unionid mussel and the largemouth bass (Table 1). Two indicators of wastewater input, DIN concentration and fraction of residential land in buffer zones (Table1), were compared with food chain length. The resulting relationships were not significant ($p > 0.05$). No significant relationship between fish species richness and food chain length was found ($p > 0.05$).

Table 4. Linear regression relationships between $\delta^{15}N$ values of fish species, mussels, and sediment and fraction of residential land in watersheds and in 91.4-m buffer zones surrounding pond sites, coefficients of determination, *p* values, and number of pond sites.

	Watershed			Buffer zone		
Sample	r^2	p	n	r^2	p	n
Largemouth bass (*Micropterus salmoides*)	0.09	0.31	14	0.33	0.03	14
Chain pickerel (*Esox niger*)	0.33	0.06	11	0.32	0.07	11
Yellow perch (*Perca flavescens*)	0.21	0.12	13	0.22	0.11	13
Pumpkinseed (*Lepomis gibbosus*)	0.15	0.19	13	0.40	0.02	13
Bluegill (*Lepomis macrochirus*)	<0.01	0.95	11	0.09	0.38	11
Brown bullhead (*Ameiurus nebulosus*)	0.33	0.06	11	0.48	0.02	11
Golden shiner (*Notemigonus crysoleucas*)	0.19	0.24	9	0.34	0.10	9
Unionid mussels (*Elliptio complanata*)[a]	0.26	0.13	10	0.36	0.07	10
Sediment	0.11	0.25	14	0.28	0.05	14

[a] Samples from Mashapaug Pond were not included.

Fig. 3. Relationships between fraction of residential land in 91.4-m buffer zones surrounding sites and $\delta^{15}N$ values of largemouth bass (diamonds), yellow perch (squares), mussels (triangles), and sediment (circles). Equations for the lines are $\delta^{15}N$ largemouth bass = 7.2(fraction residential land in buffer zones) + 12.0 ($r^2 = 0.33$, $p = 0.03$), $\delta^{15}N$ yellow perch = 4.3(fraction residential land in buffer zones) + 10.9 ($r^2 = 0.22$, $p = 0.11$) $\delta^{15}N$ mussels = 5.2(fraction residential land in buffer zones) + 6.4 ($r^2 = 0.36$, $p = 0.07$), and $\delta^{15}N$ sediment = 4.3(fraction residential land in buffer zones) + 2.5 ($r^2 = 0.28$, $p = 0.05$). Regression statistics for relationships for other fish species are given in Table 4.

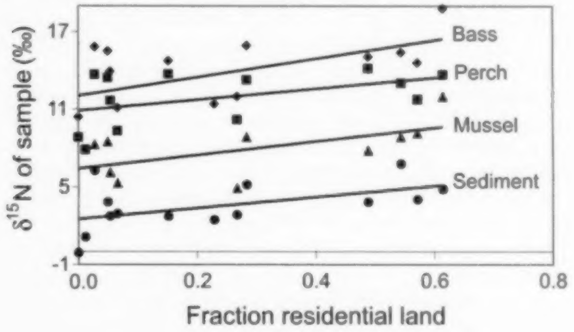

Discussion

The sampling sites in the present study encompassed a considerable range of anthropogenic influence. This range is from rural, relatively undisturbed sites to those receiving wastewater directly from sewage treatment plants. Some developed sites were near probable sources of chemical contaminants, such as former chemical manufacturing plants or municipal landfills. Sites in rural locations were far less likely to be chemically contaminated. There were large differences among sites in the types and abundance of fish. Generally, the most abundant fish was white sucker at degraded sites, while yellow perch were most abundant at the least contaminated sites.

The $\delta^{15}N$ values of unionid mussels have been used as a basis for normalization of fish $\delta^{15}N$ values because the baseline can vary between sites (Cabana and Rasmussen 1996; Vander Zanden et al. 1997). Mussels have been used as baseline indicators because they represent the same level as zooplankton (primary consumers), which are in the food webs leading to higher-level fish. At sites that contain littoral, pelagic, and profundal zones, other organisms and approaches for establishing $\delta^{15}N$ baselines have been suggested (Vander Zanden and Rasmussen 1999). Another study utilized mussels because they reflect the isotope signature of the seston (the base of the pelagic food web) and snails because they reflect the isotope signature of the detritus (the base of the littoral food web) (Post et al. 2000). In our study, we calculated differences between $\delta^{15}N$ values of fish species and those of unionid mussels, but we did not divide these differences by 3.4 to calculate quantified trophic positions. We chose to compare the normalized $\delta^{15}N$ values rather than use quantified trophic positions because "quantified trophic position" infers the number of trophic steps in food chains, yet the number of actual transfers and the exact magnitude of $\delta^{15}N$ change for each transfer are unknown at our sites. The low coefficients of variation of normalized $\delta^{15}N$ values suggest a general constancy of positioning of fish species with regard to stable nitrogen isotopes among these sites. However, Dixon's test identified six normalized $\delta^{15}N$ values for fish species as extreme. The normalized $\delta^{15}N$ values for largemouth bass, pumpkinseed, and bluegill from Mashapaug Pond were extreme. These results indicate that the one mussel sample for Mashapaug Pond, a highly enriched site, was abnormal. Normalized $\delta^{15}N$ values for pumpkinseed and brown bullhead in Tiogue Lake and brown bullhead in Mishnock Lake were also identified as extreme. The finding of two extreme values in Tiogue Lake is interesting. The site receives wastewater inputs and has high levels of anthropogenic impact. The extreme values may be the consequence of unknown baseline effects (e.g., differences in benthic- and pelagic-based food chains among sites), naturally occurring variations in $\delta^{15}N$ values in populations, or the effects of environmental perturbation. At present, it is not possible to differentiate between these possibilities to determine the specific cause of these extreme values. The coefficients of variation of normalized $\delta^{15}N$ values for predatory fish species were smaller than those for lower-level fish species, indicating a more consistent food chain for the predators. Possibly more contact with sediment and its variety of food sources is responsible for the less consistent position of the lower-level fish.

The $\delta^{15}N$ values of sediment were examined for use as a basis for predicting the $\delta^{15}N$ values of fish. Sediment has no trophic position, but it can be a long-term integrator of particles and dead organisms from the water column, and it is readily sampled. The proportions of variance in data explained by linear regressions (r^2) between $\delta^{15}N$ of sediment and $\delta^{15}N$ of fish were generally lower than those between mussels and fish. These results show that predictions of $\delta^{15}N$ values of fish made with sediment $\delta^{15}N$ values will be more variable than those made with $\delta^{15}N$ of mussels. Most of the fish to sediment $\delta^{15}N$ relationships were significant, however, which demonstrates that sediments retain the nitrogen isotope signature of the site.

Comparisons of relationships showed that the $\delta^{15}N$ in mussels accounted for 71 and 72% of the variance in the largemouth bass ($n = 12$) and yellow perch ($n = 12$), respectively. These percentages are considerably higher than the 52 and 34% found for largemouth bass versus mussels ($n = 7$) and yellow perch versus mussels ($n = 29$) in another study (Cabana and Rasmussen 1996). Ranges of $\delta^{15}N$ in the present study were 7.9–19.1‰ in largemouth bass, 7.6–16.6‰ in yellow perch, and 4.9–13.3‰ in mussels compared with 10.4–16.6‰ in largemouth bass, 7.5–12‰ in yellow perch, and 1.3–7.6‰ in mussels in the referenced work (Cabana and Rasmussen 1996). A study in a large lake found that the $\delta^{15}N$ values for some of the same species changed with location and habitat (Fry et al. 1999). Possibly, water stratification and habitat differentiation, which may have been factors contributing to higher variability in $\delta^{15}N$ values in the larger sites, were not important factors in the small, generally well-mixed sites sampled here.

No direct measures of wastewater input were available for sites in the present study; therefore, we used measured DIN concentrations (to indicate anthropogenic impact) and compared these values with the $\delta^{15}N$ values for fish species, mussels, and sediments. The relationships between $\delta^{15}N$ values of samples and DIN concentrations for sites were best described by logarithmic relationships. The initial rapid change in $\delta^{15}N$ values with DIN concentration indicates that $\delta^{15}N$ is a sensitive indicator of enrichment. A variety of fractionation processes may impact stable nitrogen isotopes at sites, but the upward deflection of $\delta^{15}N$ values is consistent with a human wastewater or barnyard waste source of these nutrients, since these materials generally have a higher $\delta^{15}N$ value than those in other inputs (e.g., synthetic fertilizers) (Heaton 1986; Aravena et al. 1993; McClelland and Valiela 1998). A barnyard was present in the shore zone of only one site; however, human development was present at varying degrees at almost all sites. These results suggest that the elevation in nutrient concentrations and $\delta^{15}N$ values resulted from inputs of human wastewater. These results are consistent with those of another study that linked elevated $\delta^{15}N$ values in primary consumers (organisms consuming phytoplankton) in aquatic systems to increases in human population and to presumptive increases in wastewater inputs in the surrounding watersheds (Cabana and Rasmussen 1996) and with results from studies that demonstrated that the $\delta^{15}N$ values of organisms have applicability as generalized measures of incipient eutrophication in estuarine environments (McClelland et al. 1997; McClelland and Valiela 1998).

Land use in the watersheds and small buffer zones surrounding the 14 ponds that we sampled was compared with $\delta^{15}N$ of samples as another method of assessing anthropogenic change. Fractions of residential, agricultural, and forest land in watersheds and buffer zones of ponds were compared with the $\delta^{15}N$ values in samples from the sites. Fraction of residential land was the only land type that gave useful relationships with $\delta^{15}N$ values of samples. These relationships were improved when only data from the buffer zone were considered; therefore, fraction of residential land was a useful surrogate for the amount of wastewater input. For these sites, watershed-scale data of land use were less useful than data of land use of the buffer zone for predicting increases in $\delta^{15}N$ values of the site.

The wide range in $\delta^{15}N$ values of lake trout (*Salvelinus namaycush*) from boreal lakes was found to be related to the length of the pelagic food chain (Cabana and Rasmussen 1994), and in another study, fish species richness was found to explain 69% of the variability in food chain length (VanderZanden et al. 1999). The food chains in our study were shorter and more littoral in character than those in the boreal lakes; however, we found considerable variation in fish species richness and abundance among sites. Despite these variations, no significant relationship between fish species richness and food chain length was found among sites. Studies of food chains of littoral zones of boreal lakes found that food chain length from mussels to largemouth bass averaged 7.1‰ (SD = ±0.6‰, $n = 7$) (Cabana and Rasmussen 1996; Vander Zanden et al. 1997). These values are close to those from the present study, which averaged 6.8‰ (SD = ±0.8, $n = 11$), and no difference in mean values was found (t test: $t = 0.95$, df = 15, $p = 0.36$). Overall food chain length from representative primary consumers (unionid mussels, at same level as primary zooplankton) through secondary zooplankton consumers to crustaceans or small fish and upward to largemouth bass shows a relatively high degree of similarity across all of these sites. This similarity is notable given the variety of sites, the differences in fish species richness, and the probable differences in zooplankton and crustacean species compositions at these sites.

We compared food chain length with DIN concentrations and with fraction of developed land in buffer zones (as indicators of anthropogenic impact) among sites because one expected trend in stressed ecosystems is the shortening of food chains (Woodwell 1983; Odum 1985; Weinstein and Birk 1989). The results showed no significant relationships between food chain length and DIN concentrations ($p > 0.05$) or fraction of developed land in buffer zones ($p > 0.05$). These findings may indicate that the variable representing anthropogenic impact is inadequate, that the level of impact is insufficient to cause a change in food chain length, or that in shallow littoral systems, breakage of pathways for protein flow (e.g., by loss of species) can be compensated for by other pathways.

In summary, the results of this study support the use of stable nitrogen isotopes as indicators of anthropogenic impact on freshwater systems. Elevations in $\delta^{15}N$ values were found in organisms and sediment from sites that had greater residential development of land (and presumed increased human wastewater inputs) in the buffer zones surrounding sites. These elevations also were consistent with increased DIN concentrations, which probably resulted from wastewater inputs. Relationships between $\delta^{15}N$ and DIN concentration indicated that $\delta^{15}N$ was a useful descriptor of eutrophication at sites with low DIN concentrations. Normalized $\delta^{15}N$ values for fish species were found to be useful for comparing trophic positions across sites and for identifying sites with extreme values. Although stress can affect food chain length, the relationships between two indicators of anthropogenic impact, DIN concentrations and fraction of developed land, and food chain length (from $\delta^{15}N$ data) were not significant. These findings may indicate that the magnitude of stress was insufficient to effect change or that overall food chain length in these communities is inherently insensitive and that species loss (e.g., from stress) may be compensated for by other pathways for protein flow to top-level predators.

Acknowledgements

The authors thank Dr. James Heltshe of the Department of Computer Science and Statistics, University of Rhode Island, Roxanne Johnson of the National Health and Environmental Effects Research Laboratory, Atlantic Ecology Division, and personnel of the Rhode Island Department of Environmental Management. This is National Health and Environmental Effects Research Laboratory, Atlantic Ecology Division, Contribution 2118. Mention of product names does not constitute endorsement for use by the U.S. Environmental Protection Agency.

References

Aravena, R., Evans, M.L., and Cherry, J.A. 1993. Stable isotopes of oxygen and nitrogen in source identification of nitrate from septic systems. Ground Water, **31**: 180–186.

Cabana, G., and Rasmussen, J.B. 1994. Modelling food chain structure and contaminant bioaccumulation using stable nitrogen isotopes. Nature (Lond.), **372**: 255–257.

Cabana, G., and Rasmussen, J.B. 1996. Comparing aquatic food chains using nitrogen isotopes. Proc. Natl. Acad. Sci. U.S.A. **93**: 10 844 – 10 849.

Ford, J. 1989. The effects of chemical stress on aquatic species composition and community structure. *In* Ecotoxicology: problems and approaches. *Edited by* S.A. Levin, M.A. Harwell, J.R. Kelly, and K.D. Kimball. Springer-Verlag, New York. pp. 99–144.

Fry, B., Mumford, P.L., Tam, F., Fox, D.D., Warren, G.L., Havens, K.E., and Steinman, A.D. 1999. Trophic position and individual feeding histories of fish from Lake Okeechobee, Florida. Can. J. Fish. Aquat. Sci. **56**: 590–600.

Guthrie, R.C., and Stolgitis, J.A. 1994. Fisheries investigations and management in Rhode Island lakes and ponds. Fish. Rep. No. 3. Rhode Island Division of Fish and Wildlife, Providence, R.I.

Hach Company. 1997. Hach water analysis handbook. 3rd ed. Hach Company, Loveland, Co.

Heaton, T.H.E. 1986. Isotopic studies of nitrogen pollution in the hydrosphere and atmosphere: a review. Chem. Geol. (Isot. Geosci. Sect.), **59**: 87–102.

Mariotti, A. 1983. Atmospheric nitrogen is a reliable standard for natural ^{15}N abundance measurements. Nature (Lond.), **303**: 685–687.

Mariotti, A., Germon, J.C., Hubert, P., Kaiser, P., Letolle, R., Tardieux, A., and Tardieux, P. 1981. Experimental determination of nitrogen kinetic isotope fractionation: some principles, illustration for the denitrification and nitrification processes. Plant Soil, **62**: 413–430.

McClelland, J.W., and Valiela, I. 1998. Linking nitrogen in estuarine producers to land-derived sources. Limnol. Oceanogr. **43**: 577–585.

McClelland, J.W., Valiela, I., and Michener, R.H. 1997. Nitrogen-stable isotope signatures in estuarine food webs: a record of increasing urbanization in coastal watersheds. Limnol. Oceanogr. **42**: 930–937.

McKinney, R.A., Lake, J.L., Allen, M., and Ryba, S. 1999. Spatial variability in mussels used to assess base level nitrogen isotope ratio in freshwater ecosystems. Hydrobiologia, **412**: 117–124.

Minigawa, M., and Wada, E. 1984. Stepwise enrichment of ^{15}N along food chains: further evidence and the relation between $\delta^{15}N$ and animal age. Geochim. Cosmochim. Acta, **48**: 1135–1140.

Odum, E.P. 1985. Trends expected in stressed ecosystems. BioScience, **35**: 419–422.

Pennock, J.R., Velinski, D.J., Ludham, D.J., Sharp, J.H., and Fogel, M.J. 1996. Isotope fractionation of ammonium and nitrate during the uptake by *Skeletonema costatum*: implications for the $\delta^{15}N$ dynamics under bloom conditions. Limnol. Oceanogr. **41**: 451–459.

Post, D.M., Pace, M.L., and Hairston, N.G., Jr. 2000. Ecosystem size determines food-chain length in lakes. Nature (Lond.), **405**: 1047–1049.

Schoeninger, M.J., and DeNiro, M.J. 1984. Nitrogen and carbon isotopic composition of bone collagen from marine and terrestrial animals. Geochim. Cosmochim. Acta, **48**: 625–639.

Snedecor, G.W., and Cochran, W.G. 1980. Statistical methods. Iowa State University Press, Ames, Iowa.

Tessier, A., Campbell, P.G.C., and Bisson, M. 1984. Relationships between the partitioning of trace metals in sediments and their accumulation in the tissues of the freshwater mollusc *Elliptio complanata* in a mining area. Can. J. Fish. Aquat. Sci. **41**: 1463–1472.

Vander Zanden, M.J., and Rasmussen, J.B. 1996. A trophic position model of pelagic food webs: impact on contaminant bioaccumulation in lake trout. Ecol. Monogr. **66**: 451–477.

Vander Zanden, M.J., and Rasmussen, J.B. 1999. Primary consumer δ^{13} C and $\delta^{15}N$ and the trophic position of aquatic consumers. Ecology, **80**: 1395–1404.

Vander Zanden, M.J., Cabana, G., and Rasmussen, J.B. 1997. Comparing trophic position of freshwater fish calculated using stable nitrogen isotope ratios ($\delta^{15}N$) and literature dietary data. Can. J. Fish. Aquat. Sci. **54**: 1142–1158.

Vander Zanden, M.J., Shuter, B.J., Lester, N., and Rasmussen, J.B. 1999. Patterns of food chain length in lakes: a stable isotope study. Am. Nat. **154**: 406–416.

Verdouw, H., van Echteld, C.J.A., and Dekkers, E.M.J. 1978. Ammonia determination based on indophenol formation with sodium salicylate. Water Res. **12**: 399–402.

Waser, N.A.D., Harrison, P.J., Nielsen, B., Calvert, S.E., and Turpin, D.H. 1998. Nitrogen isotope fractionation during the uptake and assimilation of nitrate, nitrite, ammonium and urea by a marine diatom. Limnol. Oceanogr. **43**: 215–224.

Weinstein, D.A., and Birk, E.M. 1989. The effects of chemicals on the structure of terrestrial ecosystems: mechanisms and patterns of change. *In* Ecotoxicology: problems and approaches. *Edited by* S.A. Levin, M.A. Harwell, J.R. Kelly, and K.D. Kimball. Springer-Verlag, New York. pp. 181–209.

Woodwell, G.M. 1983. The blue planet: of whole and parts of man. *In* Disturbance and ecosystems. *Edited by* H.A. Mooney and M. Gordon. Springer-Verlag, New York. pp. 1–10.

Appendix. Mean $\delta^{15}N$ values (‰) for fish species, mussels, and sediment at each site, means across sites, standard deviations, maximum and minimum values, and number of sites.

	Site No.[a]																					
Sample	1	2	3	4	5	6	7	8	9	10	11	12	13	14	15	16	17	Mean	SD	Maximum	Minimum	*n*
Largemouth bass (*Micropterus salmoides*)		7.9	10.4	11.1	11.4	12.0	13.9	14.6	14.7	15.1	15.4	15.5	15.8	15.9	15.9	18.8	19.1	14.2	3.0	19.1	7.9	16
Chain pickerel (*Esox niger*)	11.7	8.2	9.6	10.2		10.9	12.1	15.0		13.8	14.3	13.9	14.9		14.7		17.5	12.8	2.6	17.5	8.2	13
Black crappie (*Pomoxis nigromaculatus*)												14.4			14.8	17.3	18.8	16.3	2.1	18.8	14.4	4
Yellow perch (*Perca flavescens*)	11.4	7.9	8.8	9.3		10.2	11.7	11.8	13.7	14.2	13.0	13.5	13.7		13.3	13.7	16.6	12.2	2.3	16.6	7.9	15
Pumpkinseed (*Lepomis gibbosus*)		7.7	9.0	9.5	9.0	9.7	11.2	13.4	12.3	13.5	13.0	13.4			13.4	13.1	17.3	11.8	2.6	17.3	7.7	14
Bluegill (*Lepomis macrochirus*)				8.7	8.6	9.3	11.5	12.5	12.1	12.9	13.1	12.7	13.1	14.5	13.1		16.3	12.2	2.2	16.3	8.6	13
White perch (*Morone americana*)				10.3	9.1		10.6							11.3	13.6	14.0	18.3	12.5	3.1	18.3	9.1	7
White sucker (*Catostomus commersoni*)	11.0								11.5					11.7	11.9	13.5	16.5	12.7	2.1	16.5	11.0	6
Brown bullhead (*Ameiurus nebulosus*)	10.5	6.9	7.8	8.6		9.7	11.0	10.3	11.7	13.1	12.9			12.1	13.0	12.3		10.8	2.1	13.1	6.9	13
Yellow bullhead (*Ameiurus natalis*)					9.1												18.2	13.6	6.4	18.2	9.1	2
Common carp (*Cyprinus carpio*)					8.4									10.5		13.8		10.9	2.7	13.8	8.4	3
American eel (*Anguilla rostrata*)	11.3			10.0			10.3				13.5	12.6			13.5			11.9	1.6	13.5	10.0	6
Golden shiner (*Notemigonus crysoleucas*)	9.0	7.0	7.9	9.2		8.7	10.4	10.4	11.3		11.4				11.6		18.4	10.5	3.0	18.4	7.0	11
Common shiner (*Luxilus cornutus*)																	16.0	16.0		16.0	16.0	1
Alewife (*Alosa pseudoharengus*)															12.9			12.9		12.9	12.9	1
Creek chubsucker (*Erimyzon oblongus*)			7.5	8.1		8.4												8.0	0.5	8.4	7.5	3
Banded killfish (*Fundulus diaphanus*)												11.8						11.8		11.8	11.8	1
Unionid mussels (*Elliptio complanata*)	7.1			5.3	8.8	4.9	6.1	9.1		7.8	8.8	8.5	8.3		8.8	12.0	13.3	8.4	2.4	13.3	4.9	13
Bulk sediment	4.9	1.1	-0.1	2.9	2.4	2.8	2.7	4.0	2.7	3.8	6.8	3.8	6.3	3.8	5.2	4.8	6.8	3.8	1.9	6.8	-0.1	17

Changes in polyphosphate sedimentation: a response to excessive phosphorus enrichment in a hypereutrophic lake

William F. Kenney, Claire L. Schelske, and Andrew D. Chapman

Abstract: Historic changes in lake phosphorus (P) loading are often determined in paleolimnological investigations by assessing stratigraphic changes in sediment total P. Polyphosphate (poly-P) in sediments may provide additional information on historic lake trophic status, because phytoplankton store surplus P intracellularly as poly-P when supplies exceed growth requirements. We hypothesize that phytoplankton (i.e., cyanobacteria and diatoms) with stored poly-P can remain intact and viable for many decades after sedimentation and that sedimented poly-P is not geochemically reactive. We tested our hypotheses with sediment cores from Lake Apopka, Fla., U.S.A., where P loading has increased ~7-fold since the 1920s and phytoplankton biomass is nitrogen limited owing to excessive P enrichment. We show that sedimented poly-P is mobilized by sample drying (i.e., becomes water soluble, geochemically reactive, and bioavailable); that anthropogenic P enrichment is expressed in the sediment record as increasing concentrations of poly-P; and that, consequently, sedimentary poly-P is a sensitive indicator of historic excessive P enrichment. Sedimentary poly-P is not geochemically reactive; thus, it represents biological attenuation that may partially ameliorate the effects of excessive P loading.

Résumé : Les changements stratigraphiques de la quantité totale de phosphore (P) dans les sédiments sert souvent à déterminer les changements historiques de la charge de P dans les lacs lors d'études paléolimnologiques. Les concentrations de polyphosphates (poly-P) dans les sédiments apportent des informations supplémentaires sur le statut trophique du lac au cours des années parce que le phytoplancton accumule dans son milieu intracellulaire l'excédent de P sous forme de poly-P lorsque les quantités disponibles dépassent les besoins requis pour la croissance. Nous posons en hypothèse que le phytoplancton (i.e., les cyanobactéries et les diatomées) contenant des réserves de poly-P peuvent rester intactes et viables pendant plusieurs dizaines d'années après leur sédimentation et que le poly-P sédimenté n'est pas impliqué dans les réactions géochimiques. Nous avons testé notre hypothèse à l'aide de carottes de sédiments provenant du lac Apopka, Fla., U.S.A., où la charge de P a augmenté d'environ 7 fois depuis les années 1920 et où la biomasse du phytoplancton est limitée par pénurie d'azote en présence d'un enrichissement excessif en P. La mobilisation du poly-P sédimentée se fait lors du séchage des échantillons (i.e., il devient hydrosoluble, il réagit aux facteurs géochimiques et il est biodisponible); l'enrichissement en P d'origine humaine se traduit dans les sédiments par des augmentations de poly-P; en conséquence, les concentrations de poly-P dans les sédiments sont un indicateur sensible de l'enrichissement historique excessif en P. Puisque le poly-P des sédiments n'est pas impliqué dans les réactions géochimiques, il s'agit là d'une atténuation biologique qui peut compenser en partie les effets d'une charge excessive de P.

[Traduit par la Rédaction]

Introduction

Understanding the relationship between anthropogenic disturbance and water-quality problems requires research on phosphorus (P), because this nutrient is the factor most likely to limit algal growth in fresh waters (Schindler 1977). Applied studies have addressed the empirical relationships between total P (TP) and chlorophyll, without examining the components of TP (see Chapra and Auer 1999). These relationships are based on the implicit assumption that changes in chlorophyll concentration are directly proportional to changes in TP concentration, but such inferences are confounded by variable proportions of soluble reactive P (SRP), surplus P stored by algae, and refractory P (Schelske et al. 1999*a*). Although forms of P can be measured, little attention has been given to determining what TP fractions are biologically available (see Hecky and Kilham 1988; Chapra and Auer 1999). Partitioning forms of P has been advanced as a means of refining models that assess the algal-growth potential of waters (Schelske et al. 1999*a*).

In the water column, 2 common forms of biologically available P are SRP, which by definition has not been assimilated by algae, and polyphosphate (poly-P), which represents surplus storage that has been assimilated but not utilized for algal growth (Schelske et al. 1999*a*). Biological availability of sedimentary P can be determined with chemical measurements or algal bioassays. Algal bioassay (bioassay-P) is generally con-

Received March 15, 2000. Accepted February 7, 2001. Published on the NRC Research Press Web site on April 12, 2001.
J15664

W.F. Kenney[1,2] **and C.L. Schelske.** Department of Fisheries and Aquatic Sciences, University of Florida, 7922 NW 71st Street, Gainesville, FL 32653, U.S.A.
A.D. Chapman. St. Johns River Water Management District, P.O. Box 1429, Palatka, FL 32178-1429, U.S.A.

[1] Corresponding author (e-mail: kenney@gnv.ifas.ufl.edu).
[2] Present address: Department of Geological Sciences, University of Florida, P.O. Box 112120, Gainesville, FL 32611, U.S.A.

DOI: 10.1139/cjfas-58-5-879

sidered to be the ultimate test for the bioavailability of P in water and sediments (Golterman 1988; Williams et al. 1980). Sodium hydroxide extractable P (NaOH-P; Williams et al. 1980) and nitrilo triacetic acid extractable P (NTA-P; Golterman 1977) have been shown to be bioavailable by comparison with algal bioassays. NaOH-P is a large fraction of the TP (~40%) in dried Lake Apopka sediments (Schelske 1997) but NaOH-P overestimated bioassay-P by severalfold for recent sediments in this lake (Kenney 1997). It was shown previously that sample handling affects partitioning among P forms in chemical analysis (Twinch 1986). We show here that bioassay-P and water-soluble P (H_2O-P) were greater in dried sediments than in wet sediments from Lake Apopka.

We studied Lake Apopka, a large shallow hypereutrophic lake in central Florida, U.S.A., because P loading increased as much as 7-fold in the past 100 years (Battoe et al. 1999). In Lake Apopka, phytoplankton store poly-P (Newman et al. 1994; Schelske et al. 1999*a*) and are nitrogen (N) limited as a result of excessive P enrichment (Aldridge et al. 1993). Kenney (1997) found an upcore increase in sedimentary poly-P. We contend that this pattern results from surplus P stored as poly-P in phytoplankton, because resting cells of diatoms are sedimented and remain viable for decades or longer (Sicko-Goad et al. 1989) and because, in Lake Apopka, many algal species remain viable decades after sedimentation (A. Chapman, unpublished data).

Herein we show that sedimented poly-P is mobilized and becomes water-soluble and bioavailable by sample drying; that anthropogenic P-enrichment is expressed in the sediment record as increasing concentrations of poly-P; and that, consequently, sedimentary poly-P is a sensitive indicator of historic excessive P enrichment.

Materials and methods

Study site

Lake Apopka is a shallow (mean depth = 1.7 m) polymictic hypereutrophic lake (mean ± SD = 0.203 ± 0.062 mg $P{\cdot}L^{-1}$) that has been significantly impacted by anthropogenic nutrient loads (Battoe et al. 1999; Schelske et al. 2000). This subtropical lake is located ~20 km northwest of Orlando, Fla., U.S.A. Historically, the lake was macrophyte dominated with clear water (Schelske and Brezonik 1992). In the 1920s, effluent from citrus processing and municipal sewerage increased P loading to the lake (Schelske and Brezonik 1992). In the early 1940s, the lake area was reduced from 210 to 125 km^2 as "muck" farms were created on diked and drained littoral and marsh areas (Battoe et al. 1999). In the late 1940s, large standing crops of phytoplankton replaced macrophyte beds in the lake, creating a planktonic system with turbid water (Battoe et al. 1999).

Increased P loading is a major forcing factor in the development of phytoplankton dominance in Lake Apopka. In several papers, the shift to phytoplankton dominance was attributed to the effects of a hurricane, but this has not been supported by recent studies (see Battoe et al. 1999; Schelske et al. 2000). Periodic pumping of the drainage water from the P-rich and heavily fertilized farm lands was responsible for 0.42 g $P{\cdot}m^{-2}{\cdot}year^{-1}$ or 85% of the average P loading from 1989 to 1994 (Battoe et al. 1999). Since the late 1940s, basin-wide sedimentary TP accumulation has increased as much as 4-fold (Schelske 1997) and phytoplankton biomass has become N limited (Aldridge et al. 1993). A considerable amount of water column TP is poly-P stored in phytoplankton (~18%; mean = 0.036 ± 0.005 mg $P{\cdot}L^{-1}$); however, a much smaller amount of TP is SRP (~3%; mean = 0.007 ± 0.009 mg $P{\cdot}L^{-1}$; Schelske et al. 1999*a*).

Highly organic sediments deposited in Lake Apopka during the 20th century reflect 2 source materials (Olila et al. 1995). Deeper sediments (referred to as macrophyte sediments) represent the period of macrophyte dominance, and overlying sediments (referred to as phytoplankton sediments) represent the period of phytoplankton dominance (Schelske et al. 1999*b*). Macrophyte sediments are highly organic (mean loss on ignition (LOI) = 55%), with intermixed snail shells and low TP concentrations (<0.75 $mg{\cdot}g^{-1}$). Phytoplankton sediments have a mean LOI of 64% and a range in TP concentrations (~1.0 to ~2.0 $mg{\cdot}g^{-1}$) typical of many Florida lake sediments (Brenner and Binford 1988). The accumulation of phytoplankton sediments averages 47 ± 32 cm (*n* = 46) or 1.77 ± 1.56 $g{\cdot}cm^{-2}$ (*n* = 46; Schelske 1997). Phytoplankton sediments did not accumulate uniformly in the lake basin. Half the TP accumulated on only 20% of the lake bottom and ~70% of the TP accumulated on ~40% of the lake bottom (Schelske 1997).

Because of high organic matter content and a disproportionate accumulation of refractory materials in sediments, many Florida lakes, including Lake Apopka, form a subset of lakes with respect to sediment dynamics. In Lake Apopka, high rates of primary production (Schelske et al. 2000) and polymixis influence the sediment composition. Primary production by phytoplankton is sufficient to account for the organic matter sedimentation rate (Schelske et al. 2000), and total carbon to total nitrogen ratios identify its source as phytoplankton (Schelske et al. 1999*b*). The large size (125 km^2), shallow mean depth (1.7 m), and large fetch in all directions promote frequent resuspension of surface sediments (Carrick et al. 1993; Reddy et al. 1996). Frequent wind resuspension increases the time that organic particles are exposed to aerobic conditions; therefore, the material that accumulates as permanent sediment is largely refractory (<10% of the organic carbon is labile under anoxic conditions; Gale et al. 1992). Compared with Lake Okeechobee, Lake Apopka sediments have lower concentrations of extractable cations (Olila et al. 1995). In these highly organic sediments from Lake Apopka, P is not bound to Fe, Al, or Mn, and P release is not redox dependent (Olila and Reddy 1997).

Field and laboratory methods

Six sediment cores were collected with a piston corer (Fisher et al. 1992), and the depth to the sediment–water interface was determined with an infrared nephelometer (Meyers and Schelske 2000). Five core stations (LA-2H, LA-9, LA-12, LA-27, LA-43) were distributed at depositional sites over the lake basin (Fig. 1). Results from the chemical analyses and bioassays of wet sediments from these 5 locations led us to investigate the effects of freeze-drying on P fractionation and bioavailability in 20 contiguous samples from one of these locations, LA-9 (core LA-9-97). Among depositional areas, location LA-9 has an average accumulation of sediments (Schelske 1997). Cores were vertically extruded and sectioned in the field, aboard a motor-powered skiff, and samples were stored in Whirl-Pak® bags at ~5°C in ice chests for transport to the laboratory.

In the laboratory, samples were refrigerated at ~5°C. Chemical analyses of wet sediments were completed within 4 days of collection. Bioassays of wet sediments were initiated 5 days after collection. Representative subsamples were freeze-dried and ground to a maximum particle size of 100 μm for chemical analyses and bioassays.

Bioassays to determine bioavailable P were conducted according to Williams et al. (1980), with modifications from Golterman (1988). Sediment (<0.2 g dry mass equivalent$\cdot L^{-1}$) and associated P (<50 μg $P{\cdot}L^{-1}$) added were at least an order of magnitude smaller than in other studies (Golterman et al. 1969; Chiou and Boyd 1974). The initial density of algal cells (5000 cells/mL) was an order of magnitude greater than in other studies (Golterman et al.

Fig. 1. Map of Lake Apopka, Fla., U.S.A. Coring locations are plotted by station designation.

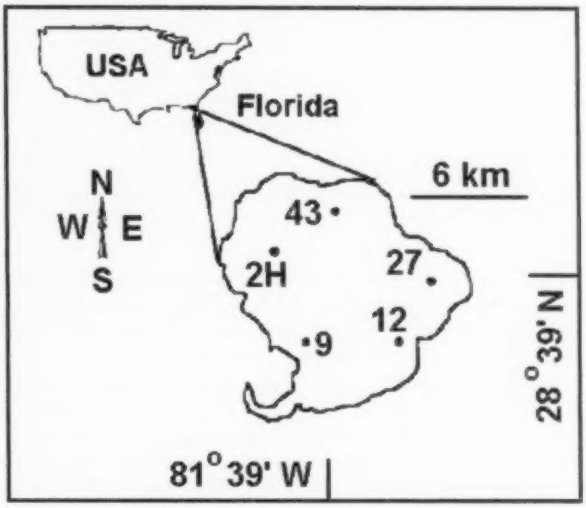

1969; Golterman 1977). These modifications minimized bias from viable algal populations in the sediment addition, including those with stored poly-P. Bioassay-P was determined in 500-mL glass flasks, using cultures of *Scenedesmus quadricauda*, obtained from E.J. Phlips, University of Florida (Gainesville, FL 32653, U.S.A). Before determinations of bioassay-P, test cultures were maintained in freshwater medium (Phlips et al. 1989), containing replete available N (>30 mg N·L^{-1}, as nitrate) and low available P (<0.005 mg P·L^{-1}, as orthophosphate), in 2 identical Percival® incubators. We conducted simultaneous duplicate bioassays in the incubators with samples replicated within each incubator. Growth responses were log-transformed in vivo fluorescence (Turner Brands® fluorometer) data collected every 48 h on diluted (1:20) test cultures. To calculate bioassay-P, growth responses of cultures with sediment as the P source were calibrated to a linear function derived from the growth responses of cultures with small additions of orthophosphate as the P source (a range of known concentrations ≤0.040 mg P·L^{-1}). Bioassays were conducted on only 6 samples. Bioassay-P concentrations for the remaining 14 samples were predicted from a linear model comparing H_2O-P with bioassay-P ($R^2 = 0.97$, $n = 6$).

We measured TP (Schelske et al. 1986) and 4 sedimentary P fractions (Table 1). The NaOH-P assay (0.1 M NaOH; Williams et al. 1980) measured sorbed Fe-, Al-, and Mn-bound P. Some organic-P/biogenic-P and possibly poly-P (Olila and Reddy 1997) are also measured by the NaOH assay. In addition, the NaOH assay partially dissolves the siliceous valves of diatoms (20–30% of diatom biogenic silica (BSi) in Lake Apopka sediments; W. Kenney, unpublished data) and releases intracellular P. Some of the organic-P/biogenic-P may be hydrolyzed to reactive P by the NaOH or the colorimetric reagents (pH <2) in the SRP analysis. The NTA-P assay (0.01 M NTA, pH = 7; Golterman 1977) measures P loosely bound to cations (e.g., Fe, Al, Mn, Ca, Mg). Although NTA-P and NaOH-P may be extracted from the same cations (e.g., Fe, Al, Mn), NaOH-P is also extracted from organic–biogenic forms that are not affected by the neutralized NTA assay. Sediment samples were equilibrated in H_2O (18 MΩ) to determine H_2O-P and were then wet-autoclaved to determine heat-extractable P. Heat extraction measures poly-P (Fitzgerald and Nelson 1966) and other intracellular reserves of P (Pettersson 1980) in phytoplankton. Because assays were not conducted sequentially, results presented for NaOH-P, NTA-P, and poly-P were corrected by subtracting the corresponding H_2O-P concentration for each sample.

The dry-mass equivalent of sediment, volume of suspension, duration of extraction, and equipment required for each chemical assay are listed in Table 1. To disperse aggregates, increase surface area, and reduce replicate error, sediment suspensions were sonicated in a Fisher Scientific® FS 110 ultrasonic cleaner. Suspensions were then equilibrated or autoclaved, diluted, neutralized, and analyzed colorimetrically for SRP with ascorbic acid and ammonium molybdate on a Bran+Luebbe® autoanalyzer (APHA 1989). Dried ground sediment samples were analyzed for diatom and sponge BSi as in Conley and Schelske (1993). We used diatom BSi as a proxy for phytoplankton contribution to sediment matter. Because macrophytes are the primary substrate for freshwater sponges in Lake Apopka, sponge BSi was used as a proxy for macrophyte contribution to sediment matter.

Sediment characterization and chronology

The interface between phytoplankton and macrophyte sediments was determined with BSi and bulk-density data. In core LA-9-97, phytoplankton sediments (n = 12) had lower bulk density (mean = 29.7 ± 9.5 mg·cm^{-3}) and lower concentrations of sponge BSi (mean = 14.3 ± 5.9 mg SiO_2·g^{-1}) than macrophyte sediments (n = 8, mean = 63.0 ± 4.5 mg·cm^{-3} and 24.4 ± 5.8 mg SiO_2·g^{-1}, respectively). The mean concentration of diatom BSi was higher in the phytoplankton sediments (38.3 ± 3.6 mg SiO_2·g^{-1}) than in the macrophyte sediments (6.5 ± 6.9 mg SiO_2·g^{-1}). For core LA-9-97, the interface between phytoplankton and macrophyte sediments was at 60 cm (Fig. 2).

Age at depth and mass sedimentation rates (MSR) for LA-9-97 were estimated on the basis of temporal patterns of sediment accumulation determined for a suite of ^{210}Pb-dated cores collected previously. Phytoplankton sediments in Lake Apopka have accumulated since ~1947, and ^{210}Pb activities were used to develop sediment chronologies (Schelske 1997). The dated sequences showed that over the past ~50 years, MSR increased 3- to 4-fold or an average annual increase of 1.0227–1.0287. We applied these end-member rates of increase to the cumulative dry mass (1.78 g·cm^{-2}) determined for phytoplankton sediments (upper 60 cm) from LA-9-97. This enabled us to compute dates for the base of each 5-cm core section using 2 rates of increase in sediment accumulation. The 2 modeling approaches yield sediment ages that differ by <3 years at the base of each 5-cm section. Ultimately, we averaged the increase in MSR between 3- and 4-fold to apply dates to depths in the core. This approach generated the age–depth pairs 1995 (10 cm), 1991 (20 cm), 1984 (30 cm), 1975 (40 cm), 1964 (50 cm), and 1947 (60 cm), as the specified initial time. Calculated MSR for the 4-fold increase ranged from 19 to 76 mg·cm^{-2}·year^{-1}.

Results

Using linear regression, we tested data from wet-sediment analyses for relationships between H_2O-P, poly-P, NaOH-P, or NTA-P and bioassay-P or TP. Unexpectedly, bioassay-P represented only a small fraction of NaOH-P and TP. Results from the 5 cores indicated that NaOH-P and poly-P were correlated with TP (Fig. 3*a*), while H_2O-P and NTA-P were correlated with bioassay-P (Fig. 3*b*). The relationships between either NaOH-P or poly-P and TP are best described by second- or third-order polynomial models, not linear models. Because similar relationships existed among P measures for LA-9-97 (Figs. 3*c* and 3*d*), we considered this core to be representative of recent Lake Apopka sediments.

That sample preparation affected the fractionation among the measured sedimentary P forms is evident from depth profiles of P fractions for LA-9-97. For phytoplankton sedi-

Table 1. Methods for the analysis of water-soluble phosphorus (H_2O-P), polyphosphate (poly-P), nitrilo triacetic acid extractable P (NTA-P), sodium hydroxide extractable P (NaOH-P), and total P (TP).

Extraction	Dry mass (g)	Volume (L)	Process	Temperature (°C)	Time (h)	Solution
H_2O-P	0.05	0.05	Equilibrate	25	20	18 MΩ water
Poly-P	0.05	0.05	Wet-autoclave	100	0.5	18 MΩ water, sequential to H_2O-P
NTA-P	0.05	0.05	Equilibrate	25	20	0.01 M nitrilo triacetic acid, pH 7
NaOH-P	0.05	0.05	Equilibrate	25	17	0.1 M sodium hydroxide
TP	0.05	0.03	Wet-autoclave	100	0.5	0.53 M sulfuric acid – 0.062 M potassium persulfate

Note: For each method, the dry mass equivalent of sediment and volume of the suspension are presented, together with the process, temperature, and time required for each analysis. All samples were equilibrated at 85 rpm in a shaker bath.

Fig. 2. Diatom biogenic silica (BSi, broken line with open diamonds), sponge-BSi (broken line with open circles), and bulk-density (solid line with open squares) data for core LA-9-97 plotted against depth. The interface between phytoplankton- and macrophyte-sediment types is indicated by the horizontal line at 60 cm.

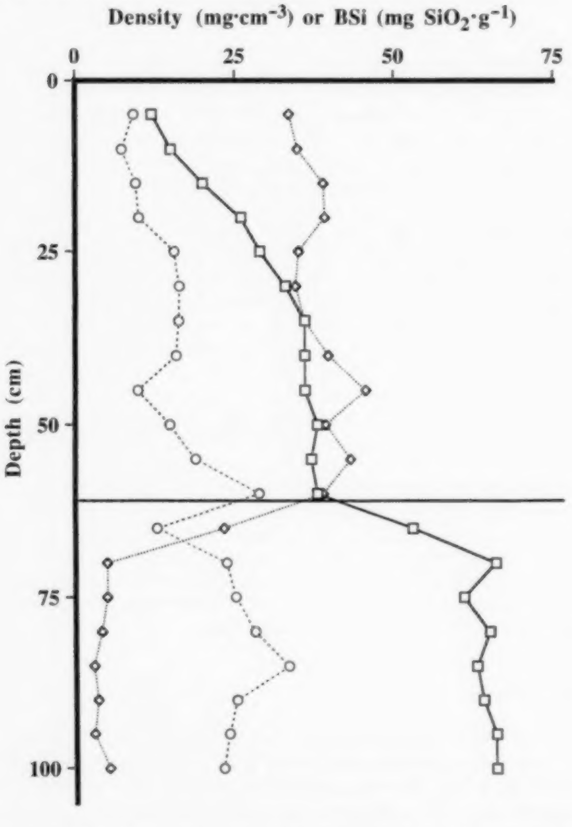

ments, H_2O-P concentrations were greater in dried samples than in wet samples, but dry and wet values were similar for macrophyte sediments (Fig. 4*a*). Poly-P was greatest in phytoplankton sediments and measurable in all wet samples but was not detectable in dried samples below 10 cm (Fig. 4*b*). The profiles of NTA-P differed from those of poly-P (Fig. 4*c*). Similarly to poly-P, concentrations of NaOH-P were greater in wet samples, with the greatest differences between wet and dry NaOH-P in phytoplankton sediments (Fig. 4*d*). Bioassay-P concentrations were larger in dried samples (relative percent difference >20%) than in wet samples in the surface 25 cm of the phytoplankton sediments (Fig. 4*e*). Wet and dry TP values varied on average by 9% (Fig. 4*f*), but the largest differences, 23 and 32%, were in the 10- and 100-cm samples, respectively.

Sediments from LA-9-97 were separated into 3 stratigraphic zones based on differences in poly-P concentration (Fig. 4*b*). Macrophyte-derived sediments below 65 cm were used to represent baseline conditions. Sediments from 40 to 65 cm are termed zone 1, and those above 40 cm are termed zone 2. We compared the changes in biological responses (BSi and poly-P) and forcing factors (TP and other P fractions) relative to baseline conditions (Fig. 5). In zones 1 and 2, diatom BSi concentrations changed more (~9-fold), relative to baseline, than any proxy investigated. In contrast, sponge spicule BSi concentrations decreased in zones 1 and 2 compared with baseline. These results show that a biological response to P enrichment in shallow lakes is an increased contribution of phytoplankton to sediment matter. The relative increase in poly-P concentration was greater than for any other P form measured: 5.6-fold greater than baseline in zone 2 and 2.5-fold greater than baseline in zone 1. The TP concentration was 2.9-fold greater than baseline in zone 2 and 2.2-fold greater than baseline in zone 1. Although the bioassay-P and NTA-P concentrations were ~1.7-fold greater than baseline in zone 1, they were not different from baseline in zone 2. These results show that poly-P was the most sensitive proxy for historic P enrichment.

Discussion

Bioassay-P concentrations determined in our experiments with wet sediments were lower than expected from chemical assays of Lake Apopka sediments. NaOH-P (Williams et al. 1980) extracted from dried sediments averaged 40% of TP in an extensive sediment survey (Schelske 1997) and 43% of TP in the present study. By contrast, bioassay-P averaged only 14% of TP in wet sediments (Kenney 1997). Williams et al. (1980) established NaOH-P as an appropriate chemical assay for estimating bioassay-P in dried sediments from the Laurentian Great Lakes. However, the 0.1 M NaOH employed in this extraction partially destroys the structural integrity of phytoplankton cells, particularly diatoms, and releases intracellular P, including poly-P, that is not externally available under bioassay conditions using wet sediments. As a result, NaOH-P overestimated bioassay-P by severalfold for the highly organic phytoplankton sediments from Lake Apopka. These results are counter-intuitive, because poly-P may support growth in the enriched phytoplankton popula-

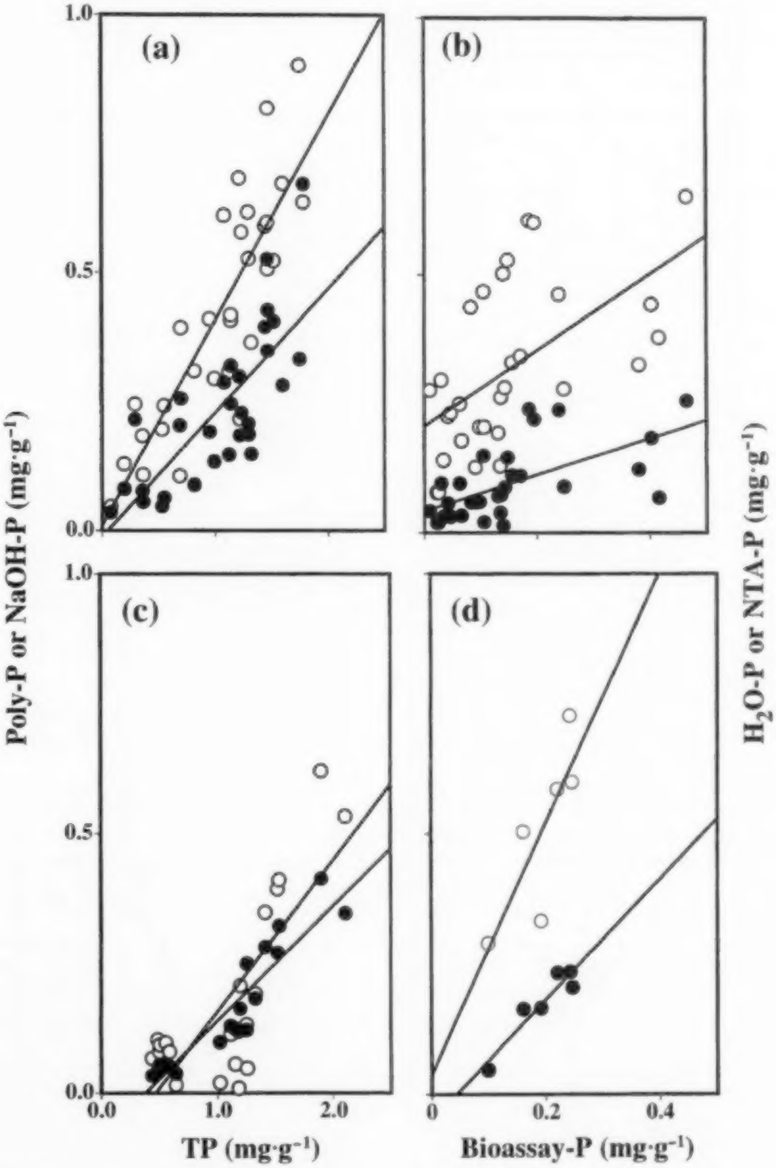

Fig. 3. Comparison of the forms of phosphorus (P; TP, total P; bioassay-P, bioavailable P (tested by algal bioassay); poly-P, polyphosphate; NaOH-P, sodium hydroxide extractable P; H_2O-P, water-soluble P; and NTA-P, nitrilo triacetic acid extractable P) in wet sediments from Lake Apopka. (*a*) Plots of poly-P (filled circles) or NaOH-P (open circles) versus TP for the initial 5-core study. Regression equations are poly-P = 0.24 × TP – 0.01, $R^2 = 0.58$, $n = 30$ and NaOH-P = 0.40 × TP + 0.01, $R^2 = 0.72$, $n = 30$. (*b*) Plots of H_2O-P (filled circles) and NTA-P (open circles) versus bioassay-P for the initial 5-core study. Regression equations are H_2O-P = 0.35 × bioassay-P + 0.04, $R^2 = 0.37$, $n = 30$ and NTA-P = 0.74 × bioassay-P + 0.21, $R^2 = 0.33$, $n = 30$. (*c*) Plots of poly-P (filled circles) or NaOH-P (open circles) versus TP for core LA-9-97. Regression equations are poly-P = 0.22 × TP – 0.08, $R^2 = 0.62$, $n = 20$ and NaOH-P = 0.29 × TP – 0.14, $R^2 = 0.86$, $n = 20$. (*d*) Plots of H_2O-P (filled circles) and NTA-P (open circles) versus bioassay-P for core LA-9-97. Regression equations are H_2O-P = 1.16 × bioassay-P – 0.05, $R^2 = 0.97$, $n = 6$ and NTA-P = 2.42 × bioassay-P – 0.04, $R^2 = 0.67$, $n = 6$.

tion but sedimented poly-P is not externally available to the test population in bioassays conducted on wet sediments.

Bioassay-P concentrations were as much as 3-fold greater in dried than in wet phytoplankton sediments. In wet sediments, concentrations of NaOH-P and poly-P were similar, indicating that these procedures extract P from the same sources. Drying the phytoplankton sediment increased H_2O-P concentrations by an amount comparable with the decrease in poly-P or NaOH-P concentration (as much as 0.6 mg P·g^{-1} dry mass equivalent or ~40% of TP). We con-

Fig. 4. Sediment phosphorus (P) fractions (reported on a dry weight basis) of both wet (filled circles) and dried (solid line) sediments plotted against depth for core LA-9-97. The interface between phytoplankton- and macrophyte-sediment types is indicated by the horizontal line at 60 cm. (*a*) Water soluble P (H_2O-P) concentrations. (*b*) Polyphosphate (poly-P) concentrations. (*c*) Nitrilo triacetic acid extractable P (NTA-P) concentrations. (*d*) Sodium hydroxide extractable P (NaOH-P) concentrations. (*e*) Bioavailable P (bioassay-P (tested by algal bioassay)) concentrations. (*f*) Total P (TP) concentrations.

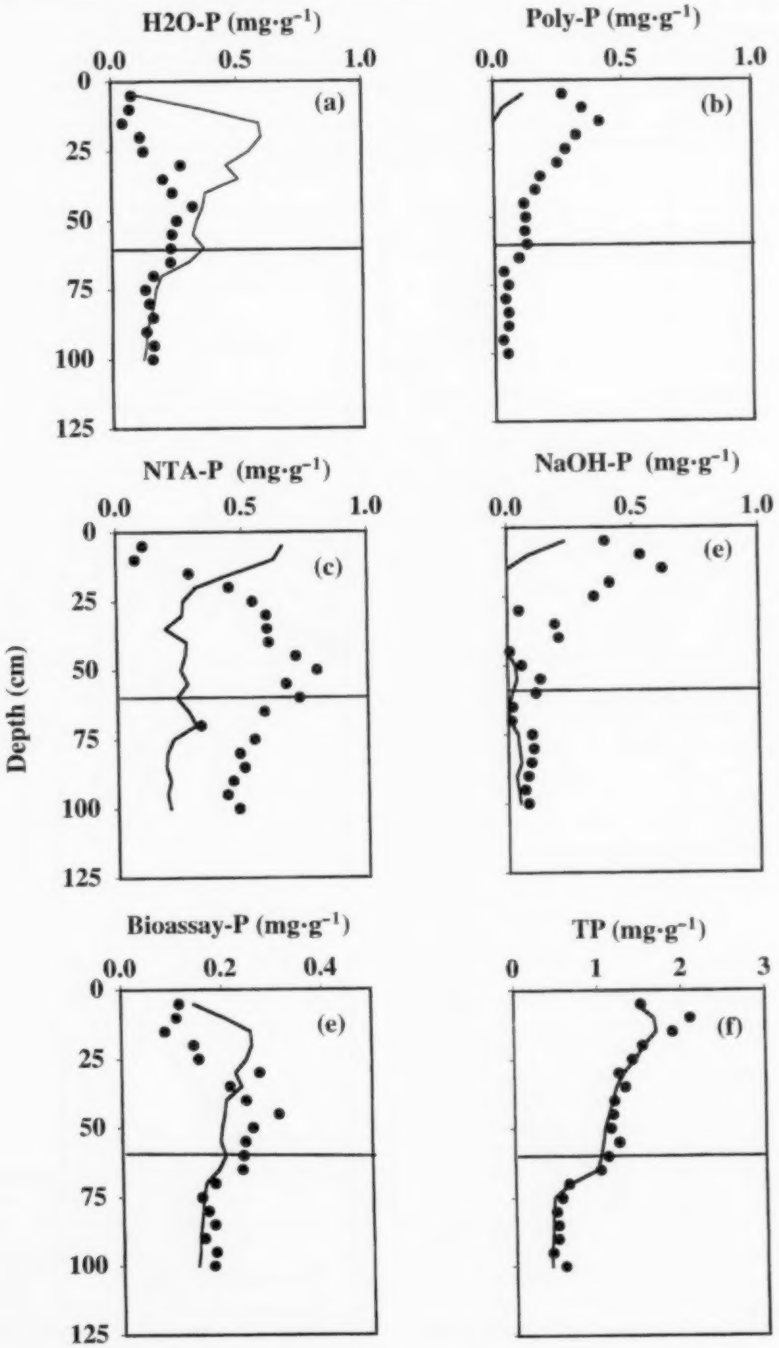

H2O-P ($mg \cdot g^{-1}$)

Poly-P ($mg \cdot g^{-1}$)

NTA-P ($mg \cdot g^{-1}$)

NaOH-P ($mg \cdot g^{-1}$)

Bioassay-P ($mg \cdot g^{-1}$)

TP ($mg \cdot g^{-1}$)

Fig. 5. Relative differences in mean phosphorus (P) and biogenic silica (BSi) concentrations for stratigraphic zones in Lake Apopka sediments. Concentrations of P (wet sediments) and BSi fractions measured on dry sediment samples from zone 1 (40–65 cm; filled bars) and zone 2 (0–40 cm; open bars) are plotted relative to baseline conditions (below 65 cm) for core LA-9-97. P fractions included are bioavailable P as determined through bioassays (bioassay-P), nitrilo triacetic acid extractable P (NTA-P), polyphosphate stored in phytoplankton (poly-P), and total P (TP). Diatom BSi (D-BSi) and sponge BSi (S-BSi) were determined as in Conley and Schelske (1993). See text for further explanation.

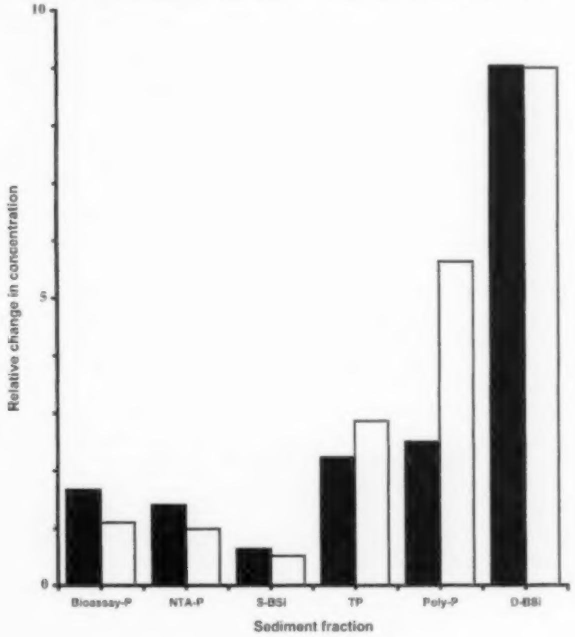

tend that poly-P originally sequestered in phytoplankton became water soluble and externally bioavailable by drying the sediment. This indicates that sample preparation (freezing, freeze-drying, and grinding) damaged cells to the extent that intracellular reserves of P became reactive with colorimetric reagents (pH <2). Some of the measured H_2O-P from dried sediments was not bioavailable under bioassay conditions run at higher pH (~8–9). Consequently, bioassay-P was less than H_2O-P for dried-sediment assays, but was roughly equal to H_2O-P for wet-sediment assays.

Our results show that sedimentary poly-P concentrations changed more relative to baseline conditions than any other P form measured. Total P has been used as a proxy for nutrient enrichment (Engstrom and Wright 1984; Schelske et al. 1986), but an increasing fraction of sedimentary poly-P provides direct evidence of historic P enrichment relative to biological demand. Increased storage of poly-P in Lake Apopka sediments corresponded stratigraphically to known increases in P loading and increased sedimentation of diatom BSi. Our data indicate that P loading and diatom sedimentation first increased at 65 cm and increased more above 40 cm. Because 65 cm is below the zone of phytoplankton sediments (60 cm) that were deposited after ~1947, the initial increase in poly-P reflects increased P loading before the onset of phytoplankton dominance. The sediment chronology indicates that the upper 40 cm of sediment in LA-9-97 was deposited since ~1975, during the period of maximum P loading in Lake Apopka. Excessive enrichment since ~1975 is evident from the relative increase in poly-P sedimentation, which was 2-fold greater than the increase in TP sedimentation. These comparisons show that, as TP loading to Lake Apopka increased relative to biological demand, the surplus available P accumulated as poly-P in phytoplankton instead of being processed geochemically. Likewise, in hypereutrophic Kis-Balaton reservoir in Hungary, nutrient uptake by phytoplankton was the dominant mechanism for removing P from the water (Istanovics 1994).

That phytoplankton and their propagules may be sedimented intact and remain viable for extended time periods, up to decades or longer, can be inferred from rejuvenation experiments conducted on sediment-core samples from Lake Apopka (A. Chapman, unpublished data) and other lakes (see Schelske et al. 1995). Resting propagules or sedimented cells were rejuvenated from all depths tested in other cores from Lake Apopka (A. Chapman, unpublished data). Microscopic examination of wet sediment from LA-9-97 confirmed that phytoplankton cells contained intact protoplasts at all depths. The long sedimentary record of poly-P from Newnans Lake, another hypereutrophic Florida lake, shows that poly-P can be permanently sedimented. Poly-P is a significant fraction of TP in the upper 128 cm, >100 years, of sediments from Newnans Lake (W. Kenney, unpublished data).

In lakes in which anthropogenic enrichment is excessive, poly-P synthesis is ecologically significant, because P is stored by phytoplankton without increasing biomass. Poly-P storage by phytoplankton provides a competitive advantage in Lake Apopka, because available inorganic nutrients (both N and P) are at times in short supply relative to the large biological demand from the large algal standing crop (Aldridge et al. 1993). Under experimental conditions, phytoplankton assemblages from Lake Apopka synthesized 83% of added reactive P as poly-P in less than 2 h (Newman et al. 1994). We hypothesize this biological uptake may limit chemical processes in the water column, because poly-P can be synthesized when SRP concentrations are low enough to prevent many inorganic precipitations. Because of excessive P enrichment, phytoplankton in Lake Apopka are sedimented with stored poly-P, thereby removing more P per unit biomass from the water column than if phytoplankton were P limited.

We suggest that burial of intact phytoplankton cells or their resting propagules is a significant contributor to P sedimentation in Lake Apopka. In the upper 40 cm of sediment, <10% of TP was bioassay-P or H_2O-P, indicating that >90% of the TP was not biologically available or chemically reactive under natural conditions. Poly-P averaged 18% of TP in both the water column and surface sediments in Lake Apopka. According to other studies, poly-P accounts for a variable percentage (<75%) of phytoplankton P (Wynne and Berman 1980; Sakamoto and Inoue 1996). These data indicate that, in Lake Apopka, between 25 and 90% of sediment TP may be sequestered in intact phytoplankton. With these data, the contribution of phytoplankton to sediment TP can only be predicted from poly-P data with a large uncertainty

(~3.6-fold range), but the range shows that phytoplankton are an important contributor to sediment TP.

The process of poly-P storage by phytoplankton removes SRP from the water column, and sedimentation of sequestered poly-P that is not geochemically reactive minimizes the potential for internal P loading. Poly-P sedimentation is a possible explanation for the large P-retention coefficient found for recent Lake Apopka sediments (Schelske 1997). Currently, the mass of P sedimented annually equals the TP reservoir in the water column (Schelske 1997) and is at least 65% of the annual P load (see Battoe et al. 1999; Schelske et al. 2000). This biological attenuation may partially ameliorate the effects of increased P loading.

The global relevance of poly-P sedimentation may be limited to eutrophic systems that support large standing crops of phytoplankton, but this will only be determined by future research. In oligotrophic, P-limited, or ephemeral systems, poly-P sedimentation may be of little ecological significance. Oligotrophic lakes not limited by P may lack the phytoplankton biomass required to store increases in available P as poly-P and, therefore, surplus available P is more likely to be processed geochemically in systems that support minimal biomass. Poly-P is not important in P-limited lakes, because it is stored primarily as a result of relaxed P limitation of phytoplankton growth. Although poly-P may be deposited in ephemeral systems, such as wetlands, periodic desiccation may prevent long-term storage in the sediments. Ecological significance in lakes can be evaluated with existing data and routine limnological techniques, even if poly-P has not been measured. If TP is in greater concentration than chlorophyll in water samples or if NaOH-P is a large fraction of TP in sediments, then poly-P sedimentation may have ecological significance. Measurable SRP in water samples may indicate surplus P in the water column and that poly-P is being stored in phytoplankton (Schelske et al. 1999*a*).

Our results demonstrate that poly-P sedimentation is an important P sink that should be considered in lakes with anthropogenic enrichment. Poly-P synthesis by phytoplankton is important in this regard, because P is stored intracellularly without increasing phytoplankton biomass. Intracellular poly-P in both phytoplankton cells and their resting propagules may be preserved in the sediment for decades or longer. This process removes SRP from enriched waters and buries it in a form that cannot diffuse into the water column, thereby providing negative feedback to P enrichment. With data from Lake Apopka, we show that anthropogenic P enrichment is expressed in the sediment record as increasing concentrations of poly-P and, consequently, that sedimentary poly-P is a sensitive indicator of historic, excessive, P enrichment.

Acknowledgements

This work was supported in part by the Carl S. Swisher Endowment, the University of Florida Foundation, and the St. Johns River Water Management District. We thank Martha Love for her administrative assistance and Peter Meyers and Christine Taylor for assistance with the collection of sediment cores. We also thank Jaye Cable for providing ^{210}Pb data. We thank Martin Auer and anonymous reviewers for their constructive criticisms of the manuscript. This contribution is journal series No. R-06266 of the Florida Agricultural Experiment Station.

References

Aldridge, F.J., Schelske, C.L., and Carrick, H.J. 1993. Nutrient limitation in a hypereutrophic Florida lake. Arch. Hydrobiol. **127**: 21–37.

American Public Health Association. 1989. Standard methods for the examination of water and wastewater. American Public Health Association, Washington, D.C.

Battoe, L.E., Coveney, M.F., Lowe, E.F., and Stites, D.L. 1999. The role of phosphorus reduction and export in the restoration of Lake Apopka, Florida. *In* Phosphorus biogeochemistry in subtropical ecosystems. *Edited by* K.R. Reddy, G.A. O'Connor, and C.L. Schelske. CRC/Lewis Publishers, New York. pp. 511–526.

Brenner, M., and Binford, M.W. 1988. Relationships between concentrations of sedimentary variables and trophic state in Florida lakes. Can. J. Fish. Aquat. Sci. **45**: 294–300.

Carrick, H.J., Aldridge, F.J., and Schelske, C.L. 1993. Wind influences phytoplankton biomass and composition in a shallow productive lake. Limnol. Oceanogr. **38**: 1179–1192.

Chapra, S.C., and Auer, M.T. 1999. Management models to evaluate phosphorus loads in lakes. *In* Phosphorus biogeochemistry in subtropical ecosystems. *Edited by* K.R. Reddy, G.A. O'Connor, and C.L. Schelske. CRC/Lewis Publishers, New York. pp. 643–666.

Chiou, C.-J., and Boyd, C.E. 1974. The utilization of phosphorus from muds by the phytoplankter, *Scenedesmus dimorphus*, and the significance of these findings to the practice of pond fertilization. Hydrobiologia, **45**: 345–355.

Conley, D.J., and Schelske, C.L. 1993. Potential role of sponge spicules in influencing the silicon biogeochemistry of Florida lakes. Can. J. Fish. Aquat. Sci. **50**: 296–302.

Engstrom, D.R., and Wright, H.E., Jr. 1984. Chemical stratigraphy of lake sediments as a record of environmental change. *In* Lake sediments and environmental history. *Edited by* E.Y. Haworth and W.G. Lund. University of Minnesota Press, Minneapolis, Minn. pp. 11–67.

Fisher, M.M., Brenner, M., and Reddy, K.R. 1992. A simple, inexpensive piston corer for collecting undisturbed sediment / water interface profiles. J. Paleolimnol. **7**: 157–161.

Fitzgerald, G.P., and Nelson, T.C. 1966. Extractive and enzymatic analysis for limiting or surplus phosphorus in algae. J. Phycol. **2**: 32–37.

Gale, P.M., Reddy, K.R., and Graetz, D.A. 1992. Mineralization of sediment organic matter under anoxic conditions. J. Environ. Qual. **21**: 394–400.

Golterman, H.L. 1977. Sediments as a source for algal growth. *In* Interactions between sediments and freshwater. Junk/Pudoc, The Hague. pp. 286–293.

Golterman, H.L. 1988. Reflections on fractionation and bioavailability of sediment bound phosphate. Verh. Internat. Ver. Limnol. **30**: 1–4.

Golterman, H.L., Bakels, C.C., and Jakobs-Mögelin, J. 1969. Availability of mud phosphates for the growth of algae. Verh. Int. Ver. Theor. Angew. Limnol. **17**: 467–479.

Hecky, R.E., and Kilham, P. 1988. Nutrient limitation of phytoplankton in freshwater and marine environments: a review of recent evidence on the effects of enrichment. Limnol. Oceanogr. **33**: 796–822.

Istanovics, V. 1994. Fractional composition, adsorption and release of sediment phosphorus in the Kis-Balaton reservoir. Water Res. **3**: 717–726.

Kenney, W.F. 1997. A comparison of chemical assays for the estimation of bioavailable phosphorus in Lake Apopka sediments. Masters thesis, University of Florida, Gainesville.

Meyers, P., and Schelske, C.L. 2000. An inexpensive, optical (infrared) detector to locate the sediment/water interface in lakes with unconsolidated sediments. J. Paleolimnol. **23**: 201–205.

Newman, S., Aldridge, F.J., Phlips, E.J., and Reddy, K.R. 1994. Assessment of phosphorus availability for natural phytoplankton populations from a hypereutrophic lake. Arch. Hydrobiol. **130**(4): 409–427.

Olila, O.G., and Reddy, K.R. 1997. Influence of redox potential on phosphate-uptake by sediments in two sub-tropical eutrophic lakes. Hydrobiologia, **345**: 45–57.

Olila, O.G., Reddy, K.R., and Harris, W.G. 1995. Forms and distributions of inorganic phosphorus in sediments of two shallow eutrophic lakes in Florida. Hydrobiologia, **302**: 147–161.

Pettersson, K. 1980. Alkaline phosphatase activity and algal surplus phosphorus as phosphorus-deficiency indicators in Lake Erken. Arch. Hydrobiol. **89**: 54–87.

Phlips, E.J., Zeman, C., and Hansen, P. 1989. Growth, photosynthesis, nitrogen fixation and carbohydrate production by a unicellular cyanobacterium, *Synechococcus* sp. (Cyanophyta). J. Appl. Phycol. **1**: 137–145.

Reddy, K.R., Fisher, M.M., and Ivanoff, D. 1996. Resuspension and diffusive flux of nitrogen and phosphorus in a hypereutrophic lake. J. Environ. Qual. **25** : 363–371.

Sakamoto, M., and Inoue, T. 1996. Typhoon-induced temporal change in plankton phosphorus in Lake Biwa. Jpn. J. Limnol. **4**: 511–522.

Schelske, C.L. 1997. Sediment and phosphorus deposition in Lake Apopka. Final Rep. SJ97-SP21 of the St. Johns River Water Management District, Palatka, Fla.

Schelske, C.L., and Brezonik, P. 1992. Restoration case studies. Can Lake Apopka be restored? *In* Restoration of Aquatic Ecosystems: Science, Technology, and Public Policy: Report of the Committee on Restoration of Aquatic Ecosystems, National Research Council. National Academy Press, Washington, D.C. pp. 393–398.

Schelske, C.L., Conley, D.J., Stoermer, E.F., Newberry, T.L., and Campbell, C.D. 1986. Biogenic silica and phosphorus accumulation in sediments as indices of eutrophication in the Laurentian Great Lakes. Hydrobiologia, **143**: 79–86.

Schelske, C.L., Carrick, H.J., and Aldridge, F.J. 1995. Can wind-induced resuspension of meroplankton affect phytoplankton dynamics? J. N. Am. Benthol. Soc. **14**: 616–630.

Schelske, C.L., Aldridge, F.J., and Kenney, W.F. 1999*a*. Assessing nutrient limitation in Florida lakes. *In* Phosphorus biogeochemistry in subtropical ecosystems. *Edited by* K.R. Reddy, G.A. O'Connor, and C.L. Schelske. CRC/Lewis Publishers, New York. pp. 321–339.

Schelske, C.L., Donar, C.M., and Stoermer, E.F. 1999*b*. A test of paleolimnological proxies for the planktonic/benthic ratio of microfossil diatoms in Lake Apopka. *In* Proceedings of the 14th International Diatom Symposium, Tokyo, Japan, September 2–8, 1996. *Edited by* S. Mayama, M. Idei, and I. Koizumi. Koeltz Scientific Books, Koenigstein, Germany. pp. 367–382.

Schelske, C.L., Coveney, M.F., Aldridge, F.J., Kenney, W.F., and Cable, J.E. 2000. Wind or nutrients: historic development of hypereutrophy in Lake Apopka, Florida. Arch. Hydrobiol. Adv. Limnol. **55**: 543–563.

Schindler, D.W. 1977. Evolution of phosphorus limitation in lakes. Science (Washington, D.C.), **195**: 260–262.

Sicko-Goad, L., Stoermer, E.F., and Kociolek, J.P. 1989. Diatom resting cell rejuvenation and formation: time course, species records and distribution. J. Plankton Res. **11**: 375–389.

Twinch, A.J. 1986. The phosphorus status of sediments in a hypereutrophic impoundment (Hartbeespoort Dam): implications for eutrophication management. Hydrobiologia, **135**: 23–34.

Williams, J.D.H., Shear, H., and Thomas, R.L. 1980. Availability to *Scenedesmus quadricauda* of different forms of phosphorus in sedimentary materials from the Great Lakes. Limnol. Oceanogr. **25**: 1–11.

Wynne, D., and Berman, T. 1980. Hot water extractable phosphorus—an indicator of nutritional status of *Peridinium cinctum* (Dinophyceae) from Lake Kinneret (Israel)? J. Phycol. **16**: 40–46.

Bioaccumulation and biomagnification of mercury in Lake Murray, Papua New Guinea

Karl C. Bowles, Simon C. Apte, William A. Maher, Matthew Kawei, and Ross Smith

Abstract: The bioaccumulation of mercury in the food webs incorporating the major piscivorous fish species of Lake Murray, Papua New Guinea, has been characterised. Methylmercury concentrations increased with trophic level and the proportion of total mercury present as methylmercury increased from <1% in plants to 94% in piscivorous fish. Methylmercury bioaccumulation factors (BAFs) were similar to those found in temperate environments, with a typical increase of 1 log unit between planktivore and piscivore trophic levels. The greatest bioaccumulation of methylmercury occurred between seston and the water column (log BAF of 5.36). The bioaccumulation of mercury to levels of regulatory concern by the lake's piscivores was attributable to the biomagnification power of the plankton-based food chain comprising four trophic levels (phytoplankton, zooplankton, planktivore, piscivore) rather than any elevated concentrations of mercury in waters or sediments. The methylmercury concentrations of individual piscivores were positively correlated with both trophic position, as indicated by $\delta^{15}N$ measurements, and fish size. Stable-isotope measurements were used to identify fish species where dietary changes occurring with age significantly augmented age-related bioaccumulation of mercury.

Résumé : La bioaccumulation du mercure a été étudiée dans le réseau alimentaire reliant les principales espèces de poissons piscivores du lac Murray en Papouasie-Nouvelle-Guinée. Les concentrations de méthylmercure croissent avec le niveau trophique et le pourcentage du mercure total présent sous la forme méthylée augmente de <1% chez les plantes à 94% chez les poissons piscivores. Les facteurs de bioaccumalation du méthylmercure (BAFs) sont semblables à ceux que l'on retrouve dans les milieux tempérés et il y a typiquement une augmentation d'une unité logarithmique entre les niveaux trophiques planctonophage et piscivore. La bioaccumulation la plus considérable a lieu entre le seston et la colonne d'eau (log BAF de 5,36). La bioaccumulation du mercure à des niveaux inquiétants (d'après les normes actuelles) par les piscivores du lac est causée par le pouvoir de bioamplification de la chaîne alimentaire à base de plancton qui couvre quatre niveaux (phytoplanctonique, zooplanctonique, planctonophage, piscivore) plutôt qu'à une augmentation des concentrations de mercure dans les eaux ou dans les sédiments. Les concentrations de méthylmercure chez les différents piscivores sont en corrélation positive à la fois avec leur position trophique, telle que déterminée par les mesures de $\delta^{15}N$, et avec leur taille. Les analyses à l'aide d'isotopes stables ont permis de reconnaître les espèces de poissons chez lesquelles des changements de régime alimentaire au cours de la vie augmentent significativement la bioaccumulation du mercure reliée à l'âge.

[Traduit par la Rédaction]

Introduction

Concerns over mercury toxicity and the ability of methylmercury (MeHg) to biomagnify to potentially harmful concentrations in aquatic food chains have led to a need to understand the cycling of mercury in aquatic environments (Clarkson 1992). To date, most studies have focussed on the cycling of mercury in northern hemisphere temperate lacustrine systems (Lee and Hultberg 1990; Watras et al. 1994; Kelly et al. 1995). Aside from the Florida Everglades (Hurley et al. 1998) and the Amazon basin (Akagi et al. 1995), both of which have been polluted by human activities, subtropical and tropical systems remain largely unstudied.

Lake Murray is situated in the remote Western Province of Papua New Guinea (PNG). The human inhabitants around the lake have some of the highest recorded concentrations of mercury in hair for people not occupationally exposed to mercury. Hair mercury concentrations in adults typically

Received July 27, 2000. Accepted January 23, 2001. Published on the NRC Research Press Web site on April 12, 2001.
J15889

K.C. Bowles. Centre for Advanced Analytical Chemistry, Commonwealth Scientific and Industrial Research Organisation, Division of Energy Technology, PMB 7, Bangor NSW 2234, Australia, and Applied Ecology Research Group, University of Canberra, P.O. Box 1, Belconnen ACT 2616, Australia.
S.C. Apte.[1] Centre for Advanced Analytical Chemistry, Commonwealth Scientific and Industrial Research Organisation, Division of Energy Technology, PMB 7, Bangor NSW 2234, Australia.
W.A. Maher. Applied Ecology Research Group, University of Canberra, P.O. Box 1, Belconnen ACT 2616, Australia.
M. Kawei. Porgera Joint Venture, Porgera, Western Province, Papua New Guinea.
R. Smith. R&D Environmental Pty. Ltd., Level 4, Lantos Place, 49 Station Road, Indooroopilly, QLD 4068, Australia.

[1] Corresponding author (e-mail: simon.apte@det.csiro.au).

Can. J. Fish. Aquat. Sci. **58**: 888–897 (2001) DOI: 10.1139/cjfas-58-5-888

range from 10–70 μg·g^{-1} (Mackenzie and Kyle 1984; Abe et al. 1995). These high hair mercury concentrations are attributed to dietary dependence on locally caught fish, which have elevated mercury concentrations. Over the past 20 years, studies have shown that the mercury concentrations of predatory fish species from Lake Murray can exceed the World Health Organisation (WHO) recommended limit for total mercury in fish intended for human consumption of 0.5 μg·g^{-1} (Sorentino 1979; Kyle and Ghani 1982). This appears to be a local phenomenon restricted to Lake Murray and, possibly, other smaller lakes in Western Province, as fish caught in other regions of PNG have much lower mercury concentrations (Sorentino 1979; Onaga 1993).

The cycling of mercury species in the waters and sediments of Lake Murray has been discussed by Bowles (1998). Although Lake Murray has the ideal physical and chemical settings for mercury methylation to occur, i.e., an extensive shallow lake with a large littoral zone, surrounding wetlands, frequent wet–dry cycles, and slightly acidic waters, the total mercury and MeHg concentrations measured in waters and sediments are generally low compared with those in other studies (Bowles 1998). As most available evidence points to dietary uptake as the dominant pathway of mercury bioaccumulation in aquatic food webs (Hall et al. 1997), the water and sediment data strongly suggest that mercury bioaccumulation is linked to the structure of the lake's food web.

In this study, mercury concentrations in fish, seston, and plant specimens, representing the key components of the Lake Murray food web, were measured. Particular focus was placed on barramundi (*Lates calcarifer*), a major food source for the human inhabitants of the area. In addition to total mercury and mercury speciation measurements, carbon and nitrogen stable isotope ratios were used as a tool to assess the modes of mercury bioaccumulation and biomagnification. This information was used to gain a better understanding of the factors leading to high mercury concentrations in piscivorous fish inhabiting the lake. Carbon and nitrogen stable isotope measurements have been widely used to elucidate food webs in aquatic ecosystems (Peterson and Fry 1987; Hamilton et al. 1992; Jarman et al. 1996). The degree of success attained with the stable-isotope technique is somewhat site specific and is largely dependent on the spread of carbon signatures observed. The ratio between the carbon isotopes ^{13}C and ^{12}C (δ^{13}C) in plants is dependent on the photosynthetic route (Peterson and Fry 1987). Since this ratio alters little (0.2–1‰) during trophic transfers (De Niro and Epstein 1978; France 1996), this parameter gives information on the carbon source of heterotrophic organisms. In contrast, the ratio between ^{15}N and ^{14}N (δ^{15}N) increases typically by about 3‰ during each trophic transfer and gives a measure of the trophic position of a given organism (Minagawa and Wada 1984).

Materials and methods

Site description

A general description of the Lake Murray region and its aquatic biology is given by Bowles (1998). Only a brief summary is given here. Lake Murray, the largest lake in PNG is situated in a shallow depression on a vast floodplain close to the confluence of the Fly and Strickland rivers (Fig. 1). The volume of Lake Murray is highly dependent on climatic conditions, and the lake has been known to dry up completely during drought conditions. The maximum depth of the lake is approximately 10 m and the mean depth is 5 m. The climate is typical of the wet tropics, with high temperatures (daily maxima: 30–32°C), high humidity, and high rainfall (annual rainfall of ca. 3000 mm (Abe et al. 1995)). The vegetation surrounding northern Lake Murray is mainly closed rainforest, whereas the land to the south of the lake is dominated by open rainforest, swamp forest, and grass swamp. The littoral areas of the lake are dominated by tropical grasses.

Over 103 fish species are known to inhabit the freshwater environments of Western Province (Roberts 1978). In view of this large number, the present study focussed on the dominant members of the major trophic guilds most commonly encountered in Lake Murray. Recent stable-isotope studies (Bowles 1998) have indicated that the food webs incorporating the major fish predators in the lake are plankton based. *Nematalosa flyensis* and *Nematalosa papuensis* are the principal planktivores in Lake Murray. Omnivores are represented by Ariidae catfishes and archerfish (*Toxotes chatareus*). *Lates calcarifer* is the most abundant large piscivore (Roberts 1978). Other piscivores include *Thryssa scratchleyi* and *Strongylura kreffti*. Benthic fauna such as oligochaetes are scarce in the main body of the lake and are unlikely to be a major food source.

Sampling

Owing to the low concentrations of mercury expected in environmental samples, trace-metal clean techniques were used throughout all stages of sampling, storage, and analysis. Aquatic macrophytes, vascular plants, and filamentous algae were sampled from the lake margins (Fig. 1) during June 1995 and November 1996 and stored frozen in acid-washed plastic vials or resealable bags. Samples of rainforest vegetation were not collected, as these were generally separated from the lake by extensive stands of littoral grasses. Subsequent stable-isotope studies (Bowles 1998) also confirmed that allocthonous carbon sources are, at best, a minor energy source for the lake's fish. Seston samples were collected by trawling a plankton net (mesh size 63 μm) at low speed for approximately 10 min. Seston was washed off the side of the net into acid-washed polyethylene or fluorinated ethylene propylene bottles with a small volume of lake water. Fish samples were collected in August 1996 and November 1996 using purse-seine or gill nets. The fish species collected comprised two planktivorous freshwater herring species (*N. flyensis* and *N. papuensis*), the omnivorous groove-snouted catfish (*Arius berneyi*), the insectivorous seven-spotted archerfish (*T. chatareus*), and three piscivores: barramundi (*L. calcarifer*), giant freshwater anchovy (*T. scratchleyi*), and Sepik garpike (*S. kreffti*). Small fish were kept as whole specimens, whereas larger fish were separated into muscle fillets or bodies, with the head and gut removed before storage. All biota samples were stored frozen.

Analytical techniques

Total mercury concentrations in fish tissues were determined by cold vapour – atomic absorption spectrometry, following digestion with a 7:3 (v/v) mixture of nitric and sulphuric acids (Bowles 1998). Because of the lower mercury concentrations in the plant samples, total mercury was quantified using cold-vapour generation with single-stage gold amalgamation and cold-vapour atomic-fluorescence detection (Liang and Bloom 1993). Two certified reference materials (National Research Council of Canada) were analysed in each batch of samples. The mean value obtained for dogfish muscle, DORM-2, was 4.52 ± 0.17 μg·g^{-1} (certified value 4.64 ± 0.26 μg·g^{-1}) and the mean value obtained for dogfish liver, DOLT-2, was 2.30 ± 0.1 μg·g^{-1} (certified value 2.14 ± 0.28 μg·g^{-1}). MeHg in tissues was determined by alkaline digestion, using a modified version of the procedure described by Fischer et al. (1993). In place of digestion in an ultrasonic bath, 50–1000 mg of wet sample was digested at 75°C for 3 h in a glass test tube fitted with an air condenser. The digests were analysed by

Fig. 1. Location of sampling sites in Lake Murray, Papua New Guinea. Sample type is denoted as *F* (fish), *P* (plants), and *S* (seston).

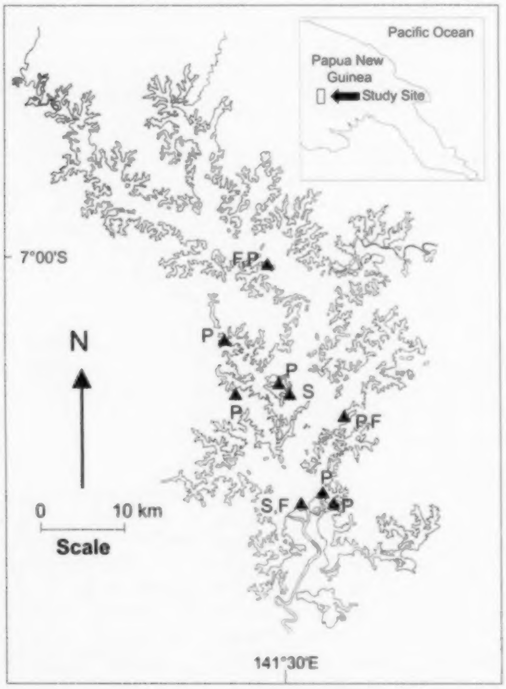

aqueous-phase ethylation and gas chromatography – atomic fluorescence spectrometry (Liang et al. 1994). The mean value obtained for MeHg in DORM-2 was 4.44 ± 0.30 $\mu g \cdot g^{-1}$ (certified value 4.47 ± 0.32 $\mu g \cdot g^{-1}$) and the mean value obtained for MeHg in DOLT-2 was 0.683 ± 0.047 $\mu g \cdot g^{-1}$ (certified value 0.693 ± 0.053 $\mu g \cdot g^{-1}$). Analytical blanks and recovery spikes were also included in all sample batches. Recoveries of MeHg and total mercury spikes were always >85%. Absolute blank values were typically less than 10% of the concentrations measured in the samples. All reported data have been corrected for the blank values.

Tissues were prepared for stable-isotope analysis by oven drying at 60°C and grinding to a fine powder using an agate mortar and pestle. The ground samples were stored in acid-washed amber glass vials fitted with aluminium-lined caps. Isotopic ratio mass spectrometry was used to measure $\delta^{13}C$ and $\delta^{15}N$ in the samples (Bunn and Boon 1993). Pee Dee belemnite carbonate and atmospheric nitrogen were used as calibration standards for carbon and nitrogen measurements, respectively. The precision of replicate measurements was typically 0.2–0.3‰ for $\delta^{13}C$ and 0.3–0.6‰ for $\delta^{15}N$.

Unless otherwise stated, all mercury data are expressed as wet-mass concentrations. Bioaccumulation factors (BAFs) were calculated using wet-mass data as follows: BAF = MeHg concentration in the organism ($\mu g \cdot g^{-1}$)/mean MeHg concentration in the water column ($\mu g \cdot g^{-1}$). A mean water column MeHg concentration of 0.067 $ng \cdot L^{-1}$ was used in these calculations (Bowles 1998).

Results

Food-web structure

Carbon and nitrogen stable isotope data are summarised in Table 1. This data is discussed in detail by Bowles et al. (1998). Overall, the data indicated that the food webs containing the major piscivorous species discussed in this paper are phytoplankton based.

Table 1. Summary of carbon and nitrogen stable isotope data.

	Sample size	$\delta^{13}C$	$\delta^{15}N$
Grasses	8	−11.9±0.7	2.9±2.3
Aquatic ferns	5	−28.0±1.2	0.12±0.36
Lilies	2	−24.6, −25.1	1.7, 1.5
Algae	10	−21.3±3.0	0.65±0.75
Weeds	2	−19.7, −26.8	−0.7, 0.1
Seston	4	−29.8±0.6	2.0±1.6
Nematalosa flyensis	11	−32.4±0.8	4.9±0.6
Nematalosa papuensis	14	−30.5±1.8	4.3±1.2
Toxotes chatareus	9	−25.9±1.7	7.5±0.5
Arius berneyi	15	−28.6±1.7	7.4±0.8
Lates calcarifer	33	−28.2±1.0	8.4±0.5
Strongylura kreffti	9	−29.2±1.5	8.8±0.5
Thryssa scratchleyi	5	−30.1±1.5	8.7±1.5

Mercury concentrations in the aquatic food web

The mercury concentrations in the biota sampled from Lake Murray are summarised in Table 2. The data showed clear evidence of biomagnification of mercury: the highest concentrations were found in piscivorous fish (0.1–1.2 $\mu g \cdot g^{-1}$), intermediate concentrations in planktivorous fish (0.03–0.09 $\mu g \cdot g^{-1}$), and the lowest concentrations in plant specimens (0.0004–0.040 $\mu g \cdot g^{-1}$). Forty-one of the 177 (23%) piscivorous and omnivorous fish specimens analysed had total mercury concentrations exceeding the WHO fish consumption guideline of 0.5 $\mu g \cdot g^{-1}$. The total mercury concentrations in *L. calcarifer* specimens were similar to concentrations observed in previous studies of Lake Murray (Sorentino 1979; Kyle and Ghani 1982). All plant samples contained MeHg concentrations below the method detection limit (<0.0003 $\mu g \cdot g^{-1}$). The mean concentration of MeHg in seston samples (a mixture of phytoplankton and some zooplankton), however, was markedly higher (0.015 $\mu g \cdot g^{-1}$). This indicated the relative importance of seston as a MeHg source for the pelagic food webs.

Mercury speciation measurements (Table 2) indicated that the proportion of total mercury present as MeHg increased with trophic level and ranged from <1% in plants to a maximum of 94% in the piscivore *S. kreffti*. This trend was illustrated by the strong linear relationship between mean percent MeHg and mean $\delta^{15}N$ values for the fish species (Fig. 2). The overall biomagnification of mercury in the aquatic food web is illustrated by the plot of MeHg concentration versus the $\delta^{15}N$ value for each fish sampled (Fig. 3). MeHg concentrations increase markedly in organisms that had a $\delta^{15}N$ value of >7. Similar relationships between Hg concentration and $\delta^{15}N$ have been found for other aquatic food webs (Kidd et al. 1995; Jarman et al. 1996). The relationship between these variables can also be expressed by the following linear equation: $\log[\mathrm{MeHg}] = 0.28[\delta^{15}N] - 2.88$ ($r^2 = 0.715$). Both the slope and the intercept of this plot bear remarkable similarity to those for the relationships derived by Kidd et al. (1995) for fish in northwest Ontario lakes and also to those for the Arctic marine food web data presented by Atwell et al. (1998). This suggests that the biomagnification

Table 2. Total mercury (HgT), methylmercury (MeHg), and inorganic mercury (inorganic Hg) concentrations in water (presented as ng·L^{-1}) and in sediments and biota (presented as µg·g^{-1}) from Lake Murray.

Component	No. of samples	Mass (g) Range	Mass (g) Mean	HgT	Inorganic Hg	MeHg	MeHg as % of HgT
Water	49		—	1.42±1.27[a]		0.067±0.115[a]	—
Surface sediments	19		—	0.111±0.062[b]		0.0009±0.00071[b]	—
Grasses	3	—	—	0.00156±0.00097	0.00156±0.00097	<0.0003	<1
Lily pads	5	—	—	0.000709±0.000343	0.000709±0.000343	<0.0003	<1
Aquatic ferns	4	—	—	0.00258±0.00211	0.00258±0.00211	<0.0003	<1
Macroalgae	11	—	—	0.00253±0.00161	0.00253±0.00161	<0.0003	<1
Seston	4		—	nd[c]	nd[c]	0.015±0.009	—
Planktivores							
Nematalosa flyensis	11	1–48	7.5	0.049±0.013	0.023±0.008	0.026±0.008	54±11
Nematalosa papuensis	14	2–64	28	0.048±0.017	0.022±0.011	0.026±0.009	56±12
Omnivores							
Arius berneyi	15	5–1005	166	0.23±0.17	0.049±0.054	0.181±0.148	75±17
Toxotes chatareus	8	29–88	59	0.36±0.18	0.067±0.040	0.289±0.149	80±6
Piscivores							
Strongylura kreffti	9	26–254	96	0.38±0.19	<0.010	0.382±0.244	94±20
Thryssa scratchleyi	5	22–142	49	0.38±0.31	0.044±0.033	0.337±0.322	79±15
Lates calcarifer	33	2400 – 13 500	7020	0.50±0.28	0.040±0.057	0.458±0.300	88±17

[a] The mean of concentrations (ng·L^{-1}) that were measured in the water column during June 1995 and November 1996.

[b] The mean of surface-sediment concentrations that were measured during June 1995.

[c] Not determined, owing to insufficient sample mass.

Fig. 2. Relationship between mean percent MeHg and $\delta^{15}N$ for (*a*) *Nematalosa papuensis*, (*b*) *Nematalosa flyensis*, (*c*) *Arius berneyi*, (*d*) *Toxotes chatareus*, (*e*) *Lates calcarifer*, (*f*) *Thryssa scratchleyi*, and (*g*) *Strongylura krefftii*.

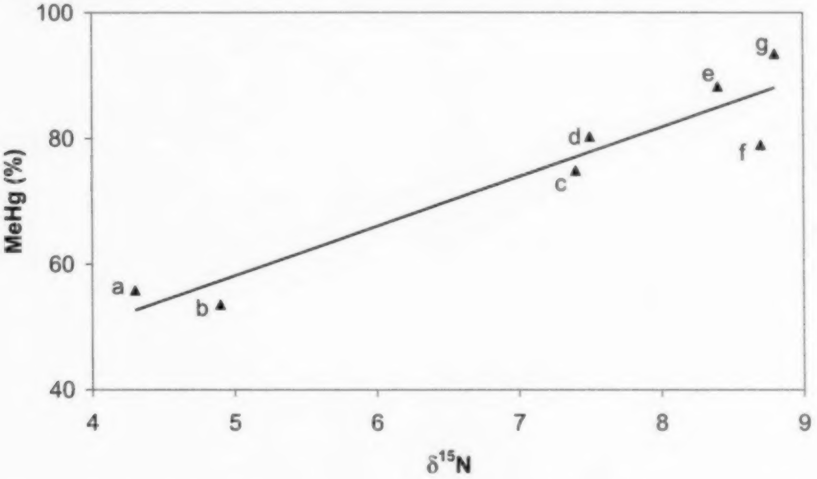

power of the Lake Murray food web is similar to that of temperate-lake and Arctic-marine systems. Such global relationships are of value in comparing different systems, although the variability in the data limits their practical utility for accurately predicting MeHg concentrations in individual organisms of known $\delta^{15}N$ value.

The mean inorganic mercury concentrations measured in all biological specimens were low and ranged from <0.01 to 0.067 $\mu g \cdot g^{-1}$. Inorganic mercury concentrations showed some evidence of increasing with trophic position (Table 2); however, unlike MeHg, there was no consistent relationship between inorganic mercury and $\delta^{15}N$. In view of the obvious importance of MeHg in determining mercury bioaccumulation, inorganic mercury is not considered further.

The BAF values for MeHg in seston and the various fish species are presented in Table 3. Similarly to studies conducted in temperate-lake systems (Watras et al. 1998), the largest BAF was observed between seston and the water column. This is consistent with the known efficient bioaccumulation of MeHg from the water column by phytoplankton (Watras and Bloom 1992; Monson et al. 1996; Watras et al. 1998). The mean log BAF for seston of 5.36 was very similar to the value of 5.43 reported by Monson et al. (1996) for plankton in lakes in Minnesota, U.S.A., and to the values reported by Watras et al. (1994) for phytoplankton in Little Rock Lake, Wisconsin (5.2 to 5.7). The difference between the BAFs of the planktivores *Nematalosa* spp. and the piscivores varied between 0.8 and 1.2 log units. This observed difference was consistent with studies conducted in North America, in which an increase in BAF of ca. 0.5–1.5 log units was typically observed between trophic levels (Watras and Bloom 1992; Hill et al. 1996). The difference in BAF values between seston and the planktivores *Nematalosa* spp. was much lower (0.23 log units), indicating that the trophic transfer of MeHg between plankton (*Nematalosa* spp. graze on a mixture of phytoplankton and zooplankton) and the planktivore is not as efficient as the transfer occurring at the next trophic level (fish to fish). Further work is required to investigate the reasons for this observation. This comparison of BAF values should be treated with some caution, as the variability of the BAFs within each of the piscivorous fish species was quite large (Table 3) and, in some cases, was greater than one log unit. All three piscivorous species contained individual specimens with log BAF values of >7. These values are extremely high and are greater than BAF values reported for organochlorine pesticide bioaccumulation by fish (Davies and Dobbs 1984).

Individual fish species

For all fish species, apart from *Nematalosa* spp. and *T. scratchleyi*, both total mercury and MeHg concentrations were significantly correlated with fish length (Fig. 4; Table 4) and fish mass (Table 4). Such relationships are commonly found in freshwater fish (Mathers and Johansen 1985; Lange et al. 1993; Watras et al. 1998). The lack of any significant relationship between MeHg and fish size for *T. scratchleyi* may, in part, be explained by the lack of intermediate-sized specimens caught for this study. Most specimens were less than 150 mm in length, while one specimen was greater than 250 mm. Although the single large specimen had a higher MeHg concentration than the smaller specimens, the overall relationship was not significant. Given the limited data set, mercury bioaccumulation in this species is not discussed further. Differences in MeHg bioaccumulation rates between *L. calcarifer*, *A. berneyi*, *S. krefftii*, and *T. chatareus* were indicated by the slopes in plots of mercury concentration versus fish length (Fig. 4). Analysis of covariance (ANCOVA) indicated significant heterogeneity of slopes ($P < 0.05$). These differences most likely reflect the different MeHg assimilation efficiencies, rates of change of trophic position with size, and growth rates of the various fish species.

Apart from the planktivores (*Nematalosa* spp.), MeHg concentrations within each fish species were positively correlated with $\delta^{15}N$ values (Fig. 5; Table 4). This correlation illustrates the importance of the trophic position of the individual fish specimens in determining MeHg concentration. Even fractional changes in trophic level affected MeHg concentrations. Only *L. calcarifer* and *A. berneyi* displayed sta-

Fig. 3. Relationship between MeHg concentration and $\delta^{15}N$ values of all fish specimens: *Nematalosa* spp.(△), *Arius berneyi* (▲), *Toxotes chatareus* (□), *Strongylura kreffti* (●), *Thryssa scratchleyi* (○), and *Lates calcarifer* (■).

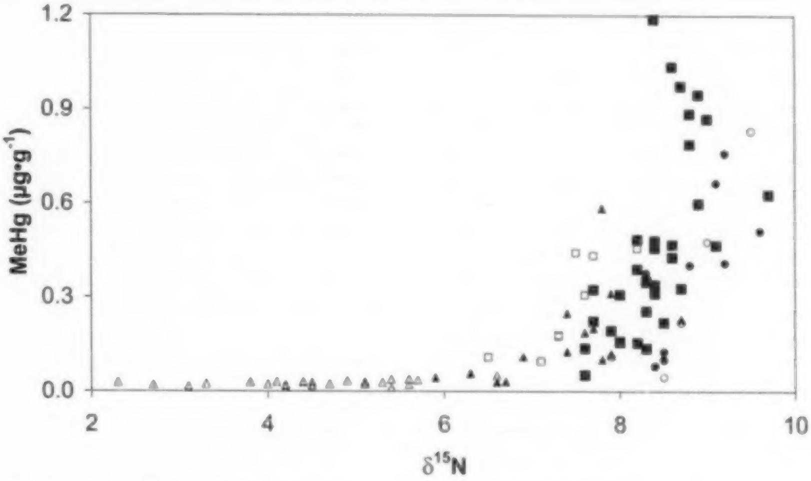

Table 3. Bioaccumulation factors (BAFs) for fish species and seston from Lake Murray.

Ecosystem component	MeHg ($\mu g \cdot g^{-1}$)	Mean log BAF	Range
Water	6.7×10^{-8}		
Seston	0.0154	5.36	4.92–5.65
Nematalosa spp.	0.026	5.59	5.28–5.87
Arius berneyi	0.181	6.43	5.63–6.94
Toxotes chatareus	0.289	6.63	6.16–6.83
Strongylura kreffti	0.382	6.76	6.08–7.06
Thryssa scratchleyi	0.281	6.62	5.84–7.09
Lates calcarifer	0.458	6.83	5.89–7.25

Fig. 4. Relationship between total mercury concentration and fish length for each fish species. (*a*) *Nematalosa flyensis* (■) and *N. papuensis* (△). (*b*) *Arius berneyi* (▲), *Toxotes chatareus* (□), *Strongylura kreffti* (△), and *Lates calcarifer* (■). (*c*) *Thryssa scratchleyi*. Total mercury (Hg) was used in place of MeHg in these plots, owing to the greater number of data points.

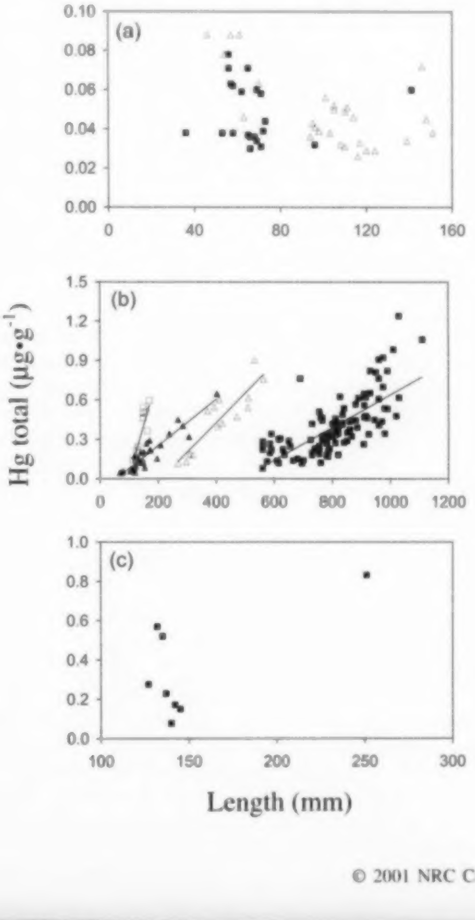

tistically significant positive correlations between $\delta^{15}N$ and fish size (Table 4), which indicate that trophic position increases for these fish as they grow. The lack of a relationship between $\delta^{15}N$ values and fish size for the *S. kreffti* and *T. chatareus* specimens (Bowles 1998) indicates that these species do not change their trophic position as they grow larger. Coupled with the MeHg versus $\delta^{15}N$ relationship data presented above, this suggests that some of the variability in MeHg concentrations in these fish was linked to differences in the trophic position of the individual fish, irrespective of their size.

A statistically significant relationship between MeHg and $\delta^{13}C$ was seen only in *A. berneyi* (Table 4). The factors influencing the bioaccumulation of MeHg by *A. berneyi* are hard to unravel, owing to the covariance of MeHg, $\delta^{13}C$, $\delta^{15}N$, and fish size (Table 4; Bowles 1998). This indicates that *A. berneyi* simultaneously changes diet (which incorporates a change in the primary carbon source) and trophic position with size. Any one of these changes, or a combination of them, will contribute to the observed increase in MeHg concentration with size.

The concentrations of mercury in *T. chatareus* were relatively high, with 4 of the 10 specimens analysed having total mercury concentrations greater than $0.5\ \mu g \cdot g^{-1}$. This fish also had the steepest gradient in the plots of MeHg versus fish

Table 4. Pearson product–moment correlations between total mercury (HgT), methylmercury (MeHg), fish length, fish mass, and stable-isotope ratios ($\delta^{13}C$ and $\delta^{15}N$).

Species	No. of samples[a]	HgT vs. length	HgT vs. mass	MeHg vs. length	MeHg vs. mass	No. of samples[b]	MeHg vs. $\delta^{13}C$	MeHg vs. $\delta^{15}N$	MeHg vs. HgT	$\delta^{15}N$ vs. length
Nematalosa flyensis	21	–0.103	0.605	0.392	0.455	11	0.524	0.255	0.808	0.231
		(0.965)	(0.795)	(0.233)	(0.160)		(0.098)	(0.449)	(0.003)	(0.495)
Nematalosa papuensis	27	–0.635*	–0.431*	–0.554*	–0.337	14	–0.289	0.380	0.788*	–0.504
		(<0.001)	(0.025)	(0.040)	(0.239)		(0.317)	(0.200)	(0.001)	(0.066)
Arius berneyi	35	0.936*	0.849*	0.904*	0.896*	15	0.783*	0.613*	0.949*	0.655*
		(<0.001)	(<0.001)	(<0.001)	(<0.001)		(0.001)	(0.015)	(<0.001)	(0.008)
Toxotes chatareus	10	0.769*	0.804*	0.725*	0.768*	9	–0.627	0.823*	0.985*	0.612
		(0.009)	(0.005)	(0.027)	(0.016)		(0.071)	(0.006)	(<0.001)	(0.080)
Lates calcarifer	113	0.712*	0.719*	0.683*	0.703*	33	0.215	0.613*	0.982*	0.666*
		(<0.001)	(0.001)	(<0.001)	(<0.001)		(0.229)	(<0.001)	(<0.001)	(<0.001)
Strongylura kreffti	14	0.893*	0.825*	0.813*	0.753*	9	–0.567	0.723*	0.970*	0.654
		(<0.001)	(<0.001)	(0.008)	(0.019)		(0.112)	(0.028)	(<0.001)	(0.232)
Thryssa scratchleyi	8	0.681	0.742*	0.855	0.811	5	0.447	0.887*	0.995*	0.431
		(0.063)	(0.035)	(0.065)	(0.096)		(0.451)	(0.045)	(<0.001)	(0.247)

Note: Values in parentheses are confidence level. Relationships that are significant at the 95% confidence level are indicated by an asterisk (*).

[a] For length and mass correlation data.

[b] For $\delta^{13}C$ and $\delta^{15}N$ correlation data.

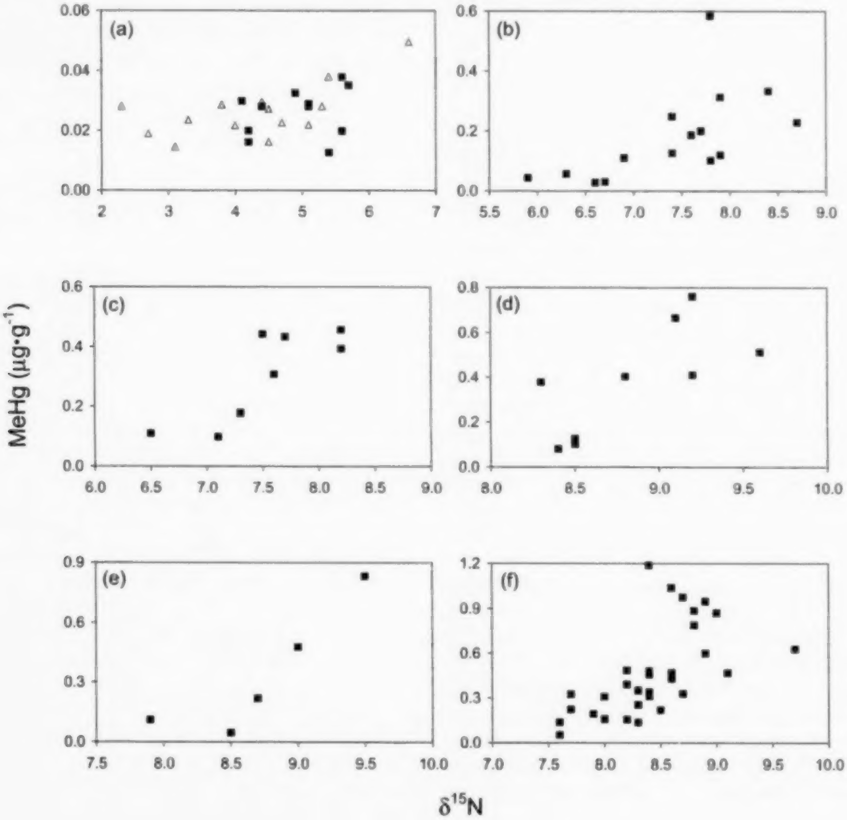

Fig. 5. Relationship between MeHg concentration and $\delta^{15}N$ value for each fish species. (*a*) *Nematalosa flyensis* (■) and *N. papuensis* (△). (*b*) *Arius berneyi*. (*c*) *Toxotes chatareus*. (*d*) *Strongylura kreffti*. (*e*) *Thryssa scratchleyi*. (*f*) *Lates calcarifer*.

length. The pathway of mercury bioaccumulation is of interest, as *T. chatareus* is predominantly a specialised insectivore. Stable-isotope measurements (Table 1; Bowles 1998) showed that the food web of *T. chatareus* was partly influenced by energy derived from aquatic macrophytes. However, compared with seston, these plants were very low in MeHg (Table 2) and would not account for the MeHg concentrations observed in *T. chatareus*. This suggests either a slow rate of growth with age (time-dependent mercury bioaccumulation) or a very efficient mercury biomagnification pathway via aquatic insects. An additional possibility, supported by the high $\delta^{15}N$ values of some individual specimens, is that *T. chatareus* may be partly piscivorous. To better understand mercury bioaccumulation in this species, mercury concentrations and stable-isotope ratios need to be measured in their insect prey.

The *L. calcarifer* data displayed a distinct curvilinear relationship between total mercury and fish length, with little change in mercury concentration in fish between 550 and 750 mm long. This trend was not accounted for by similar trends in the $\delta^{15}N$ value versus length relationship for this fish, which was reasonably linear over the entire size range (Bowles 1998). The *L. calcarifer* data displayed covariance between MeHg, fish length, and $\delta^{15}N$ (Table 4). This is consistent with an increase in trophic position with size and, hence, an increase in the amount of MeHg in prey. There are, however, several factors that complicate the interpretation of the data. *Lates calcarifer* are migratory and regularly move from Lake Murray to the Gulf of Papua to spawn (Moore and Reynolds 1982). Juveniles remain in salt water until they are 200–300 mm in length before they migrate to fresh waters (Moore and Reynolds 1982). No data exist on the amount of time the fish spend out of the lake during migration, but it is reasonable to assume that mercury concentrations would be lower in *L. calcarifer* than in nonmigratory fish species that are exposed to higher concentrations of mercury for longer periods of time—assuming that MeHg concentrations are lower in the riverine and estuarine environments downstream of Lake Murray. This appears reasonable, considering that *L. calcarifer* from other rivers that also spawn in the same coastal region have lower concentrations of MeHg (Sorentino 1979; Kyle and Ghani 1982). This may explain, in part, why the slope of the plot of total mercury versus fish length was lowest for *L. calcarifer* among the fish species studied. *Lates calcarifer* is a protandrous hermaphrodite (Moore 1979), beginning its life cycle as a male and changing sex when it grows larger. Any change in metabolism associated with the change in sex could conceivably cause a change in the accumulation of MeHg. Using a length of 870 mm as the criterion to delineate male from female fish (Moore 1979), around 30% of the fish sampled in the current study are female. Aside from some increased variability in the plot of mercury concentration versus fish length at lengths of >900 mm (Fig. 4), sexual transformation appears to have little detectable effect on MeHg bioaccumulation.

Discussion

The data presented in this paper, together with previous studies (Sorentino 1979; Kyle and Ghani 1982), show that mercury is accumulated to levels of regulatory concern by the piscivorous fish of Lake Murray. Over 23% of the piscivorous fish sampled had mercury concentrations exceeding 0.5 $\mu g \cdot g^{-1}$. This is in spite of there being no conspicuously elevated concentrations of inorganic mercury or MeHg in the lake's water column or sediments (Bowles 1998). How can the relatively high concentrations of MeHg in fish be reconciled with the low concentrations of MeHg in the water column? There are two key factors that account for this apparent inconsistency. First, stable-isotope studies indicate that, in spite of the abundance of aquatic and terrestrial vascular plants in Lake Murray, the food webs incorporating the main piscivorous fish are phytoplankton based. The mean seston MeHg concentration of 0.015 $\mu g \cdot g^{-1}$ was at least 50 times that of the aquatic plants sampled. This enrichment is entirely consistent with studies conducted in temperate systems, in which phytoplankton are known to efficiently bioaccumulate MeHg from the water column (Watras and Bloom 1992; Monson et al. 1996; Watras et al. 1998). Second, the stable-isotope studies showed that the food webs incorporating the key piscivorous fish comprise four trophic levels (phytoplankton, zooplankton, planktivore, piscivore). The length of the food chain and the associated biomagnification factors between trophic levels were sufficient to biomagnify MeHg concentrations approximately 30-fold between the seston and piscivorous fish. The relatively high MeHg concentrations in the lake's piscivorous fish are therefore explicable by the efficient bioaccumulation of MeHg at the base of the food web, and the amplification of mercury concentrations afforded by the length of the food chain. Several workers have noted the critical role of pelagic food chain length in mercury bioaccumulation by piscivorous fish in temperate systems (Rask and Metsala 1991; Cabana et al. 1994; Futter 1994). For instance, in Canadian lakes, a five trophic level food chain, which includes forage fish and the crustacean *Mysis relicta*, results in higher mercury concentrations in lake trout (*Salvelinus namaycush*) than do much shorter food chains found in lakes in which trout feed directly on zooplankton (Cabana et al. 1994; Futter 1994).

It was not possible to make many direct comparisons with other tropical-lake systems, owing to the lack of studies conducted in uncontaminated environments. Nevertheless, there are close similarities with temperate-lake systems. Biomagnification factors (a typical range of 6- to 16-fold between piscivores and their prey) in Lake Murray were comparable with those measured in temperate systems (Watras et al. 1998). There was no indication of any anomalously efficient accumulation of mercury by any component of the food web. The greatest biomagnification occurred at the bottom of the food chain and involved the transfer of MeHg from the water column to seston. Lucotte et al. (1999) recently presented detailed food web data for uncontaminated lakes in northern Quebec. The mean dissolved MeHg concentration for these lakes was 0.049 $ng \cdot L^{-1}$ (compared with 0.067 $ng \cdot L^{-1}$ in Lake Murray) and MeHg concentrations in piscivores ranged from 0.3 to 1.41 $\mu g \cdot g^{-1}$. These results are very similar to those reported in this study. In terms of assessing the risk of mercury bioaccumulation, the measurement of MeHg concentrations in waters and sediments alone is of limited value, unless the biomagnification power of the food web is also considered. It is clear that aquatic food chains in both temperate and tropical environments have sufficient biomagnification power to amplify water column MeHg concentrations from very low levels to levels of regulatory concern in piscivorous fish.

Owing to the remote nature of the study location, no data exist to demonstrate whether the observed bioaccumulation of MeHg by piscivorous fish is a phenomenon specific to Lake Murray or whether this phenomenon is also common to the numerous smaller lakes of the region. Given that the food webs and BAFs are likely to be similar in other lowland lakes, similar MeHg concentrations in piscivorous fish may be expected. It is interesting to use the BAFs identified for the Lake Murray system to calculate the fish mercury concentrations that would arise as a consequence of increases in MeHg concentrations in the water column. Hurley et al. (1998) measured water column MeHg concentrations of 0.5–0.8 ng·L^{-1} in the Florida Everglades (a subtropical area of wetlands and lakes known to be contaminated with mercury). These values represent an order of magnitude increase over the concentrations typically observed in Lake Murray. Assuming a MeHg concentration of 0.5 ng·L^{-1} in the water column of Lake Murray and a log BAF of 6.83, the resulting mercury concentration in a 6-kg barramundi would be 3.4 μg·g^{-1}. This value is comparable with the upper range observed for piscivorous fish in the Florida Everglades (Fleming et al. 1995). This calculation illustrates the sensitivity of the system to increases in mercury concentration.

The data for individual piscivore species were notable for the correlations between MeHg, fish length, and δ^{15}N. Importantly, the results indicated that fractional changes in trophic status had a significant effect on the mercury concentrations of individual piscivores. Aside from Kidd et al. (1995), few workers have attempted to make use of stable-isotope data to unravel the role of food web effects in mercury bioaccumulation. It is well established that mercury concentrations increase with fish age (and hence fish size) because of the very slow rate of elimination of MeHg from tissues compared with its rate of uptake (Clarkson 1992). This is the basic process by which MeHg is bioaccumulated. Most available evidence points to dietary uptake as the dominant pathway for mercury bioaccumulation in fish (Hall et al. 1997). Fish that occupy the same trophic position throughout their life are exposed to relatively constant mercury concentrations in their food, and MeHg concentrations will gradually increase with age. Fractional increases in trophic position potentially result in an increase in the MeHg content of prey, with a corresponding increase in the flux of MeHg to the predator and, hence, an increased concentration of MeHg in tissue. Increases in trophic position therefore augment the time-related bioaccumulation of MeHg. Carefully designed studies are required to determine the relative importance of exposure time related and trophic position related MeHg bioaccumulation.

It is worthy of note that, in the planktivores *Nematalosa* spp., there was no relationship between MeHg concentration and δ^{15}N, despite there being well over a one trophic level range in the δ^{15}N data. The large range in δ^{15}N values (2.7–6.6) is a consequence of these fish feeding off a mixture of zooplankton and phytoplankton. A possible explanation for the lack of relationship may be the relatively poor biomagnification in MeHg on trophic transfer between phytoplankton and zooplankton. This is worthy of further investigation.

Most mercury bioaccumulation studies focus on surveying contaminant concentrations and do not usually examine food-web interactions and changes in trophic position within individual fish species. At best, broad assignments of trophic level are given, and change of trophic status with organism age is assumed to be unimportant. This study further illustrates the utility of carbon and nitrogen stable isotope measurements in understanding food-web interactions, and their importance in unravelling the processes of mercury bioaccumulation. Used in conjunction with mercury-concentration and fish-size data, these parameters allow deductions to be made on the processes affecting bioaccumulation in individual fish species.

Acknowledgements

Charles Tabua, Exon Waingut, Jim McNamara, Billy Sari, Bruce Ambrose (Environment Department, Porgera Joint Venture), and Denise Peggs are thanked for their assistance with field work and project planning. Total mercury in fish samples was analysed by Matthew Higham (CSIRO). Stable isotope ratio analyses were performed at the Division of Environmental Sciences, Griffith University, Australia. This project was funded, in part, by Porgera Joint Venture and through an Australian Postgraduate scholarship awarded to Karl Bowles.

References

Abe, T., Ohtsuka, R., Hongo, T., Suzuki, T., Tohyama, C., Nakano, A., Akagi, H., and Akimichi, T. 1995. High hair and urinary mercury levels of fish eaters in the nonpolluted environment of Papua New Guinea. Arch. Environ. Health, **50**: 367–373.

Akagi, H., Malm, O., and Kinjo, Y. 1995. Methylmercury pollution in the Amazon, Brazil. Sci. Total Environ. **175**: 85–95.

Atwell, L., Hobson, K.A., and Welsh, H.E. 1998. Biomagnification and bioaccumulation of mercury in an artic marine food web: insights from stable nitrogen isotope analysis. Can. J. Fish Aquat. Sci. **55**: 1114–1121.

Bowles, K.C. 1998. The cycling of mercury in Australasian aquatic systems. Ph.D. thesis, University of Canberra, Australia.

Bunn, S.E., and Boon, P.I. 1993. What sources of organic carbon drive food webs in billabongs? A study based on stable isotope analysis. Oecologia, **96**: 85–94.

Cabana, G., Tremblay, A., Kalff, J., and Rasmussen, J.B. 1994. Pelagic food chain structure in Ontario lakes: a determinant of mercury levels in lake trout (*Salvelinus namaycush*). Can. J. Fish. Aquat. Sci. **51**: 381–389.

Clarkson, T.W. 1992. Mercury: major issues in environmental health. Environ. Health Perspect. **100**: 31–38.

Davies, R.P., and Dobbs, A.J. 1984. The prediction of bioconcentration in fish. Water Res. **18**: 1253–1262.

De Niro, M., and Epstein, S. 1978. Influence of diet on the distribution of carbon isotopes in animals. Geochim. Cosmochim. Acta, **42**: 495-506.

Fischer, R., Rapsomanikis, S., and Andreae, M.O. 1993. Determination of methylmercury in fish samples using GC/AA and sodium tetraethylborate derivatization. Anal. Chem. **65**: 763–766.

Fleming, L.E., Watkins, S., Kaderman, R., Levin, B., Ayyar, D.R., Bizzio, M., Stephens, D., and Bean, J.A. 1995. Mercury exposure in humans through food consumption from the Everglades of Florida. Water Air Soil Pollut. **80**: 41–48.

France, R.L. 1996. Carbon-13 conundrums: limitations and cautions in the use of stable isotope analysis in stream ecotonal research. Can. J. Fish. Aquat. Sci. **53**: 1916-1919.

Futter, N.M. 1994. Pelagic food-web structure influences probability of mercury contamination in lake trout (*Salvelinus namaycush*). Sci. Total Environ. **145**: 7–12.

Hall, B.D., Bodaly, R.A., Fudge, R.J., Rudd, J.W., and Rosenberg, D.M. 1997. Food as the dominant pathway of methylmercury uptake by fish. Water Air Soil Pollut. **100**: 13–24.

Hamilton, S.K., Lewis, W.M., and Sippel, S.J. 1992. Energy sources for aquatic animals in the Orinoco River floodplain: evidence from stable isotopes. Oecologia, **89**: 324-330.

Hill, W.R., Stewart, A.J., and Napolitano, G.E. 1996. Mercury speciation and bioaccumulation in lotic primary producers and primary consumers. Can. J. Fish. Aquat. Sci. **53**: 812–819.

Hurley, J.P., Krabbenhoft, D., Cleckner, L.B., King, S.A., and Olsen, M.L. 1998. System controls on the aqueous mercury distribution in the northern Everglades. Biogeochemistry (Dordr.), **40**: 293–311.

Jarman, W.M., Hobson, K.A., Sydeman, W.J., Bacon, C.E., and McLaren, E.B. 1996. Influence of trophic position and feeding location on contaminant levels in the Gulf of Farallones food web revealed by stable isotope analysis. Environ. Sci. Technol. **30**: 654–660.

Kelly, C.A., Rudd, J.W.M., St. Louis, V.L., and Heyes, A. 1995. Is total mercury concentration a good predictor of methyl mercury concentration in aquatic systems? Water Air Soil Pollut. **80**: 715–724.

Kidd, K.A., Hesslein, R.H., Fudge, R.J.P., and Hallard, K.A. 1995. The influence of trophic level as measured by δ^{15}N on mercury concentrations in freshwater organisms. Water Air Soil Pollut. **80**: 1011–1015.

Kyle, J.H., and Ghani, N. 1982. Mercury concentrations in ten species of fish from Lake Murray, western province. Sci. New Guinea, **9**: 48–58.

Lange, T.R., Royals, H.E., and Connor, L.L. 1993. Influence of water chemistry on mercury concentration in largemouth bass from Florida lakes. Trans. Am. Fish. Soc. **122**: 74–84.

Lee, Y.-H., and Hultberg, H. 1990. Methylmercury in some Swedish waters. Environ. Toxicol. Chem. **9**: 833–841.

Liang, L., and Bloom, N.S. 1993. Determination of total mercury by single-stage gold amalgamation with cold vapour atomic spectrometric detection. J. Anal. At. Spectrom. **8**: 591–594.

Liang, L., Horvat, M., and Bloom, N.S. 1994. An improved speciation method for mercury by GC/CVAFS after aqueous phase ethylation and room temperature precollection. Talanta, **41**: 371–379.

Lucotte, M., Schetagne, R., Therien, N., Langlois, C., and Tremblay, A. 1999. Mercury in the biogeochemical cycle. Natural environments and hydroelectric reservoirs of Northern Quebec, Canada. Springer-Verlag, Berlin, Heidelberg, New York.

Mackenzie, C.J.G., and Kyle, J.H. 1984. Two examples of environmental problems occurring in remote sparsely populated areas. Ann. Acad. Med. Singapore, **13**: 237–246.

Mathers, R.A., and Johansen, P.H. 1985. The effects of feeding ecology on mercury accumulation in walleye (*Stizostedion vitreum*) and pike (*Esox lucius*) in lake Simcoe. Can. J. Zool. **63**: 2006–2012.

Minagawa, M., and Wada, E. 1984. Stepwise enrichment of ^{15}N along food chains: further evidence and the relation between δ^{15}N and animal age. Geochim. Cosmochim. Acta, **48**: 1135-1140.

Monson, B., Brezonik, P., Strassman, R., and Swain, E. 1996. Seasonal patterns of mercury species in water and plankton from low softwater lakes in northeastern Minnesota. Biogeochemistry (Dordr.), **40**: 147–162.

Moore, R. 1979. Natural sex inversion in the giant perch (*Lates calcarifer*). Aust. J. Mar. Freshw. Res. **30**: 803–813.

Moore, R., and Reynolds, L.F. 1982. Migration patterns of Barramundi, *Lates calcarifer* (Bloch), in Papua New Guinea. Aust. J. Mar. Freshw. Res. **33**: 671–682.

Onaga, I.I. 1993. The total mercury concentrations in fish from certain southern coastal waters and North Solomons Province of Papua New Guinea. P. N. G. J. Agric. For. Fish. **36**: 22–28.

Peterson, B.J., and Fry, B. 1987. Stable isotopes in ecosystem studies. Annu. Rev. Ecol. Systematics, **18**: 293-320.

Rask, M., and Metsala, T.R. 1991. Mercury concentrations in northern pike *Esox lucius* L., in small lakes of the Evo area, Southern Finland. Water Air Soil Pollut. **56**: 369–378.

Roberts, T.R. 1978. An icthyological survey of the Fly River in Papua New Guinea with descriptions of new species. Smithsonian Contrib. Zool. No. 281.

Sorentino, C. 1979. Mercury in marine and freshwater fish of Papua New Guinea. Aust. J. Mar. Freshw. Res. **30**: 617–623.

Watras, C.J., and Bloom, N.S. 1992. Mercury and methylmercury in individual zooplankton: implications for bioaccumulation. Limnol. Oceanogr. **37**: 1313–1318.

Watras, C.J., Bloom, N.S., Hudson, R.J.M., Gherini, S., Munson, R., Claas, S.A., Morrison, K.A., Hurley, J.P., Wiener, J.G., Fitzgerald, W.F., Mason, R.P., Vandal, G.M., Powell, D.E., Rada, R.G., Rislov, L., Winfrey, M.R., Elder, J., Krabbenhoft, D., Andren, A.W., Babiarz, C.L., Porcella, D.B., and Huckabee, J.W. 1994. Sources and fates of mercury and methylmercury in Wisconsin lakes. *In* Mercury pollution: integration and synthesis. *Edited by* C.J. Watras and J.W. Huckabee. Lewis Publishers, Boca Raton. pp. 153–179.

Watras, C.J., Back, R.C., Halvorsen, S., Hudson, R.J.M., Morrison, K.A., and Wente, S.P. 1998. Bioaccumulation of mercury in pelagic freshwater foodwebs. Sci. Total Environ. **219**: 183–208.

Dreissena distribution in commercial waterways of the U.S.: using failed invasions to identify limiting factors

Yvonne C. Allen and Charles W. Ramcharan

Abstract: Preventing the introduction of an invasive species and managing the ecological and economic effects of successful invasions often rely on accurate predictions of the potential distribution of the species in its new habitat. Instances of failed invasion can highlight factors other than dispersal that limit range expansion in an invasive species. The commercially available waterways (CAWs) of the U.S. are a network of interconnected rivers that support a regular traffic of commercial and maintenance vessels. As such, they are at extremely high risk of infestation from *Dreissena*, yet not all the rivers are infested. We used traffic, water chemistry, and impoundment characteristics of the rivers in this system to develop a set of logistic-regression models to predict the occurrence of *Dreissena*. Four single variable models correctly classified 20 out of 24 (83%) river systems. The best two-variable models had only one misclassified river, for an overall accuracy of 96%. Among rivers to which *Dreissena* has successfully dispersed, permanent populations are most likely to establish in systems that have moderate ionic strength and that also have some impoundment areas to increase long-term population persistence. We use this hierarchy of factors to extend predictions to four systems that currently lack the high dispersal intensity of the CAWs.

Résumé : Des prédictions précises sur le potentiel de dispersion d'une espèce envahissante dans son nouvel habitat permettent souvent de prévenir l'introduction de l'espèce et de gérer les effets écologiques et économiques en cas d'invasion réussie. Des exemples d'invasions manquées peuvent mettre en lumière des facteurs autres que le pouvoir de dispersion qui limitent l'aire d'expansion d'une espèce envahissante. Les cours d'eau ouverts au commerce (CAWs) aux États-Unis forment un réseau de rivières interconnectées qui supportent un trafic régulier de navires commerciaux et de navires d'entretien. Ils sont ainsi à très haut risque d'infestation par *Dreissena*, bien que tous n'aient pas été envahis. Des données sur le trafic maritime, la chimie de l'eau et les caractéristiques des barrages dans ces rivières ont servi à élaborer une série de modèles de régression logistique pour prédire la présence de *Dreissena*. Quatre modèles à une seule variable ont classifié correctement 20 des 24 (83%) systèmes hydrographiques. Les meilleurs modèles à deux variables n'ont fait qu'une seule erreur de classification, pour une précision générale de 96%. Parmi les rivières où *Dreissena* s'est établi avec succès, les populations permanentes sont le plus susceptibles de se retrouver dans les systèmes qui ont une charge ionique modérée et qui possèdent des réservoirs qui favorisent la persistance à long terme. Cette hiérarchie de facteurs a servi à faire des prédictions au sujet de quatre systèmes hydrographiques qui ne présentent pas le potentiel élevé de dispersion des CAWs.

[Traduit par la Rédaction]

Introduction

Preventing the introduction of an invasive species and managing the ecological and economic effects of successful invasions often rely on accurate predictions of the potential distribution of the invasive species. Presently, the most reliable predictive models incorporate a detailed understanding of the pathway of introduction, as well as species-specific information on life-history traits, tolerance limits, and potential biotic interactions of the invasive species (Simberloff 1989). Analyses of successful invasions highlight the situations in which the requirements for invasion were met. That a species is not found in a particular environment can be the result of either nondispersal or failed invasion. If dispersal criteria were not met, analysis of distribution patterns will reveal little about species-specific requirements. Failed invasion, on the other hand, implies that dispersal requirements have been met but that the invasion failed, owing to a mismatch of factors related to species-specific limitations. By identifying the importance of factors that cause failed invasions, we can build more accurate models to determine the risk of invasion into novel habitats (Drake et al. 1989).

The invasion of North America by the zebra mussel, *Dreissena polymorpha*, provides an example of an invasive organism that has infested a large geographic area representing a diversity of habitat types. *Dreissena polymorpha* was introduced into the Great Lakes in the mid-1980s. Range expansion through the freshwater ecosystems of the Great Lakes and into the connected waterways of the Mississippi

Received March 8, 2000. Accepted February 16, 2001. Published on the NRC Research Press Web site on April 12, 2001.
J15654

Y.C. Allen.[1] Coastal Fisheries Institute, Louisiana State University, Baton Rouge, LA 70803, U.S.A.
C.W. Ramcharan. Department of Biological Sciences, Louisiana State University, Baton Rouge, LA 70803, U.S.A.

[1] Corresponding author (e-mail: allenyc@lsu.edu).

Can. J. Fish. Aquat. Sci. **58**: 898–907 (2001) DOI: 10.1139/cjfas-58-5-898

Fig. 1. The maximum extent of river kilometres infested by *D. polymorpha* in the commercially available waterways (CAWs) of the Mississippi River drainage basin in the 1990s. The total number of infested river kilometres for each year was determined by noting the farthest upstream *D. polymorpha* population (United States Geological Survey 1998). If *D. polymorpha* was found at an upstream location, the remainder of the downstream system was also presumed to be infested. The total number of river kilometres in the system (see Fig. 2) is indicated by the top line. *Dreissena polymorpha* remains absent from 37% of the interconnected CAWs.

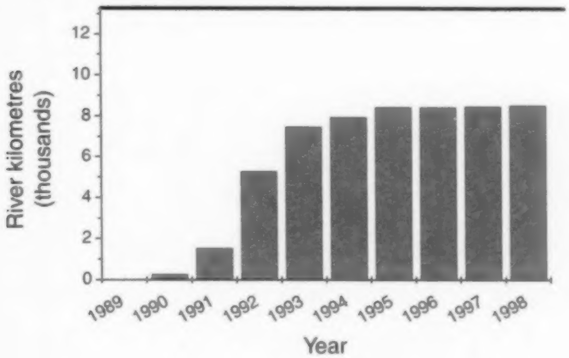

River drainage basin was extremely rapid in the early 1990s (United States Geological Survey 1998; Fig. 1). Maps of *D. polymorpha* distribution in North America needed to be updated every few months in the early 1990s, and it appeared as though all the major river systems and lakes in the eastern United States and Canada would rapidly be plagued by population explosions of *D. polymorpha* (Ludyanskiy et al. 1993).

While the range of *D. polymorpha* continued to expand into suitable inland lakes through 1998 (United States Geological Survey 1998), in recent years, expansion into rivers in the Mississippi River drainage that are open to commercial navigation through direct traffic has slowed dramatically (Fig. 1). This decline in the rate of invasion has occurred despite the fact that eight uninfested river systems are directly connected to heavily infested waterways (United States Geological Survey 1998; Fig. 2). Therefore, there must be some characteristics of the vector of dispersal, or of the interaction of the organism with its environment, that has limited the expansion of *D. polymorpha* into these rivers.

Models to predict *D. polymorpha* occurrence have generally considered either human-activity patterns as a surrogate for dispersal (Johnson and Padilla 1996; Schneider et al. 1998; Buchan and Padilla 1999) or the physiological tolerance limits of *D. polymorpha* (Ramcharan et al. 1992; Mellina and Rasmussen 1994; but see Neary and Leach 1992). Many other studies have identified individual factors that impact *D. polymorpha* growth and survival and may influence distribution (McMahon 1996; Karateyev et al. 1998; Madon et al. 1998). A successful invasion implies, however, that all minimal dispersal, physiological, and ecological tolerance requirements have been met.

In this study, we focus on the commercially available waterways (CAWs) of the U.S. in which *D. polymorpha* dispersal is intense and continuous. In this system, commercial and maintenance vessels regularly travel between river systems with *D. polymorpha* attached to their hulls. Any absence of *D. polymorpha* in the river can, therefore, be considered a failed invasion. We used logistic regression to further examine the factors that appeared to critically limit *D. polymorpha* distribution within the CAWs. This study is the first large-scale empirical evaluation of factors influencing *D. polymorpha* distribution since its introduction into North American waters. Unlike European systems, which have been the focus of other predictive efforts (Strayer 1991; Ramcharan et al. 1992), the CAWs cover a very wide range of hydrology, water quality, and climatic characteristics. We use the results from our analyses to gauge the risk of *D. polymorpha* colonization of presently uninfested waters in four river systems that lack high dispersal intensity.

Methods

Area of analysis

Dispersal is the primary factor limiting *D. polymorpha* expansion into novel environments. To focus on failed invasions, we sought to limit our analysis to waters that have had certain opportunity for infestation, through either passive or active dispersal. Passive dispersal occurs through an obligate planktonic larval (veliger) stage that is directed by water flow. *Dreissena polymorpha* produces abundant propagules (Borcherding 1992) and can rapidly colonize suitable areas, both within a lake and in other lakes and rivers downstream (Griffiths et al. 1991; Horvath et al. 1996). Upstream dispersal by passive transport may be very slow or impossible in rivers, but active dispersal via human activities can greatly accelerate the transport of *D. polymorpha* upstream. Human activities also provide overland dispersal and access to isolated watersheds (Morton 1993; Johnson and Padilla 1996; Buchan and Padilla 1999).

The CAWs of the U.S. are a network of rivers that support a regular traffic of commercial and maintenance vessels (Fig. 2). The extent of the CAWs was defined by the presence of a 9-ft minimum channel depth (1 ft = 0.3048 m) maintained for navigation and the existence of reported commercial-traffic statistics (United States Army Corps of Engineers 1998). The majority of this network lies within the Mississippi River drainage basin. Commercial navigation is limited at the most-upstream reaches of the network by fixed dams, with no opportunity for direct vessel passage.

The operation and structure of commercial and maintenance vessels provide an ideal mechanism for *D. polymorpha* dispersal. Most commercial vessels are in continual operation and are brought into dry dock only for repairs or scheduled maintenance. *Dreissena polymorpha* is typically removed at dry-docking (Y. Allen, unpublished data), but the time between dry-docking can be 6 months to a year or more. During this period, *D. polymorpha* can attach to the sea chest, internal piping, and hull (Keevin et al. 1992; Stafford 1995; Allen 1999). The typical range of operation for many commercial and maintenance vessels includes multiple river systems, so an infested vessel can disperse *D. polymorpha* widely, and an uninfested vessel faces a high probability of acquiring *D. polymorpha* by passing through an infested area.

Because of the nature of traffic patterns, we can assume that *D. polymorpha* has been introduced into that portion of the CAWs that is open to unimpeded traffic from other infested fresh waters. We therefore restricted further analysis to 24 river systems within the CAWs that have had the opportunity to be infested by *D. polymorpha* (Table 1). The Columbia, Chattahoochee, Connecticut, and Savannah rivers were not used to generate the predictive models.

Fig. 2. The extent of the commercially available waterways (CAWs) in the U.S. are indicated with thick lines. CAWs having a *D. polymorpha* population are indicated in black and uninfested waters are indicated in grey. The Mohawk River is not part of the CAWs but its location is indicated to highlight the connection of the Hudson River to infested areas in the Great Lakes. Open triangles indicate the location of United States Geological Survey sampling stations (Alexander et al. 1996) used in the logistic-regression analyses. Filled triangles indicate United States Geological Survey sampling locations for rivers outside of the CAWs.

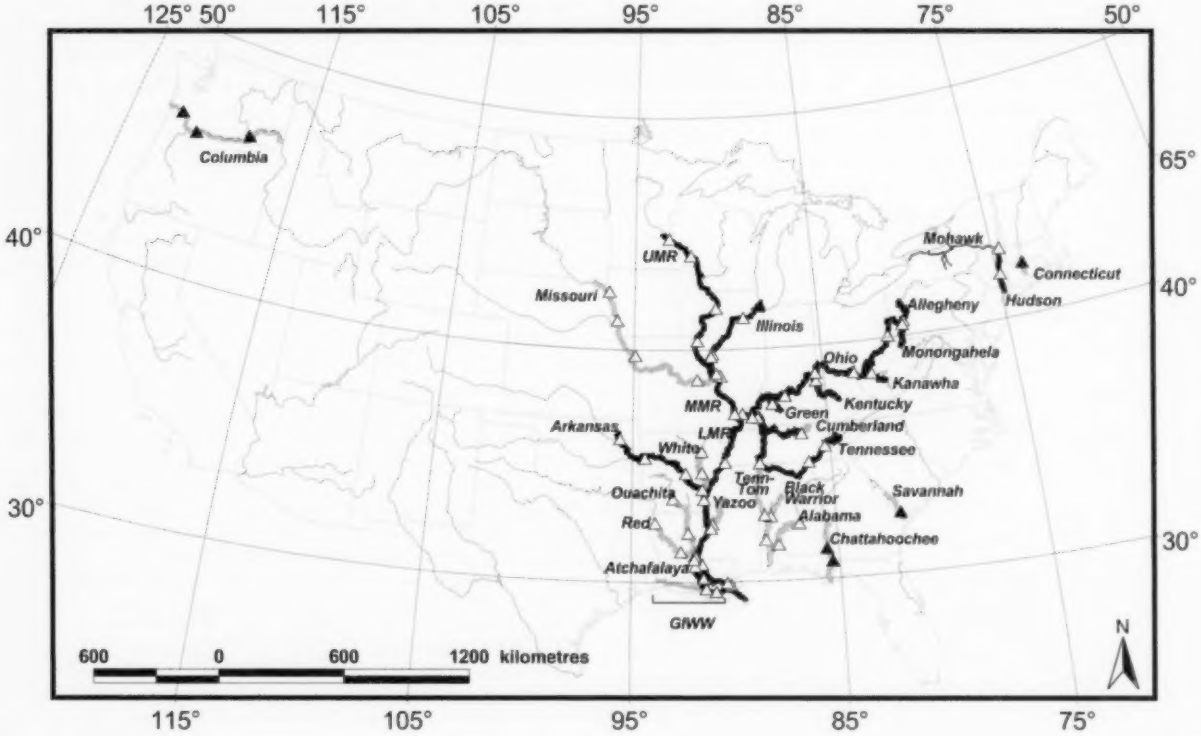

Logistic regression

We used logistic regression (Hosmer and Lemeshow 1989; Statistica version 5.1, StatSoft Inc.) to identify the factors, other than dispersal, that affect *D. polymorpha* population establishment. The advantages of logistic regression over other methods, such as linear regression and discriminant-function analysis, are that independent variables can be binary or dichotomous, non-normality of variables does not seriously affect the model outcomes, and the response variable can be binary. In our study, the response variable was presence or absence of *D. polymorpha* in 24 river systems. Explanatory variables were related to water quality, hydrology, and traffic (Table 2). All explanatory variables were continuous, except for the presence of impoundments, which was dichotomous. Biases in a regression analysis that may be caused by extreme values can be reduced by log-transformation. However, models using untransformed variables are often easier to interpret. Therefore, we performed our logistic-regression analyses on both log-transformed and untransformed variables. If the results were the same, we present the models constructed using untransformed data and only use models based on log-transformed variables when classification accuracy is improved.

Classification was based on the estimated probability, P (scaled from 0 to 1), of a river system supporting *D. polymorpha*. Formally, P values below 0.5 indicate absence of *D. polymorpha*, and values equal to and above 0.5 indicate presence of *D. polymorpha*. However, P values that are near 0.5 are more correctly interpreted as an ambiguous classification.

Although our data set included 35 variables, we chose not to use stepwise logistic regression. In a stepwise approach, the importance of each predictor variable is determined by a loglikelihood ratio χ^2 test. Unfortunately, with the low degrees of freedom available in a data set with only 24 cases, we could not be confident of the statistical rigor of the stepwise method (Hosmer and Lemeshow 1989). Instead, we developed our models to predict presence and absence of *D. polymorpha* using a purposeful rather than a statistical selection of variables. We chose variables based on biological relevance. In Results, we present all the one- and two-variable models that correctly classified the greatest number of river systems, rather than selecting models based strictly on statistical significance level.

We used the best of our models to predict presence or absence of *D. polymorpha* in currently uninfested waterways. Several inland navigable waterways are not connected to the CAWs of the Mississippi River basin (Fig. 2) and, as such, lack the high dispersal intensity of rivers in the CAWs. We have limited our predictions to these rivers, because they fall under the purview of the United States Army Corps of Engineers and, therefore, we have good information about configuration of impoundments.

Water-quality parameters

Previous models have focused on the importance of various water-quality variables to predict *D. polymorpha* distribution (Strayer 1991; Ramcharan et al. 1992; Mellina and Rasmussen 1994). Analyses of empirical European water quality data (Strayer 1991; Ramcharan et al. 1992) have, however, had to rely on sporadic published accounts of water quality. For our analysis, we used a comprehensive water quality data set collected by the United States Geological Survey from 1975 to 1995 at riverine

Table 1. Summary of selected water-quality, traffic, and hydrologic data.

					Water chemistry					
River system	L&D	Drift	Traffic (1995)	WQ stns	Ca^{2+} ($mg \cdot L^{-1}$)	Mg^{2+} ($mg \cdot L^{-1}$)	Total hardness ($mg \cdot L^{-1}$)	T (°C)	Total suspended sediments ($mg \cdot L^{-1}$)	Conductivity ($\mu S \cdot cm^{-1}$)
Connected river systems with *D. polymorpha*										
UMR	28		11 962	5	49 (39–62)	18.7 (15.0–23.7)	199 (162–253)	12.4 (10.9–14.2)	96 (21–205)	434 (347–546)
MMR	1	Drift	12 549	1	51.5	18.8	207	14.7	377	516
LMR	0	Drift	36 612	6	39 (38–39)	12 (11.5–12.5)	148 (142–152)	17.3 (16.0–18.3)	208 (169–275)	387 (367–407)
Illinois	8	Drift	4 966	3	66 (63–67)	25.6 (24.6–26.9)	269 (268–270)	13.9 (13.3–14.4)	195 (143–247)	604 (370–757)
Ohio	20	Drift	42 514	5	35 (33–37)	9.4 (8.9–10.2)	126 (118–136)	15.3 (14.4–16.2)	105 (77–143)	340 (301–355)
Hudson	1	Drift	4 054	2	22.1 (22–24)	4.1 (4.0–4.4)	72 (69–75)	11.9 (11.7–12.2)	24 (17–41)	198 (193–202)
Allegheny	8		2 575	1	25	6.8	91	12.5	38	252
Monongahela	10		8 563	1	33	8.4	116	14.5	48	357
Kanawha	3		4 764	1	16	5.3	61	15	57	207
Kentucky	4		100	1	38	8.4	129	15.4	86	299
Green	2		1 214	1	40	9.3	137	16.4	89	310
Cumberland	4		1 395	2	26 (23–28)	4.6 (4.3–5.0)	83 (78–87)	15.3 (13.8–16.7)	22 (20–23)	188 (176–200)
Tennessee	9		5 615	4	19.7 (19–20)	4.1 (3.5–4.7)	66 (64–68)	17.1 (16.4–17.8)	13 (9–17)	163 (160–166)
Atchafalaya	1	Drift	3 486	4	34 (31–35)	10.2 (9.5–10.7)	126 (118–131)	19.5 (18.6–21.2)	259 (123–334)	362 (331–376)
Arkansas	15		6 900	3	36.6 (31–45)	8.0 (7.5–8.2)	126 (113–147)	17.3 (16.4–18.0)	70 (57–94)	484 (432–528)
Connected river systems without *D. polymorpha*										
Tenn-Tom	10		944	2	15.4 (15.2–15.6)	2.2 (1.4–3.0)	50	19.3 (19.1–19.5)	71	140 (123–158)
Black Warrior	4		3 216	1	11.5	6	53	19.6	38	173
Alabama	3		195	2	10.7 (9.3–12.0)	2.8 (2.7–2.8)	38 (35–41)	19.4 (19.1–19.8)	40 (28–51)	110 (99–120)
Ouachita	3		278	2	8.3 (7.3–9.2)	1.8 (1.5–2.2)	28 (24–32)	18.6 (17.3–19.9)	47 (43–49)	134 (84–185)
Yazoo	0		142	1	10.4	3.5	40	19.6	222	121
Missouri	0		11 136	5	61 (54–65)	21.5 (17.4–24.1)	240 (205–261)	12.8 (12.1–15.2)	690 (356–1102)	702 (576–750)
White	0		90	2	31 (28–33)	12.5 (11.3–13.6)	128 (140–115)	15.9 (15.4–16.8)	73 (63–83)	256 (235–277)
Red	5		536	2	38 (28–46)	10.2 (7.4–12.7)	137 (100–168)	19.9 (19.3–20.4)	447 (268–626)	540 (432–656)

Note: Only connected river system data were used in the logistic-regression analyses. L&D and drift indicate the number of locks and dams present on the river system and whether there is potential for passive veliger drift into the system from *D. polymorpha* populations located in an upstream lake or impoundment within the commercially available waterways. The volume of commercial traffic was determined from waterborne-commerce statistics compiled by the United States Army Corps of Engineers and is expressed as the number of self-propelled upbound tow and tug trips. WQ stns indicates the number of water quality stations incorporated into the analysis. Water-chemistry variables are average annual values within a river system. Values in parentheses are minimum and maximum annual averages from stations within a river system (see text). UMR, MMR, and LMR indicate the upper, middle, and lower sections of the Mississippi River, respectively (see Fig. 2).

sites across the U.S. (Alexander et al. 1996). We selected all sampling stations located within the CAWs on the 24 river systems open to active dispersal (Fig. 2). For each station, we determined monthly averages for each variable. We used the monthly values to determine an annual average for each station and variable. We then summarized all the annual averages from all stations within a river system, to assign a single value for each variable and river system. We chose to use annual rather than seasonal averages to reduce problems associated with defining a "season" over such a broad geographic range. In the logistic regression, we included only chemical and physical variables that have been shown to variously affect *D. polymorpha* survival, growth, and reproduction (McMahon 1996; Table 2).

Hydraulic considerations

We included a dichotomous variable, impoundment, to reflect whether each river system had the potential to support a persistent

Table 2. Correlation matrix of selected variables used in the logistic regression.

Variable	Log(traffic)	*T* (°C)	Conductivity (µS·cm^{-1})	pH	Alkalinity (mg·L^{-1})	Ca^{2+} (mg·L^{-1})	Total hardness (mg·L^{-1})	Mg^{2+} (mg·L^{-1})	Total suspended sediments (mg·L^{-1})
Log(traffic)	1.00								
T	–0.37	1							
Conductivity	0.47	–0.32	1.00						
pH	0.25	–0.32	*0.57*	1.00					
Alkalinity	0.27	–0.35	*0.81*	*0.80*	1.00				
Ca^{2+}	0.44	–0.49	*0.92*	*0.63*	*0.89*	1.00			
Total hardness	0.43	–0.48	*0.92*	*0.64*	*0.92*	*0.99*	1.00		
Mg^{2+}	0.40	–0.45	*0.87*	*0.62*	*0.93*	*0.93*	*0.98*	*1.00*	
Total suspended sediments	0.17	–0.03	*0.74*	0.43	*0.59*	*0.59*	*0.60*	*0.60*	1

Note: Selected variables are those discussed in the text. Additional variables considered in the logistic regression include bicarbonate, dissolved chloride, total nitrogen, dissolved nitrogen, dissolved nitrite, dissolved nitrate, dissolved ammonia, total phosphorus, dissolved phosphorus, dissolved oxygen, fluoride, potassium, sodium, sulfate, silica dioxide, total carbon, total organic carbon, and dissolved organic carbon. Values in italics are statistically significant correlations at $\alpha = 0.01$. Traffic was log-transformed, because the values covered a very wide range. Correlations for log-transformed values of the other variables showed the same trends as the untransformed data and are not presented here. The volume of commercial traffic is expressed as the number of self-propelled upbound tow and tug trips in 1995.

population of *D. polymorpha*. Maintenance of a population under free-flowing conditions is difficult, because *D. polymorpha* has an obligate planktonic stage that would be continually swept downstream. The inoculation of *D. polymorpha* into a river system could result in a persistent population, if the river system contains some areas of low or no flow during at least some portions of the year to allow for larval development and resettlement. Several authors have found that impoundments (Horvath et al. 1996; Walz and Welker 1998), storage areas (Reynolds et al. 1991), shallow reaches (Reckendorfer et al. 1999), backwaters, and lock and dam systems (Kern et al. 1994) can provide suitable areas for maintaining plankton populations within a river. Sparks et al. (1998) indicate that the locks and dams on the Upper Mississippi River system have enlarged the extent of backwaters present during summer low-flow periods. Systems of locks and dams were built on many river systems within the CAWs (Table 1), to maintain a minimum pool depth for navigation, particularly during summer low flow conditions. The seasonally increased backwater and impoundment areas created by the system of locks and dams may, therefore, allow *D. polymorpha* populations to more easily develop in rivers. Based on the above, we considered the requirement of impoundment satisfied if a system of locks and dams was present on the river system.

A *D. polymorpha* population in a river could also be apparently persistent if an upstream lake, impoundment, or tributary was also infested. The upstream population could then resupply both a local and a downstream population (Horvath et al. 1996). Although the lower Mississippi River does not have a series of locks and dams, and there may not be any means of establishing a persistent population strictly within it, the requirement of impoundment was satisfied because it has infested tributaries.

Traffic

The volume of commercial and maintenance traffic may also affect the opportunity for *D. polymorpha* dispersal into the CAWs. Rivers that are infrequently visited by commercial and maintenance traffic may be more resistant to infestation by *D. polymorpha*. The variable "traffic volume" used in our analysis was defined as the number of self-propelled upbound vessel trips reported for each river (United States Army Corps of Engineers 1998).

Current distribution

Current *D. polymorpha* distribution patterns were used to determine the value of the response variable in the logistic regression. Presence–absence values were derived from data and maps provided by the Biological Resource Division of the United States Geological Survey (United States Geological Survey 1998) and National Zebra Mussel Clearinghouse maps (New York Sea Grant 1998). Officials from state and federal agencies were contacted by telephone to confirm the presence or absence and extent of *D. polymorpha* infestation in each river. Where data showed only a single record from a river, the original source of the report was contacted to determine the current status of *D. polymorpha* in that system. If follow-up investigations showed no subsequent sitings, the waterway was classified as not currently having a *D. polymorpha* population. Where data showed no *D. polymorpha* in a river, agency personnel were queried to determine whether current monitoring efforts were adequate to find *D. polymorpha*. Perhaps because of high interest in *D. polymorpha* infestation, monitoring activities had been conducted in each of the 24 river systems used in the logistic-regression analyses. The activities were usually conducted by United States Army Corps of Engineers personnel at locks and dams. On river systems without locks and dams, navigation buoys or concrete blocks were used to monitor for *D. polymorpha*.

Although the uppermost reaches of the navigable Cumberland River are not infested with *D. polymorpha* (Fig. 2), the Cumberland River system was classified as having *D. polymorpha*, since the most upstream water-quality station is within the infested reach of river (Fig. 2). Likewise, the western reach of the Gulf Intracoastal Waterway (GIWW) remains uninfested; however, the only available water-quality data are from stations in the infested eastern portion of the waterway and, therefore, we classified the GIWW as infested.

Because of its great length and changing character, the Mississippi River was considered as three separate systems—the upper, middle, and lower Mississippi Rivers. The upper Mississippi River (UMR) runs from the head of navigation to the confluence with the Missouri River. This section of river has a large series of lock and dams, extensive backwater areas, and moderate suspended sediment. At St. Louis, the sediment-rich waters from the Missouri River join the Mississippi and contribute a volume of water approximately equal to the UMR (Meade 1995), dramatically changing the character of the Mississippi to the confluence with the Ohio River. Because of the change in water quality and the number of lock and dams, we have designated this section of river as the middle Mississippi River (MMR). The character of the Mississippi changes again at the confluence with the Ohio River. The waters of the Ohio are similar to those of the UMR (Table 1) and contribute an equal volume of water. Additionally, there are no locks and dams on the Mississippi River below its confluence with the Ohio River. We therefore consider the lower Mississippi River (LMR) to be the reach of the Mississippi from the confluence of the Ohio River to the mouth at the Gulf of Mexico. All other rivers were considered as single river systems (Fig. 2).

Results

Four single-variable models correctly classified 20 out of 24 (83%) river systems (Table 3). The Missouri, Red, and White rivers were all predicted to have *D. polymorpha* but do not, according to these models (Missouri, $P = 0.92–0.93$; Red, $P = 0.77–0.85$; White, $P = 0.67–0.79$, for the four models). Only single sitings and not established populations have been reported for each of these three rivers (United States Geological Survey 1998). *Dreissena polymorpha* was also weakly predicted to be absent from the Kanawha River ($P = 0.47–0.49$ for the four models), but *D. polymorpha* has, in fact, been found there. Three of the four single variables were related to ionic concentration, indicating the robustness of this characteristic in describing *D. polymorpha* presence or absence. These three variables were strongly correlated with one another (Table 2) and, therefore, indicate redundant results.

We were able to increase the number of correctly classified rivers by considering two-variable models that included a variable related to ionic strength and the impoundment variable. Other than impoundment, no second variable improved classification over the single-variable models. Adding a second variable did not improve the classification of models that included traffic volume. The best two-variable models had only one misclassified river for an overall accuracy of 96%.

Using the two-variable models, the Missouri and White rivers were correctly classified as not sustaining a *D. polymorpha* population ($P < 0.01$). Within the extent of the CAWs, the Missouri and White rivers have neither a system of locks and dams nor any other natural or man-made impoundment areas, making persistent-population development difficult or impossible. Each of these rivers has a system of dams, but they occur above the reach of navigation.

The Kanawha River was also correctly classified as having *D. polymorpha* in the two-variable models including total hardness, conductivity, and magnesium ($P = 0.50$, 0.66, and 0.67, respectively), but the Kanawha River remained misclassified in the two-variable model that included calcium ($P = 0.41$). The Kanawha River has the lowest average calcium concentration of any river having *D. polymorpha*, but it also has an unusually high concentration of magnesium (Table 1), which has also been shown to strongly affect *D. polymorpha* survival (Dietz et al. 1994).

The only river system that remained misclassified by the two-variable models was the Red River ($P > 0.9$ for each model). *Dreissena polymorpha* has been found in the Red River but only sporadically on the locks and commercial vessels plying the river (Stafford 1995). No permanent populations have been identified.

Using the results from the best-fitting two-variable models, *D. polymorpha* are unlikely to establish persistent populations in three of the four rivers outside of the CAWs. The lack of impoundments within the reach that we considered is limiting for both the Connecticut and Savannah rivers. Ionic composition is likewise limiting for the Chattahoochee, Connecticut, and Savannah rivers (Table 4). If, however, *D. polymorpha* are effectively dispersed to the Columbia River, a persistent population might become established. Impoundments are present on the Columbia, and ionic composition is comparable with that found in the Tennessee River, which supports a light to moderate *D. polymorpha* population.

Discussion

By analyzing environmental conditions in areas of failed invasions, we have identified a set of factors that restrict the establishment of *D. polymorpha* populations. We found that, once adequate dispersal is ensured in an area, *D. polymorpha* distribution appears to depend primarily on ionic conditions and the presence or absence of an upstream source or other impoundment that will ensure population stability.

Dispersal

Although *D. polymorpha* may be dispersed by a wide array of different vectors, the effectiveness of the dispersal vector appears to vary tremendously. Johnson and Carlton (1996) indicated that rapid range expansion appeared to occur primarily between directly interconnected water bodies. Overland dispersal occurs relatively more slowly, indicating the difficulties of overland transport, or perhaps indicating that prevention efforts have been effective in discouraging new invasions (Buchan and Padilla 1999).

Dreissena polymorpha expansion through interconnected waterways, such as the CAWs in the Mississippi River drainage basin, has been extremely rapid. In Europe, *D. polymorpha* spread rapidly through the interconnected canals that were contiguous with infested waters (Morton 1993). In North America, *D. polymorpha* likewise moved rapidly through the Rideau Canal and Trent–Severn Waterway in Ontario, and through the Erie Canal and Mohawk River in New York State (United States Geological Survey

Table 3. The most accurate one- and two-variable models from the logistic-regression analyses.

Model	Variables	*P*	Constant	Coefficient 1	Coefficient 2	Observed–predicted P/P	A/A	P/A	A/P	Overall accuracy (%)
1	$[Ca^{2+}]$	0.061	–1.0551	0.0612		5	15	1	3	83.3
2	Log(traffic)	0	–5.6889	1.9665		5	15	1	3	83.3
3	Log(total hardness)	0.019	–8.0433	4.4876		5	15	1	3	83.3
4	Log(conductivity)	0.046	–9.1640	4.1151		5	15	1	3	83.3
5	Upstream impoundment + log(total hardness)	0	–50.2237	32.8200	9.9354	7	16	0	1	95.8
6	Upstream impoundment + log(conductivity)	0	–49.5910	32.2429	7.9335	7	16	0	1	95.8
7	Upstream impoundment + $[Mg^{2+}]$	0	–331.3354	329.5115	0.4853	7	16	0	1	95.8
8	Upstream impoundment + $[Ca^{2+}]$	0	–167.0434	164.4482	0.1543	7	15	1	1	91.7

Note: Upstream impoundment indicates the presence of upstream impoundments such as locks and dams on a river. *P* provides the statistical significance of each logistic-regression model. Coefficient 1 and coefficient 2 refer to the coefficients of the first and second variables in each model, respectively. The form of one-variable models is the probability of *D. polymorpha* = $e^{(\text{constant} + \text{coefficient 1} \times \text{variable 1})}/(1 + e^{(\text{constant} + \text{coefficient 1} \times \text{variable 1})})$ and the form of two-variable models is the probability of *D. polymorpha* = $e^{(\text{constant} + \text{coefficient 1} \times \text{variable 1} + \text{coefficient 2} \times \text{variable 2})}/(1 + e^{(\text{constant} + \text{coefficient 1} \times \text{variable 1} + \text{coefficient 2} \times \text{variable 2})})$. P/P indicates the number of rivers with *D. polymorpha* that were correctly predicted by the model to have *D. polymorpha*. A/A indicates the number of rivers without *D. polymorpha* that were correctly predicted to not support *D. polymorpha*. Both P/A and A/P indicate discrepancies between the observed data and the predictions of the models. Overall accuracy is the number of correct classifications per number of incorrect classifications × 100%.

1998). These waterways allow no commercial traffic but receive heavy recreational traffic directly from the infested waters of lakes Ontario and Erie. Large numbers of *D. polymorpha* can be attached to the hulls of vessels moving among interconnected waterways. These mussels are not desiccated by overland transport and are not subject to visual inspection and removal before a boat is moved to a new water body. The probability of dispersal through an interconnected waterway system appears, therefore, to be very high (much higher than via overland transport). In our analysis, however, connectedness alone did not indicate that the invasion would be successful.

Abiotic constraints

Some measure of ionic strength, usually calcium, has been a common feature of all models that predict the potential distribution of *D. polymorpha* (e.g., Strayer 1991; Neary and Leach 1992; Hincks and Mackie 1997). The degree of sensitivity to low ionic strength waters depends on life stage, where the limitation of the most sensitive life stage defines a threshold for population establishment. In laboratory experiments, Sprung (1987) found that minimum threshold calcium for successful rearing of healthy veligers fell in the range of 12–24 $mg \cdot L^{-1}$. Much greater rearing success and fewer crippled veligers were found at higher calcium concentrations. Compared with veligers, adult *D. polymorpha* will tolerate lower ionic strength waters, and can tolerate deionized water in the laboratory for a few days or longer (Ram and Walker 1993). Dietz et al. (1994) found that minimal concentrations of Na, Cl, K, and particularly Mg were required to maintain adult *D. polymorpha* in the laboratory for longer than 2 months. In North America, populations of adult mussels have been found at very low densities in rivers with calcium concentrations as low as but not lower than 16 $mg \cdot L^{-1}$ (St. Lawrence River; Mellina and Rasmussen 1994; this study).

This concentration is much lower than the presence–absence threshold of 28.3 $mg \cdot L^{-1}$ reported for European lakes by Ramcharan et al. (1992). The difference in level may be due to differences in dispersal. Dispersal opportunity may be much lower for isolated lakes than for interconnected waters that are continually open for reinoculation. Frequent reinoculations may have the effect of supporting a population in waters that might otherwise have a much lower risk for invasion.

Constraints on data availability restricted our analyses to the freshwater portions of the CAWs; however, *D. polymorpha* is also generally intolerant of waters having extremely high ionic strength. *Dreissena polymorpha* is primarily a freshwater organism and, although this species can tolerate mildly brackish waters, the high ionic strength of sea water is completely restrictive (Ludyanskiy et al. 1993; Karateyev et al. 1998). Accordingly, *D. polymorpha* has not been found in the CAWs of the U.S. in areas where salinity is greater than 2–6‰ (United States Geological Survey 1998).

Static flow

Dreissena polymorpha has an obligate planktonic life stage, and establishing a population in a riverine environment poses a substantial challenge. Strong unidirectional flow can wash a large proportion of propagules downstream, thereby reducing the chances of perpetuating a local population within free-flowing reaches of the river.

Previous empirical models to predict the occurrence of *D. polymorpha* have focused on environments that already satisfy the requirement of an impoundment as defined by the current study (lakes, Ramcharan et al. 1992; rivers, Mellina and Rasmussen 1994). From an analysis of river systems in Europe and Michigan, Horvath et al. (1996) found a significant association between *D. polymorpha* presence in streams and their presence in upstream lakes. Our results support the conclusion of Horvath et al. (1996) and further maintain that the availability of upstream impoundment areas combined with effective dispersal and suitable water quality characteristics define waters that are most vulnerable to *D. polymorpha* invasion.

Other factors

Temperature is such an important factor affecting *D. polymorpha* growth and survival (McMahon 1996; Allen et al. 1999) that it has also been considered potentially critical in determining *D. polymorpha* distributions (Strayer

Table 4. Summary of selected water-quality, traffic, and hydrologic data for commercially navigable rivers *not* connected to infested waters.

					Water chemistry						*P*			
	L&D	Drift	Traffic (1995)	WQ stns	Ca^{2+} (mg·L^{-1})	Mg^{2+} (mg·L^{-1})	Total hardness (mg·L^{-1})	*T* (°C)	Total suspended sediments (mg·L^{-1})	Conductivity (µS·cm^{-1})	Model 5	Model 6	Model 7	Model 8
Savannah	0	—	na	1	4.9	1.2	17–18.3	18.3	18	80	<0.01	<0.01	<0.01	<0.01
Connecticut	0	—	na	1	13.4	1.5	40	10.1	8	108	<0.01	<0.01	<0.01	<0.01
Chattahoochee	2	—	na	1	12.7	1.2	36	14	20.8	106	0.13	0.21	0.22	0.34
Columbia	5	—	na	3	18.9 (15.9–20.6)	5.2 (4.4–7.0)	69 (58–81)	11.4 (9.4–12.5)	12.9 (5.8–17.4)	169 (143–226)	0.68	0.55	0.67	0.58

Note: L&D and drift indicate the number of locks and dams present on the river system and whether there is potential for passive veliger drift into the system from *D. polymorpha* populations located in an upstream lake or impoundment within the commercially available waterways. The volume of commercial traffic was determined from waterborne-commerce statistics compiled by the United States Army Corps of Engineers and is expressed as the number of self-propelled upbound tow and tug trips. WQ stns provides the number of water quality stations incorporated into the analysis. Water-chemistry variables are average annual values within a river system. *P* is the predicted probability for *D. polymorpha* population establishment and is given for each of the best-fitting models (see Table 3).

1991; Karateyev et al. 1998). Our study encompassed the largest range of temperatures ever considered in an empirical model to determine *D. polymorpha* distribution and, within the temperature range examined in this study, temperature either alone or in combination with other variables could not be used to accurately predict the presence or absence of *D. polymorpha*. It is possible, however, that temperatures higher than those examined in our study may prove limiting to *D. polymorpha*.

High concentrations of suspended sediment have also been shown to affect *D. polymorpha* growth (Madon et al. 1998). Like temperature, it could not accurately predict *D. polymorpha* distribution in this study. In the Red River, however, the values for both temperature and suspended sediment are some of the highest values in the entire data set. We suspect that the combination of extreme levels of these two stressors with low traffic volume may be restricting *D. polymorpha* from the Red River.

The effect of traffic volume on the presence and absence of *D. polymorpha* is unclear. On average, rivers with *D. polymorpha* had higher traffic volumes than those without (9504 and 2067 vessel trips, respectively). However, the variability was high (12 300 and 3807 vessel trips, respectively). The Kentucky and Green rivers were fairly low traffic volume systems that had *D. polymorpha*, while the Missouri, Tenn-Tom, and Black Warrior were high to medium traffic volume rivers from which *D. polymorpha* was absent. This inconsistency is likely the reason that traffic volume appeared significant in the single-variable models but was not retained in any of the two-variable models.

Some level of traffic is necessary for upstream inoculation, and increased commercial and maintenance traffic may certainly increase the likelihood of early inoculation. However, infestation is apparently possible even with very low traffic volumes. Indeed, a single vessel may be sufficient to inoculate a water body that has suitable impoundment and water-quality characteristics (see Kentucky River, Table 1). Conversely, inoculation does not occur in rivers receiving heavy traffic from infested water bodies, if suitable impoundment and water-quality criteria are not met (see Missouri and Black Warrior rivers, Table 1).

Although we did not explicitly consider it in our analysis, the availability of suitable substrate for settlement has also been identified as an important physical requirement defining small-scale *D. polymorpha* distribution patterns within lakes and streams (Stanczykowska 1977; Mellina and Rasmussen 1994). However, while substrate is certainly a mitigating factor influencing *D. polymorpha* density, it has not been shown to restrict *D. polymorpha* from occurring in a system—even when the substrate is composed of sand and mud (Mellina and Rasmussen 1994; Berkman et al. 1998). Available substrate is not likely to be a factor limiting *D. polymorpha* distribution in our analysis. Where natural substrate is lacking in the CAWs, man-made features, such as locks, dams, jetties, buoys, stationary barges, bridge pilings, bank stabilization, sea walls, and water intake structures, provide ample stable substrate.

Ecological constraints

Although some invasions of other species have been thwarted by characteristics of the native biological community (Case 1991), ecological interactions with other species are unlikely to explain the *D. polymorpha* distribution patterns that we found. *Dreissena polymorpha* has been a notorious invader, because of several characteristics that give it an advantage in the freshwater environment. Among these are a high reproductive rate and the ability to exploit a previously underutilized niche. While predators do remove some portion of *D. polymorpha* production, intense predation is not likely to restrict *D. polymorpha* from colonizing a habitat (Hamilton and Bailey 1994; Ray and Corkum 1997). Likewise, competition with other freshwater mussels is unlikely to exclude *D. polymorpha*. In fact, the opposite is true. *Dreissena polymorpha* has been implicated in substantial declines of native freshwater bivalves (Haag et al. 1993).

Implications for future spread

A clear understanding of the complementary roles of dispersal, life history, and physiological tolerance in determining *D. polymorpha* distribution patterns is critical for making an accurate assessment of infestation risk. Once risk is put into perspective, control efforts can be more accurately focused on particularly vulnerable areas. From our analysis, we can see that an interconnected waterway system with appropriate hydrology and ionic composition is at greatest risk of *D. polymorpha* infestation. We purposely did not focus on overland dispersal events, because we have no information about the relative frequency of nondispersal versus failed invasions in these cases. Overland transport of *D. polymorpha* through recreational boating may, however, represent the most common vector for dispersal into novel habitats, thereby creating new interconnected systems. Other studies have addressed the likelihood of overland dispersal through gravity models (Schneider et. al 1998). Perhaps the best regional predictive model would incorporate features of both this type of dispersal model and the current analysis to determine a more realistic estimate of potential infestation risk.

It is important to note that risk of invasion to any ecosystem is variable not fixed. Risk can change dramatically with changes to system configuration. For example, a persistent *D. polymorpha* population has not yet developed in the Missouri River. Since this river is within the CAWs, dispersal is adequate and the only barrier to population development appears to be the absence of some impoundment areas to provide an area for progagule retention. Plans are currently underway to construct extensive wetland areas along the Missouri, to restore a more natural hydrology and reduce the impacts of flooding. An inadvertent result of this restoration may be to create stable habitats for *D. polymorpha*. Installing control measures on vessels entering the Missouri River may protect this system from infestation.

Acknowledgements

Funding for this work was provided by Louisiana Sea Grant (A/ZM-2, Zebra Mussel Subprogram). We particularly thank Amy Benson (United States Geological Survey) and the other numerous state- and federal-agency personnel contacted during the course of this study. Early versions of the manuscript benefitted greatly from critical reviews by Drs. D.K. Padilla and K.A. Rose and two anonymous reviewers.

References

Alexander, R.B., Slack, J.R., Ludtke, A.S., Fitzgerald, K.K., and Schertz, T.L. 1996. Data from selected U.S. Geological Survey National Stream Water-Quality Monitoring Networks (WQN). U.S. Geol. Surv. Digital Data Ser. DDS-37.

Allen, Y.C. 1999. Zebra mussels in commercial vessels on inland waterways. Louisiana Sea Grant Publ. Available at <http://www.laseagrant.org/common/zm_pubs.html#zm_commvessels>.

Allen, Y.C., Thompson, B.A., and Ramcharan, C.W. 1999. Growth and mortality of the zebra mussel, *Dreissena polymorpha*, in the lower Mississippi River. Can. J. Fish. Aquat. Sci. **56**: 748–759.

Berkman, P.A., Haltuch, M.A., Tichnich, E., Garton, D.W., Kennedy, G.W., Gannon, J.E., Mackey, S.D., Fuller, J.A., and Liebenthal, D.L. 1998. Zebra mussels invade Lake Erie muds. Nature (London), **393**: 27–28.

Borcherding, J. 1992. Morphometric changes in relation to the annual reproductive cycle in *Dreissena polymorpha*—a prerequisite for biomonitoring studies with zebra mussels. *In* Limnologie Aktuell **4**: The zebra mussel (*Dreissena polymorpha*)—ecology, biological monitoring and first applications in the water quality management. *Edited by* D. Neumann and H.A. Jenner. Gustav Fischer, Stuttgart. pp. 87–99.

Buchan, L.A.J., and Padilla, D.K. 1999. Estimating the probability of long-distance overland dispersal of invading aquatic species. Ecol. Appl. **9**: 254–265.

Case, T. 1991. Invasion resistance, species build-up and community collapse in metapopulation models with interspecies competition. Biol. J. Linn. Soc. **42**: 239–266.

Dietz, T.H., Lessard, D., Silverman, H., and Lynn, J.W. 1994. Osmoregulation in *Dreissena polymorpha*: the importance of Na, Cl, K, and particularly Mg. Biol. Bull. (Woods Hole, Mass.), **187**: 76–83.

Drake, J.A., Mooney, H.A., diCastri, F., Groves, R., Kruger, F., Rejmanek, M., and Williamson, M. (*Editors*). 1989. Biological invasion: a SCOPE program overview. *In* Biological invasions: a global perspective. Wiley & Sons, New York. pp. 491–506.

Griffiths, R.W., Schloesser, D.W., Leach, J.H., and Kovalak, W.P. 1991. Distribution and dispersal of the zebra mussel (*Dreissena polymorpha*) in the Great Lakes region. Can. J. Fish. Aquat. Sci. **48**: 1381–1388.

Haag, W.R., Berg, D.J., Garton, D.W., and Farris, J.L. 1993. Reduced survival and fitness in native bivalves in response to fouling by the introduced zebra mussel (*Dreissena polymorpha*) in western Lake Erie. Can. J. Fish. Aquat. Sci. **50**: 13–19.

Hamilton, D.J., and Bailey, R.C. 1994. Predation of zebra mussel by diving ducks: an exclosure study. Ecology, **75**: 521–531.

Hincks, S.S., and Mackie, G.L. 1997. Effects of pH, calcium, alkalinity, hardness, and chlorophyll on the survival, growth, and reproductive success of zebra mussel (*Dreissena polymorpha*) in Ontario lakes. Can. J. Fish. Aquat. Sci. **54**: 2049–2057.

Horvath, T.G., Lamberti, G.A., Lodge, D.M., and Perry, W.L. 1996. Zebra mussel dispersal in lake–stream systems: source–sink dynamics? J. North Am. Benthol. Soc. **15**: 564–575.

Hosmer, D.W., Jr., and Lemeshow, S. 1989. Applied logistic regression. John Wiley & Sons, New York.

Johnson, L.E., and Carlton, J.T. 1996. Post-establishment spread in large-scale invasions: dispersal mechanisms of the zebra mussel, *Dreissena polymorpha*. Ecology, **77**: 1686–1690.

Johnson, L.E., and Padilla, D.K. 1996. Geographic spread of exotic species: ecological lessons and opportunities from the invasion of the zebra mussel *Dreissena polymorpha*. Biol. Conserv. **78**: 23–33.

Karateyev, A.Y., Burlakova, L.E., and Padilla, D.K. 1998. Physical factors that limit the distribution and abundances of *Dreissena polymorpha* (Pall.). J. Shellfish Res. **17**: 1219–1235.

Keevin, T.M., Yarborough, R.E., and Miller, A.C. 1992. Long-distance dispersal of zebra mussels (*Dreissena polymorpha*) attached to hulls of commercial vessels. J. Freshw. Ecol. **7**: 437.

Kern, R., Borcherding, J., and Neumann, D. 1994. Recruitment of a freshwater mussel with a planktonic life-stage in running waters—studies on *Dreissena polymorpha* in the River Rhine. Arch. Hydrobiol. **131**: 385–400.

Ludyanskiy, M.L., McDonald, D., and MacNeill, D. 1993. Impact of the zebra mussel, a bivalve invader—*Dreissena polymorpha* is rapidly colonizing hard surfaces throughout waterways of the United States and Canada. BioScience, **43**: 533–544.

Madon, S.P., Schneider, D.W., Stoeckel, J.A., and Sparks, R.E. 1998. Effects of inorganic sediment and food concentrations on energetic processes of the zebra mussel, *Dreissena polymorpha*: implications for growth in turbid rivers. Can. J. Fish. Aquat. Sci. **55**: 401–413.

McMahon, R.T. 1996. The physiological ecology of the zebra mussel, *Dreissena polymorpha*, in North America and Europe. Am. Zool. **36**: 339–363.

Meade, R.H. 1995. Setting: geology, hydrology, sediments, and engineering of the Mississippi River. *In* Contaminants of the Mississippi River. *Edited by* R.H. Meade. U.S. Geol. Surv. Circ.1133.

Mellina, E., and Rasmussen, J. 1994. Patterns in the distribution and abundance of zebra mussel (*Dreissena polymorpha*) in rivers and lakes in relation to substrate and other physicochemical factors. Can. J. Fish. Aquat. Sci. **51**: 1024–1036.

Morton, B. 1993. The anatomy of *Dreissena polymorpha* and the evolution and success of the heteromyarian form in the Dreissenoidea. *In* Zebra mussels: biology, impacts and control. *Edited by* T.F. Nalepa and D.W. Schloesser Lewis Publishers, Boca Raton, Fla. pp. 185–215.

Neary, B.P., and Leach, J.H. 1992. Mapping the potential spread of the zebra mussel (*Dreissena polymorpha*) in Ontario. Can. J. Fish. Aquat. Sci. **49**: 406–415.

New York Sea Grant. 1998. National Zebra Mussel Clearinghouse maps. Available via http://www.entryway.com/seagrant/maps.cfm.

Ram, J.L., and Walker, J.U. 1993. Effects of deionized water on viability of the zebra mussel, *Dreissena polymorpha*. Comp. Biochem. Physiol. C, Pharmacol. Toxicol. Endocrinol. **105**: 409–414.

Ramcharan, C.W., Padilla, D.K., and Dodson, S.I. 1992. Models to predict potential occurrence and density of the zebra mussel (*Dreissena polymorpha*). Can. J. Fish. Aquat. Sci. **49**: 150–158.

Ray, W.J., and Corkum, L.D. 1997. Predation of zebra mussel by round gobies (*Neogobius melanostomus*). Environ. Biol. Fishes, **50**:267–273.

Reckendorfer, W., Keckeis, H., Winkler, G., and Schiemer, F. 1999. Zooplankton abundance in the river Danube, Austria: the significance of inshore retention. Freshw. Biol. **41**: 583–591.

Reynolds, C.S., Carling, P.A., and Beven, K.J. 1991. Flow in river channels—new insights into hydraulic retention. Arch. Hydrobiol. **121**: 171–179.

Schneider, D.W., Ellis, C.D., and Cummings, K.S. 1998. A transportation model assessment of the risk to native mussel communities from zebra mussel spread. Conserv. Biol. **12**: 788–800.

Simberloff, D. 1989. Which insect introductions succeed and which fail? *In* Biological invasions: a global perspective. *Edited by* J.A. Drake, H.A. Mooney, F. diCastri, R. Groves, F. Kruger, M. Rejmanek, and M. Williamson. Wiley & Sons, New York. pp. 61–75.

Sparks, R.E., Nelson, J.C., and Yin, Y. 1998. Naturalization of the flood regime in regulated rivers. BioScience, **48**: 706–720.

Sprung, M. 1987. Ecological requirements of developing *Dreissena polymorpha* eggs. Archiv. Hydrobiol. Suppl. **79**: 69–86.

Stafford, P. 1995. Zebra mussel observation during 1994–95. US Army Corps of Engineer District, Vicksburg. *In* Abstracts of Zebra Mussel Workshop '95, held 27–30 November 1995, New Orleans, La. U.S. Army Corps of Engineers, Vicksburg, Miss.

Stanczykowska, A. 1977. Ecology of *Dreissena polymorpha* (Pall.) (Bivalvia) in lakes. Pol. Arch. Hydrobiol. **24**: 461–530.

Strayer, D.L. 1991. Projected distribution of the zebra mussel, *Dreissena polymorpha*, in North America. Can. J. Fish. Aquat. Sci. **48**: 1389–1395.

United States Army Corps of Engineers. 1998. Navigational Data Center Publications and U.S. Waterway CD. Vol. 4. CEWRC-NDC Water Resources Support Center, Navigation Data Center, Alexandria, Va. (Also available at <http://www.wrsc.usace.army.mil/ndc/cdinfo.htm>.)

United States Geological Survey. 1998. Nonindigenous aquatic species (NAS) information resource. Available from Florida Carribean Sciences Center, Gainesville, Fla., and via <http://nas.nfrcg.gov/zebra.mussel/index.html>.

Walz, N., and Welker, M. 1998. Plankton development in a rapidly flushed lake in the river Spree system (Neuendorfer See, Northeast Germany). J. Plankton Res. **20**: 2071–2087.

Estimating predation mortality in the Georges Bank fish community

Tien-Shui Tsou and Jeremy S. Collie

Abstract: Multispecies virtual population analysis (MSVPA) is one of the most successful methods of including predation in fishery models. By applying MSVPA to nine important fish species on Georges Bank, we estimated predation mortality of prey species, fishing mortality, and population abundance from 1978 to 1992. One of the inputs to the MSVPA, relative stomach content, was estimated by fitting gamma distributions to the logarithmic predator-to-prey size ratios. Chi-square tests indicated that the gamma distributions fit the observed ratios well. Predation mortality was highest at ages 0 and 1. Total biomass of all species remained relatively constant with decreasing predator biomass and increasing prey biomass. MSVPA requires extensive input data, and the uncertainty in the inputs will propagate into the model output. The sensitivity of MSVPA to perturbations in the inputs was assessed with a two-level fractional factorial design. Results of the sensitivity test indicated that MSVPA outputs were most sensitive to predator consumption rates and terminal fishing mortalities. With ±25% perturbations to the input parameters, MSVPA outputs varied within ±10% of the levels from the base run. Therefore, MSVPA appears to be relatively robust to uncertainty in the input data.

Résumé : L'analyse des populations plurispécifiques virtuelles (MSVPA) est l'une des méthodes les plus efficaces pour inclure la prédation dans les modèles des pêches. L'application de la MSVPA à neuf espèces importantes de poissons du banc Georges a permis d'estimer la mortalité due à la prédation, la mortalité due à la pêche et la densité des populations de 1978 à 1992. L'une des données d'entrée du MSVPA, le contenu relatif de l'estomac, a pu être estimée en ajustant des distributions gamma aux rapports logarithmiques des tailles prédateurs–proies; des tests de chi-carré confirment que les distributions gamma s'accordent bien aux rapports observés. La mortalité due à la prédation est maximale aux âges 0 et 1. La biomasse totale de toutes les espèces reste relativement constante lorsque la biomasse des prédateurs diminue et que la biomasse des proies augmente. La MSVPA exige une grande quantité de données d'entrée et l'incertitude dans ces données se répercute dans les sorties du modèle. La sensibilité de la MSVPA aux perturbations dans les données d'entrée a été évaluée par un plan d'analyse fractionnel factoriel à deux niveaux. Les résultats du test de sensibilité indiquent que les sorties de la MSVPA sont surtout sensibles aux taux de consommation des prédateurs et aux mortalités terminales dues à la pêche. Des perturbations de ±25% dans les données d'entrée entraînent des sorties de la MSVPA qui se situent à moins de ±10% des valeurs obtenus lors des exécutions de base du programme. La MSVPA semble donc relativement robuste même lorsqu'il y a de l'incertitude dans les données d'entrée.

[Traduit par la Rédaction]

Introduction

Large-scale exploitation has reduced the abundance of commercially valuable species and led to a reduction in the mean trophic level of world fisheries (Pauly et at. 1998). In some marine ecosystems, overexploitation has led to dramatic changes in community structure (Fogarty and Murawski 1998). Although the exploitation rates, abundances, and distributions of commercially important species are generally well documented, the impacts of species interactions through competition and predation are poorly understood. Understanding the role of species interactions in regulating community and population dynamics is therefore required, to explain past population trajectories and to project the rates of recovery of severely depleted populations. Since the 1980s, the development of quantitative ecosystem approaches has been a priority in fisheries science (Larkin 1996). One of the approaches taken by the International Council of the Exploitation of the Sea (ICES) has been to estimate the combined effects of species interactions (especially predation) and exploitation with multispecies virtual population analysis (MSVPA).

MSVPA was developed and implemented by the ICES Multispecies Assessment Working Group (Pope 1991). The method integrates the suitability concept of Andersen and Ursin (1977) for describing predator–prey relationships with the traditional form of virtual population analysis (VPA) implemented by Gulland (1965). MSVPA provides useful insight into the role of predator–prey interactions by quantifying food consumption of major predators (Sparre 1980). As an extension of single-species VPA (SSVPA), MSVPA treats consumed biomass as part of the virtual population. It simultaneously estimates fishing and predation mortalities by year and age group of predator and prey species on the basis of

Received February 22, 2000. Accepted January 24, 2001. Published on the NRC Research Press Web site on April 12, 2001.
J15625

T.-S. Tsou[1,2] and J.S. Collie. University of Rhode Island, Graduate School of Oceanography, Narragansett, RI 02882, U.S.A.

[1] Corresponding author (e-mail: theresa.tsou@fwc.state.fl.us).

[2] Present address: Florida Marine Research Institute, Fish and Wildlife Conservation Commission, 100 8th Avenue SE, St. Petersburg, FL 33701, U.S.A.

DOI: 10.1139/cjfas-58-5-908

catch-at-age and stomach-content data. The analysis also produces suitability coefficients that can be used to project consumption under differing abundances of both predators and prey. MSVPA has been applied primarily to the North Sea by the ICES Multispecies Assessment Working Group. Preliminary applications have also been made in other areas, such as the Baltic Sea (Sparholt 1991), Southwest African waters (Blinov 1991), and the eastern Bering Sea (Livingston and Jurado-Molina 2000). In theory, MSVPA can reduce the uncertainty in natural mortality, but the expanded data requirements raise the concern that "we are adding uncertainty to an already too-uncertain approach" (Christensen 1996). Following the example of Finn et al. (1991), we performed a sensitivity analysis of the reliability of MSVPA in our application to the Georges Bank fish community.

Georges Bank is a highly productive marine ecosystem with a long history of exploitation. It has been an important fishing area for groundfish, including Atlantic cod, haddock, and several species of flounder. Sharply increased exploitation levels with the advent and expansion of distant-water fisheries on Georges Bank in the early 1960s resulted in major perturbations to the community structure and fishery production (Fogarty and Murawski 1998). The most apparent change to the Georges Bank fish community is the shift in species composition (Murawski and Idoine 1992), in particular the rapid and significant increases in principal pelagics and elasmobranchs and the record low abundance of principal groundfish and flounders in the early 1990s (Fogarty and Murawski 1998).

To evaluate these structural changes, multispecies models of the Georges Bank ecosystem have been explored since the mid-1970s (Foster 1982). It was found that species interactions (predation and competition) could substantially influence both the structure and energy flow within the ecosystem (Clark and Brown 1977) and could account for some of the variability in fish biomass and abundance (Sissenwine et al. 1984; Overholtz and Tyler 1986). The main interactions identified by Collie and Delong (1999) were predation on pelagics by gadoids and elasmobranchs and apparent competition between gadoids and elasmobranchs.

As part of the Coastal Ocean Program Georges Bank predation study, we constructed a nine-species MSVPA of the fish community on Georges Bank, to investigate the trophic dynamics between predator and prey. To perform MSVPA, detailed-food habit information is required. Beginning in 1968, thousands of stomach samples from marine fish along the northeast coast of North America have been gathered and analyzed by the National Marine Fisheries Service (NMFS), Northeast Fisheries Science Center (NEFSC). However, only a small fraction of the stomach contents has been classified by size–age group of prey. To circumvent this problem, we used predator-specific size-preference functions to distribute the ingested prey into size categories. Size preference has generally been assumed to be a lognormal function of the predator-to-prey weight ratio (Ursin 1973). In reality, the shape of size-preference distributions varies with predator species: some are symmetric but most are skewed. Owing to this skewness, gamma distributions were applied in this study. In addition to food-habit and consumption-rate data, MSVPA requires other input information, as described below. To evaluate the level at which uncertainty in the inputs propagates into the outputs, a sensitivity test was performed with a fractional factorial design.

Materials and methods

Model

The methodology of MSVPA is well documented. Helgason and Gislason (1979), Pope (1979), and Sparre (1980) took the first steps in developing MSVPA. A detailed derivation of its equations was given in Gislason and Helgason (1985) and the method was summarized by Sparre (1991). Pope (1991) gave overviews of the applications of MSVPA to the North Sea. Magnusson (1995) presented a comprehensive picture of the mathematical aspects and the underlying assumptions. In MSVPA, age-specific survivorship and catch are calculated with the well-established equations for SSVPA, except that natural mortality is partitioned into two components, predation mortality and residual natural mortality (Sparre 1991). Predation mortality (*P*) is equal to the consumption rates (*I*) of all predator species (*j*) and age-classes (*b*) times the fraction of the total food that consists of prey species *i*, age *a*, divided by the biomass of prey (*i*,*a*):

$$(1)\qquad P_{i,a} = \frac{1}{N_{i,a} \cdot w_{i,a}} \cdot \sum_{j} \sum_{b} I_{j,b} \cdot N_{j,b} \frac{\Phi_{i,a:j,b}}{\Phi_{j,b}}$$

where *N* is number of fish, *w* is mean body weight at age, and Φ represents available food. The fraction of each prey in the total food is a function of the abundance of that particular prey and all other possible prey weighted by a prey-specific suitability index (*v*):

$$(2)\qquad \Phi_{i,a:j,b} = v_{i,a:j,b} \cdot N_{i,a} \cdot w_{i,a}$$

$$(3)\qquad \Phi_{j,b} = \left(\sum_{i} \sum_{a} \Phi_{i,a:j,b} \right) + v_{r:j,b} \cdot B_{r}$$

where the subscript *r* indicates "other food" and *B* refers to biomass.

Starting with the most recent year, the cohorts of all species are reconstructed back in time, with three iteration loops, to solve for fishing mortality, predation mortality, and suitability. The following assumptions are made in the MSVPA program. The fraction of a particular prey in the diet of a particular predator is the ratio of the suitable biomass of the prey over the total suitable biomass available to the predator. The suitability coefficients (*v*) are assumed to be constant over time, which implies that the feeding preference is time invariant. Although not required by MSVPA, growth rate, consumption rate, and residual natural mortality are assumed to be constant over time in this study.There are three alternative assumptions related to how "other food" is treated: (1) constant fraction in predator's diet (Pope 1979), (2) constant amount in the environment (Helgason and Gislason 1979), and (3) constant ecosystem biomass (Sparre 1980).

A nine-species MSVPA for the Georges Bank fish community for the years 1978–1992 was constructed. As predators, we included Atlantic cod, *Gadus morhua*; silver hake, *Merluccius bilinearis*; haddock, *Melanogrammus aeglefinus*; spiny dogfish, *Squalus acanthias*; and winter skate, *Raja ocellata* and, as prey, we included Atlantic cod; silver hake; haddock; Atlantic herring, *Clupea harengus*; Atlantic mackerel, *Scomber scombrus*; yellowtail flounder, *Limanda ferruginea*; and sand lance, *Ammodytes* sp. Cod, silver hake, haddock, mackerel, herring, and yellowtail flounder are referred to as the MSVPA species in this paper, because their population structures are reconstructed within the MSVPA. Spiny dogfish and winter skate are referred to as "other predators" and sand lance as "other prey," because their abundance was estimated outside the MSVPA. Information needed to perform the MSVPA includes quarterly catch at age, terminal fishing mortality rates, residual natural mortality rates, predator consumption rates, body weights at age, predator stomach contents, and an assumption of "other food."

Data preparation

Stock information

Annual catch-at-age data and terminal fishing mortalities were adopted from single-species stock-assessment documents. Catches and terminal fishing mortalities of cod, haddock, and yellowtail flounder on Georges Bank were taken from the documents (Northeast Fisheries Science Center 1997) without modification. The catches of silver hake, herring, and mackerel were assessed over a wider geographic area than Georges Bank. Collie and DeLong (1999) used the spring trawl survey data to prorate the amount of biomass that occurred on Georges Bank for these three species. The average biomass proportions on Georges Bank of silver hake, herring, and mackerel were 0.19, 0.121, and 0.126, respectively. Catch-at-age data for silver hake (Northeast Fisheries Science Center 1994*a*), mackerel (Northeast Fisheries Science Center 1995), and herring (Northeast Fisheries Science Center 1996) from the northwest Atlantic coast were multiplied by these proportions to obtain estimates for Georges Bank only. Factors to split annual catch into quarterly catch for the MSVPA species were estimated from the NMFS commercial fisheries database by calculating the overall averages of the proportions of catch in each quarter in every year. These factors were assumed to be constant over age and time. Terminal fishing mortalities for herring and mackerel were set to be the same as in the tuned SSVPA, assuming that the average fishing mortality on Georges Bank was similar to the fishing mortality for the entire range of these species. As there was no recent stock assessment for silver hake, terminal fishing mortalities were tuned so that the biomasses of silver hake in Collie and DeLong (1999) were the lower bounds of the estimates from MSVPA and the trends in biomass over time were the same.

Spiny dogfish and winter skate were incorporated as "other predators," whose minimum abundances were estimated from the NEFSC survey database. Spiny dogfish were classified by sex and their abundance was estimated for spring and fall. Winter skate were not separated by sex and only the fall survey was used to estimate their abundance. The minimum abundance by 10 cm length interval was calculated by multiplying the total survey area on Georges Bank (215×10^3 km^2) by mean numbers per tow and dividing by the average area swept by a 30 min trawl haul (0.033 km^2). Sand lance were included as "other prey" in a run separate from the base run, to examine the influence of sand lance abundance on the MSVPA prey species. We calculated the minimum abundance of sand lance, not including size information, from the NEFSC spring-survey database and multiplied this estimate by an expansion factor, so that there were enough sand lance for the predators.

Body weights at age were taken to be time invariant. Mean body weights at age for cod, silver hake, haddock, mackerel, herring, and yellowtail flounder were adopted from Grosslein et al. (1980). For spiny dogfish, mean weight (W) in grams by sex and 10 cm length (L) interval was calculated from the length frequency in each 10-cm interval and the length–weight regressions: $W = \exp(-15.025) \times L^{3.607}$ for female dogfish and $W = \exp(-13.002) \times L^{3.098}$ for male dogfish (Northeast Fisheries Science Center 1998). For winter skate, mean body weights for 10 cm length classes were adopted from Nelson (1993) and were assumed to be equal in all the seasons.

One of the original objectives of MSVPA was to reduce uncertainty in the natural mortality rate and to take account of variability among years and ages by calculating a part of the mortality, predation, inside the model. In MSVPA, residual natural mortality, M, is given externally as in SSVPA, but predation mortality (P) is calculated inside the model. In single-species stock assessments, natural mortalities were set at 0.2 for all the species on Georges Bank. In this study, M equaled 0.2 for age-1 and older fish, so that predation mortality was in addition to the residual natural mortality (M) assumed in SSVPA. This choice was made so that the natural mortality rate for older fish (for which predation mortality is low) would be the same in the single and multispecies VPA. For age-0 fish, M equaled 0.3 or 0.1 per quarter, assuming each cohort was born in the second quarter (spring) for all the MSVPA species, irrespective of the actual spawning seasons of these species.

Consumption rates

An important input to the MSVPA, the food consumption rate, may be calculated from the energy requirements of the predator, or it may be estimated from stomach contents. Grosslein et al. (1980) applied the former approach to six major finfish (cod, silver hake, yellowtail flounder, haddock, herring, and mackerel) on Georges Bank during 1963–1972; Cohen and Grosslein (1981) applied the latter approach to five species (cod, silver hake, haddock, yellowtail flounder, and pollock) on Georges Bank during 1972–1976. Garrahan (1994) also estimated gastric-evacuation rate of Atlantic cod by fitting a general model (Temming and Andersen 1992) and obtained an average consumption of 1.04% body weight per day. In our base run, quarterly consumption rates of cod, silver hake, and haddock were from Grosslein et al. (1980). The values in Cohen and Grosslein (1981) were used in the sensitivity test.

In stomach-sample models, the total daily ration, R, was calculated by

$$(4) \qquad R = 24\alpha\bar{S}$$

where α is the evacuation rate and $\bar{S}$ equals the mean stomach content (in weight or percent body weight) over the 24-h period (Elliot and Persson 1978). Evacuation rates (α) were related to temperature (t) by Elliot (1972) as

$$(5) \qquad \alpha = a\,e^{bt}$$

The exponent (b) of this relationship appears to be fairly constant for different prey types and predator species ($b = 0.111$; Elliot 1972), but the coefficient a may change significantly according to prey type. The quarterly α values of cod, silver hake, and haddock were derived from their annual values in Cohen and Grosslein (1981), adjusted by the quarterly mean sea surface temperatures on Georges Bank over 1946–1990 obtained from the National Climate Data Center.

Mean stomach content ($\bar{S}$, in percent body weight) of silver hake and haddock by age group were adopted from Cohen and Grosslein (1981) for the sensitivity test. Daily ration, R, for a given predator age group was then multiplied by 90 days, to estimate the quarterly consumption rates. Daily ration of winter skate by season for 10 cm length classes was adopted from Nelson (1993). Jones and Geen (1977) reported quarterly consumption rates by size and sex for spiny dogfish based on an energy budget. Their estimates were applied in the base run. Tanasichuk et al. (1991) estimated the dogfish consumption rate in August to be 2.6% of body weight per day based on stomach samples; this higher estimate is used in the sensitivity test.

Diet composition

NEFSC food-habit data from 1981–1990, which include detailed information on the size of predators, were examined to estimate the diet composition of each predator species in two seasons. Owing to the limited sample sizes, we averaged the stomach-content data over the sampling years for the five predator species in this study and designated the "representative years" (Table 1) to be those years that had the highest numbers of samples, so that the sum of sample sizes in these years constituted more than 50% of the total sample size. This assignment is necessary, because prey biomass in these "representative years" affects the estimates of suitability. Since the stomach contents were measured by volume, we assumed that the density of stomach contents equaled one to convert from volume to weight units. The diet data for predators in the spring were applied to winter, and the fall diet data were applied to summer. To incorporate the growth of predators, the weighted mean relative stomach contents were grouped differently according to the predator's length-at-age categories in the spring and fall. The relative stomach contents of each predator species – age and prey species – age combination were estimated by fitting gamma distributions to the predator-to-prey size ratios.

The gamma distribution is a flexible curve that can be used to model asymmetric distributions. This distribution has only two parameters, α and β, to be estimated in its probability density function:

$$(6)\qquad f(x) = \frac{1}{\beta^{\alpha} \cdot \Gamma(\alpha)} \cdot x^{\alpha-1} \cdot \exp\left[\frac{-x}{\beta}\right], \qquad \text{for } x > 0$$

For any positive mean and variance we can find α and β so that $\alpha\beta$ is the mean and $\alpha\beta^2$ is the variance (Freund 1992). Because of this flexibility, we used the gamma distribution to reconstruct the size structure of fish prey. The random variable (x) of the gamma distribution is

$$(7)\qquad x = \ln\left(\frac{c_j \cdot L_j}{c_i \cdot L_i}\right)^3$$

where i is the subscript for prey and j is the subscript for predator. Prey weight (w_i) was converted from prey length (L_i) based on the length–weight relationship $w_i = c_i \cdot L^3$ because prey weights were not measured. We assumed $c_j = c_i$ because length–weight relationships were not available for all of the ingested prey species.

Five predator species, cod, silver hake, haddock, spiny dogfish, and winter skate, and their fish prey, were included for fitting the size-ratio data with the gamma distribution. Body length of the predators and their ingested prey were measured by the NEFSC. There were 497 measurements of predator-to-prey size ratio for cod, 173 for silver hake, 16 for haddock, 227 for dogfish, and 700 for winter skate. These were a small subset of the stomach database that had length information for predators and ingested prey. We used the method of least squares to estimate α and β, and tested the goodness of fit of the results with a χ^2 statistic.

The fitted distributions were then applied to the whole stomach data set for distributing the relative stomach content of each predator age-class by prey-species and -age categories. Length-at-age information of predator and prey species was from Penttila et al. (1989). The size preference of a given predator age for a prey age group with a size ratio corresponding to x_i equals the probability area under the gamma distribution between $(x_{i-1} + x_i)/2$ and $(x_i + x_{i+1})/2$. For each predator age-class (L_j fixed), the amount of each eaten prey species was distributed into different age groups (L_i changing) according to these probabilities.

Other food

The last input parameter to be estimated was the amount of "other food." The constant ecosystem-biomass assumption was adopted, so that the expected changes in "other food" would compensate for changes in the exploited prey. Using an energy budget from Sissenwine et al. (1984), we estimated the total biomass of fish and their prey on Georges Bank to be 15 million t. The effect of the assumptions concerning "other food" was evaluated in preliminary runs; the results indicated that MSVPA was insensitive to alternative assumptions of "other food."

Table 1. Representative years for the predator species that accounted for at least 50% of the stomach samples for each species–season combination.

	Representative years	
Species	Spring	Fall
Cod	1985	1987
	1986	1983
	1990	1990
Silver hake	1985	1986
	1986	1989
	1987	1990
Haddock	1987	1987
	1989	1989
Dogfish	1985	1981
	1986	1988
	1987	1989
	1989	1990
Winter skate	1989	1989
	1990	1990

Sensitivity test

The MSVPA requires extensive data and involves the estimation of many parameters. It is important to know the response of the model to small perturbations in the input data, especially to those input parameters that are uncertain. To test the sensitivity of the model, we followed the approach of Finn et al. (1991) for the North Sea. Ten of the most important input parameters were varied: terminal fishing mortalities for all six species; age-0 residual natural mortality (M) values of cod, silver hake, and haddock; and the consumption rates of all predators. The nine response variables were age-0 and age-1 predation mortality (P) for cod, silver hake, and herring; age-0 P for haddock; age-1 P for yellowtail flounder; and the mean r^2 from regression of the MSVPA abundance estimates on the respective survey estimates from 1978–1990. A two-level fractional factorial (2^{10-5}_{IV}) design was used to reduce the redundancy from a full two-level design (Box et al. 1978). A fractional factorial design eliminates the need to test all possible combinations of parameters, while still allowing the main effects to be estimated. For terminal fishing mortalities (Fs), the two levels were set to be 25% higher or lower than in the base run; the same range was also applied to the residual natural mortality rates (Ms). Consumption rates by age for cod from Garrahan (1994) and for silver hake and haddock from Cohen and Grosslein (1981) were defined as the upper levels and those used in the base run were the lower levels (Table 2). Consumption rates of dogfish from Jones and Geen (1977) were used as the low level and the rates from Tanasichuk et al. (1991) were adopted as the high level. No variation of consumption rates was applied for winter skate, because only a single estimate of its ration was available. The results of 32 MSVPA runs were analyzed with nine linear regression models with no interaction between factors.

Results

The two main inputs of the MSVPA that were calculated in this study were the quarterly consumption rates by predator age based on stomach samples and the relative stomach contents by predator age–size categories distributed by predator size-preference functions. Consumption rates in each quarter for cod, silver hake, and haddock were determined

Table 2. Range of daily-ration estimates (percent body weight per day) of cod, silver hake, and haddock reported in prior studies and the ration values used in Georges Bank multispecies virtual population analysis; the ranges correspond to different age–size classes.

Cod	Silver hake	Haddock	Spiny dogfish	Winter skate	Source
0.5–1.1	1.0–1.4	0.7–1.2			Grosslein et al. 1980
1.2–2.0	0.6–2.2	1.9–2.9			Cohen and Grosslein 1981
2.3	3.1				Edwards and Bowman 1979
0.9–1.5	0.8–3.2				Durbin et al. 1983
1.04					Garrahan 1994
0.5–1.1	1.0–1.4	0.7–1.2	0.5–1.9	0.1–2.0	Values used in base run
1.04	0.6–2.2	1.9–2.9	2.8	0.1–2.0	Upper values for sensitivity analysis

Fig. 1. Observed predator-to-prey size ratios (solid circles) and predicted gamma distributions (lines) of cod (χ^2 = 27.1, df = 14, p = 0.006) (*a*), silver hake (χ^2 = 14.5, df = 13, p = 0.067) (*b*), dogfish (χ^2 = 70.3, df = 11, p < 0.0001) (*c*), haddock (no goodness-of-fit test, owing to small sample size) (*d*), and winter skate (χ^2 = 126.6, df = 12, p < 0.0001) (*e*). The x-axis is 3·ln(predator length/prey length) and the y-axis is the value of the probability function (eq. 4).

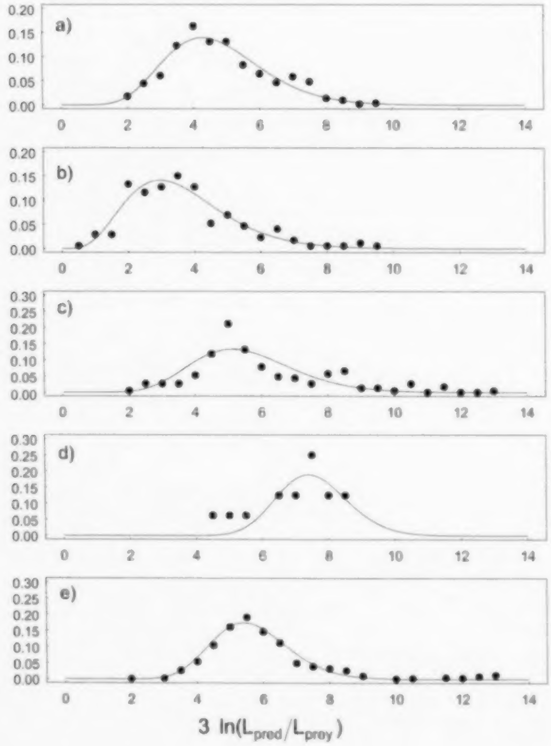

Fig. 2. Trophic relationships for the nine important fish species on Georges Bank. The arrows lead from prey species to predator species.

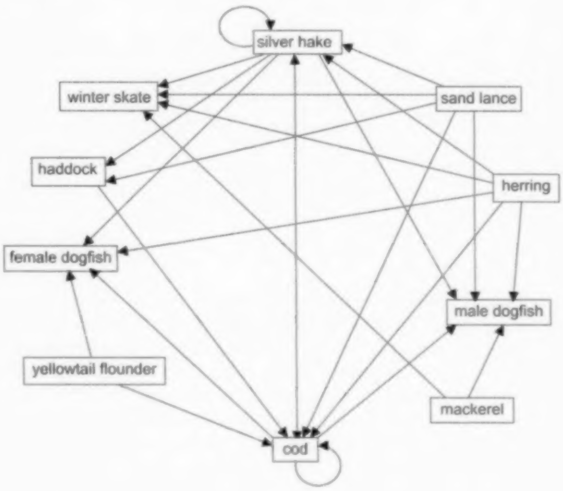

by the values of *a* and α in eq. 5. The estimated *a* value was 0.037 for cod, 0.015 for silver hake, and 0.107 for haddock. Stomach-evacuation rates were higher in quarters three and four, owing to warmer temperature. Based on the estimated *a* values, daily rations in each quarter, *R*, by predator age–size classes were calculated (available from the authors) and used as input parameters in the MSVPA.

The gamma distribution provided a good fit to the observed logarithmic predator-to-prey size ratios (Fig. 1), which justifies its use as a size-preference function. All distributions were noticeably skewed toward higher size ratios. The results of goodness-of-fit tests indicated that the fit for silver hake was significant (at $p = 0.05$). The size ratios of cod and winter skate also conformed to the gamma distribution, but the fits were not statistically significant, owing to lack of fit in the right-hand tails of the distribution. The distribution of size ratios for spiny dogfish appeared bimodal, and the distribution for haddock was highly variable, because of small sample sizes. From the predicted curves, the mean values of the predator-to-prey size ratio (3·ln(predator length/prey length)) for cod, silver hake, haddock, dogfish, and winter skate as predators were 4.8, 3.6, 7.5, 5.4, and 5.7, respectively. This means that, relative to its own body weight, silver hake ate the largest prey and haddock ate the smallest prey. The shape of the gamma distributions demonstrated the range of a predator's preference relative to the mean size ratio. This range is positively related to the variance of the gamma distribution. A sharp peak with low variance indicated a strong preference for a narrow range of prey size and vice versa. Our results indicated that silver hake had the widest range of preference and haddock the narrowest, although the estimate for haddock was the most uncertain.

Fig. 3. Mean relative stomach contents of cod (*a*), silver hake (*b*), and haddock (*c*) by age and of male dogfish (*d*), female dogfish (*e*), and winter skate (*f*) by size. Prey items are described in the key.

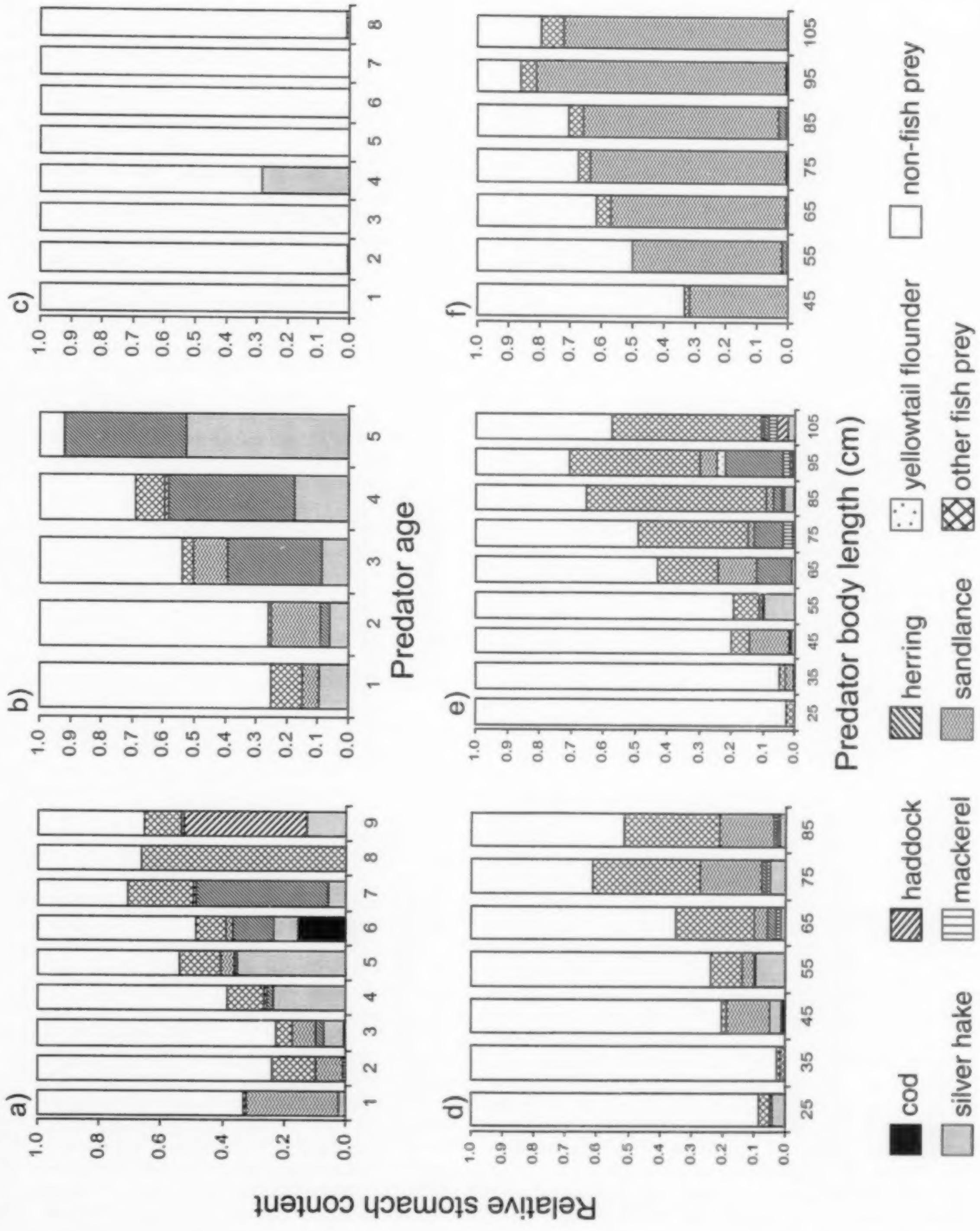

Fig. 4. Predation mortality by age of cod (- -▲- -), silver hake (—△—), haddock (- -■- -), mackerel (—□—), herring (- -●- -), and yellowtail flounder (—○—) averaged over years.

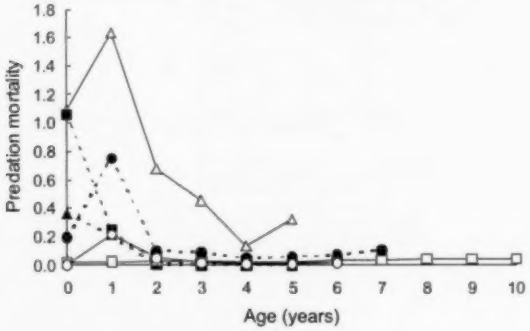

To evaluate the effects of using length instead of weight in fitting gamma distributions, the mean values of ln(predator weight/prey weight) for cod and silver hake were calculated from a much smaller sample. The mean of the logarithmic size ratios equaled 3.98 for cod and 2.27 for silver hake. These values were lower than the values based on length ratios. The fitted gamma distributions were applied to the entire stomach-data set for distributing the relative stomach content of each predator age group. The detailed stomach content data files (by predator-species age-class and prey-species age-class in the spring and fall) used as input to the MSVPA are available from the authors.

The trophic relationships of the nine species in our model (Fig. 2) were identified from the NMFS food-habits database. The most important predators were cod, silver hake, and spiny dogfish; the most important prey species were sand lance, silver hake, and herring. The relative stomach contents of predators by age–size categories have been averaged to give an overview of the diet composition (Fig. 3). Seasonal food habits data were used in the MSVPA and seasonal differences in the diet composition are noted below. Cod preyed on all the prey species in our model, except mackerel (Fig. 2). Nonfish prey was the major food for younger cod, whereas older cod consumed more fish prey (Fig. 3). On a seasonal basis, cod consumed more of the MSVPA species in the fall and more "other fish" in the spring. Silver hake preyed on cod, silver hake, herring, and sand lance (Fig. 2). Like cod, nonfish prey was the dominant component in the diet of younger silver hake, while fish prey was most important in the diet of older silver hake (Fig. 3). Silver hake consumed more fish in the fall, and herring was its major prey species in that season. Cannibalism of silver hake was important, although more significant in the spring than in the fall. Haddock consumed mostly nonfish prey, except for age-4 haddock, in whose diet silver hake accounted for more than 50% in the fall (Fig. 3). Conclusions drawn about the age-specific feeding habits of haddock are tentative, because the sample sizes for each age category were small. Diet compositions for female and male dogfish were similar, except that female dogfish preyed on all the prey species and male dogfish did not consume either mackerel or yellowtail flounder (Fig. 2). The seven prey species included in this study did not constitute a significant amount of the dogfish diet (Fig. 3). Nonfish prey was the most important prey item of smaller dogfish and was important for larger dogfish in the fall. "Other fish" was important for older dogfish, more so in the spring than in the fall. Winter skate preyed on silver hake, mackerel, herring, and sand lance (Fig. 2). For skates smaller than 50 cm, nonfish prey were most important; for skates larger than 50 cm, sand lance was the most important prey species (Fig. 3). MSVPA species and "other fish" constituted less than 10% of the winter skate diet.

Predation mortality caused by the six predators in this study was high compared with residual natural mortality, except for mackerel. Predation mortality of cod ranged from 0.3 at age 0 to 0.003 at age 3 (Fig. 4). Silver hake was the most important prey species and was preyed upon by all the predators. Its predation mortality ranged from 1.6 at age 1 to 0.13 at age 4. Haddock experienced high predation mortality at age 0 (1.05) and age 1 (0.24), even though its predators, cod and female dogfish, only consumed a small amount of haddock in their diet. Predation mortality of mackerel was lower than 0.05 for all age groups. Predation mortality of herring ranged from 0.75 at age 1 to 0.06 at age 5 (Fig. 4). For yellowtail flounder, predation was not high, except that age-1 fish experienced a slightly higher predation mortality (0.22). Sand lance was not included in the base run, because its abundance was uncertain.

Biomass consumed by predators varied among years (Fig. 5), owing to the changes of predator and prey biomass over time. Biomass of cod consumed was low compared with its yield. Cod was consumed more in the early years when cod abundance was higher; consumption of cod peaked in 1981. Cannibalism accounted for 60–90% of the consumed biomass and silver hake accounted for another 10–30%. Consumption of cod by dogfish increased slightly after the mid-1980s. Silver hake was the most important prey species and its consumed biomass was about 10 times its yield. Consumed biomass was highest in 1978 and 1979 when silver hake was most abundant. It decreased sharply in the early 1980s and peaked again in the late 1980s. These changes in the amount of silver hake eaten coincided with the changes in biomass over time. Cod and silver hake were the most important predators of silver hake and accounted for 20–50% and 30–80% of the predation, respectively. Predation from elasmobranchs increased slightly when their abundance increased in the late 1980s and early 1990s. For haddock, predation came from cod and female dogfish, and its biomass consumed was the same magnitude as its yield. Cod was the major predator of haddock in the early 1980s; female dogfish became more important in the late 1980s. Total consumed biomass of mackerel increased over time with the increase in elasmobranch biomass. Herring became more important as prey in the latter years as its abundance increased sharply. Total herring biomass consumed increased from five to 10 times its yield over these years. The increase in consumption of herring in the 1990s may account for the coincident declines in consumption of the other prey species. Silver hake was the dominant predator of herring, accounting for 50–90% of consumed biomass. Predation from dogfish increased over time with the increase in dogfish biomass. Yellowtail flounder was not an important prey species. Its biomass consumed was highest in 1978 and then de-

Fig. 5. The biomass of cod (*a*), silver hake (*b*), haddock (*c*), mackerel (*d*), herring (*e*), and yellowtail flounder (*f*) consumed in each year by predators (see key).

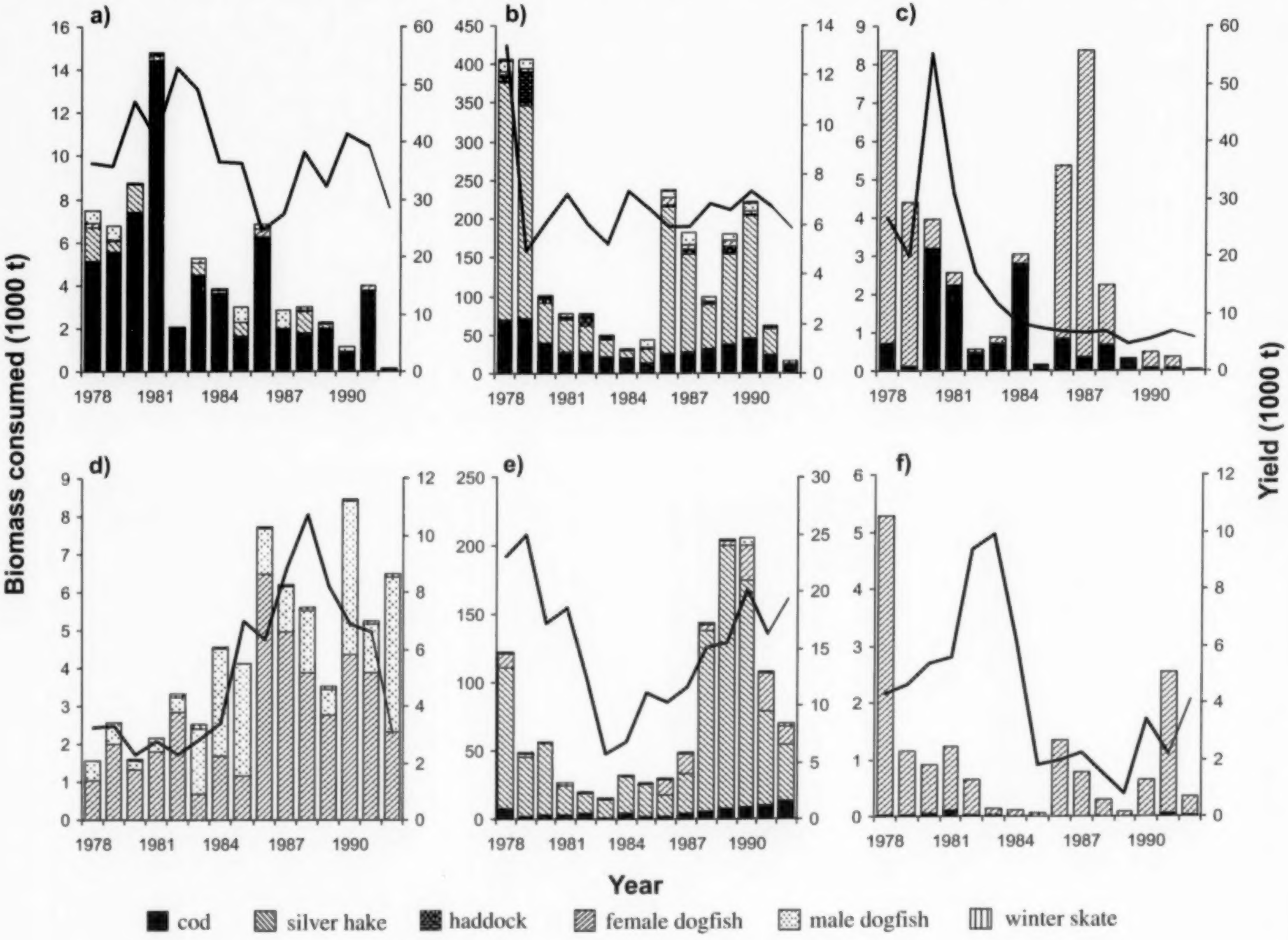

Fig. 6. (*a*) Total biomass of predator species. (*b*) Total biomass of prey species.

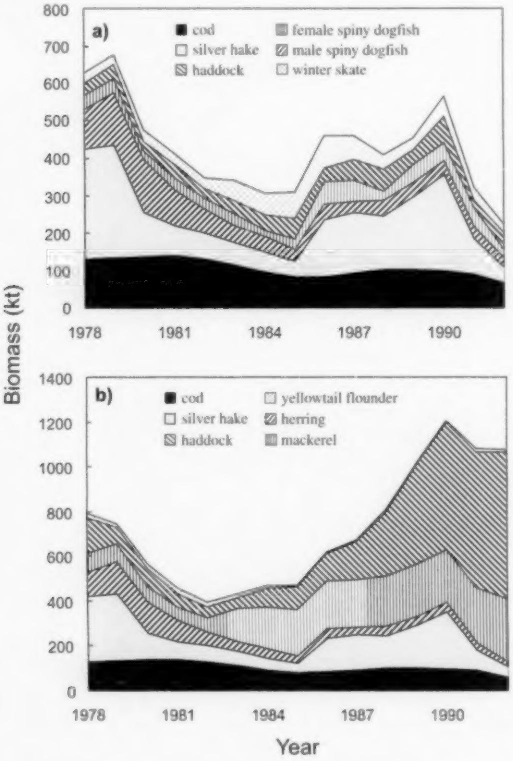

creased over time as flounder abundance decreased. The slight increase in the biomass of flounder consumed in the late 1980s was due to the increased abundance of its major predator, female spiny dogfish.

Total biomass of the eight base-run species remained relatively constant over the years, with a slight increase in the latter years due to the sharp increase in mackerel and herring abundance. Total predator biomass decreased over time (Fig. 6*a*), with peaks in the 1970s and late 1980s, owing to the very high abundance of silver hake in these years. Total prey biomass (Fig. 6*b*) decreased from 1978 to 1982. After 1982, the increasing biomass of mackerel and herring compensated for the declining biomass of other prey species, which resulted in an increasing total prey biomass.

MSVPA also accounts for the changes in predator diet as the abundance of predators and prey changes (Fig. 7). The MSVPA species together constituted 10–20% of the biomass consumed by each predator. "Other food" was the major component in the predators' diet and compensated for the biomass changes of the MSVPA species. The changes in the consumed biomass of silver hake coincided with changes in silver hake biomass, which peaked in the late 1970s and again in the late 1980s. In the 1990s, silver hake abundance declined while herring abundance increased sharply. Consequently, herring became the dominant prey in the predators' diet and constituted more than 50% of the total biomass eaten. Cannibalism was important for cod and silver hake and accounted for more than 50% of their predation rates. The rate of cannibalism by cod was relatively low and showed no clear pattern with stock size (Fig. 8*a*). The cannibalism rate of silver hake was higher and was an increasing function of stock size (Fig. 8*b*), as would be predicted from eq. 1.

Sand lance was abundant from 1979 to 1983, after which its abundance declined sharply (Wallace Morse, Northeast Fisheries Science Center, 100 Water Street, Woods Hole, MA 02543, U.S.A., unpublished data). Its minimum biomass estimates were multiplied by a factor of 50 to support the predators in this study. By adding sand lance as "other prey," the predation mortalities of the MSVPA species decreased about 10–20%, depending on the age and year. The amount of sand lance provided did not affect the predation estimates much, as long as there were enough sand lance for the predators. The predation mortality on sand lance itself is tentative, because sand lance abundance was relative.

The results of our sensitivity test indicated that, although the MSVPA outputs varied with small perturbations in the input parameters, the variation was within 10% of the values in the base run. All the response variables, except for mean r^2, were most sensitive to the consumption rate estimates (Fig. 9); the higher consumption estimates caused higher predation mortalities. In addition to the consumption estimates, terminal fishing mortalities for a given species were positively related to estimates of predation mortality for the same species. In addition to the two major factors, the first response variable, predation mortality of age-0 cod, was negatively related to the terminal fishing mortalities of silver hake and the residual natural mortality of age-0 cod (Fig. 9*a*). The third response variable, predation mortality of age-0 silver hake, was sensitive to the terminal fishing mortalities of cod and the residual natural mortality of cod (Fig. 9*c*). Higher terminal fishing mortalities of cod and lower residual natural mortality of cod caused higher predation mortality of age-0 silver hake. Predation of age-1 silver hake was positively related to the terminal fishing mortalities of cod (Fig. 9*d*), whereas predation mortality of age-0 haddock was negatively related to the terminal fishing mortalities of cod and the residual natural mortality of cod (Fig. 9*e*). Predation of age-0 and age-1 herring was sensitive and negatively related to the terminal fishing mortalities of silver hake (Figs. 9*f* and 9*g*). Predation mortality of age-1 yellowtail flounder was positively related to the terminal fishing mortalities of yellowtail flounder but insensitive to the other factors (Fig. 9*h*). The regression between the MSVPA abundance estimates and the survey indices did not improve much with different parameter combinations. Mean r^2 values varied between 0.52 and 0.54 for the 32 MSVPA runs. Mean r^2s were negatively related to the terminal fishing mortalities of all the species, except for cod and silver hake. Lower consumption estimates also had higher mean r^2 values.

Discussion

This application of MSVPA builds upon previous age-structured analyses of the Georges Bank fish community (Foster 1982; Overholtz and Tyler 1986). MSVPA integrates the conventional age-structured stock assessments with the extensive stomach-content database collected by the NEFSC. Unlike the earlier multispecies analyses of Georges Bank, MSVPA calculates suitability coefficients, which can be

Fig. 7. Proportion of each prey species (see key) in the biomass of these six prey species consumed by predators in each year.

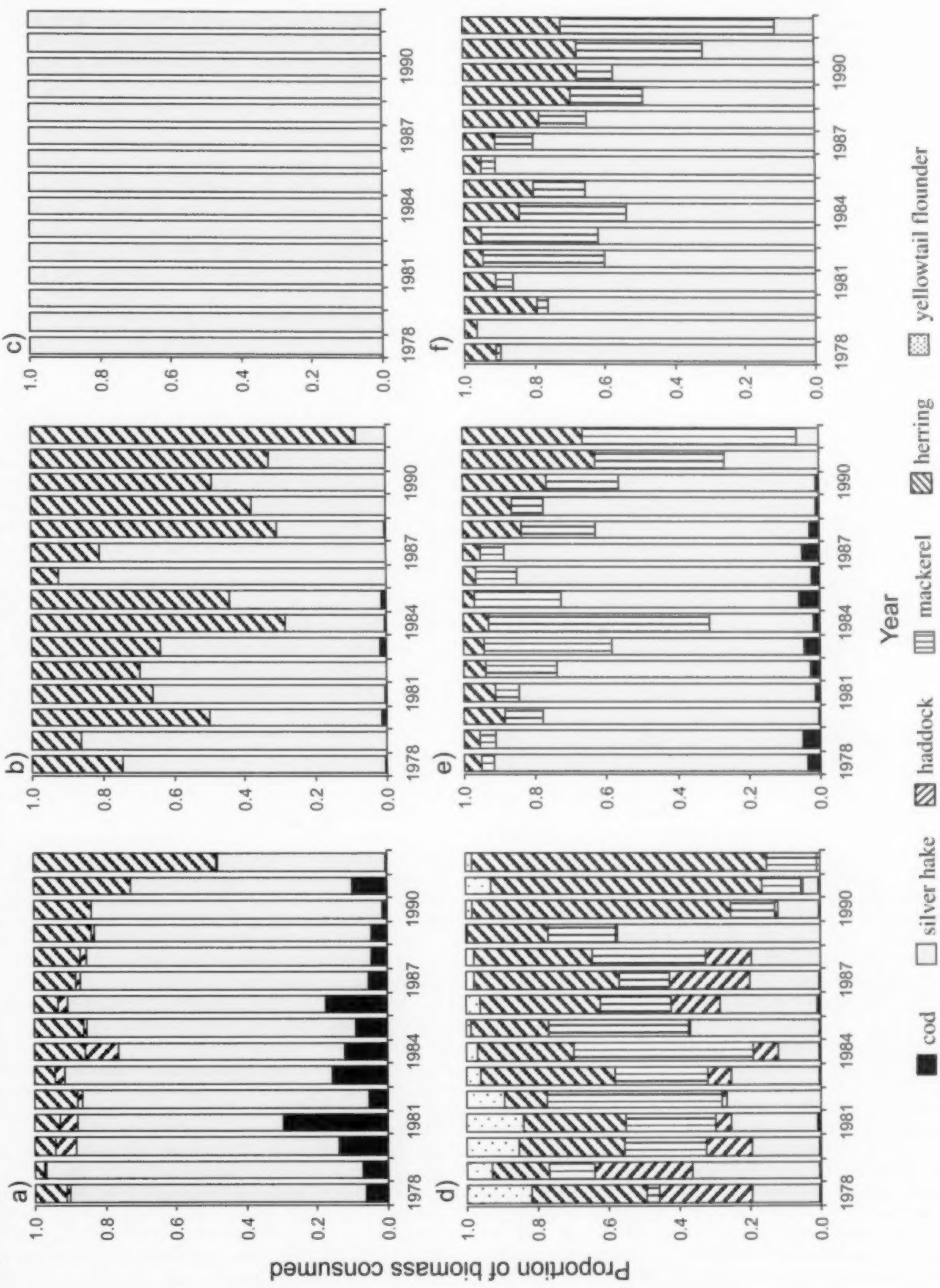

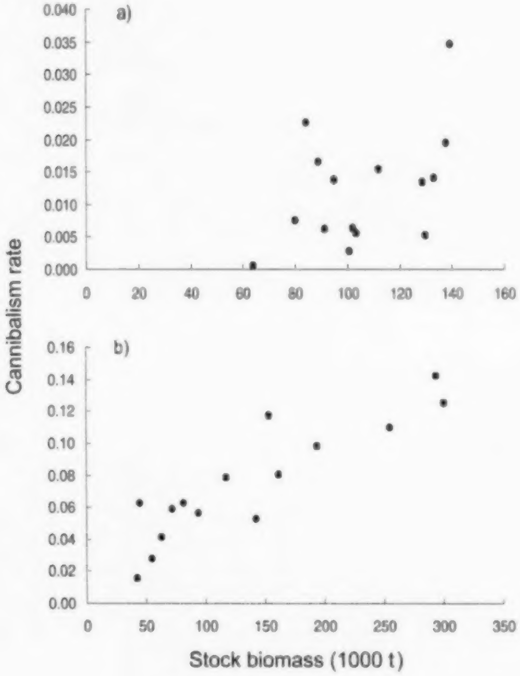

Fig. 8. Cannibalism rate versus stock biomass of cod (*a*) and silver hake (*b*). The cannibalism rate of cod (silver hake) is defined as the biomass of cod (silver hake) consumed by cod (silver hake) divided by total prey biomass consumed by cod (silver hake), including other food.

used in forward simulations with programs such as MSFOR (International Council of the Exploitation of the Sea 1988).

The results of our MSVPA agree with previous conclusions that predation is a dominant source of mortality in the Georges Bank fish community (Sissenwine et al. 1984; Fogarty and Murawski 1998; Collie and DeLong 1999). Cod and silver hake were the most important predators, but were replaced by elasmobranchs as the dominant piscivores in the latter years. However, spiny dogfish eat more "other fish" and invertebrates than the gadoids and, hence, have a lower predation impact on the MSVPA species. The predator diet composition shifted to herring and mackerel as these prey species became more abundant in the late 1990s, but the predation pressure was insufficient to prevent these pelagic species from increasing to record levels of abundance.

Predation by elasmobranchs does not appear to be a significant source of mortality for cod and haddock. Most of the predation on the gadoid species is inflicted by other gadoids, and includes cannibalism. The gadoids and elasmobranchs may compete for mackerel, herring, and sand lance. Yellowtail flounder constituted a small proportion of the spiny dogfish diet, yet there was substantial predation mortality, because dogfish far outnumbered the flounder. The predators in our model had a wide range of alternative prey species, which justifies the assumption of constant consumption rates made in the MSVPA. Given this model structure, prey abundance was not a limiting factor for the predators, but predation had considerable impact on the prey species, particularly silver hake, haddock, and herring.

The main differences between the results of MSVPA and SSVPA were the abundance estimates for young fish. The influence of predation is principally on age-0 to age-2 fish, whereas the influence of the fishery is principally on older fish. Therefore, the abundance estimates for young fish are considerably higher from MSVPA than from SSVPA; however, there were no major differences among the abundance estimates for older fish. Fishing mortality estimates from MSVPA and SSVPA were very close, because fishing mortality was more important for older fish when predation was not a major concern. For some prey species, such as herring, predation remained important for adults. Their MSVPA abundances were higher than VPA abundances for all age groups, while the fishing mortalities from MSVPA tended to be slightly lower than those from VPA.

The lognormal distribution has traditionally been used to measure size preference (Ursin 1973), despite evidence of asymmetric frequency distributions. To our knowledge, ours is the first application of the gamma distribution to fish size preference data. This flexible distribution may prove to be more useful than other functions that have been fitted to skewed size-preference distributions (International Council of the Exploitation of the Sea 1996). Size-preference functions, estimated from a subset of the stomach-content data, have been shown to be widely applicable, and should facilitate application of MSVPA to areas for which extensive stomach-content data are not available (Christensen 1996). A drawback of this approach is that the ingested prey size distributions are assumed to stay unchanged regardless of variations in prey availability. The fitted gamma distributions are not actually size-preference functions, because the size distribution of available prey was not measured coincidentally with the stomach-content analyses. As a result, the gamma distribution can attribute the ingested prey material to prey age-classes that were actually not abundant in the sea. A flat-topped growth curve, such as those for herring and silver hake, gives both young and old prey the same probability of being ingested, although the abundance of a cohort decreases with age. This resulted in somewhat high predation mortalities for older herring age groups being estimated by the MSVPA. This overestimation of predation mortality for older prey came from the calculation of suitability coefficients. In MSVPA, when a prey species or age group with low abundance was consumed, a high value was assigned to its suitability, which then caused a high predation mortality. This bias can only be avoided by measuring the age of ingested prey or by reverting to a multispecies model that is not age structured.

Hahm and Langton (1984) examined logarithmic predator-to-prey weight ratios for 11 northwest Atlantic fishes. For the predators on Georges Bank, the mean values were 7.2 for silver hake, 8.15 for cod, and 9.5 for haddock. These values are higher than ours, because we only included fish prey, which gave smaller logarithmic size ratios. The final estimate used in this study was 3·ln(predator length/prey length) instead of ln(weight ratios), because of the limited information on length–weight relationships for all the fish prey. Most of the prey items that could be converted from length to weight were silver hake and sand lance. The mean values

Fig. 9. Design plots of the response variables in relation to 10 factors: fishing mortality of cod (cF), silver hake (sF), haddock (hF), mackerel (mF), herring (rF), and yellowtail flounder (yF); residual natural mortality of age-0 cod (cM), silver hake (sM), and haddock (hM); and different consumption rates (cn). The horizontal line in each panel is the mean of each response variable: predation mortality of age-0 cod (cod0P), age-1 cod (cod1P), age-0 silver hake (shk0P), age-1 silver hake (shk1P), age-0 haddock (had0P), age-0 herring (her0P), age-1 herring (her1P), and age-1 yellowtail flounder (ytf1P), and mean r^2 values from regressing the multispecies virtual population analysis abundance estimates against trawl-survey data. The vertical lines show the sensitivity of each response variable to an increase or decrease in each factor.

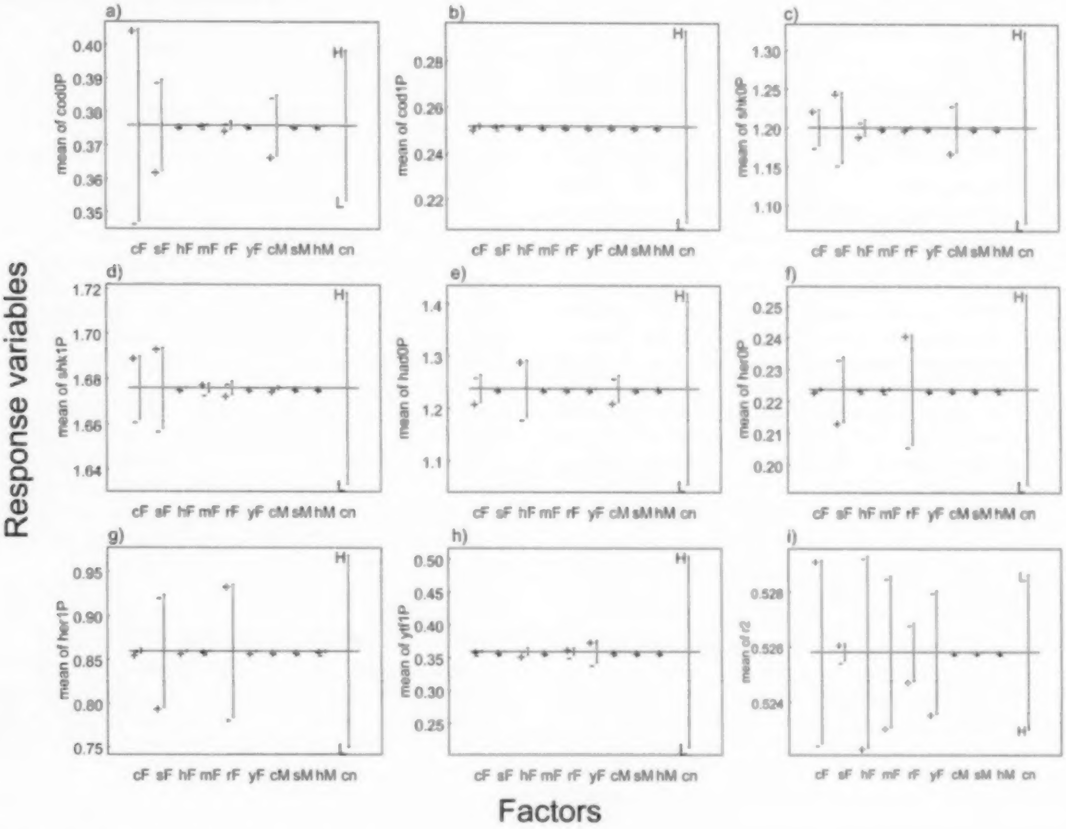

of logarithmic size ratios from the length ratios and weight ratios for these two prey species were very close. However, when the mean ln(weight ratio) from these two prey species was compared with the mean ln(length ratio) from all the consumed fish prey species, the former estimates had lower values. This may mean that the assumption of similar body shapes of predator and prey was not met. If lower mean logarithmic size ratios were used, predation on young fish would decrease and predation on older fish would increase.

According to our sensitivity test, the consumption rates input to MSVPA have the most influence on the magnitude of estimated predation mortalities. This can be seen from eq. 1, in which predation mortality is linearly related to the predator consumption rates (I). In contrast, a sensitivity analysis of MSVPA for the North Sea (Finn et al. 1991) indicated that MSVPA biomass estimates were less sensitive to food consumption levels than to terminal fishing mortalities and residual natural mortalities. This is because the highest consumption levels in Finn et al. (1991) were only 3.5 times the values in their base run, whereas our consumption rates in the sensitivity test can differ by one order of magnitude for some predators. Comparing the daily ration estimates from the different studies, the values used in the base run were on the lower end and, thus, the predation mortalities may be underestimated as a consequence.

Relative stomach content data are the foundation of MSVPA and, therefore, the accuracy of this information is essential. Potential errors in this information may come from the identification of prey species and the measurement of the amount consumed. Mis-identifying the prey species in the stomach will lead to structural errors in the MSVPA output. However, identifying partially digested prey items is not an easy task and unidentified fish remains constituted a considerable proportion of the diet data. We distributed the amount of unidentified fish remains to the identified fish prey according to their relative portions in the stomach, to prevent underestimating predation. The accuracy of this redistribution is uncertain, especially when the amount of unidentified fish remains is much higher than that of identified fish prey. Furthermore, the density of the stomach content was assumed to be one, a convenient way to convert relative volume to relative weight of the stomachs. The actual density may be greater than one and vary with prey types. This assumption may underestimate the predation mortality of prey species with high body density.

Our lack of information on 0-group (young-of-the-year) abundance also contributes to the uncertainty in the abundance and predation estimates for the 0 groups. As there was no 0-group catch, the abundances of the 0 groups were determined by predation mortalities (estimated inside the model) and residual natural mortalities (inputs to the model). Lower values of residual natural mortality caused higher predation mortality and vice versa. The uncertainty of 0-group residual mortality transferred into the 0-group predation estimates. Predation on 0-group mackerel and herring was low in our model. This is because these prey sizes were not selected by the predators according to our size-preference distributions. In the base run, only age-0 silver hake and haddock experienced the highest predation mortality (>1.0). Silver hake was preyed upon by all the predators and constituted a considerable portion of their diets. Therefore, a high predation rate was expected. However, the magnitude of this high predation is uncertain, because the abundances of silver hake were uncertain. Haddock was preyed upon by cod and female dogfish, but was not a major prey item for these species. Its high predation mortality was caused by its lower abundance.

Spiny dogfish was one of the major predators in our model and its abundance estimates should have considerable impact on the MSVPA outputs. The "swept-area estimates" of stock abundance used in this study are considered to be minima, because vulnerability of the stock to the trawls is not incorporated. Compared with the biomass-corrected estimates (total stock biomass in Northeast Fisheries Science Center (1994*b*)) multiplied by the Georges Bank proportion, 0.124 (Collie and DeLong 1999), the "swept-area estimates" were about 1/3 to 3/4 of the biomass-corrected estimates. Thus, by using minimum abundances in MSVPA, predation mortalities might be underestimated, especially for mackerel and yellowtail flounder. The consumption rates used in this study were for Pacific spiny dogfish. Differences in the consumption rates between dogfish populations from two oceans might be expected.

MSVPA requires intensive data input, and the uncertainties in the input parameters will propagate into the outputs, as discussed above. Therefore, it is important to know how sensitive the analysis is to perturbations in input parameters that are uncertain. Results of our sensitivity test indicate that MSVPA was sensitive to the inputs, but the outputs remained within ±10% of the values in the base run while the input parameters varied in a ±25% range. Of our nine response variables, predation mortalities for the prey species were positively related to their own terminal fishing mortalities and negatively related to their own residual natural mortalities. These relationships were expected, because high terminal fishing mortality and low residual natural mortality resulted in lower abundance, which increased the predation mortality. High predation was also caused by high predator abundance that came from lower terminal fishing mortalities of the predators. Alternative prey for a predator was revealed to be important as well. For instance, the predation mortalities of age-0 and age-1 silver hake were positively related to the terminal fishing mortality of cod and negatively related to the residual natural mortality of age-0 cod. This does not mean that fewer predators cause higher predation, but may indicate that cod and silver hake are the alternative prey for predators. It was notable that the MSVPA results were most sensitive to predator consumption rates and that higher consumption-rate estimates created higher predation mortalities for all the prey species. Sensitivity tests on the overall fit of the MSVPA abundance estimates to the survey indices showed that the MSVPA agreed more with the survey indices when the MSVPA created more prey and fewer predators. This is a reasonable result, because higher prey abundance and lower predator abundance can avoid extreme predation estimates and stabilize the system.

MSVPA is one of the more successful multispecies fishery models, but its extensive data requirements may prohibit its application and increase the uncertainty in the outputs. Securing proper data is thus the crucial problem, especially so for consumption-rate estimates that are the major source of uncertainty. For the Georges Bank fish community, the MSVPA results are consistent with the hypothesis of Georges Bank as a predator-controlled ecosystem (Sissenwine et al. 1984). Predators on Georges Bank have a wide choice of prey species, so the abundance of prey does not appear to limit predator consumption rates. In contrast, predation had a considerable impact on prey abundance. Projection of recruitment for prey species that suffer high pre-recruit predation (silver hake, haddock, herring) needs to account for future predator abundance. The MSVPA results were reasonable and varied within a small range, given the assumptions made to create input files, and with small perturbations to some of the input parameters. Therefore, the MSVPA outputs were fairly precise, even if the accuracy remains unknown. Furthermore, different input parameter combinations, such as predator consumption rates, can be considered as alternative models in an adaptive management framework, which can be used to identify robust management strategies.

Acknowledgements

We thank Michael Fogarty, Patricia Livingston, and Jesus Jurado-Molina for their advice on multispecies analysis and Rodney Rountree, Jason Link, and Lance Garrison for their help in accessing the NEFSC food-habits database; Jack Finn provided the original MSVPA FORTRAN program. This study was funded by the National Oceanic and Atmospheric Administration Coastal Ocean Program, Georges Bank Predation Study, NA36RG0474.

References

Andersen, K.P., and Ursin, E. 1977. A multispecies extension to the Beverton and Holt theory of fishing: with accounts of phosphorus, circulation and primary production. Medd. Dan. Fisk.-og Havunders. **7**: 319–435.

Blinov, V.V. 1991. A robust approach to the analysis of feeding data and an attempt to link multispecies virtual population analysis and Volterra predator–prey analysis. ICES Mar. Sci. Symp. **193**: 80–85.

Box, G.E.P, Hunter, W.G., and Hunter, J.S. 1978. Statistics for experimenters: an introduction to design, data analysis and model building. Wiley, New York.

Christensen, V. 1996. Virtual population reality. Rev. Fish Biol. Fish. **6**: 243–247.

Clark, S.H., and Brown, B.E. 1977. Changes in biomass of finfish and squids from the Gulf of Maine to Cape Hatteras, 1963–1974, as determined from research vessel survey data. Fish. Bull. U.S. **75**(1): 1–21.

Cohen, E., and Grosslein, M. 1981. Food consumption in five species of fish on Georges Bank. ICES CM 1981/G:68. (Available from ICES, Palagade 2-4, DK-1261 Copenhagen K, Denmark.)

Collie, J.S., and DeLong, A.K. 1999. Multispecies interactions in the Georges Bank fish community. *In* Ecosystem considerations in fisheries management. Alaska Sea Grant College Program, AK-SG-99-01, Fairbanks, Alaska. pp.187–210.

Durbin, E.G., Durbin, A.G., Langton, R.W., and Bowman, R.E. 1983. Stomach contents of silver hake, *Merluccius bilinearis*, and Atlantic cod, *Gadus morhua*, and estimation of their daily rations. Fish. Bull. U.S. **81**(3): 437–454.

Edwards, R.L., and Bowman, R.E. 1979. Food consumed by continental shelf fishes. *In* Predator–prey systems in fisheries management. *Edited by* H. Cleper. Sport Fishing Institute, Washington, D.C. pp. 387–406.

Elliot, J.M. 1972. Rates of evacuation of brown trout, *Salmo trutta* L. Freshw. Biol. **2**: 1–18.

Elliot, J.M., and Persson, L. 1978. The estimation of daily rates of food consumption for fish. J. Anim. Ecol. **47**: 977–991.

Finn, J.T, Idoine, J.S, and Gislason, H. 1991. Sensitivity analysis of multispecies assessments and predictions for the North Sea. ICES CM 1991/D:7. (Available from ICES, Palagade 2-4, DK-1261 Copenhagen K, Denmark.)

Fogarty, M.J., and Murawski, S.A. 1998. Large-scale disturbance and the structure of marine systems: fisheries impacts on Georges Bank. Ecol. Appl. **8**(1): S6–S22.

Foster, K. 1982. An application of a multispecies cohort analysis to six fish stocks located on Georges Bank. ICES CM 1982/G:37. (Available from ICES, Palagade 2-4, DK-1261 Copenhagen K, Denmark.)

Freund, J.E. 1992. Mathematical statistics. 5th ed. Prentice Hall, Englewood Cliffs, N.J.

Garrahan, P.R. 1994. Gastric evacuation in Atlantic cod. M.Sc. thesis, University of Rhode Island, Narragansett, R.I.

Gislason, H., and Helgason, T. 1985. Species interaction in assessment of fish stocks with special application to the North Sea. Dana, **5**: 1–44.

Grosslein, M.D., Langton, R.W., and Sissenwine, M.P. 1980. Recent fluctuations in pelagic fish stocks of the northwest Atlantic, Georges Bank region, in relation to species interactions. Rapp. P.-V. Reun. Cons. Int. Explor. Mer, No. 177. pp. 374–404.

Gulland, J.A. 1965. Estimation of mortality rates. Annex to Arctic Fisheries Working Group report. ICES CM Gadoid Fish Commission (3). (Available from ICES, Palagade 2-4, DK-1261 Copenhagen K, Denmark.)

Hahm, W., and Langton, R. 1984. Prey selection based on predator/prey weight ratios for some northwest Atlantic fish. Mar. Ecol. Prog. Ser. **19**: 1–5.

Helgason, T., and Gislason, H. 1979. VPA-analysis with species interaction due to predation. ICES CM 1977/G:52. (Available from ICES, Palagade 2-4, DK-1261 Copenhagen K, Denmark.)

ICES. 1988. Report of the Multispecies Assessment Working Group. ICES CM 1988/Assess:23. (Available from ICES, Palagade 2-4, DK-1261 Copenhagen K, Denmark.)

ICES. 1996. Report of the Multispecies Assessment Working Group. ICES CM 1996/Assess:3. (Available from ICES, Palagade 2-4, DK-1261 Copenhagen K, Denmark.)

Jones, B.C., and Geen, G.H. 1977. Food and feeding of spiny dogfish (*Squalus acanthias*) in British Columbia waters. J. Fish. Res. Board Can. **34**: 2067–2078.

Larkin, P.A. 1996. Concepts and issues in the marine ecosystem management. Rev. Fish Biol. Fish. **6**: 139–164.

Livingston, P.A., and Jurado-Molina, J. 2000. Multispecies virtual population analysis of the eastern Bering Sea. ICES J. Mar. Sci. **57**: 294–299.

Magnusson, K.G. 1995. An overview of the multispecies VPA—theory and applications. Rev. Fish Biol. Fish. **5**: 195–212.

Murawski, S.A., and Idoine, J.S. 1992. Multispecies size composition: a conservative property of exploited fishery systems? J. Northwest Atl. Fish. Sci. **14**: 79–85.

Nelson, G.A. 1993. The potential impacts of skate abundances upon the invertebrate resources and growth of yellowtail flounder (*Pleuronectes ferrugineus*) on Georges Bank. Ph.D. thesis, University of Massachusetts, Amherst, Ma.

Northeast Fisheries Science Center. 1994*a*. Report of the 17th Northeast Regional Stock Assessment Workshop: Stock Assessment Review Committee (SARC) consensus summary of assessments. Northeast Fisheries Science Center Ref. Doc. 94-6. National Oceanic and Atmospheric Administration – National Marine Fisheries Service, Woods Hole, Mass.

Northeast Fisheries Science Center. 1994*b*. Report of the 18th Northeast Regional Stock Assessment Workshop: Stock Assessment Review Committee (SARC) consensus summary of assessments. Northeast Fisheries Science Center Ref. Doc. 94-22. National Oceanic and Atmospheric Administration – National Marine Fisheries Service, Woods Hole, Mass.

Northeast Fisheries Science Center. 1995. Report of the 20th Northeast Regional Stock Assessment Workshop: Stock Assessment Review Committee (SARC) consensus summary of assessments. Northeast Fisheries Science Center Ref. Doc. 95-18. National Oceanic and Atmospheric Administration – National Marine Fisheries Service, Woods Hole, Mass.

Northeast Fisheries Science Center. 1996. Report of the 21st Northeast Regional Stock Assessment Workshop: Stock Assessment Review Committee (SARC) consensus summary of assessments. Northeast Fisheries Science Center Ref. Doc. 96-05D. National Oceanic and Atmospheric Administration – National Marine Fisheries Service, Woods Hole, Mass.

Northeast Fisheries Science Center. 1997. Report of the 24th Northeast Regional Stock Assessment Workshop: Stock Assessment Review Committee (SARC) consensus summary of assessments. Northeast Fisheries Science Center Ref. Doc. 97-12. National Oceanic and Atmospheric Administration – National Marine Fisheries Service, Woods Hole, Mass.

Northeast Fisheries Science Center. 1998. Report of the 26th Northeast Regional Stock Assessment Workshop: Stock Assessment Review Committee (SARC) consensus summary of assessments. Northeast Fisheries Science Center Ref. Doc. 98-03. National Oceanic and Atmospheric Administration – National Marine Fisheries Service, Woods Hole, Mass.

Overholtz, W.J., and Tyler, A.V. 1986. An exploratory simulation model of competition and predation in a demersal fish assemblage on Georges Bank. Trans. Am. Fish. Soc. **115**: 805–817.

Pauly, D., Christensen, V., Dalsgaard, J., Froese, R., and Torres, F., Jr. 1998. Fishing down marine food webs. Science (Washington, D.C.), **279**: 860–863.

Penttila, J.A., Nelson, G.A., and Burnett, J.M. 1989. Guidelines for estimating lengths at age for 18 northwest Atlantic finfish and shellfish species. NOAA Tech. Mem. NMFS-F/NEC-66.

Pope, J.G. 1979. A modified cohort analysis in which constant natural mortality is replaced by estimates of predation levels. ICES CM 1979/H:16. (Available from ICES, Palagade 2-4, DK-1261 Copenhagen K, Denmark.)

Pope, J.G. 1991. The ICES Multispecies Assessment Working Group: evolution, insights, and future problems. ICES Mar. Sci. Symp. **193**: 22–33.

Sissenwine, M.P., Cohen, E.B., and Grosslein, M.D. 1984. Structure of the Georges Bank ecosystem. Rapp. P.-V. Reun. Cons. Int. Explor. Mer, No. 183. pp. 243–254.

Sparholt, H. 1991. Multispecies assessment of Baltic fish stocks. ICES Mar. Sci. Symp. **193**: 64–79.

Sparre, P. 1980. A goal function of fisheries (legion analysis). ICES CM 1980/G:40. (Available from ICES, Palagade 2-4, DK-1261 Copenhagen K, Denmark.)

Sparre, P. 1991. Introduction to multispecies virtual population analysis. ICES Mar. Sci. Symp. **193**: 12–21.

Tanasichuk, R.W., Ware, D.M., Shaw, W., and McFarlane, G.A. 1991. Variations in diet, daily ration, and feeding periodicity of Pacific hake (*Merluccius productus*) and spiny dogfish (*Squalus acanthias*) off the lower west coast of Vancouver Island. Can. J. Fish. Aquat. Sci. **48**: 2118–2128.

Temming, A., and Andersen, N.G. 1992. Modeling gastric evacuation in cod. ICES CM 1992/G:6. (Available from ICES, Palagade 2-4, DK-1261 Copenhagen K, Denmark.)

Ursin, E. 1973. On the prey size preferences of cod and dab. Medd. Dan. Fisk.-og Havunders. **7**: 95–98.

Isotopic turnover in aquatic predators: quantifying the exploitation of migratory prey

Stephen E. MacAvoy, Stephen A. Macko, and Greg C. Garman

Abstract: In the tidal freshwaters of Virginia, U.S.A., the blue catfish (*Ictalurus furcatus*), an introduced piscivore, derives a significant proportion of its nutrition from spawning anadromous fish (genus *Alosa*, including blueback herring (*A. aestivalis*), American shad (*A. sapidissima*), and alewife (*A. pseudoharengus*)). Because the *Alosa* are not continually available to *I. furcatus*, there is an isotopic turnover, defined as change in isotope composition due to growth and metabolic tissue replacement, in *I. furcatus* tissues associated with the diet switch from freshwater to anadromous fishes. However, isotopic turnover rates for ictalurid fish are unknown. This study determined the maximum isotopic turnover rate of channel catfish (*Ictalurus punctatus*) tissues and compared this maximum rate with that of *I. furcatus* captured in the field over the 3-month *Alosa* spawning run. Maximum turnover rates for $\delta^{13}C$ were 0.014 and 0.017‰ per day in muscle and blood. For $\delta^{34}S$, rates were 0.017 and 0.020‰ per day in muscle and blood, respectively. Isotopic turnover of muscle carbon reflected growth rate, but sulfur did not match growth as well. *Ictalurus furcatus* captured in the field showed no enrichment during the *Alosa* spawning run owing to slow turnover and variable diet. In aquatic ecosystems that have migrating prey, exploitation by predators may be underestimated using isotopes because of slow tissue turnover.

Résumé : Dans les eaux douces intertidales de la Virginie, aux États-Unis, *Ictalurus furcatus*, un poisson piscivore introduit, retire une proportion significative de son alimentation des poissons anadromes du genre *Alosa*, dont le l'Alose d'été (*A. aestivalis*), l'Alose savoureuse (*A. sapidissima*) et le Gaspareau (*A. pseudoharengus*), qui viennent y frayer. Parce que les *Alosa* ne sont pas toujours disponibles à *I. furcatus*, il se produit un virement isotopique dans les tissus de la barbue, c'est à dire un changement dans la composition isotopique reliée à la croissance et au renouvellement métabolique des tissus consécutif à un remplacement dans le régime des poissons d'eau douce par des poissons anadromes. Cependant, les taux de renouvellements isotopiques chez les poissons ictaluridés sont inconnus. Noua avons déterminé le taux maximal de renouvellement isotopique dans les tissus de la Barbue de rivière (*Ictalurus punctatus*) et l'avons comparé avec le taux maximum observé chez les *I. furcatus* capturés en nature durant les 3 mois de la montaison de reproduction des *Alosa*. Les taux maximaux de renouvellement du $\delta^{13}C$ sont respectivement de 0,014 et de 0,017‰ par jour dans le muscle et dans le sang, alors que les taux maximaux de $\delta^{34}S$ sont respectivement de 0,017 et de 0,020‰ par jour dans les mêmes tissus. Le taux de renouvellement isotopique du carbone musculaire reflète le taux de croissance, mais celui du soufre ne suit pas la croissance d'aussi près. Les *I. furcatus* capturés en nature ne font preuve d'aucun enrichissement durant la montaison des *Alosa* à cause du faible taux de renouvellement et du régime alimentaire variable. Dans les écosystèmes aquatiques où il y a des proies migratrices, l'utilisation des isotopes peut sous-estimer l'exploitation par les prédateurs à cause du faible taux de renouvellement des tissus.

[Traduit par la Rédaction]

Introduction

Stable isotopes are useful in the study of food webs because they can often be used to differentiate among nutrient sources contributing to consumers' diets. The carbon, nitrogen, and sulfur isotope ratios of prey animals are assumed to be relatively constant over time. Therefore, the isotopic signature of the consumer organisms is assumed to reflect the available prey items at any given time. Often, this assumption may be valid; however, it may be violated in ecosystems that occasionally experience migrations of animals, such as birds, mammals, and fish. The migratory animals may have unique carbon, nitrogen, or sulfur isotopic signatures relative to resident animals in the system they enter. In such a system, the predators that consume the migrating prey should have their own isotopic signatures shift toward that of the prey species (Kline et al. 1998; Persson and Hansson 1999). However, the isotopic turnover rate of most animals, especially large vertebrates, is unknown (Gannes et al. 1997).

Isotopic turnover is defined in this paper as the isotopic change due to growth and metabolic tissue replacement associated with a change in diet. Isotopic turnover studies on brine shrimp (Fry and Arnold 1982) and krill (Frazer et al. 1997) have shown high rates of isotopic turnover owing to the quick growth of these invertebrates. Herzka and Holt

Received August 14, 2000. Accepted January 26, 2001. Published on the NRC Research Press Web site on April 17, 2001.
J15917

S.E. MacAvoy[1,2] and S.A. Macko. Department of Environmental Sciences, University of Virginia, Charlottesville, VA 22903, U.S.A.
G.C. Garman. Center for Environmental Studies, Virginia Commonwealth University, Richmond, VA 23284, U.S.A.

[1] Corresponding author (e-mail: sem7e@arches.uga.edu).

[2] Present address: Department of Marine Sciences, University of Georgia, Athens, GA 30601, U.S.A.

DOI: 10.1139/cjfas-58-5-923

(2000) also found quick turnover rates in larval red drum (*Sciaenops ocellatus*) owing to growth. Hesslein et al. (1993) found slow turnover rates in broad whitefish (*Coregonus nasus*). In their study, Hesslein et al. (1993) determined that more than a year was required for *C. nasus* muscle tissue $\delta^{13}C$ and $\delta^{34}S$ to completely reflect consumed food, and they hypothesized that in slow-growing wild populations, it could take longer. Because of the uncertainties about tissue turnover rates, it becomes difficult to determine isotopically the extent to which a migrating population is being preyed upon by local predators. Additionally, if the predator is migratory, then its role in the ecosystem it moves through would be difficult to determine isotopically. Determination of isotopic turnover rate is also important for understanding the temporal relationship between the isotopic signature of a predator and that of its prey. Some period of time may be required for a predator to reflect the isotope signature of a new prey item.

Many coastal river systems worldwide experience a seasonal influx of spawning anadromous fish. The large influx of anadromous fish may be an important nutrient source to freshwater ecosystems, particularly if the species are semelparous (Kline et al. 1993; Bilby et al. 1996; Ben-David et al. 1998; MacAvoy et al. 1998). The anadromous fish are enriched in ^{13}C, ^{15}N, and ^{34}S relative to freshwater animals and plants because they have spent the majority of their lives in the marine environment and have acquired its relatively enriched isotopic signal. Therefore, the nutrients (in the form of their biomass) that they deliver to freshwater are detectable using stable isotope techniques as shown in Alaska and the Pacific Northwest by Kline et al. (1990, 1993), Bilby et al. (1996), and Ben-David et al. (1998).

In the coastal rivers of the eastern United States, the dominant anadromous fishes are *Alosa* (including blueback herring (*A. aestivalis*), American shad (*A. sapidissima*), and alewife (*A. pseudoharengus*)), and they have been found to be substantially enriched in ^{34}S and ^{13}C relative to freshwater species (Garman and Macko 1998; MacAvoy et al. 1998). Enriched $\delta^{13}C$ and $\delta^{34}S$ values associated with *Alosa* have been detected in the introduced piscivorous blue catfish (*Ictalurus furcatus*) (MacAvoy et al. 2000); however, the changing isotope signature that should occur in a predator consuming seasonally available isotopically distinct prey has not been examined.

The purpose of this study was to determine the isotopic turnover rate of ictalurid catfish in a controlled laboratory experiment and compare it with isotope data collected from *I. furcatus* in the field. It was hypothesized that *I. furcatus* at the beginning of the *Alosa* spawning run should reflect the isotope values of the resident freshwater fish. Then, as the spawning run progressed and *Alosa* became a regular component of the *I. furcatus* diet, the isotope signature of the *I. furcatus* should increasingly resemble that of *Alosa*.

The maximum isotope turnover could be defined as the result of a 100% diet change from foods with a freshwater isotope signature to foods with a marine isotope signature. We hypothesized that the maximum isotope turnover rate in the laboratory could be compared with turnover rates observed in the field and thereby estimate the amount of marine material being consumed at any point in time (see Fig. 1 for an illustration of this point). The isotope change observed in the laboratory was divided into growth and metabolic tissue replacement components in order to address the relative importance of these two components (Hesslein et al. 1993). Ideally, documenting isotopic turnover allows temporal interpretation of the percentage of marine carbon, sulfur, and nitrogen consumed by *I. furcatus* during the course of the *Alosa* spawning run and would augment estimates of *I. furcatus* exploitation of marine material derived from isotope mixing equations (MacAvoy et al. 2000).

Materials and methods

Turnover determination

Channel catfish (*Ictalurus punctatus*) were used in this experiment as a surrogate for *I. furcatus* because they could be obtained locally with minimal transport and handling stress and the growth rates of the two ictalurids are similar (Conder and Hoffarth 1962; Webster et al. 1992, 1995). On 7 April 1999, 36 *I. punctatus* were obtained from Hale Farm, Oilville, Va. Seven fish were sacrificed to determine initial isotopic values. All fish were transported to the University of Virginia and, once there, were measured (total length in inches), tagged, and placed in a Living Stream model LSW-900 (190 gal; Frigid Units, Inc., Toledo, Ohio). The catfish were fed a marine fish diet (100% tuna meat) of known isotopic composition beginning on 8 April 1999 and ending on 17 June 1999; over the 90 days of the study, food was added so that it was always visible (Fry and Arnold 1982). Ninety days is the approximate length of the *Alosa* spawning run in Virginia and was chosen as the optimal length for the turnover experiment because it would encompass the time that *Alosa* adults and *I. furcatus* share the tidal freshwater. Fish were placed on ice prior to sampling. For all fish, muscle and skin were sampled. Most fish had blood samples taken (in some cases, blood could not be obtained), and catfish with barbels had those sampled as well.

As a control group, 19 *I. punctatus* obtained from Hale Farm were kept in the Living Stream for 60 days and were fed the commercial fish food (Big Strike floating fish food, SSC-338220) they had been raised on. This food had 32.0% crude protein and 4.0% fat (Southern States Cooperative Inc., Richmond, Va.). The fish had their total length and fork length measured prior to being placed in the Living Stream.

Water temperature in the Living Stream was raised slowly from 11 to 19°C over a 60-day period during both the experimental and the control procedures. This was done to approximate the water temperature change in the tidal freshwater areas of Virginia during the spring months.

Isotopic analysis

Samples of dorsal muscle, blood, skin, and barbel were dried at 60°C for 3 days and homogenized with a mortar and pestle in preparation for analysis. A Carlo Erba elemental analyzer coupled to a Micromass Optima isotope ratio mass spectrometer (Micromass, Manchester, U.K.) was used to obtain $\delta^{13}C$, $\delta^{15}N$, and $\delta^{34}S$ values (Fry et al. 1992; Giesemann et al. 1994). The $\delta^{13}C$ and $\delta^{15}N$ were obtained concurrently and $\delta^{34}S$ was determined during separate analysis runs.

The isotope compositions are reported relative to standard material and follow the same procedure for all stable isotopic measurements as follows:

$$(1) \qquad \delta^{x}E = ([(^{x}E/^{y}E)_{\text{sample}}/(^{x}E/^{y}E)_{\text{standard}}] - 1) \times 1000$$

where E is the element analyzed (carbon, nitrogen, or sulfur), x is the molecular weight of the heavier isotope, and y is the molecular weight of the lighter isotope (x = 13, 15, and 34 and y = 12, 14, and 32 for carbon, nitrogen, and sulfur, respectively). The standard

Fig. 1. Example of theoretical maximum turnover rate, resulting from a 100% diet switch from freshwater to marine foods (top line), versus a hypothetical turnover rate that may be observed in the field (bottom line). The field rate would probably be less than the maximum rate because the predator would not be forced to undertake a 100% diet switch. The figure illustrates that any isotopic turnover observed in the field should be interpreted relative to a measured maximum turnover rate. This is necessary in order to understand the extent that a predator is feeding upon a migratory population at any given time.

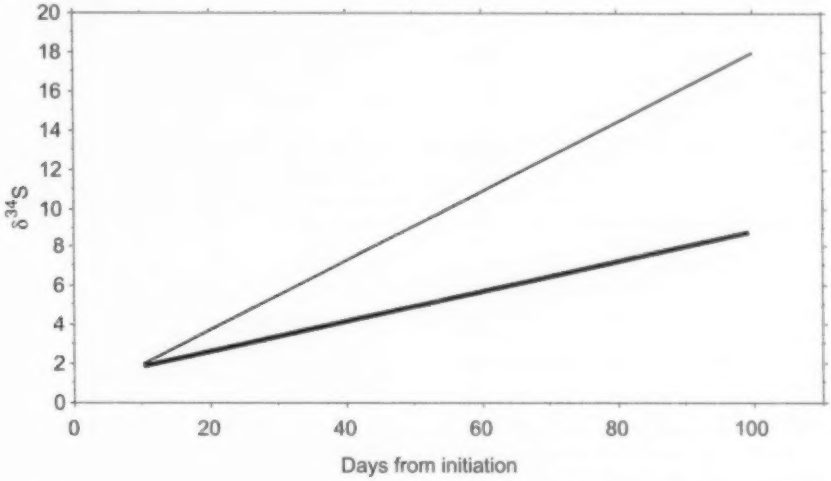

materials with which the samples are compared are Pee Dee Beleminte for carbon, air N_2 for nitrogen, and Canyon Diablo Troilite for sulfur. The reproducibility of all measurements was typically 0.3‰ or better.

Normalization of turnover rates

The rate of turnover observed for the different isotopes is relative to the separation of the isotope endmembers. The greater the separation, the greater is the observed change over time. Therefore, when turnover rates are compared between field and laboratory situations or different field situations, the degree of separation of isotopic endmembers should be addressed.

Field measurements, where predators are not expected to switch prey completely, should display a fraction of the maximum turnover rate, obtained from a 100% diet switch. If, hypothetically, a laboratory a turnover rate of 0.017‰ per day was observed and the endmembers were 7‰ apart, then if in the field there was a 14‰ separation, the expected shift would be 0.034‰ per day.

Subsequently, the expected maximum in the field situation can be found by the following equation:

$$(2)\qquad y = x([\mathrm{Fa} - \mathrm{Fb}]/[\mathrm{La} - \mathrm{Lb}])$$

where y is the maximum isotope turnover rate for ictalurids caught in the field (unknown), x is the turnover rate measured in the laboratory for a particular tissue, [Fa – Fb] is the absolute value of the difference between isotopic endmembers in the field, and [La – Lb] is the absolute value of the difference between isotopic endmembers in the laboratory. In this study, the isotope endmembers in the field were approximately equivalent to laboratory endmembers (Table 1).

Turnover modeling

The turnover model was divided into two components, growth and metabolic tissue replacement. This was done in order to identify whether metabolic tissue replacement was important relative to growth. It is important to know this because isotope turnover in mammals may have a substantial metabolic component (Hobson and Clark 1992). However, it was hypothesized that growth would be the major contributor to isotopic change because the metabolism of the poikilothermic catfish is low relative to that of mammals. The observed isotopic turnover can be better predicted if knowledge of what contributes to it exists.

The turnover model used was based on that of Hesslein et al. (1993), which contained both a growth and a metabolic tissue replacement component. Growth can be described by the following equation:

$$(3)\qquad k = (\ln(W_s/W_0)/t)$$

where k is the specific growth rate constant, t is days, W_s is the weight of the fish at any given time, and W_0 is the initial fish weight (Webster et al. 1992).

In an equation where metabolism (m) and growth (k) contribute to isotope turnover, the following equation holds true:

$$(4)\qquad dC/dt = -(k + m)(C - C_n)$$

where dC/dt is change in isotope value over time, C is the isotope value of the fish when sampled, C_n is the expected isotopic value for a fish in equilibrium with its new diet, and k is the specific growth rate constant (from eq. 3).

Let $(C - C_n) = C'$; then, integrate eq. 4:

$$(5)\qquad \ln C' = -(k + m)t$$

and

$$(6)\qquad C' = \alpha e^{-(k+m)t}$$

where α is the difference between the initial isotope value of the fish (C_0) and the expected isotopic value for a fish in equilibrium with its new diet (C_n), which is a constant. Therefore, eq. 6 becomes

$$(7)\qquad C = C_n + (C_0 - C_n)e^{-(k+m)t}$$

To solve eq. 7, values for k must be determined. Webster et al. (1995) observed that, generally, the more fish in a catfish feed, the larger the k. They observed a k of 0.00218 fish per day in juvenile *I. furcatus* consuming the most fish protein of those in their treatments (14% menhaden); therefore, this value was used as a first ap-

Table 1. Equating the maximum turnover measured in the laboratory to the theoretical maximum possible in the field.

	Laboratory rate (‰ per day)	La	Lb	Fa	Fb	Field rate (‰ per day)
$\delta^{13}C$						
Muscle	0.014	–23.1	–16.7	–25.6	–18.6	0.015
Blood	0.017	–23.4	–16.7	–25.6	–18.6	0.018
$\delta^{34}S$						
Muscle	0.017	3.7	15.9	4.8	18.4	0.019
Blood	0.020	5.3	15.9	4.8	18.4	0.026

Note: La, initial isotope signature (carbon and sulfur) for *I. punctatus* kept in the laboratory; Lb, isotope signature of the laboratory food; Fa, freshwater isotope signature recorded in the field; Fb, marine isotope signal of anadromous *Alosa* in the freshwater field area. Based on the relative difference between the isotopic endmembers, the maximum expected turnover rate in the field is calculated.

proximation of k; however, a range of k values derived from the experimental data were also used (see below). The metabolic tissue replacement component of the turnover (m) was to be arrived at by fitting predicted values (using eq. 7) to the measured data and minimizing the mean difference between the two by estimating various values for m (Hesslein et al. 1993).

Measuring the total length of the fish was problematic because of fin abrasion. For some of the experimental fish where total length could not be determined, fork length was measured instead. Total length is highly correlated with fork length ($r^2 = 0.97$) for the *I. punctatus*, and a simple regression of fork length (FL) with total length (TL) yielded the equation

$$(8)\qquad \mathrm{TL} = 1.04(\mathrm{FL}) + 0.63$$

Therefore, an estimated change in total length was obtained from some experimental fish, and from those values, weight was estimated using the following equation:

$$(9)\qquad Y = 0.152299(\mathrm{TL}) - 0.013302(\mathrm{TL})^2 + 0.000706(\mathrm{TL})^3 - 0.5834$$

where Y is weight in pounds and TL is in inches (Kelly 1969). From these weights, experimental values of k ($\ln(W_t/W_0)/t$) were estimated. The k values calculated for the fish in both the experimental and the control groups ranged between 0.0037 and 0.009, which were in the range observed in other ictalurid growth studies (Conder and Hoffarth 1962; Webster et al. 1992).

Field collections

In the spring (between March and May) of 1997 and 1998, coincident with the anadromous *Alosa* spawning run, 22 *I. furcatus* (≥38 cm total length) were captured from the upper tidal freshwater reaches of the Rappahannock River in Virginia (64–113 km upstream from where the Rappahannock meets the Chesapeake Bay) by boat electrofishing. Resident freshwater fish and spawning anadromous *Alosa* were also collected to provide freshwater and marine examples of fish that the piscivorous *I. furcatus* may have been consuming. Samples of dorsal muscle were either taken in the field or obtained from whole fish in the laboratory. All fish were prepared for isotope analysis and analyzed using the method described above.

Kruskal–Wallis nonparametric procedures were used to test for differences in isotopic values among the three groups of fish captured in the field (native resident freshwater, anadromous fish, and *I. furcatus*) ($\alpha = 0.05$). The Dunn procedure was used to examine differences between groups (Rosner 1990). Simple regressions were used to examine isotope change over time. Statview SE + Graphics (Abacus Concepts, Inc.) and Microsoft Excel version 5.0 (Microsoft, Inc.) were used for statistical tests.

Results

Carbon isotopes

From the laboratory study, regressions of $\delta^{13}C$ versus time indicated turnover rates of 0.014‰ per day in muscle tissue and 0.017‰ per day in blood (Fig. 2). Both regressions were statistically significant ($p = 0.0001$ and 0.0004, respectively) (Table 2). The mean initial $\delta^{13}C$ values of the *I. punctatus* muscle and blood were –23.1 and –23.4‰, respectively. The $\delta^{13}C$ of the marine diet was –16.7 ± 0.5‰. Over the course of the 84-day experiment, the isotope signatures of the *I. punctatus* muscle and blood became enriched by 1.3 and 1.5‰, respectively (Fig. 2). Skin tissue showed larger variability, and regressions of $\delta^{13}C$ versus time were not significant. Barbels were sampled from only a few *I. punctatus* because most of them were missing the tissue. The regression of barbel versus time was significant ($p < 0.001$, $r^2 = 0.87$); however, owing to the limited samples available, only the regressions of muscle and blood were considered for the turnover models. Among the controls, the $\delta^{13}C$ values of all tissues did not change significantly ($p > 0.05$). Skin tissue $\delta^{13}C$ was variable among controls as it was among fish in the experimental group. If the observed turnover rates were to remain reasonably consistent over time, it would take approximately 400 or 450 days for a complete $\delta^{13}C$ turnover of blood or muscle tissue, respectively.

Sulfur isotopes

As hypothesized, there was a significant enrichment in ^{34}S among laboratory-held *I. punctatus* muscle tissue over time ($p = 0.05$) (Table 2). The mean initial muscle $\delta^{34}S$ among *I. punctatus* was 3.7 ± 0.7‰ ($n = 5$). The $\delta^{34}S$ of the marine diet was 15.9 ± 2.1‰. Over the course of the 84-day experiment, the muscle $\delta^{34}S$ values increased by 1.5‰ (Fig. 3). The regressions of blood, skin, and barbel tissue versus time were not significant. There was considerable scatter in the observed $\delta^{34}S$ values, and, although significant in the case of muscle tissue, the r^2 values for the regressions for all tissues were very low. Some of the variability observed in the $\delta^{34}S$ values may be due to the variability in $\delta^{34}S$ of the food that they were fed (standard deviation of 2.1‰, see above). Slopes of 0.02 and 0.017 were measured for blood and muscle $\delta^{34}S$ versus time, respectively, which were similar to the slopes observed with $\delta^{13}C$. This indicates that carbon is replaced faster than sulfur in *I. punctatus* because the degree of separation between the experimental marine feed and

Fig. 2. Simple regressions showing *I. punctatus* tissue $\delta^{13}C$ turnover rate from the laboratory study. (*a*) Muscle; (*b*) blood. The rate is the observed change in stable isotope value starting when the diet was switched (day 0) from commercial catfish food (see Materials and methods) to a marine food (tuna). The initial $\delta^{13}C$ value of the *I. punctatus* muscle and blood was −23.1 and −23.4‰, respectively. The marine food that the *I. punctatus* were being fed had a $\delta^{13}C$ of −16.7 ± 0.5‰.

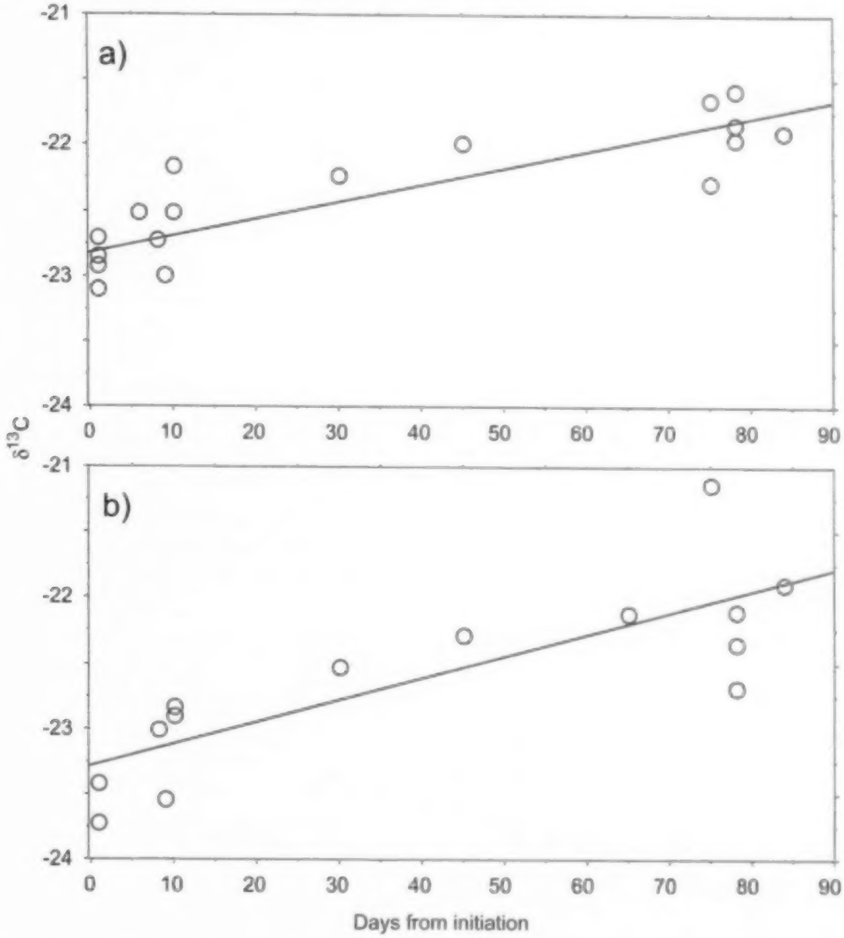

Table 2. Regression analysies of isotope change versus time.

	‰ per day	*p*
Muscle tunover		
$\delta^{13}C$	0.014	≤0.0001
$\delta^{34}S$	0.017	≤0.05
$\delta^{15}N$	0.014	≤0.0026
Blood turnover		
$\delta^{13}C$	0.017	≤0.0004
$\delta^{34}S$	ns	ns
$\delta^{15}N$	0.018	≤0.0074

Note: ns, not significant.

baseline values is roughly 6‰ for $\delta^{13}C$ and 12‰ for $\delta^{34}S$. If the turnover rate was the same for the two elements, then the regression slopes would only be equal once normalized for differences in endmember isotope values. Among the controls, $\delta^{34}S$ values of all tissues did not change significantly ($p > 0.05$). At the observed turnover rates, it would take well over 450 days for the $\delta^{34}S$ of the *I. punctatus* blood and muscle tissue to completely turn over.

Nitrogen isotopes

There was considerable scatter in the nitrogen data among *I. punctatus* in the laboratory study. However, the muscle ($p = 0.0026$, $r^2 = 0.41$), blood ($p = 0.0074$, $r^2 = 0.46$), and barbel ($p = 0.009$, $r^2 = 0.64$) tissues showed statistically significant enrichment over time. The turnover rate measured for $\delta^{15}N$ was equal to that measured for $\delta^{13}C$ in muscle (0.014‰ per day) and blood (0.018‰ per day). However, the $\delta^{15}N$ isotopic endmembers were farther apart than the $\delta^{13}C$ endmembers. Therefore, the actual isotopic turnover was slower than that of $\delta^{13}C$ (as with $\delta^{34}S$ above). The $\delta^{15}N$ of the marine diet was 13.1 ± 0.9‰. The mean initial muscle $\delta^{15}N$ among the laboratory-held *I. punctatus* was 6.2 ± 0.8‰. The blood and skin tissues fell within the same $\delta^{15}N$ range as did muscle (Fig. 4). The barbel tissue $\delta^{15}N$ turnover

Fig. 3. Simple regressions showing *I. punctatus* muscle tissue $\delta^{34}S$ turnover rate from the laboratory study. The rate is the observed change in stable isotope value starting from when the diet was switched (day 0) from commercial catfish food (see Materials and methods) to a marine food (tuna). The initial $\delta^{34}S$ value of the *I. punctatus* muscle tissue was 3.7 ± 0.7‰. The marine food that the *I. punctatus* were being fed had a $\delta^{34}S$ of 15.9 ± 2.1‰.

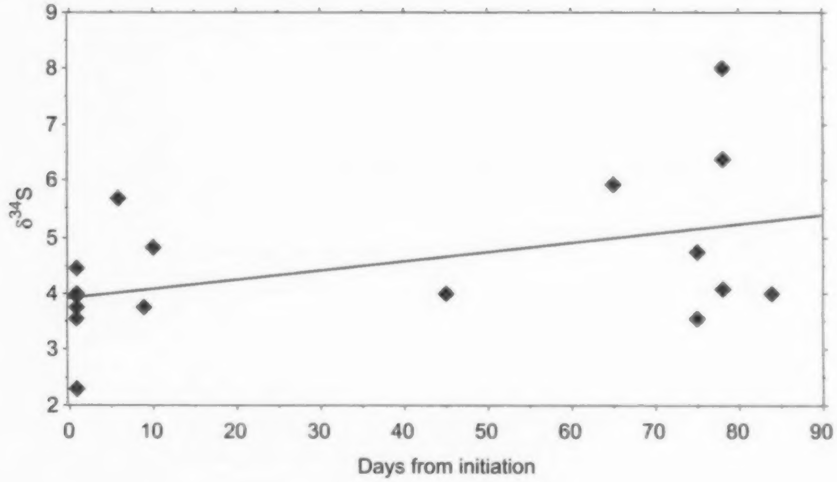

Fig. 4. Simple regressions showing *I. punctatus* muscle tissue $\delta^{15}N$ turnover rate from the laboratory study. The rate is the observed change in stable isotope value starting from when the diet was switched (day 0) from commercial catfish food (see Materials and methods) to a marine food (tuna). The initial $\delta^{15}N$ of the *I. punctatus* muscle tissue was 6.2 ± 0.8‰. The marine food that the *I. punctatus* were being fed had a $\delta^{15}N$ of 13.1 ± 0.9‰.

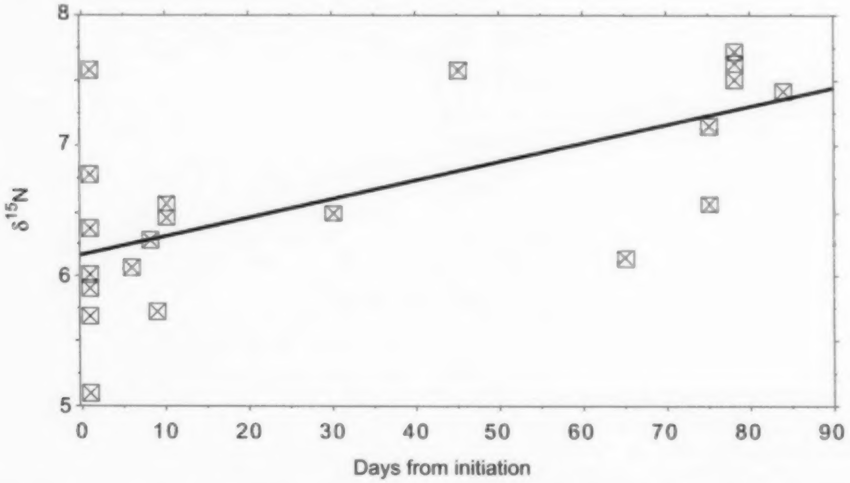

rate was roughly equivalent to that of $\delta^{13}C$ muscle and blood (measured rate = 0.035‰ per day). As with the $\delta^{13}C$ measurements, the skin $\delta^{15}N$ values exhibited a high degree of variability. Although the regression of $\delta^{15}N$ versus time was statistically significant ($p \leq 0.05$), the r^2 was very poor (0.22).

Field data

Regressions of field $\delta^{13}C$, $\delta^{34}S$, and $\delta^{15}N$ showed no statistically significant enrichment of *I. furcatus* muscle tissue during the anadromous *Alosa* spawning run ($p > 0.05$) (Fig. 5). Although there is no obvious isotopic enrichment over time in $\delta^{13}C$ and $\delta^{34}S$ among the *I. furcatus*, their isotopic signatures were significantly enriched ($p < 0.05$) relative to freshwater fish captured within the same stream (the Rappahannock) (Fig. 6). The *I. furcatus* $\delta^{15}N$ values were also significantly higher ($p < 0.05$) than resident fish values (Fig. 6). Relative to anadromous fish captured in the Rappahannock, the *I. furcatus* and resident freshwater fishes were significantly depleted ($p < 0.05$) in ^{13}C and ^{34}S (–21.7 ± 1.8 and 10.6 ± 2.1‰ and –25.6 ± 2.3 and 4.8 ± 1.6‰, respectively) (Fig. 6).

Discussion

Observed versus modeled turnover: isotope change due to growth

Based on eq. 7, the expected $\delta^{13}C$ change in muscle tissue

Fig. 5. Isotopic signatures of *I. furcatus* (>37 cm total length) caught in the Rappahannock River, Virginia, between March and June 1997–1998. (*a*) $\delta^{13}C$; (*b*) $\delta^{34}S$; (*c*) $\delta^{15}N$. Days from initiation indicates the time from when the *Alosa* spawning run begins during the last week of February. The isotopic signatures of the *Alosa* were –18.6 ± 1.4‰ for $\delta^{13}C$, 18.4 ± 1.1‰ for $\delta^{34}S$, and 12.9 ± 0.6‰ for $\delta^{15}N$.

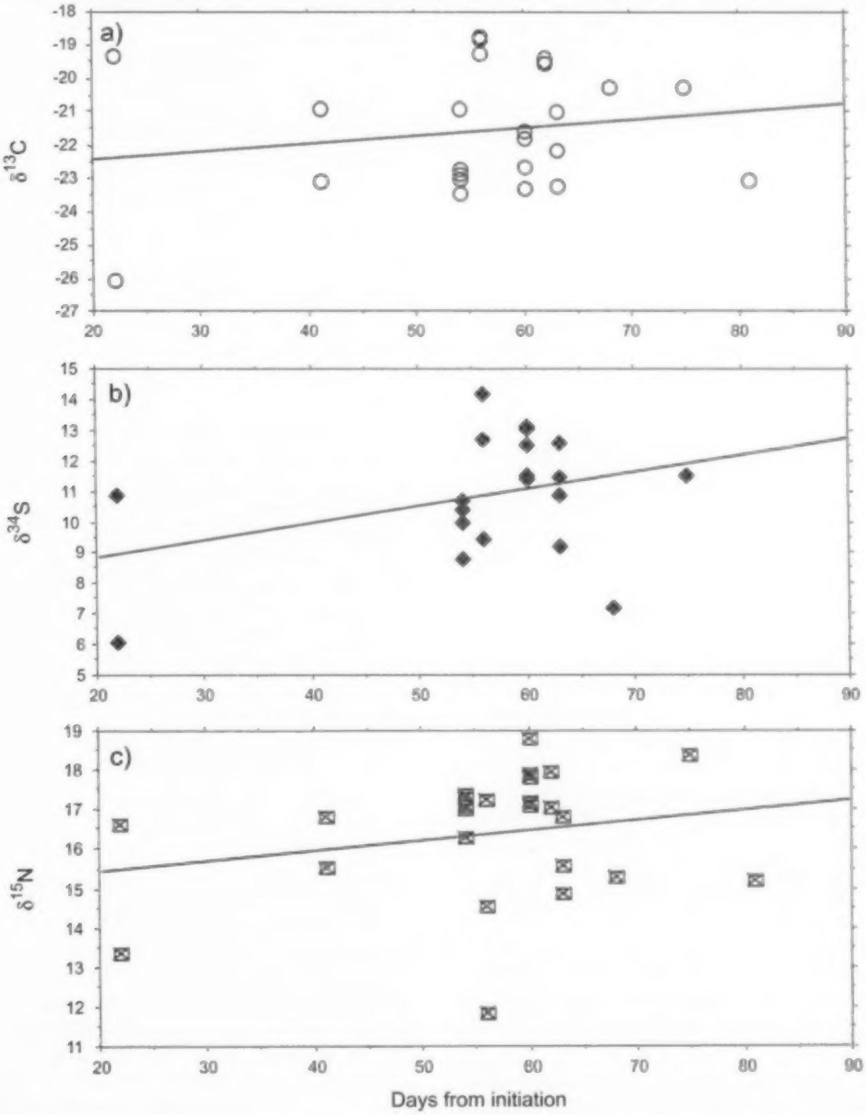

due to growth alone was compared with that actually measured in the laboratory (Table 3). Using the specific growth rate k measured by Webster et al. (1995) for juvenile *I. furcatus* (0.00218), there was fairly good agreement between the predicted isotope change (calculated from eq. 7) and the actual isotope change ($r^2 = 0.72$). One source of variability was that the *I. punctatus* obtained from Hale Farms did not all have identical $\delta^{13}C$ values. Their $\delta^{13}C$ values ranged from –22.9 to –23.7‰. However, eq. 7 assumes that the initial isotope value of the *I. punctatus* would all be equal at time 0. Because this was not the case, there was some variability associated with the violation of this assumption.

Various values of k were used in eq. 7 ranging between 0.00218 and 0.009. The low value (0.00218) was measured in *I. furcatus* fed a diet with 14% fish meal (Webster et al. 1995). The highest growth rate observed in this study was 0.009 and reflected both the greater proportion of fish protein used in the feed and the competitive feeding among the *I. punctatus*. Using the range of k values changed the slope of the predicted δ values versus the measured δ values. However, there was not a large improvement in the r^2 for the regressions using the various k values. In general, the larger values of $k + m$ resulted in large mean differences between predicted and modeled results. The $k + m$ value that yielded the best r^2 (0.74) was 0.004. This value was within the measured range of the k values, which accounted only for growth. Therefore, relative to growth, metabolic tissue replacement was probably minimal. It would come to be important only

Fig. 6. δ^{34}S versus δ^{13}C for fish captured in the tidal freshwater of the Rappahannock River, Virginia. Anadromous fish (×) include *A. pseduoharengus* and one *A. aestivalis*. Native resident freshwater fish (+) include *Hyboganthus regios*, *Perca flavescens*, and *Erimizon oblongus*. The apex predator *I. furcatus* (△) is significantly enriched (p = 0.05) in δ^{13}C and δ^{34}S relative to other freshwater fishes, indicating the importance of anadromous *Alosa* in their diet. Figure adapted from MacAvoy et al. (2000).

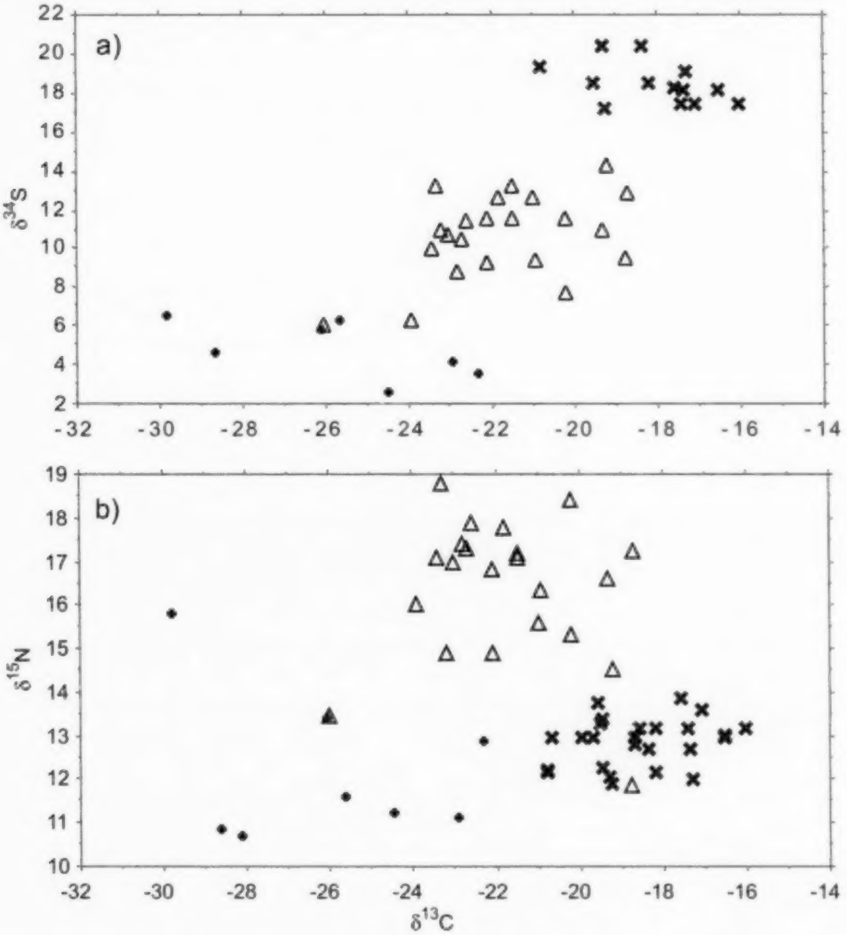

when growth rate would not account for the observed isotope turnover, such as in the case of small mammals and birds (Tieszen et al. 1983; Hobson and Clark 1992).

The observed δ^{34}S values were also compared with predicted values using eq. 7. The modeled δ^{34}S isotopic change did not fit the laboratory data as well as the modeled δ^{13}C, and the r^2 values for $k + m$ values of 0.00218 and 0.004 were only 0.27 and 0.28, respectively. The poor correlation was due to two factors: first, the variability in initial δ^{34}S values among the farm-raised *I. punctatus* (as noted for δ^{13}C above) and, second, a large variation in the δ^{34}S of the marine fish that were used to feed the *I. punctatus* in the laboratory (range 13–17‰, mean ± SD = 15.9 ± 2.1‰). Nitrogen isotope turnover was not modeled against what would be expected due to growth because of the variability among individual *I. punctatus* and the high fractionation expected for nitrogen isotopes relative to carbon and sulfur isotopes. There is a 3–4‰ enrichment of ^{15}N in a predator's muscle tissue relative to its prey, and when combined with the initial variability of the δ^{15}N in the *I. punctatus*, carbon and sulfur isotope signatures probably are a superior method for documenting turnover of tissue due to growth.

As expected, the isotope turnover of the *I. punctatus* tissue was slow relative to that of Japanese quail (Hobson and Clark 1992), gerbils (Tieszen et al. 1983), brine shrimp (Fry and Arnold 1982), and krill (Frazer et al. 1997). In the cases of the birds and gerbils, their growth rates and metabolism were orders of magnitude higher than those of the *I. punctatus* in this study. The krill quickly assume the isotope composition of their food because they have a high growth rate (Frazer et al. 1997). When krill are starved or kept at low temperatures, they show no turnover of δ^{13}C. In brine shrimp, Fry and Arnold (1982) measured half-lives of δ^{13}C turnover to be between 4 and 19 days depending on their diet. Herzka and Holt (2000) found rapid turnover of δ^{13}C and δ^{15}N in red drum larvae, which generally matched the very high growth rate of these very young fish (doubling of biomass occurred in 1 or 2 days). Hesslein et al. (1993) is

Table 3. Measured versus calculated isotope turnover.

		$\delta^{13}C$ calculated (‰)			$\delta^{34}S$ calculated (‰)	
Time (days)	$\delta^{13}C$ measured (‰)	$k + m = 0.00218$	$k + m = 0.004$	$\delta^{34}S$ measured (‰)	$k + m = 0.00218$	$k + m = 0.004$
1	–23.1 ± 0.3	–22.98	–22.87	3.7 ± 0.7	3.70	3.72
6	–22.5	–22.90	–22.73	5.7	3.83	3.96
8	–22.7	–22.87	–22.67			
9	–23.0	–22.86	–22.64	3.7	3.91	4.10
10	–22.3 ± 0.2	–22.84	–22.61	4.8	3.93	4.15
30	–22.2	–22.53	–22.07			
45	–22.0	–21.31	–21.70	4.0	4.81	5.68
65				5.9	5.29	6.47
75	–22.0 ± 0.4	–21.88	–21.01	4.1 ± 0.8	5.51	6.84
78	–21.8 ± 0.2	–21.84	–20.94	6.0 ± 2.8	5.58	6.95
84	–21.9	–21.76	–20.82			

Note: Calculated values were arrived at using eq. 7 ($C = C_n + (C_0 - C_n)e^{-(k+m)t}$), where C is the isotope signature at time of sampling, C_n is the signature of a fish in equilibrium with the new food, C_0 is the initial signature of the fish, and $k + m$ is growth rate per day plus metabolic turnover. Initial $\delta^{13}C$ and $\delta^{34}S$ values of the *I. punctatus* muscle were –23.1 and 3.7‰, respectively. The marine food (tuna muscle) that they were fed had a $\delta^{13}C$ of –16.7‰ and a $\delta^{34}S$ of 15.9‰.

the only study that we are aware of that examined juvenile fish (broad whitefish (*Coregonus nasus*)), and they found very slow turnover rates, comparable with those measured in this study. They attributed most of the observed isotope change to growth. However, they estimated that metabolic turnover might have accounted for 0.0013‰ per day for $\delta^{34}S$ and 0.0018‰ per day for $\delta^{13}C$. It should be noted that Hesslein et al. (1993) estimated the k of *C. nasus* to be between 0.03 and 0.07 in their study, which is somewhat higher than that observed among ictalurids in this study. Factors contributing to the slow isotopic turnover of fish are, first, the slow metabolism of poikilotherms and, second, slow growth rates. In addition, ictalurid catfish may reduce feeding during the winter months as their metabolism slows, therefore reducing growth rate.

Application of laboratory results to field data

Isotopic turnover rates measured in the laboratory could not be uniformly applied to the accumulated field data due to the variability of the *I. furcatus* isotopic signatures. Determining a maximum isotopic turnover rate in the laboratory would have yielded fine-scale information about the importance of marine nutrients during the *Alosa* run instead of coarse-scale approximations arrived at by proportionation equations. However, the field data did not support the hypothesis that *I. furcatus* isotope values would be depleted at the beginning of the *Alosa* run and would become steadily enriched over the course of the spring as *Alosa* are consumed. However, it should be noted that there was a limited number of captures of large (>38 cm) *I. furcatus* in the first several weeks of the study.

The fact that no significant enrichment trend with time was seen in the isotope values of *I. furcatus* in the field, although there was a clear isotopic enrichment associated with marine influences in these same *I. furcatus*, led to two conclusions. First, some *I. furcatus* heavily utilize the anadromous resource when it is available and others clearly consume only freshwater material (MacAvoy et al. 2000). Therefore, since the population as a whole does not consume *Alosa* at the same rate or with the same frequency, there is considerable variation in their isotope signature at any given time. Second, at the maximum rate, isotopic turnover will be between 1 and 2‰ for $\delta^{34}S$ and $\delta^{13}C$, respectively, over a 90-day period. The maximum turnover rate is so slow that it made observing a significant enrichment among the *I. furcatus* population as a whole during the 3 months of the *Alosa* spawning run unlikely. Isotopic variability among individual *I. furcatus* masks any enrichment trend. The more enriched isotope signatures of the *I. furcatus* were likely a result of years of feeding upon the migratory *Alosa* populations. Using isotope mixing equations, MacAvoy et al. (2000) estimated that approximately 40% of the biomass carbon and sulfur in adult *I. furcatus* was derived from marine sources.

It is important to note that in systems that experience migrations of prey species, the consumption of these prey items by predators may be underestimated using isotopes if predator tissue turnover is slow. This may be particularly true if the prey species is not a regular migrant. Conversely, the impact or influence of a migrating predator on resident prey populations may be underestimated if isotopic turnover in the predator is slow. It follows that the often-assumed equilibrium in isotopic signature between predator and prey may be violated if predator tissues have slow isotope turnover.

Acknowledgments

We would like to thank Dr. Stephen McIninch of Virginia Commonwealth University for his efforts in the field. We thank Nicole Cortese, Snoopy Dawson, Dr. Samantha Joye, Stefania Korontzi, Dr. Tom O'Donnell, Dr. Vaughan Turekian, Peter Yanik, three referees, and an anonymous Associate Editor for their helpful suggestions. This project was funded in part by a Moore Award granted to S.E. MacAvoy by the Department of Environmental Sciences, University of Virginia.

References

Ben-David, M., Hanley, T.A., and Schell, D.M. 1998. Fertilization of terrestrial vegetation by spawning Pacific salmon: the role of flooding and predator activity. Oikos, **83**: 47–55.

Bilby, R.E., Fransen, B.R., and Bisson, P.A. 1996. Incorporation of nitrogen and carbon from spawning coho salmon into the trophic system of small streams: evidence from stable isotopes. Can. J. Fish. Aquat. Sci. **53**: 164–173.

Conder, J.R., and Hoffarth, R. 1962. Growth of channel catfish, *Ictalurus punctatus*, and blue catfish, *Ictalurus furcatus*, in the Kentucky lake portion of the Tennessee River in Tennessee. Proc. Annu. Conf. Southeast. Assoc. Game Fish Comm. **16**: 348–354.

Frazer, T.K., Ross, R.M., Quetin, L.B., and Montoya, J.P. 1997. Turnover of carbon and nitrogen during growth of larval krill, *Euphausia superba* Dana: a stable isotope approach. J. Exp. Mar. Biol. Ecol. **212**: 259–275.

Fry, B., and Arnold, C. 1982. Rapid $^{13}C/^{12}C$ turnover during growth of brine shrimp (*Penaeus aztecus*). Oecologia, **54**: 200–204.

Fry, B., Brandt, W., Mersch, F.J., Tholke, K., and Garritt, R. 1992. Automated analysis system for coupled $\delta^{13}C$ and $\delta^{15}N$ measurements. Anal. Chem. **64**: 288-291.

Gannes, L.Z., O'Brien, D.M., and del Rio, C.M. 1997. Stable isotopes in animal ecology: assumptions, caveats, and a call for more laboratory experiments. Ecology, **78**: 1271–1276.

Garman, G.C. 1992. Fate and potential significance of postspawning anadromous fish carcasses in an Atlantic coastal river. Trans. Am. Fish. Soc. **121**: 390–394.

Garman, G.C., and Macko, S.A. 1998. Contribution of marine-derived organic matter to an Atlantic coast, freshwater, tidal stream by anadromous clupeid fishes. J. North Am. Benthol. Soc. **17**: 277–285.

Giesemann, A., Jager, H-J., Norman, A.L., Krouse, H.R., and Brand, W.A. 1994. On-line sulfur isotope determination using an elemental analyzer coupled to a mass spectrometer. Anal. Chem. **66**: 2816.

Herzka, S.Z., and Holt, G.J. 2000. Changes in isotopic composition of red drum (*Sciaenops ocellatus*) larvae in response to dietary shifts: potential applications to settlement studies. Can. J. Fish. Aquat. Sci. **57**: 137–147.

Hesslein, R.H., Hallard, K.A., and Ramlal, P. 1993. Replacement of sulfur, carbon, and nitrogen in tissue of growing broad whitefish (*Coregonus nasus*) in response to a change in diet traced by $\delta^{34}S$, $\delta^{13}C$, and $\delta^{15}N$. Can. J. Fish. Aquat. Sci. **50**: 2071–2076.

Hobson, K.A., and Clark, R.G. 1992. Assessing avian diets using stable isotopes I: turnover of ^{13}C in tissues. Condor, **94**: 181–188.

Kelly, J.R. 1969. Growth of blue catfish *Ictalurus furcatus* (LeSueur) in the Tombigbee River of Alabama. Proc. Annu. Conf. Southeast. Assoc. Game Fish Comm. **23**: 248–255.

Kline, T.C., Goering, J.J., Mathisen, O.A., Poe, P.H., and Parker, P.L. 1990. Recycling of elements transported upstream by runs of Pacific salmon: I. $\delta^{15}N$ and $\delta^{13}C$ evidence in Sashin Creek, southeastern Alaska. Can. J. Fish. Aquat. Sci. **47**: 136–144.

Kline, T.C., Goering, J.J., Mathisen, O.A., Poe, P.H., and Parker, P.L. 1993. Recycling of elements transported upstream by runs of Pacific salmon: II. $\delta^{15}N$ and $\delta^{13}C$ evidence in the Kvichak River watershed, Bristol Bay, southwestern Alaska. Can. J. Fish. Aquat. Sci. **50**: 2350–2365.

Kline, T.C., Wilson, W.J., and Goering, J.J. 1998. Natural isotope indicators of fish migration at Prudhoe Bay, Alaska. Can. J. Fish. Aquat. Sci. **55**: 1494–1502.

MacAvoy, S.E., Macko, S.A., and Garman, G.C. 1998. Tracing marine biomass into tidal freshwater ecosystems using stable sulfur isotopes. Naturwissenschaften, **85**: 544–546.

MacAvoy, S.E., Macko, S.A., McIninch, S.P., and Garman, G.C. 2000. Marine nutrient contributions to freshwater apex predators. Oecologia, **122**: 568–573.

Persson, A., and Hansson, L.-A. 1999. Diet shift in fish following competitive release. Can. J. Fish. Aquat. Sci. **56**: 70–78.

Rosner, B. 1990. Fundamentals of biostatistics. 3rd ed. PWS-Kent Publishing Company, Boston, Mass.

Tieszen, L.L., Boutton, T.W., Tesdahl, K.G., and Slade, N.A. 1983. Fractionation and turnover of stable carbon isotopes in animal tissues: implications for $\delta^{13}C$ analysis of diet. Oecologia, **57**: 32–37.

Webster, C.D., Yancey, D.H., and Tidwell, J.H. 1992. Effect of partially or totally replacing fish meal with soybean meal on growth of blue catfish (*Ictalurus furcatus*). Aquaculture, **103**: 141–152.

Webster, C.D., Tidwell, J.H., Tiu, L.S., and Yancey, D.H. 1995. Use of soybean meal as partial or total substitute of fish meal in diets for blue catfish (*Ictalurus furcatus*). Aquat. Living Resour. **8**: 379–384.

Patterns in abundance of fishes in main channels of the upper Mississippi River system

John M. Dettmers, Steve Gutreuter, David H. Wahl, and Daniel A. Soluk

Abstract: Abundance of fishes of the main channels of the upper Mississippi River system and of other large North American rivers is largely unknown because historic sampling methods have been inadequate. We used a bottom trawl to estimate spatial and temporal patterns in abundance in the navigation channels of Pool 26 of the Mississippi River and the lower Illinois River. Total biomass density averaged 21 and 29 $kg \cdot ha^{-1}$ in the navigation channels of Pool 26 and the lower Illinois River, respectively. We identified spatial and temporal patterns in catches of key species using a generalized linear model based on the negative binomial distribution. Some species, including shovelnose sturgeon (*Scaphirhynchus platorynchus*), are persistent residents of the main channel. Multiple-season residents, including freshwater drum (*Aplodinotus grunniens*), rely heavily on the main channel during most of the year but leave it briefly, for example to seek thermal refugia in backwaters during winters. We suggest revision of the prevailing notion that main channels of large temperate rivers serve mainly as corridors for movement among other habitat types.

Résumé : L'abondance des poissons dans les chenaux principaux du réseau supérieur du Mississippi et des autres grandes rivières de l'Amérique du Nord reste mal connue parce que, dans le passé, les méthodes d'inventaire ont été inadéquates. Nous avons utilisé un chalut de fond pour estimer les structures spatiales et temporelles d'abondance dans les chenaux de navigation du bassin 26 du Mississippi et du cours inférieur de l'Illinois. La densité totale en biomasse était en moyenne de 21 $kg \cdot ha^{-1}$ dans le bassin 26 du Mississippi et de 29 $kg \cdot ha^{-1}$ dans l'Illinois inférieur. Un modèle linéaire généralisé basé sur la distribution binômiale négative a permis d'identifier les structures spatiales et temporelles des captures des espèces principales. Quelques espèces, dont l'Esturgeon à museau plat (*Scaphirhynchus platorynchus*), résident en permanence dans le chenal principal. D'autres y demeurent pendant plusieurs saisons, dépendant du chenal principal pendant presque toute l'année, mais le quittent pour une courte période, par exemple en quête de refuges d'eau plus chaude en hiver dans les eaux dormantes; c'est le cas, entre autres, du Malachigan (*Aplodinotus grunniens*). Il faut donc revoir la conception actuelle qui veut que les chenaux principaux des grandes rivières tempérées servent surtout de corridors pour des déplacements vers d'autres types d'habitat.

[Traduit par la Rédaction]

Introduction

River–floodplain ecosystems are typically productive in both temperate and tropical regions (Bayley 1995). Rivers may be more productive than lakes due to greater fish density and production to biomass ratio (Randall et al. 1995). Two broad theories, the river continuum and flood-pulse concepts, have been invoked to describe production processes in streams and rivers (Johnson et al. 1995). The river continuum concept (Vannote et al. 1980) was developed from observations in unperturbed, forested temperate watersheds and states that a predictable longitudinal gradient of physical forces determines the relative importance of various production pathways. Because this concept assumes a longitudinal structure, it relates primarily to major channels of rivers and may help describe production pathways in large rivers that are predominantly composed of channels. More recently, the high productivity of floodplain rivers has been attributed, in large part, to the connection of the river with its floodplain during annual flood cycles that permit fish and other organisms to move onto the floodplain to take advantage of the latent (to riverine species) productivity available there (Junk et al. 1989). The flood-pulse concept states that predictable annual inundation is "the principal driving force responsible for the existence, productivity, and interactions of the major biota in river–floodplain systems" (Junk et al. 1989) and emphasizes the importance of the moving littoral zone.

A key component of the flood-pulse concept is the seasonal dynamic of the flood (Junk et al. 1989). Rainfall and spring snowmelt (in temperate rivers) typically provide an extended flood that joins the flowing river with its floodplain, allowing fishes and other organisms to colonize productive habitat for spawning and feeding. After taking advantage of the flood-

Received September 20, 2000. Accepted February 16, 2001. Published on the NRC Research Press Web site on April 17, 2001.
J15983

J.M. Dettmers.[1,2] Illinois Natural History Survey, Great Rivers Field Station, 8450 Montclair, Brighton, IL 62012, U.S.A.
S. Gutreuter. U.S. Geological Survey, Upper Midwest Environmental Sciences Center, 2630 Fanta Reed Road, La Crosse, WI 54603, U.S.A.
D.H. Wahl. Illinois Natural History Survey, Kaskaskia Biological Station, RR 1, Box 157, Sullivan, IL 61951, U.S.A.
D.A. Soluk. Illinois Natural History Survey, Center for Aquatic Ecology, 607 E. Peabody Drive, Champaign, IL 61820, U.S.A.

[1] Corresponding author (e-mail: dettmers@mail.inhs.uiuc.edu).
[2] Present address: Illinois Natural History Survey, Lake Michigan Biological Station, 400 17th Street, Zion, IL 60099, U.S.A.

DOI: 10.1139/cjfas-58-5-933

plain, fishes and other organisms retreat to in-channel habitats or floodplain lakes during late summer and autumn as flood waters recede (Junk et al. 1989). However, little is known about how seasonal changes might affect fish assemblages in other aquatic areas like the main channel.

The main channels of large river–floodplain systems typically have been considered less productive and less hospitable to many organisms than floodplain backwaters (Junk et al. 1989). In particular, the main channel has been considered primarily as a highway used by most fishes to move between suitable habitats (Junk et al. 1989), although it is recognized that some fishes do spend at least some of their time in the main channel (Nielsen et al. 1986; Fremling et al. 1989). Such movement might occur as a means of dispersal or as fishes move from summer and autumn habitats to overwintering areas or from wintering habitats to spawning areas (Junk et al. 1989).

Unfortunately, assemblage composition and spatial and seasonal patterns in abundance of fishes from the major channels of large rivers are poorly known (Baker et al. 1991), mainly because sampling is difficult (Casselman et al. 1990). Carefully monitored trawling (Gunderson 1993) has the potential to provide estimates of abundance of fishes in river channels, but trawling has not been commonly used in large rivers (Casselman et al. 1990). As a result, historic perceptions of patterns of abundance of fishes in large rivers have been shaped mainly by observations from more easily sampled shallow aquatic areas. Without adequate sampling of the main channel, scientists and managers are unable to fully determine either the seasonal or the spatial importance of this aquatic area to the fish community.

Identification of patterns of fish abundance in the main channel is central to understanding the mechanisms that permit fishes to reside in the main channel, either seasonally or year-round. In addition, it is important to understand the linkages between main channels and other aquatic areas of river–floodplain ecosystems. For example, large-scale movements through channels can create linkages among food webs in distant floodplains (Winemiller and Jepsen 1998). From a management perspective, understanding seasonal and spatial patterns of fish abundance in the main channel is valuable information for managers that seek to mitigate the impacts of continued regulation of rivers by dams or by channelization and potentially harmful impacts of commercial navigation on fishes.

Our objectives were to (*i*) evaluate the general feasibility and effectiveness of bottom trawling in the navigation channels of rivers, (*ii*) estimate and model spatial and seasonal patterns in catches of important riverine species, and (*iii*) obtain initial estimates of numeric density and biomass density for comparison with previous estimates from shallow floodplain aquatic areas to begin the process of understanding the importance of the main channel for seasonal and spatial use by fishes of the upper Mississippi River system.

Materials and methods

Study area

We follow the hierarchical nomenclature of Wilcox (1993) for definition of aquatic areas of the upper Mississippi River system. Among major channels in a river cross section, one usually predominates and is therefore called the main channel. The main channel is composed of the main channel borders, which are riverine littoral areas, the main channel trough, sandbars, and tailwaters below dams. In commercially navigated rivers, the navigation channel is typically the deepest portion of the main channel trough and is delineated by buoys.

We sampled about 65 km of the Mississippi River comprising Navigation Pool 26 between river kilometer (rkm) 388 above the confluence with the Ohio River to rkm 323 and about 32 km of the Illinois River above the confluence with the Mississippi River (Fig. 1). The confluence of the Illinois River with the Mississippi River occurs near the middle of Pool 26, at Mississippi rkm 350. The Mississippi River is characterized by relatively higher discharge, lower turbidity, and steeper gradient than the Illinois River. Within our study area, the Mississippi River has a more complex form, with relatively extensive side channels compared with the Illinois River. The bed of the main channel of the Mississippi River is predominantly sand structured in dunes that vary in amplitude with discharge (Vanoni and Nomicos 1960). The bed of the Illinois River consists mainly of a 1- to 9-m-deep layer of fine sediments overlaying sand, with only occasional patches of exposed sand (Butzer 1977). Dunes do not form in fine sediments (Patrick 1995). Large woody debris and other hard debris are common in both river beds.

Discharge was distinctly greater through Pool 26 of the Mississippi River than through its tributary, the Illinois River (Fig. 2). The seasonal discharge regimen during the course of this study was fairly typical for these rivers, showing a distinct increase from late winter to early summer and much smaller increases during autumn. Mean water temperatures in the main channel trough of Pool 26 ranged from nearly 0°C to over 28°C (Fig. 2).

Sampling

We sampled during August–December 1996 and March–October 1997 as equipment, weather, and current velocities permitted. Sampling occurred at least monthly but occurred weekly during October 1996 and every other week during November 1996. We sampled at predetermined fixed sites in the main channel troughs that maximized our line of site to ensure that our trawling operations were safe in the presence of commercial navigation traffic.

Because most rheophilic fishes are benthic or epibenthic, we used a four-seam bottom trawl with a footrope length of 10.2 m and a headrope length of 8.0 m to sample fish in the main channel. Mesh of the trawl mouth and cod end consisted of No. 21 nylon with a bar measure mesh size of 2.54 cm. The footrope was equipped with rockhopper rollers consisting of 25-cm-diameter disks cut from tire tread salvage and spaced approximately every 61 cm by 7.6-cm disks. The length of the cod end was approximately 2.4 m, and the distance from the wings to the cod end was approximately 10.7 m. Paired "V" doors were constructed of steel and measured 96 cm long by 69 cm high.

The trawl was towed upstream at an average speed, relative to the ground, of 4.0 $km \cdot h^{-1}$ for a nominal duration of 20 min. Upon gear retrieval, all fishes collected were identified, measured, weighed, and immediately released. Regular sampling sites in Pool 26 were located at rkm 326.5, 333.4, 343.7, 347.1, 358.8, 365.6, 370.9, 375.7, and 383.3 during 1996. Sampling sites during 1997 were the same as for 1996 except that the site at rkm 370.9 was abandoned after we lost a net there during April and that sampling occasionally was done at rkm 386.5. Sampling sites in the Illinois River were located at rkm 8.8, 15.0, 21.7, and 30.1 during both 1996 and 1997. Our goal was to sample all of the sites within a 1-week time frame before starting another cycle of sampling.

During some trawl hauls, the wingspread and headrope height was monitored with a Northstar Technical Netmind^{TM} acoustic trawl monitoring system. The wingspread and headrope sensors

Fig. 1. Upper Mississippi River system showing the study area in Pool 26 of the Mississippi River and the lower 32 km of the Illinois River.

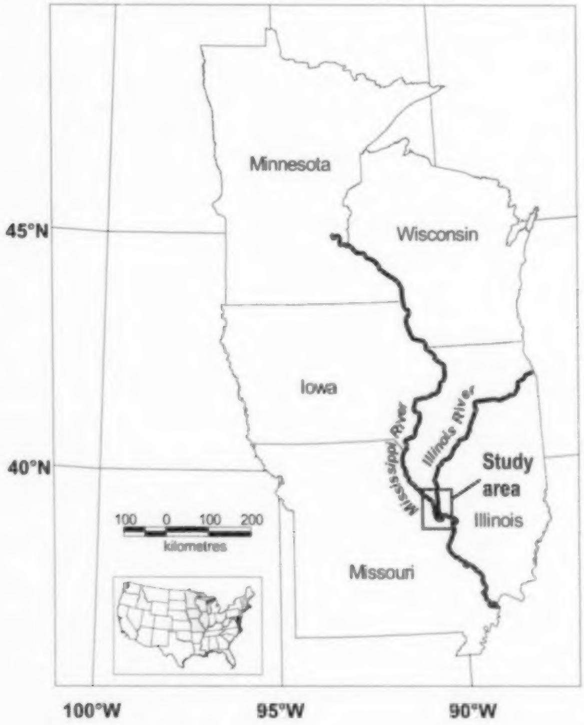

were not installed during all samples to minimize the cost of gear loss on irretrievable snags. Measurements from the trawl monitoring system were recorded at approximately 1-min intervals during the course of 18 trawl hauls. The durations of some hauls were abbreviated because of snags or development of hazards. Further, signal interference or other factors occasionally caused measurements of headrope height and wingspread to be missed. In total, we obtained 265 recordings of headrope height and 258 recordings of wingspread. For the trawl hauls that were monitored by using the trawl monitoring system, we computed the bottom area swept A_b as the product of the length of the haul and the mean wingspread from measurements recorded during the particular haul. For the hauls that were not monitored with the trawl monitoring system, we computed the bottom area swept A_b as the length of the haul times the mean wingspread from all 258 measurements obtained during the 18 monitored hauls.

Estimation of density and biomass of fish in the main channel trough

We estimated the numeric density (number per hectare) and biomass density (kilograms per hectare) of fishes by dividing the catch count and mass, respectively, from each sample by A_b. For some fish, we measured individual mass (grams) in the field with a spring-loaded scale. For the others, we estimated mass with conventional weight–length equations. The resulting estimates of density and biomass are conservative because we could not estimate trawl avoidance and escapement during this study. For the relatively few pelagic species, such as gizzard shad (*Dorosoma cepedianum*), density was underestimated because we did not estimate the fraction of the stock that was located above the headrope.

Fig. 2. Daily water discharge (solid lines) measured at U.S. Geological Survey gauging stations (*a*) near the midpoint of Pool 26 of the Mississippi River at Grafton, Ill., and (*b*) on the Illinois River near rkm 113 at Valley City, Ill. Smoothed water temperatures (broken line) for Pool 26 are from the Long Term Resource Monitoring Program of the upper Mississippi River system.

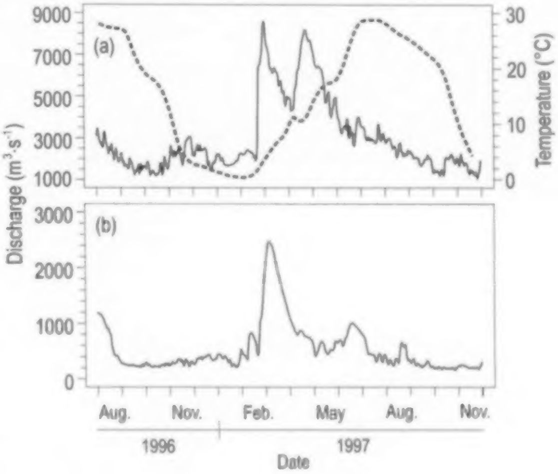

Analysis of spatial and temporal pattern in trawl catch counts

We present detailed analyses of spatial and temporal patterns in trawl catches for three species that were abundant in both rivers: freshwater drum (*Aplodinotus grunniens*), gizzard shad, and smallmouth buffalo (*Ictiobus bubalus*). We also selected shovelnose sturgeon (*Scaphirhynchus platorynchus*) because of their abundance in the Mississippi River and because they are ecologically similar to the endangered pallid sturgeon (*Scaphirhynchus albus*). Except for gizzard shad, an important prey species, these species are exploited by commercial fishers and (or) anglers.

Catch data are counts that are naturally modeled by the Poisson distribution with overdispersion (Smith et al. 1991) or the negative binomial distribution (Power and Moser 1999). We assumed the negative binomial distribution for catch counts and formulated a statistical model of spatial and temporal pattern based on the conventional catch equation given by

$$(1) \qquad C = fqN$$

where C denotes catch, f is sampling effort, q is the catchability coefficient, and N represents abundance (Ricker 1975). Our goal here was not to estimate q and N but rather to formulate a statistical model for spatial and temporal patterns in catch that is consistent, in general form, with this conventional catch equation. We modeled qN as an exponential function of the sum of spatial and temporal effects because, consistent with qN, the exponential function is multiplicative in that $\exp(X_1 + X_2) = \exp(X_1)\exp(X_2)$. Spatial patterns of interest were differences between rivers and effects of longitudinal position within Pool 26 of the Mississippi River. Temporal patterns of interest were effects of year and of seasonal cycles within years. For identification of seasonal cycles, we used the general sinusoidal function given by $\alpha\cos(\omega t + \phi)$, where t represents time, herein measured in months, α represents amplitude (height of peaks), ω represents the frequency (reciprocal of wavelength), and ϕ represents the phase shift (angle by which peaks are shifted). For fixed frequency ω, this functional form is nonlinear in the parameters α and ϕ and therefore is unsuited for our purpose. However, because $\cos(\omega t + \phi) = \cos(\phi)\cos(\omega t) - \sin(\phi)\sin(\omega t)$, we used the alternative form $\nu_1 \cos(\omega t) + \nu_2 \sin(\omega t)$, where $\nu_1 = \alpha_1 \cos(\phi)$ and $\nu_2 = -\alpha_2 \sin(\phi)$ because it is linear in ν_1 and ν_2 for any *specified* frequency ω. Therefore, our conditional mean response function for catch counts from trawl samples $i = 1,\ldots,I$, denoted μ, is given by

$$(2) \qquad \mu = f_i \exp[\lambda_0 + \tau_y + \tau_r + \tau_{r(s)} + g_1(t) + g_2(t)]$$

where λ_0 is the baseline (Illinois River during 1997) log$C$, τ_y is the incremental effect for 1997, τ_r is the incremental effect of the Mississippi River, $\tau_{r(s)}$ is the nested incremental effect of the upper longitudinal segment within Pool 26 of the Mississippi River, and $g_1(t)$ and $g_2(t)$ are sums of mutually orthogonal terms in time t describing half- and full-sinusoidal cycles per year given by

$$g_1(t) = \sum_{j=1}^{2}\left[\beta_{2j-1}\sin\left(\frac{j\pi t}{12}\right) + \beta_{2j}\cos\left(\frac{j\pi t}{12}\right)\right]$$

and

$$g_2(t) = \sum_{j=1}^{2}\sum_{k=1}^{2}\left[\beta_{2j-1,k}\sin\left(\frac{j\pi t}{12}\right)_{\mathrm{r(s),k}} + \beta_{2j,k}\cos\left(\frac{j\pi t}{12}\right)_{\mathrm{r(s),k}}\right]$$

where $\beta_1,\ldots,\beta_4$ in $g_1(t)$ are parameters for seasonal responses at frequencies $\omega(j) = j\pi$ radians·year^{-1} = $0.5j$ cycles·year^{-1}, $j \in \{1,2\}$, and $\beta_{1,1},\ldots,\beta_{4,2}$ in $g_2(t)$ are eight parameters for interactions between longitudinal segment within river and seasonal responses at frequencies of $0.5j$ cycles·year^{-1}. This modeling of seasonal cycles as sinusoidal functions is efficient in that it requires at most 12 parameters to describe plausible seasonal responses, whereas use of categorical indicator variables for month would have required as many as 33.

The parameters in eq. 2 have natural interpretations. The lower Illinois River in 1997 is the baseline from which other effects may be compared. Therefore, $\exp(\lambda_0)$ is interpreted as the expected catch per effort from the lower Illinois River during 1997, ignoring seasonal effects. For the categorical effects of year, river, and longitudinal segment within river, exponentials of the corresponding parameters represent the multipliers against the baseline. For example, if $\tau_y = 3$, then, ignoring other effects, expected catch per effort would be $\exp(3) \cong 20$ times greater during 1996 than during 1997. Similarly, the expected catch per effort in the Illinois River during 1996, ignoring other effects, is given by $\exp(\lambda_0 + \tau_y)$. For the continuous effects of season, the parameters β_j and $\beta_{j,k}$ are interpreted as the multiplicative change relative to baseline for each unit change in time.

We completed our statistical model of catch by assuming that catch, C_i, follows a negative binomial distribution having mean μ (eq. 2) and dispersion parameter κ. From properties of the negative binomial distribution, $\mathrm{Var}(C_i) = \mu + \kappa\mu^2$ (Lawless 1987). For $\kappa \equiv 0$, $\mathrm{Var}(C_i) = \mu$, which is a characteristic of the Poisson distribution. Hence, the negative binomial distribution models the Poisson distribution as a special case. Our modeling approach differs from that of Power and Moser (1999) with our accommodation of sampling effort, wherein, consistent with eq. 1, the "regression" coefficient for f is held fixed at 1 and hence, log f is said to be an "offset" (McCullagh and Nelder 1989).

Let $\theta = (\lambda_0, \tau_y, \tau_r, \tau_{r(s)}, \beta_1, \ldots, \beta_4, \beta_{1,1}, \ldots, \beta_{4,2}, \kappa)^{\mathrm{T}}$, where $\mathbf{x}^{\mathrm{T}}$ denotes the transpose of $\mathbf{x}$, denote the vector of parameters to be estimated from the data. Lawless (1987) gives the general form of the log likelihood ℓ and the partial derivatives of ℓ with respect to the parameter vector. We obtained maximum likelihood estimates $\hat{\theta}$ of θ with the Newton–Raphson algorithm implemented in SAS 8.0 (http://www.sas.com/). We estimated the covariance matrix Σ of θ as the inverse of the observed Fisher information matrix (McCullagh and Nelder 1989). We evaluated goodness of fit using the deviance (McCullagh and Nelder 1989) and deleted unimportant terms one by one using likelihood ratio χ^2 tests and Akaike's information criterion $\mathrm{AIC} = -2\ell + 2d$ (Burnham and Anderson 1998), where d denotes the number of parameters in θ. Nonsignificant main effects were retained whenever they were involved in a significant interaction or where their elimination resulted in a poorer overall fit or an inferior AIC. Our goal was to identify the simplest submodel that fit the data.

Results

The fish assemblages sampled by bottom trawling in navigation channels differed distinctly between Pool 26 of the Mississippi River and the lower 32 km of the Illinois River. We detected 26 species in 114 trawl hauls from the navigation channel of Pool 26 and 15 species in 37 hauls from the lower Illinois River (Table 1). Species that were captured in Pool 26 but not in the lower Illinois River were lake sturgeon, shovelnose sturgeon, goldeye, skipjack herring, bighead carp, speckled chub, silver chub, quillback, blue sucker, black buffalo, and black crappie (Table 1).

Numeric and biomass dominants also differed between rivers. We defined dominant species as those with densities approximately 10% or more of total community density. The biomass dominants in the navigation channel of Pool 26 were, in descending order, smallmouth buffalo, freshwater drum, and shovelnose sturgeon, whereas the biomass dominants in the lower Illinois River were freshwater drum, smallmouth buffalo, and common carp (Table 1). Numeric dominants in Pool 26 were freshwater drum, gizzard shad, and smallmouth buffalo and in the lower Illinois were freshwater drum and gizzard shad.

The rheophilic shovelnose sturgeon was not collected in the low-gradient Illinois River. Therefore, we excluded samples from the lower Illinois River from our analysis of spatial and temporal patterns. Our final negative binomial model of shovelnose sturgeon catch included only effects of longitudinal segment within Pool 26; the ratio of the deviance to the degrees of freedom was approximately 1 and indicated a reasonable fit (Table 2). Catch differed between longitudinal segments ($P < 0.01$) and in the lower half of Pool 26 was 0.08 (exp(–2.460); likelihood ratio confidence interval: 0.04–0.17) times the catch in the upper half. This species clearly is more abundant in the swifter currents of the upper half of the pool than in the slower waters of the partly impounded lower half. Conversely, effects of year and seasonal cycle were not significant descriptors of pattern in the data and were eliminated prior to the final fit. Our final model for shovelnose sturgeon describes temporally constant catches that differ markedly between the upper and lower halves of Pool 26 (Fig. 3*a*). The lack of a detectible difference between years is unlikely to be an enduring pattern, and we would expect to observe significant yearly variation over longer time scales. Although sample mean densities of shovelnose sturgeon apparently increased during autumns and perhaps during spring (Fig. 3*b*), the model indicated that

Table 1. Estimates of numeric density and biomass density of fishes captured in 114 trawl hauls from Pool 26 of the Mississippi River and 37 trawl hauls from the lower Illinois River, 1996–1997.

		Pool 26, Mississippi River		Lower Illinois River	
Species	Season	Numeric density (no.·ha^{-1} (SE))	Biomass density (kg·ha^{-1} (SE))	Numeric density (no.·ha^{-1} (SE))	Biomass density (kg·ha^{-1} (SE))
Lake sturgeon (*Acipenser fulvescens*)	saw	0.17 (0.06)	0.41 (0.15)	0 (0)	0 (0)
Shovelnose sturgeon (*Scaphirhynchus platorynchus*)	vsaw	4.12 (0.77)	2.02 (0.35)	0 (0)	0 (0)
Shortnose gar (*Lepisosteus platostomus*)	a	0.03 (0.02)	0.03 (0.02)	0.05 (0.05)	0.06 (0.06)
Goldeye (*Hiodon alosoides*)	vsaw	0.24 (0.07)	0.04 (0.01)	0 (0)	0 (0)
Mooneye (*Hiodon tergisus*)	aw	3.32 (1.68)	0.09 (0.03)	0.07 (0.07)	0.00 (0)
Skipjack herring (*Alosa chrysochloris*)	a	0.07 (0.04)	0.00 (0.00)	0 (0)	0 (0)
Gizzard shad (*Dorosoma cepedianum*)	aw	25.56 (10.95)	0.38 (0.08)	27.71 (24.08)	0.54 (0.34)
Common carp (*Cyprinus carpio*)	saw	2.56 (0.88)	1.98 (0.64)	3.41 (0.86)	4.43 (1.05)
Bighead carp (*Hypophthalmichthys nobilis*)	s	0.02 (0.02)	0.00 (0.00)	0 (0)	0 (0)
Speckled chub (*Macrhybopsis aestivalis*)	s	0.07 (0.07)	0.00 (0.00)	0 (0)	0 (0)
Silver chub (*Macrhybopsis storeriana*)	a	0.04 (0.02)	0.00 (0.00)	0 (0)	0 (0)
River carpsucker (*Carpiodes carpio*)	a	1.17 (0.49)	1.06 (0.45)	0.17 (0.10)	0.14 (0.08)
Quillback (*Carpiodes cyprinus*)	a	1.16 (0.40)	0.73 (0.24)	0 (0)	0 (0)
Highfin carpsucker (*Carpiodes velifer*)	aw	0.17 (0.07)	0.09 (0.04)	0.10 (0.10)	0.04 (0.04)
Blue sucker (*Cycleptus elongatus*)	a	0.09 (0.05)	0.04 (0.04)	0 (0)	0 (0)
Smallmouth buffalo (*Ictiobus bubalus*)	saw	8.58 (1.49)	7.29 (1.14)	8.46 (2.24)	5.72 (1.59)
Bigmouth buffalo (*Ictiobus cyprinellus*)	a	1.37 (0.54)	1.07 (0.36)	0.29 (0.18)	0.20 (0.12)
Black buffalo (*Ictiobus niger*)	a	0.11 (0.08)	0.14 (0.10)	0 (0)	0 (0)
Shorthead redhorse (*Moxostoma macrolepidotum*)	saw	0.33 (0.10)	0.23 (0.09)	0.12 (0.08)	0.05 (0.03)
Blue catfish (*Ictalurus furcatus*)	saw	1.73 (0.46)	0.29 (0.11)	0.73 (0.27)	0.04 (0.02)
Channel catfish (*Ictalurus punctatus*)	vsaw	8.02 (1.40)	1.30 (0.22)	15.19 (3.82)	1.34 (0.40)
Flathead catfish (*Pylodictis olivaris*)	sa	0.31 (0.08)	0.63 (0.22)	0.53 (0.22)	0.48 (0.22)
White bass (*Morone chrysops*)	a	0.35 (0.13)	0.02 (0.01)	0.78 (0.35)	0.01 (0.01)
Black crappie (*Pomoxis nigromaculatus*)	a	0.02 (0.02)	0.00 (0.00)	0 (0)	0 (0)
Sauger (*Stizostedion canadense*)	aw	0.52 (0.12)	0.27 (0.07)	0.31 (0.16)	0.11 (0.07)
Freshwater drum (*Aplodinotus grunniens*)	saw	25.88 (4.57)	3.13 (0.48)	108.22 (21.83)	15.79 (3.15)
Totals		86.00 (14.69)	21.22 (2.60)	166.13 (32.46)	28.98 (4.58)

Note: Season qualitatively indicates time of the year primarily encountered as March–April (v), June–August (s), September–October (a), and November–December (w).

chance alone could explain the apparent seasonal pattern in catch. Shovelnose sturgeon younger than age 1 were uncommon in our samples (Fig. 3*c*). The rheophilic blue sucker showed a similar but more pronounced spatial pattern in abundance, and catch rates averaged nearly 1 fish·h^{-1} in the upper segment of Pool 26 but zero elsewhere.

Catches of gizzard shad exhibited a complex spatial and seasonal pattern (Fig. 4*a*). The estimate of the negative binomial dispersion parameter was nearly twice that of other species (Table 2; likelihood ratio confidence interval: 3.165–5.926), indicating an unusually high degree of spatial and temporal aggregation. Most catches of gizzard shad were small, but occasional catch rates approached 1500 fish·h^{-1} and expected catch rates approached 150 fish·h^{-1}. Catches of gizzard shad differed between longitudinal segments nested within Pool 26 ($P < 0.01$). Although the main effect of river was not significant ($P = 0.90$), it was retained because the nested effect of longitudinal position is a related interaction. Seasonal pattern in catch was apparent through the effects of $\sin(\pi t \cdot 12^{-1})$ ($P < 0.01$), $\cos(2\pi t \cdot 12^{-1})$ ($P < 0.01$), $\sin(2\pi t \cdot 12^{-1})$ ($P = 0.11$), $\cos(2\pi t \cdot 12^{-1})$ ($P < 0.01$), and the interactions between longitudinal segment and $\sin(2\pi t \cdot 12^{-1})$ and $\cos(2\pi t \cdot 12^{-1})$ ($P < 0.01$ and $P = 0.20$, respectively), where t denotes month. The fitted negative binomial model of catch counts (Fig. 4*a*) differs somewhat from the spatial and temporal pattern in the observed mean numeric densities (Fig. 4*b*) and wrongly predicted autumnal increases during 1996 in the Illinois River and during 1997 in the upper half of Pool 26. These discrepancies could be resolved using either arbitrary polynomials in month or high-order interactions with sinusoidal functions, but those models resulted in inferior AIC scores and were more difficult to interpret. In contrast, our final model indicates the presence of a strong autumnal pulse in abundance with a high degree of aggregation. During autumns, most of our catches of gizzard shad were relatively small, but occasionally, very large schools of age-0 fish were encountered, particularly during October 1996 and November 1997 (Fig. 4*c*). The spatial distribution of these occasional large schools could not be predicted reliably, however. The autumnal pulse in catch of gizzard shad almost certainly resulted from increased vulnerability of age-0 cohorts to trawling. The reduced catches the following spring and summer are likely due to depletion by overwinter mortality, which is frequently large for gizzard shad in the upper Mississippi River system.

Smallmouth buffalo showed a consistent pattern in abundance. Any effect of year had been excluded as unimportant prior to the final fitting. There was no detectable difference in catch between rivers ($P = 0.95$), but catches differed sig-

Table 2. Maximum likelihood estimates (±1 SE) of parameters in the final models that were reduced from the full negative binomial generalized linear model given by eq. 2.

xParameter (effect)	Shovelnose sturgeon	Gizzard shad	Smallmouth buffalo	Freshwater drum
λ_0 (baseline, Illinois River, 1997)	–1.605 (0.189)	–27.906 (7.715)	–3.569 (0.471)	–0.743 (0.331)
τ_y (year, 1996)				
τ_r (river, Pool 26)		–2.356 (1.427)	–0.583 (0.353)	–2.370 (0.343)
τ_s (lower segment within Pool 26)	–2.460 (0.345)	0.680 (0.798)	0.578 (0.314)	0.915 (0.315)
β_1 ($\sin(\pi t \cdot 12^{-1})$)		38.573 (10.666)	0.956 (0.537)	
β_2 ($\cos(\pi t \cdot 12^{-1})$)		–10.775 (4.865)		
β_3 ($\sin(2\pi t \cdot 12^{-1})$)		9.141 (3.588)	–2.330 (0.361)	–2.844 (0.372)
β_4 ($\cos(2\pi t \cdot 12^{-1})$)		14.606 (2.726)		
$\beta_{1,1}$ ($\sin(\pi t \cdot 12^{-1})$ in lower Pool 26)				
$\beta_{1,2}$ ($\sin(\pi t \cdot 12^{-1})$ in upper Pool 26)				
$\beta_{2,1}$ ($\cos(\pi t \cdot 12^{-1})$ in lower Pool 26)				
$\beta_{2,2}$ ($\cos(\pi t \cdot 12^{-1})$ in upper Pool 26)				
$\beta_{3,1}$ ($\sin(2\pi t \cdot 12^{-1})$ in lower Pool 26)		–1.571 (1.752)		
$\beta_{3,2}$ ($\sin(2\pi t \cdot 12^{-1})$ in upper Pool 26)		–3.907 (1.820)		
$\beta_{4,1}$ ($\cos(2\pi t \cdot 12^{-1})$ in lower Pool 26)		–1.753 (0.979)		
$\beta_{4,2}$ ($\cos(2\pi t \cdot 12^{-1})$ in upper Pool 26)		–0.582 (1.100)		
κ (dispersion)	1.730 (0.400)	4.304 (0.690)	2.094 (0.336)	2.355 (0.307)
Deviance (df)	98.6 (112)	120.9 (140)	144.5 (146)	158.7 (147)

Note: Empty cells indicate that the parameter had been eliminated prior to the final model. See text for an explanation of the parameters (effects) and of the model fitting and reduction process.

nificantly between longitudinal segments within Pool 26 ($P = 0.04$) and were 1.8 times greater (exp(0.578)) in the lower segment of Pool 26 than in the upper segment (Table 2). Model-based estimates of mean catches from the lower segment of Pool 26 and the Illinois River were visually indistinguishable and distinctly greater than those from the upper segment of Pool 26 (Fig. 5*a*). Although smallmouth buffalo are considered a riverine species, the reduced abundance in the upper segment of Pool 26 suggests that they prefer lower current velocities than, for example, shovelnose sturgeon. Catches of smallmouth buffalo showed a strong seasonal cycle through $\sin(\pi t \cdot 12^{-1})$ ($P = 0.07$) and $\sin(2\pi t \cdot 12^{-1})$ ($P < 0.01$) and peaked from August to October when mean water temperatures were declining from 28 to 12°C and current velocities were low and generally decreasing (Fig. 2). Sample mean densities showed patterns similar to those in the raw catch data (Fig. 5*b*). Our trawl catches of smallmouth buffalo were composed entirely of fish older than age 0 (Fig. 5*c*). Therefore, we conclude that the increase in abundance in the main channel that occurred from August to September is likely a consequence of a predictable seasonal movement of this species that includes an influx into the main channel from other aquatic areas.

Abundance of freshwater drum showed a seasonal pattern and tended to be greatest from the lower Illinois River and least from the upper segment of Pool 26 (Fig. 6). The effect of year had been eliminated prior to fitting the final model. Trawl catches of freshwater drum differed between rivers ($P < 0.01$) and between segments in Pool 26 ($P < 0.01$). Mean catches from the upper segment of Pool 26 tended to be only 0.09 times those in the Illinois River (exp(–2.37)) and 2.5 times greater (exp(0.915)) in the lower segment of Pool 26 than in the upper segment (Table 2). The seasonal pattern in abundance was described by $\sin(\pi t \cdot 12^{-1})$ ($P < 0.01$). Abundance of freshwater drum in the main channel peaked from August to October when water temperatures and discharges were declining (Fig. 2). Juveniles often comprised substantial fractions of the catch of freshwater drum (Fig. 6*c*), and the percentage of adults seemed inversely related to catch and numeric density. Therefore, at least some of the seasonal increase in catch of freshwater drum may be explained by recruitment of juveniles.

Discussion

The main channel trough is used by a large subset of the species present in this part of the Mississippi and Illinois rivers. We collected 26 species of fish in the navigation channel of the Mississippi River during 1996 and 1997, comprising 31% of the total number of species collected by long-term monitoring of Pool 26 (84 species; E. Ratcliff, Illinois Natural History Survey, personal communication).

Within the Mississippi River, catch rates of freshwater drum, gizzard shad, and shovelnose sturgeon were greater in the upper segment of Pool 26, whereas catch rates of smallmouth buffalo and channel catfish were greater in the lower segment of Pool 26. These results suggest that certain fishes may prefer regions within navigation pools with either relatively high or low current velocity. For instance, the lower abundance of smallmouth buffalo in the upper segment of Pool 26 suggests that this species prefers lower current velocities than the shovelnose sturgeon, which were caught primarily in the upper segment of Pool 26. These patterns of fish distribution suggest that numerous behavioral cues may influence the locations and seasons that certain fishes use the main channel.

Fig. 3. Shovelnose sturgeon (*a*) catch per effort (×, upper Pool 26 of the Mississippi River; +, lower Pool 26 of the Mississippi River) and the fitted negative binomial model given by eq. 2 (short-dashed line, upper Pool 26 of the Mississippi River; long- and short-dashed line, lower Pool 26 of the Mississippi River), (*b*) mean population density, and (*c*) percentage of catch comprising adults (older than age 0, total length ≥25 cm; Carlander 1969) from both areas. Shovelnose sturgeon were not encountered in the lower Illinois River.

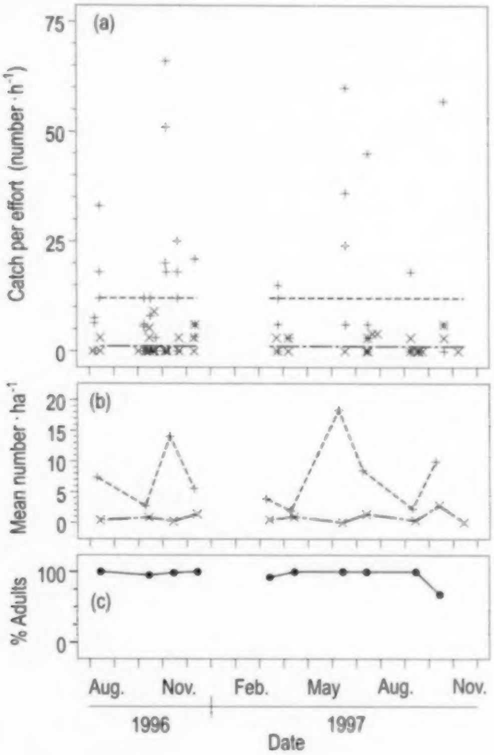

Fig. 4. Gizzard shad (*a*) catch per effort (×, upper Pool 26 of the Mississippi River; +, lower Pool 26 of the Mississippi River; ○, lower Illinois River) and the fitted negative binomial model given by eq. 2 (short-dashed line, upper Pool 26 of the Mississippi River; long- and short-dashed line, lower Pool 26 of the Mississippi River; solid line, lower Illinois River), (*b*) mean population density, and (*c*) percentage of catch comprising adults (older than age 0, total length ≥18 cm; Carlander 1969) from all three areas.

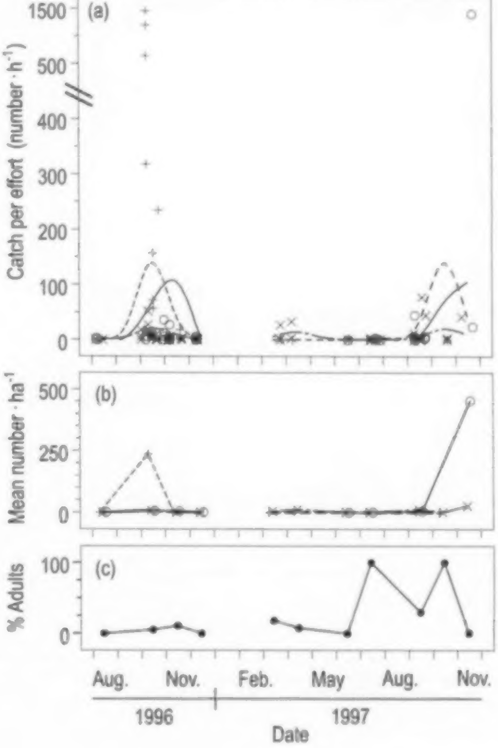

Although the estimated biomass density of fish in the main channel trough was considerable, it was far less than values recorded from other aquatic areas of the upper Mississippi River system (Table 3). Among extant biomass estimates, the largest values were recorded from main channel borders and side channels, whereas the lowest values were recorded from the main channel trough. Biomass density estimates from backwaters were intermediate between channel borders and the main channel trough. Several possibilities may explain this pattern. First, deep riverine channels may support less biomass than other aquatic areas. Second, our biomass estimates may be biased low, since we do not have estimates of our trawling efficiency. Determination of trawl efficiency in large turbid rivers is difficult and was outside our objectives for this study. Third, frequent and persistent disturbance by commercial tow traffic may effectively deny use of some main channel habitat by fishes, which may result in reduced biomass in the navigation channels. Fourth, the frequent barge traffic also limited our ability to sample certain areas, especially near large bends in the river. The resulting uncertainty over spatial bias in sampling is problematic for river management because commercial navigation is projected to increase. Differences in biomass density between the navigation channel and main channel borders (Table 3) also suggest spatial bias. However, this comparison is confounded by between-habitat differences in depth, current velocity, and bottom composition. Important questions remain about fish biomass in these navigation channels and about the influence of barge traffic. We determined, however, that the main channel trough supports substantial biomass of some characteristically riverine species such as shovelnose sturgeon, lake sturgeon, blue sucker, and blue catfish that are uncommon in other aquatic areas of the Mississippi River (Baker et al. 1991). Because lake sturgeon and blue sucker are species of special concern, the importance of the main channel trough is greater than revealed by collective fish abundance. In addition, relatively deep (>3 m) areas, consisting mostly of the main channel, constitute about 65% of the total aquatic area in Pool 26. Therefore, the ecological importance of these relatively deep channels, as measured by total biomass, is greater than indicated by biomass density alone.

Fig. 5. Smallmouth buffalo (*a*) catch per effort (×, upper Pool 26 of the Mississippi River; +, lower Pool 26 of the Mississippi River; ○, lower Illinois River) and the fitted negative binomial model given by eq. 2 (short-dashed line, upper Pool 26 of the Mississippi River; long- and short-dashed line, lower Pool 26 of the Mississippi River; solid line, lower Illinois River), (*b*) mean population density, and (*c*) percentage of catch comprising adults (older than age 0, total length ≥20 cm; Carlander 1969) from all three areas.

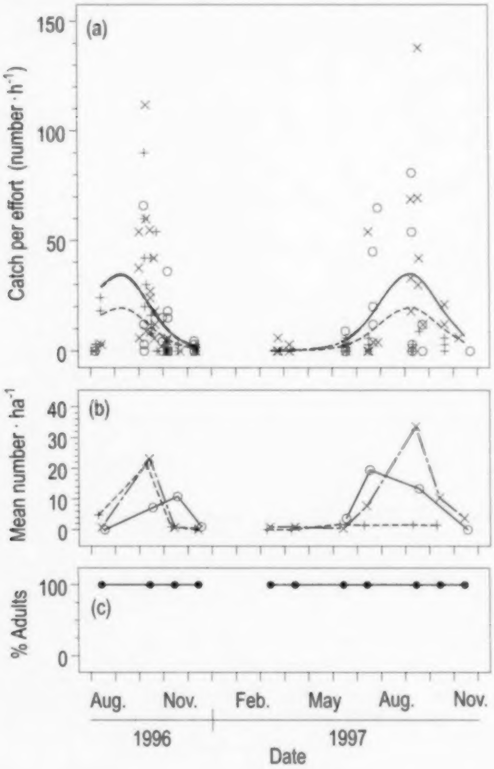

Fig. 6. Freshwater drum (*a*) catch per effort (×, upper Pool 26 of the Mississippi River; +, lower Pool 26 of the Mississippi River; ○, lower Illinois River) and the fitted negative binomial model given by eq. 2 (short-dashed line, upper Pool 26 of the Mississippi River; long- and short-dashed line, lower Pool 26 of the Mississippi River; solid line, lower Illinois River), (*b*) mean population density, and (*c*) percentage of catch comprising adults (older than age 0, total length ≥20 cm; Carlander 1969) from all three areas.

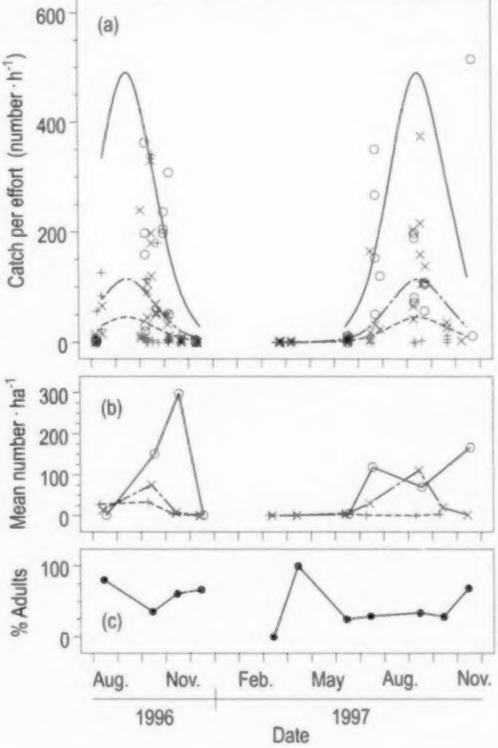

Despite these unresolved issues regarding biomass estimation, our trawling gear managed to catch fishes under a wide range of river conditions. Several species clearly use the river channel across the great range of surface current velocity and temperature conditions present in the upper Mississippi and Illinois rivers. Some fishes residing in the main channel trough during extreme temperature or flow conditions posess behavioral and morphological adaptations that minimize energetic expenditures. Many fishes in the main channel trough of the Mississippi River probably select areas of low current velocity directly downstream of sand dunes. In fishes like the sturgeons, such behavioral adaptations coupled with morphological adaptations (wide, flat head, large pectoral fins, flat ventral surface; Adams et al. 1997), may allow occupation of the channel with relatively low energetic cost.

Our data suggest at least four patterns of use of main channel troughs in the upper Mississippi River system. Some species (highway users, e.g., black crappie, shortnose gar) appear to use the main channel trough primarily as a highway (sensu Junk et al. 1989) to move among various habitats. We collected these species only in the autumn, and only a single individual was collected each year. This low frequency of catch of species that are abundant in other aquatic areas suggests transient use of the main channel trough.

A second group of fishes (single-season users, e.g., bigmouth buffalo, carpsuckers) used the main channel trough primarily during a single season, usually autumn. These fishes remain in the main channel trough for 1–2 months each year but were not collected in the main channel during the rest of the year. We hypothesize that these fishes opportunistically use the main channel trough during the period of low discharge and moderate temperatures that provides a more favorable energetic balance.

A third group of fishes (multiple-season users, e.g., freshwater drum, smallmouth buffalo) uses the main channel trough for multiple, but not all, seasons within each year. These fishes are well adapted to conditions in the main channel trough during most of the year but appear to leave for at least one season. These fishes may leave the main channel trough for purposes associated with spawning or overwinter habitat requirements. For instance, freshwater drum may reside in the main channel trough during summer and autumn because of favorable food resources (Wahl et al. 1988) but move into backwaters during winter to avoid pro-

Table 3. Estimates of biomass density (kg·ha^{-1}) from the upper Mississippi River system.

Aquatic area classification	Mean (SE)	Range
Contiguous backwaters (*n* = 23)[a]	385 (56)	41–931
Secondary and tertiary channel borders (*n* = 2)[b]	536 (477)	79–1035
Main channel borders (*n* = 7)[c]	641 (322)	0–3015
Main channel trough, navigation channel (*n* = 151)[d]	23 (2)	0–130

[a] Rotenone sampling, 1946–1984, Mississippi River Pools 5A–18 (Pitlo 1987).

[b] Rotenone sampling, 1976 and 1981, Pool 22 and unimpounded Mississippi River (Pitlo 1987).

[c] Primacord sampling, 1983 and 1984, Mississippi River Pool 13 (Pitlo 1987).

[d] Trawling (this study).

longed exposure to near-freezing temperatures (Bodensteiner and Lewis 1992).

A final group (residents, e.g., shovelnose sturgeon) is present in the main channel trough during the entire year. Shovelnose sturgeon have been reported primarily either in areas of fast current (Pflieger 1975) or in the main channel (Curtis et al. 1997). When spring current velocities were high in Pool 13 of the Mississippi River, only 9% of locations of radiotagged shovelnose sturgeon were in the main channel, whereas when current velocities were lower during summer, 30% of fish locations were in the main channel (Hurley et al. 1987). Conversely, under conditions of low spring discharge, 54% of radiotagged locations occurred either in tailwaters or in the main channel trough (Curtis et al. 1997). These field observations, coupled with laboratory observations that shovelnose sturgeon cannot maintain their position at focal current velocities >0.4 m·s^{-1} (Adams et al. 1997), suggest that fewer shovelnose sturgeon may persist in the main channel trough during periods of high discharge. However, we commonly captured shovelnose sturgeon when surface current velocities exceeded 1 m·s^{-1}, indicating that shovelnose sturgeon do remain in the main channel trough under high-discharge conditions, possibly in microhabitats with reduced current velocities such as troughs behind sand dunes.

Results from our study reveal a need to modify the prevailing view of the ecological role of the main channel of river–floodplain ecosystems (sensu Junk et al. 1989). Importantly, many fishes do not merely use the main channel as a highway to move between more desirable habitats. Instead, the main channel provides important feeding and (or) spawning habitat for many riverine fishes. As evidenced by the high species richness and abundance of fish in the main channel trough during autumn, the channel trough is at least seasonally important to many fishes. In the Ohio River, sauger fed aggressively on abundant gizzard shad during autumn and grew fastest during October–January (Wahl and Nielsen 1982). Certain species even occupy the main channel trough during the cold months. Shorthead redhorse and sauger were more common in the main channel trough during winter than during other seasons. Lake sturgeon, shovelnose sturgeon, blue sucker, and channel catfish, which are species of interest to river managers and conservationists, are present in the main river channel during all sampling seasons.

The main channel cannot simply be considered a highway for riverine fishes. Although it is unlikely that the main channel trough is more productive than inundated floodplains, it may play an ecologically important role in maintaining the abundance and diversity of fishes present in river–floodplain systems (sensu Winemiller and Jepsen 1998). Clearly, the role of the main channel as fish habitat needs to be better understood and integrated into our understanding of river–floodplain dynamics. For too long, perceptions about ecological processes in large floodplain rivers have been biased by the convenience of sampling in relatively accessible marginal areas. We need to develop a better understanding of the physical features that create habitat for channel-dwelling species, the forces that regulate the abundance and production of these species, and the trophic pathways that sustain biological production in channels.

Acknowledgments

This study was funded by the U.S. Army Corps of Engineers through contract NCR-94-175 with the U.S. Geological Survey, S.G., Principal Investigator. The Illinois Natural History Survey was funded by the U.S. Geological Survey through cooperative agreement 1434-HQ-97-AG-01771. The U.S. Geological Survey Upper Midwest Environmental Science Center provided additional administrative and scientific support. We thank Randy Claramunt, Marc Desjardins, Chad Dolan, Eric Larsen, John Rader, and Frank Wadda for their work in the field. We thank the many scientists who contributed ideas and helpful comments, and particularly Webster Van Winkle, A. L. Jensen, David Schaeffer, Mark Sandheinrich, Randy Burkhardt, Joe Wlosinski, and two anonymous reviewers.

References

Adams, S.R., Parsons, G.R., Hoover, J.J., and Kilgore, K.J. 1997. Observations of swimming ability in shovelnose sturgeon. J. Freshwater Ecol. **12**: 631–633.

Baker, J.A., Kilgore, K.J., and Kasul, R.L. 1991. Aquatic habitats and fish communities in the lower Mississippi River. Rev. Aquat. Sci. **3**: 313–356.

Bayley, P.B. 1995. Understanding river–floodplain ecosystems. BioScience, **45**: 153–158.

Bodensteiner, L.R., and Lewis, W.M. 1992. Role of temperature, dissolved oxygen, and backwaters in the winter survival of freshwater drum (*Aplodinotus grunniens*) in the Mississippi River. Can. J. Fish. Aquat. Sci. **49**: 173–184.

Burnham, K.P., and Anderson, D.R. 1998. Model selection and inference: a practical information-theoretic approach. Springer-Verlag, New York.

Butzer, K.W. 1977. Geomorphology of the lower Illinois Valley as a spatial–temporal context for the Koster archaic site. Rep. Invest. No. 34. Illinois State Museum, Springfield, Ill.

Carlander, K.D. 1969. Handbook of freshwater fishery biology. Vol. 1. Iowa State University Press, Ames, Iowa.

Casselman, J.M., Penczak, T., Carl, L., Mann, R.H.K., Holcik, J., and Woitowich, W.A. 1990. An evaluation of fish sampling methodologies for large river systems. Pol. Arch. Hydrobiol. **37**: 521–551.

Curtis, G.L., Ramsey, J.S., and Scarnecchia, D.L. 1997. Habitat use and movements of shovelnose sturgeon in Pool 13 of the upper Mississippi River during extreme low flow conditions. Environ. Biol. Fishes, **50**: 175–182.

Fremling, C.R., Rasmussen, J.L., Sparks, R.E., Cobb, S.P., Bryan, C.F., and Claflin, T.O. 1989. Mississippi River fisheries: a case history. *In* Proceedings of the International Large River Symposium. *Edited by* D.P. Dodge. Can. Spec. Publ. Fish. Aquat. Sci. No. 106. pp. 309–351.

Gunderson, D.R. 1993. Surveys of fisheries resources. John Wiley & Sons, New York.

Hurley, S.T., Hubert, W.A., and Nickum, J.G. 1987. Habitats and movements of shovelnose sturgeon in the upper Mississippi River. Trans. Am. Fish. Soc. **18**: 327–336.

Johnson, B.L., Richardson, R.L., and Naimo, T.J. 1995. Past, present, and future concepts in large river ecology. BioScience, **45**: 134–141.

Junk, W.L., Bayley, P.B., and Sparks, R.E. 1989. The flood pulse concept in river–floodplain systems. *In* Proceedings of the International Large River Symposium. *Edited by* D.P. Dodge. Can. Spec. Publ. Fish. Aquat. Sci. No. 106. pp. 110–127.

Lawless, J.F. 1987. Negative binomial and mixed Poisson regression. Can. J. Stat. **15**: 209–225.

McCullagh, P., and Nelder, J.A. 1989. Generalized linear models. 2nd ed. Chapman and Hall, London, U.K.

Nielsen, L.A., Sheehan, R.J., and Orth, D.J. 1986. Impacts of navigation on riverine fish production in the United States. Pol. Arch. Hydrobiol. **33**: 277–294.

Patrick, R. 1995. Rivers of the United States. Vol. 2. Chemical and physical characteristics. John Wiley & Sons, New York.

Pflieger, W.L. 1975. The fishes of Missouri. Missouri Department of Conservation, Jefferson City, Mo.

Pitlo, J., Jr. 1987. Standing stock of fishes in the Upper Mississippi River. Upper Mississippi River Conservation Committee Fisheries Section, Rock Island, Ill.

Power, J.H., and Moser, E.B. 1999. Linear model analysis of net catch data using the negative binomial distribution. Can. J. Fish. Aquat. Sci. **56**: 191–200.

Randall, R.G., Kelso, J.R.M., and Minns, C.K. 1995. Fish production in freshwaters: are rivers more productive than lakes? Can. J. Fish. Aquat. Sci. **52**: 631–643.

Ricker, W.E. 1975. Computation and interpretation of biological statistics of fish populations. Bull. Fish. Res. Board Can. No. 191.

Smith, S.J., Perry, R.I., and Fanning, L.P. 1991. Relationships between water mass characteristics and estimates of fish population abundance from trawl surveys. Environ. Monit. Assess. **17**: 227–245.

Vannote, R.L., Minshall, G.W., Cummins, K.W., Sedell, J.R., and Cushing, C.E. 1980. The river continuum concept. Can. J. Fish. Aquat. Sci. **37**: 130–137.

Vanoni, V.A., and Nomicos, G.N. 1960. Resistant properties of sediment-laden streams. Am. Soc. Civ. Eng. Trans. **125**: 1140–1175.

Wahl, D.H., and Nielsen, L.A. 1982. Feeding ecology of the sauger (*Stizostedion canadense*) in a large river. Can. J. Fish. Aquat. Sci. **39**: 120–128.

Wahl, D.H., Brunner, K., and Nielsen, L.A. 1988. Trophic ecology of freshwater drum in large rivers. J. Freshwater Ecol. **4**: 483–491.

Wilcox, D.B. 1993. An aquatic habitat classification system for the Upper Mississippi River system. Tech. Rep. 93-T003. U.S. Fish and Wildlife Service, Environmental Management Technical Center, Onalaska, Wis.

Winemiller, K.O., and Jepsen, D.B. 1998. Effects of seasonality and fish movement on tropical river food webs. J. Fish Biol. **53**(Suppl. A): 267–296.

Effect of spawning day and temperature on salmon emergence: interpretations of a growth model for Methow River chinook

W. Nicholas Beer and James J. Anderson

Abstract: A mechanistic temperature-dependent model for preemergent growth coupled with spawning and river temperature data is used to evaluate early life history strategies for chinook salmon (*Oncorhynchus tshawytscha*) in the Methow River, Washington, U.S.A. Since the model provides a predictable coupling between time of spawning and fry emergence, it helps explain the spatial and temporal patterns observed for the sympatric stocks. The model suggests that progeny of August-spawning chinook in upper river habitats emerge at button-up (no visible yolk sac) over a wide range of days in the early spring. The eggs grow efficiently, which maximizes fry mass. The progeny of October-spawning downstream chinook can exploit a wide range of habitats in the river because their emergence mass is not sensitive to location in the river, but the adults must spawn later in the season to avoid summer high temperatures. Late spawning forces fry to emerge prior to button-up to avoid scouring flows but synchronizes their emergence times. The trade-offs between the spawning strategies of these two salmon runs are complex and the seasonal and spatial distribution of temperatures plays a critical role in these trade-offs.

Résumé : Un modèle mécaniste de la croissance avant l'émergence en fonction de la température combiné à des données sur la fraye et la température de la rivière a servi à évaluer les stratégies du début du cycle biologique chez le Saumon quinnat (*Oncorhynchus tshawytscha*) de la rivière Methow dans l'état de Washington aux États-Unis. Puisque le modèle relie, comme on s'y attend, le moment de la fraye et l'émergence des alevins, il aide à expliquer les structures spatiales et temporelles observées chez ces stocks sympatriques. Le modèle indique que la progéniture des saumons qui frayent en août dans les habitats d'amont émerge au stade de la résorption totale du sac vitellin au début du printemps sur une période étendue de plusieurs jours. Les oeufs croissent activement, ce qui maximise la masse des alevins. La progéniture des saumons qui frayent en aval en octobre peut exploiter une gamme étendue d'habitats dans la rivière, parce que la biomasse de l'émergence n'est pas fonction de la position dans la rivière; les adultes doivent frayer tard dans la saison pour éviter les températures élevées de l'été. La fraye tardive force les alevins à émerger avant la résorption totale du sac vitellin pour éviter les débits d'affouillement, mais cela synchronise leur période d'émergence. Les compromis dans les stratégies de fraye de ces deux montaisons de saumons sont complexes et la répartition saisonnière et spatiale de la température y joue un rôle crucial.

[Traduit par la Rédaction]

Introduction

The final act of semalparous salmon spawning sets the stage for growth and survival of their progeny. Their fate is a function of mechanisms that are mostly independent of behavior prior to emergence: temperature profile, embryonic developmental rates, embryonic yolk conversion efficiencies, and timing and frequency of gravel scour. The ability of fry to survive is a function of the timing of emergence and the frys' physical condition upon emergence.

In the Methow River, on the eastern slope of the Cascade Mountains in Washington, two distinct runs of chinook salmon (*Oncorhynchus tshawytscha*) spawn at different times and locations. The early-arriving adults begin their run in the Columbia River in the spring, wait in the Methow River and its tributaries until August, and spawn in upstream portions of the river. The fry emerge the following spring and are assumed to smolt as yearlings, although multiple life histories have been observed in geographically similar stocks. The second run begins with adult passage in late summer and spawning during November in the lower reaches of the Methow. Progeny of the downstream spawners are assumed to smolt as subyearlings (Mullan et al. 1993).

Environmental controls and selection pressure affecting this separation are unclear, although we speculate that fitness of the two stocks is optimized in distinct ways. Natural selection ensures that the timing of spawning will optimize fry survival in response to environmental cycles that include lethal high temperatures during early incubation, flood cycles that scour the gravel, timing of migration-promoting freshets used by fry, growth potential, food availability, and predator susceptibility (Burger et al. 1985; Brannon 1987). Large size almost always confers survival potential (Lundvall et al. 1999), since swimming speeds are generally higher and

Received June 8, 2000. Accepted February 28, 2001. Published on the NRC Research Press Web site on April 17, 2001.
J15823

W.N. Beer[1] and J.J. Anderson. Columbia Basin Research, School of Aquatic and Fishery Sciences, University of Washington, Box 358218, Seattle, WA 98195, U.S.A.

[1] Corresponding author (e-mail: nick@cbr.washington.edu).

DOI: 10.1139/cjfas-58-5-943

gape-limited predators fewer, but this may only have benefits if emergence timing is synchronized with the environmental events of their habitat.

In this paper, we apply a mechanistic model of preemergent growth to understand the effect of spawning time and location on fry emergence timing for these wild salmon.

Methods

Model for embryonic salmon growth

A model based on basic growth mechanisms identified by Marr (1966) and Heming and Buddington (1988) is used to simulate embryonic growth. Three specific mechanisms are expressed through the yolk–embryo system geometry, which constrains nutrient flow and utilization: (*i*) yolk absorption rate is a function of the surface area of the absorptive layer, (*ii*) surface area changes as the yolk is absorbed, and (*iii*) temperature is the most important abiotic variable affecting yolk absorption. Details of the model are provided in Beer and Anderson (1997) and in the reference notes on an internet site where the user can run the complete model online with full control (http://www.cbr.washington.edu/egg_growth/).

The model characterizes the following growth stages. Embryos in fertilized eggs hatch in 1–3 months to produce larvae. Each larva carries a large yolk sac that provides most if not all of its food until the juvenile fish emerges into the free-flowing waters of the stream as a fry. Together, the yolk sac and larva constitute the alevin. We refer to a developing fish in this sequence of subgravel stages as a "preemergent." There are two physiological landmarks of interest. First, when the alevin's mass has reached a maximum (prior to exogenous feeding), it has attained "maximum alevin wet weight," which we will refer to as the alevin maximum (AM). Second, when the yolk is sufficiently absorbed, the fry has reached button-up (BU), and we assume that this is when 98% of the original yolk has been absorbed.

Emergence is controlled by environmental and developmental variables rather than a specific physiological state because fry emerge with various amounts of yolk remaining and hence are at different developmental stages. At the earliest, fry are not likely to emerge prior to reaching AM due to the comparative benefit of remaining in the gravel while still growing on the yolk. At the latest, fry are not likely to emerge after BU because they will be starving. Emergent fry may still have unabsorbed yolk. Heming (1982) reported that laboratory-grown chinook fry emerge with 10–40% weight in yolk. Other chinook studies (Rombough 1985; Murray and Beacham 1987; Beacham and Murray 1989) reported 9–30% with a higher percentage at warmer temperatures, but field studies (Shelton 1955; Thomas et al. 1969; Field-Dodgson 1988) generally reported less (<2.5% or BU) or were unspecific. As a reference point for our "base case" simulations, the yolk percentage at AM varied between 7 and 16%, which is well within the range of possible states for emergence. However, our purpose is to examine patterns in the timing of development to AM or BU and we assume that emergence is constrained to be between these events.

Water temperature profiles

Methow River temperature profiles are generated with a U.S. Fish and Wildlife model based on temperature records collected along the Methow for several years by different agencies including the U.S. Geological Service, U.S. Fish and Wildlife Service, and Winthrop National Fish Hatchery (Mullan et al. 1993). River temperature (T) is described as a harmonic function of elevation (elev) and day (t):

$$T = \max\begin{bmatrix} (b_0 + b_1 \cdot \text{elev}) + (b_2 + b_3 \cdot \text{elev})\ \sin(c(t + b_4)) \\ 0 \end{bmatrix}$$

where $b_0 = 12.25$, $b_1 = -0.009$, $b_2 = 13.0323$, $b_3 = -0.016$, $b_4 = 248$, and $c = 2\pi/365$. The parameters were fitted to existing data. The b_0 and b_1 terms determine the average annual temperature, the b_2 and b_3 terms determine the magnitude of seasonal fluctuations, and the b_4 term determines the phase shift of the function. For the Methow, elevation is a good surrogate for river kilometer, the distance along the river from the mouth.

The model captures the observed pattern in which lower elevation water temperatures are colder in the winter than the higher elevation temperatures. This counterintuitive pattern occurs because in the winter, ground and surface water from beneath the snowpack flows to the river and is exposed to cool (often subfreezing) air temperatures as it moves downstream and loses heat to the atmosphere. In the summer, the opposite is the case, as water in the mainstem of the river is exposed to warm air and gains heat from the atmosphere. The result is relatively stable temperatures upstream and wider fluctuations downstream. Actual stream temperatures may reach freezing in winter and be significantly warmer than modeled in the summer, but this serves only to shift the growth patterns presented here and does not change their character.

Thermal barrier

There is a thermal barrier above which significant prehatch mortality occurs. Studies have reported that prehatch mortality exceeds 50% at temperatures over 14°C (Alderdice and Velsen 1978; Murray and McPhail 1988). We use 12°C as a prehatch thermal barrier. Temperatures below this are within the recommended range (5.6–12.8°C) for Columbia River basin chinook spawning (McCullough 1999). Note that temperatures are more moderate at higher elevations, allowing earlier spawning, while the thermal barrier extends later in the season at lower elevations. Given these criteria, there may not be a significant thermal barrier for chinook spawning above 530 m, but this does not imply that temperature at the time of spawning is not important.

Scour probability

In the Methow River as in other eastern slope rivers, scouring floods generally occur with the spring run-off. The probability of scour is a function of substrate composition, gradient, suspended load, local hydraulics, and flow. We assume that the probability of scour is proportional with flow based on a 25-year record of weekly averaged flows. Weekly flow exceedance probabilities were defined as the proportion of years where the flow exceeded a given threshold. For example, an exceedance probability of 0.4 for a 300 $m^3 \cdot s^{-1}$ flow on day 130 means that the average flow for that week exceeded 300 $m^3 \cdot s^{-1}$ for 40% of the years in the historic record.

Spawning

The index area for the August-spawning chinook in the Methow River is about 10 km long, starting at the Weeman bridge (96 km from mouth) at an elevation of approximately 560 m. During each spawning season from 1987 to 1993, the index area was surveyed between one and nine times (Kohn 1989; Edson 1990; Scribner et al. 1993). Counts were aggregated to the center of the nearest week of collection and the peak of spawning computed. Between 1987 and 1993, the average spawning peak was day 243 (August 31) with two thirds of all spawning falling in a 15-day period centered on this day. The earliest year was 1988 with the peak on day 232, and the latest year was 1991 (Meekin 1991) with the peak occurring on day 256. Ranges of spawning (two thirds of all new redds deposited) varied from a low of 7 days in 1990 to 21 days in 1988 (Kohn 1988). In our analysis, we use a 15-day window as a typical range.

The October-spawning chinook index area is in the lower river along 80 km from the head of the Wells pool at the mouth of the river to the Winthrop Hatchery dam. The center of the spawning area is near elevation 444 m. For most years, only one or two

Fig. 1. AM (solid line) and BU (broken line) mass as a function of spawning day for (*a*) October-spawned summer chinook fry and (*b*) August-spawned spring chinook fry. The vertical lines mark typical Methow River spawning dates.

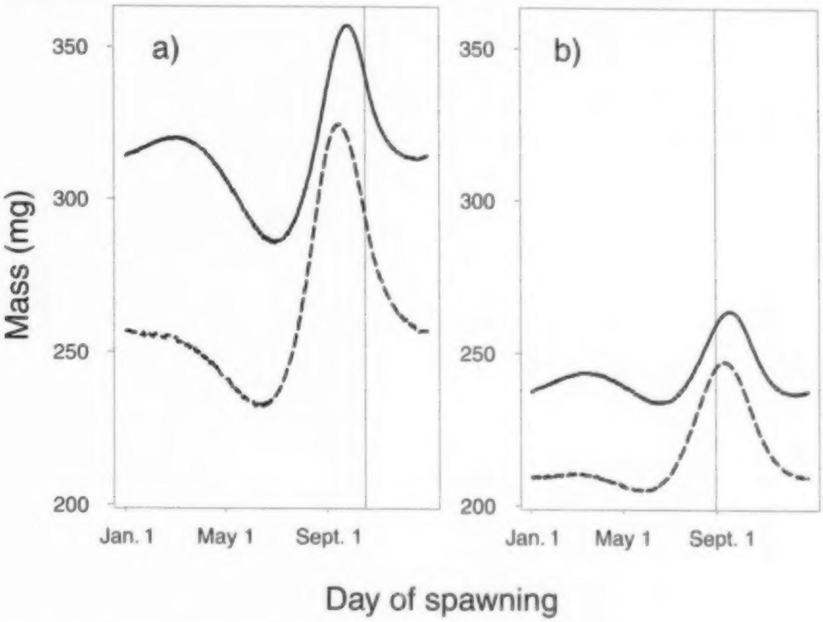

Table 1. Parameters and results for Methow River chinook salmon egg growth.

Parameter	Downstream, October-spawning, summer-run chinook		Upstream, August-spawning, spring-run chinook
Egg mass	284 mg		218 mg
Day of year of spawning	290		243
Elevation	560 m		444 m
Range of spawning time		15 days	
Initial embryo mass		1 mg	
Time step (Δt)		0.25 days	
AM mass	344 mg		259 mg
BU mass	302 mg		245 mg
AM time (month/day)	53 (2/22)		10 (1/10)
BU time (month/day)	160 (5/10)		133 (4/14)

counts were made of these lower areas. The peak of spawning is later, near day 290 (October 17), while the temporal spread of spawning is assumed to be similar to that of the upstream chinook.

Modeled egg mass is based on the mean egg mass for the two runs from the hatchery brood stock: 284 mg for October-spawning downstream chinook and 218 mg for August-spawning upstream chinook (Bartlett and Bugert 1994; H. Bartlett, Washington Department of Fish and Wildlife, P.O. Box 83, Twisp, WA 98856-0912, U.S.A., personal communication).

Daily U.S. Geological Survey flow records (gauging station No. 12449950, 1970–1993) for Pateros at the mouth of the Methow were averaged over a 1-week period, and the proportion of years that had values over a given level determine the flow exceedance probability for that particular week.

Simulations

A single simulation involves setting the temperature profile, spawning time, and egg size and then calculating the time and mass at AM and BU. The model runs reported here examine the sensitivity of emergent fry mass and time to a range of inputs, e.g., day of spawning, and interpreting the results in terms of survival or growth potential for the emergent fish.

Results

October-spawning downstream chinook spawn too late to optimize the mass of their progeny (Fig. 1*a*). After AM, the alevins shrink quickly in the warming waters, losing 18% of their AM mass by BU. August-spawned upstream chinook (Fig. 1*b*) come closer to reaching their greatest possible mass at either AM and BU and lose only 8% of their AM mass by BU. Table 1 summarizes the input parameters and these base-case results.

A range of spawning dates results in a range of emergent masses and emergent times. The range of emergence times is

Fig. 2. Ranges of chinook salmon alevin emergence date and mass for a 15-day spawning interval about mean spawning date. The solid and broken lines depict emergence at AM and BU, respectively. The vertical lines mark typical spawning dates and hence identify typical emergence ranges.

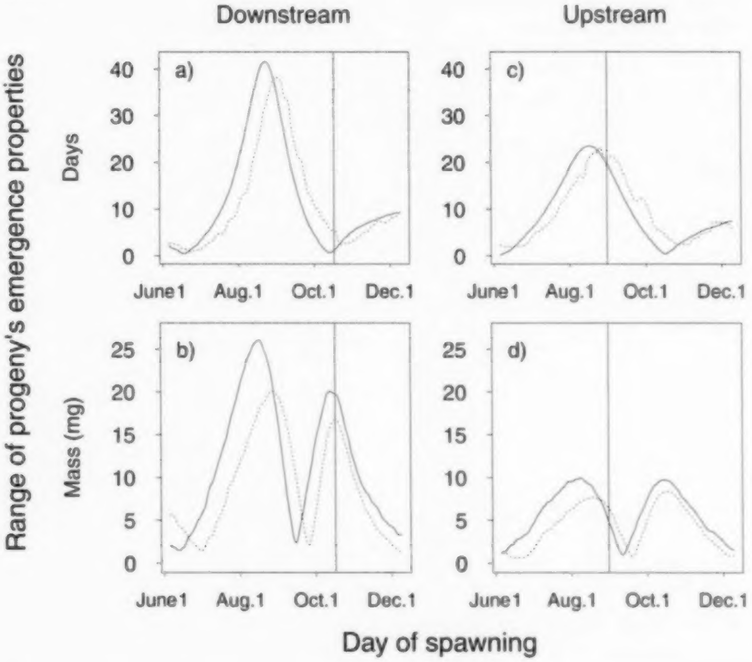

Fig. 3. Sensitivity of progeny's AM and BU emergence mass and developmental period (days from fertilization to emergence) to spawning elevation for October spawners (solid lines) and August spawners (broken lines). Vertical lines show typical spawning elevations of the stocks. The sets of three curves show the mean and range of outcomes for the fish spawning over a 15-day range.

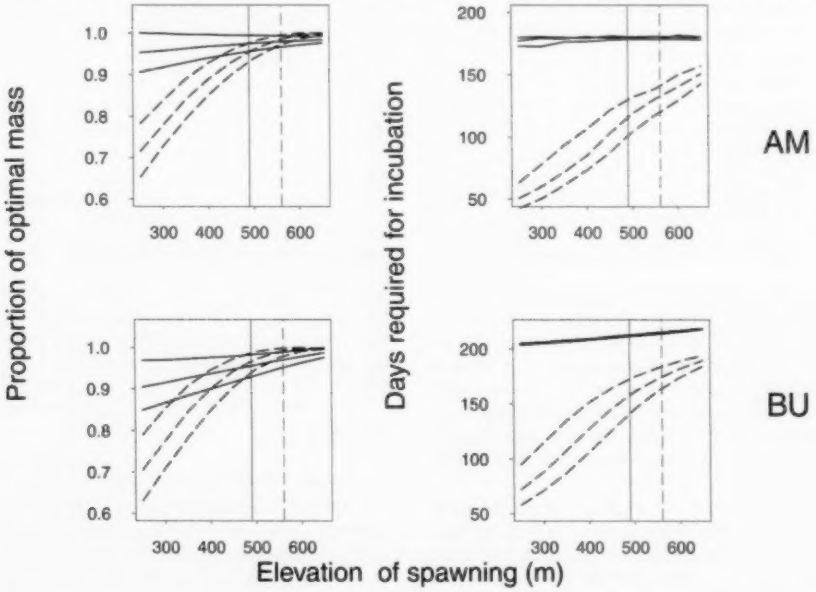

a function not only of the range of spawning times but also of the temperature profile and the time of hatching because most growth occurs after hatching. If spawning is early enough such that hatching occurs during a period of rapidly fluctuating temperatures, the spread of emergence masses and times is greater than if spawning is later and hatching

Fig. 4. (*a*) Relationship of AM and BU emergence day to adult chinook salmon spawning day and location (elevation). The base case is drawn with a horizontal broken line. The boxes show the typical spawning time range (15 days) and location of the index area for the August-spawning spring chinook (upstream) and October-spawning summer chinook (downstream). The times to AM and BU corresponding to the typical spawning times and elevations are shown as labeled polygons. The spawning time for maximum fry emergence mass at any elevation is shown as a heavy broken line. A 12°C thermal barrier defines the earliest spawning date (marked), and a scour barrier defines the latest emergence date (vertical line through both panels). The shaded area about the line illustrates the range of spawning times that give fry emergence mass greater than 95% of the maximum possible. (*b*) Methow River seasonal temperatures for upstream (broken line, 560 m) and downstream (solid line, 444 m) spawning locations and the probability of flow exceedance at three different flows (75, 150, and 300 $m^3 \cdot s^{-1}$).

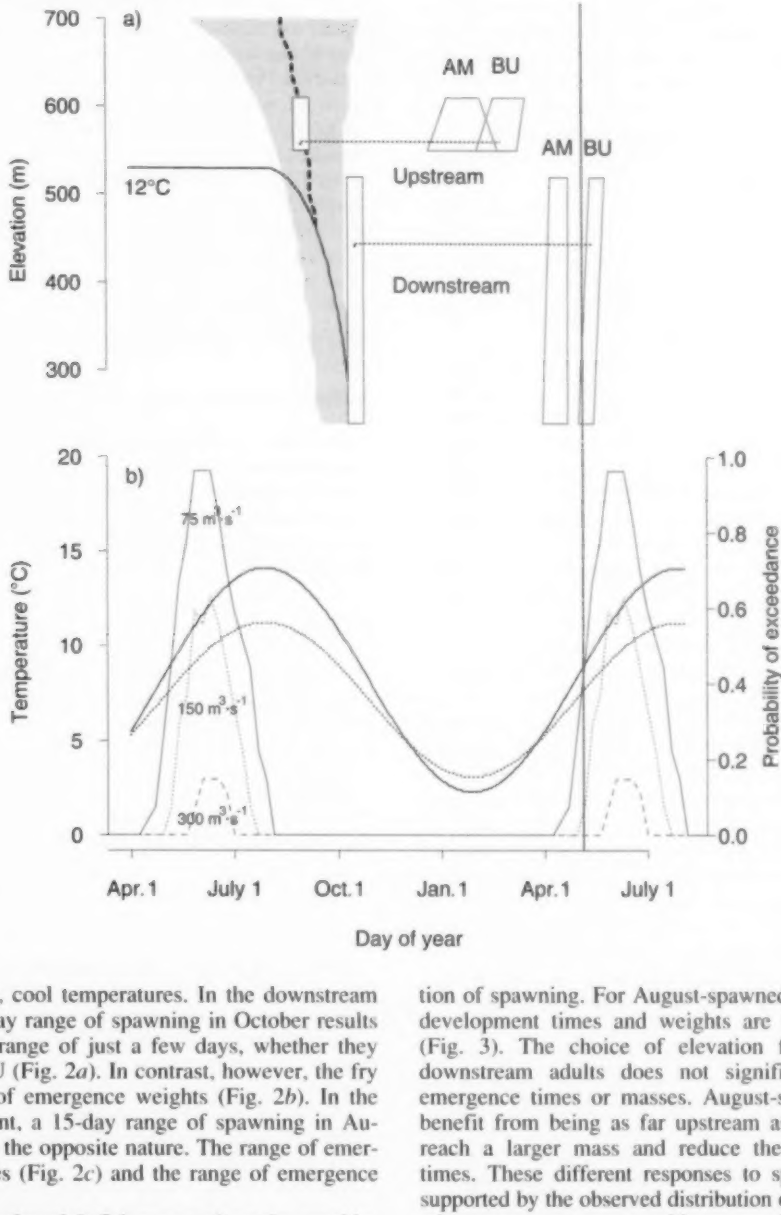

occurs during stable, cool temperatures. In the downstream environment, a 15-day range of spawning in October results in a fry emergence range of just a few days, whether they emerge at AM or BU (Fig. 2*a*). In contrast, however, the fry have a wide range of emergence weights (Fig. 2*b*). In the upstream environment, a 15-day range of spawning in August exhibits exactly the opposite nature. The range of emergence times increases (Fig. 2*c*) and the range of emergence weights is narrow.

The time at which the adult fish spawn alters the sensitivity of their progeny's emergence properties to river location. The masses and development times to AM and BU of October-spawned fry are generally independent of the elevation of spawning. For August-spawned fry, the AM and BU development times and weights are sensitive to elevation (Fig. 3). The choice of elevation for October-spawning downstream adults does not significantly alter progeny emergence times or masses. August-spawned upstream fry benefit from being as far upstream as possible where they reach a larger mass and reduce the range of emergence times. These different responses to spawning elevation are supported by the observed distribution of spawners. Thus, October spawners cover a wide range of elevations, while the August spawners are confined to a small upstream area. Farther upstream, habitat quality may be limiting for nonthermal reasons.

The upstream spawners exhibit more spread in emergence times than the downstream spawners. In fact, upstream spawners maximize the spread of their progeny's emergence times by spawning in August, while the downstream spawners minimize the spread of emergence times by spawning in October.

Discussion

The interactions of the biological and environmental constraints that determine spawning strategies are illustrated in Fig. 4. The upstream fry are constrained by elevation (physical habitat becomes limiting farther upstream) but not by time, so spawning can occur at a time that results in the most efficient egg development and emergence weight. Since time is not an issue, the alevins likely remain in the gravel until BU and lose only 5% of their AM mass.

Downstream fry are constrained more in time than in elevation. The thermal barrier blocks early spawning and the scour barrier blocks late emergence, so they fail to optimize their size and may be forced to emerge closer to AM. Since location has little effect on development time or AM mass, spawning is broadcast over a wide area.

The optimal growth line (heavy dashed line in Fig. 4*a*) meets the thermal barrier near elevation 475 m around the beginning of September. This may be the spatial and temporal boundary that separates the two life histories strategies. High summer temperatures below this elevation can induce egg mortality, which negates the benefit of the optimum growth strategy of the typical upstream-spawning chinook. Above this elevation, the typical downstream-spawning strategy is suboptimal because the fry of adults that spawned earlier will have higher growth. Therefore, attempts by adults with either life history strategy to spawn close to this boundary result in suboptimal survival for the progeny.

Although egg size is a factor in growth, there are no clear ecological benefits to any particular egg size based on this model. The August-spawning upstream chinook have small eggs and the fry emerge in early spring. Large egg size would in theory be beneficial at emergence, and there is no obvious detriment to longer developmental times. In the opposite manner, the October-spawning downstream chinook have larger eggs and longer development times that make them susceptible to scouring. Smaller eggs could shorten their development time, which may be beneficial to survival. However, the small size of the high-elevation alevins may facilitate their motion in the gravel to find water during low flow years and (or) escape from anchor ice that can form in the gravel during very cold, dry winters (Caldwell and Catterson 1992).

A spread of emergence time could allow for a broader variety of life history patterns. In the Methow basin on the Chewuck River, Hubble and Sexauer (1994) observed juvenile chinook salmon outmigration throughout the spring and summer (as smolts or parr). Lichatowich and Mobrand (1995) identified six different life history patterns historically present in the Yakima River. Of these six, five of them are associated with stream-type chinook. Upstream fry emerge during a low productivity time, so niche separation may be enhanced by a wide range of emergence times. In contrast, the downstream fry may be emerging together in order to saturate the predators (Brännäs 1995). This may be particularly advantageous if they emerge near AM and have limited predator avoidance capabilities because the yolk sac is not completely absorbed (Thomas et al. 1969).

This analysis demonstrates the complexity of trade-offs in spawning strategies faced by chinook salmon and suggests that the seasonal and spatial distribution of temperature plays a critical role in these trade-offs. In particular, some habitats that may be physically suitable for fish may be inaccessible because of seasonal temperature patterns. Although population differences in development rates could allow late- or cold-temperature-spawned eggs to develop more quickly (Brannon 1987), behavioral differences and life history variations allow a very wide range of responses and adaptations.

The possibility that some of the complex effects of temperature on preemergent growth can be quantitatively established has been largely unexplored and needs to be further considered for enhancing fish spawning success. Finally, since our work suggests that the natural spawning times of a stock and the postspawning temperature pattern together can affect the fitness of emergent fry in a particular habitat, these factors should be considered when planning habitat restoration and fish supplementation activities.

Acknowledgments

We thank A. Hendry, H. Bartlett, and J. Hubble for their insights and information and extend gratitude to the editors and two anonymous reviewers for helpful comments that improved earlier drafts of this manuscript. This work was supported by Bonneville Power Administration contract DE-BI79-89BP02347.

References

Alderdice, D.F., and Velsen, F.P. 1978. Relation between temperature and incubation time for eggs of chinook salmon. J. Fish. Res. Board Can. **35**: 69–75.

Bartlett, H., and Bugert, B. 1994. Methow River basin spring chinook salmon hatchery program evaluation. Prepared for Douglas County Public Utilities District, Washington Department of Fish and Wildlife, Olympia, Wash.

Beacham, T.D., and Murray, C.B. 1989. Variation in developmental biology of sockeye salmon (*Oncorhynchus nerka*) and chinook salmon (*Oncorhynchus tshawytscha*) in British Columbia. Can. J. Zool. **67**: 2081–2089.

Beer, W.N., and Anderson, J.J. 1997. Modeling the growth of salmonid embryos. J. Theor. Biol. **189**: 297–306.

Brännäs, E. 1995. First access to territorial space and exposure to strong predation pressure: a conflict in early emerging Atlantic salmon (*Salmo salar*) fry. Evol. Ecol. **9**: 411–420.

Brannon, E.L. 1987. Mechanisms stabilizing salmonid fry emergence timing. *In* Sockeye salmon (*Oncorhynchus nerka*) population biology and future management. *Edited by* H.D. Smith, L. Margolis, and C.C. Wood. Can. Spec. Publ. Fish. Aquat. Sci. No. 96. pp. 120–124.

Burger, C.V., Wilmot, R.L., and Wangaard, D.B. 1985. Comparison of spawning times for two runs of chinook salmon (*Oncorhynchus tshawytscha*) in the Kenai River, Alaska. Can. J. Fish. Aquat. Sci. **42**: 693–700.

Caldwell, B., and Catterson, D. 1992. Methow River basin fish habitat analysis using the instream flow incremental methodology. Water Resources Program, Department of Ecology, Olympia, Wash.

Edson, S.A. 1990. Spring chinook spawning ground surveys of the Methow River basin. Yakima Indian Nation, Fisheries Resource Management, Toppenish, Wash.

Field-Dodgson, M.S. 1988. Size characteristics and diet of emergent chinook salmon in a small, stable, New Zealand stream. J. Fish Biol. **32**: 27–40.

Heming, T.A. 1982. Effects of temperature on utilization of yolk by chinook salmon (*Oncorhynchus tshawytscha*) eggs and alevins. Can. J. Fish. Aquat. Sci. **39**: 184–190.

Heming, T.A., and Buddington, R.K. 1988. Yolk absorption in embryonic and larval fishes. *In* Fish physiology. Vol. XI. *Edited by* W.S. Hoar and D.J. Randall. Academic Press, New York. pp. 408–446.

Hubble, J., and Sexauer, H. 1994. Methow basin spring chinook salmon supplementation plan, natural production study, 1994 annual report. Prepared for Douglas County Public Utilities District, East Wenatchee, Wash. Yakima Indian Nation, Toppenish, Wash.

Kohn, M.S. 1988. Spring and summer chinook spawning ground surveys, Methow and Okanogan River basins, 1988. Report to Chelan County Public Utilities District. Yakima Indian Nation, Toppenish, Wash.

Kohn, M.S. 1989. Spring and summer chinook spawning ground surveys, Wenatchee, Methow and Okanogan River basins, 1989. Report to Chelan County Public Utilities District. Yakima Indian Nation, Toppenish, Wash.

Lichatowich, J.A., and Mobrand, L.E. 1995. Analysis of chinook salmon in the Columbia River from an ecosystem perspective. DOE/BP-25105-2. Research report prepared for Bonneville Power Administration, Environment, Fish and Wildlife, P.O. Box 3621, Portland, OR 97208-3621, U.S.A.

Lundvall, D., Svanbäck, R., Persson, L., and Byström, P. 1999. Size-dependent predation in piscivores: interactions between predator foraging and prey avoidance abilities. Can. J. Fish. Aquat. Sci. **56**: 1285–1292.

Marr, D.H.A. 1966. Influence of temperature on the efficiency of growth of salmonid embryos. Nature (Lond.), **212**: 957–959.

McCullough, D.A. 1999. A review and synthesis of effects of alterations to the water temperature regime on freshwater life stages of salmonids, with special reference to chinook salmon. EPA Region 10, 1200 Sixth Avenue, Seattle, WA 98101, U.S.A.

Meekin, T.K. 1991. Spring chinook spawning ground surveys of the Methow River basins, 1991. Report to Chelan County Public Utilities District. Yakima Indian Nation, Toppenish, Wash.

Mullan, J.W., Williams, K.R., Rhodus, G., Hillman, T.W., and McIntyre, J.D. 1993. Production and habitat of salmonids in mid-Columbia River tributary streams. U.S. Fish and Wildlife Service, Leavenworth Wash.

Murray, C.B., and Beacham, T.D. 1987. The development of chinook (*Oncorhynchus tshawytscha*) and chum salmon (*Oncorhynchus keta*) embryos and alevins under varying temperature regimes. Can. J. Zool. **65**: 2672–2682.

Murray, C.B., and McPhail, J.D. 1988. Effects of incubation temperature on the development of five species of Pacific salmon (*Oncorhynchus*) embryos and alevins. Can. J. Zool. **66**: 266–273.

Rombough, P.J. 1985. Initial egg weight, time to maximum alevin wet weight, and optimal ponding times for chinook salmon (*Oncorhynchus tshawytscha*). Can. J. Fish. Aquat. Sci. **42**: 287–291.

Scribner, T., Meekin, T.K., Hubble, J., and Fiander, W. 1993. Spring chinook spawning ground surveys of the Methow River basin, 1993. Yakima Indian Nation, Fisheries Resource Management, Toppenish, Wash.

Shelton, J.M. 1955. The hatching of chinook salmon eggs under simulated stream conditions. Prog. Fish-Cult. **17**: 20–35.

Thomas, A.E., Banks, J.L., and Greenland, D.C. 1969. Effect of yolk sac absorption on the swimming ability of fall chinook salmon. Trans. Am. Fish. Soc. **98**: 406–410.

Identifying cause in sediment assessments: bioavailability and the Sediment Quality Triad

U. Borgmann, W.P. Norwood, T.B. Reynoldson, and F. Rosa

Abstract: Application of the Sediment Quality Triad approach to non-pH-stressed Sudbury area lakes clearly demonstrated increased metal (Cd, Co, Cu, and Ni) contamination, decreased abundances of some benthic invertebrates (amphipods, pisidiid clams, and tanytarsiid midges), and severe sediment toxicity to amphipods and mayflies. However, the bioavailability of metals and the cause of biological effects cannot be identified from these data. Bioaccumulation measurements, however, clearly demonstrated increased Cd, Co, and Ni bioavailability to *Hyalella*. Copper concentrations in *Hyalella* were not elevated, in spite of much higher sediment Cu concentrations. Nickel was the only metal accumulated in sufficient amounts to cause toxicity. Toxicity in *Hyalella* caged above the sediments was equivalent to that of animals exposed directly in sediment, demonstrating that effects were due to dissolved metal and not metals in the solid phase. Copper concentrations in overlying water were much lower than Ni concentrations and insufficient to account for toxicity. Including bioaccumulation data with traditional measurements of sediment chemistry, benthic community composition, and sediment toxicity allows quantification of metal bioavailability and identification of the cause of toxicity. This approach results in a much more complete assessment of the biological impacts of metals in sediments.

Résumé : L'application d'une approche basée sur les «trois critères de qualité des sédiments» à des lacs de la région de Sudbury qui ne subissent pas de stress dû au pH a clairement révélé une contamination plus importante par les métaux (Cd, Co, Cu, Ni), des densités plus faibles chez certains invertébrés benthiques (amphipodes, moules Pisidiidae et diptères Chironomidae Tanytarsini) et une grande toxicité des sédiments aux amphipodes et aux éphéméroptères. Cependant, les résultats ne permettent pas de déterminer la biodisponibilité des métaux et d'identifier les causes des effets biologiques. Des mesures de la bioaccumulation indiquent clairement une biodisponibilité accrue du Cd, du Co et du Ni à *Hyalella*. Les concentrations de Cu chez *Hyalella* ne sont pas élevées, même si les concentrations de Cu dans les sédiments se sont fortement accrues. Le Ni est le seul métal accumulé en quantité suffisante pour produire une toxicité. La toxicité chez des *Hyalella* gardés dans des cages au-dessus des sédiments est la même que chez des animaux exposés directement aux sédiments, ce qui indique que les effets sont dus aux métaux dissous et non aux métaux en phase solide. Les concentrations de Cu dans l'eau surnageante sont beaucoup plus faibles que celles du Ni et insuffisantes pour expliquer la toxicité. L'addition de données sur la bioaccumulation aux mesures classiques de chimie des sédiments, de composition de la communauté benthique et de toxicité des sédiments permet la quantification de la biodisponibilité des métaux et l'identification de la cause de la toxicité. Une telle approche produit une évaluation plus complète des impacts biologiques des métaux dans les sédiments.

[Traduit par la Rédaction]

Introduction

The Sediment Quality Triad (Chapman 1990; Chapman et al. 1997) represents the "state of the art" for most current sediment assessments. It consists of sediment chemical analysis, examination of in situ benthic community composition, and measurement of sediment toxicity. Traditionally, correlations between these three components are examined in an attempt to define the significance of chemical measurements and to provide clues to the causes of biological effects. Chapman (1996, 2000) and Chapman et al. (1997) have called for improvements to the Triad approach, including the possible addition of bioaccumulation measurements, but most environmental assessments have not yet been expanded to do this.

The information needed to make sound environmental decisions is conveniently summarized in the four key questions posed in the Aquatic Effects Technology Evaluation (AETE) program (ESG International Inc. 1999). This program was a major Canadian government and industry initiative established to evaluate potential monitoring tools for the mining industry. Monitoring tools were evaluated with respect to their ability to address one of these four guiding questions. (*i*) Are contaminants getting in the system? (*ii*) Are contaminants bioavailable? (*iii*) Is there a measurable response? (*iv*) Are the contaminants causing this response? These questions summarize succinctly what needs to be asked in environmental assessments of chemicals, not just for metals but for any contaminants. They also provide a useful means of assessing the adequacy of the Sediment Quality Triad approach and for identifying what needs to be added to the Triad to ensure that sediment assessments are complete.

A research program initiated by the National Water Research Institute in 1996 to examine the biological impacts

Received July 5, 2000. Accepted February 28, 2001. Published on the NRC Research Press Web site on April 17, 2001.
J15853

U. Borgmann,[1] W.P. Norwood, T.B. Reynoldson, and F. Rosa. Environment Canada, National Water Research Institute, Burlington, ON L7R 4A6, Canada.

[1] Corresponding author (e-mail: uwe.borgmann@cciw.ca).

Can. J. Fish. Aquat. Sci. **58**: 950–960 (2001) DOI: 10.1139/cjfas-58-5-950

of the atmospheric deposition of metals from Sudbury area smelters on lake ecosystems provides an opportunity to test the adequacy of the Sediment Quality Triad in answering the four AETE questions. Although smelting activities in the Sudbury area have resulted in extensive atmospheric deposition of S and metals and concomitant environmental degradation (Jeffries 1984; Keller 1992; Winterhalder 1995), the relative importance of metals specifically in biological impacts has not been examined extensively. Yan et al. (1996) did, however, conclude that metals slowed the recovery of populations of *Daphnia galeata mendotae* in two lakes near Sudbury that had been limed to increase pH. Metals bind strongly to sedimenting particulate matter, and benthic communities are therefore likely to be vulnerable to metal contamination. Examination of the biological impacts of metals in Sudbury area sediments included analysis of the standard Sediment Quality Triad components in 1996. In addition, metal bioavailability (bioaccumulation in *Hyalella azteca*) was measured under laboratory conditions with fresh sediments collected in 1998. The results from this study were used to examine the adequacy of the Sediment Quality Triad in answering the four key questions in the AETE program. This provides an opportunity to identify what needs to be added to the Triad to provide a more complete assessment of sediments contaminated with metals.

Materials and methods

Water, sediment, and benthic invertebrate samples were collected from 12 lakes at 6–154 km from the smelter stacks at Copper Cliff in August 1996 and again in August 1998 (Table 1). These included four lakes in the immediate Sudbury area (<13 km from the smelter stacks at Copper Cliff), four reference lakes at considerable distance from Sudbury (94–154 km), and four lakes at intermediate distance (32–52 km) (i.e., high-, low-, and intermediate-impact areas) (Table 1). Two sampling depths were selected in each lake, including the deepest location and a site at 10 m depth if the deep site was >10 m. Only a single (deep) site was chosen for Ramsey Lake. This lake is within the city of Sudbury and sediment contamination by metals is not necessarily entirely due to atmospheric deposition. This site was included, since it was very close to the site of emissions, known to be heavily contaminated, and might show effects even if the other lakes did not (i.e., a positive control). The pH, specific conductance, dissolved oxygen concentration, and temperature were recorded with a HYDROLAB profiling system, model DataSonde® 3 (Hydrolab Corp. 1991), at each site. All lakes were circumneutral with pH values of 6.6–8.3 near the surface, although lower values were observed near the bottom (Table 1).

In addition to the reference lakes indicated above, two control sediments were used in the toxicity and bioaccumulation tests, one from Hamilton Harbour (HH1) and another from Lake Erie (LE303), near Long Point. The Lake Erie sediment is low in metals. Although the Hamilton Harbour sediment is not a "clean" sediment, it has consistently supported excellent growth and survival of *Hyalella* in our laboratory and is a good control sediment for toxicity in this species.

Sediment chemistry

Surface sediment samples for metal analysis were obtained from within the top 5 cm of sediment collected with a box corer in 1996. In addition, in 1996 at the deep stations only, a 20-cm sediment core was taken using a Technical Operations corer (modified combination of Kajak–Brinkhurst and benthos gravity corers) and carefully sectioned using a hydraulic extruder (Mudroch and MacKnight 1991) into 1-cm intervals for the first 10 cm and 2-cm intervals for the next 10 cm to obtain a sediment profile of metal concentrations. Sediment samples were freeze-dried and ground with a mortar and pestle before analysis for total metals following methods modified slightly from Environment Canada (1994). A 0.5-g subsample was digested with concentrated nitric acid (5 mL) and hydrofluoric acid (3 mL) in teflon beakers on a hotplate at 95°C and evaporated to dryness. Residues were redissolved in hydrogen peroxide (30%, 1 mL) and nitric acid (0.4 M, 5 mL) and gently heated for 1 h. Samples were then cooled, diluted to 50 mL with 0.4 M nitric acid, centrifuged at 5000 rpm for 30 min, and analyzed on a JY 74 inductively coupled argon plasma optical emission system (ICAP-OES). Recovery of metals from certified reference material (NIST-2704 Buffalo River sediment) was within 10% of the certified values. Particle size was determined by sieving to remove sand and gravel (62.4-μm mesh). The material passing through the sieve was suspended in a dispersant solution and analyzed on a Sedigraph analyzer (Duncan and LaHaie 1979) for particle size. Sediments contained 25–50% silt (>3.91 μm), 29–75% clay (<3.91 μm), and no sand except for two sites (RAF10 at 41% and TRO10 at 2%). Organic C in sediments, measured by infrared analysis of combusted C from dried sediment samples using a LECO-12 carbon determinator (Dalton 1994), ranged from 3.5 to 8.7%.

Benthic community structure

In 1996, in situ benthic invertebrates were collected using a box corer (38 × 38 × 46 cm) from which five core tubes (10 cm deep, 33.2 cm^2 area each) of sediment were sampled, sieved through a 250-μm mesh, and fixed in 5% formalin. The samples were transferred to 70% ethanol after several days to prevent decalcification. Due to the low abundance of invertebrates obtained from the core tubes, animals were collected by miniponar grab sampler (224 cm^2 area) in 1998. Three replicate grabs were collected from each station. These were sieved through a 500-μm-mesh screen because of the larger sediment volume collected in 1998. The entire invertebrate samples were identified and counted in both years.

Sediment toxicity

Sediment toxicity tests were conducted under standardized laboratory conditions (constant temperature, aeration, water–sediment volume ratios, and test species) to determine if these reflect differences observed in benthic communities seen in the field. Such tests cannot mimic all natural in situ conditions, and no attempt was made to do so. Five replicate miniponar sediment samples were collected at each sampling site and stored separately in polyethylene bags at 4°C until analyzed. Four toxicity tests were conducted on sediments collected in 1996, a 10-day survival and growth test with *Chironomus riparius*, a 21-day survival and growth test with *Hexagenia limbata*, a 28-day survival and growth test with *H. azteca*, and a 28-day survival and reproduction test with *Tubifex tubifex* (Day et al. 1995). Experiments were conducted at 23°C with dechlorinated Burlington city tap water (originating from Lake Ontario, hardness 130 $mg \cdot L^{-1}$, alkalinity 90 $mg \cdot L^{-1}$, dissolved organic C 2.3 $mg \cdot L^{-1}$, pH 7.8–8.6) overlying the test sediments. In initial static tests, conducted in beakers with a sediment to water ratio of 1 to 4, the pH quickly dropped to around 4 in most of the test containers, except for those with control sediments. This resulted in high or complete mortality of *Hexagenia* and *Hyalella* in all test sediments, including reference sediments. All further experiments were therefore conducted in Imhoff settling cones with 15 mL of sediment and 1 L of overlying water using methods described in Borgmann and Norwood (1999*a*). The test containers were aerated and oxygen concentrations in the overlying water averaged 8 $mg \cdot L^{-1}$ (minimum recorded = 7.1 $mg \cdot L^{-1}$, $n = 72$). The pH averaged 8.29 (SD 0.22, $n = 671$). Each cone contained 15 *Hyalella*, 15 *Chironomus*, two *Hexagenia*, or two *Tubifex*. Nine

Table 1. Sampling site locations and characteristics and Cu and Ni in surface (0–5 cm) sediment samples.

Site code[a]	Latitude (°)	Longitude (°)	Distance from Copper Cliff (km)	Water depth (m)	Oxygen directly above bottom ($mg \cdot L^{-1}$)[b]	Temperature near bottom (°C)[c]	pH near bottom[c]	Conductivity near bottom ($\mu S \cdot cm^{-1}$)[c]	Cu ($\mu mol \cdot g^{-1}$)	Ni ($\mu mol \cdot g^{-1}$)
Sudbury area lakes										
RAMD	46.4806	80.9758	6	20.4	5.6	7.8	6.98	306	27.01	34.53
MCF10	46.4233	80.9494	10	9.6	0.8	10.7	7.32	326	16.95	34.34
MCFD	46.4136	80.9689	10	19.3	0.5	7.0	6.78	327	18.73	99.10
RAF10	46.4125	80.9406	11	10.1	8.7	11.5	6.62	38	11.40	14.89
RAFD	46.4128	80.9514	11	15.2	2.5	8.0	6.17	40	34.42	39.06
RICD	46.4378	80.9167	12	9.3	2.3	18.2	7.16	184	27.26	54.39
Intermediate lakes										
NEPD	46.3333	80.6956	32	9.9	2.4	19.4	6.35	46	3.95	6.52
KAK10	46.1917	80.7894	38	10.3	3.7	8.7	6.20	64	2.66	5.58
KAKD	46.1900	80.7908	38	23.6	1.1	5.1	6.07	70	3.28	5.51
TRO10	46.2283	80.6408	43	8.9	6.7	10.0	6.41	30	3.06	6.37
TROD	46.2278	80.6169	43	47.3	5.8	5.8	5.82	31	3.21	3.91
LOS10	46.1269	80.6006	52	9.8	7.4	6.0	6.36	31	1.35	4.00
LOSD	46.1353	80.6081	52	45.4	4.2	4.2	5.95	31	2.20	2.61
Reference lakes										
TOM10	46.5383	79.8333	94	9.8	6.2	16.9	6.43	33	1.09	1.74
TOMD	46.5439	79.8142	94	22.5	4.2	10.4	5.68	32	1.03	1.53
RES10	46.0561	79.7953	107	10.4	5.6	10.7	6.20	32	0.64	1.18
RESD	46.0569	79.8061	107	28.5	5.1	6.2	5.66	32	0.68	0.87
NOS10	46.2167	79.2228	144	10.4	1.9	17.4	6.59	61	0.59	0.88
NOSD	46.2183	79.2181	144	13.8	0.5	12.3	6.63	83	0.68	0.87
TAL10	46.2964	79.0436	154	10.7	7.8	10.8	6.84	47	0.72	1.47
TALD	46.3014	79.0647	154	38.1	7.3	5.7	6.13	45	0.66	1.08

[a] Lake names associated with these codes are Ramsey (RAM), McFarlane (MCF), Raft (RAF), Richard (RIC), Nepewassi (NEP), Kakakiwaganda (KAK), Trout (TRO), Lower Sturgeon (LOS), Tomiko (TOM), Restoule (RES), Nosbonsing (NOS), and Talon (TAL).

[b] Oxygen at 1 m below surface = 7.73–8.29 $mg \cdot L^{-1}$ for all lakes.

[c] 1 m above bottom. Temperature = 21.6–23.9°C and pH = 6.59–8.29 at 1 m below the surface for all lakes.

separate experiments were conducted with sediments collected in 1996, two with each of *Chironomus*, *Hexagenia*, and *Tubifex* and three with *Hyalella*. Each experiment included one test container with sediment from each site (21 sites) plus two control sediments (Hamilton Harbour and Lake Erie). This was the maximum number of experimental containers that could be processed in 1 day. Repeat experiments with the same species were conducted using sediments from a different miniponar grab sample. Some of the toxicity tests with *Hyalella* were conducted with the addition of caged animals to determine the effect of direct contact with the sediment on toxicity. Cages consisted of a 250-mL polypropylene specimen container with the bottom cut out and replaced with a 200-μm-mesh nylon screen (Borgmann and Norwood 1999*b*). A 5 × 5 cm piece of cotton gauze was added to the cage to provide a substrate for the animals.

Due to delays incurred while the Imhoff settling cone method was being developed, some of the tests were not completed until a year after collection of the sediments. As a check, some toxicity tests with *Chironomus* and *Hyalella* were repeated in 1998 within 3 months of sediment collection. Although some minor differences were observed, the general pattern of toxicity was the same as observed in 1996. In addition, some of the original sediments collected in 1996 were retested after 2.5 years of storage at 4°C to check for long-term storage effects. This resulted in an increase in toxicity of some sediments which were moderately toxic when initially tested (KAKD). Prolonged storage resulted in an increased concentration of Ni in overlying water during toxicity testing, but this effect was only clearly pronounced after several years of storage. Storage of a variety of sediment types for up to 101 weeks at 4°C did not result in any systematic changes in toxicity to *Hyalella* or *Chironomus* (DeFoe and Ankley 1998).

Bioaccumulation

Hyalella were used for bioaccumulation measurements because these were one of the two species showing the greatest sensitivity to Sudbury area sediments, because *Hyalella* can be cultured in the laboratory, and because a database on critical body concentrations of metals already exists for this species. Amphipods were cultured in dechlorinated Burlington city tap water as described in Borgmann et al. (1989). Culture and experimental conditions were the same as those used for the toxicity tests. Bioaccumulation was measured using fresh sediments collected in 1998 because over a year had passed by the time all of the Sediment Quality Triad measurements had been completed with samples collected in 1996. Tests were set up within 6 weeks of sediment collection. To maintain overlying water quality, bioaccumulation experiments were also conducted in Imhoff settling cones with 15 mL of sediment and 1 L of overlying water. The overlying water in the test chambers was gently aerated and allowed to equilibrate for 10–14 days before test animals were added. Aeration is essential because *Hyalella* cannot tolerate anoxic conditions. This equilibration period results in the oxidation of a thin section (approximately 5 mm) of surface sediment and the potential release of some sulfide-bound metals to pore and overlying water. Oxygen concentrations in the overlying water were usually about 8 $mg \cdot L^{-1}$ and always above 7.5. The pH averaged 8.40 (SD 0.19, $n = 122$). Fifteen adult *Hyalella* (4–6 weeks old) were added to each test container and exposed for 1 week. This is sufficient time for *Hyalella* metal body concentrations to come to equilibrium; Ni turnover rates, for example, are about 0.5 per day in *Hyalella* (Borgmann et al. 2001). Two experiments were conducted. Each included one test container with sediment from each site plus two control sediments (Hamilton Harbour and Lake Erie) and an additional container without sediment but with cotton gauze as a substrate. This approaches the maximum number of experimental containers that could be processed in 1 day. The second experiment was conducted using sediments from a different miniponar grab sample from each site.

At the end of the incubation period, a sample of overlying water was filtered through a 0.4-µm polycarbonate membrane filter and preserved with nitric acid. The surviving amphipods were sorted from the sediment by sieving, rinsed in clean water, and placed in 120-mL plastic specimen containers with 50 µM EDTA and cotton gauze for 24 h to clear their guts. They were then dried at 60°C for 72 h. Groups of four dried amphipods (approximayely 0.5–3 mg total dry mass) were digested with 70% nitric acid at room temperature for 6 days, after which 30% hydrogen peroxide was added and digestion allowed to continue for another 24 h. Each sample was then made up to 6 mL with Milli-Q deionized water for analysis by inductively coupled plasma mass spectrometry (ICP-MS) or to 0.5–2 mL (depending on tissue mass) for analysis by graphite furnace atomic absorption spectrophotometry (GFAAS). Acid and peroxide volumes were 25 and 20 µL per 1 mL of total volume, respectively. Digested amphipods and overlying water were analyzed on a Varian SpectraAA 400 graphite furnace atomic absorption spectrophotometer with Zeeman background correction using a partition tube or by ICP-MS by the National Laboratory for Environmental Testing in Burlington, Ont. Metal concentrations in the sediments to which the amphipods were exposed were measured by ICAP-OES as described above under sediment chemistry.

Statistical methods

Statistical analysis was performed using Systat 7.0. All chemical data were log transformed before curve fitting by least squares. Comparisons of benthic invertebrate abundances by region was done using the Kruskal–Wallis test to determine if regional differences were significant and the Mann–Whitney *U* test for comparison of Sudbury area benthos with that of reference sites. The Mann–Whitney *U* test was also used for comparing toxicity in Sudbury area sediments with that in reference sediments, especially for *Hexagenia* and *Tubifex* survival because 100% survival in all reference sediments precluded calculation of variance. Growth in *Chironomus*, *Hexagenia*, and *Hyalella*, reproduction in *Tubifex*, and survival in *Chironomus* and *Hyalella* were also analyzed by analysis of variance. Dunnett's test was used to compare effects in Sudbury area, intermediate or control sediments to reference sediments. Data used for analysis of variance were first checked for normality and homogeneity of variances.

Results

Sediment chemistry

Surface sediments from lakes in the immediate Sudbury area (<13 km from Copper Cliff) had substantially higher metal concentrations, especially for Cu and Ni, than those from the reference or intermediate lakes (Table 1). Maximum metal concentrations were generally found in the top 5–10 cm of sediment. Metal concentrations in the deep sediments (below 15 cm) were substantially lower than in surface sediments in lakes near Sudbury (Fig. 1) and similar to both deep and surface sediments of the reference lakes. In contrast, metal concentrations in surface sediments (above 5 cm) were much higher in the Sudbury area than in the reference lakes. The strongest profiles (greatest range in metal concentrations with depth) were observed for Cu and Ni in lakes close to Sudbury, but higher concentrations of Cd, Co, Pb, and Zn were also observed in surface sediments.

The relative magnitude of metal enrichment in the surface sediments was estimated for each sediment core by dividing the mean metal concentration of the top three sections (0–3 cm depth) by the mean of the bottom three core sections (14–20 cm). This enrichment factor (EF) was then plotted against distance (*d*) from Copper Cliff and fitted to the equation

$$(1)\qquad \mathrm{EF} = \max \mathrm{e}^{(-kd)} + 1$$

where max is the maximum EF less 1 and k (per kilometre) is the rate at which EF approaches 1 as d increases. The maximum EF expected at 0 km from Copper Cliff was about 40 for Cd, Cu, and Ni and approximately 8 for Co (Fig. 2). The distance from Copper Cliff at which EF – 1 equals max/2 (i.e., ln(2)/k) was 12–15 km for Co, Cu, and Ni and 25 for Cd. The higher value for Cd could be partly due to the greater variability in the estimates of EF because Cd concentrations were much lower than those of the other metals and were, in fact, below the calculated detection limit of the analytical method (0.03 $\mu\mathrm{mol{\cdot}g^{-1}}$) in the deep sediments. It appears, therefore, that excess metal in the sediment, as judged by comparison with the deeper sediments, decreases by half with every 12- to 15-km increase in distance from Copper Cliff.

Benthic community structure

The number of benthic organisms collected at each site was relatively small. Consequently, statistical comparisons were made by region (lakes near Sudbury, reference lakes, and intermediate lakes) on the total number of animals collected in both years. Phantom midges (Chaoboridae), midges belonging to the tribe Chironomini (including *Chironomus* sp.), and oligochaetes were the most frequently observed organisms overall. Their abundance did not correlate with distance from Sudbury (Fig. 3). Quite marked, however, was the complete absence of fingernail clams (Pisidiidae, formerly Sphaeriidae) from any of the sites in the Sudbury area. Clams were collected at all but one of the sites in both the reference and the intermediate lakes. The only other statistically significant difference was the absence of Tanytarsini midges from all but one of the Sudbury lakes. Amphipods were also mostly absent from the Sudbury lakes. Only one individual was collected from Richard Lake, but the absence of amphipods from six of the reference and intermediate lakes makes statistical differences of abundance between the three regions not significant (Fig. 3).

Sediment toxicity

Growth in the mayfly *Hexagenia* and the amphipod *Hyalella* and survival in *Hyalella* were drastically reduced in sediments collected from the Sudbury area. Deepwater sediments from Ramsey, McFarlane, and Richard lakes (RAMD, MCFD, and RICD) were most toxic and resulted in weight loss rather than growth in *Hexagenia* and complete mortality in *Hyalella*. *Hexagenia* growth in Raft Lake sediments (RAF10 and RAFD) and 10-m-deep sediments from McFarlane Lake (MCF10) was less than twofold (final/initial weight), whereas growth in all reference and intermediate lake sediments exceeded a fourfold increase in body mass

Fig. 1. Sediment core profiles for four metals in McFarlane Lake. One concentration unit equals 0.002 µmol Cd·g^{-1} (+), 0.05 µmol Co·g^{-1} (✳), 0.4 µmol Cu·g^{-1} (▲), or 1 µmol Ni·g^{-1} (○).

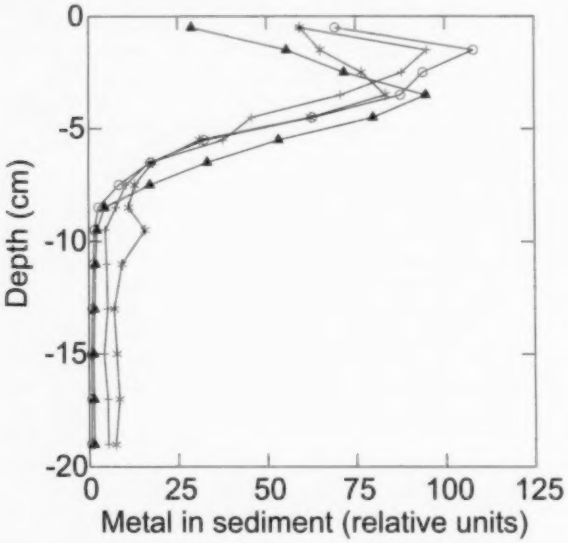

Fig. 2. Enrichment factor for Cd (+), Co (✳), Cu (▲), and Ni (○) in sediments as a function of distance from Copper Cliff. Lines represent least square regressions to an exponential drop towards unity at infinite distance.

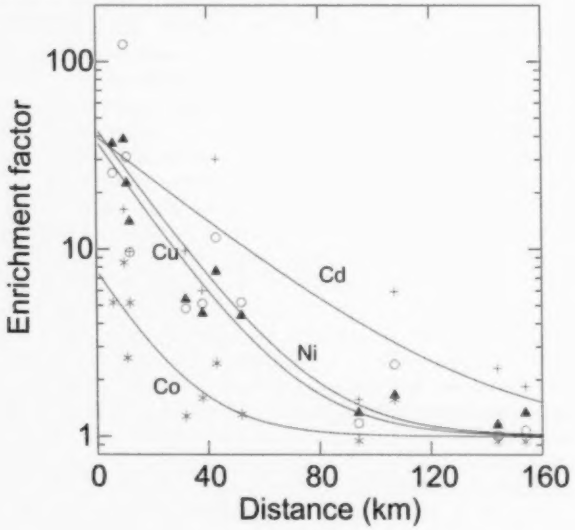

Fig. 3. Abundance (total number of animals collected per site) of pisidiid clams (●), amphipods (▲), tanytarsid midges (▼), chironomids of the tribe Chironomini (○), phantom midges (*Chaoborus*) (△), and oligochaetes (▽) as a function of distance from the smelters in Sudbury.

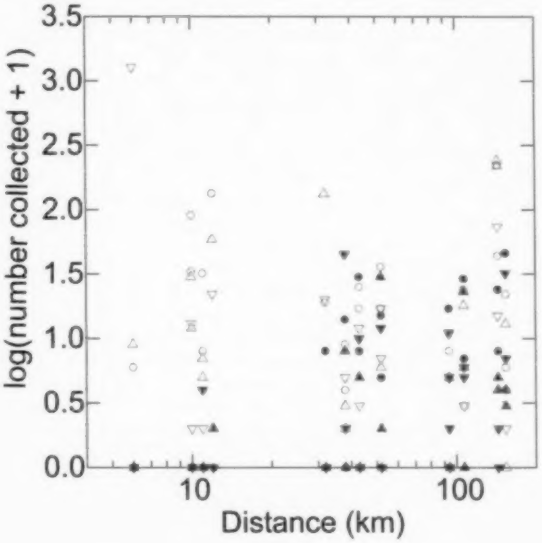

Fig. 4. Toxicity of sediments to four species of benthic invertebrates as a function of distance from the smelters in Sudbury. Response units equal percent survival for *Chironomus* (○) and *Hyalella* (▲), growth for *Hexagenia* ($W/W_0 \times 10$) (■), and reproduction for *Tubifex* (young produced per two adults) (▽). Data at 440 and 500 km represent Lake Erie and Hamilton Harbour control sediments, respectively.

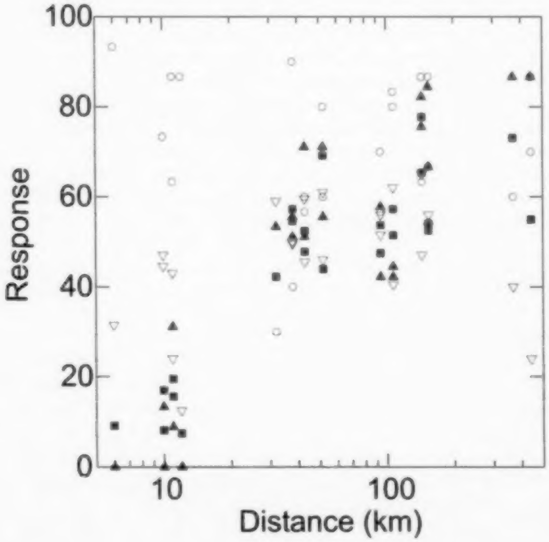

(Fig. 4). Survival of *Hyalella* never exceeded 31% in any Sudbury area sediments, whereas survival in reference and intermediate lake sediments ranged from 42 to 82% (Fig. 4). Sediments collected from lakes near Sudbury were, therefore, highly toxic to both *Hexagenia* and *Hyalella*.

In contrast with the above species, growth and survival of the midge *C. riparius* did not differ significantly between sediments collected from lakes near Sudbury, reference lakes, intermediate lakes, or control sediments from Hamilton Harbour and Lake Erie (Fig. 4). Growth and survival were, in fact, slightly higher in the Sudbury area sediments than in reference sediments. Tubificid worms produced fewer young in sediments from Sudbury area lakes, but survival was not affected. There were almost 40% fewer young *Tubifex* in sediments from the Sudbury area compared with reference or intermediate sediments. However, reproduction in Lake Erie and Hamilton Harbour sediments was also low and equal to that in Sudbury area sediments (Fig. 4). *Tubifex* was the only species for which reproduction or growth was poorer in control than in reference sediments. Using the fifth percentile of reproduction in Great Lakes reference sediments as an indicator of toxicity (35 young per four adults for fed animals; Day et al. 1995), only the sediments from Richard Lake would be declared toxic (13 young produced per two adults).

Metal bioaccumulation

The increased concentrations of metals in sediments from the Sudbury area lakes resulted in increased bioaccumulation for Cd, Co, and Ni in *Hyalella* exposed to those sediments in the laboratory. Bioaccumulation increased rapidly with increasing sediment concentrations, resulting in slopes ≥1 in log–log plots (Fig. 5). On average, amphipods exposed to Sudbury area sediments had body concentrations of Ni, Co, and Cd that were, respectively, 17-, 4.5-, and 3.7-fold greater than in amphipods exposed to sediments from reference lakes (Table 2). In contrast, As, Cr, Mn, Pb, Se, and Tl concentrations in *Hyalella* did not differ significantly among amphipods exposed to sediments from the Sudbury, reference, and intermediate locations, although Mn concentrations were extremely high in some amphipods (e.g., MCFD, Table 2). Copper and Zn in *Hyalella* also did not differ significantly, in spite of the much higher Cu concentrations in Sudbury area sediments (Table 1). However, Cu and Zn are regulated by *Hyalella* and body concentrations remain relatively constant until sediment concentrations are high enough to cause toxicity (Borgmann and Norwood 1997*a*). Copper concentrations in sediment-exposed *Hyalella* were consistently higher than in amphipods not exposed to sediments (gauze controls, Table 2), but there was no relationship between Cu in *Hyalella* and Cu in sediment (Fig. 5*c*). Increased bioaccumulation of metals in response to increased sediment concentrations was, therefore, observed for several (Cd, Co, and Ni), but not all, metals.

Critical body concentrations and the cause of sediment toxicity

The cause of sediment toxicity can be determined by comparing metal bioaccumulation with critical body concentrations previously shown to cause toxicity. The maximum amount of metal accumulated by *Hyalella* in the 1-week exposures exceeded the critical body concentrations resulting in 25% mortality in 4-week exposures (LBC25) for Ni but not for Cd, Co, Cu, Pb, Tl, or Zn (Table 2). LBC25s are not yet available for As, Cr, Mn, or Se, but the maximum body concentrations of these metals, except Mn, were always below 50 nmol·g^{-1}. This is well below any LBC25 determined so far (Table 2). Furthermore, As, Cr, Mn, and Se bioaccumulation were just as high in the nontoxic reference and intermediate area sediments as in the Sudbury area sediments. The only metal that can, therefore, clearly be identified as contributing to toxicity in chronic tests with *Hyalella* exposed to Sudbury area sediments is Ni.

One weakness in the above analysis is the difficulty in interpreting body concentrations of Cu. Copper and Zn are regulated by *Hyalella*, and increases in sediment concentrations do not necessarily result in significant increases in body concentrations until toxicity is relatively severe (e.g., mortality is observed in adults in 1-week exposures; Borgmann and Norwood 1997*a*, 1997*b*). Although Sudbury area sediments were extremely toxic to young *Hyalella* exposed for 4 weeks, mortality was negligible in the 1-week metal bioaccumulation experiments. Although Cu bioaccumulation provides no evidence that Cu contributed to toxicity (Table 2), it is not possible to state categorically that Cu did not contribute somewhat to total metal toxicity in the chronic studies.

Metals in overlying water: supplemental information on the cause of toxicity

Although metal concentrations in overlying water in toxicity tests are not as direct an indicator of metal bioavailability as are body concentrations, they can provide supplemental information and are particularly useful when investigating the potential contribution of Cu to toxicity because of the difficulty in interpreting body concentrations of this metal. To relate metal toxicity to concentration in the overlying water, it is first necessary to demonstrate that toxicity is due to dissolved metal and not metal in the solid phase. This was done in chronic exposure experiments in which some animals were exposed directly to sediment and others were exposed in cages above the sediment in the same containers. The caged animals were exposed to the same overlying water but did not have access to the sediments themselves. Survival in the cages, although slightly lower on average, correlated well with survival of amphipods exposed directly to the sediment (Fig. 6). In particular, there were no cases in which high mortality in the sediment was not also associated with high mortality in the cage. This demonstrates that toxicity was indeed due to a dissolved substance and that metal concentrations in the overlying water may, therefore, be useful in interpreting toxicity data.

The relative importance of Cu and Ni in contributing to toxicity can now be compared by examining overlying water concentrations. The 4-week LC25 for Cu in water is about 330 nmol·L^{-1} (Borgmann et al. 1998), and the LC25 for Ni in water is about 440 nmol·L^{-1} (Borgmann et al. 2001). Copper in overlying water in the chronic toxicity tests (1996 toxicity tests plus repeated tests in 1998 with cages) ranged from nondetectable to 535 nmol·L^{-1}, and Ni ranged from nondetectable to 16500 nmol·L^{-1}. Copper exceeded the LC25 in only four of 112 test containers. Nickel exceeded the LC25 in 34 containers, including the four containers with high Cu. Complete mortality was observed in 33 containers; Ni exceeded the LC25 in 29 of these and Cu in only four (Table 3). This leaves four other containers with unexplained mortality. The data indicate, therefore, that Ni was responsible for most of the toxicity observed, although Cu may also have contributed to toxicity in the four containers with high Cu in solution. All containers with >33% survival had Ni concentrations <440 nmol·L^{-1} and Cu concentrations <330 nmol·L^{-1}, with the exception of one container, which had 80% survival and a Ni concentration of 680 nmol·L^{-1}.

Fig. 5. Body concentrations of (*a*) Cd, (*b*) Co, (*c*) Cu, and (*d*) Ni in *H. azteca* after 1-week exposures to sediments as a function of sediment concentration. Solid circles represent data for Sudbury area lakes and open circles are from reference and intermediate lakes.

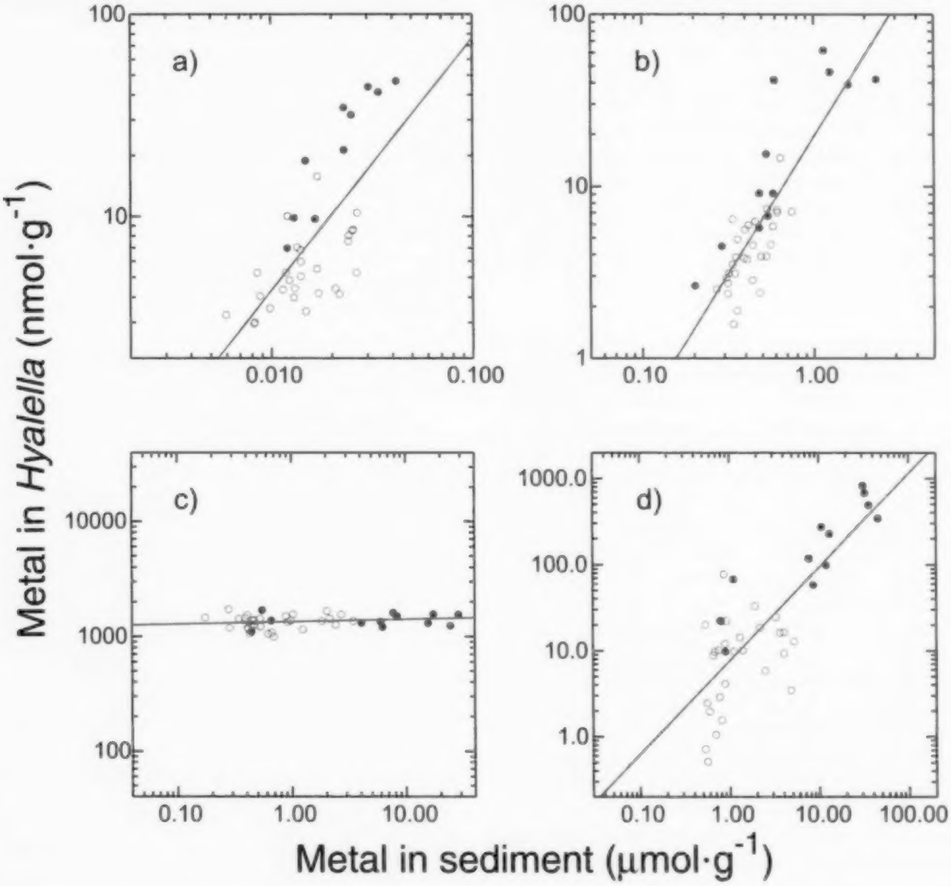

This was the only case of unexplained survival, possibly due either to an error in measured Ni or to the presence of an unknown factor that reduced Ni bioavailability. This suggests that toxicity in the chronic tests with *Hyalella* was primarily due to Ni, with the exception of occasional unexplained mortality that could not be attributed to either Ni or Cu.

Discussion

The Sediment Quality Triad, which forms the basis for most current state-of-the-art sediment assessments, is not necessarily sufficient to address all key questions regarding sediment impacts. In the present study, the Triad has been supplemented with measurements of metal bioaccumulation by *Hyalella* and metals in overlying water during toxicity tests. The ability of our data to address the four key AETE questions is summarized below.

Are contaminants getting in the system?

The sediment chemistry data clearly show that metals have been deposited in lakes near Sudbury. Sediment metal concentrations decrease rapidly with distance from Sudbury. Furthermore, sediment core profiles indicate that only the top sediment layers are heavily contaminated with metals, and enrichment factors decrease with distance from Sudbury, implying that contamination occurred following industrialization and is not from natural sources. Similar levels of metal contamination in lake sediments in the Sudbury area have been demonstrated previously (Semkin and Kramer 1976; Jeffries 1984), including enrichment of recent sediments in core profiles (Nriagu et al. 1982; Nriagu and Rao 1987; Belzile and Morris 1995).

Are contaminants bioavailable?

This question cannot be answered directly using only the Sediment Quality Triad. This is one of the weaknesses of the Sediment Quality Triad approach. It can be argued that if metals are responsible for observed effects, then they must be bioavailable (Chapman 1990). This question is therefore addressed indirectly if the final question can be answered in the affirmative. However, no direct estimates of metal bioavailability are included in Sediment Quality Triad assessments.

In the present study, bioaccumulation of metals by *Hyalella* clearly showed that the bioavailability of Cd, Co, and Ni was elevated in sediments from Sudbury area lakes. Increased metals in overlying water in the toxicity tests, coupled with

Table 2. Mean metal concentrations (nmol·g^{-1}) in adult *Hyalella* exposed for 1 week to sediments collected by miniponar grab from each sampling site in 1998[a] or exposed to cotton gauze without sediment and LBC25s in chronic (4-week) toxicity tests.

Site[b]	As	Cd	Co	Cr	Cu	Mn	Ni	Pb	Se	Tl	Zn
Sudbury area lakes											
RAMD	7	28	24	25	1390	670	306	2.1	18	0.6	850
MCF10	20	14	7	24	1350	300	63	0.4	26	0.5	1330
MCFD	14	24	42	26	1300	29 600	309	0.5	29	0.3	1090
RAF10	17	6	4	24	1400	150	16	0.3	29	0.4	920
RAFD	13	28	11	26	1560	270	164	1.2	30	0.7	910
RICD	5	43	54	28	1440	410	757	1.8	28	1.2	890
Intermediate lakes											
NEPD	11	4	4	24	1500	480	18	0.6	31	0.5	890
KAK10	13	6	4	23	1260	620	15	0.6	23	0.5	960
KAKD	13	6	6	25	1360	1 250	18	0.4	28	0.5	900
TRO10	13	8	4	27	1470	410	6	0.8	27	1.3	940
TROD	6	7	7	25	1540	460	9	0.9	28	0.5	950
LOS10	9	4	7	26	1270	2 880	12	1.0	18	1.3	930
LOSD	10	5	10	27	1400	1 300	11	2.2	20	0.5	930
Reference lakes											
TOM10	11	13	3	31	1330	730	11	1.3	22	3.0	1050
TOMD	12	5	5	24	1290	360	5	1.2	33	0.7	890
RES10	3	6	6	22	1330	3 420	6	0.3	31	1.8	930
RESD	10	5	3	25	1240	500	6	0.6	31	0.5	1260
NOS10	11	4	3	23	1300	470	17	0.3	28	0.5	890
NOSD	12	4	3	24	1340	500	7	0.4	28	0.3	940
TAL10	14	6	3	25	1230	550	5	0.7	21	0.8	1080
TALD	16	4	3	22	1220	1 450	41	0.6	23	0.4	890
Controls											
HH1	12	10	3	26	1940	490	14	1.7	45	2.0	1140
LE303	7	8	5	23	1400	270	25	0.3	26	0.9	940
Gauze	11	6	6	23	900	110	10	0.6	26	0.1	890
Enrichment ratio (geometric mean, Sudbury sites/reference sites)											
	1.15	3.7***	4.5***	1.05	1.09	0.93	17***	1.4	0.99	0.77	1.00
Maximum body concentration (gauze corrected)											
	20	43	54	31	1940 (1040)	29 600	**757**	2	45	3	1330 (440)
LBC25 (gauze corrected)											
	—	270[c]	>100[d]	—	2380[e] (1050)	—	**194**[f]	126[g]	—	290[c]	4420[e] (3080)

Note: ***Significant at $P < 0.001$. Dashes indicate no available data.

[a] Mean of two experiments with separate sediment grab samples used in each experiment.

[b] Lake names associated with these codes are Ramsey (RAM), McFarlane (MCF), Raft (RAF), Richard (RIC), Nepewassi (NEP), Kakakiwaganda (KAK), Trout (TRO), Lower Sturgeon (LOS), Tomiko (TOM), Restoule (RES), Nosbonsing (NOS), and Talon (TAL).

[c] Borgmann et al. (1998).

[d] W.P. Norwood and U. Borgmann (unpublished data).

[e] Borgmann and Norwood (1997*a*); spiked sediment exposure.

[f] Borgmann et al. (2001).

[g] Borgmann and Norwood (1999*b*).

the demonstration that toxicity was due to contaminant(s) in the dissolved phase, also suggested possible increased metal bioavailability.

Metal bioaccumulation can be measured either following laboratory exposures or in field-collected animals. Concentrations of Cd, Cu, and Ni in abdominal muscles of crayfish collected from Ramsey Lake (27, 1600, and 450 nmol·g^{-1}, respectively; Bagatto and Alikhan 1987) were similar to those in *Hyalella* exposed to sediments from the same lake (28, 1390, and 306 nmol·g^{-1}, Table 2). The same metals in crayfish muscle from a reference lake (16, 790, and 17 nmol·g^{-1}, respectively) were also within a factor of 2 or 3 of those in *Hyalella* exposed to sediments from our reference lakes. Laboratory bioaccumulation measurements with *Hyalella* seem, therefore, to reflect in situ bioavailability of metals to at least some species. The laboratory bioaccumulation measurements are more useful for identifying cause, however, because the critical body concentrations have been established for the population of *Hyalella* used in these measurements.

The question regarding metal bioavailability is therefore answered affirmatively, but only by supplementing the Triad with bioaccumulation measurements.

Is there a measurable response?

This question is addressed through a combination of in situ community assessment and laboratory toxicity tests. Analysis of benthic community composition can demonstrate whether populations in contaminated areas differ from those in reference locations, but this difference is not neces-

Fig. 6. Survival of *Hyalella* after 4 weeks of exposure to overlying water in cages compared with survival of amphipods exposed directly to the sediment. Numbers beside a data point indicate multiple values. Note there are 11 data points superimposed on the origin.

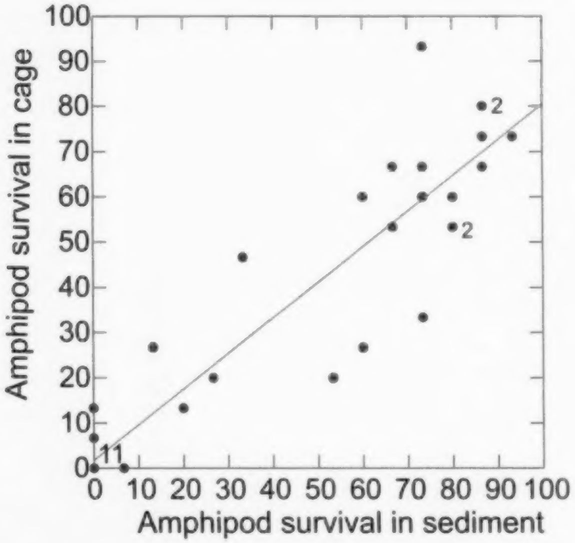

Table 3. Summary of survival results in all chronic (4-week) toxicity tests conducted with *Hyalella* and the number of times Cu and Ni exceeded the LC25.

	Frequency of occurrence		
Survival (%)	Total	Cu > 330 nmol·L^{-1}	Ni > 440 nmol·L^{-1}
0	33	4[a]	29
7–27	14	0	4[b]
>33	65	0	1[c]
0–100	112	4	34

[a] Cu = 331–535 nmol·L^{-1}; Ni = 820 – 16 500 nmol·L^{-1}.
[b] Ni = 800–2300 nmol·L^{-1}.
[c] Ni = 680 nmol·L^{-1}.

sarily due to toxic chemicals. Toxicity testing can demonstrate whether sediments are toxic, but laboratory conditions are rarely identical to exposure conditions in the field. For example, toxicity testing with metal-sensitive invertebrates requires aeration of the test containers to prevent death from anoxia. Test sediments may come from anoxic environments, but even if they do not, sediment mixing during collection and test initiation often results in exposure of underlying anoxic sediments to oxygenated overlying water. This can alter sediment toxicity by, for example, solubilizing metals bound to insoluble metal sulfides upon oxidation of sulfide to sulfate. It is therefore difficult to prove environmental impairment by toxic chemicals from either in situ benthic community composition or sediment toxicity alone. Taken together, however, changes in benthic composition coupled with a demonstration of sediment toxicity are a strong indication of a measurable response due to poor sediment quality.

Good concordance was observed between the benthic survey and sediment toxicity, demonstrating severe effects to some organisms and nondetectable effects in other species. There were no observed differences in abundance of chironomids belonging to the Chironomini between the three study regions, and no sediment toxicity was detected using *Chironomus*. Severe sediment toxicity was, however, detected using *Hyalella*, and this coincided with an absence of amphipods in Sudbury area sediments with the exception of one amphipod caught in Richard Lake. Unfortunately, mayflies were absent from most sites, but the abundance of pisidiid clams and tanytarsid midges matched the toxicity of sediments to *Hyalella* and *Hexagenia*. Although a difference in reproduction among sediments was detected in *Tubifex*, reproductive inhibition was only partial, and this coincided with the lack of a clear difference in oligochaete abundance between regions. Consequently, both abundance in the field and sediment toxicity demonstrated effects to some, but not all, species, and field abundance matched sediment toxicity whenever the same, or closely related, species were examined in the field and laboratory studies. Taken together, in situ invertebrate abundances and toxicity tests indicate that there are biological impacts in the deep sediments (≥10 m) of lakes in the Sudbury area, and these are probably the result of sediment toxicity.

Are the contaminants causing this response?

This question, along with the second question, is not addressed directly by Sediment Quality Triad data, but inferences about cause can sometimes be made if biological effects correlate with chemical measurements (Chapman 1990; Chapman et al. 1997). In the Sudbury area, biological effects associated with sediment toxicity were observed, and sediments were clearly contaminated with several metals. However, the concentrations of all the metals are closely correlated with each other. It is therefore not possible to determine which of the metals is responsible for the observed effects based on the Triad data alone, or even if toxicity is due to any one of the measured metals. Toxicity could be due to some other contaminant, the concentration of which correlates with that of the metals measured here. It was, however, possible to answer the final AETE question affirmatively in the present study by comparing metal bioaccumulation with LBC25s. This demonstrated that Ni was the primary cause of sediment toxicity. It also demonstrates the value of adding bioaccumulation measurements to the ususal Sediment Quality Triad when conducting sediment assessments for metals. Chapman (2000) has already suggested that bioaccumulation can be considered part of the Triad provided that the context for its use and for the evaluation of tissue residue data is clear. Comparison of bioaccumulation with LBC25s provides such a context.

Comparison of bioaccumulation and overlying water concentrations as tools for cause identification

Metal bioaccumulation is the most direct and reliable method of estimating bioavailable metal for nonregulated metals, and comparison with critical body concentrations provides a means of identifying the cause of toxicity. Changes in water chemistry (pH, major ions, and organic matter) can affect both metal accumulation and toxicity, but the body concentrations at which effects are observed in *Hyalella* tend to remain relatively constant (Borgmann et al.

1991, 1998, 2001). This makes body concentration a more reliable indicator of effects than water concentration. This approach will only work, however, if the metal concentration in the body is related to metal bioavailability in the medium. Regulation of internal concentrations of the essential metals Cu and Zn results in little variation in body concentration until metal bioavailability approaches toxic levels for *Hyalella*. This makes it difficult to infer low-level chronic effects from Cu and Zn measured in *Hyalella*, but it is possible to identify these metals as the cause of severe mortality (e.g., mortality of adults within 1 week) in sediments (Borgmann and Norwood 1997*b*). Furthermore, the relatively rapid equilibrium between metals in *Hyalella* and water allows accumulation to be measured in adult animals in exposures of only a 1-week duration. Since 1-week exposures with adults result in much lower mortality than chronic exposures with young amphipods, bioavailability can often be quantified in 1-week exposures even if chronic exposures result in complete mortality (e.g., this study). Body concentrations are, therefore, the preferred method of identifying cause, where possible.

In cases where low-level chronic effects of Cu are suspected, or if body concentrations cannot be measured because all of the animals have died and 1-week repeat experiments with adults are not possible, overlying water concentrations in toxicity tests can provide an alternative method of quantifying metal bioavailability and identifying cause. For Cd (Warren et al. 1998), Cu (Deaver and Rodgers 1996), Pb (Borgmann and Norwood 1999*b*), and Ni (Borgmann et al. 2001), metal toxicity in sediments to *Hyalella* appears to be due to dissolved metal and not the solid phase. It is essential, however, that overlying water quality is not affected substantially by the sediment. Otherwise, changes in ionic composition, pH, or dissolved organic matter can alter the toxicity of dissolved metal. One way of reducing the impact of sediments on overlying water chemistry is to use a large water to sediment ratio, as in the present experiments with Imhoff settling cones (15 mL of sediment plus 1 L of overlying water). Dissolved metals in overlying water are much better predictors of bioavailable metal in experiments with Imhoff cones than in more typical experiments with beakers and lower water to sediment ratios (Borgmann and Norwood 1999*a*; Borgmann et al. 2001).

In conclusion, a full assessment of the biological impact of metals in sediments cannot be completed using only sediment chemistry, in situ benthic community composition, and sediment toxicity testing because metal bioavailability cannot be quantified accurately and the cause of toxicity cannot be identified with certainty. Measurement of metal bioaccumulation, supplemented with measurement of metals in overlying water in toxicity tests, can help resolve these problems. The Sediment Quality Triad approach should, therefore, be augmented with such bioavailability measurements. Adding bioaccumulation and overlying water measurements to the Triad has demonstrated that the major metal of concern in sediments from Sudbury area lakes appears to be Ni.

Acknowledgments

The field work was done by M. Mawhinney, M. Dahl, and M. Benner of the Technical Operations Section and C. Logan and W. Norwood. Total metal concentrations in sediment and water were measured by J. Rajkumar. ICP-MS analysis for metals in overlying water and *Hyalella* was done by the National Laboratory for Environmental Testing. Identification and enumeration of benthos were done by C. Logan, S. Hughson, and R. Gould. D. Milani assisted with the sediment toxicity tests.

References

Bagatto, G., and Alikhan, M.A. 1987. Copper, cadmium, and nickel accumulation in crayfish populations near copper–nickel smelters at Sudbury, Ontario, Canada. Bull. Environ. Contam. Toxicol. **38**: 540–545.

Belzile, N., and Morris, J.R. 1995. Lake sediments: sources or sinks of industrially mobilized elements? *In* Restoration and recovery of an industrial region. *Edited by* J.M. Gunn. Springer-Verlag, New York. pp. 183–204.

Borgmann, U., and Norwood, W.P. 1997*a*. Toxicity and accumulation of zinc and copper in *Hyalella azteca* exposed to metal-spiked sediments. Can. J. Fish. Aquat. Sci. **54**: 1046–1054.

Borgmann, U., and Norwood, W.P. 1997*b*. Identification of the toxic agent in metal-contaminated sediments from Manitouwadge Lake, Ontario, using toxicity–accumulation relationships in *Hyalella azteca*. Can. J. Fish. Aquat. Sci. **54**: 1055–1063.

Borgmann, U., and Norwood, W.P. 1999*a*. Sediment toxicity testing using large water–sediment ratios: an alternative to water renewal. Environ. Pollut. **106**: 333–339.

Borgmann, U., and Norwood, W.P. 1999*b*. Assessing the toxicity of lead in sediments to *Hyalella azteca*: the significance of bioaccumulation and dissolved metal. Can. J. Fish. Aquat. Sci. **56**: 1494–1503.

Borgmann, U., Ralph, K.M., and Norwood, W.P. 1989. Toxicity test procedures for *Hyalella azteca*, and chronic toxicity of cadmium and pentachlorophenol to *H. azteca*, *Gammarus fasciatus*, and *Daphnia magna*. Arch. Environ. Contam. Toxicol. **18**: 756–764.

Borgmann, U., Norwood, W.P., and Babirad, I.M. 1991. Relationship between chronic toxicity and bioaccumulation of cadmium in *Hyalella azteca*. Can. J. Fish. Aquat. Sci. **48**: 1055–1060.

Borgmann, U., Cheam, V., Norwood, W.P., and Lechner, J. 1998. Toxicity and bioaccumulation of thallium in *Hyalella azteca*, with comparison to other metals and prediction of environmental impact. Environ. Pollut. **99**: 105–114.

Borgmann, U., Néron, R., and Norwood, W.P. 2001. Quantification of bioavailable nickel in sediments and toxic thresholds to *Hyalella azteca*. Environ. Pollut. **111**: 189–198.

Chapman, P.M. 1990. The sediment quality triad approach to determining pollution-induced degradation. Sci. Total Environ. **97/98**: 815–825.

Chapman, P.M. 1996. Presentation and interpretation of Sediment Quality Triad data. Ecotoxicology, **5**: 327–339.

Chapman, P.M. 2000. The Sediment Quality Triad: then, now and tomorrow. Int. J. Environ. Pollut. **13**: 351–356.

Chapman, P.M., Anderson, B., Carr, S., Engles, V., Green, R., Hameedi, J., Harmon, M., Haverland, P., Hyland, J., Ingersoll, C., Long, E., Rodgers, J., Jr., Salazar, M., Sibley, P.K., Smith, P.J., Swartz, R.C., Thompson, B., and Windom, H. 1997. General guidelines for using the Sediment Quality Triad. Mar. Pollut. Bull. **34**: 368–372.

Dalton, J.A. 1994. Introduction and troubleshooting manual for the LECO CR-12 carbon analyzer. NWRI Tech. Note No. AER-TN-94-14.

Day, K.E., Dutka, B.J., Kwan, K.K., Batista, N., Reynoldson, T.B., and Metcalfe-Smith, J.L. 1995. Correlations between solid-phase microbial screening assays, whole-sediment toxicity tests with macroinvertebrates and *in situ* benthic community structure. J. Gt. Lakes Res. **21**: 192–206.

Deaver, E., and Rodgers, J.H., Jr. 1996. Measuring bioavailable copper using anodic stripping voltammetry. Environ. Toxicol. Chem. **15**: 1925–1996.

DeFoe, D.L., and Ankley, G.T. 1998. Influence of storage time on toxicity of freshwater sediments to benthic macroinvertebrates. Environ. Pollut. **99**: 123–131

Duncan, G.A., and LaHaie, G.G. 1979. Size analysis procedures used in the Sedimentology Laboratory, NWRI, CCIW, Hydraulics Division. Manual, September 1979. Available from the Library, National Water Research Institute, Burlington, Ont.

Environment Canada. 1994. Manual of analytical methods. Vol. 2. Trace metals. National Laboratory for Environmental Testing, Burlington, Ont.

ESG International Inc. 1999. Aquatic Effects Technology Evaluation (AETE) program synthesis report of selected technologies for cost-effective environmental monitoring of mine effluent impacts in Canada. Report prepared for the AETE program, CANMET, Natural Resources Canada, Ottawa, Ont.

Hydrolab Corp. 1991. Operating manual, DataSonde® 3, Multi-parameter Datalogger. Hydrolab Corp., Austin, Tex.

Jeffries, D.S. 1984. Atmospheric deposition of pollutants in the Sudbury area. *In* Environmental impacts of smelters. *Edited by* J.O. Nriagu. John Wiley & Sons, New York. pp. 117–154.

Keller, W. 1992. Introduction and overview to aquatic acidification studies in the Sudbury, Ontario, Canada, area. Can. J. Fish. Aquat. Sci. **49**(Suppl. 1): 3–7.

Mudroch, A., and MacKnight, S.D. 1991. CRC handbook of techniques for aquatic sediments sampling. CRC Press, Boca Raton, Fla.

Nriagu, J.O., and Rao, S.S. 1987. Responses of lake sediments to changes in trace metal emissions from the smelters at Sudbury, Ontario. Environ. Pollut. **44**: 211–218.

Nriagu, J.O., Wong, H.K., and Coker, R.D. 1982. Deposition and chemistry of pollutant metals in lakes around the smelters at Sudbury, Ontario. Environ. Sci. Technol. **16**: 551–560.

Semkin, R.G., and Kramer, J.R. 1976. Sediment geochemistry of Sudbury-area lakes. Can. Mineral. **14**: 73–90.

Warren, L.A., Tessier, A., and Hare, L. 1998. Modelling cadmium accumulation by benthic invertebrates in situ: the relative contributions of sediment and overlying water reservoirs to organism cadmium concentrations. Limnol. Oceanogr. **43**: 1442–1454.

Winterhalder, K. 1995. Early history of human activities in the Sudbury area and ecological damage to the landscape. *In* Restoration and recovery of an industrial region. *Edited by* J.M. Gunn. Springer-Verlag, New York. pp. 17–31.

Yan, N.D., Welsh, P.G., Lin, H., Taylor, D.J., and Filion, J.-M. 1996. Demographic and genetic evidence of the long-term recovery of *Daphnia galeata mendotae* (Crustacea: Daphniidae) in Sudbury lakes following additions of base: the role of metal toxicity. Can. J. Fish. Aquat. Sci. **53**: 1328–1344.

Stability of physiological and behavioural determinants of performance in Arctic char (*Salvelinus alpinus*)

C.J. Cutts, C.E. Adams, and A. Campbell

Abstract: The physiological and behavioural mechanisms that confer behavioural dominance are poorly understood. Although recent studies have shown a link between metabolism and dominance, these studies relied on single measurements of both, and assumed that inter-individual variation of physiology and behaviour were repeatable over time. This paper demonstrates that standard metabolic rate is a repeatable trait in Arctic char (*Salvelinus alpinus* L.) and that relative differences between individuals are consistent across a range of environmental conditions. Furthermore, there were positive associations between metabolic rate, aggression, and competitive ability that were also repeatable over time. However, there was no relationship between competitive ability (measured as feeding attempts) and subsequent growth. This may be due to an energetic cost of dominance: high rates of food capture were only attainable through high rates of effort. This, in addition to elevated aggression, was thought to exert an energetic cost that could not be fully offset by the increased food intake.

Résumé : Les mécanismes physiologiques et comportementaux qui procurent la dominance dans les comportements restent mal connus. Bien que des études récentes aient établi un lien entre le métabolisme et la dominance, ces études se basent sur des mesures individuelles des deux facteurs et elles supposent que la variation de la physiologie et du comportement entre les individus se maintient dans le temps. On trouvera ici une démonstration que le taux de métabolisme standard chez l'Omble chevalier (*Salvelinus alpinus* L.) est une caractéristique stable et que les différences relatives entre les individus se maintiennent sur une gamme étendue de conditions du milieu. De plus, il existe des associations positives entre le taux du métabolisme, l'agression et la compétitivité qui se maintiennent dans le temps. Cependant, il n'y a pas de relation entre la compétitivité (telle que mesurée en nombre de tentatives d'alimentation) et la croissance subséquente. Cela peut sans doute s'expliquer par le coût énergétique relié à la dominance: en effet, de forts taux de capture de nourriture ne s'atteignent que par des taux élevés d'effort. S'ajoutant à une agression plus grande, cela entraîne un coût énergétique important qui ne peut être entièrement compensé par l'ingestion accrue de nourriture.

[Traduit par la Rédaction]

Introduction

The physiological and behavioural mechanisms through which certain individuals are able to outcompete conspecifics are poorly understood. Recent studies have shown a link between metabolism and dominance in Atlantic salmon (*Salmo salar* L.): individuals with higher than expected standard metabolic rates (SMRs; controlling for body size) are more aggressive and are dominant over their conspecifics (Metcalfe et al. 1995; Cutts et al. 1998, 1999). SMR is the minimal maintenance or resting metabolic rate of unfed fish below which physiological function is impaired (Brett and Groves 1979; Priede 1985). It is more likely that differences in dominance are a consequence of differences in metabolic rate rather than a cause, since, in studies reported by Metcalfe et al. (1995) and Cutts et al. (1999), metabolic rate measurements were taken at first feeding, prior to the development of aggressive behaviour (Dill 1977). SMR was the first physiological determinant of competitive ability to be demonstrated in fish; previous studies relied on a single measure of metabolic rate before examining behaviour, and conclusions were derived from the tacit assumption that inter-individual variation in this physiological trait and its effect on behaviour were repeatable over time in salmonids. This assumption has never been tested in salmonids (or fish) but is particularly important, since extrapolating long-term behavioural fitness from a single measurement of physiological performance may not be possible if there is a deterministic relationship between physiology and competitive performance, and physiological performance changes with time. With the recent studies of causal links between physiological and behavioural performance and the lack of any data on how these traits co-vary with time, the present study provides a timely analysis of how physiology influences behaviour and whether the relationship persists over a period of several months.

Therefore, the aims of this study were (*i*) to investigate the relationship between SMR, competitive ability (food

Received July 14, 2000. Accepted February 15, 2001. Published on the NRC Research Press Web site on April 19, 2001.
J15872

C.J. Cutts,[1,2] C.E. Adams, and A. Campbell. Fish Biology Group, University Field Station, Institute of Biomedical and Life Sciences, University of Glasgow, Rowardennan, Glasgow G63 0AW, U.K.

[1] Corresponding author (e-mail: c_cutts@seafish.co.uk).

[2] Present address: Seafish Marine Farming Unit, Ardtoe, Acharacle, Argyll PH36 4LD, U.K.

DOI: 10.1139/cjfas-58-5-961

acquisition and aggression), and subsequent success (i.e., growth) in Arctic char (*Salvelinus alpinus*); (*ii*) to test the hypothesis that SMR, aggression, and growth are stable traits in Arctic char; and (*iii*) to assess whether it is reasonable to predict long-term fitness from a single set of physiological measurements.

Materials and methods

Experimental animals

The Arctic char used in this study were the offspring of four female and two male pelagic Arctic char collected by gill net at Loch Luichart, Rosshire, Scotland. Eggs were incubated in the laboratory, and reared fry were held in tangential-flow holding tanks (at the University Field Station, Loch Lomond) at ambient light and temperature (56°N) and fed ad libitum. At age 8 months, Arctic char were allocated to four replicate groups of 10 fish each, given an individual Alcian blue tattoo mark on the fins, and moved from holding tanks and placed in four replicate 0.5 m diameter tangential flow tanks, in which individual respiration rate, aggression rate, and growth were determined over the following 6 months.

Respirometry

SMRs at ambient temperature (see Table 1), which was held constant for the duration of each measurement of each group, were measured four times in total: during September 1997 (at age 8 months), November 1997, February 1998, and March 1998. Oxygen consumption rates of Arctic char were measured by placing individual fish in Perspex respirometry chambers through which water continually flowed at a known rate. Water temperature was noted, to estimate the capacitance of oxygen in the water ($\beta W\mathrm{O}_2$; mL $\mathrm{O_2 \cdot L^{-1}}$) during a series of oxygen-consumption measurements, and was kept constant throughout each trial. The water was kept fully saturated with oxygen by aeration in the header tank and flowed by gravity from the header tank through the respirometry chambers.

A rack of 10 such chambers allowed the oxygen consumption rates of 10 Arctic char to be measured on the same day. Fish were placed in the respirometry chambers overnight; measurements commenced 24 h later, by which time they had settled and evacuated their guts (Higgins and Talbot 1985) and any oxygen debt due to differences in activity before and after being placed in the chambers would have been paid off. Pilot experiments on juvenile salmon indicated that oxygen consumption was stable after this period of acclimation (Cutts 1997). In addition, to minimise activity, the fish were kept in semidarkness and the low flow rates (1.6 $\mathrm{L \cdot h^{-1}}$ for the first trial to 3.7 $\mathrm{L \cdot h^{-1}}$ during the last trial) through the chambers precluded any active swimming against a current. Oxygen consumption ($\dot{V}\mathrm{O}_2$; mL $\mathrm{O_2 \cdot h^{-1}}$) was measured by first injecting 5 mL of 100% oxygen saturated water from the header tank (representative of the water flowing into each chamber) into an oxygen electrode and then injecting a 5-mL sample of water from the respirometry chamber outflow and noting the percentage reduction in oxygen saturation from 100%. The percentage reduction in oxygen concentration was converted to oxygen consumption ($\dot{V}\mathrm{O}_2$) using the equation:

$$(1) \qquad \dot{V}\mathrm{O}_2 = V_\mathrm{W} \cdot \Delta C_\mathrm{W}\mathrm{O}_2$$

where V_W is the flow rate ($\mathrm{L \cdot h^{-1}}$; measured by collecting the water outflow from each tube in a beaker over a measured period of time (a minimum of 2 min) and weighing it) of water through the respirometry chamber and $\Delta C_\mathrm{W}\mathrm{O}_2$ is the difference in oxygen concentration between the inflow and outflow water ((0.01 × percent reduction)$\cdot\beta W\mathrm{O}_2$ mL $\mathrm{O_2 \cdot L^{-1}}$, where $\beta W\mathrm{O}_2$ is the capacitance of oxygen in the water; Steffensen 1989).

During each sampling period, this procedure was repeated three times for each fish (with a minimum interval of 30 min between measurements); a fourth reading was taken if the initial three values did not agree closely (i.e., if the values were not within 10% of the mean value). This provided a mean oxygen consumption value for each fish for each of the four separate sampling periods. The mean values from each sampling period were used to generate a regression equation specific for each sampling period. The entire procedure was identical for each Arctic char, resulting in comparable measures of SMR for individuals. For a fuller account of the respirometry methodology, see Cutts et al. (1998). After measuring metabolic rate, each fish was measured (fork length; mm) and weighed (g), to calculate specific growth rate ($\% \cdot \mathrm{day^{-1}}$).

To determine whether fish had relatively high or low respiration rates for their size, the double ln-transformed regression of oxygen consumption (mL $\mathrm{O_2 \cdot h^{-1}}$) on weight (g) (specific for each sampling period) was used to calculate the expected metabolic rate of a fish of a particular weight. This was then compared with its observed metabolic rate (the mean oxygen consumption of each fish during each sampling period). Weight and oxygen-consumption data were both ln-transformed, since double-log plots are more appropriate when using a large range of animal sizes (Yamamoto 1991). Absolute rather than weight-specific values were used, since weight-specific values usually decrease with increasing body size, that is, larger fish respire less on a per gram basis than smaller fish. The confounding effects of body weight were removed by regressing the oxygen-consumption data on body weight and then testing for relationships among the residuals. The importance of residual variation has recently received great attention (Hayes and Shonkwiler 1996). The difference between the observed and expected SMR of a fish was therefore termed the residual SMR (rSMR; mL $\mathrm{O_2 \cdot h^{-1}}$); a positive value indicated that a fish had a higher than expected oxygen consumption rate for its size, while a negative value indicated a relatively low consumption rate (Metcalfe et al. 1995; Cutts et al. 1998, 1999). Residuals were recalculated for each experimental fish from the regression equations specific for each sampling period. Each equation was derived from the measurements of a minimum of 36 Arctic char during any one sampling period, providing a wide size range with which to calculate an accurate regression equation of body weight against SMR.

Behavioural observations

Immediately following measurement of SMR, every fish from each group was placed in an individual isolation chambers for 2 weeks and hand-fed ad libitum. Each isolation chamber consisted of a wedge-shaped section of a 1.5 m diameter holding tank (the tank was sectioned into 35 such chambers), and each chamber had its own water inlet draining away to a central drain. These conditions resulted in a prolonged period without exposure to a competitive environment and, together with the introduction to the novel experimental tanks, reduced the effect of previous experience of social interactions in the holding tank (Gómez-Laplaza and Morgan 1993). After the isolation period, each group of 10 fish were placed in identical circular (diameter 0.5 m) tangential flow tanks and hand-fed from a point source, six times a day, to promote a competitive hierarchy.

Each tank was filmed directly from above with a video camera for 2 h on four occasions between October 1997 and March 1998 on the third day following re-introduction to the holding tank. Each tank was screened off during filming, to exclude any external stimuli, and was lit from below, to highlight fin marks. Once every 5 min during filming, individual bloodworms were introduced into the tank at a point source, providing 24 food items per 2-h film. Thus, at the end of the experiment, there was 32 h of video footage in total.

Each video was subsequently analysed to determine individual fish aggression and food-acquisition rate; if the intensity of aggressive interactions exceeded 100 interactions over the 2-h period, only

Table 1. Results of standard metabolic rate (SMR) measurements of juvenile Arctic char (*Salvelinus alpinus*) from September 1997 to March 1998.

Date	T (°C)	n	Regression equation ($y = \ln(\mathrm{SMR})(\mathrm{mL\ O_2 \cdot h^{-1}})$, $x = \ln(\mathrm{weight})$ (g))	df	F	r^2	P
September 1997	13.0	139	$y = 0.296 + 0.294x$	1,138	17.97	0.109	<0.0001
November 1997	9.0	58	$y = -0.831 + 0.560x$	1,57	7.67	0.105	<0.01
February 1998	5.0	36	$y = -2.270 + 0.938x$	1,35	22.31	0.378	<0.0001
March 1998	6.5	40	$y = -0.332 + 0.474x$	1,39	6.01	0.114	<0.02

100 aggressive interactions were noted, from segments at the beginning, middle, and end of each 2-h sample. If there were fewer than 100 aggressive interactions, the whole 2-h video was sampled. For each aggressive interaction, the fish initiating and receiving aggression was noted. The aggressive act was normally very polarised, involving only a pair of fish (the aggressor and the attacked fish). In a similar way, every observable feeding attempt was noted: which fish acquired the bloodworm and which fish (if any) also attempted to acquire the bloodworm but were outcompeted. The total time sampled per 2-h video and the number of fish were noted, to calculate a standardised measure of individual aggression (aggressive acts per fish/min). Since some of the 24 bloodworms offered per observation period were obscured (e.g., by air bubbles or fish), individual feeding success was measured as a percentage of the total number of bloodworms that were consumed by identifiable individual fish within the 2 h video segments. Following metabolic-rate determination, each group of fish was transferred to a tank different from their previous one, to remove possible tank effects.

Results

SMR

The mean weights of each group at the start of the experiment (the first measurement of SMR) were 6.60 ± 0.49 (SE) g (range 4.79–8.52 g; $n = 10$), 10.37 ± 0.27 g (9.45–11.82 g; $n = 10$), 7.68 ± 0.59 g (4.85–9.82 g; $n = 10$), and 14.71 ± 0.74 g (11.34–18.05 g; $n = 9$ (one of the experimental animals died at the start of the experiment). Table 1 presents data from this and each subsequent sampling period. The sample size is in excess of the number of experimental animals in three of the four cases. The reason for this is that the regression equations based simply on the data from the experimental animals alone were not significant, and it was therefore necessary to include data from more animals to derive reliable equations. Fortunately, for all three times, additional fish from the same stock that had been held under the same ambient conditions were available, and these fish were subjected to identical respirometric measurements in groups of 10. The criterion for deciding how many more fish to include was the achievement of a satisfactory level of significance ($p < 0.02$ in all cases) while maintaining an equal size range among the experimental animals. There was considerable variation in rSMR; it varied from –1.043 to 2.917 mL $\mathrm{O_2 \cdot h^{-1}}$ in the first sampling period and from –2.439 to 4.783 mL $\mathrm{O_2 \cdot h^{-1}}$ in subsequent sampling periods. The mean weights for each group at the end of the experiment were 36.96 ± 2.27 g (range 25.11–46.56 g), 44.51 ± 3.19 g (32.82–57.68 g), 44.31 ± 5.27 g (33.16–49.03 g), and 66.00 ± 5.34 g (37.01–87.7 g).

To test the variance of rSMR over time, each fish was ranked on a scale from 1 to 10 according to its rSMR value during the first sampling period (1 = highest; 10 = lowest). Their initial ranked value was subsequently compared with their ranks for the following three sampling periods (Fig. 1). Individual rSMR was relatively invariant, with high- and low-ranking individuals tending to remain so over the course of the experiment (Kendall coefficient of concordance W = 0.747, df = 29, $p < 0.01$(data derived from the 30 fish that were alive at the end of the experiment)).

Aggression and food acquisition in trial 1

Since the first observation period may be very important in determining how the Arctic char will behave over the course of the experiment, it is dealt with in detail here. In trial 1, mean aggression (aggressive acts per fish/min) was highly polarised, with two individual fish delivering 43% of all attacks on average in each tank and the remaining fish being significantly less aggressive (Kruskal–Wallis test H = 26.65, df = 9, $p < 0.005$).

In trial 1, the fish were ranked with regard to initial weight (g), as well as for aggression (aggressive acts per fish/min), and the relationship between the two variables was compared. There was no significant relationship between weight at the start of the experiment and subsequent aggression in trial 1. However, there was a correlation between aggression and rSMR in trial 1 after ranking both sets of variables (Spearman's coefficient of rank correlation $r_s = 0.564$, $p < 0.05$; Fig. 2). The lowest-ranked fish in terms of rSMR were also the lowest ranked in terms of aggression.

Furthermore, aggression in trial 1 varied significantly with feeding attempts (measured as a percentage of total feeding attempts allocated to each fish in each group). Individual share of feeding attempts ranged from 0 to 90%. However, the relationship between aggression and feeding in trial 1 can best be described as curvilinear (Fig. 3), and the significance after double ln-transforming the axes was $F_{(1,27)}$ = 14.093, $r^2 = 0.319$, $p < 0.001$, $n = 29$ (10 fish were excluded, since their scores were zero, and untransformed). Figure 3 represents fish from all four groups. Attempts at feeding are therefore closely correlated with aggression.

The relationship between feeding attempts and feeding success was also investigated. Figure 4 shows the relationship between mean (from all four trials) individual percent feeding attempts and mean individual percent successful feeding attempts (percentage of food items actually acquired; $F_{(1,37)}$ = 137.077, $r^2 = 0.782$, $p < 0.0001$). The slope of the line (m) equals 0.507. That is, regardless of effort, each fish gets approximately half the food items for which it competes. Fish that put more effort into competing for food are more successful at actually acquiring food items, but only through increased effort.

Fig. 1. Mean residual standard metabolic rate (rSMR) ranking from trials 2, 3, and 4 of individual Arctic char from each of four experimental groups against their rSMR-rate rank in trial 1. Error bars denote ±SE.

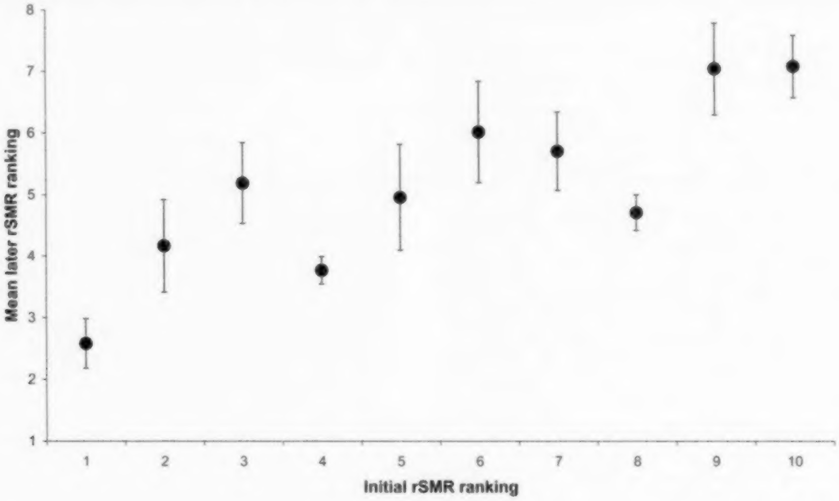

Fig. 2. Mean initial aggression ranking of Arctic char from each of four groups against their initial residual standard metabolic rate (rSMR) rank in trial 1. Error bars denote ±SE.

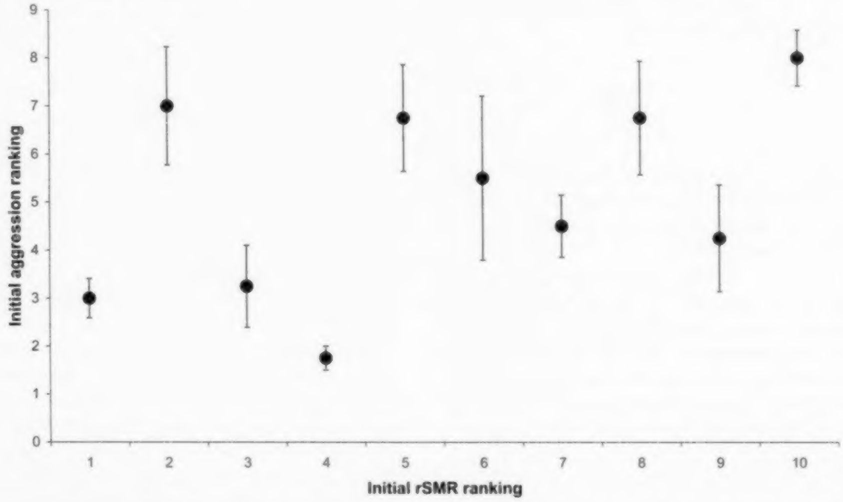

Does food acquisition translate into improved growth? The results are ambiguous. Since ranked food acquisition in trial 1 was very skewed towards very few successful individuals (leaving the less successful individuals ranked at sixth equal), growth rate was tested against feeding attempts. Fish were ranked with regard to their specific growth rate (%·day^{-1}) and the rankings correlated with their level of feeding attempt. Ranked feeding attempts had no overall significant effect on ranked growth (Kruskal–Wallis test $H = 10.25$, df = 9, $p = 0.330$).

Subsequent stability of aggression and growth

As for rSMR in Fig. 1, we can test the stability of feeding hierarchies over time. There was a significant relationship between initial ranked attempts at feeding and mean attempts in subsequent trials, when treated similarly to the above (Kendall coefficient of concordance W = 0.891, df = 29, $p < 0.05$; Fig. 5*a*). Arctic char also tended to maintain their relative aggression over the course of the experiment, with the most and least aggressive fish remaining so over the 6 months (Kendall coefficient of concordance W = 0.737, df = 29, $p < 0.05$; Fig. 5*b*). Hierarchies in terms of specific growth rate (%·day^{-1}) also tended to be fairly stable over time (Kendall coefficient of concordance W = 0.922, df = 29, $p < 0.05$; Fig. 5*c*), although the significant result seemed to be brought about by significantly lower growth in the lowest ranks only (fish 7–10 in trial 1; Fig. 5*c*).

Discussion

This study examined whether the relative SMRs of individual Arctic char were maintained over a period of 6 months and

Fig. 3. Mean attempts at feeding (% total number of food items) against mean aggression (aggressive acts per fish/min) for 39 Arctic char (data from all four trials were pooled). Error bars denote ±SE.

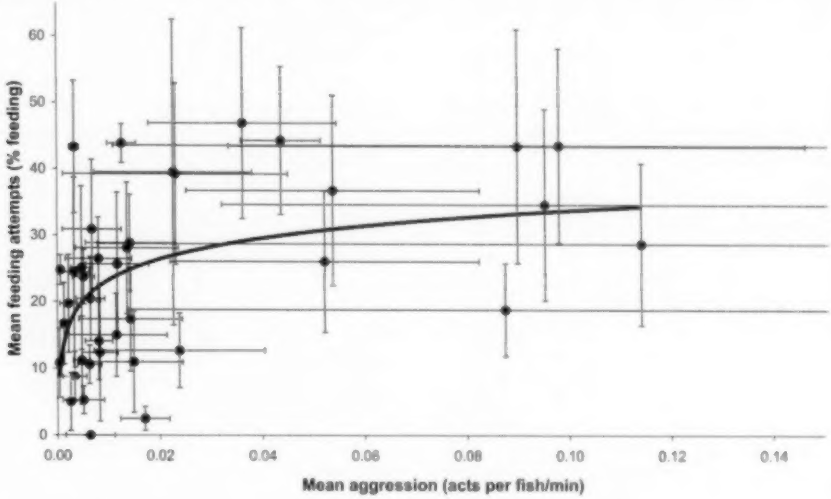

Fig. 4. Mean feeding success (% total number of food items successfully competed for) against mean feeding attempts (% total number of feeding opportunities) for 39 Arctic char (data from all four trials were pooled). Error bars denote ±SE.

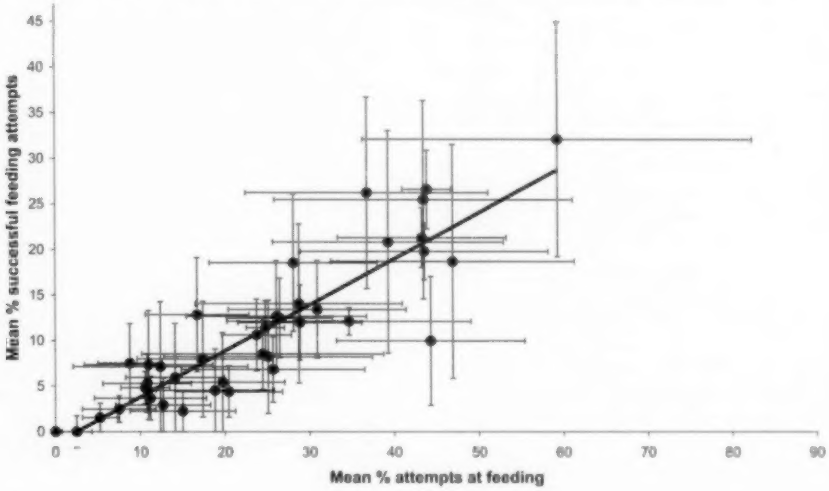

whether the differences in relative SMR had any effect on their subsequent behaviour and growth, and tested the null hypothesis that differences in behaviour would not be similarly repeatable. Measurements of physiological performance in one set of conditions to predict the same physiological performance in another set of conditions are routinely used by physiologists and ecologists (Hayes and Chappell 1990). However, the use of measurements of physiological performance to predict a different performance parameter (e.g., behaviour) is not so routine, and has been applied to few species (African dung beetles (*Scarabaeus laevistriatus*), Heinrich and Bartholomew 1979; spinyhead and roughhead blennies (*Acanthemblemaria spinosa* and *A. aspera*), Clarke 1992; Atlantic salmon, Metcalfe et al. 1995; Cutts et al. 1998, 1999; Masu salmon (*Oncorhynchus masou*), Yamamoto et al. 1998). Both methodologies suffer from the fundamental assumption that individual performance relative to the group remains repeatable and consistent over long time periods and across a range of environmental conditions. Despite the importance of testing this assumption, it has received little attention (Bennett 1987).

Here we demonstrate that aerobic metabolic performance is a repeatable trait in Arctic char. Previous studies have tended to concentrate on locomotor traits in fish (Gibson and Johnston 1995; Gregory and Wood 1998), lizards (Garland 1985), and mammals (e.g., Hayes and Chappell 1990; Chappell et al. 1995), where repeatability between individuals over time was also found. The consistency of individual relative SMR in this study is particularly relevant, since its relationship with aggression and dominance in salmonids (highlighting the selective importance of this trait) has previously relied on a single measure of relative SMR (Cutts et al. 1998, 1999; Yamamoto et al. 1998). Moreover, measure-

Fig. 5. Mean ranks from trials 2, 3, and 4 of individual Arctic char from each of four experimental groups against their rank in trial 1 for feeding attempts (% total feeding opportunities) (*a*), aggression (acts per fish/min) (*b*), and specific growth rate (%·day^{-1}) (*c*). Error bars denote SE.

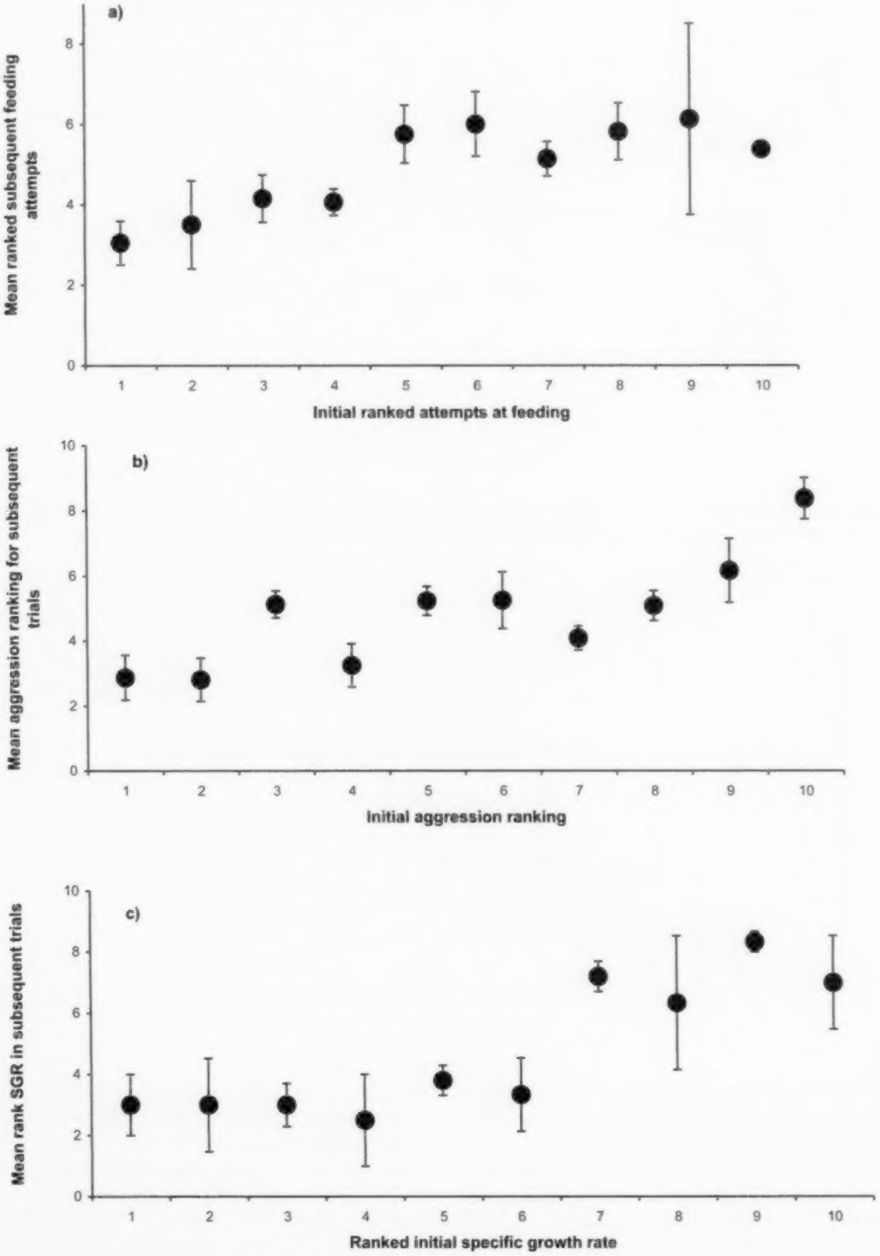

ments of SMR were taken across four different ambient temperatures, showing consistency of relative SMR across a range of environmental conditions. Consistency of individual performance has been shown previously across a range of conditions, such as variations in temperature (Kolok 1992) and altitude (Hayes and Chappell 1990).

In accordance with previous studies on salmonids (Metcalfe et al. 1995; Cutts et al. 1998, 1999), a link between relative SMR and subsequent aggression and food-acquisition performance has been shown. Size can often be a potent indicator of competitive ability (Maynard Smith 1982; Turner and Huntingford 1986) but, by deliberately minimising the size range in each experimental group, relative SMR was shown to be a good predictor of aggression and, in turn, competitive ability. Nevertheless, there was still size variability within each group, and its lack of effect on competitive ability agrees with other salmonid studies (Huntingford et al. 1990; Adams and Huntingford 1996) where differences in size will often be a consequence of dominance rather than a cause.

There was a clear association between aggression and feeding attempts in the replicated trials (when ranked), but no relationship between feeding attempts and subsequent growth. Furthermore, the nonlinear relationship between aggression and feeding attempts implies that very aggressive fish are not correspondingly more successful than less aggressive fish, since attempts at feeding reach an asymptote as aggression continues to increase. It has been noted in other salmonid species that high levels of aggression are extremely costly in terms of feeding: Elliott (1990), for example, observed that, for large territorial brown trout (*Salmo trutta*), the time left for feeding after the time costs of aggression would be greatly reduced and probably inadequate to obtain an adequate energy intake. Indeed, there may be an optimum strategy for growth exhibited by subordinates of minimizing energetic expenditure (through low levels of aggression and attempts at feeding) at the expense of maximising food intake (Metcalfe 1986).

Moreover, the striking relationship between feeding attempts and feeding success, where each fish, regardless of its position in the hierarchy, captures half the food items it attempts to capture, may contribute to the relatively poor growth of dominant fish. Dominant Arctic char with increased rates of food capture only achieved greater energy intake through greater effort. This, in addition to their greater aggression, may exert an energetic cost that the increased food intake could not fully offset.

Acknowledgements

The authors thank John Eccles of John Eccles Hatcheries, Orkney, for collecting Arctic char eggs, David Tierney of Yorkshire Salmon Ltd. for fish husbandry prior to their removal to the University Field Station, Vivien Cameron for fish husbandry thereafter, and two anonymous reviewers for helpful comments on an early draft of the manuscript. This study was funded by European Union "Aquachar" grant No. FAIR-CT96-1981.

References

Adams, C.E., and Huntingford, F.A. 1996. What is a successful fish? Determinants of competitive success in Arctic char (*Salvelinus alpinus*) in different social contexts. Can. J. Fish. Aquat. Sci. **53**: 2446–2450.

Bennett, A.F. 1987. Interindividual variability: an underutilised resource. *In* New directions in ecological physiology. *Edited by* M.E. Feder, A.F. Bennett, W.W. Burggren, and B.B. Huey. Cambridge University Press, Cambridge. pp. 147–166.

Brett, J.R., and Groves, T.D.D. 1979. Physiological energetics. *In* Fish physiology. Vol. VIII. *Edited by* W.S. Hoar and D.J. Randall. Academic Press, New York. pp. 279–352.

Chappell, M.A., Bachmann, G.C., and Odell, J.P. 1995. Repeatability of maximal aerobic performance in Belding's ground squirrel, *Spermophilus beldingi*. Funct. Ecol. **9**: 498–504.

Clarke, R.D. 1992. Effects of microhabitat and metabolic rate on food intake, growth and fecundity of two competing coral reef fishes. Coral Reefs, **11**: 199–205.

Cutts, C.J. 1997. Metabolic rate, territoriality and life-history strategies of juvenile Atlantic salmon (*Salmo salar* L.). Ph.D. thesis, University of Glasgow, Glasgow, U.K.

Cutts, C.J., Metcalfe, N.B., and Taylor, A.C. 1998. Aggression and growth depression in juvenile Atlantic salmon: the consequences of individual variation in standard metabolic rate. J. Fish Biol. **52**: 1026–1037.

Cutts, C.J., Metcalfe, N.B., and Taylor, A.C. 1999. Competitive asymmetries in territorial juvenile Atlantic salmon, *Salmo salar*. Oikos, **86**: 479–486.

Dill, P. 1977. Development of behaviour in alevins of Atlantic salmon. Anim. Behav. **25**: 116–121.

Elliott, J.M. 1990. Mechanisms responsible for population regulation in young migratory trout, *Salmo trutta* III: the role of territorial behaviour. J. Anim. Ecol. **59**: 803–819.

Garland, T., Jr. 1985. Ontogenetic and individual variation in size, shape, and speed in the Australian agamid lizard *Amphibolurus nuchalis*. J. Zool. Ser. A, **207**: 425–439.

Gibson, S., and Johnston, I.A. 1995. Scaling relationships, individual variation and the influence of temperature on maximum swimming speed in early settled stages of the turbot *Scophthalmus maximus*. Mar. Biol. (Berlin), **121**: 401–408.

Gómez-Laplaza, L.M., and Morgan, E. 1993. Social isolation, aggression, and dominance in attacks in juvenile angelfish, *Pterophyllum scalare*. Aggress. Behav. **19**: 213–222.

Gregory, T.R., and Wood, C.M. 1998. Individual variation and interrelationships between swimming performance, growth rate, and feeding in juvenile rainbow trout (*Oncorhynchus mykiss*). Can. J. Fish. Aquat. Sci. **55**: 1583–1590.

Hayes, J.P., and Chappell, M.A. 1990. Individual consistency of maximal oxygen consumption in deer mice. Funct. Ecol. **4**: 495–503.

Hayes, J.P., and Shonkwiler, J.S. 1996. Analyzing mass-independent data. Physiol. Zool. **69**: 974–980.

Heinrich, B., and Bartholomew, G.A. 1979. Roles of endothermy and size in inter- and intraspecific competition for elephant dung in an African dung beetle, *Scarabaeus laevistriatus*. Physiol. Zool. **52**: 484–496.

Higgins, P.J., and Talbot, C. 1985. Feeding and growth in juvenile Atlantic salmon. *In* Nutrition and feeding in fish. *Edited by* C.B. Cowey, A. Mackie, and J.G. Bell. Academic Press, London. pp. 243–263.

Huntingford, F.A., Metcalfe, N.B., Thorpe, J.E., Graham, W.D., and Adams, C.E. 1990. Social dominance and body size in Atlantic salmon parr, *Salmo salar* L. J. Fish Biol. **36**: 877–881.

Kolok, A.S. 1992. The swimming performance of individual largemouth bass (*Micropterus salmoides*) are repeatable. J. Exp. Biol. **170**: 265–270.

Maynard Smith, J. 1982. Evolution and the theory of games. Cambridge University Press, London.

Metcalfe, N.B. 1986. Intraspecific variation in competitive ability and food intake in salmonids: consequences for energy budgets and growth rates. J. Fish Biol. **28**: 525–531.

Metcalfe, N.B., Taylor, A.C., and Thorpe, J.E. 1995. Metabolic rate, social status and life-history strategies in Atlantic salmon. Anim. Behav. **49**: 431–436.

Priede, I.G. 1985. Metabolic scope in fishes. *In* Fish energetics: new perspectives. *Edited by* P. Tytler and P. Calow. Croom Helm, London. pp. 33–64.

Steffensen, J.F. 1989. Some errors in respirometry of aquatic breathers and how to avoid and correct for them. Fish Physiol. Biochem. **6**: 49–59.

Turner, G.F., and Huntingford, F.A. 1986. A problem for game theory analysis: assessment and intention in male mouthbrooder contests. Anim. Behav. **34**: 961–970.

Yamamoto, K.-I. 1991. Relationship of respiration to body weight in the carp *Cyprinus carpio* under resting and normoxic conditions. Comp. Biochem. Physiol. A, **100**: 113–116.

Yamamoto, T., Ueda, H., and Higashi, S. 1998. Correlation among dominance, metabolic rate and otolith size in Masu salmon. J. Fish Biol. **52**: 281–290.

Estimation and analysis of biological parameters in elasmobranch fishes: a comparative life history study

Michael G. Frisk, Thomas J. Miller, and Michael J. Fogarty

Abstract: Published life-history parameters for sharks, skates, and rays over a wide geographic range were used to develop predictive models to estimate parameters that are difficult to measure or have not been previously estimated in elasmobranch species. We determined empirical relationships between body size (total length) and length at maturity (L_m) and age at maturity (T_m). The data used in determining these empirical relationships, the von Bertalanffy parameters asymptotic length (L_∞) and growth rate (k), and natural mortality (M) and maximum age (T_{max}) were used to describe the life-history strategies of elasmobranch fishes. M/k and Beverton's growth–maturity–longevity plots were used to make comparisons between teleost fishes, reptiles, and elasmobranchs. We found that the M/k ratio in elasmobranchs is significantly different from those for other fish and reptile taxa. We linked elasmobranch species fecundity (f) and T_m to potential vulnerability to population decline under exploitation. We found that larger species of elasmobranchs have lower growth rates (k) and potential population increases (r'). Elasmobranchs can be categorized by species maximum length to determine susceptibility of decline under exploitation. Generally, species greater than 100 cm are characterized by life-history and population traits that place them at greater risk of population decline.

Résumé : Des paramètres démographiques de requins, de raies et de torpilles tirés de la littérature et couvrant une large échelle géographique ont servi à élaborer des modèles prédictifs pour estimer les paramètres qui sont difficiles à mesurer ou qui n'ont pas encore été estimés chez les sélaciens. Nous avons déterminé les relations empiriques entre la taille corporelle (longueur totale) et la longueur à la maturité (L_m) et l'âge à la maturité (T_m). Les données utilisées en déterminant ces empiriques rapports, les paramètres de von Bertalanffy longueur asymptotique (L_∞) et taux de croissance (k), et la mortalité naturelle (M) et l'âge maximal (T_{max}) ont servi à décrire les stratégies démographiques des poissons sélaciens. Des graphiques de M/k et des graphiques croissance–maturité–longévité de Beverton ont permis de faire des comparaisons entre les poissons téléostéens, les reptiles et les sélaciens. Le rapport M/k des sélaciens diffère significativement de ceux des autres poissons et des reptiles. Il existe, chez les sélaciens, un lien entre la fécondité de l'espèce (f) et T_m, d'une part, et la vulnérabilité potentielle au déclin démographique dans des conditions d'exploitation, d'autre part. Les espèces les plus grandes de sélaciens ont des taux de croissance (k) et des potentiels biotiques (r') plus faibles. Un classement des espèces de sélaciens d'après leur longueur maximale reflète leur vulnérabilité au déclin sous exploitation: règle générale, les espèces de taille supérieure à 100 cm possèdent des caractéristiques de leur cycle biologique et de leur démographie qui les placent à un risque plus élevé de déclin démographique.

[Traduit par la Rédaction]

Introduction

Elasmobranch fishes comprise 700–800 species occupying a wide range of habitats distributed throughout the oceans of the world (Bone and Marshall 1982). More than 700 000 t of cartilaginous fish are harvested annually worldwide. Although this number is on the rise, it accounts for less than 1% of world fish catch (Bonfil 1994). The responses of elasmobranch species to increased harvest pressure have differed. Off New England, the winter skate, *Leucoraja ocellata*, population increased dramatically in the late 1980s, despite high overall levels of fishing pressure in a multispecies fishery, apparently in response to broader changes in fish community structure (Fogarty and Murawski 1998). The basking shark, *Cetorhinus maximus*, declined sharply off the Irish coast, owing to fishing in the 18th century (Taylor et al. 1997). The Norwegian porbeagle shark, *Lamna nasus*, declined similarly under fishing pressure in the 1980s (Taylor et al. 1997). The extirpation of the common skate, *Dipturus batis*, in the Irish Sea (Brander 1981) and the decline of the barndoor skate, *Dipturus laevis*, in the western Atlantic (Casey and Meyers 1998) highlight the need to gain the knowledge necessary to develop conservation strategies for elasmobranch

Received April 11, 2000. Accepted January 25, 2001. Published on the NRC Research Press Web site on April 25, 2001.
J15719

M.G. Frisk,[1] T.J. Miller, and M.J. Fogarty.[2] Chesapeake Biological Laboratory, University of Maryland Center for Environmental Science, P.O. Box 38, Solomons, MD 20688, U.S.A.

[1] Corresponding author (e-mail: frisk@cbl.umces.edu).

[2] Present address: National Oceanic and Atmospheric Administration, National Marine Fisheries Service, Northeast Fisheries Science Center, Woods Hole, MA 02543, U.S.A.

DOI: 10.1139/cjfas-58-5-969

species. Developing methods to determine life-history parameters of elasmobranchs is the first step in understanding their life strategies and in making sound policy decisions.

Limited biological information for elasmobranchs has made it difficult to determine the resilience of elasmobranch populations to harvesting and has complicated the development of conservation policies. Further, the paucity of knowledge regarding elasmobranchs has made it difficult to compare their life histories with those of other taxonomic groups.

Although it is preferable to determine biological parameters for species individually, the conservation of elasmobranch resources requires that we use the best information available to make sound management decisions. The annuli of elasmobranch vertebrae have been used successfully in aging studies (Cailliet 1990). In some species, annuli have been validated; however, the accuracy of using vertebral rings to determine age has not been validated in many elasmobranch species (Cailliet 1990). Ossified otoliths are commonly used to age bony fish; however, these are not present in elasmobranchs, which possess placoid scales that have yet to be used successfully to age individuals. As most traditional fisheries models are tied to size or stage-at-age relationships, they cannot easily be applied to some elasmobranchs.

Empirical predictive models have been used to estimate vital parameters for species lacking demographic or life-history data. For example, Pauly (1978) used mean water temperature and growth parameters to estimate natural mortality in 175 fish species. Hoenig (1983) predicted total mortality based on the maximum age of fish, cetacean, and mollusk stocks. Holden (1974) related weight at birth to annual fecundity, and estimated growth rate based on fecundity, length at birth, duration of pregnancy, and maximum size in elasmobranchs species. The applicability of Holden's method was questioned by Pratt and Casey (1990).

Beverton and Holt (1959) pioneered comparative life history studies of fish, using von Bertalanffy parameters for growth rate (*k*) and asymptotic size (L_∞) and natural mortality (*M*) and age and length at maturation (T_m and L_m, respectively). They quantified life-history patterns within taxonomic groups and populations and analyzed how these patterns varied over different environmental conditions and geographic locations. Beverton and Holt (1959) found consistent patterns within taxonomic groups. Moreover, several ratios and key life-history traits (e.g., M/k, L_m/L_∞) were relatively invariant. Beverton (1963) recognized that a trade-off in growth and mortality existed. Fish species that reached their asymptotic size in a short period of time tended to die at a younger age than slower-growing species. Beverton (1963) suggested that the age at first maturation should be adjusted to life-span, so that the maximum contribution to reproduction could be achieved. This strategy would yield the patterns observed for the ratios of age at maturity and longevity (T_m/T_{max}) and length at maturity and total length (L_m/L_∞) (Beverton 1963, 1992).

Charnov and colleagues (Charnov and Berrigan 1991; Charnov 1993; Charnov et al. 1993) extended Beverton's (1963) early recognition of the importance of life-history invariants in evolutionary theory. Based on the premise that "invariances imply deeper symmetries," and noting the invariance in the M/k ratio, Charnov and Berrigan (1991) and Charnov et al. (1993) examined the trade-offs in growth and mortality that influence life-history evolution. Charnov et al. (1993) found that the M/k ratio was invariant for fish and reptiles. Shine and Charnov (1992) related the selection for age at maturity to growth and mortality expressed in the constant ratio of M/k among different taxonomic groups. Invariance of the M/k ratios among widely different taxonomic groups suggests a fundamental evolutionary constraint.

Here we expanded the work of Beverton and Holt (1959) and Charnov (1993) to include elasmobranchs. We quantified relationships among important biological parameters (size and age at maturity) and species-specific maximum lengths for dogfish (Squalidae) and skates and rays (Rajidae) from different geographic areas. We then compared life-history traits of elasmobranchs with those of other fish groups, using Charnov's (1993) invariant M/k ratio and Beverton's (1992) growth–maturity–longevity plots based on data derived for the empirical relationships. The goals of this study were to (*i*) develop predictive equations for estimating vital parameters in elasmobranchs; (*ii*) compare life-history relationships in elasmobranchs with those in other taxa; and (*iii*) provide a life-history approach for assessing the risk of species to potential population decline under exploitation.

Methods

Data sources

Data used in our analyses came from many different sources and we attempted to use data from diverse geographic areas. If parameter values were specified by a range, the midpoint was used in the analyses. If multiple estimates were given for one location, the values were averaged and this single value used. In a few cases, the same species had published parameter estimates from different locations. Data for total length were obtained from previous estimates of maximum total length (L_{max})—either the largest specimen found in the wild or the published von Bertalanffy parameter (L_∞) was used. Data on age at maturity (T_m), length at maturity (L_m), and fecundity (*f*) were also collected from previously published studies. Although many areas are represented, it should be noted that Last and Stevens's (1994) book provided many estimates of L_m, all coming from waters surrounding Australia. Life-span estimates were generally not sex-specific. In some cases, total maximum length was given for sexes combined, but length at maturity was given for sexes individually. In a few cases, parameter estimates for different life-history traits were given in different studies of the same species; in these cases, the estimates were combined for the species as a whole.

Estimates of natural mortality (*M*) and growth rate (*k*) follow the same guidelines as above, with the following exceptions: (*i*) if both natural mortality and growth rate were given in one study, they were used together and (*ii*) remaining estimates for that area (usually areas are defined as oceans) were averaged and used separately. Natural mortality was also determined using Hoenig's regression method that relates total mortality (*Z*) to maximum age of the species. Since we were using estimates of maximum age—the oldest individual determined from rings or extrapolations of the von Bertalanffy equation—we assumed that the estimates of *Z* from Hoenig's method represented *M*. Data for empirical analyses can be obtained by contacting the lead author.

Predictive models

We analyzed relationships among L_{max} and two life-history traits: length at maturity (L_m) and age at maturity (T_m). Maximum total length was used as the independent variable. Maximum total length was assumed to be estimated without error and all other parameters were used as sample estimates. We used linear and log-linear models to develop predictive equations throughout.

We examined regional differences for dogfish, skates, and rays using analysis of covariance (ANCOVA). The data for dogfish sharks were divided into the following five regions: (1) Australia, (2) Eastern Pacific, (3) Western Pacific, (4) South Atlantic, and (5) Western Atlantic. The data for skates were divided into four regions: (1) Australia, (2) Eastern Pacific, (3) Eastern Atlantic, and (4) Western Atlantic.

Survivorship after maturity and the reproductive strategy of elasmobranchs

The relationship between average adult life-span and female age at maturity was determined and compared with that in other taxonomic groups. Following Charnov (1993), average adult life-span was estimated as $1/M$. The results for elasmobranchs were compared with those found for birds, mammals, snakes, lizards, and fish by Charnov. The analysis adds to a cross-taxa comparison of maturation and life-span over different taxa.

Life-history invariants

The ratio of M to k for elasmobranchs was determined and compared with this ratio for other taxonomic groups. Growth rate, k, is a parameter in the von Bertalanffy equation. L_∞ is the asymptotic size determined from the von Bertalanffy equation and is used to estimate the theoretical maximum age of the species. Often natural mortality, M, is estimated using Hoenig's method based on the maximum age corresponding to asymptotic size. Since both parameter estimates are based, at least indirectly, on the same data set, a confounding effect potentially exits between estimates of M and k. Estimates of M determined by this method are not independent of estimates of k. However, independent estimates of M can be derived by tagging studies and from direct estimates of age. We separated data into dependent and independent estimates of M to yield 14 independent and 16 dependant data points. We have included all data points in our analysis, as have many other authors, including Beverton and Holt (1959), Pauly (1978), and Charnov (1993).

If we assume that cohorts decline exponentially in abundance over time and that the growth of individuals in weight can be expressed by a von Bertalanffy function, we may write total population biomass at time t as

$$(1) \qquad N_t w_t = N_0 e^{(-M\cdot t)} \cdot W_\infty (1 - e^{-k\cdot t})^3$$

where N_t, w_t, M, and k are age-specific population number, weight, natural mortality, and growth rate, respectively, and W_∞ is the asymptotic weight. Total biomass of a cohort is a dome-shaped function of age. The age at which cohort biomass is maximal is termed T_{opt} (Beverton 1992). Maximum possible yield would be attained if the entire cohort could be harvested immediately when it reaches T_{opt} (Holt 1958). Holt set the first derivative of eq. 1 to zero to yield a new expression describing W_{opt}, given by

$$(2) \qquad W_{\mathrm{opt}} = W_\infty \left(\frac{3}{\left(3 + \frac{M}{k}\right)} \right)^3$$

A similar expression can be developed to express the point of maximum population biomass with regard to the optimal length (L_{opt}), using the M/k ratio and assuming that $L = W^{1/3}$, where L is the length of individual fish, as

$$(3a) \qquad L_{\mathrm{opt}} = L_\infty \left(\frac{3}{3 + \frac{M}{k}} \right)$$

or

$$(3b) \qquad \frac{L_{\mathrm{opt}}}{L_\infty} = \frac{3}{3 + \frac{v}{k \cdot T_{\mathrm{max}}}}$$

Where v is a constant reflecting the products of natural mortality (M) and life-span (T_{max}).

We analysed the trade-offs among growth, maturity, and life-span by regressing L_{m}/L_∞ on $k \cdot T_{\mathrm{max}}$. When plotted, these data display an optimal strategy zone for length at maturity calculated from using extreme values of v in eq. 3b over a range of $k \cdot T_{\mathrm{max}}$ (Beverton 1992).

Comparison of life-history parameters

The ratio of age at maturity (T_{m}) and life-span (T_{max}), the products of natural mortality (M) and life-span, and the products of age at maturity and natural mortality were compared across fish groups and with those of birds, mammals, and reptiles. This provided an analysis of the relationships between maturation, life-span, and mortality among life histories of different animal groups.

Life history and potential population increase

Von Bertalanffy growth rate estimates (k) were regressed on species' maximum total length (L_{max}), to compare the relationship among species. Jennings et al. (1999) related fecundity at length of 50% maturity (L_{m}) and T_{m} to produce potential population increase (r') in the following expression:

$$(4) \qquad r' = \frac{\mathrm{In(fecundity)}}{T_{\mathrm{m}}}$$

Midpoints of fecundity estimates were used as approximate annual fecundities for elasmobranchs when calculating r', while minimal levels were used for teleosts. Jennings et al. (1998) related the variation in potential population increase (r') within different populations of the same species and between species. They associated lower r' values with population declines in response to exploitation. In the present analysis, we contrasted r' in elasmobranchs with this value for other fishes and used elasmobranch species L_{max} as a predictor of r'. Associations between r' and growth and T_{m} were also determined.

Elasmobranch species were broken into three groups based on total length (L_{max}): (1) $L_{\mathrm{max}} < 100$ cm, (2) 100 cm $< L_{\mathrm{max}} <$ 200 cm, and (3) $L_{\mathrm{max}} > 200$ cm. Even though these size groups were arbitrary, they can provide managers with information on how vital rates likely differ over the size range of elasmobranchs. Arithmetic means for each group were determined for size at maturity, maximum life-span, age at maturity, growth rate, and potential population increase. Risk of vulnerability to overexploitation was assessed with population measurements and life-history indicators of population productivity, to rank the potential risk of population vulnerability.

Results

Predictive models

Length at maturity for elasmobranch fishes was significantly related to total length, L_{max} (Fig. 1). Females and males showed very similar relationships for length at matu-

Fig. 1. The relationship between length at maturity (L_m) and maximum length (L_{max}) for 150 elasmobranch species and one species of chimaeroid. Data for males and females are shown separately: diamonds, females; circles, males; squares, mixed-sex estimates. The least-squares relationship between L_m and L_{max} is $L_m = 0.70 \cdot L_{max} + 3.29$ ($n = 151$, $r^2 = 0.84$, $p = 0.0001$).

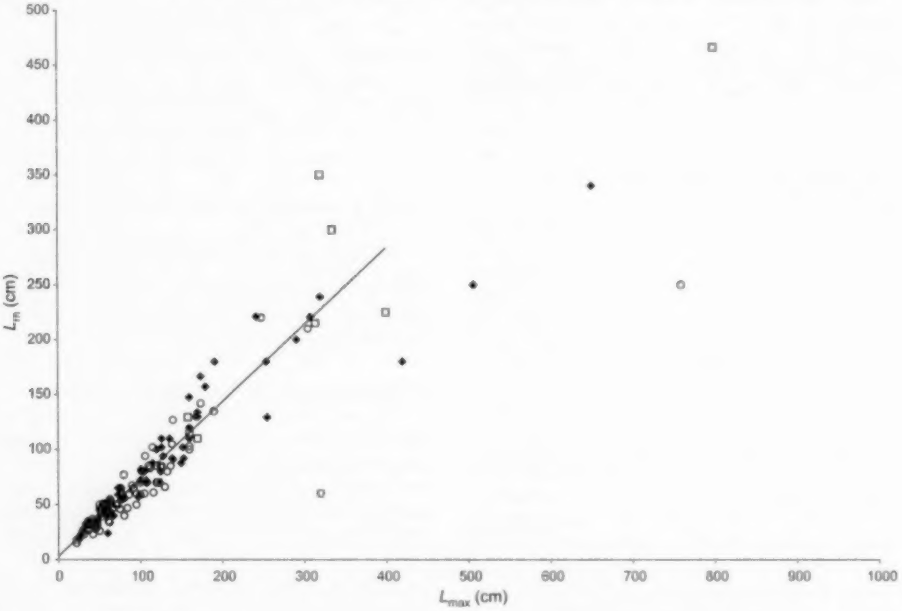

rity. Regression analysis was only performed for species with L_{max} less than 400 cm, as there was less confidence in data for larger species. Similar significant relationships were found for dogfishes, skates, and rays (dogfish: $L_m = 0.59 \cdot L_{max} + 9.35$, $n = 65$, $r^2 = 0.80$, $p = 0.0001$; skates: $L_m = 0.71 \cdot L_{max} + 5.17$, $n = 40$, $r^2 = 0.89$, $p = 0.0001$; rays: $L_m = 0.61 \cdot L_{max} + 2.67$, $n = 17$, $r^2 = 0.84$, $p = 0.001$.). For skates and rays there were no significant differences in either slopes or intercepts with location (ANCOVA: skates and rays: location, $p < 0.38$; L_{max}: location, $p < 0.43$). These results indicate that the proportion of total length achieved at maturation remained constant over the geographic regions used in these analyses. A difference with location and slope for dogfish was detected (ANCOVA: dogfish: location, $p < 0.028$; L_{max}: location, $p < 0.002$). The ratio of length at maturity to total length was 0.73 ± 0.022, with values ranging from 0.19 to 1.0.

We quantified the relationship between age at maturity in elasmobranchs using maximum total length and maximum life-span as independent variables. Only two families, the rays and skates (Rajidae) and the requiem sharks (Carcharhinidae), exhibited strong relationships between age at maturity and total length. Only a few estimates of age at maturity for skates have been determined. However, the few estimates available are statistically significantly related to total length (skates: $T_m = 5.06 \cdot \ln(L_{max}) - 15.70$, $n = 15$, $r^2 = 0.58$, $p = 0.001$). Requiem sharks also showed a significant relationship between age at maturity and total maximum length (requiem sharks: $T_m = 5.92 \cdot \ln(L_{max}) - 23.25$, $n = 14$, $r^2 = 0.33$, $p = 0.0325$). We found significant relationships between maximum life-span and age at maturity for elasmobranchs as a group (Fig. 2).

Life-history invariants for elasmobranchs

Natural mortality, M, was significantly related to growth rate, k (Fig. 3). However, the relationship between M and k for elasmobranchs was significantly different from that for fishes and reptiles. Natural mortality in elasmobranchs appears not to change with growth at the same rate as it does in other animal groups. Welch's approximate t test of equality of the slopes of two samples with unequal variances was used to compare elasmobranchs with other fishes and reptiles. In both cases, it was found that the slope and intercepts for elasmobranchs were significantly different from those for the other taxa (slope: elasmobranchs/fish, $F_{0.05[30,173]} = 0.32$, $F_s = 0.97$; elasmobranchs/reptiles, $F_{0.05[30,45]} = 0.95$, $F_s = 3.25$; intercept: elasmobranchs/fish, $F_{0.05[30,173]} = 0.32$, $F_s = 2.60$; elasmobranchs/reptiles, $F_{0.05[30,45]} = 0.95$, $F_s = 7.55$) (Fig. 3).

To investigate whether the observed differences are a result of the limited range in M and k exhibited by elasmobranchs relative to other fishes, we made comparisons with species falling within the range for elasmobranchs only. The slope for elasmobranchs was still significantly different from that for other fish species occupying a similar range of values ($F_{0.05[22,116]} = 0.66$, $F_s = 3.88$).

The M/k ratio for the Rajidae followed a trend similar to the one found for bony fishes and reptiles ($\ln M = 1.10 \cdot \ln k - 0.8$, $n = 8$, $r^2 = 0.81$, $p = 0.002$). In general, long-lived species of elasmobranchs drive the lower regression. Requiem sharks have a much lower slope than other elasmobranchs, although it was not significant ($\ln M = 0.19 \cdot \ln k - 1.25$, $n = 9$, $r^2 = 0.14$, $p = 0.32$). With more data, the M/k ratio for families could be further developed, to see if these groups continue to differ from other elasmobranchs.

Fig. 2. The relationship between age at maturity (T_m) and maximum life-span (T_{max}) for 35 elasmobranch species. The least-squares regression model is elasmobranch $T_m = 7.20 \cdot \ln(T_{max}) - 12.68$ ($n = 35$, $r^2 = 0.57$, $p = 0.0001$).

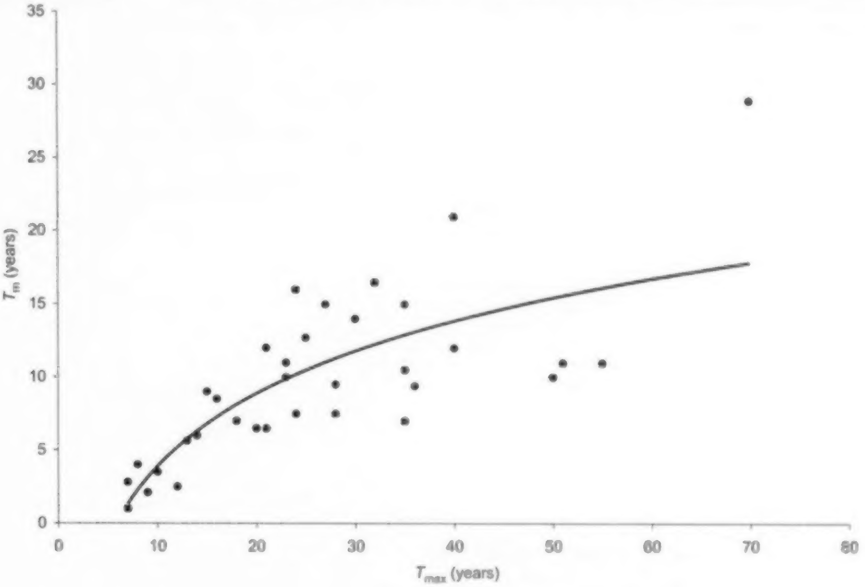

Fig. 3. The relationship between natural mortality (M) and growth rate (k) for 30 elasmobranch species. In the figure, the data points presented are separated for family groups. The least-squares relationship between M and k is $M = 0.42 \cdot k - 0.83$ ($n = 30$, $r^2 = 0.30$, $p = 0.002$).

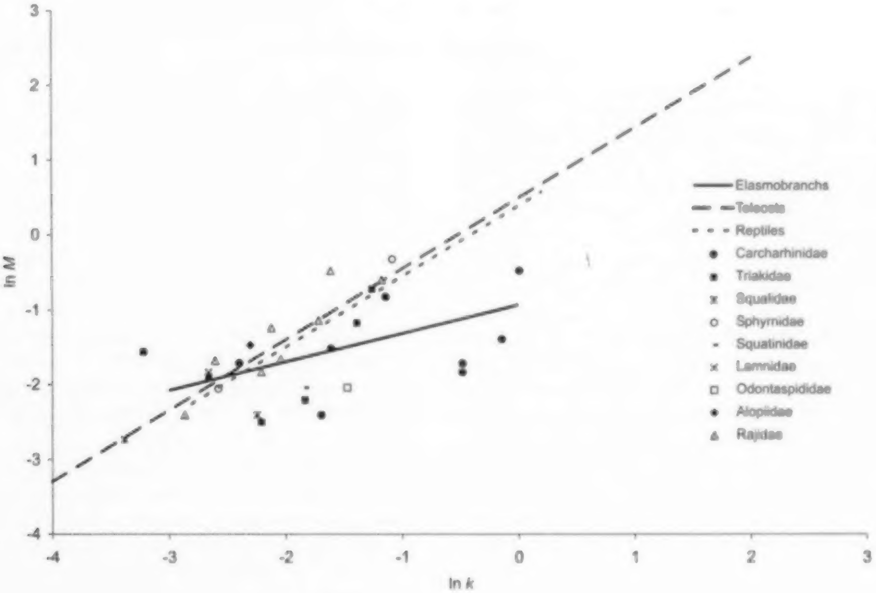

Survivorship after maturity and the reproductive strategy of elasmobranchs

Average adult life expectancy was significantly related to age at maturity (Fig. 4). We compared the relationship developed for elasmobranchs with patterns in other taxonomic groups published by Charnov (1993) and Charnov and Berrigan (1991). The slope for elasmobranchs fell close to those for fishes and reptiles.

Beverton growth–maturity–longevity plots

The growth–maturity–longevity relationships for elasmobranchs are presented in Fig. 5. The observed L_m values, as a

Fig. 4. The relationship between average adult life expectancy ($1/M$) and age at maturity (T_m) for female elasmobranchs. The graph shows comparisons of elasmobranchs with teleost fishes, reptiles, mammals, and birds. The data points (filled circles) shown in the graph are for elasmobranchs. The least-squares relationship between average $1/M$ and T_m for female elasmobranchs is $(1/M) = 0.44 \cdot T_m + 1.87$ ($n = 30$, $r^2 = 0.49$, $p = 0.0001$).

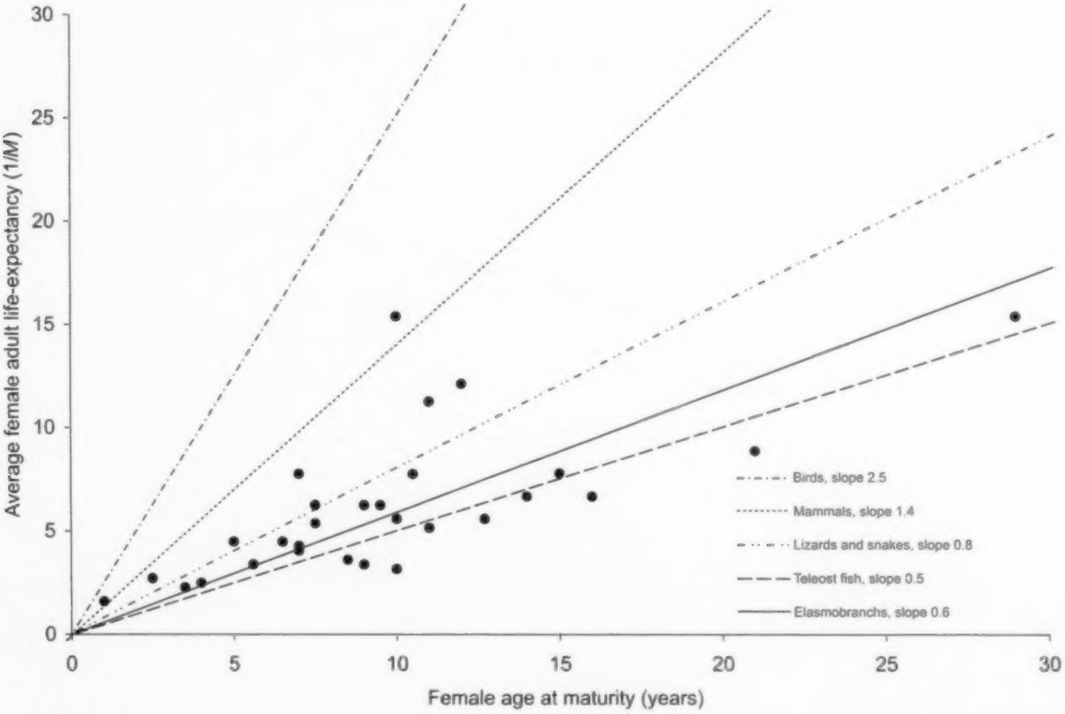

group, fell fairly close to those calculated by eq. 3. The life histories of skates appear similar to the optimal-strategy zone, although all but one of the species fell above the optimal-strategy zone, indicating that skates may be maturing later and (or) at a larger size than the predicted optimal zone. The data scatter for the requiem sharks fell below the optimal-strategy zone, indicating that they are maturing at a smaller size and or a younger age than their calculated optimum.

Comparison of life-history parameters

Beverton (1992) provided a comparison of reproductive strategies of different taxonomic groups using dimensionless numbers. Dimensionless numbers for several fish and animal groups, including elasmobranchs, are provided in Table 1. The invariant ratios for elasmobranchs were high in relation to the Clupeidae and to the genus *Sebastes*, but were similar in relation to the Gadiformes and the Pleuronectiformes. The product of T_m and M was substantially different from reproductive values for birds and mammals and somewhat higher than values for poikilotherms (snakes and lizards).

Life history and population stability

Sufficient data on the life-history parameters L_{max} and k were available to compare the relation between maximum body size and growth rate for the families Rajidae and Triakidae (Fig. 6). There were insufficient data for sharks in the family Squalidae, and the family Carcharhinidae had too much variability, to produce significant results. We found a significant relationship between potential population increase (r') and species maximum total length for elasmobranchs (Fig. 7). The regression was also run without the blue shark, *Prionace glauca*, an apparent outlier ($r' = 0.89 \cdot \ln L_{max} - 0.13$, $n = 33$, $r^2 = 0.28$, $p = 0.002$). Length at maturity was significantly associated with r' (with the blue shark included: $r' = 0.82 \cdot \ln L_m - 0.12$, $n = 33$, $r^2 = 0.20$, $p = 0.008$; without the blue shark: $r' = 0.89 \cdot \ln L_m - 0.14$, $n = 32$, $r^2 = 0.30$, $p = 0.001$). The family Carcharhinidae was the source of much of the variation in relationships involving r' and k and, as a group, did not produce significant results. A comparison of elasmobranch r' values with those for groundfish is shown in Table 2.

There was a significant relationship between age at maturity and species growth rate (with the requiem sharks included: $k = 0.40 \cdot \ln T_m - 0.10$, $n = 53$, $r^2 = 0.21$, $p = 0.001$; without the requiem sharks: $k = 0.35 \cdot \ln T_m - 0.10$, $n = 39$, $r^2 = 0.62$, $p = 0.0001$). Species growth rates were related to the potential rate of population increase only when the requiem shark data were removed ($r' = 1.0 \cdot k + 0.10$, $n = 20$, $r^2 = 0.31$, $p = 0.008$). It appears that requiem sharks as a group constitute an outlier. However, in the absence of requiem sharks, a rather large and important group, elasmobranchs exhibited several key patterns in species growth, maturation, and potential rate of population increase. Still, further data are needed to determine if the deviance in re-

Fig. 5. Growth–maturity–longevity relationships, L_m/L_∞ versus $k{\cdot}T_{max}$ (where L_m is length at maturity, L_∞ and k are the von Bertalanffy parameters for asymptotic length and growth rate, respectively, and T_{max} is maximum age (life-span)), for all elasmobranchs (*a*), skates (*b*), and requiem sharks (*c*). The graphs also show the optimal-strategy zone for maturation (L_{opt}) calculated using the function: $L_{opt}/L_\infty = 3/(3 + v/k{\cdot}T_{max})$, where v is a constant reflecting the products of natural mortality (M) and T_{max}.

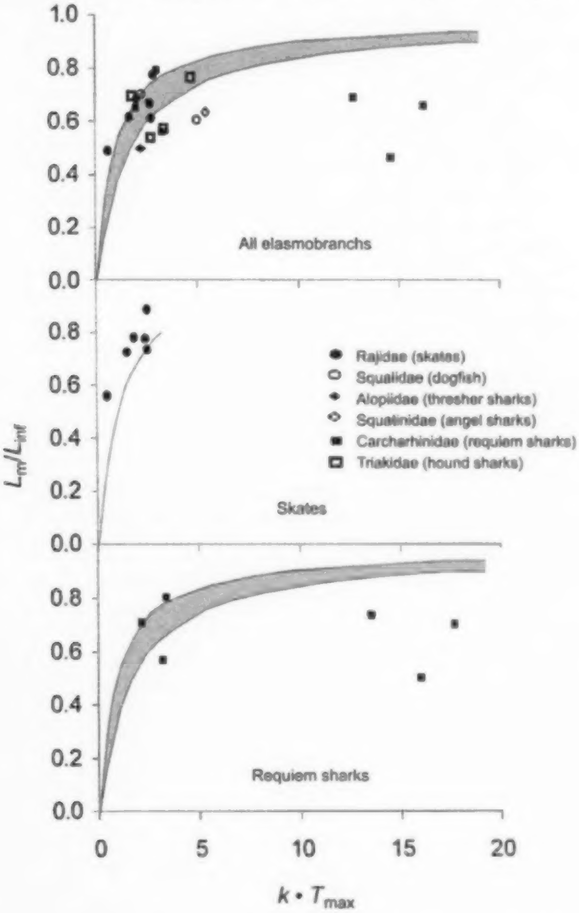

quiem sharks is due to poor data or truly distinguishes the group from other elasmobranchs.

The relation of size to measurements of potential risk was determined, associating larger species with increased vulnerability to exploitation (Table 3). Life-span and age at maturity increase with the average size of a species. Fecundity, growth rate, and the population potential rate of increase all decrease in the larger-size groups. These results provide a view of the average vital rates for size groups of elasmobranchs; however, the size groupings are qualitative and do not provide predictive results.

Discussion

Elasmobranchs now face increased exploitation as overall market demand increases (Bonfil 1994). This trend has been driven by an increased demand for elasmobranchs as a food and by redirected fishing effort following declines in other commercially valuable fish. Extirpation of the common skate in the Irish Sea (Brander 1981) and declines in the barndoor skate in the western North Atlantic (Casey and Myers 1998) have emphasized the need to better understand the biology and ecology of elasmobranchs. The lack of data for these species motivated our use of empirically based life-history models.

Table 1. Comparison of elasmobranch reproductive parameters with those of other fishes, birds, snakes, lizards, and mammals.

	T_m/T_{max}	$M{\cdot}T_{max}$	$T_m{\cdot}M$
Fish			
Elasmobranchs	0.38	4.2	1.7
Genus *Sebastes*	0.16	2.5	0.4
Pacific species	0.16	2.5	0.4
Atlantic species	0.23	3.0	0.7
Clupeidae	0.24	3.0	0.7
Gadiformes	0.30	5.0	1.5
Pleuronectiformes	0.39	4.0	1.6
Birds			0.4
Mammals			0.7
Lizards and snakes			1.4

Note: Estimates for fishes other than elasmobranchs are from Beverton (1992) and estimates for birds, mammals, lizards, and snakes are from Charnov and Berrigan (1991). Abbreviations used: T_m, age at maturity; T_{max}, life-span (maximum age); M, natural mortality. For the elasmobranchs, 38 estimates of T_m/T_{max}, 40 estimates of $M{\cdot}T_{max}$, and 33 estimates of $T_m{\cdot}M$ were used. Estimates of M came from previously published estimates and were calculated using Hoenig's (1983) method for estimating total instantaneous mortality based on longevity data.

Significant regressions were found for predicting length at maturity (L_m) for elasmobranchs and age at maturity (T_m) for the families Rajidae and Carcharhinidae. The mean of the ratio of maximum total length (L_{max}) and L_m for elasmobranchs is 0.73, similar to values for other fish groups (Beverton and Holt 1959). Moreover, the extreme values (0.19–1.0) cover the entire range Beverton and Holt (1959) found for other fish groups. A significant relationship for predicting age at maturity was also found by regressing age at maturity on total life-span. The mean ratio of T_m to maximum age, T_{max}, is 0.38, also consistent with values for other fish groups (Beverton 1992). These values represent the proportion of time and growth that occurs before the onset of maturation, prior to the energy investment adults allocate to reproduction. If an elasmobranch lives to an age near its maximum age of 25 years, it will have partitioned 27% of its growth and have lived 62% of its life-span after maturation. This enables cartilaginous fishes to invest energy and time in reproduction, potentially over many spawning seasons.

The ratio of natural mortality, M, to the von Bertalanffy growth coefficient, k, for elasmobranchs is significantly different from those of other taxonomic groups. But many of the individual elasmobranch species have M/k ratios similar to those for other fish and animal groups. Similarly, other fish species have shown departure from the slope of M/k found by Charnov (1993). Our study identified a class of animals with a wide range of values—from 0 to 3.5 for the natural log of both parameters—and a M/k ratio that is significantly lower

Fig. 6. The relationship between growth rate (k) and total length (L_{max}) for the families Rajidae (filled circles) and Triakidae (open diamonds). The least-squares relationships are given by $k = -0.17 \cdot \ln(L_{max}) + 0.97$ ($n = 16$, $r^2 = 0.68$, $p = 0.0001$) for the Rajidae and $k = -0.11 \cdot \ln(L_{max}) + 0.72$ ($n = 18$, $r^2 = 0.45$, $p = 0.002$) for the Triakidae.

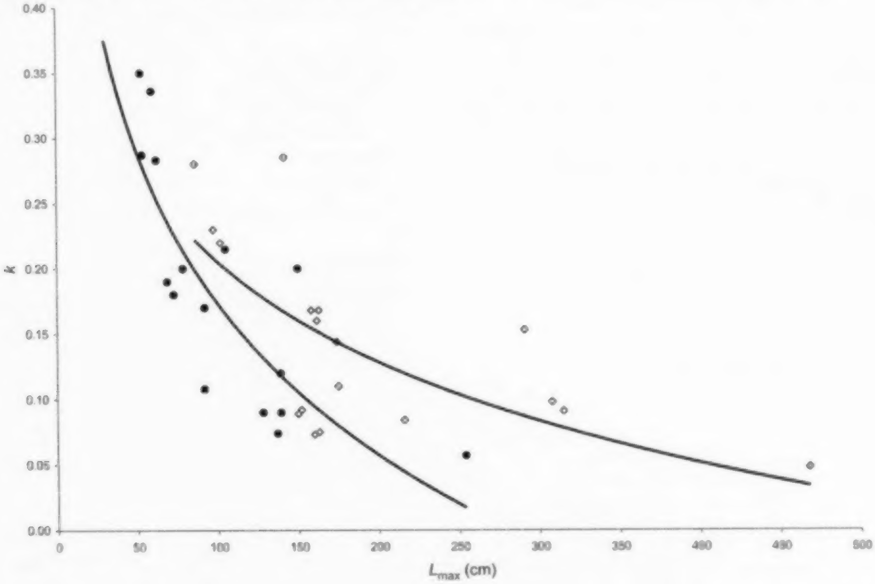

Fig. 7. The relationship between potential rate of population increase (r') and maximum total length (L_{max}) for elasmobranchs. The least-squares relationship is given by $r' = -0.11 \cdot \ln(L_{max}) + 0.81$ ($n = 34$, $r^2 = 0.17$, $p = 0.01$). One potential outlier, the blue shark, *Prionace glauca*, is shown (open square). The regression run without the blue shark is $r' = -0.13 \cdot \ln(L_{max}) + 0.93$ ($n = 33$, $r^2 = 0.28$, $p = 0.001$).

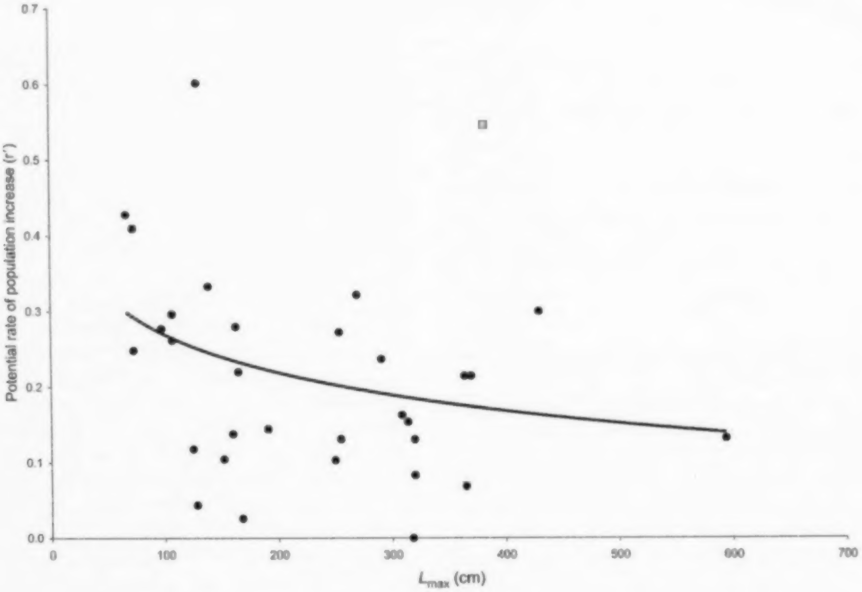

than Pauly's (1978) cross-family analysis. In general, the longer-lived species of elasmobranchs have a lower ratio than other animal groups, and these strongly influence the regression.

Lack of attention to elasmobranchs and the lack of anatomical features commonly used to age fish may have increased the uncertainty in estimates of M. Estimates of k and Hoenig's method for estimating total mortality (Z) are based on age determination. Aging methods for cartilaginous species have been verified in only a few species (Cailliet 1990). Since the M/k ratio is very sensitive to changes in growth rate, minor aging errors could cause profound differences in

Table 2. Comparison of potential population increase (r') between elasmobranchs and groundfish of the North Sea and Western Atlantic.

Common name	Scientific name	T_m (years)	f	r'
Elasmobranchs				
Common thresher	*Alopias vulpinus*	5	4	0.14
Grey reef shark	*Carcharhinus amblyrhynchos*	7	5	0.13
Silky shark	*Carcharhinus falciformis*	9	8	0.15
Galapagos shark	*Carcharhinus galapagenis*	7.5	10	0.21
Bull shark	*Carcharhinus leucas*	15	6.5	0.08
Black tip shark	*Carcharhinus limbatus*	7	5.5	0.14
Oceanic whitetip	*Carcharhinus longimanus*	4.5	8.5	0.32
Dusky shark	*Carcharhinus obscurus*	21	8.5	0.07
Sandbar shark	*Carcharhinus plumbeus*	14	8.5	0.10
Sandtiger shark	*Carcharias taurus*	7	2	0.0
White shark	*Carcharodon carcharias*	10.5	7	0.13
Tiger shark	*Galeocerdo cuvier*	9.5	34.5	0.30
School/Soupfin	*Galeorhinus galeus*	12	28	0.22
Mako shark	*Isurus oxyrinchus*	7.5	10	0.21
Gray smooth-hound	*Mustelus californicus*	2	3.6	0.28
Brown smooth-hound	*Mustelus henlei*	2.5	4	0.28
Lemon shark	*Negaprion brevirostris*	12.7	11.5	0.13
Sevengill	*Notorynchus cepedianus*	16	88.5	0.24
Blue shark	*Prionace glauca*	6.5	69.5	0.55
Common skate	*Dipturus batis*	11	40	0.27
Blonde ray	*Raja brachyura*	9	40	0.33
Thornback skate	*Raja clavata*	11	52	0.30
Little skate	*Leucoraja erinacea*	4	30	0.68
Spotted ray	*Raja montagui*	9.5	24	0.25
Cuckoo ray	*Leucoraja naevus*	9	80	0.41
Thorny skate	*Amblyraja radiata*	5	17	0.43
Atlantic sharpnose shark	*Rhizoprionodon terraenovae*	3.5	5	0.26
Lesser spotted dogfish	*Scyliorhinus canicula*	5	23	0.63
Scalloped hammerhead	*Sphyrna lewini*	15	23	0.16
Bonnethead shark	*Sphyrna tiburo*	2.5	9	0.60
Spiny dogfish shark (Pacific)	*Squalus acanthias*	29	7.14	0.04
Spiny dogfish shark (Atlantic)	*Squalus acanthias*	10	6.5	0.12
Spurdog shark	*Squalus acanthias*	6.5	5	0.25
Angel shark	*Squatina californica*	10	6	0.10
Whitetip reef shark	*Triaenodon obesus*	8.5	2.5	0.03
Leopard shark	*Triakis semifasciata*	13	12	0.14
Average		9.40	19.60	0.24
Teleosts				
Western Atlantic				
Cod	*Gadus morhua*	2.2	94 000	2.26
Haddock	*Melanogrammus aeglefinus*	2.2	169 050	5.47
Silver hake	*Merluccius bilinearis*	1.7	343 000	7.50
Pollock	*Pollachius virens*	2	200 000	6.10
Yellowtail flounder	*Limanda ferruginea*	1.8	400 000	7.17
Winter flounder	*Pseudopleuronectes americanus*	3.5	500 000	3.75
Goosefish	*Lophius americanus*	4	1 300 000	3.52
Average		2.53	485 342	5.60
North Sea				
Whiting	*Merlangius merlangus*	1.5	83 900	7.56
Lemon sole	*Microstomus kitt*	4.0	95 000	2.86
Witch	*Glyptocephalus cynoglossus*	4.5	100 000	2.56
Plaice	*Pleuronectes platessa*	2.5	69 700	4.56
Dab	*Limanda limanda*	2.3	80 500	4.91
Halibut	*Hippoglossus hippoglossus*	5.8	171 200	2.08
Long rough dab	*Hippoglossoides platessoides*	2.6	21 100	3.83
Average		3.31	88 771.4	4.05

Note: Data for the North Sea are from Jennings et al. (1999), data for age at maturity (T_m) for the Western Atlantic are from National Oceanic and Atmospheric Administration (1998), and data for fecundity (f) are from Hardy (1978).

Table 3. Elasmobranch vital rates grouped by species total length.

Length category	L_{max} (cm)	T_{max} (years)	T_m (years)	*f*	*k*	*r′*
Small	0–99	14	5	31	0.25	0.41
Medium	100–199	24	11	21	0.13	0.21
Large	200 +	27	10	13	0.17 (0.11)	0.19 (0.16)

Note: Medium-sized and large species have characteristics associated with greater "risk" of vulnerability to population decline under exploitation compared with small species. Low population productivity and growth rate have been associated with species that are vulnerable to fisheries decline (Musick 1999; Stevens 1999). Large size has been associated with vulnerability to population decline in elasmobranchs (Jennings et al.1998; Walker and Hislop 1998; and Duvly 2000) and is a predictor of age at maturity and life-span, which are indirectly related to population productivity. Values in parentheses are values for large species calculated without values for the requiem sharks. Abbreviations used: T_m, age at maturity; T_{max}, maximum age; L_{max}, maximum total length; *f*, fecundity; *k*, growth rate; *r′*, potential rate of population increase.

the resulting *M* to *k* ratio. The method of combining point estimates may increase the chance of drawing data from populations of the same species that are growing under different environmental conditions, which affect the physiological timing of maturation and allocation of energy to survival and growth.

Survival, particularly juvenile survival, is often the major contributor to growth rate in population analyses of long-lived species. In a cross-taxa analysis of long-lived species, including the leopard shark, *Triakis semifasciata*, and the angel shark, *Squatina californica*, Heppell et al. (1999) found that among age-0, juvenile, and adult stages, juvenile and early adult survival made the highest contribution to variation in population growth rate. Large values of elasticity indicate which elements of life-history parameters show the greatest selective pressure (Caswell 2000). Brewster-Geisz and Miller (2000), using a stage-based model, found that juvenile survival was the major contributor to population growth in the sandbar shark, *Carcharhinus plumbeus*. From these examples, it can be argued that there should be strong selective pressure in elasmobranchs for low juvenile mortality. High survival, the delayed energetic needs of maturation, and relatively fast growth may allow elasmobranchs species to reach a larger size and decrease their risk of predation. Thus, their relatively fast growth and low mortality may not allow for the *M*/*k* ratio common in other groups.

We found that elasmobranchs have a lower *M*/*k* ratio than other taxa. In an evolutionary sense, our findings relating to the *M*/*k* ratio and growth–maturation–longevity plots appear logical for a group of fishes that has low fecundity. Elasmobranchs appear to make up for low fecundity by investing in large offspring with high survival rates. They also have higher adult survival than the average teleost fish. Bony fishes appear to have selected a life-history strategy that relies on high fecundity and chance events resulting in high recruitment, while elasmobranchs appear to have a life-history strategy that relies on higher offspring survival and longevity after maturation. More data, especially for longer-lived species, are needed to resolve whether the lower *M*/*k* ratio we found is due to sample size or estimation error, or is a true evolutionary distinction between elasmobranchs and other fishes.

Beverton's growth–maturity–longevity plots indicate that some elasmobranch species, notably the requiem sharks, have high values for the products of growth rate and longevity ($k \cdot T_{max}$). Beverton (1992) found $k \cdot T_{max}$ values ranging from 1 in Gadiformes to 12 in *Sebastes*. We found that the product of $k \cdot T_{max}$ ranges from 0.9 in skates to 17.0 in requiem sharks. Generally, *k* and T_{max} are negatively related; a fish that lives long will likely have a lower growth rate. For elasmobranchs, as life-span increases, growth rate does not decrease at the same rate as it does in other taxonomic groups, as shown by the *M*/*k* ratio. Another interesting aspect of the growth–maturity–longevity plots is that the optimal-strategy zone indicates where the maximum possible yield is reached if the entire cohort is harvested (Holt 1958). Skates reach maturity at a larger or later stage then would produce the maximum possible yield. These plots do not directly relate to the sustainability of populations. However, if maturity is not occurring at stages where the greatest potential harvest would be attained, it may suggest that balancing exploitation and a healthy skate population may be difficult. For other elasmobranchs, this is not as clear, with species values above and below the optimal-strategy zone.

The ratio of age at maturity and maximum life-span (T_m/T_{max}) and the products of natural mortality and maximum life-span ($M \cdot T_{max}$) and age at maturity and natural mortality ($T_m \cdot M$) for elasmobranchs are higher than those commonly found in other fish groups. For elasmobranchs, the ratio of age at maturity to the average adult life expectancy (1/*M*) for females was 0.6, very close to that for teleost fishes but substantially less than those for mammals and birds (Charnov 1993). There is an important difference between elasmobranchs and birds and mammals. Lizards, snakes, and most birds and mammals are not heavily exploited species. Exploited species often show compensatory effects in age at maturity, growth rate, and mortality. Thus, differences between elasmobranchs and reptiles may be an artifact of exploitation. However, it seems that the magnitude of the difference between elasmobranch and bird and mammal values is too high to be explained solely by compensatory behavior.

Often little information is available for determining management options for non-targeted fishes. In such cases, comparative analyses of life histories have yielded valuable insights. Life-history strategy has been linked to the resilience of populations to fishing pressure in the North Sea (Jennings at al. 1999). Jennings at al. (1999) provided quantitative evidence that later-maturing, slower-growing, larger species are more susceptible to declines when exploited. Comparing nearest phylogenetic relatives, Jennings et al. (1999) found that species with larger body size, slower growth, and larger and older maturation were significantly more susceptible to population decline under exploitation. In addition, phylogenetic relatives with lower r' values were associated with decreasing trends in abundance. Although similar trends were observed for life history and population decline in cross-species analyses, significant results were only found for age at maturity and population decline.

Productivity of fish populations can be gauged by the intrinsic rate of increase (r) or the potential rate of population increase (r') developed by Jennings et al. (1999). Stevens (1999) found that for two shark species harvested together in an Australian shark fishery, the school shark, *Galeorhinus galeus*, with a lower productivity (r), declined, while the gummy shark, *Mustelus antarcticus*, with a higher productivity, supported a sustainable fishery. Direct estimates of r have not been determined for many elasmobranch species. However, over a wide group of taxa, a negative relationship has been found relating generation time and adult body size (weight or length) to r (Hoenig and Gruber 1990). Recently Smith et al. (1998) provided estimates of r and found that larger Pacific shark species were associated with low values of r. A similar relationship was estimated for the elasmobranch group for $L_{\max}$ and r' in this study.

We have estimated r' values for elasmobranchs as a group and compared them with values for groundfish in the western Atlantic and North Sea. Using the method of Jennings et al. (1998), the values of r' for elasmobranchs estimated in this study are low to moderate. There appears to be a size dependency in r'. For example, the little skate, *Leucoraja erinacea*, and the bonnethead shark, *Sphyrna tiburo*, are small elasmobranchs and exhibit high r' values, whereas large elasmobranchs have lower r' values. However, there are inconsistencies in the pattern. The r' value for the blue shark is much higher than expected based upon size. A higher potential rate of population increase (r') was also significantly associated with lower length at maturity and species growth rate. Using r' as a measure of the ability of a population to compensate for exploitation, larger elasmobranchs, which are associated with large and (or) late maturation, lower growth rates, and early vulnerability to fisheries, appear more susceptible to population declines.

Musick (1999) suggests that slower-growing species from the taxonomic groups chondrosteans, teleosts, elasmobranchs, and sea turtles appear at high risk of population decline under exploitation. Musick notes that species with k coefficients below 0.1 are at particular risk. We were not able to find a significant relationship associating declining growth rate with species maximum size for elasmobranchs as a group, but were able to find a relationship for two families, the Rajidae and the Carcharhinidae. As with r' values, larger species were associated with lower growth rate values in these two families.

Moving beyond these basic generalizations and determining the resilience of species to harvest is a difficult and complex problem without species-specific life-history and fishery data. We explored many different combinations of life-history parameters and population-productivity measures and did not find a strong link for categorizing a species' risk of overexploitation. Total length was not a particularly good indicator and only produced a weak association with the potential rate of population increase (r'). Using Charnov's (1993) approximation of r (which uses the product of T_m with the reciprocal of M to produce average generation length divided into the net reproductive rate R_0), no association was found with species total length. Lower k values were significantly related to lower r' values, suggesting that slower-growing species have less potential to rebound from population depletion. Age of maturity was negatively related to growth, indicating that larger, later-maturing elasmobranchs have lower growth rates. Generalizations linking life-history traits and vulnerability should be used with caution. However, in many cases there are insufficient data to develop detailed models, and life history based methods provide the only available information for managers.

With these caveats, we arbitrarily divided elasmobranch species into three groups based on their total length, to examine how life-history traits differ by species size. The first group of species ranges in size from 0 to 99 cm and includes many species from the families Rajidae, Torpedinidae, Dasyatidae, Urolophidae, and Squalidae. The second group of species ranges in total length from 100 to 199 cm and includes larger species of skates, rays, and dogfish, as well as families of the larger sharks, such as the Alopiidae, Carcharhinidae, Chlamydoselachidae, Hexanchidae, Lamnidae, Odontaspididae, Orectolobidae, Pristiophoridae, Sphyrnidae, Squatinidae, and Triakidae. The third group consists of species greater then 200 cm and is represented by the families Alopiidae, Carcharinidae, Hexanchidae, Lamnidae, Odontaspididae, Orectolobidae, and Pristiophoridae. In several studies, it has been determined that the maximum size of species in the Rajidae is an indicator of low resilience to fishing pressure (Walker and Hislop 1998; Dulvy et al. 2000; Stevens et al. 2000). This study adds to these findings, increasing the importance of species size (and its relation to other life-history traits) to the risk of potential decline under exploitation. Life-history traits consistent with a species' vulnerability to decline, such as delayed age of maturity, species maximum age, lower growth rate, and lower rate of potential population increase, are common in elasmobranchs species greater than 100 cm. Average vital rates place large elasmobranch species at potentially greater risk of decline than smaller species. Combination of the species groupings and life-history regressions indicates that larger species, given a fixed size of recruitment to the fishery, are more likely to be vulnerable to the fishery before maturation and have low rebound potentials. It should be noted that small elasmobranch species have the fewest data points in this analysis, as research has often been devoted to larger species.

Relating life history and species response to ecosystem perturbations, Winemiller and Rose (1992) expanded the traditional r–k continuum to a triangular ordination of three evolved strategies: (1) small, rapidly maturing, short-lived fishes (opportunistic strategists), (2) larger, highly fecund fishes with longer life-spans (periodic strategists), and (3) fishes of intermediate size that often exhibit parental care and produce fewer but large offspring (equilibrium strategists). The equilibrium strategy is characterized by fish with high juvenile survival, late maturation, and low fecundity (Winemiller and Rose 1992). Elasmobranchs are most similar to equilibrium strategists, owing to their high parental investment, represented by large eggs or embryos, gestation periods of several months to over a year, young born as juveniles, high juvenile survival, and low fecundity. Winemiller and Rose (1992) found most large species were not equilibrium strategists but they did not include elasmobranchs in their study. Conservative management options can be formed by combining the relationships presented in this paper, Winemiller and Rose's (1992) triangular ordination, and Jennings at al. (1999) quantitative evidence of life-history-dependent susceptibility to decline.

We recommend that managers take the following precautionary measures to conserve elasmobranchs: (*i*) size-based fishery limits should be implemented for species with either a large size at maturation or late maturation, (*ii*) large species (>100 cm) should be monitored with increased interest and conservative fishing limits implemented, (*iii*) adult stocks should be maintained, as has been recommended for other equilibrium strategists (Winemiller and Rose 1992).

The present analysis develops a preliminary understanding of life-history traits in elasmobranchs. Variations in population parameters over different spatial and temporal scales are not well known for the vast majority of these species. Little is known about the effect that exploitation or temperature has on age and length at maturity, fecundity, and mortality in elasmobranchs. In our analysis, we looked at how the ratio of length at maturity and total length varied over large geographic regions and found there were no significant differences. However, we did not look at intraspecific differences across populations and ranges. Research characterizing population differences within elasmobranch species under different environmental and exploitation scenarios would be an important step toward their conservation.

The paucity of estimates of annual fecundity, periodicity, and the range of annual egg and (or) neonate production in many elasmobranch species has made it difficult to develop relationships for predicting fecundity. More information on fecundity, age, mortality, and growth rates is necessary to further our ability to set conservation goals for elasmobranchs. Until further methods are developed, the relationships in this paper can help fill in biological parameters that are not known and serve as a guide for the conservation of elasmobranchs.

Acknowledgements

Many of the initial leads in compiling the data used in our analyses came from Fish Base 97 (International Center for Living Aquatic Resources Management (ICLARM), Manila, Philippines). We thank W.E. Morrison, D.A. O'Brien, M.A. Chenery, R.T. Kraus, and three anonymous reviewers for constructive comments on early versions of the manuscript. This is contribution number 3408 from the University of Maryland Center for Environmental Science.

References

Beverton, R.J.H. 1963. Maturation, growth and mortality of clupeid and engraulid stocks in relation to fishing. Rapp. P.-V. Reun. Cons. Int. Explor. Mer, No. 154. pp. 44–67.

Beverton, R.J.H. 1992. Patterns of reproductive strategy parameters in some marine teleost fishes. J. Fish Biol. **41**(Suppl. B): 137–160.

Beverton, R.J.H., and Holt, S.J. 1959. A review of the life-spans and mortality rates of fish in nature, and their relationship to growth and other physiological characteristics. Ciba Found. Colloq. Ageing, **54**: 142–180.

Bone, Q., and Marshall, N.B. 1982. Biology of fishes. Blackie Academic & Professional, New York.

Bonfil, R. 1994. Overview of world elasmobranch fisheries. FAO Fish. Tech. Pap. No. 341.

Brander, K. 1981. Disappearance of common skate *Raja batis* from the Irish Sea. Nature (London), **290**: 48–49.

Brewster-Geisz, K.K., and Miller, T.J. 2000. Management of the sandbar shark, *Carcharhinus plumbeus*: implications of a stage-based model. Fish. Bull. (U.S.), **98**: 236–249.

Cailliet, G.M. 1990. Elasmobranch age determination and verification: an updated review. NOAA (Natl. Ocean Atmos. Adm.) Tech. Rep. NMFS (Natl. Mar. Fish. Serv.) No. 90. pp. 157–165.

Cailliet, G.M., Yudin, K.G., Tanaka, S., and Taniuchi, T. 1990. Growth characteristics of two populations of *Mustelus manazo* from Japan based upon cross-readings of vertebral bands. NOAA (Natl. Ocean Atmos. Adm.) Tech. Rep. NMFS (Natl. Mar. Fish. Serv.) No. 90. pp. 167–176.

Casey, J.M., and Myers, R.A. 1998. Near extinction of a large widely distributed fish. Science (Washington, D.C.), **281**: 690–692.

Charnov, E.L. 1993. Life history invariants: some explorations of symmetry in evolutionary ecology. Oxford University Press, Oxford.

Charnov, E.L., and Berrigan, D. 1991. Dimensionless numbers and the assembly rules for life histories. Philos. Trans. R. Soc. B, Biol. Sci. No. 332. pp. 41–48.

Charnov, E.L., Berrigan, D., and Shine, R. 1993. The M/k ratio is the same for fish and reptiles. Am. Nat. **142**: 707–711.

Dulvy, N.K., Metcalfe, J.D., Gianville, J., Pawson, M.G., and Reynolds, J.D. 2000. Fishery stability, local extinctions, and shifts in community structure in skates. Conserv. Biol. **14**: 283–293.

Fogarty, M.J., and Murawski, S.A. 1998. Large-scale disturbance and the structure of marine system: fishery impacts on Georges Bank. Ecol. Appl. **8**: S6–S22.

Hardy, J.D., Jr. 1978. Development of fishes of the mid-Atlantic Bight. Vols. I–VI. U.S. Department of the Interior, Fish and Wildlife Service, Washington D.C.

Heppell, S.S., Crowder, L.B., and Menzel, T.R. 1999. Life table analysis of long-lived marine species with implications for conservation and management. *In* Life in the slow lane. *Edited by* J.A. Musick. Am. Fish. Soc. Symp. **23**: 137–146.

Hoenig, J.M. 1983. Empirical use of longevity data to estimate mortality rates. Fish. Bull. (U.S.), **82**: 898–903.

Hoenig, J.M., and Gruber, S.H. 1990. Life-history patterns in the elasmobranchs: implication for fisheries management. NOAA (Natl. Ocean Atmos. Adm.) Tech. Rep. NMFS (Natl. Mar. Fish. Serv.) No. 90. pp. 1–16.

Holden, M.J. 1974. Problems in the rational exploitation of elasmobranch populations and some suggested solutions. *In* Sea fisheries research. *Edited by* F.R. Harden-Jones. Logos Press, London. pp. 117–137.

Holt, S.J. 1958. The evaluation of fisheries resources by the dynamic analysis of stocks, and notes on the time factors involved. Spec. Publ. No. 1 of the International Commission for the Northwest Atlantic Fisheries, Halifax, N.S., Canada. pp. 77–95.

Jennings, S., Reynolds, J.D., and Mills, S.C. 1998. Life history correlates of responses to fisheries exploitation. Proc. R. Soc. Lond. Ser. B, Biol. Sci. **265**: 333–339.

Jennings, S., Greenstreet, S.R.P., and Reynolds, J.D. 1999. Structural change in an exploited fish community: a consequence of differential fishing effects on species with contrasting life histories. J. Anim. Ecol. **68**: 617–627.

Last, P.R., and Stevens, J.D. 1994. Sharks and rays of Australia. Commonwealth Scientific and Industrial Research Organisation, Australia.

Musick, J.A. 1999. Ecology and conservation of long-lived marine animals. *In* Life in the slow lane. *Edited by* J.A. Musick. Am. Fish. Soc. Symp. **23**: 1–7.

National Oceanic and Atmospheric Administration. 1998. Status of the fishery resources off northeastern United States for 1998. NOAA (Natl. Ocean. Atmos. Adm.) Tech. Mem. NMFS (Natl Mar. Fish. Serv.) NE-15. Northeast Fisheries Science Center, Woods Hole, Mass.

Pauly, D. 1978. A preliminary compilation of fish length growth parameters. Ber. Inst. Meereskd. Christian Albrechts Univ. Kiel, **55**: 200.

Pratt, H.L., and Casey, J.G. 1990. Shark reproductive strategies as a limiting factor in directed fisheries, with a review of Holden's method of estimating growth parameters. NOAA (Natl. Ocean Atmos. Adm.) Tech. Rep. NMFS (Natl. Mar. Fish. Serv.) No. 90. pp. 97–110.

Shine, R., and Charnov, E.L. 1992. Patterns of survivorship, growth and maturation in snakes and lizards. Am. Nat. **139**: 1257–1269.

Smith, S.E., Au, D.W., and Show, C. 1998. Intrinsic rebound potentials of 26 species of Pacific sharks. Mar. Freshw. Res. **49**: 663–678.

Stevens, J.D. 1999. Variable resilience to fishing pressure in two sharks: the significance of different ecology and life history parameters. *In* Life in the slow lane. *Edited by* J.A. Musick. Am. Fish. Soc. Symp. **23**: 11–14.

Stevens, J.D., Bonfil, R., Dulvy, N.K., and Walker, P.A. 2000. The effects of fishing on sharks, rays, and chimaeras (chondrichthyans), and the implications for marine ecosystems. ICES (Int. Counc. Explor. Sea) J. Mar. Sci. **57**: 475–494.

Taylor, L., Walker, T.I., and Sowden, C. 1997. Our relationship with sharks and rays. *In* The nature conservancy guides: sharks and rays. *Edited by* L. Taylor. Time-Life Books, San Francisco. pp. 12–30.

Walker, P.A., and Hislop, J.R.G. 1998. Sensitive skates or resilient rays? Spatial and temporal shifts in ray species composition in the central and north-western North Sea between 1930 and the present day. ICES (Int. Counc. Explor. Sea) J. Mar. Sci. **55**: 392–402.

Winemiller, K.O., and Rose, K.A. 1992. Patterns of life-history diversification in North America fishes: implications for population regulation. Can. J. Fish. Aquat. Sci. **49**: 2196–2218.

Microsatellite evaluation of haddock (*Melanogrammus aeglefinus*) stocks in the northwest Atlantic Ocean

Christopher Lage, Maureen Purcell, Michael Fogarty, and Irv Kornfield

Abstract: The goal of this study was to gain insight about the impact of intensive fishing on a single haddock (*Melanogrammus aeglefinus*) stock, and examine the genetic structuring of spatially discrete spawning aggregations in the northwest Atlantic. We analyzed genetic change at four microsatellite loci for Georges Bank haddock over a 40-year time span in which significant changes in demographics and abundances have occurred in the population. Allelic diversities have changed little, indicating that, although the commercial fishery has collapsed, stock sizes have remained large enough to insulate against major reductions in genetic variation due to drift. Results indicate significant genetic divergence among decadally separated samples. Potential causes for these differences include admixture from other spawning regions, fluctuations in the effective number of spawners contributing to a single spawning event, drift, or a combination of these. Examination of discrete spawning aggregations from Georges Bank, Browns Bank, the Scotian Shelf, and Nantucket Shoals indicated significant differences among stocks. Genetic distance based measures supported the clustering of Scotian Shelf, Browns Bank, and Georges Bank haddock to the exclusion of Nantucket Shoals haddock. Haddock spawning on Nantucket Shoals may be genetically discrete from other haddock populations in the northwest Atlantic.

Résumé : Le but de notre étude est d'explorer les effets de la pêche intensive sur un stock particulier d'Aiglefins (*Melanogrammus aeglefinus*) et d'examiner la structuration génétique de regroupements isolés de reproducteurs dans l'Atlantique Nord. Nous avons analysé les changements génétiques à quatre locus microsatellites chez les Aiglefins du banc Georges sur une période de 40 ans, pendant laquelle la population a subi d'importants changements de démographie et de densité. La diversité des allèles a peu varié, ce qui laisse croire qu'en dépit de l'effondrement de la pêche commerciale, les densités des stocks se sont maintenues à un niveau suffisant pour les protéger contre une réduction de la variation génétique due à la dérive. Il y a cependant une divergence génétique significative entre les échantillons lorsqu'on les regroupe en classes de 10 ans. Ces différences peuvent avoir été causées par l'immixtion de reproducteurs d'autres régions, par la fluctuation du nombre effectif de reproducteurs qui contribuent à un épisode individuel de reproduction, par la dérive génétique, ou par une combinaison de ces facteurs. L'examen des regroupements particuliers de reproducteurs du banc Georges, du banc Browns, de la plate-forme néo-écossaise et des hauts-fonds de Nantucket révèle des différences significatives entre les stocks. Des indices basés sur la distance génétique permettent de regrouper les Aiglefins de la plate-forme néo-écossaise, du banc Browns et du banc Georges, mais excluent ceux des hauts-fonds de Nantucket. Les Aiglefins qui fraient sur les hauts-fonds de Nantucket sont peut-être isolés génétiquement des autres populations de nord-ouest de l'Atlantique.

[Traduit par la Rédaction]

Introduction

The Atlantic haddock, *Melanogrammus aeglefinus*, is a commercially important species endemic to both sides of the North Atlantic. In the northwest Atlantic, haddock range from Cape Hatteras to Greenland, with the highest concentration off the U.S. coast on the Northeast Peak of Georges Bank. This species spawns in distinct areas, in particular, on offshore banks, and is characterized by extensive variability in annual recruitment (Clark et al. 1982). While there is some indication of seasonal movement in the western Gulf of Maine, a variety of tagging, meristic, and life-history studies suggest that there is very little adult mixing between Georges Bank and other stocks in the northwest Atlantic, including Browns Bank, Scotian Shelf, Nantucket Shoals, and the western Gulf of Maine (Schroeder 1942; Clark and Vladykov 1960; Bowen 1987). The Northeast Channel may be a significant barrier to adult migration between Georges Bank and areas to the northeast, as haddock are not usually found in waters deeper than 200 m (Bigelow and Schroeder 1953).

Haddock have been selectively fished throughout their range, and declines have affected stocks on Georges Bank,

Received May 2, 2000. Accepted November 21, 2000. Published on the NRC Research Press Web site on April 19, 2001.
J15742

C. Lage and I. Kornfield.[1] University of Maine, School of Marine Sciences, Orono, ME 04469, U.S.A.
M. Purcell. Western Fisheries Research Center, 6505 N.E. 65th Street, Seattle, WA 98115-5016, U.S.A.
M. Fogarty. Center for Environmental and Estuarine Studies, Chesapeake Biological Laboratory, University of Maryland System, P.O. Box 38, Solomons, MD 20688, U.S.A.

[1] Corresponding author (e-mail: irvk@maine.edu).

DOI: 10.1139/cjfas-58-5-982

in the Gulf of Maine, and on the Scotian Shelf (Gavaris and VanEeckhaute 1994). A subsequent switch in species dominance has occurred on Georges Bank, with a replacement of gadid and flounder species by elasmobranchs, such as dogfish and skate (Fogarty and Murawski 1998). The cumulative long-term consequences for haddock stocks resulting from overharvesting and damage to benthic habitat from fishing gear, as well as predation and competitive pressures from shifts in species dominance, are not yet fully understood. Commercial fisheries for haddock have collapsed in some areas. A variety of regulations designed to minimize impact on remaining groundfish stocks have been implemented in the U.S. and Canada and include closed areas, catch quotas, and trip limits (Fogarty and Murawski 1998). Insight into the population biology of commercial species is particularly critical when management decisions involve recovery plans for overexploited populations. Large fluctuations in population size due to variability in recruitment or overexploitation may lead to changes in genetic population structure and possible reductions in overall genetic variability. Intensive exploitation of haddock stocks may result in life-history changes, such as an increased age-specific weight and reduced time to reproductive maturity (Clark et al. 1982); such changes are most likely compensatory physiologic responses to overfishing, but may also be due to a shift in underlying genetic control (Policansky 1993). The determination of population structure and genetic variability is of paramount importance to the long-term viability of haddock as a commercial species.

Techniques for the genetic identification of stocks of marine fish and shellfish have been reviewed by Shaklee and Bentzen (1998). Molecular techniques implemented to determine population structure in Atlantic haddock have included the use of allozymes (Jamiesen and Birley 1989; Giaever et al. 1995) and mitochondrial DNA (mtDNA) (Zwanenburg et al. 1992; Purcell et al. 1996). These mitochondrial studies suggest that mtDNA may not be sensitive enough to identify fine-scale population structure in Atlantic haddock if, in fact, it exists. This study utilizes microsatellite markers to infer population structure in Atlantic haddock, as they have been found useful in a number of population studies including that of Atlantic cod, *Gadus morhua*, a closely related gadid species (Bentzen et al. 1996; Ruzzante et al. 1996*a*, 1998). Three microsatellite loci used in this study were developed specifically for haddock (Lage and Kornfield 1999) and one cod-specific marker was modified for use in haddock (Brooker et al. 1994).

The goal of this project was to gain insight about the impact of intensive fishing on a single haddock stock, that of Georges Bank, as well as to study genetic structuring of spatially discrete spawning aggregates in the northwest Atlantic. This study analyzes changes in a single population over decadal periods, a time span in which significant changes in demographics and abundances have occurred in the population.

Materials and methods

Sampling

Historic samples were obtained from a collection of archived scales held at the National Marine Fisheries Service in Woods Hole, Mass. We used these scales to extract DNA dating back to 1958, and to genetically characterize this stock over decadal increments. Scale samples used in this study were taken from the Northeast Peak of Georges Bank, and were restricted to individuals collected between February and May, a time interval when spawning aggregations are usually present. Scale samples were sorted by year-class; individuals from the 1963 and 1975 year-classes were taken from multiple collections of age 5 fish made in 1968 and 1980, respectively, while the 1985 year-class came from fish aged 2–5 years collected over several years. Prior to the 1960s, aging of the scales was not recorded on the individual archived packages, consequently the 1958 sample represents multiple year-classes. All samples postdating 1985 also represent multiple year-classes.

Multiple temporally separated samples were obtained from each of the following northwest Atlantic spawning sites during peak spawning times: Georges Bank, Nantucket Shoals, Browns Bank, and the Scotian Shelf. For comparison, single collections were obtained from the Grand Banks and Norway (Fig. 1; Table 1). Fin clips and muscle tissue were obtained from individual fish and preserved in 95% ethanol for subsequent DNA extraction. Collection was provided by the combined efforts of the U.S. National Marine Fisheries Service, the Canadian Department of Fisheries and Oceans, and Professor Jarle Mork of Norway.

DNA extraction, amplification, and visualization

Published protocols were followed for DNA extraction from ethanol-preserved tissue samples and dried scale samples (Purcell et al. 1996). Haddock-specific dinucleotide microsatellite loci Mae-111, Mae-211, and Mae-249 were exploited in this study (Lage and Kornfield 1999). Initial screening suggested that these loci may prove useful for population discrimination due to high levels of variability and heterozygosity. Multiplex polymerase chain reactions (PCR) of all three loci were performed, following the published protocol for a Hybaid OMN-E thermal cycler. Fluorescent PCR products were visualized on an ABI377 automated DNA sequencer (Perkin Elmer). Fluorescent-peak data were analyzed using the GeneScan (version 2.1) and Genotyper (version 2.1) software programs (Perkin Elmer).

A microsatellite locus originally developed for cod (Brooker et al. 1994) was also exploited. PCR fragments for locus Gmo-132 were cloned using the PGEM-T kit (Promega Co.), following the manufacturer's instructions. Multiple bands were sequenced in a single direction and probed with a (CA)$_{10}$ repeat. New haddock-specific primers were designed by moving in both primers at least 4 base pairs (bp). Original Gmo-132 cod primer sequences are indicated with underlining, while new haddock primer sequences (Gmo-132.1) are indicated in bold: GG AAC CCA **TTG GAT TCA GGC TCC GTA** CCA TGT AAC GGT CTG CAC ACT CAC AAT CTC GTT TTT TCT CTC (GT)$_{15}$ GCG CTG **ATT TGT TAT TGG CTC GTC CTT TCG**.

PCR amplification and visualization of Gmo-132.1 was performed using [$\gamma-^{32}$P]dATP labeled reverse primer, electrophoretic separation, and exposure to x-ray film (Kodak). The final concentrations of the PCR reagents in a volume of 25 µL were as follows: 10 ng genomic DNA, 1× PCR buffer (pH 9.5; 10 mM KCl, 20 mM Tris-HCl (pH 8.3), 10 mM $(NH_4)_2SO_4$), 2 mM $MgCl_2$, 200 µM each dNTP, 1 µM unlabelled forward primer, 0.5 µM unlabelled reverse primer, 0.5 µM [$\gamma-^{32}$P]dATP labeled reverse primer, and 0.75 U of Taq polymerase (Gibco BRL). PCR reactions were carried out in a PTC-100 programmable thermal cycler (MJ Research) as follows: an initial denaturation of 4 min at 94°C, followed by 35 cycles of 94°C for 45 s, 55°C for 1 min, 72°C for 1 min, with a final extension of 72°C for 10 min. Electrophoretic separation was performed on a 6.5% denaturing polyacrylamide gel electrophoresed at 70 W. Gmo-132.1 produced crisp low-stutter products. Size was determined using a M13 control DNA sequence ladder from the Sequenanase kit (USB/Amersham Co.).

Fig. 1. Map of the northwest Atlantic sampling regions. Broken lines indicate the 100-m isobath.

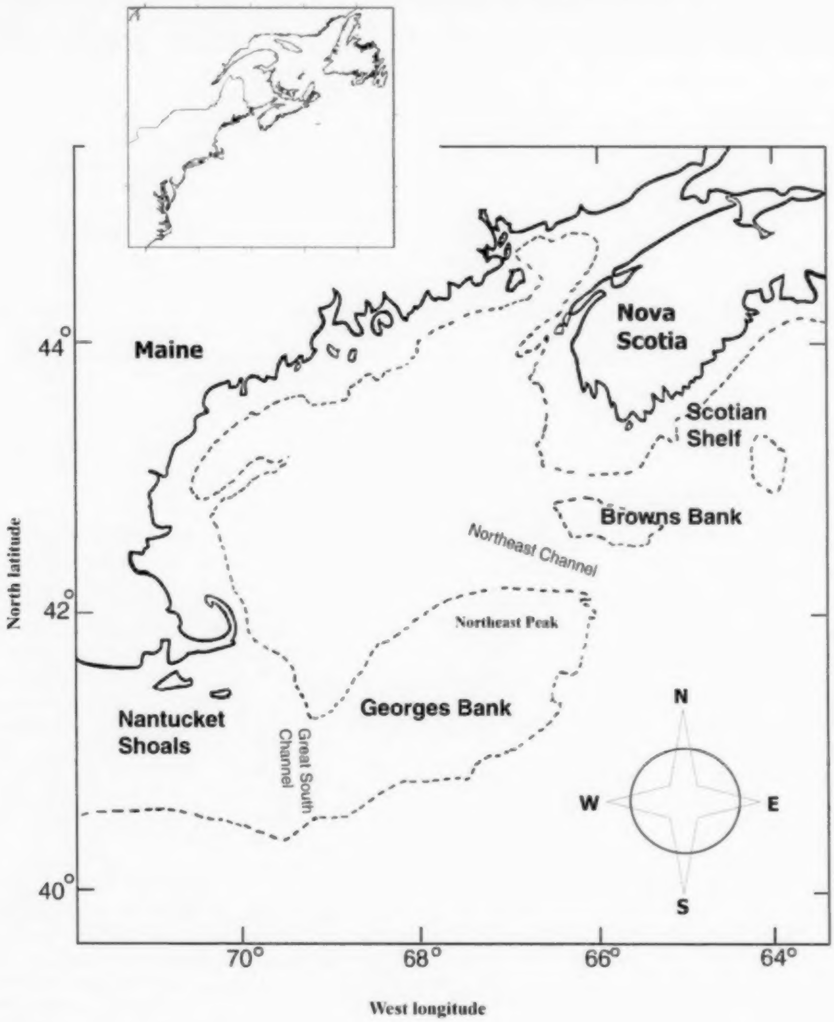

Genetic analysis

Populations were tested for conformation to Hardy–Weinberg expectations by the Markov chain method (Guo and Thomson 1992), resampling 10 000 iterations per batch for 200 batches in GENEPOP 3.1c (Raymond and Rousset 1995); the null hypothesis tested was the random union of gametes within a population. All loci were tested for genotypic disequilibrium across the entire data set, as well as for individual populations, using the Markov chain method, resampling 10 000 iterations per batch for 200 batches; the null hypothesis tested was that the genotypes at one locus are independent from the genotypes at the other locus (within each individual population and within the global population).

Population comparisons were tested for divergence of allelic and genotypic distribution, in which the null hypothesis tested was that the distribution is identical across populations. At each geographic location in which multiple temporal samples were collected, exact tests for allelic and genotypic divergence were performed among and between samples. When homogeneity was confirmed within individual geographic locations in the northwest Atlantic, the multiple samples were then combined to form a single population sample. Every location was tested among and between each other for geographic stock structuring. Comparisons among and between the 1963, 1975, and 1985 Georges Bank year-classes were performed, as well as comparisons between the 1958 and 1990s mixed year-classes, to test for long-term genetic stability of this stock (see Discussion). We calculated an unbiased estimate of the value of a log-likelihood-based exact test by the Markov chain method (Goudet et al. 1996). To correct for simultaneous comparisons, standard Bonferroni corrections were applied, using a global significance level of 0.05 (Rice 1989).

Temporally separated Georges Bank samples were tested for differences in mean heterozygosity across all loci via ANOVA (α = 0.05) and pairwise t tests (α = 0.05). Tests between the 1958 and 1990s mixed year-class samples, as well as between and among the 1963, 1975, and 1985 year-class samples, were performed.

Different genetic-distance measures perform better under different conditions. Some measures are more appropriate for hypervariable loci and follow different mutational assumptions, thus, data from these loci need to be carefully evaluated (Goldstein et al. 1995; Ruzzante 1998; Hedrick 1999). Sample size, number of loci, number

Table 1. Sample information and Hardy–Weinberg equilibria.

Sampling location	Year-class	N	ΣN	HWE
Georges Bank	1963	113	113	Mae-111
	1975	105	105	None
	1985	114	114	None
	1958 mixed	105	105	None
	1996 mixed	120	437	Mae-249
	1997 mixed	128		
	1998 mixed	90		
	1999 mixed	99		
Browns Bank	1996 mixed	99	229	None
	1999 mixed	130		
Nantucket Shoals	1996 mixed	104	184	Mae-111
	1997 mixed	80		
Scotian Shelf	1995 mixed	90	150	None
	1997 mixed	60		
Grand Banks	1996 mixed	28	28	None
Norway	1992 mixed	91	91	None

Note: N = the number of individuals; ΣN = the number of pooled individuals; in the column headed HWE (Hardy–Weinberg equilibrium), locus names are given for deviations of ΣN after Bonferroni correction for six populations (mixed year-classes) and three temporal samples (single year-classes). Sampling location and latitude and longitude ranges are as follows: Georges Bank (41°52′ ± 19′N, 66°36′ ± 46′W), Browns Bank (42°44′ ± 9′N, 66°3′ ± 1′W), Nantucket Shoals (40°45′ ± 24′N, 69°9′ ± 30′W), Scotian Shelf (43°11′ ± 19′N, 62°29′ ± 42′W), and Grand Banks (46°3′ ± 1°N, 56°22′ ± 1°39′W).

of alleles, and allelic-size range may all affect estimations of genetic distances. For instance, $\delta\mu^2$ (Goldstein et al. 1995), a genetic-distance measure developed specifically for microsatellite loci under the stepwise mutational model (SMM) of evolution, may be extremely sensitive to individual loci that contribute extreme values, even when the number of loci used to estimate the distance is >200 (Cooper et al. 1999). Ruzzante (1998) showed that $\delta\mu^2$ and D_{sw} (Shriver et al. 1995), a stepwise-weighted distance measure, may be biased at small sample sizes. In terms of bias and variance, it has been shown that $\delta\mu^2$, D_{sw}, R_{ST} (Slatkin 1995), and F_{ST} (Wright 1951) may be the best performers for microsatellite loci (Ruzzante 1998). Various measures of population subdivision and genetic distance were calculated, including $\delta\mu^2$, D_{sw}, D_c (Cavalli-Sforza and Edwards 1967), F_{ST}, and R_{ST}. D_{sw} and $\delta\mu^2$ are distances based on SMM, while D_c is simply based on differences in allele frequencies and is idependent of any mutational model. Estimates of F_{ST} were generated following Weir and Cocherham (1984). Strict consensus trees were generated via the neighbor-joining method, with 1000 bootstrap samples for each measure in PHYLIP 3.5c (Felsenstein 1993).

Results

Single-locus statistics

Allelic-size ranges, numbers of alleles, and observed and expected heterozygosities (H_o and H_e, respectively) are presented in Table 2. Size ranges, numbers of alleles, and heterozygosities for each temporal Georges Bank sample were similar, except for the combined 1990s mixed year-class sample (N = 437), for which an increased number of total and unique alleles were observed at multiple loci (Table 3). The 1958 Georges Bank mixed year-class sample was not analyzed at locus Mae-111, as template quality and primer specificity resulted in poor amplification of larger-sized alleles at this locus.

Table 2. Single-locus statistics.

Locus	N	n	Range (bp)	H_o	H_e
Gmo-132.1	1100	16	96–132	0.779	0.778
Mae-111	1037	65	193–411	0.902	0.945
Mae-211	1365	47	93–202	0.966	0.960
Mae-249	1385	70	106–267	0.955	0.950

Note: N = the total number of individuals genotyped; n = the total number of alleles observed; range (bp) = the allelic-size range in base pairs; H_o = heterozygosity observed; H_e = heterozygosity expected.

Tests of heterozygosity change

There were no significant differences in mean observed heterozygosities among temporally separated Georges Bank samples. Single factor ANOVA analysis between the 1958 and 1990s mixed year-class samples (df = 1, $\alpha = 0.05$, P = 0.975), as well as among the 1963, 1975, and 1985 single year-class samples (df = 2, $\alpha = 0.05$, $P = 0.878$) indicated no significant differences in mean heterozygosity values. All pairwise t tests (1958 vs. 1990s, $P = 0.905$; 1963 vs. 1975, $P = 0.484$; 1975 vs. 1985, $P = 0.847$; 1963 vs. 1985, P = 0.669) were not significant for $\alpha = 0.05$. Heterozygosity tests between the 1963, 1975, and 1985 samples included all loci. Heterozygosity tests between the 1958 and 1990s mixed year-class samples did not include locus Mae-111, owing to poor amplification in the 1958 population sample.

Exact tests of allelic and genotypic divergence

Exact tests of genetic divergence were performed between temporally separated mixed year-class samples at each individual spawning location. Homogeneity was observed for each location at all loci, except between the Browns Bank 1996 versus 1999 samples at Mae-249 ($P_{\text{allelic}} = 0.010$; $P_{\text{genotypic}} = 0.001$). Temporally separated mixed year-class samples for each spawning location were pooled in an effort to facilitate statistical analyses. Pairwise comparisons between all pooled northwest Atlantic, Grand Banks, and Norway samples were tested for both allelic and genotypic divergence. When Bonferroni corrections for 15 pairwise comparisons were applied to measures of divergence (α = 0.05, $P < 0.003$), all significance was lost, except at locus Mae-249 for comparisons between Norway versus Georges Bank, Browns Bank, Nantucket Shoals, and Scotian Shelf, and at locus Gmo-132.1 for the comparison between Norway versus Browns Bank.

Exact tests of allelic divergence among all pooled mixed year-class samples (Table 4), including Georges Bank, Browns Bank, Scotian Shelf, Nantucket Shoals, Grand Banks, and Norway, indicate significance ($P < 0.0167$) for Gmo-132.1, Mae-249, and overall. Tests of allelic divergence among pooled mixed year-class samples excluding Norway indicate significance for Gmo-132.1 and overall. Tests of allelic divergence for all pooled mixed year-class samples excluding Norway and Grand Banks indicate significance for Gmo-132.1 and overall.

Exact tests of allelic divergence (Table 4) were performed among and between single year-class samples, as well as between the mixed year-class samples from Georges Bank. Significance was observed among all single year-class samples ($P < 0.025$) for Mae-111 and overall. Pairwise comparisons of single year-class samples showed significance after

Table 3. Genetic variation of Georges Bank haddock stock.

		Gmo-132.1			Mae-111			Mae-211			Mae-249		
Year	*N*	*n*	*n**	H_o	*n*	*n**	H_o	*n*	*n**	Ho	*n*	*n**	H_o
1958	105	10	0	0.784	—	—	—	31	0	0.920	46	4	0.968
1963	113	12	2	0.859	23	0	0.753	34	0	0.971	41	2	0.944
1975	105	10	0	0.806	20	1	0.865	38	4	0.987	40	0	0.977
1985	114	11	1	0.737	23	2	1.000	32	1	0.977	39	0	0.958
1990s	437	10	0	0.769	49	17	0.864	41	0	0.956	59	8	0.939

Note: N = sample size; n = total number of alleles; n^* = number of unique alleles observed; H_o = heterozygosity observed. The 1958 mixed year-class sample did not have scorable amplification at locus Mae-111.

Table 4. Exact tests of allelic differentiation among North Atlantic haddock stocks.

(A) Exact tests of allelic differentiation among spatially separated samples; P values significant after Bonferroni correction ($\alpha = 0.05$, $P < 0.0167$) are indicated in bold.

	All spatial samples	All spatial samples excluding Norway	All spatial samples excluding Norway and the Grand Banks
Gmo-132.1	**0.0016**	**0.0106**	**0.0113**
Mae-111	0.6086	0.7575	0.6067
Mae-211	0.0598	0.0883	0.2239
Mae-249	**0.0000**	0.0579	0.2156
All Loci	**0.0000**	**0.0096**	0.0422

(B) Exact tests of allelic differentiation among temporally separated Georges Bank samples; P values significant after Bonferroni correction ($\alpha = 0.05$, $P < 0.025$) are indicated in bold.

	Georges Bank single year-class comparison	Georges Bank mixed year-class comparison
Gmo-132.1	0.1770	0.9311
Mae-111	**0.0016**	—
Mae-211	0.0694	0.3547
Mae-249	0.0362	**0.0173**
All Loci	**0.0004**	0.1117

Bonferroni correction ($P < 0.0167$) at Mae-249 (1963 vs. 1975) and Mae-111 (1963 vs. 1985 and 1975 vs. 1985). Significant ($P < 0.025$) allelic divergence was observed between the 1990s pooled mixed year-class sample and the 1958 mixed year-class sample at locus Mae-249.

Hardy–Weinberg equilibrium and linkage disequilibrium

Pooled mixed year-class samples and individual single year-class samples were tested for comformation to Hardy–Weinberg expectations. When Bonferroni corrections for multiple tests were applied, no population sample was out of Hardy–Weinberg equilibrium (HWE) at more than one locus (Table 1). The pooled 1990s Nantucket Shoals sample and the 1963 Georges Bank single year-class sample were out of HWE at Mae-111. The pooled 1990s Georges Bank mixed year-class was out of HWE at Mae-249. Nonconformity was due to minor heterozygote deficiencies for the 1990s Nantucket Shoals sample at Mae-111 ($H_e = 0.947$; $H_o = 0.932$) and for the 1990s Georges Bank sample at Mae-249 ($H_e = 0.947$; $H_o = 0.939$). A more pronounced heterozygote deficiency was observed for the 1963 Georges Bank year-class sample at Mae-111 ($H_e = 0.929$; $H_o = 0.753$). Population samples that generally conform to expectations of random mating but show a lack of HWE at a single locus may indicate some amount of sampling bias, drift, or admixture. A possible explanation of observed heterozygote deficiency may be sample admixture; however, this is unlikely, as one would expect to see similar results at all loci. A more likely explanation is that there is a certain amount of scoring error and (or) null alleles present at these hypervariable loci, especially for the 1963 Georges Bank year-class sample, that had routinely difficult DNA amplification at locus Mae-111. All other population samples were in HWE at all loci.

Tests of genotypic linkage disequilibrium were performed for all population samples, as well as globally. The global test of linkage disequilibrium between Gmo-132.1 and Mae-249 was highly significant ($P < 0.001$), most likely owing to the analysis of a single mixture composed of multiple reproductively isolated populations with differing gametic frequencies. After Bonferroni correction, significance was observed only between Gmo-132.1 and Mae-249 for the 1996 mixed year-class Nantucket Shoals sample ($P < 0.0001$). When pooled with the 1997 mixed year-class Nantucket Shoals sample, significance was lost. This suggests that the significant results from the 1996 Nantucket Shoals sample may be due to drift or sampling bias. No other significance was observed either at a global or a population scale.

F_{ST} and R_{ST}

F_{ST} and R_{ST} values were generated for all pairwise comparisons between spatially separated samples in the North Atlantic. F_{ST}- and R_{ST}-based strict consensus trees indicate the clustering of Georges Bank, Browns Bank, and Scotian

Shelf populations to the exclusion of the Nantucket Shoals population, with bootstrap support of 77 and 98%, respectively (Fig. 2). The Norway and Grand Banks populations clustered separately from the rest of the northwest Atlantic samples, with 71 and 65% bootstrap support, respectively. Values of R_{ST} were generally higher than values of F_{ST}, indicating that variation in allele size among samples may be more indicative of population structuring than differences among heterozygosities alone for the loci examined. Although low F_{ST} values are expected when examining hypervariable loci, this does not preclude this measure as an estimate of population structuring. Higher values of R_{ST} indicate that population structure may be underestimated when using only F_{ST}.

Fig. 2. Strict consensus neighbor-joining trees. Numbers indicate percent bootstrap support of each branch node for $\delta\mu^2$, D_{sw}, D_c, R_{ST}, and F_{ST} (top to bottom, respectively).

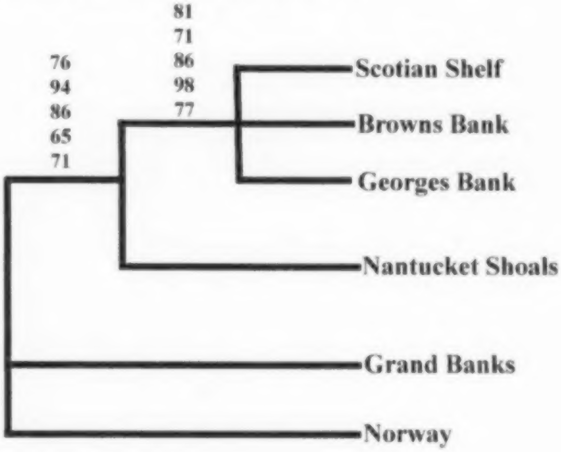

D_{sw}, D_c, and $\delta\mu^2$

Genetic-distance measures were employed between all geographically separated samples in the North Atlantic. Strict consensus trees based on D_{sw}, D_c, and $\delta\mu^2$ distances were concordant with each other and with the F_{ST}- and R_{ST}-based trees, supporting the clustering of Georges Bank, Browns Bank, and Scotian Shelf populations to the exclusion of the Nantucket Shoals population, with bootstrap support of 71, 86, and 81% for the D_{sw}-, D_c-, and $\delta\mu^2$-based trees, respectively (Fig. 2). The Norway and Grand Banks populations clustered away from the rest of the northwest Atlantic samples, with 94, 86, and 76% bootstrap support for the D_{sw}-, D_c-, and $\delta\mu^2$-based trees, respectively. Regardless of mutational-model dependency, all distance measures produced concordant trees with significant bootstrap values.

Discussion

In the last 30 years, the use of molecular markers in fisheries science has become common (Shaklee and Bentzen 1998). High dispersive capabilities of many marine fish are often correlated with low levels of population divergence and slight genetic divergence over vast areas (Graves 1998). This may be particularly true when the species is characterized by high fecundity, large population size, and potentially long-distance egg and larval dispersal. However, examples have been found where dispersal alone may not be correlated with high levels of gene flow (Palumbi 1994). When ecological and evolutionary processes are responsible for stock structuring, it is necessary to incorporate them into strategies designed to manage commercially exploited species (Avise 1998).

Temporal evaluation of the Georges Bank population

Georges Bank, a large submerged offshore bank located along the U.S. and Canadian coasts, once supported an incredibly rich fishery. Georges Bank is shallow and highly productive, supporting a large fish biomass. The high productivity and tightly bound system energetics of Georges Bank tend to result in relatively stable levels of overall biomass and total fish production, although major shifts in species composition routinely occur (Fogarty and Murawski 1998). The largest spawning aggregation of haddock on Georges Bank is found on the Northeast Peak. The gravel region on the Northeast Peak is an important habitat for the early demersal phase of haddock and may represent a limiting resource for this stock (Lough and Bolz 1989; Langton et al. 1996). Georges Bank maintains its own circulation pattern in a slow clockwise gyre that may act as a transportation and retention mechanism for planktonic eggs and larvae (Smith and Morse 1984; Lough and Bolz 1989; GLOBEC 1992). This subsurface clockwise circulation around Georges Bank exists throughout the year, however the flow is strongest in late summer through early fall and is weakest and most variable in winter (Butman and Beardsley 1987). Haddock larvae are advected away from the spawning grounds and, at age 2, the haddock migrate back to the spawning areas where they tend to remain. Long-term monitoring of haddock stocks has revealed dramatic fluctuations in recruitment on Georges Bank (Clark et al. 1982).

The Georges Bank stock is thought to be distinct from the nearby Gulf of Maine and Canadian stocks. Evidence for stock divergence is based on a variety of tagging, meristic, and life-history studies (Schroeder 1942; Clark and Vladykov 1960; Bowen 1987). Tagging studies indicate that adult haddock are not highly mobile and do not tend to migrate large distances (Schroeder 1942; Halliday and McCracken 1970).

Many approaches have been used to evaluate the temporal stability of populations of marine fish with overlapping generations. Our goal was to examine long-term temporal stability of the Georges Bank population. In particular, we were interested in gross as well as minor changes in allelic-frequency distributions and diversities that might be consequential to commercial overharvesting or the combined effects of genetic drift and admixture. We examined this in two ways. First, we examined individual year-classes that were separated by decadal increments. Second, we examined mixed year-class samples that were temporally separated by roughly 40 years. Sampling adults from two successive years at a particular location does not necessarily result in two distinct temporal samples. For instance, when generations overlap and individuals spawn in multiple years, it is difficult to compare temporal samples separated by only short periods of time relative to the life-span of the organism. This is because samples may consist of the same proportions of individuals from particular year-classes and, thus, it can be argued that they are not temporally distinct. To compare unambiguously temporally separated samples, we examined mixed year-class samples that were separated by roughly 40 years. We examined individual year-classes separated by relatively long periods of time (i.e., decadal periods), to evaluate the temporal stability of resulting cohorts derived from individual spawning events on Georges Bank. Given that only a subsection of potential parents contribute gametes to the gene pool each year, we expected that fluctuations in the genetic composition of temporal samples would be most pronounced among individual year-class samples rather than among mixed year-class samples. Although single year-class samples have analytical limitations, they have been exploited in many temporal genetic studies of population structure in marine fish (Bentzen et al. 1996; Ruzzante et al. 1996*b*). Ruzzante (1998) determined that sample sizes of 50–100 individuals are necessary for such analyses.

Genetic analysis of four microsatellite loci indicates that, although there have been dramatic fluctuations in recruitment and spawning-stock biomass over time, there has been an overall maintenance of genetic variability in this stock, as indicated by only small changes in both heterozygosities and allelic diversities (Tables 3 and 4). If these loci are representative of the overall genetic background of this stock, it would seem that little reduction in variability has occurred, even though substantial reductions in population sizes have repeatedly occurred through history. This may be fostered by this species' large population sizes, albeit reduced from historical counts, and extremely high fecundity—a 2-kg female may produce more than 800 000 eggs (Bigelow and Schroeder 1953). At its lowest, the Georges Bank haddock population numbered in the millions, not a level associated with genetic drift or loss of diversity. Measures of divergence suggest that gene frequencies of Georges Bank year-classes have changed from 1963 to 1985. Results suggest that gene frequencies of the mixed year-class Georges Bank population have changed between 1958 and the 1990s, although not as strongly as individual cohorts.

Unique alleles were observed at every temporal sample at one or more loci (Table 3). Most likely this is a sampling artifact of hypervariable loci rather than an indicator of temporal heterogeneity in the Georges Bank stock. Allelic frequencies at each locus examined in this study follow a roughly normal distribution, in which alleles closer to the mean size have increased frequencies. All unique and rare alleles are represented near the edges of their size ranges. A greatly increased number of total alleles and unique alleles were observed at the 1990s mixed year-class sample; this expected result is most certainly due to it's increased sample size (roughly four times) compared with the other Georges Bank samples, although temporal changes in allele frequencies may also play a minor role.

The results presented here are concordant with a previous genetic study (Purcell et al. 1996) that revealed significant heterogeneity in the frequencies of mtDNA control region haplotypes between decadally separated cohorts. Purcell et al. (1996) suggested that the haddock population spawning on Georges Bank may not be genetically discrete and that, with respect to Atlantic haddock, Georges Bank may not be viewed as a closed system. Albeit unlikely, this may be due to some level of gene flow associated with migration of reproductive adults. More likely, this may be due to episodic influxes of planktonic eggs or larvae from other spawning aggregations (Cohen et al. 1991; Polacheck et al. 1992), to fluctuations in the effective number of spawners contributing to a single spawning and subsequent recruitment event (Hedgecock 1994), or to other mechanisms of drift. Given the great fecundity of haddock, it is possible that a relatively small number of highly successful females could give rise to an entire year-class; however, this is unlikely as one would expect to observe significant reductions in genetic variation within the stock over time and within individual cohorts compared with the population as a whole. The combined effects of density-independent influences on the survival of larval haddock (Fogarty 1993), the fine-scale spatial and temporal patchiness of shelf ecosystems (Leising and Franks 1999), and hydrographic effects on egg and larval distribution (Frank et al. 1989; Page and Frank 1989; Page et al. 1989) may result in a stochastic pattern of reproductive success. Disproportionate contributions to the gene pool through demographic stochasticity or differential survival of larvae or egg masses (Hedgecock 1994; Ruzzante et al. 1996*b*) may have similar genetic consequences: it may change a population's genetic structuring so that populations or cohorts may appear to be heterogeneous over time. In theory, a single dominant year-class of Atlantic haddock may be able to support an entire commercial fishery. High fecundity and prolonged spawning events (Page and Frank 1989; Hedgecock 1994) may be an evolutionary response to variations in oceanographic conditions and food resources at a particular spawning area, to increase the probability of larval success and the maintenance of genetic variation.

Spatial stock structuring of haddock in the northwest Atlantic

Previous genetic work using mitochondrial markers did not detect a significant difference between the Georges Bank stock and stocks to the north (Zwanenburg et al. 1992). However, that study did detect a cline in frequency from north to south, indicating that stock structure may exist, but that mitochondrial markers may not be sensitive enough to detect it with statistical significance. Other mitochondrial studies suggest that the Georges Bank stock may not be a genetically closed system with regard to haddock populations (Purcell et al. 1996). Gadid species such as cod and haddock share similar reproductive biologies, life histories, and ecological constraints that may result in similar patterns of population genetic structuring. Recent studies using microsatellite markers have demonstrated a significant difference between cod on Georges Bank and cod on the Scotian Shelf (Ruzzante et al. 1998). Interestingly, the highest level of significance was reported for locus Gmo-132, the cod-specific locus from which the haddock-specific primers used in this study were redesigned.

Exact tests of allelic divergence among geographically separated samples showed overall significance ($P < 0.0167$) when all samples were analyzed and when the Norwegian sample was excluded. When both the Norwegian and Grand Banks samples were excluded, significance ($P < 0.05$) was observed—however it was lost after Bonferroni correction. Most of this significance comes from Gmo-132.1 and Mae-249. Pairwise comparisons of all geographically separated samples showed Bonferroni-corrected significant differences ($P < 0.003$) only for Norway versus Georges Bank, Browns Bank, Nantucket Shoals, and Scotian Shelf comparisons at Gmo-132.1, and for Norway versus Browns Bank comparisons at Mae-249.

Measures of F_{ST}, R_{ST}, D_{sw}, D_c, and $\delta\mu^2$ support the Fisher's exact test results of stock divergence. Measures of F_{ST} were generally very low, indicating that this metric may not be appropriate for loci with such high heterozygosities and variation (Hedrick 1999). Measures of R_{ST} were generally higher than those of F_{ST}, although similar in result, indicating that R_{ST} may be a more reliable measure for such loci or simply that levels of population structure may be underestimated when using F_{ST} alone. All strict consensus trees were generally concordant with each other: all trees supported the clustering of Georges Bank, Browns Bank, and Scotian Shelf populations to the exclusion of the Nantucket Shoals population with high bootstrap support. The Norway and Grand Banks populations clustered away from the rest of the northwest Atlantic samples with high bootstrap support.

These results indicate that the Georges Bank, Browns Bank, Scotian Shelf, and Nantucket Shoals haddock populations are genetically distinct from those populations to the north (i.e., the Grand Banks) and in the eastern Atlantic (i.e., Norway). Results also indicate that Nantucket Shoals haddock are genetically distinct from Georges Bank, Browns Bank, and Scotian Shelf haddock. Episodic fluxes of eggs and larvae from the Scotian Shelf and Browns Bank onto Georges Bank may act to homogenize the genetic structure of these three spawning regions (Cohen et al. 1991; Polacheck et al. 1992). Once on Georges Bank, planktonic eggs and larvae may be entrained and would then be transported to gravel settlement sites (Smith and Morse 1984; GLOBEC 1992). There is a possibility that adult haddock may move between these regions; however, it is extremely unlikely, as these areas are separated by deep channels that are regarded as significant barriers to migration (Bigelow and Schroeder 1953).

The Nantucket Shoals population may be genetically distinct, owing to isolation from entrainment in the Georges Bank gyre, as well as limited movement of adults between Nantucket Shoals and other regions. Eggs and larvae spawned on Nantucket Shoals most likely do not enter this gyre system; thus, they do not settle on Georges Bank but rather on the shoals itself or are transported by prevailing circulation to the southwest (Fogarty and Murawski 1998). Tagging studies suggest that there is very little mixing between Georges Bank and nearby areas such as Nantucket Shoals and the Scotian Shelf (Schroeder 1942; Halliday and McCracken 1970). Haddock from the Gulf of Maine may migrate seasonally along the coast to Nantucket Shoals where there is no barrier to movement. If this is true, the Nantucket Shoals sample that we analyzed may actually be representative of a Gulf of Maine – Nantucket Shoals mixed population. Additional analyses are needed to evaluate the hypothesis that Nantucket Shoals haddock are genetically distinct from those spawning along the coast of the Gulf of Maine. Our research suggests that the haddock spawning on Nantucket Shoals are genetically differentiated from haddock spawing in other regions of the northwest Atlantic and should be managed as such.

Acknowledgements

Several primers were generously donated by the Dalhousie University Marine Gene Probe Laboratory for use in initial screening. We thank the captains and crew of the R/V *Needler* and R/V *Albatross IV*, as well as the scientists from the Canadian Department of Fisheries and Oceans and the U.S. National Marine Fisheries Service (NMFS). In particular, we thank Nina Shepard, John Galbraith, and Dan DenDanto for assistance in obtaining samples. We also thank Frank Almeida and staff at the Northeast Fisheries Science Center, NMFS, who generously assisted our examination of archived material. This work was funded in part by the University of Maine and the University of New Hampshire Sea Grant Program (NA56RG0159 and NA76RG0084).

References

Avise, J.C. 1998. Conservation genetics in the marine realm. J. Hered. **89**: 377–382.

Bentzen, P., Taggart, C.T, Ruzzante, D.E., and Cook, D. 1996. Microsatellite polymorphism and the population structure of Atlantic cod (*Gadus morhua*) in the northwest Atlantic. Can. J. Fish. Aquat. Sci. **53**: 2706–2721.

Bigelow, H.B., and Schroeder, W.C. 1953. Fishes of the Gulf of Maine. Fish. Bull. (U.S.), **53**: 199–213.

Bowen, W.D. 1987. A review of stock structure in the Gulf of Maine area: a workshop report. Canadian Atlantic Fisheries Scientific Advisory Committee Res. Doc. No. 21.

Brooker, A.L., Cook, D., Bentzen, P., Wright, J.M., and Doyle, R.W. 1994. The organization of microsatellites differs between mammals and cold water fishes. Can. J. Fish. Aquat. Sci. **51**: 1959–1966.

Butman, B., and Beardsley, R. 1987. Long-term observations on the southern flank of Georges Bank. Part I: a description of the seasonal cycle of currents, temperature, stratification, and wind stress. J. Phys. Oceanogr. **17**: 367–384.

Cavalli-Sforza, L., and Edwards, A.W.F. 1967. Phylogenetic analysis: models and estimation procedures. Am. J. Hum. Genet. **19**: 233–257.

Clark, J.R., and Vladykov, V.D. 1960. Definition of haddock stocks of the northwestern Atlantic. Fish. Bull. (U.S.), **60**: 283–296.

Clark, S.H., Overholtz, W.J., and Hennemuth, R.C. 1982. Review and assessment of the Georges Bank and Gulf of Maine haddock fishery. J. Northwest Atl. Fish. Sci. **3**: 1–27.

Cohen, E.B., Mountain, D.G., and O'Boyle, R. 1991. Local-scale versus large-scale factors affecting recruitment. Can. J. Fish. Aquat. Sci. **48**: 1003–1006.

Cooper, G., Amos, W., Bellamy, R., Siddiqui, M.R., Frodsham, A., Hill, A.V.S., and Rubinsztein, D.C. 1999. An empirical exploration of the ($\delta\mu^2$) genetic distance for 213 human microsatellite markers. Am. J. Hum. Genet. **65**: 1125–1133.

Felsenstein, J. 1993. PHYLIP (phylogeny inference package) v.3.5c. Code available via http://evolution.genetics.washington.edu/phylip/html.

Fogarty, M.J. 1993. Recruitment in randomly varying environments. ICES J. Mar. Sci. **50**: 247–260.

Fogarty, M.J., and Murawski, S.A. 1998. Large-scale disturbance and the structure of marine systems: fishery impacts on Georges Bank. Ecol. Appl. **8**: S6–S22.

Frank, K.T., Page, F.H., and McRuer, J.K. 1989. Hydrographic effects on the vertical distribution of haddock (*Melanogrammus aeglefinus*) eggs and larvae on the Southwestern Scotian Shelf. Can. J. Fish. Aquat. Sci. **46**: 82–92.

Gavaris, S., and VanEeckhaute, L. 1994. Assessment of haddock on Eastern Georges Bank. Department of Fisheries and Oceans Atlantic Fisheries Res. Doc. 1994/31:38. Available from Canadian Stock Assessment Secretariat, Fisheries and Oceans (Station 1256), 200 Kent St., Ottawa, ON K1A OE6, Canada.

Giaever, M., Forthun, J.K.B., and Mork, J. 1995. Genetic variability at isozyme loci in haddock (*Melanogrammus aeglefinus*) from Norwegian fjord and coastal waters. ICES (International Council for the Exploration of the Sea) Demersal Fish Committee 1995/G:16.

GLOBEC. 1992. US GLOBEC: northwest Atlantic implementation plan. Rep. No. 6. <http://globec.whoi.edu/globec.html>

Goldstein, D.B., Ruiz-Linares, A., Cavalli-Sforza, L.L., and Feldman, M.W. 1995. An evaluation of genetic distances for use with microsatellite loci. Genetics, **139**: 463–471.

Goudet, J., Raymond, M., De Meeus, T., and Rousset, F. 1996. Testing divergence in diploid populations. Genetics, **144**: 933–940.

Graves, J.E. 1998. Molecular insights into population structure of cosmopolitan marine fishes. J. Hered. **89**: 427–437.

Guo, S.W., and Thomson, E.A. 1992. Performing the exact test test of Hardy–Weinberg proportions for multiple alleles. Biometrics, **48**: 361–372.

Halliday, R.G., and McCracken, F.D. 1970. Movements of haddock tagged off Digby, Nova Scotia. International Commission for the Northwest Atlantic Fisheries Res. Bull. No. 7. pp. 8–14.

Hedgecock, D. 1994. Does variance in reproductive success limit effective population sizes of marine organisms? *In* Genetics and evolution of aquatic organisms. *Edited by* A.R. Beaumont. Chapman and Hall, London. pp. 122–134.

Hedrick, P.W. 1999. Perspective: highly variable loci and their interpretation in evolution and conservation. Evolution, **53**: 313–318.

Jamiesen, A., and Birley, A.J. 1989. The distribution of transferrin alleles in haddock stocks. J. Cons. Cons. Int. Explor. Mer, **45**: 248–262.

Lage, C.R., and Kornfield, I. 1999. Isolation and characterization of microsatellite loci in Atlantic haddock (*Melanogrammus aeglefinus*). Mol. Ecol. **8**: 1355–1357.

Langton, R.W., Steneck, R.S., Gotceitas, V., Juanes, F., and Lawton, P. 1996. The interface between fisheries research and habitat management. N. Am. J. Fish. Manag. **16**: 1–7.

Leising, A.W., and Franks, P.J.S. 1999. Larval Atlantic cod (*Gadus morhua*) and haddock (*Melanogrammus aeglefinus*) growth on Georges Bank: a model with temperature, prey size, and turbulence forcing. Can. J. Fish. Aquat. Sci. **56**: 25–36.

Lough, R.G., and Bolz, G.R. 1989. The movements of cod and haddock larvae onto the shoals of Georges Bank. J. Fish Biol. **35**(Suppl. A): 71–79.

Page, F.H., and Frank, K.T. 1989. Spawning time and egg stage duration in Northwest Atlantic haddock (*Melanogrammus aeglefinus*) stocks with emphasis on Georges and Browns Bank. Can. J. Fish. Aquat. Sci. **46**: 68–81.

Page, F.H., Frank, K.T., and Thomson, K.R. 1989. Stage dependent vertical distribution of haddock (*Melanogrammus aeglefinus*) eggs in a stratified water column: observations and model. Can. J. Fish. Aquat. Sci. **46**: 55–67.

Palumbi, S.R. 1994. Genetic divergence, reproductive isolation and marine speciation. Annu. Rev. Ecol. Syst. **25**: 547–572.

Polacheck, T., Mountain, D., McMillan, D., Smith, W., and Berrien, P. 1992. Recruitment of the 1987 year-class of Georges Bank haddock (*Melanogrammus aeglefinus*): the influence of unusual larval transport. Can. J. Fish. Aquat. Sci. **49**: 484–496.

Policansky, D. 1993. Fishing as a cause of evolution in fishes. *In* The exploitation of evolving populations. *Edited by* T.K. Stokes, J.M. McGlade, and R. Law. Springer-Verlag, Berlin. pp. 2–18.

Purcell, M.K., Kornfield, I., Fogarty, M., and Parker, A. 1996. Interdecadal heterogeneity in mitochondrial DNA of Atlantic haddock (*Melanogrammus aeglefinus*) from Georges Bank. Mol. Mar. Biol. Biotechnol. **5**: 185–192.

Raymond, M., and Rousset, F. 1995. GENEPOP (version 1.2): population genetics software for exact tests and eumenism. J. Hered. **86**: 248–249.

Rice, W.R. 1989. Analyzing tables of statistical tests. Evolution, **43**: 223–225.

Ruzzante, D.E. 1998. A comparison of several measures of genetic distance and population structure with microsatellite data: bias and sampling variance. Can. J. Fish. Aquat. Sci. **55**: 1–8.

Ruzzante, D.E., Taggart, C.T., Cook, D., and Goddard, S. 1996*a*. Genetic divergence between inshore and offshore Atlantic cod (*Gadus morhua*) off Newfoundland: microsatellite DNA variation and antifreeze level. Can. J. Fish. Aquat. Sci. **53**: 634–645.

Ruzzante, D.E., Taggart, C.T., and Cook, D. 1996*b*. Spatial and temporal variation in the genetic composition of a larval cod (*Gadus morhua*) aggregation: cohort contribution and genetic stability. Can. J. Fish. Aquat. Sci. **53**: 2695–2705.

Ruzzante, D.E., Taggart, C.T., and Cook, D. 1998. A nuclear basis for shelf- and bank-scale population structure in northwest Atlantic cod (*Gadus morhua*): Labrador to Georges Bank. Mol. Ecol. **7**: 1663–1668.

Schroeder, W.C. 1942. Results of haddock tagging in the Gulf of Maine from 1923 to 1932. J. Mar. Res. **5**: 1–19.

Shaklee, J.B., and Bentzen, P. 1998. Genetic identification of stocks of marine fish and shellfish. Bull. Mar. Sci. **62**: 589–621.

Shriver, M.D., Jin, L., Boerwinkle, E., Deka, R., Ferell, R.E., and Chakraborty, R. 1995. A novel measure of genetic distance for highly polymorphic tandem repeat loci. Mol. Biol. Evol. **12**: 914–920.

Slatkin, M. 1995. A measure of population subdivision based on microsatellite allele frequencies. Genetics, **139**: 457–462.

Smith, W., and Morse, W.W. 1984. Retention of larval haddock *Melanogrammus aeglefinus* in the Georges Bank region, a gyre-influenced spawning area. Mar. Ecol. Prog. Ser. **24**: 1–13.

Weir, B.S., and Cockerham, C.C. 1984. Estimating F-statistics for the analysis of population structure. Evolution, **38**: 1358–1370.

Wright, S. 1951. The genetical structure of populations. Ann. Eugen. **15**: 323–354.

Zwanenburg, K.C.T., Bentzen, P., and Wright, J.M. 1992. Mitochondrial DNA divergence in Western North Atlantic populations of haddock (*Melanogrammus aeglefinus*). Can. J. Fish. Aquat. Sci. **49**: 2527–2537.

The interaction between shellfish culture and ecosystem processes

Aad Smaal, Marnix van Stralen, and Egbertha Schuiling

Abstract: The carrying capacity of the Oosterschelde ecosystem for the production of mussels (*Mytilus edulis*) was evaluated before and after completion of a large-scale coastal engineering project in 1987. This project caused hydrodynamic and water-quality changes; hence, phytoplankton-species composition changed and phytoplankton turnover increased, but primary production remained the same. In the prebarrier period (1980–1986), condition of mussels showed a significant negative correlation with the annual shellfish standing stock and a significant positive correlation with the annual primary production. The system was exploited at maximum capacity. In the postbarrier period (1987–1997), the significant correlation between mussel condition and primary production remained, but there was no longer a negative correlation between standing stock and condition. This indicates overstocking, but yields were maintained. This was explained by (*i*) feedbacks of the mussels in the Oosterschelde ecosystem—through their large filtration and nitrogen-regeneration capacity, increased phytoplankton turnover was induced; and (*ii*) adaptation to the new conditions by the shellfish farmers in their management of the mussel stocks. It was concluded that feedbacks by filter feeders and farmers have to be addressed in estimating the exploitation capacity of ecosystems.

Résumé : Le stock limite de la production de moules (*Mytilus edulis*) de l'écosystème d'Oosterschelde a été évalué avant et après la réalisation d'un ouvrage côtier d'ingénierie de grande envergure en 1987. La projet a entraîné des changements dans l'hydrodynamique et dans la qualité de l'eau; la composition spécifique du phytoplancton s'est donc modifiée, le taux de remplacement du phytoplancton a augmenté, mais la production primaire est restée la même. Avant la présence de l'ouvrage (1980–1986), la condition des moules affichait une corrélation négative significative avec la densité annuelle des mollusques et une corrélation positive significative avec la production primaire annuelle. Le système était alors exploité à sa capacité maximale. Après l'installation de l'ouvrage (1987–1997), il y avait encore une corrélation significative entre la condition des moules et la production primaire, mais il n'y avait plus de corrélation négative entre la densité et la condition. Cela indique une densité excessive, mais les rendements se sont maintenus. Une telle condition s'explique par (*i*) des rétroactions des moules dans l'écosystème d'Oosterschelde qui, à cause de leur grand potentiel de filtration et de régénération de l'azote, peuvent générer un taux plus élevé de renouvellement du phytoplancton, ainsi que par (*ii*) l'adaptation des éleveurs de mollusques aux conditions nouvelles dans leur gestion des stocks de moules. En conclusion, il faut tenir compte des rétroactions des organismes filtreurs et des éleveurs lorsqu'on veut estimer le potentiel d'exploitation d'un écosystème.

[Traduit par la Rédaction]

Introduction

Bivalve filter feeders, such as mussels (*Mytilus edulis*), cockles (*Cerastoderma edule*), oysters (*Crassostrea gigas*; *Ostrea edulis*), and beach clams (*Spisula* spp.), play a dominant role in many estuarine and coastal waters, owing to their great abundance, their extensive filtration activity, and their role as prey for higher trophic levels (Gosling 1992; Dame 1996). Their commercial exploitation has led to both increased and decreased abundance in many coastal waters, thereby raising questions about management and the carrying capacity of the ecosystem (Héral 1993; Grant et al. 1993; Smaal and Héral 1998). Application of the carrying-capacity concept in the exploitation of natural resources, such as shellfish populations, introduces growth rate and annual yield as important parameters. Carver and Mallet (1990) define the carrying capacity of a coastal inlet for mussel cultivation as the stock density at which production levels are maximized without negatively affecting growth rates (see also Incze et al. 1981). However, production is not necessarily maximized at a given growth rate. An increased stock may result in both low individual growth rates and maximum production. Bacher et al. (1998) define carrying capacity for shellfish culture as the standing stock at which the annual production of the marketable cohort is maximized. This is a basic rule of exploitation: maximum yield is obtained from populations at less than maximum density (see Krebs 1972). As a consequence, the exploitation carrying capacity of an ecosystem may be quite different from the ecological carrying capacity, which is the population size supported for a given time in a given ecosystem without ex-

Received January 11, 2000. Accepted November 30, 2000. Published on the NRC Research Press Web site on April 25, 2001.
J15527

A. Smaal,[1] M. van Stralen, and E. Schuiling. Netherlands Institute for Fisheries Research RIVO–DLO, Centre for Shellfish Research, P.O. Box 77, 4400 AB Yerseke, The Netherlands.

[1]Corresponding author (e-mail: a.c.smaal@rivo.wag-ur.nl).

DOI: 10.1139/cjfas-58-5-991

Fig. 1. The Oosterschelde estuary (southwest Netherlands), showing the sampling stations for chlorophyll *a*, suspended-matter, and primary-production measurement, and mussel-culture plots (shaded) in the western (A) and central (B) regions; the re-watering area (hatched) is shown in region C. Region D, northern region.

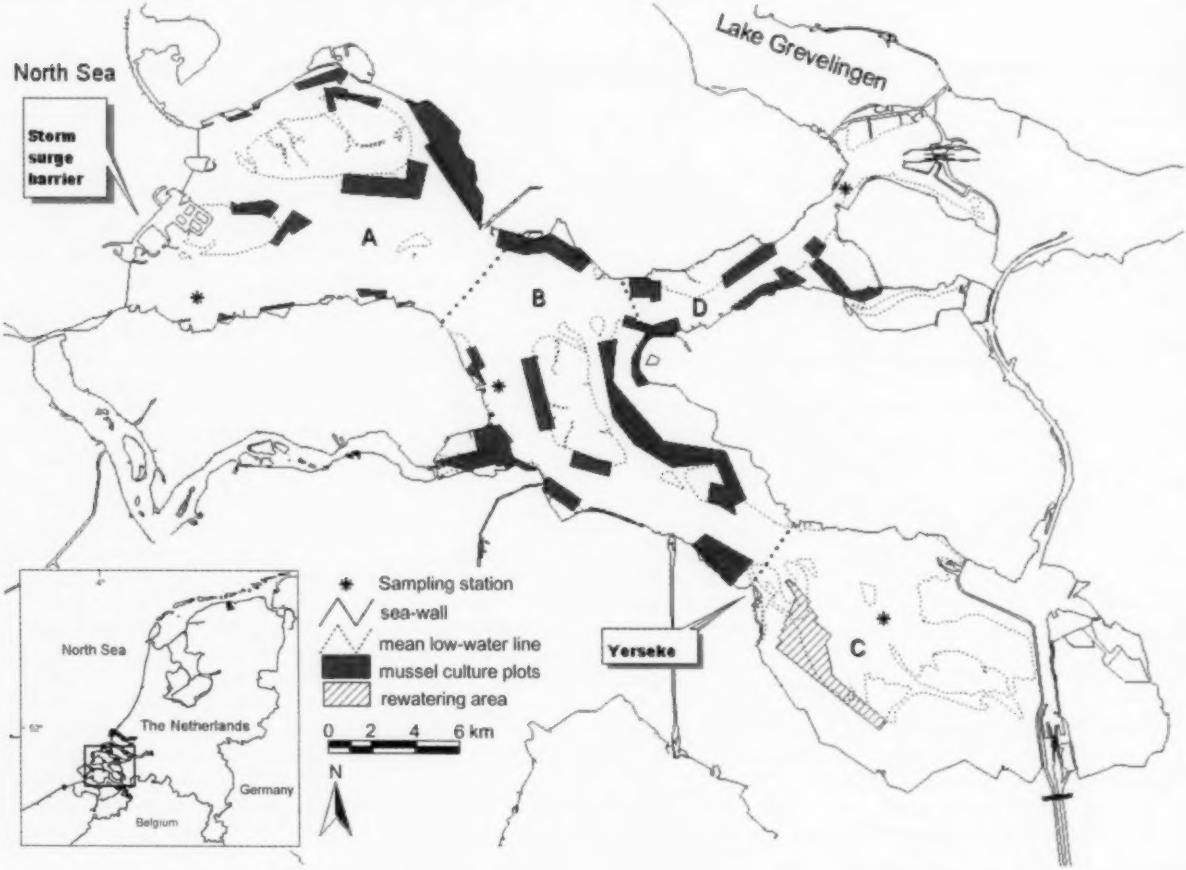
North Sea
Storm surge barrier
Lake Grevelingen
A
B
C
D
Yerseke
North Sea
The Netherlands
Germany
Belgium
Sampling station
sea-wall
mean low-water line
mussel culture plots
rewatering area
0 2 4 6 km
N

Table 1. Main characteristics (total, average, or range) of the Oosterschelde estuary before (Pre) and after (Post) completion of the coastal engineering project (after Smaal and Boeije 1991).

	Western region		Central region		Total	
	Pre	Post	Pre	Post	Pre	Post
Total surface area (km^2)	106	106	107	107	452	351
Tidal-flat area (km^2)	24.5	23.9	34.8	33.3	170	114
Depth (m)	12.15	12.15	10.35	10.35	8.93	9.01
Volume (10^6 m^3)	1150	1150	996	996	3015	2741
Mean tidal range (cm)	284	247	329	290	374	325
Maximum current velocity (m·s^{-1})	1.5	1	1.5	1	1.5	1
Residence time (days)	10	20	80	140	5–50	10–150
Freshwater load (m^3·s^{-1})	—	—	—	—	70	25
Nitrate–nitrite (winter) (mg·L^{-1})	0.9	0.5	1.1	0.5	1.4	0.5
Phosphate (mg·L^{-1})	0.07	0.05	0.09	0.07	0.08	0.06

ploitation. We therefore define the exploitation carrying capacity as the stock size at which a maximum yield of the marketable cohort is achieved (Smaal et al. 1998).

In the Oosterschelde estuary (southwest Netherlands; Fig. 1), shellfish production is based on bottom culture of mussels and oysters and fisheries of wild cockles. Mussel spat and half-grown mussels are imported from the Wadden Sea and further cultivated on lease sites, mainly in the western and central regions of the estuary. The cockle fishery depends entirely on wild stocks living mainly on the tidal flats. Owing to the Bonamia disease, flat oysters (*Ostrea edulis*) have been decimated, and the cupped oyster (*C. gigas*) is now cultured on a limited scale in the eastern region of the estuary (Dijkema 1997). A significant positive

Fig. 2. Total standing stock (kg ash-free dry weight) in all regions of the Oosterschelde estuary: for mussels (solid bars) and cockles (open bars) since 1980 and for oysters (hatched bar) in 1998.

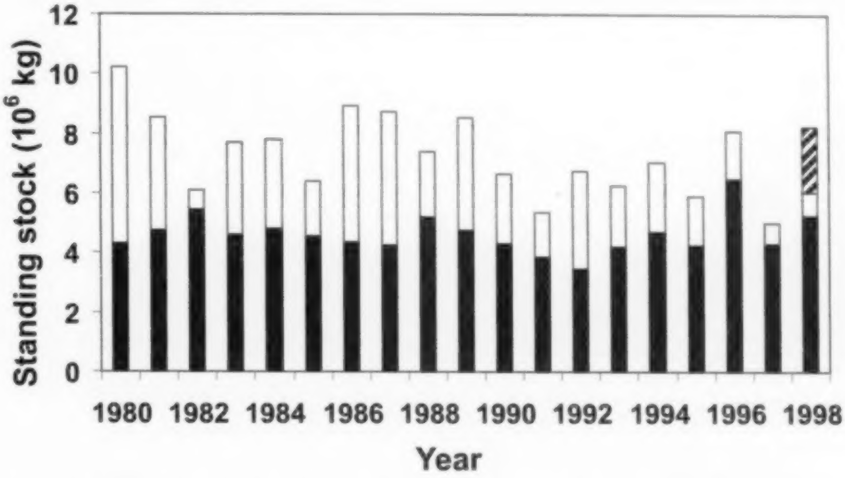

Fig. 3. Annual yield (kg fresh weight) of mussels since 1980 in the period August–December from the western (solid bars) and central (open bar) regions of the Oosterschelde estuary.

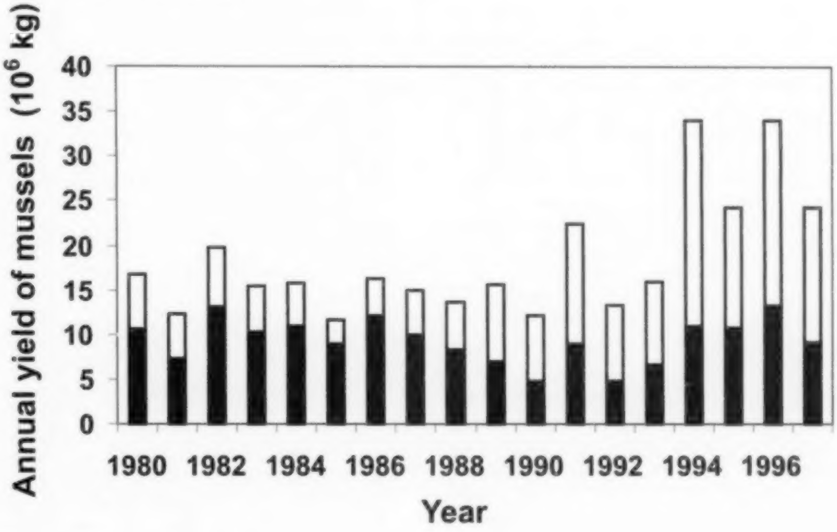

correlation between the annual primary production and the condition of mussels cultured in the Oosterschelde estuary was described by Smaal and Van Stralen (1990), indicating that mussels were food limited in the period 1980–1987.

Owing to a large-scale coastal engineering project, finalised in 1987, that entailed the erection of a storm-surge barrier in the seaward mouth of the estuary and two compartmentalisation dams on the northern and eastern boundaries, the ecosystem has changed: increased water residence time, increased water transparency, increased salinity, decreased current velocities, and decreased nutrient inputs (Nienhuis and Smaal 1994). Exchange with other systems (the North Sea, the rivers Rhine and Meuse) has decreased dramatically, and the system depends mainly on internal nutrient cycles. It was demonstrated that the mussel stock plays a dominant role in nutrient regeneration (Smaal and Prins 1993; Prins and Smaal 1994). Van Stralen and Dijkema (1994) showed that food limitation of mussels continued in the postbarrier period (1987–1990). In addition, they demonstrated a significant negative correlation between bivalve standing stock and mussel condition, indicating that the system was exploited at maximum capacity. Bivalve stocks dominate the ecosystem processes, and it is hypothesised that feedbacks through these filter feeders are now very important in the Oosterschelde ecosystem, owing to the increased water residence time and decreased nutrient loads (Prins and Smaal 1994; Prins et al. 1998).

In the postbarrier period, cultivation methods have been slightly modified and mussel yield has increased (Smaal and Lucas 2000). In this paper, the response of the shellfish

Fig. 4. Average annual values (±SE) for flesh content of harvested mussels (1980–1997) as percentage of total fresh weight (*a*), chlorophyll *a* concentration (central region, 1980–1995; western region, 1981–1997) (*b*), and total suspended particulate matter concentration (1981–1997) (*c*) in the western (circles) and central (squares) regions of the Oosterschelde estuary.

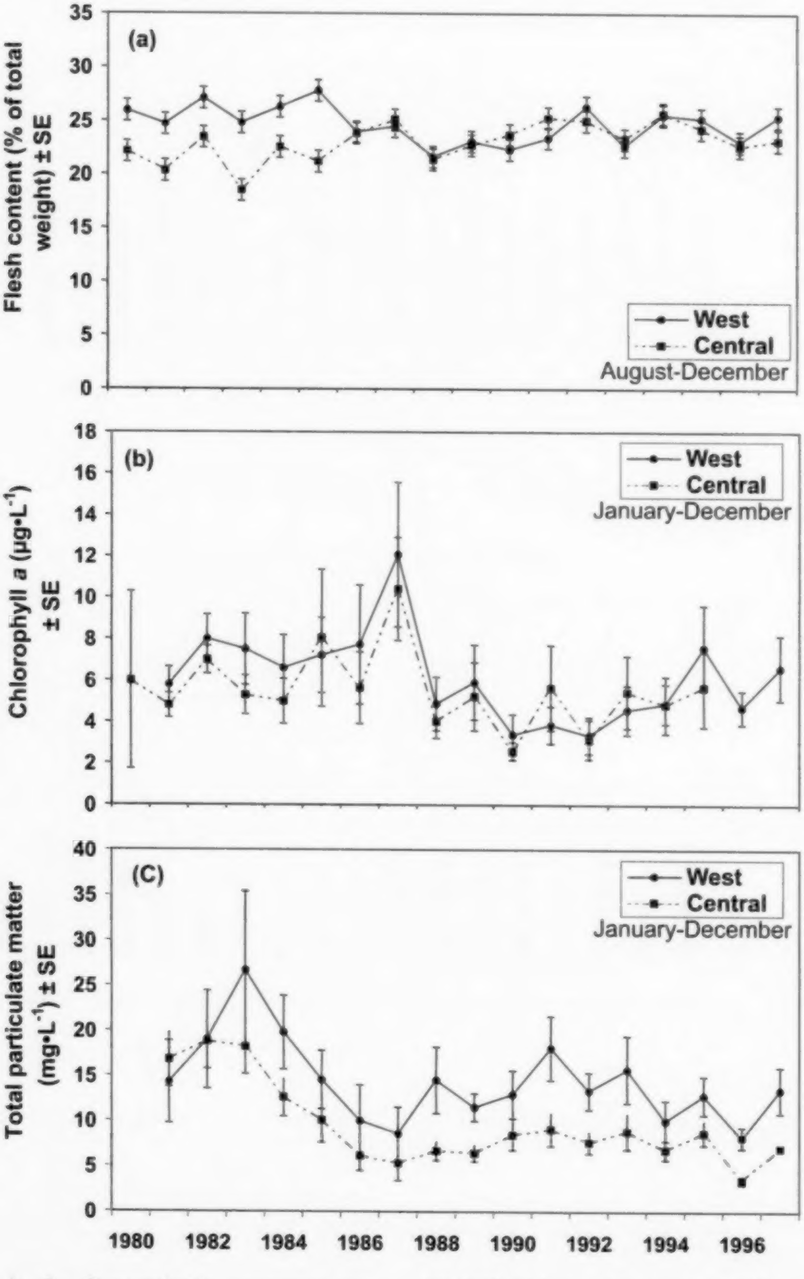

farmers to changes in the Oosterschelde ecosystem processes by anticipating the increased feedbacks between the mussel population and the ecosystem is analysed.

Materials and methods

Study area

The Oosterschelde estuary is a macrotidal system with an average depth of 9 m, a tidal range of 3.25 m, and a surface area of 350 km^2, of which 30% is tidal flats. Owing to a large-scale coastal engineering project, the estuary has changed considerably (Table 1), and is now characterized by high salinity, high water transparency, long water residence time, and low inorganic-nutrient concentrations (Nienhuis and Smaal 1994).

The Oosterschelde estuary has an extensive bottom culture of mussels on cultivation plots that are leased by the farmers from the state. In the eastern region, lease sites are in use by mussel traders

Fig. 5. Total annual primary production in the western (solid bar) and central (open bar) regions of the Oosterschelde estuary for the period 1980–1997.

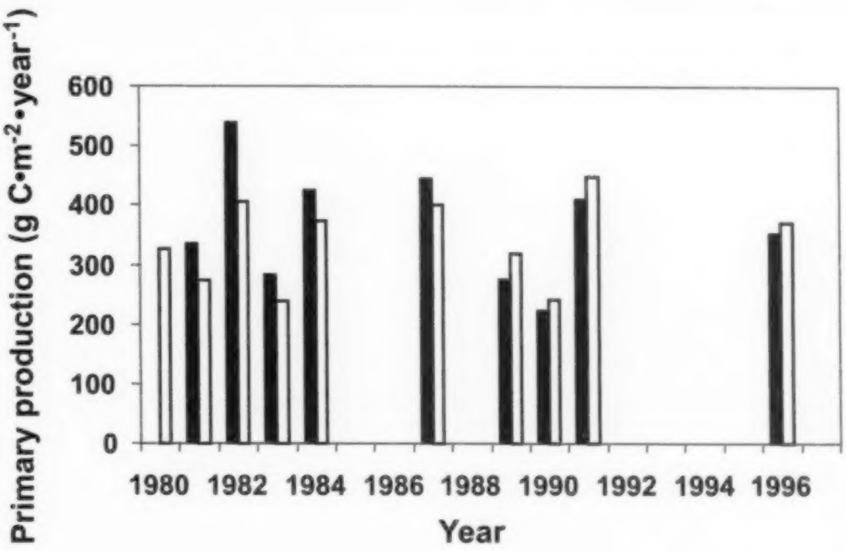

for storage and re-watering of mussels after transport and sale through the auction. Owing to the coastal engineering project, reduced current velocities allowed shellfish culture to be extended to previously unstable sites. Nowadays 22.5 km^2 is in use as subtidal bottom lease sites for mussel culture, 3.4 km^2 for re-watering, and 11 km^2 for bottom culture of oysters. The cultivation time of mussels is 14–33 months.

Cockle fisheries rely on wild stocks that are found in the intertidal areas. These areas are also important for wading birds, and parts of the estuary are now closed to the cockle fishery. Furthermore, a minimum stock of cockles has to be reserved as food for the birds (Smaal and Lucas 2000).

Primary-production, seston, chlorophyll, and nutrient concentrations

For the period 1980–1990, data on primary production and water-quality parameters were derived from Wetsteijn and Kromkamp (1994); later data were derived from Van Berchum and Wattel (1997). Primary-production data after 1990 are unpublished results collected by the same method as previously (J. Kromkamp, Netherlands Institute of Ecology, Centre for Estuarine and Coastal Ecology, P.O. Box 140, 4400 AC Yerseke, The Netherlands, personal communication). Primary production was measured in the western and central regions in the prebarrier period in 1981, 1982, 1983, 1984, and 1987 and in the postbarrier period in 1989, 1990, 1991, and 1996. Water samples for analysis (1.2 L for primary production, 1 L for seston and chlorophyll, 0.1 L for nutrients) of all parameters were taken from the different regions (at a depth of ca. 1 m) randomly in the tidal period. Samples were taken every week in the growing season (April–September), once in 2 weeks in March and October, and monthly in the remaining period. After 1990, primary production was measured biweekly in the growing season and monthly during the rest of the year. The number of observations for suspended particulate matter (SPM) varied from 8 in 1986 to 21 in 1996 (average $n = 13$), and for chlorophyll from 7 in 1987 to 19 in 1996 (average $n = 12$). Samples were brought to the laboratory for immediate primary-production incubation or were processed on board the research vessel. Total primary production (particulate + dissolved production) was measured in a laboratory incubator for 2 h, using the ^{14}C method (Wetsteijn et al. 1990). Column production was calculated according to Wetsteijn and Kromkamp (1994). Primary production is expressed as accumulated column production per year. Seston, chlorophyll *a*, and inorganic-nutrient concentrations were analysed by gravimetric, high performance liquid chromatographic (HPLC), and auto-analyser methods, respectively (Wetsteijn and Kromkamp 1994; Smaal and Haas 1997). Sampling stations used in this study are located in the western and central regions; as the Oosterschelde estuary is a well-mixed system (Klepper 1989), one station per region is considered sufficient to provide representative sampling (Fig. 1).

For correlations with mussel growth, chlorophyll data for the mussel-growing season (June–November) were used. Calculation of the phytoplankton fraction of total particulate matter is based on a carbon to chlorophyll ratio of 40 and a particulate organic matter to particulate organic carbon ratio of 2.5.

Bivalve standing stocks

Data on the standing stocks of mussels and cockles are based on annual stock assessments. Prior to 1990, data were derived from various sources, as described by Van Stralen and Dijkema (1994) and Coosen et al. (1994). Since 1990, extensive surveys for cockles have been carried out in spring on 350 stations in the Oosterschelde estuary. A special cockle-sampling device was constructed with a sample surface of 70 cm^2. Mussel surveys were performed with a Van Veen grab on 500 stations on culture plots in the Oosterschelde estuary. Nearly 100% of the mussels sampled are from cultivated stocks. For wild oysters, only preliminary data since 1998 were available from a stock assessment on tidal flats. This is based on estimations of the area covered by oysters in density classes and in subsamples per class. Subsamples of collected shellfish were analysed for ash-free dry weight by drying for 48 h at 80°C, weighing, ashing at 520°C for 2 h, and re-weighing.

Mussel yield and condition

As all mussels are traded through the auction, total gross yield, net yield, and fish content are registered; hence, a large database of annual yield and condition is available. The annual net yield for a certain year is based on the accumulated yield of the market deliveries throughout the harvesting season (from 1 July until 1 April of the following year). The yield is registered separately for different

Fig. 6. The relationship between condition of harvested mussels and annual primary production in different years (shown as data labels) in the western (*a*) and central (*b*) regions of the Oosterschelde estuary. In the western region, $r^2 = 0.586$ ($p < 0.05$, $n = 9$); in the central region, $r^2 = 0.587$ ($p < 0.01$, $n = 10$).

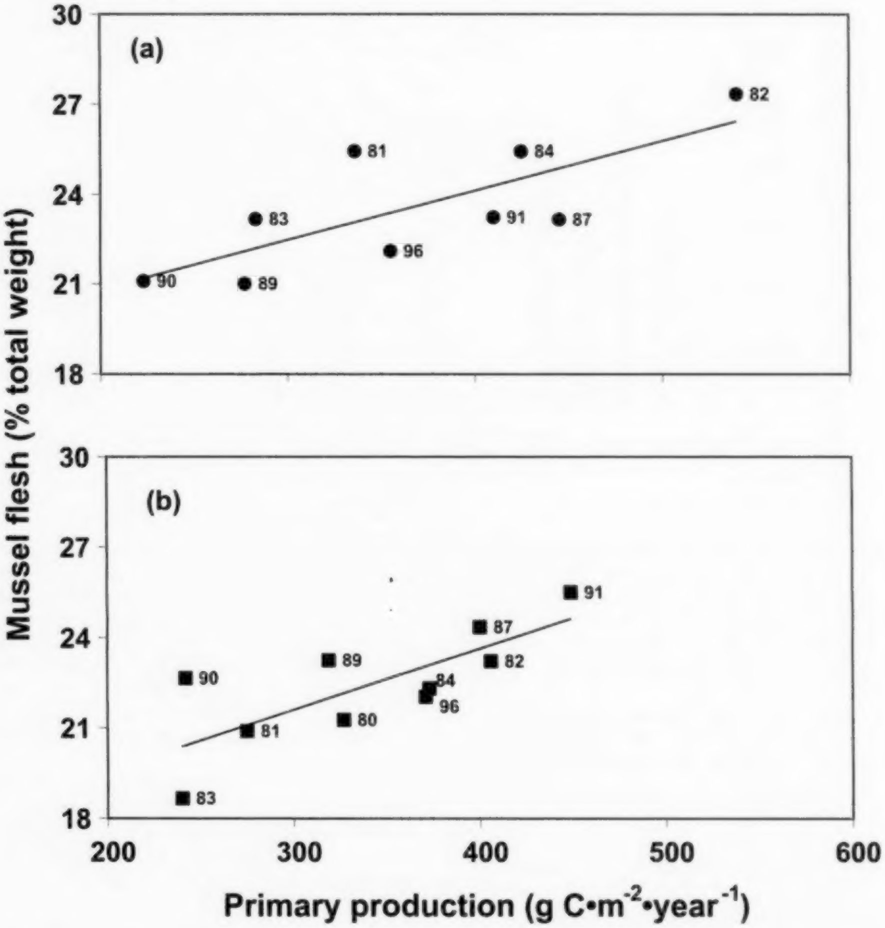

cultivation areas. In this paper, data for the western (Fig. 1, area A) and central (Fig. 1, area B) regions are compared for the period August–December; this period was chosen for comparison with standing stock and condition data over the same period. Data on yield are fresh weight, including the shell. The condition of mussels is estimated as the amount of flesh, when weighed after 5 min of cooking, relative to the total weight, and expressed as percent. It was shown that this condition parameter is significantly correlated with the growth rate (Van Stralen and Dijkema 1994). Mussel-condition data were averaged per area for the period August–December. The number of market deliveries varied between years from 25 in 1992 to 297 in 1994. The average number of observations is 64.

Results

Shellfish stocks and mussel yield

The standing stock of mussels and cockles is shown for the period 1980–1998 (Fig. 2). Data on the stock of wild oysters *C. gigas* are available for 1998 only. Since completion of the coastal engineering project in 1987, the cockle stock has decreased to about 0.7×10^6 kg ash-free dry weight (AFDW). The oyster stock now partly occupies former cockle habitats in the Oosterschelde estuary, and has a stock size of 2×10^6 kg AFDW. The mussel stock has not changed dramatically and is still the major shellfish species (5×10^6 kg AFDW; 100×10^6 kg fresh weight).

From 1994–1997, the production of mussels in the period August–December from the main cultivation areas in the Oosterschelde estuary was about 30×10^6 kg fresh weight. There was an increase in yield in the central region (Fig. 3). In the prebarrier period, the western region delivered the major part of the production, while in the postbarrier period, the central region is the main production area.

In the prebarrier period, the condition of harvested mussels was better in the western region than in the central region (Fig. 4*a*). In the postbarrier period, the differences have completely vanished.

Seston, phytoplankton, and primary production

The chlorophyll *a* concentration has decreased since the

Fig. 7. The relationship between condition of harvested mussels and annual average chlorophyll *a* concentration for the growing season (June–November) in western (*a*) and central (*b*) regions of the Oosterschelde estuary in the postbarrier period (years shown as data labels). In the western region, $r^2 = 0.72$ ($p < 0.05$, $n = 10$); in the central region, $r^2 = 0.344$ ($p = 0.126$, $n = 8$).

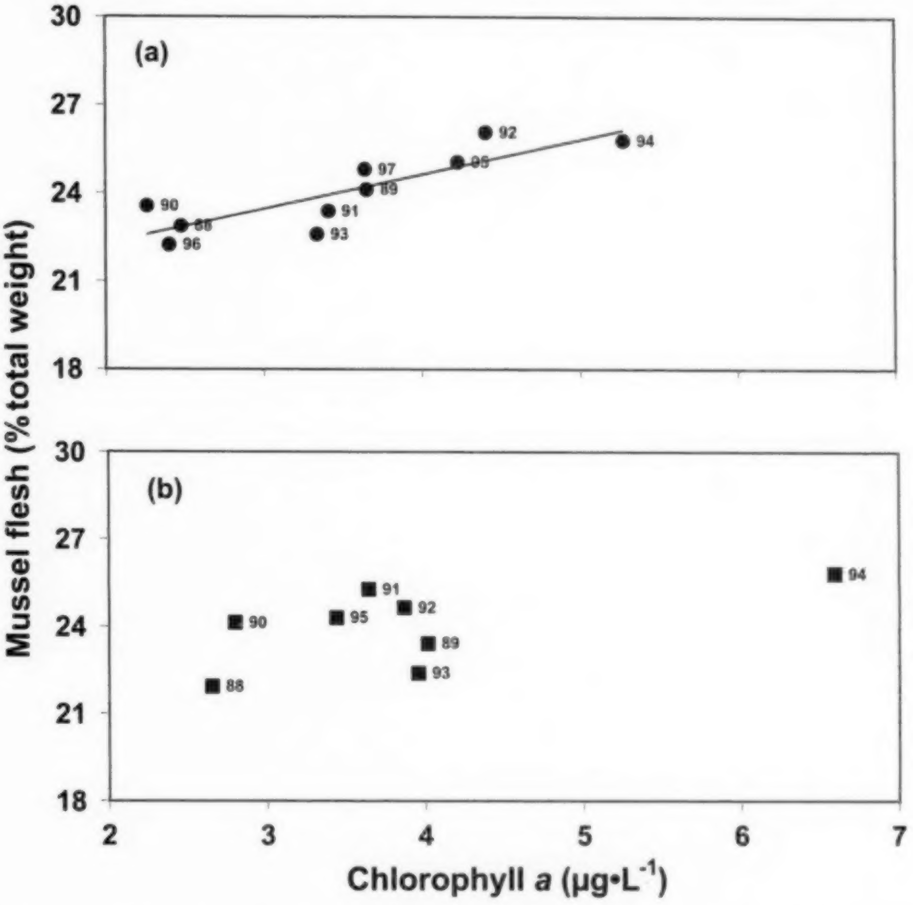

completion of the Oosterschelde project in 1987, and the differences between the western and central regions have disappeared (Fig. 4*b*). Also, the total SPM concentration has decreased since 1984, as a response to coastal engineering works in the mouth and at the eastern boundary of the Oosterschelde estuary. However, differences in the concentration of total SPM between the western and central regions have been maintained (Fig. 4*c*). The phytoplankton fraction of seston has increased in the central region only. In contrast with these changes, primary production has not shown any dramatic change (Fig. 5).

As a consequence of maintained primary production and decreased chlorophyll *a* concentrations, phytoplankton turnover in the postbarrier period has increased from 0.3 to 0.6 times per day in the western region and from 0.4 to 0.8 times per day in the central region.

Exploitation capacity

The exploitation capacity of ecosystems depends on the availability of food and the number of competitors. The relationship between mussel condition and food availability is shown in Figs. 6 and 7. There is a significant correlation between mussel condition and annual primary production in western ($r^2 = 0.59$, $n = 9$, $p < 0.05$) and central ($r^2 = 0.587$, $n = 10$, $p < 0.01$) regions over the whole period. For the postbarrier period, the correlation between mussel condition and annual average chlorophyll a concentration is significant in the western ($r^2 = 0.72$, $n = 10$, $p < 0.01$) but not in the central ($r^2 = 0.34$, $n = 8$, $p = 0.126$) region (Fig. 7). Figures 6 and 7 show that the condition of market-size mussels is reduced in years with low primary production and low chlorophyll *a* concentration.

The relationship between mussel condition and the standing stock of filter feeders (mussels and cockles together) shows a significant correlation in the prebarrier period in the western region ($r^2 = 0.72$, $n = 8$, $p < 0.01$) (Fig. 8*a*). This relationship is not significant for the postbarrier period ($p = 0.957$). For the central region, this correlation is not significant in either period (prebarrier: $p = 0.79$; postbarrier: $p = 0.29$; Fig. 8*b*). At the present time, the growth of mussels seems to be related only to food availability and not to stock size. Lower stocks do not correspond to better mussel condi-

Fig. 8. The relationship between condition of harvested mussels and total standing stock of mussels and cockles in the western (*a*) and central (*b*) regions of the Oosterschelde estuary (prebarrier period, solid symbols; postbarrier period, open symbols). In the western region in the prebarrier period, $r^2 = 0.72$ ($p < 0.01$, $n = 8$).

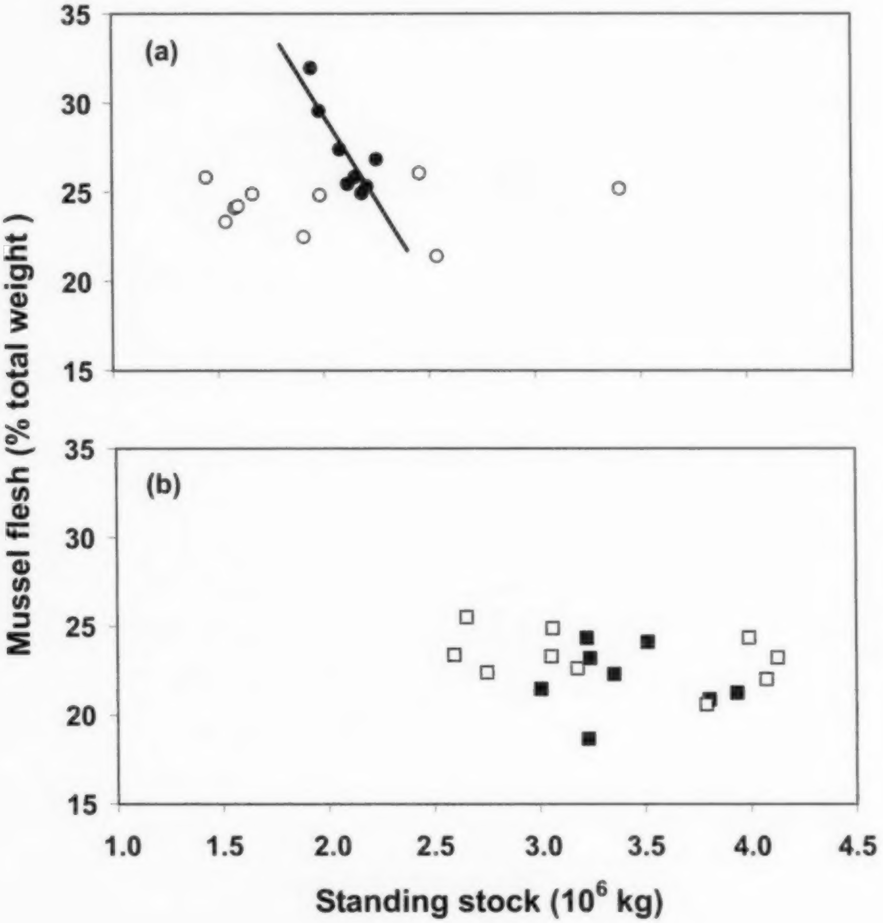

tion, indicating overstocking of the system and density-dependent growth limitation.

As shown in Fig. 9, yield has increased only in the central region, and there is no significant correlation between the annual yield of mussels and the corresponding shellfish stock (western: prebarrier, $p = 0.29$; postbarrier, $p = 0.64$; central: prebarrier, $p = 0.27$; postbarrier, $p = 0.63$). The absence of a stock–yield relation can be ascribed to the fact that mussels are brought in by the farmers and harvested after a certain growth period. Nowadays, this is a continuous process: new stocks are supplied to the system as a function of harvesting. The culture practise has changed and now the central region is used as a market production area rather than for storage and for growing from juvenile to medium-sized mussels, as was the case before 1990.

Figure 10 shows that the yield per stock in the western region has recovered after a short period of decreased yields just after completion of the coastal engineering project in 1987; in the central region, the yield per stock has increased to a level similar to that in the western region. Meanwhile, the percent flesh of produced mussels has stabilized at about 21–26% (Fig. 4*a*).

Discussion

Changes in the Oosterschelde ecosystem

The changes in the Oosterschelde ecosystem in response to the coastal engineering project have been extensively studied and are documented in Nienhuis and Smaal (1994). It was concluded that dominant ecosystem processes showed a resilient response, owing to adaptations in the structure of communities and spatial shifts of habitats (Nienhuis et al. 1994). Primary production is maintained in response to opposite changes in light and nutrient availability: light conditions improved and nutrient concentrations decreased. Bakker et al. (1994) demonstrated adaptations of the phytoplankton community to the new light–nutrient–salinity conditions: the phytoplankton growth season started earlier and lasted longer; the original succession of spring and summer species vanished and the plankton community became domi-

Fig. 9. The annual yield of mussels in total fresh weight as a function of the total standing stock of mussels and cockles in ash-free dry weight, in the western (*a*) and central (*b*) regions of the Oosterschelde estuary (prebarrier period, solid symbols; postbarrier period, open symbols).

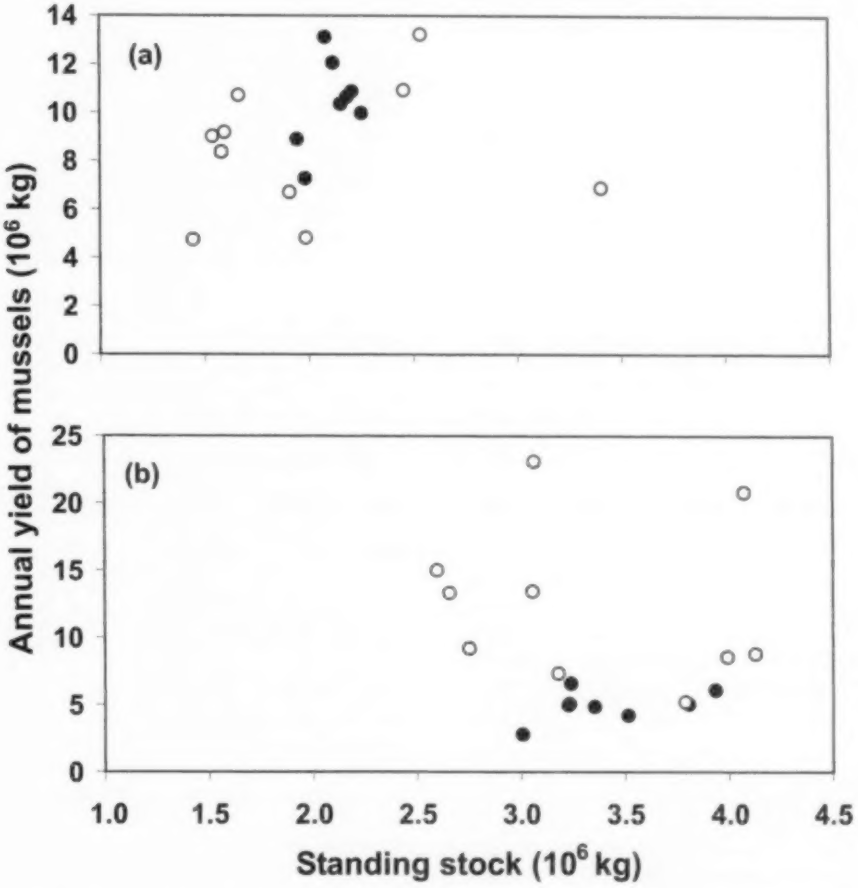

nated by small flagellates and weakly silicified diatoms. As we show in this paper, phytoplankton turnover has increased from 0.3 to 0.6 times/day in the western region and from 0.4 to 0.8 times/day in the central region. Decreased seston concentrations have improved food quality in the central region since 1987, despite decreased chlorophyll *a* concentrations.

Food-limited growth

Despite these changes, the relationship between mussel condition and primary production or chlorophyll concentration has been conserved. A highly significant positive correlation between mussel condition and annual primary production was described by Smaal and Van Stralen (1990) for the prebarrier period and by Van Stralen and Dijkema (1994) for the period 1981–1990; Van Stralen and Dijkema (1994) describe a highly significant positive correlation between mussel condition and chlorophyll *a* concentration in this period, as well.

In this paper, we confirm a significant correlation between mussel condition and primary production for the whole period 1980–1997, and between mussel condition and chlorophyll *a* concentration in the western region for the postbarrier period. As shown by Van Stralen and Dijkema (1994), the relationship between chlorophyll *a* concentration and percent flesh was also significant in the prebarrier period in the western region. In the central region, the relationship was not significant in the pre- and post-barrier periods. This is explained by the fact that chlorophyll is an intermediate variable between production and consumption; hence, a relationship with growth or condition is less likely than for primary production. Primary production gives the best indication of food production. Therefore, it is concluded that mussel condition and growth are food limited at the ecosystem level.

A similar observation was made by Blanton et al. (1987) for the Ria de Arosa, Spain, another important area of extensive mussel culture in Europe. They describe a significant positive relationship between mussel condition and the upwelling of nutrients from the ocean; nutrient-limited food production is stimulated through upwelling and, hence, mussels grow faster in years with a better upwelling index.

A synthesis of the relationship between food production and benthos is given by Herman et al. (1999). These authors showed a significant relationship between system-averaged

Fig. 10. Changes in yield as a fraction of the stock of mussels on a fresh weight basis in the western (circles) and central (squares) regions of the Oosterschelde estuary over the period 1980–1997.

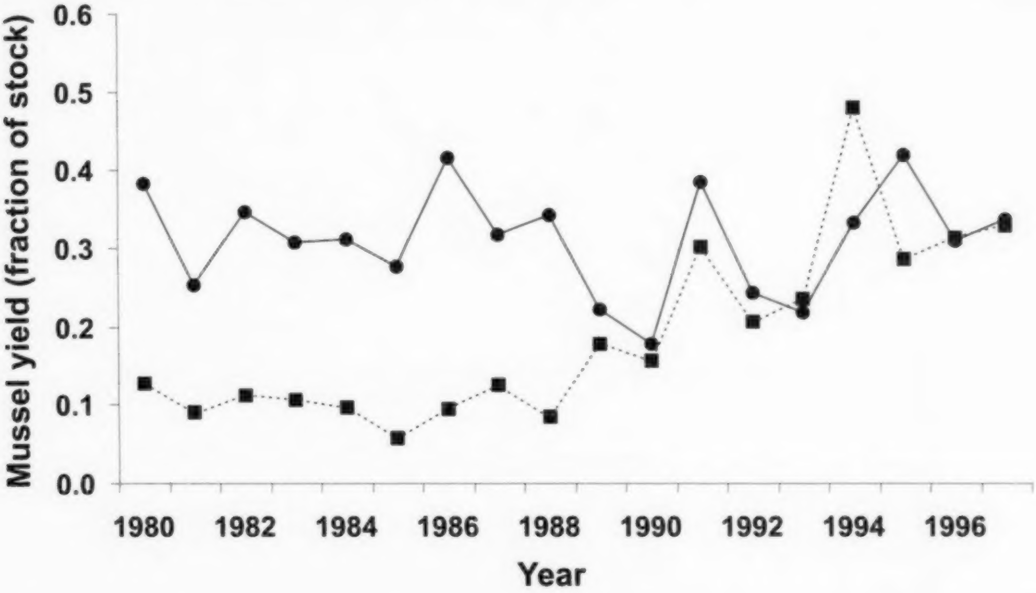

macrobenthic biomass and primary production for a large number of estuarine ecosystems. As suspension feeders dominate total benthos (in the Oosterschelde estuary their contribution was estimated at 74%), there is a clear indication that suspension feeders are food limited at the ecosystem level.

Standing stock, growth, and yield

In the prebarrier period, a negative relationship between standing stock and growth was demonstrated for the western region by Van Stralen and Dijkema (1994). They concluded that the carrying capacity of the Oosterschelde estuary was fully exploited, depending mainly on the annual primary production and the stock size. In this period, the western region was the most important production area and the central region was used predominantly for the cultivation of half-grown mussels.

In contrast with these earlier findings, we show in this paper that, for the postbarrier period, the relationship between the condition and standing stock of shellfish could no longer be demonstrated. This is an indication that the exploitation of the Oosterschelde system may exceed its maximum capacity, and that there might be density-dependent growth limitation, unless stocks of other filter feeders have changed.

Our standing-stock estimates prior to 1998 do not include benthic and pelagic suspension feeders other than mussels and cockles. No quantitative data are available for the cupped oyster (*C. gigas*), but there are clear indications that this stock has increased steadily since the first introduction in 1965 (Drinkwaard 1999). New data for this oyster show a contribution to total shellfish biomass of about 30%. Owing to their large filtration capacity, the contribution to total clearance time (time to potentially filter the water column) is probably more than 30% (see Bougrier et al. 1995). However, cockle stocks have decreased and total bivalve stock has been maintained.

Data on zooplankton are only available for the Oosterschelde estuary for the period 1982–1988 (Bakker and van Rijswijk 1994). However, there are indications that the impact of zooplankton is inferior to that of benthic suspension feeders, and that zooplankton can be outcompeted to a certain extent (Herman and Scholten 1990). Studies based on empirical data and simulations with the Oosterschelde-ecosystem model have shown a limited and rather constant impact of other benthic suspension feeders, such as tunicates and sponges (Klepper et al. 1994). It is therefore concluded that mussels and cockles are the dominant filter feeders, and that the relationship between standing stock and mussel growth will not be improved by including other suspension feeders.

Exploitation capacity was defined as the stock that gives maximum yield. This is based on an analysis of oyster production in Marennes-Oléron (France) (Héral 1993; Bacher et al. 1998). For the Oosterschelde estuary, the relation between stock and yield does not show a clear optimum, indicating that the exploitation may exceed the capacity of the system. Yet, yields have increased in the postbarrier period. This can be explained by a cultivation technique that is based on growing mussels in both the Wadden Sea and the Oosterschelde estuary. Mussel seed is harvested in the Wadden Sea and brought to lease sites. Most farmers have lease sites in both areas and can decide what area they prefer, depending on the quality of their lease sites, their actual stock, and the amount of mussel seed (Van Stralen and Dijkema 1994). The general practice is to bring mussels from the Wadden Sea to the Oosterschelde, as the estuary is a less storm-sensitive area. Therefore, the strategy of the farmers, i.e., changes in mussel culture, have to be included in the analysis of exploitation capacity.

Changes in mussel culture

We have shown that the yield per stock has increased in the postbarrier period, particularly in the central region. After 1987, new lease sites were exploited, to compensate for a decrease of quality in some areas due to a decrease in current velocity. After a test-period redistribution of lease sites took place, higher yields were achieved. Particularly in the central region, lease sites are now used for culture from half-grown to consumption-sized mussels rather than to produce half-grown mussels. The farmers adapted to the new Oosterschelde and shifted the lease sites to new locations. This can be considered a response to system changes. However, the adaptations also have an impact on the system, owing to the role of shellfish in ecosystem processes.

Feedbacks

Prins et al. (1998) present a review of the interactions between benthic suspension feeders and ecosystem processes. They identify a number of positive and negative feedbacks that are relevant for carrying-capacity estimations. It was shown for the Oosterschelde estuary, on the basis of in situ measurements and mesocosm studies, that grazing, production, and resuspension of biodeposits, and retention and remineralisation of nutrients, are the main processes in the interaction between mussels and their food (Prins 1996). Grazing is important, as the filtration by the bivalves is estimated at 2 $m^3 \cdot m^{-2} \cdot d^{-1}$, which is a clearance time of about 5 days. As the water residence time has doubled to 50–100 days, phytoplankton is controlled by bivalve grazing (Dame and Prins 1998). In addition, external nutrient loads decreased by 60%. Based on empirical and model studies, it was estimated that the contribution of mussel beds to total nitrogen mineralisation is now about 30% (Prins and Smaal 1994), which must have a positive effect on the availability of nitrogen as a limiting nutrient after the spring bloom. Lower chlorophyll *a* concentrations and maintained primary production are induced by the bivalves. Filtration and nutrient regeneration stimulate phytoplankton turnover, and this is considered to be an important feedback of the bivalves on their own food source.

The relationship between water residence time, primary-production time, and clearance time was described by Dame and Prins (1998) as a framework for the evaluation of the carrying capacity of ecosystems for bivalve filter feeder populations. Water residence time in the Oosterschelde estuary has increased, and exchange with other systems has decreased. Primary-production time has decreased and the rate of phytoplankton turnover has increased. Increased water residence time is compensated for by faster phytoplankton turnover and, hence, clearance time, i.e., bivalve stock, could be maintained. As the mussel stocks are managed by the farmers, it is concluded that their strategy can be considered to be a feedback to the system changes.

Acknowledgements

The authors are grateful to the Dutch mussel board for the use of yield and condition data. We also thank Rijkswaterstaat for chlorophyll *a* and total particulate matter concentration data, and J. Kromkamp for primary-production data since 1990. The comments of three anonymous reviewers were valuable in improving the manuscript. Part of this work was supported by EU-ESSENSE contract No. FAIR-CT98-4201.

References

Bacher, C., Duarte, P., Ferreira, J.G., Héral, M., and Raillard, O. 1998. Assessment and comparison of the Marennes-Oléron Bay (France) and Carlingford Lough (Ireland) carrying capacity with ecosystem models. Aquat. Ecol. **31**: 379–394.

Bakker, C., and van Rijswijk, P. 1994. Zooplankton biomass in the Oosterschelde (SW Netherlands) before, during and after the construction of a storm-surge barrier. Hydrobiologia, **282/283**: 127–144.

Bakker, C., Herman, P.M.J., and Vink, M. 1994. A new trend in the development of the phytoplankton in the Oosterschelde (SW Netherlands) during and after the construction of a storm-surge barrier. Hydrobiologia, **282/283**: 79–100.

Blanton, J.O., Tenore, K.R., Castillejo, F., Atkonson, L.P., Schwing, F.B., and Lavin, A. 1987. The relationship of upwelling to mussel production rias on the western coast of Spain. J. Mar. Res. **45**: 497–511.

Bougrier, S., Geairon, P., Deslous-Paoli, J.M., Bacher, C., and Jonquieres, G. 1995. Allometric relationships and effects of temperature on clearance and oxygen consumption rates of *Crassostrea gigas* (Thunberg). Aquaculture, **134**: 143–154.

Carver, C.E.A., and Mallet, A.L. 1990. Estimating the carrying capacity of a coastal inlet for mussel culture. Aquaculture, **88**: 39–53.

Coosen, J.C., Twisk, F., Van der Tol, M.W.M., Lambeck, R.H.D., Van Stralen, M.R., and Meire, P.M. 1994. Variability in stock assessment of cockles (*Cerastoderma edule* L.) in the Oosterschelde (in 1980–1990) in relation to environmental factors. Hydrobiologia, **282/283**: 381–396.

Dame, R.F. 1996. Ecology of marine bivalves: an ecosystem approach. CRC Press, Boca Raton.

Dame, R.F., and Prins, T.C. 1998. Bivalve carrying capacity in coastal ecosystems. Aquat. Ecol. **31**: 409–421.

Dijkema, R.D. 1997. Molluscan fisheries and culture in the Netherlands. NOAA (Natl. Ocean Atmos. Adm.) Tech. Rep. NMFS (National Marine Fisheries Service) 129. pp. 115–134.

Drinkwaard, A.C. 1999. Introductions and developments of oysters in the North Sea area: a review. Helgol. Meeresunters. **52**: 301–308.

Gosling, E. (*Editor*). 1992. The mussel *Mytilus*: ecology, physiology, genetics and culture. Elsevier, Amsterdam.

Grant, J., Dowd, M., Thompson, K., Emerson, C., and Hatcher, A. 1993. Perspectives on field studies and related biological models of bivalve growth and carrying capacity. *In* Bivalve filter feeders in estuarine and coastal ecosystem processes. *Edited by* R.F. Dame. Springer-Verlag, Berlin. pp. 371–420.

Héral, M. 1993. Why carrying capacity models are useful tools for management of bivalve molluscs culture. *In* Bivalve filter feeders in estuarine and coastal ecosystem processes. *Edited by* R.F. Dame. Springer-Verlag, Berlin. pp. 455–477.

Herman, P.M.J., and Scholten, H. 1990. Can suspension-feeders stabilise estuarine ecosystems? *In* Trophic Relationships in the Marine Environment: Proceedings of the 24th European Marine Biology Symposium. Vol. 35. *Edited by* M. Barnes and R. Gibson. Aberdeen University Press, Aberdeen. pp. 104–116.

Herman, P.M.J., Middelburg, J.J., Van de Koppel, J., and Heip, C.H.R. 1999. Ecology of estuarine macrobenthos. Adv. Ecol. Res. **29**: 195–240.

Incze, L.S., Lutz, R.A., and True, E. 1981. Modelling carrying capacities for bivalve molluscs in open, suspended culture systems. J. World Maric. Soc. **12**: 143–155.

Klepper, O. 1989. A model of carbon flows in relation to macrobenthic food supply in the Oosterschelde estuary (SW Netherlands). Ph.D. thesis, Wageningen University, The Netherlands.

Klepper, O. Van der Tol, M.W.M., Scholten, H., and Herman, P.M.J. 1994. SMOES: a simulation model for the Oosterschelde ecosystem. Part I: description and uncertainty analysis. Hydrobiologia, **282/283**: 437–452.

Krebs, J. 1972. Ecology—the experimental analysis of distribution and abundance. Harper and Row, New York. p. 694.

Nienhuis, P.H., and Smaal, A.C. (*Editors*). 1994. The Oosterschelde estuary (The Netherlands). A case study of a changing ecosystem. Kluwer Academic Publishers, Dordrecht, The Netherlands.

Nienhuis, P.H., Smaal, A.C., and Knoester, M. 1994. The Oosterschelde estuary: an evaluation of changes at the ecosystem level induced by civil-engineering works. Hydrobiologia, **282/283**: 575–592.

Prins, T.C. 1996. Bivalve grazing, nutrient cycling and phytoplankton dynamics in an estuarine ecosystem. Ph.D. thesis, Wageningen University, The Netherlands.

Prins, T.C., and Smaal, A.C. 1994. The role of the blue mussel *Mytilus edulis* in the cycling of nutrients in the Oosterschelde estuary (The Netherlands). Hydrobiologia, **282/283**: 413–429.

Prins, T.C., Smaal, A.C., and Dame, R.F. 1998. A review of feedbacks between bivalve grazing and ecosystem processes. Aquat. Ecol. **31**: 349–359.

Smaal, A.C., and Boeije, R.C. 1991. Veilig getij, de effecten van de waterbouwkundige werken op het getijdemilieu van de Oosterschelde. [In Dutch.] GWWS 911.088 DGW, Middelburg, The Netherlands. p. 131.

Smaal, A.C., and Haas, H.A. 1997. Seston dynamics and food availability on mussel and cockle beds. Estuar. Coast. Shelf Sci. **45**: 247–259.

Smaal, A.C., and Héral, M. (*Editors*). 1998. Modelling bivalve carrying capacity. Aquat. Ecol. **31**(4).

Smaal, A.C., and Lucas, L. 2000. Regulation and monitoring of marine aquaculture in the Netherlands. J. Appl. Ichthyol. **16**: 187–191.

Smaal, A.C., and Prins, T.C. 1993. The uptake of organic matter and the release of inorganic nutrients by bivalve suspension feeder beds. *In* Bivalve filter feeders in estuarine and coastal ecosystem processes. *Edited by* R.F. Dame. Springer-Verlag, Berlin. pp. 271–298.

Smaal, A.C., and Van Stralen, M.R. 1990. Average annual growth and condition of mussels as a function of food source. Hydrobiologia, **195**: 179–188.

Smaal, A.C., Prins, T.C., Dankers, N., and Ball, B. 1998. Minimum requirements for modelling bivalve carrying capacity. Aquat. Ecol. **31**: 423–428.

Van Berchum, A., and Wattel, G. 1997. De Oosterschelde, van estuarium naar zeearm. [In Dutch.] RIKZ-97.034. DGW, Middelburg, The Netherlands.

Van Stralen, M.R., and Dijkema, R.D. 1994. Mussel culture in a changing environment: the effects of a coastal engineering project on mussel culture (*Mytilus edulis* L.) in the Oosterschelde (SW Netherlands). Hydrobiologia, **282/283**: 359–379.

Wetsteijn, L.P.M.J., and Kromkamp, J. 1994. Turbidity, nutrients and phytoplankton primary production in the Oosterschelde (The Netherlands) before, during and after a large-scale coastal engineering project (1980–1990). Hydrobiologia, **195**: 163–177.

Wetsteijn, L.P.M.J., Peeters, J.C.H., Duin, R.N.H.M., Vegter, F., and De Visscher, P.R.M. 1990. Phytoplankton primary production and nutrients in the Oosterschelde (The Netherlands) during the pre-barrier period 1980–1984. Hydrobiologia, **195**: 163–177.

A numerical model of flow modification induced by suspended aquaculture in a Chinese bay

Jon Grant and Cedric Bacher

Abstract: A finite element circulation model of flow was constructed for Sungo Bay, China, a site of dense cultivation of both marine bivalves and kelp, to assess the magnitude of friction due to culture structure and its implications for particle exchange. In the model, parameterization of friction was modified to reflect the patterns of culture configuration in the bay and the results compared with the default case with no culture. Results of model output indicate that suspended aquaculture results in a 20% reduction in current speed in the main navigation channel and a 54% reduction in speed in the midst of a culture area. In the channel, reduced flow had little effect on tracer exchange under mid-ebb conditions, but the presence of culture structure caused a 41% decrease in exchange rate compared with the absence of culture. These results indicate that disregard for physical barriers associated with culture will result in a serious overestimation of the particle renewal term and thus an overestimation of carrying capacity. Further work is required to measure the characteristics of culture (spacing, length scale), quantify their magnitude of flow retardation in the field, and improve model parameterization of the frictional effects of various types of culture.

Résumé : Un modèle de circulation du flux aux éléments finis a été élaboré pour la baie de Sungo en Chine, un site d'intense culture de bivalves marins et de varech, afin d'évaluer la friction générée par l'équipement d'élevage et ses répercussions sur l'échange des particules. La configuration des paramètres de friction dans le modèle a permis de simuler la structure d'élevage dans la baie et de comparer les résultats avec la situation par défaut, donc en l'absence de culture. Il en ressort que la présence d'élevages en suspension cause une réduction de 20% de la vitesse du courant dans le principal chenal de navigation et une réduction de 54% dans la zone d'élevage. Dans le chenal, cette réduction a peu d'effet sur les échanges de traceurs en pleine marée descendante; en revanche, la présence de l'équipement d'élevage cause une réduction de 41% du taux d'échange. Ces résultats indiquent que de ne pas tenir compte des barrières physiques associées à l'élevage résultera en une surestimation importante du taux de renouvellement des particules et, ainsi, du stock limite. Il reste à déterminer les caractéristiques de l'élevage (espacement, échelle de longueur), mesurer sur le terrain leur effet de ralentissement du débit et améliorer la configuration dans le modèle des paramètres décrivant les effets de friction générés par divers types de culture.

[Traduit par la Rédaction]

Introduction

Suspended mariculture of marine bivalves involves dense aggregations of animals in cages, nets, or other containment systems hung from floats or rafts. Bivalve suspension feeding can deplete ambient water of particulate food and thus become self-limiting for expansion of culture. The balance between particle depletion and renewal is the basis for most models of carrying capacity developed for suspended culture (Grant 1996; Wildish and Kristmanson 1997). However, in addition to suspension feeding, it is apparent that the suspended structure should impact particle renewal by retarding ambient flow via enhanced drag. Despite the intuitive importance of this frictional effect, there is only a single comprehensive field study of currents through culture leases (Boyd and Heasman 1998) and no models that incorporate this source of drag. Analogous effects have been examined for natural mussel beds (Fréchette et al. 1989) and for canopies of macroalgae (Andersen et al. 1996; Jackson 1997), but these are sources of roughness that originate from the seabed rather than from the water surface. Existing models of flow through culture ecosystems are parameterized in the absence of the culture itself (Raillard and Menesguen 1994), except for bottom culture in which the roughness of the animals is explicit (Campbell and Newell 1998). In many cases, this deletion is appropriate, since the areal extent of culture is small and its impact difficult to measure. However, in large-scale culture practiced in countries such as China, entire bays may be dominated by suspended culture, making inclusion of these structures mandatory in consideration of particle renewal. Although we have emphasized bivalve culture, suspended culture of kelp and other seaweeds will have a similar impact on flow. In one of the main Chinese culture sites (Sungo Bay), Zhao et al. (1996) suggested that there has been a 50% decrease in current speed over an 11-year period of increasing mariculture development.

In the present study, we include culture in a two-dimensional finite element model of circulation in Sungo Bay to predict the effects of scallop and kelp culture on tidal current speed and flow pattern and their implications

Received January 11, 2000. Accepted November 18, 2000. Published on the NRC Research Press Web site on April 25, 2001.
J15525

J. Grant.[1] Department of Oceanography, Dalhousie University, Halifax, NS B3H 4J1, Canada.
C. Bacher. CREMA, B.P. 5, Place du séminaire, 17137 L'Houmeau, France.

[1] Corresponding author (e-mail: jon.grant@dal.ca).

DOI: 10.1139/cjfas-58-5-1003

Fig. 1. Bathymetry of Sungo Bay and its location in People's Republic of China.

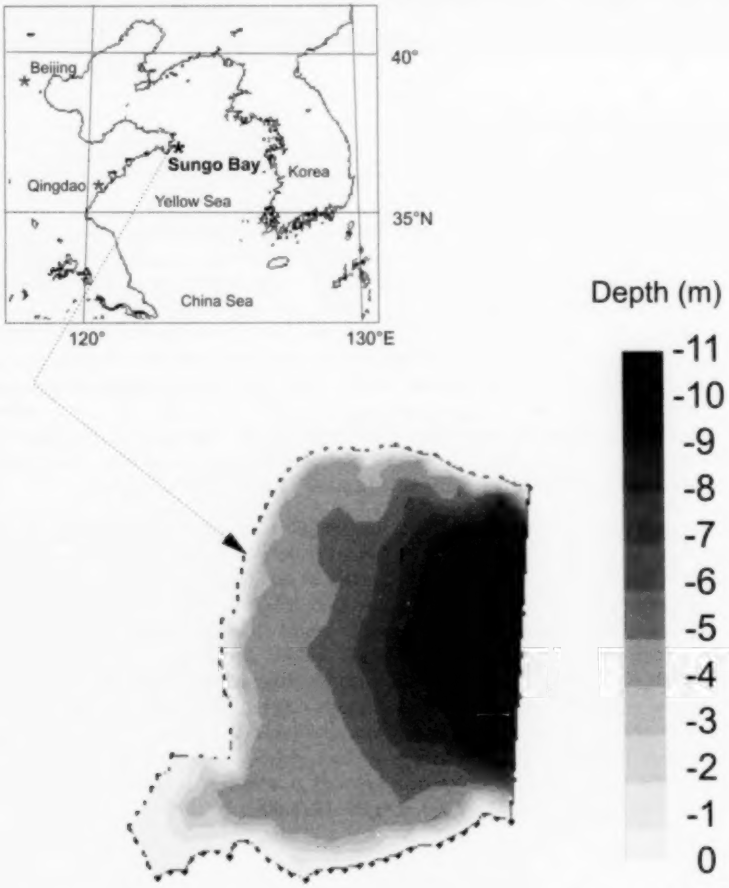

for food provision to scallops. This is achieved by varying drag in locations in the bay based on culture maps and comparing circulation with the default case of no culture. We do not attempt to develop a temporally comprehensive model of this bay, since there are limited data for the boundary conditions. Instead, we concentrate on producing an accurate representation for several tidal cycles in order to examine the effects of culture on circulation.

Materials and methods

Study area

Sungo Bay, located in Shandong Province (37°01′–37°09′N, 122°24′–122°35′E), has been under culture for more than 20 years and is among the largest aquaculture production sites in China (Guo et al. 1999). The bay is approximately 140 km^2 with a fairly evenly graded depth distribution ranging to 15 m (Fig. 1). Seasonal temperatures range from 2 to 26°C and suspended particulate material from 5 to 40 mg·L^{-1}, with organic contents of 14–41% and chlorophyll *a* levels of 2–10 μg·L^{-1} (Kuang et al. 1996). Virtually the entire bay is used for culture of invertebrates and plants, the two main species being kelp (*Laminaria japonica*) and scallops (*Chlamys farreri*). According to 1994 culture statistics, there were 3300 and 1333 ha of culture for these two species, respectively (Zhao et al. 1996). They are cultured in both mono- and polyculture from suspended longlines (Fang et al. 1996*c*). Scallops are contained either in lantern nets or by ear-hanging and kelps tied freely to ropes. In polyculture areas, kelp ropes may be suspended across longlines. Three trends in culture are an increase in scallop culture relative to kelps, an enlargement in the seaward extent of kelp culture, and a decrease in ear-hanging relative to lantern nets. More recently, increased mortality of scallops has led to greater emphasis on oyster culture. The effects of the culture structures on flow are obvious to the casual observer; ocean swells travel through the bay, but rarely are there whitecaps within the culture areas. Sungo Bay has been studied for about 20 years, with extensive studies of bivalve ecophysiology, seston, circulation, and carrying capacity (e.g., Fang et al. 1996*a*, 1996*b*). There are existing numerical models of Sungo Bay circulation published in the Chinese literature (Zhao et al. 1996), indicating that there is a gyre circulation from north to south.

Model of Sungo Bay

A numerical model of Sungo Bay was developed using Aquadyn 3.0, a Windows-based program that provides construction of the model finite element mesh as well as a hydrodynamic model based on the vertically averaged St. Venant equations (HydroSoft Energie; http://www.hydrosoftenergie.com). The model also allows introduction of tracers at any node. Tidal differences in phase measured with pressure gauges at the mouth of the bay were input to the model as a time series to produce barotropic flow. Wind data are

Fig. 2. Distribution of drag due to aquaculture of scallops and kelp in Sungo Bay parameterized as Manning coefficients. (*a*) Culture configuration 1; (*b*) culture configuration 2. Marked node 60 is in the main channel and node 115 is in the midst of culture areas. See text for details on culture configurations

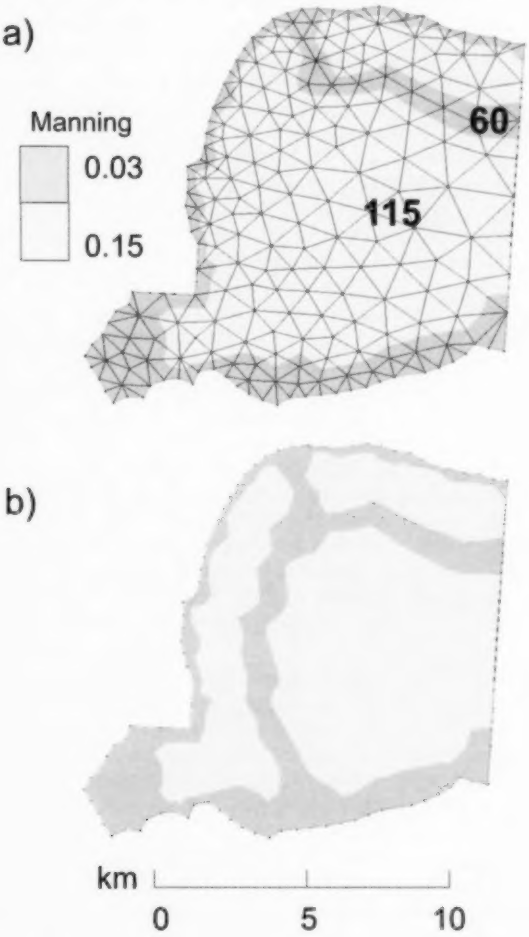

limited in this region and wave transport was not included. Moreover, application of the model to wind waves requires detailed parameterization of surface roughness in culture areas. The level of uncertainty associated with these processes does not justify their inclusion relative to the better constrained tidal circulation. Turbulent diffusion was set to zero, such that the model is purely advective. A map of the bay was digitized and the coordinates for the boundary and depths imported to Aquadyn, which interpolates into a standardized *XYZ* grid based on the finite element mesh. The triangular mesh of 227 nodes was generated with user selection of mesh fineness. Elements were on the order of 0.5 km near the coastline and 2 km near the bay mouth (Fig. 2).

Maps of the aquaculture areas were used to assign values of bottom drag coefficient to specific elements. Because model drag is applied to vertically averaged flow, a drag coefficient is an appropriate method of simulating the effects of structure in the water column on flow retardation. This frictional force is parameterized as the Manning coefficient, the most convenient format for input to Aquadyn:

Fig. 3. Boundary tidal conditions in the north and south of Sungo Bay used as input to the finite element model. ■, time series for the north boundary of the bay; □, time series for the south boundary of the mouth of the bay.

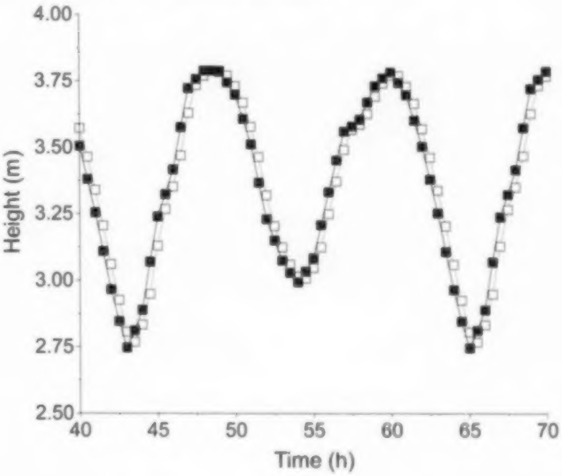

(1) $C_d = (gn^2)/H^{1/3}$

where C_d is the drag coefficient, n is the Manning coefficient, H is water column depth, and g is acceleration due to gravity. A default value for the Manning coefficient of 0.03 (C_d = 0.004) is appropriate for a bottom substrate consisting of gravel beds with no larger scale roughness (Roberson et al. 1988). The bay has a mixture of substrates, and this value will average out the variety of substrates that occur. The absolute Manning value is less important than the gradient that is imposed between culture and nonculture areas.

Following Jackson and Winant (1983) and Grant et al. (1998), the drag (D) exerted by individual culture drop ropes is described as

(2) $D = C_D \rho u^2 dl$

where C_D is the drag coefficient (0.5 for flow approaching a cylinder), ρ is seawater density (1.03 g·cm^{-3}), u is ambient velocity, d is the diameter of the cluster of bivalves surrounding the rope (~50 cm), and l is rope length (5 m). Values of D for culture rafts in South Africa were calculated to be $0.43u^2$, 30 times greater than drag on a sand bottom as estimated in Jackson and Winant (1983).

Beyond this calculation, limited empirical data exist on appropriate values for C_d in the presence of culture, and we employ information from the only detailed example. In field studies of suspended mussel culture on rafts, Boyd and Heasman (1998) found that ambient flow was reduced by a factor of 6 within the rafts. Again invoking the squared scaling between velocity and drag, the latter would be increased by 30- to 40-fold in the presence of culture, giving some empirical weight to the calculation from eq. 2. To be conservative with this parameter, we assume that culture in Sungo Bay increases the Manning coefficient fivefold from 0.03 to 0.15, an increase in drag by a factor of 23. We then derived contours of Manning coefficients (Fig. 2) corresponding to culture configurations reported in Zhao et al. (1996) and from Prof. Fang Jianguang (Yellow Sea Fisheries Research Institute, Qingdao, People's Republic of China, personal communication). The two culture configurations differ mainly in the presence of an additional inner navigation channel in configuration 2. In Zhao et al. (1996), the offshore block of culture was largely kelp, whereas inshore was dominated by scallops. Polyculture areas were in between, but no attempt was made to resolve the culture-specific areas of drag.

Fig. 4. (*a*) Model time series of net tidal velocity in the northern navigation channel of Sungo Bay (node 60) compared with (*b*) measured tidal currents for the same site from Zhao et al. (1996). Site location is shown in Fig. 2.

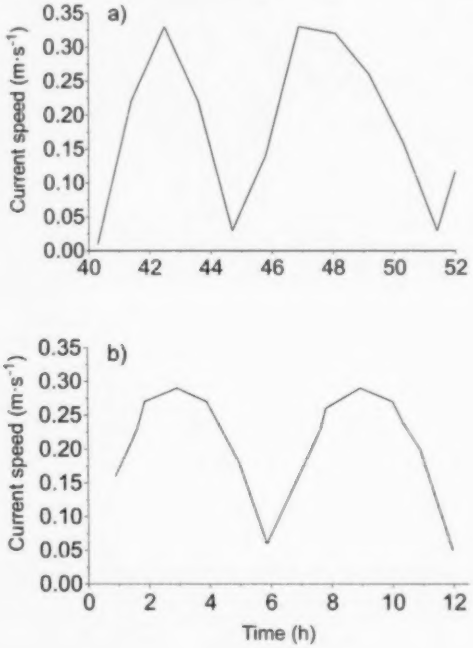

Fig. 5. Time series of model output for net current velocity (*a*) in the northern navigation channel (node 60) and (*b*) in the midst of scallop and kelp culture of Sungo Bay (node 115). ■, default case with no culture; △, culture configuration 1; ○, culture configuration 2. Node locations and culture configurations are shown in Fig. 2.

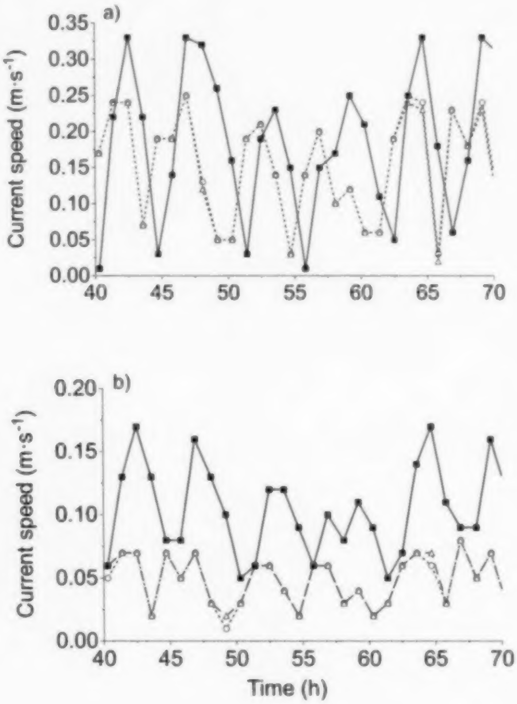

Barotropic flow was generated from a phase difference (600 s) relative to a pressure gauge deployed for 1 year in the northern mouth of the bay (Fig. 3) (Prof. Mingyuan Zhu, First Institute of Oceanography, Qingdao, People's Republic of China, personal communication). In order to produce reasonable model current velocities, the northern time series was linearly interpolated over this phase range for the nine north–south nodes across the mouth of the bay as the boundary conditions for Aquadyn, which uses Galerkin's method to solve the St. Venant equations over the triangular grid (Fig. 2*a*). In the following section, we verify that model output is a reasonable approximation of observed current data and focus on flows at a station in the main channel (node 60) and in the centre of the culture area (node 115) for the different culture configurations and attendant drag. For vector and contour maps of the bay, we present only ebb tide results, since these are the strongest flows and most demonstrative of potential differences between culture arrangements.

In order to compare periodicity of observed and model flows, Fourier spectra of detrended data (minus the mean) were plotted using a Kaiser–Bessel data window (Emery and Thomson 1998) with Autosignal software (SPSS Inc.). A 0.05 significance criterion was established for peak magnitude such that only 5% of random noise signals would produce a peak of this height. The spectral plots are not shown for brevity.

As a measure of flushing, we modelled the introduction of a constant source of conservative tracer at the mouth of the bay and examined the time at which a given node achieved 95% of this external concentration. At present, Aquadyn simulates this advection using a constant velocity field over the grid, for which we chose mid-ebb conditions. External concentration was imposed at 10 (arbitrary units), with initial internal concentration at 1. Longitudinal and transversal dispersion were both set at 5 $m^2 \cdot s^{-1}$.

Results

Circulation

To verify that the model output was reasonable in describing the circulation in Sungo Bay, we compare the modulus of *X* and *Y* velocity (vector sum) with groundtruth data from Zhao et al. (1996). These data consist of current meter records as well as the results of numerical model output. In the former case, we limit comparisons to node 60 in the northern navigation channel, since this location is least dependent on culture conditions measured or assumed in the various data and model results. Their model results do not contain friction estimates caused by longline culture and are thus comparable with our default model case.

Although the current measurements are short in duration, they indicate a range of 0.05–0.3 $m \cdot s^{-1}$, similar to the range predicted in our model output for the default case at this location (Figs. 4 and 5). A second time series (4.5 days) of 1983 data from the northern mouth shows higher velocities, with speeds frequently >0.75 $m \cdot s^{-1}$ (Prof. Mingyuan Zhu, First Institute of Oceanography, Qingdao, People's Republic of China, personal communication). As indicated below, this region is one of steep gradients in velocity, and these maxima are consistent with the spatial variation in our model results for this region. The latter field data show a significant spectral peak at 6.1 h, as expected from a semidiurnal tide. Our modelled current results for this location have a significant spectral peak at 5.5 h, reflecting the periodicity of the boundary conditions. Taken together, these comparisons suggest reasonable agreement between the model output and available field data.

Numerical model output from Zhao et al. (1996) shows a dominant gyre near the mouth that follows the depth contours and weakens inshore. The default output of our Sungo Bay model shows similar cyclonic circulation, with velocities near the mouth also at 0.4 m·s^{-1} or more. (Fig. 6*a*). However, our results are less radially symmetrical, with more of a jet flow at the northern and southern entrances to the bay and localized areas of high flow as observed in the currents for this site (see above). Although these comparisons are limited by a lack of other groundtruth data such as water level curves in the interior of the bay, we consider the magnitude and pattern of circulation predicted by Aquadyn to be sufficient to justify examination of friction effects due to culture.

The pattern of friction due to culture imposed on the model bay as in Fig. 2 indicates significant effects on flow speeds, especially in the midst of the cultivated areas. In the main navigation channel (node 60), tidal speeds for both culture configurations are always less than in the default case, with ~20% mean reduction in both culture cases (Fig. 5*a*). Current speeds in the culture area (node 115) show an even greater differential in magnitude, with a 54% reduction in current speed compared with the default case (Fig. 5*b*). Again, the two culture configurations showed identical patterns in speed (Fig. 5).

Vector diagrams of circulation in the bay also reflect the effects of culture (Fig. 6). In comparison with the default output (Fig. 6*a*), flow at the northern mouth is reduced in both culture configurations, and speed exiting the southern mouth is greatly weakened in the presence of culture (Figs. 6*b* and 6*c*). In all cases, flow is attenuated in the shallow water near the shore. Contour plots of speed provide more insight into the changes in circulation caused by culture, especially between the two culture arrangements and at the lower end of the velocity range inshore. While currents across the mouth of the bay reach 0.1–0.5 m·s^{-1} in the absence of culture (Fig. 7*a*), higher speeds (0.1–0.3 m·s^{-1}) are restricted to the northern entrance and the main navigation channel when culture is present (Figs. 7*b* and 7*c*).

The default contours show speeds from 0.05 to 0.1 m·s^{-1} in the inner parts of the bay (Fig. 7*a*). Although culture configuration 1 has speeds <0.05 m·s^{-1} in the inner margin (Fig. 7*b*), culture configuration 2 displays distinct elevation of current speed along the inner navigation channel through the culture (Fig. 7*c*). Shallowing of the bay is responsible for observed reduction in flows in the inner part of the bay (Figs. 6*a* and 7*a*), but increased attenuation of flow through high-drag culture regions accentuates this effect (also see Jackson 1997). This process is seen in the hindrance of high flows at the mouth (Figs. 7*b* and 7*c*), restricting them to the main navigation channel compared with the default case without culture (Fig. 7*a*). Our results thus indicate that culture of shellfish and kelp has a substantial influence on both the magnitude and the spatial pattern of flow in Sungo Bay. The implications of these frictional effects for the transport of food particles are considered with conservative tracer simulations within the model grid.

Fig. 6. Vector plot of mid-ebb tidal currents in Sungo Bay for three culture configurations: (*a*) default case with no aquaculture, (*b*) culture configuration 1, and (*c*) culture configuration 2. Culture configurations refer to those in Fig. 2.

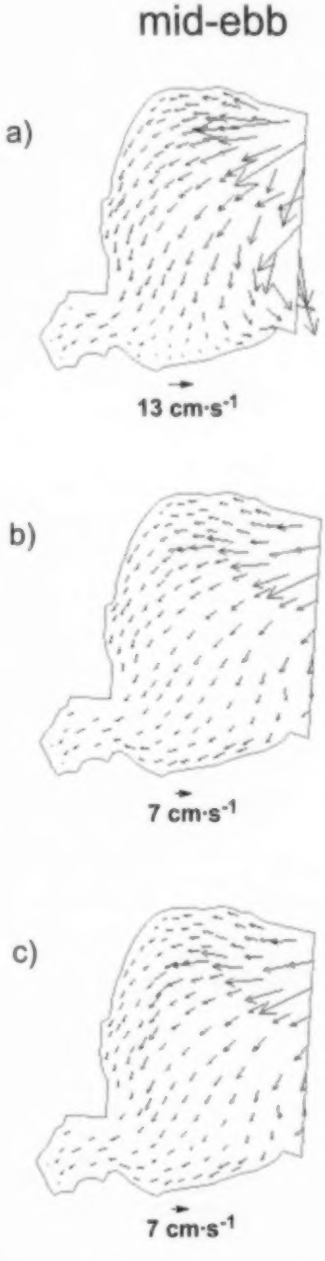

Flushing times

Plots of concentration versus time in the northern naviga-

Fig. 7. Tidal current speed contour plots for three culture configurations in Sungo Bay at mid-ebb tide: (*a*) default case with no aquaculture, (*b*) culture configuration 1, and (*c*) culture configuration 2. Culture configurations refer to those in Fig. 2.

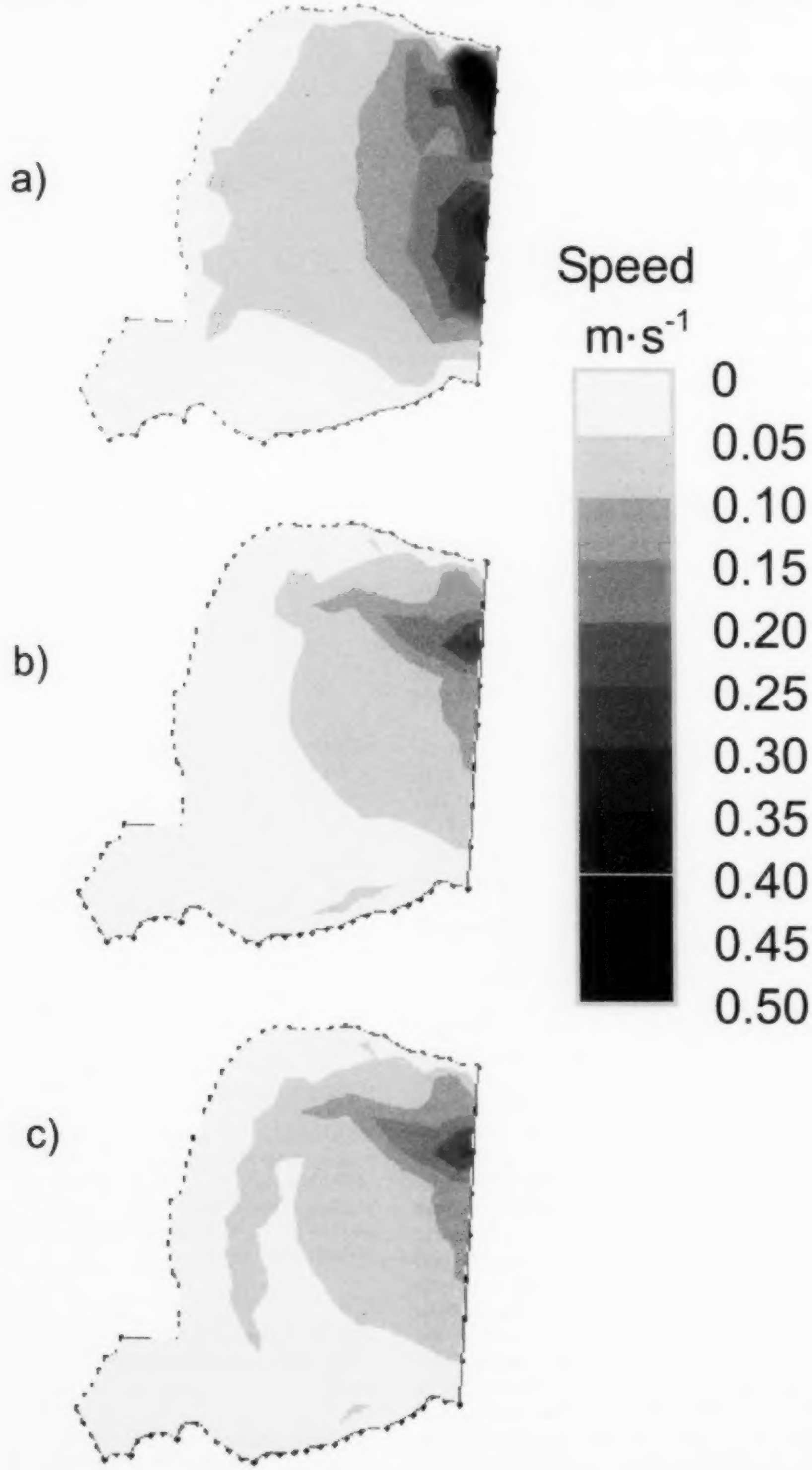
a)
b)
c)
Speed
m·s^{-1}
0
0.05
0.10
0.15
0.20
0.25
0.30
0.35
0.40
0.45
0.50

Fig. 8. Model results of tracer transport in Sungo Bay for a conservative tracer introduced as a constant supply of 10 arbitrary concentration units across the mouth of the bay. Curves are shown for the northern navigation channel (node 60) and in the midst of scallop and kelp culture of Sungo Bay (node 115) for both the default case (no culture, solid line) and culture configuration 1 (dashed line). Node locations and culture configuration are shown in Fig. 2. The horizontal line at concentration = 9.5 is 95% of the imposed tracer concentration.

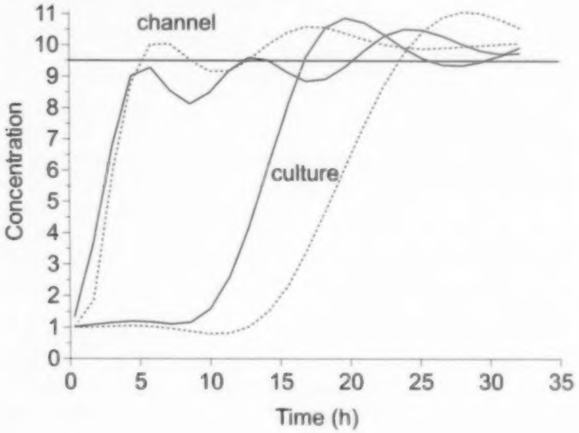

tion channel (node 60) demonstrated a steep increase in tracer addition due to the rapid flushing at this location (Fig. 8). Instantaneous maxima of 11 (arbitrary units) are possible, since internal water started with a concentration of 1. The oscillations near the asymptote reflect input contributions of adjacent nodes with differing concentration (+ or –) from the tracer content at node 60. In the default case (no culture), the channel node displays a temporal pattern similar to that of configuration 1, with a flushing time of about one-half tide (~6 h). Although the default case does not actually cross the 95% concentration level until ~13 h, these curves do not show major differences in flushing time for average ebb conditions. The interior of the longline area (culture) displays greater difference between the default and configuration 1, although both remain stagnant for the first 10 h (Fig. 8). Flushing time is increased from 17 h in the default model to 24 h in culture configuration 1. In terms of water turnover (per day), the presence of culture causes a 41% decrease in exchange rates within the culture area. Although absolute values of exchange rate are dependent on the magnitude of the outside concentration imposed, the proportional differential in exchange between the presence and absence of culture is not sensitive to initial values. Results for culture configuration 2 were identical to those for configuration 1 for nodes 60 and 115. It should be emphasized that these simulations are for a constant flow field and so represent a static view of flushing.

Discussion

The frictional effects of aquaculture on water and particle flux are one of the most neglected areas of study in culture systems. Finite element models have been used to characterize circulation patterns in bays in relation to the transport of wastes from aquaculture, but usually in the context of dispersion of food and feces from salmon cages (Panchang et al. 1997; Wu et al. 1999). No special consideration has been given to the presence of the cages, except at the container scale where it is known that mesh and biofouling interfere with local flow and bivalve food delivery and growth (Claereboudt et al. 1994; Hodson et al. 1997). No numerical models used to predict food transport to suspended bivalves (e.g., Raillard and Menesguen 1994; Ferreira et al. 1998) attempt to include this physical effect. The only influence of culture considered therein is the removal of particles due to suspension feeding.

Our simulations provide a reasonable picture of circulation in Sungo Bay in which to explore these flow alterations, given the limitations imposed by input data for this site. Finite element models are extremely sensitive to boundary conditions (Bills and Noyes 1987), making the presence of any uncertainty in the original data significant. Ongoing studies will attempt to confirm boundary conditions in the bay mouth. At present, the small north–south gradient in tidal phase was sufficient to drive the gyre circulation of the bay. The juncture between the bay and open coastline is a region of steep velocity gradients, potentially a result of topographic steering. This region is a complex portion of the model domain but critical in driving circulation in Sungo Bay. It is likely that wind is also important in water flux in the bay (Geyer 1997), although there are insufficient data available to include this in the model. Estuarine circulation is likely unimportant in Sungo Bay, since the rivers are barricaded or dry and there is little freshwater input to the bay. The Yellow Sea is a tidally dominated system (Lee and Jung 1999), and the tidal model is sufficiently robust compared with observed flow fields to allow estimation of frictional effects of culture animals and hardware. We have attempted to be conservative with respect to the magnitude of friction in demonstrating that it is an aspect of exchange that cannot be ignored.

There are few studies from which information on frictional effects of culture can be gleaned. The only direct study of suspended culture on tidal currents is that of Boyd and Heasman (1998). Using current meters inside and outside raft culture, they determined that flow was reduced by a factor of 6 within the rafts, dependent on rope spacing and ambient speed. They modelled this process by considering flow separation by individual rafts. When extrapolated to the farm scale, this approach requires inclusion of interraft spacing which is on the order of 20% of raft size. Despite this spacing, Boyd and Heasman (1998) estimated that current reduction at the farm scale (30 rafts) was 28%. Pilditch et al. (2001) determined from field measurements that currents through suspended scallop culture were reduced by 40% compared with ambient currents. Gibbs et al. (1991) found that currents within New Zealand longline mussel culture were reduced by 30% compared with ambient flows. Our model results indicate that the spatially denser culture of Sungo Bay reduced current by 54%. Zhao et al. (1996) suggested that velocities in Sungo Bay were reduced by 50% over the period from 1983 to 1994. The degree of current reduction is dependent on the type of culture and its spatial arrangement, but it is an effect that is so substantial as to be readily measured in the field. The implications of reduced advection for particle exchange are also severe, although there are no values in the literature that can be compared with our model results.

A well-studied natural feature analogous to suspended aquaculture is the kelp forest, a situation obviously relevant to kelp culture. Natural kelp beds are somewhat different in that they originate in the benthos and cover the whole water column. As indicated above, on the basis of kelp studies by Jackson and Winant (1983), Grant et al. (1998) suggested that drag due to mussel raft culture should be ~30 times that of a bare substrate, confirmed as the value estimated from the square of velocity retardation in Boyd and Heasman (1998). A similar drag coefficient has been applied to bottom culture or natural bivalve populations on the bottom (Fréchette et al. 1989; Green et al. 1998). In suspended culture, drag will vary with rope geometry but also with culture type (plants versus animals), age of culture, and harvest status. Polyculture of scallops and kelps is likely to be particularly opaque to flow, since plants are hung between rows of scallops. Substantial seasonal changes in culture influence on flow fields would also occur as a result of kelp harvest in Sungo Bay, which takes place in summer and fall (Fang et al. 1996*a*).

In order to maintain conservation of water flux in Sungo Bay, altered velocities in culture must be accounted for by increased flows elsewhere. In a two-dimensional model, this increase must occur in the unobstructed main channels. However, in three-dimensional space, we anticipate that flow will be enhanced between the culture and the bottom, as found by Gibbs et al. (1991), and in some of the smaller secondary flow channels that exist within the culture area. Depending on how far below the longlines their frictional effect is felt, the drag of the plants or culture containers may interact with the benthic boundary layer, especially in shallow water. This situation sets up a complex near-bottom flow, with potential increases in bottom shear and thus resuspension. This flow field is further complicated by the sedimentation of biodeposits beneath bivalve culture, which alters both bottom roughness and the critical threshold for transport (Widdows et al. 1998).

Particle incursions into dense culture will be hindered by reduced advection in these areas. This issue has been similarly addressed in kelp forests. Despite reduced delivery of larvae and detrital particles, the departure of material is also reduced from kelp stands, such that they tend to be particle accumulation zones (Eckman et al. 1989). Bivalve culture has the added feature of intense particle consumption by suspension feeding, so that the consequences of reduced delivery may be severe. Some of the effects of increased friction may be offset by the local advection through small channels (Grant 1996) or increased turbulent diffusion that assists in renewal of particle-depleted water (Fréchette et al. 1989). Pilditch et al. (2001) constructed a model of seston depletion through a suspended scallop culture lease. They examined lease geometry relative to tidal flow to optimize lease orientation and aspect ratio, such that seston depletion was offset by turbulent particle renewal for various lease configurations. Geyer and Signell (1992) indicated that horizontal dispersion (inclusive of mixing at larger scales than turbulent diffusion) increases at abrupt topographic transitions, and it may be that the arrangement of longlines and access channels produces a complex array of dispersion values.

It is apparent that further field measurements and parameterization of both friction and diffusivity due to culture will contribute significantly to the development of appropriate models for use in the management of shellfish aquaculture. Renewal versus consumption terms form the conceptual basis for food limitation in bivalve populations (Wildish and Kristmanson 1997) and for models of carrying capacity (Grant 1996). Our tracer simulations indicate that in culture areas, exchange rates forced by tidal advection may be reduced by 41% due to the retardation influence of culture organisms and containers. Disregard for the frictional effects of culture physical and biological structure will result in a serious overestimation of the renewal term and thus an overestimation of carrying capacity. Further work is required to measure the characteristics of culture (spacing, length scale) that determine its retardation of the flow and the magnitude of these effects in the field and to improve the theoretical parameterization of the frictional effects of various types of culture.

In terms of management, seston depletion is not the only consideration. Previous work on scallop feeding has indicated that higher flows induce feeding inhibition (Wildish and Kristmanson 1997). Reduced flow due to fouling has been shown to allow positive scallop growth in areas where current velocity was otherwise too high (Claereboudt et al. 1994). In this context, the modified flow of culture arrays might allow scallop cultivation in areas in which growth would be flow inhibited.

Acknowledgements

This research was supported by a NATO collaborative research grant and by the Natural Sciences and Engineering Research Council of Canada. We thank the reviewers for helpful comments.

References

Andersen, K.H., Mork, M., and Nilsen, J.E.O. 1996. Measurement of the velocity-profile in and above a forest of *Laminaria hyperborea*. Sarsia, **81**: 193–196.

Bills, P., and Noyes, J. 1987. An investigation of open boundary conditions for tidal models of shallow seas. *In* Numercial modelling: applications to marine systems. *Edited by* J. Noyes. North-Holland, Amsterdam, the Netherlands. pp. 159–194.

Boyd, A.J., and Heasman, K.G. 1998. Shellfish mariculture in the Benguela System: water flow patterns within a mussel farm in Saldanha Bay, South Africa. J. Shellfish Res. **17**: 25–32.

Campbell, D.E., and Newell, C.R. 1998. MUSMOD(c), a production model for bottom culture of the blue mussel, *Mytilus edulis* L. J. Exp. Mar. Biol. Ecol. **219**: 171–203.

Claereboudt, M.R., Bureau, D., Cote, J., and Himmelman, J.H. 1994. Fouling development and its effect on the growth of juvenile giant scallops (*Placopecten magellanicus*). Aquaculture, **121**: 327–342.

Eckman, J.E., Duggins, D.O., and Sewell, A.T. 1989. Ecology of understory kelp environments. I. Effects of kelps on flow and particle transport near the bottom. J. Exp. Mar. Biol. Ecol. **129**: 173–187.

Emery, W.J., and Thomson, R.E. 1998. Data analysis methods in physical oceanography. Pergamon, Oxford, U.K.

Fang, J., Sun, H., Kuang, S., Sun, Y., Zhou, S., Song, Y., Cui, Y., Zhao, J., Yang, Q., Li, F., Grant, J., Emerson, C., Wang, X., and Tang, T. 1996*a*. Assessing the carrying capacity of Sanggou Bay for culture of kelp *Laminaria japonica*. Mar. Fish. Res. **17**: 7–17. (In Chinese.)

Fang, J., Sun, H., Kuang, S., Sun, Y., Zhou, S., Song, Y., Cui, Y., Zhao, J., Yang, Q., Li, F., Grant, J., Emerson, C., Wang, X., and Tang, T. 1996*b*. Study on the carrying capacity of Sanggou Bay for the culture of scallop *Chlamys farreri*. Mar. Fish. Res. **17**: 18–31. (In Chinese.)

Fang, J., Sun, H., Yan, J., Kuang, S., Li, F., Newkirk, G.F., and Grant, J. 1996*c*. Polyculture of scallop *Chlamys farreri* and kelp *Laminaria japonica* in Sungo Bay. Chin. J. Oceanogr. Limnol. **14**: 322–329.

Ferreira, J.G., Duarte, P., and Ball, B. 1998. Trophic capacity of Carlingford Lough for oyster culture — analysis by ecological modelling. Aquat. Ecol. **31**: 361–378.

Fréchette, M., Butman, C.A., and Geyer, W.R. 1989. The importance of boundary layer flows in supplying phytoplankton to the suspension feeder, *Mytilus edulis* L. Limnol. Oceanogr. **34**: 19–36.

Geyer, W.R. 1997. Influence of wind on dynamics and flushing of shallow estuaries. Estuarine Coastal Shelf Sci. **44**: 713–722.

Geyer, W.R., and Signell, R.P. 1992. A reassessment of the role of tidal dispersion in estuaries and bays. Estuaries, **15**: 97–108.

Gibbs, M.M., James, M.R., Pickmere, S.E., Woods, P.H., Shakespeare, B.S., Hickman, R.W., and Illingworth, J. 1991. Hydrodynamics and water column properties at six stations associated with mussel farming in Pelorus Sound, 1984–85. N.Z. J. Mar. Freshwater Res. **25**: 239–254.

Grant, J. 1996. The relationship of bioenergtics and the environment to the field growth of cultured bivalves. J. Exp. Mar. Biol. Ecol. **200**: 239–256.

Grant, J., Stenton-Dozey, J., Monteiro, P., Pitcher, G., and Heasman, K. 1998. Shellfish culture in the Benguela system: a carbon budget of Saldanha Bay for raft culture of *Mytilus galloprovincialis*. J. Shellfish Res. **17**: 41–49.

Green, M.O., Hewitt, J.E., and Thrush, S.F. 1998. Seabed drag coefficient over natural beds of horse mussels (*Atrina zelandica*). J. Mar. Res. **56**: 613–637.

Guo, X., Ford, S., and Zhang, F. 1999. Molluscan aquaculture in China. J. Shellfish Res. **18**: 19–32.

Hodson, S.L., Lewis, T.E., and Burke, C.M. 1997. Biofouling of fish-cage netting: efficacy and problems of in situ cleaning. Aquaculture, **152**: 77–90.

Jackson, G.A. 1997. Currents in the high drag environment of a coastal kelp stand off California. Continental Shelf Res. **17**: 1913–1928.

Jackson, G.A., and Winant, C.D. 1983. Effect of a kelp forest on coastal currents. Continental Shelf Res. **2**: 75–80.

Kuang, S., Fang, J., Sun, H., and Li, F. 1996. Seston dynamics in Sanggou Bay. Mar. Fish. Res. **17**: 60–67. (In Chinese.)

Lee, J.C., and Jung, K.T. 1999. Application of eddy viscosity closure models for the M-2 tide and tidal currents in the Yellow Sea and the East China Sea. Continental Shelf Res. **19**: 445–475.

Panchang, V., Cheng, G., and Newell, C. 1997. Modeling hydrodynamics and aquaculture waste transport in coastal Maine. Estuaries, **20**: 14–41.

Pilditch, C.A., Grant, J., and Bryan, K.R. 2001. Seston supply to sea scallops (*Placopecten magellanicus*) in suspended culture. Can. J. Fish. Aquat. Sci. **58**: 241–253.

Raillard, O., and Menesguen, A. 1994. An ecosystem box model for estimating the carrying capacity of a macrotidal shellfish system. Mar. Ecol. Prog. Ser. **115**: 117–130.

Roberson, J.A., Cassidy, J.J, and Chaudhry, M.H. 1988. Hydraulic engineering. Houghton Mifflin Co., Boston, Mass.

Widdows, J., Brinsley, M.D., Bowley, N., and Barrett, C. 1998. A benthic annular flume for in situ measurement of suspension feeding/biodeposition rates and erosion potential of intertidal cohesive sediments. Estuarine Coastal Shelf Sci. **46**: 27–38.

Wildish, D., and Kristmanson, D. 1997. Benthic suspension feeders and flow. Cambridge University Press, New York.

Wu, R.S.S., Shin, P.K.S., MacKay, D.W., Mollowney, M., and Johnson, D. 1999. Management of marine fish farming in the sub-tropical environment: a modelling approach. Aquaculture, **174**: 279–298.

Zhao, J., Zhou, S., Sun, Y., and Fang, J. 1996. Research on Sanggou Bay aquaculture hydroenvironment. Mar. Fish. Res. **17**: 68–79. (In Chinese.)

Assessing the production and the impact of cultivated oysters in the Thau lagoon (Mediterranee, France) with a population dynamics model

A. Gangnery, C. Bacher, and D. Buestel

Abstract: The Thau lagoon (France) has been studied for many years because of its ecological interest related to economic activities: shellfish cultivation, tourism, and industry. The standing stock of cultivated filter feeders is around 20 000 t and consists of two main species, the Japanese oyster *Crassostrea gigas* and the Mediterranean mussel *Mytilus galloprovincialis*. To predict changes in the standing stock and the annual production, a mathematical model of the population dynamics was defined. It was based on the continuous equation of the density as a function of the mortality rate, the individual growth rate, and the interindividual variability. The daily growth rate was derived from field surveys and depended on the phytoplankton concentration and individual weight. The model also took into account the rearing strategy of the producers defined by the timetable of seeding and harvesting, obtained by an inquiry among the producers and used to simulate real cases of standing stock changes. The model was also used to assess the potential impact on the environment through the computation of the food consumption, which was compared with the residence time and the primary production.

Résumé : Ses nombreuses activités économiques (élevage conchylicole, tourisme et industrie) font de l'étang de Thau (France), un site intéressant d'un point de vue écologique. C'est pourquoi, des études y sont menées depuis plusieurs années. La biomasse de mollusques en élevage dans l'étang est de l'ordre de 20 000 tonnes. Deux espèces y sont élevées : l'huître creuse, *Crassostrea gigas*, et la moule de Méditerranée, *Mytilus galloprovincialis*. Un modèle mathématique de dynamique de population a été élaboré permettant de prédire les variations temporelles de la biomasse ainsi que la production annuelle du bassin. Ce modèle est basé sur une équation continue de la densité, fonction de la mortalité, de la croissance individuelle et de la variabilité inter individuelle. Le taux de croissance dépend de la concentration en phytoplancton et du poids total individuel. Le modèle intègre également les stratégies d'élevage, i.e., l'ensemencement et la récolte, définies à partir d'enquêtes réalisées auprès des producteurs. Il permet ainsi de simuler des cas réels de variations de biomasse. Dans un second temps, le calcul de la consommation phytoplanctonique par les bivalves permet d'estimer leur impact sur l'écosystème. La consommation est comparée au temps de résidence et à la production primaire dans l'étang.

Introduction

The Thau lagoon is an important shellfish centre for both Japanese oysters (*Crassostrea gigas*) and Mediterranean mussels (*Mytilus galloprovincialis*) (Fig. 1). The annual production is not known accurately but is estimated to be around 12 000 t for oysters only, representing most of the regional production and roughly 10% of the national production (Anonymous 1998). This situation has led to a large number of scientific studies. Among others, the National Coastal Oceanographic Programme, launched in 1991, has a dual objective: a general analysis of the behaviour of this lagunar ecosystem and the creation of tools both to monitor and to simulate the changes in such systems. The present work is carried out within the scope of this programme.

Shellfish farming is part of the ecosystem and interacts with the other components of the environment. The impact of shellfish farming on the ecosystem depends on the quantities reared (Mazouni et al. 1998), and its assessment requires an accurate knowledge of the standing stock of cultivated bivalves and of the weight distribution. Evaluations of the standing stock of cultivated shellfish were undertaken in the Thau lagoon from 1980 to 1987 (Hamon and Tournier 1980, 1984, 1990). A new sampling strategy was developed in 1998 (Gangnery 1998) and tested in July 1998 and April 1999. The estimates of standing stock yield discrete values, whereas there are, all year-round, important variations in both the total biomass and its distribution, depending on season, environment, and rearing practices.

From this perspective, a modelling effort has been undertaken, and this work is devoted to deriving a preliminary model of the population dynamics. The population is struc-

Received January 11, 2000. Accepted January 24, 2001. Published on the NRC Research Press Web site on April 25, 2001.
J15526

A. Gangnery and D. Buestel. Laboratoire Conchylicole de Méditerranée, IFREMER, Boulevard Jean Monnet, BP 171, 34203 Sète Cedex, France.
C. Bacher.[1] CREMA, B.P. 5, 17137 L'Houmeau, France.

[1]Corresponding author (e-mail: cbacher@ifremer.fr).

DOI: 10.1139/cjfas-58-5-1012

Fig. 1. Map of the Thau lagoon showing the six geographic strata and the five sampling sites (solid squares) of the oyster growth monitoring network (REMORA).

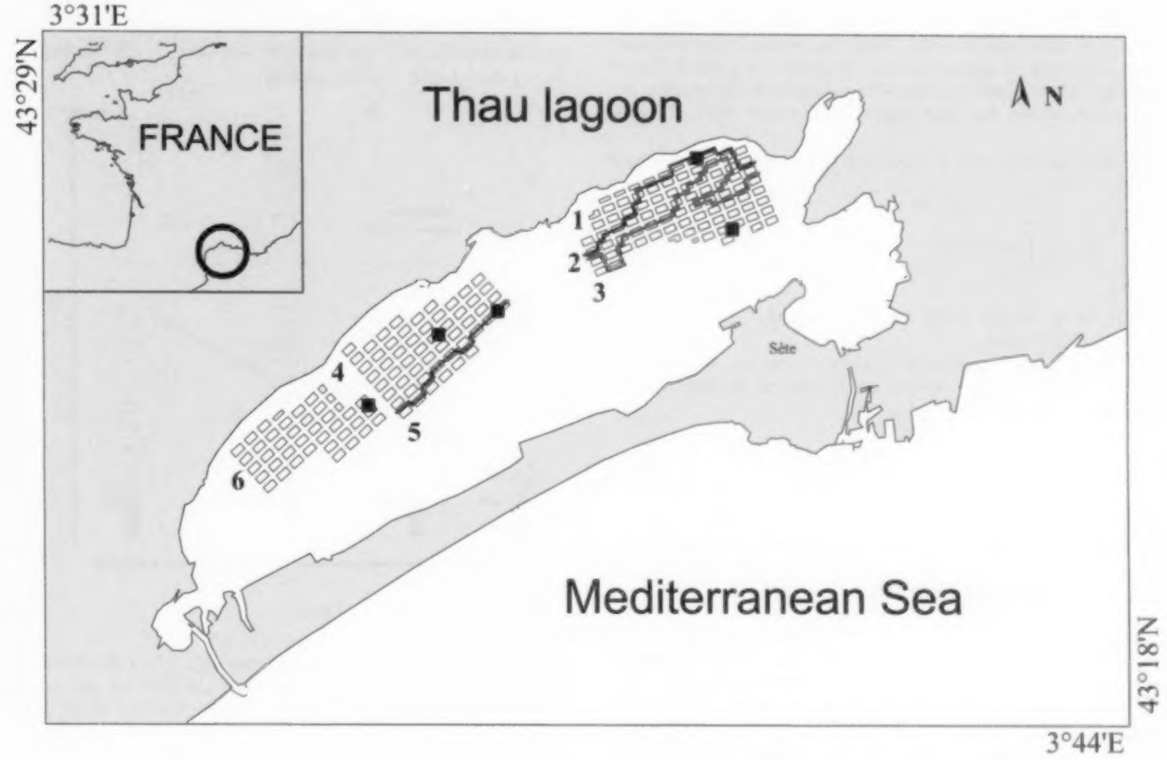

tured in weight classes and the model simulates the variation in time of the abundances in each weight class, the total standing stock, and the production of the system. The mathematical background can be found in Gurney and Nisbet (1998), and applications of such models have been carried out on cultivated mussels in Saint Brieuc Bay (Guarini 1994) to quantify the energy needs of the standing stock and the flux of particulate matter with the other parts of ecosystem (water column and sediment). The same type of population model has been coupled with an ecosystem model to estimate the carrying capacity of Carlingford Lough (Ireland) (Ferreira et al. 1998). In our study, we focused on the detailed description of the short-term variability and the weight distribution of the population and how the production is related to the population dynamics. The driving processes are the individual growth, the variation between individuals, the seeding (which is the input into the model), and the harvest and mortality (which are the outputs). The model accounts for geographical location but is not yet able to account for the mussels and the different rearing methods of oysters due to insufficient data on growth. As a first step, this study concerns only a fraction of the oyster standing stock, corresponding to one culture method that represents about 60% of the total oyster biomass in the lagoon. Then, the model is used to simulate the variations in the biomass in 1999, the initial conditions being those given by the estimate of the standing stock in April 1999. The model is applied to assess the impact of the population in terms of consumption of the available food.

Material and methods

Population dynamics model

The model chosen for this study is a continuous temporal model of the demographic structure of the *C. gigas* standing stock. The character chosen as representative of the demographic structure was the total individual fresh weight (including shell). The standing stock dynamics were described with the standard equation based on growth and mortality (Gurney and Nisbet 1998). The equation was augmented with a harvesting rate and individual growth variation expressed as a random dispersion of the weight; this formulation is commonly used in physics to quantify the random diffusion of particles. Equation 1 expresses the variation in the number of individuals whose weight is w at time t:

$$(1) \qquad \frac{\delta}{\delta t} n(w,t) + \frac{\delta}{\delta w} G(w,t)n(w,t) = K \frac{\delta^2}{\delta w^2} n(w,t) - mn(w,t) - r(w,t)n(w,t)$$

where $n(w,t)\mathrm{d}w$ is the number of individuals whose weight is in the range w to $w + \mathrm{d}w$ at time t, $G(w,t)$ is the growth rate (grams per day) and is a function of the weight of the individuals and of the chlorophyll a concentration in the environment, K is the diffusion coefficient (grams squared per day) and is related to the individual growth variance, m is the mortality rate (per day) and is independent of both individual weight and time, and $r(w,t)$ is the harvest rate (grams per day) and is a function of individual weight and time. The population level is maintained through the seeding $e(t)$ (per day) of new individuals of weight w_0, which is the minimum weight class (Fig. 2). Equation 1 has no analytical solution. In the following, the semiimplicit Crank–Nicholson method, which is unconditionally stable, has been used (Churchhouse 1981; Koutitas 1988).

The total standing stock S (tonnes) in the lagoon can be obtained for time t with

$$(2) \qquad S(t) = \int_{w_0}^{w_{\max}} n(w,t)w\mathrm{d}w$$

where w_0 is the weight of the new animals and $w_{\max}$ is the maximum individual weight.

Similarly, the instantaneous production P (tonnes), which represents the fraction of the standing stock that can be harvested at time t, can be derived with

$$(3) \qquad P(t) = \int_{w_{\min}}^{w_{\max}} r(w,t)n(w,t)w\mathrm{d}w$$

where $w_{\min}$ is the minimum weight for the beginning of the harvest.

Seeding, harvest, and mortality

Seeding

Seeding parameters have been gathered from the oyster farmers through inquiries concerning the timing of farming activities. The main aim of these inquiries was to clarify the farming strategy of the Thau lagoon oyster farmers during the different rearing stages: seeding of young oysters, growth duration with the different rearing techniques, harvesting periods, and marketing characteristics of oysters (weight).

Based on this inquiry, a preliminary timetable of oyster farming has been established. These inquiries have also given some data on the quantities and characteristics of young individuals being bred, have helped to formulate the harvest model, and have given insights into mortality. For the sake of simplicity, seeding has been considered to be constant year-round, except during the summer (July, August, and September) when it is zero.

Harvest

The harvest depends on the weight of the individuals and the period of the year. The dependency with weight has been taken into account with the sigmoid function given by

$$(4) \qquad r = \left(\frac{w - w_{\min}}{w_{\max} - w_{\min}}\right)^{\alpha}$$

where w is the total individual fresh weight (grams) of the animals, $w_{\min}$ is the minimum weight set for harvest (60 g), $w_{\max}$ is the maximum weight set for an individual in the lagoon (120 g), and α is the curvature parameter for the sigmoid.

The animals can be harvested from 60 g up, and all the animals above 120 g are harvested. The curvature of the sigmoid has been set at 3, implying an average weight at harvesting of about 90 g. The probability of harvest during different periods of the year as given by the sigmoid function is corrected by a coefficient. According to the inquiries, it was considered that 50% of the harvest takes place at the end of the year (October 1 to December 31), 30% in summer (July 1 to September 30), and the remaining 20% spread out during the rest of the year. The following coefficients have been chosen for each of these periods: $r_1 = r$ for the end of the year (October 1 to December 31), $r_2 = 0.5r$ for the summer (July 1 to September 30), and $r_3 = 0.1r$ for the rest of the year.

Fig. 2. Conceptual scheme of the population dynamics model, where n is the number of individuals whose weight is in the range w to w + dw at time t, G is the growth rate (g·day^{-1}), K is the diffusion coefficient (g^2·day^{-1}) and is related to the individual growth variance, m is the mortality rate (day^{-1}), r is the harvest rate (g·day^{-1}), and e is the seeding.

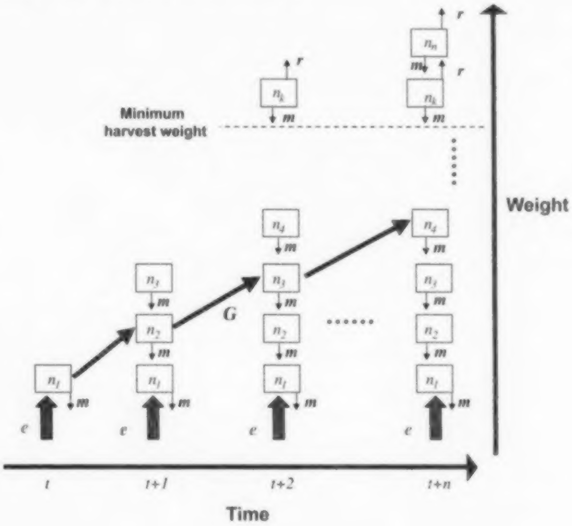

Mortality

Save for exceptional events, such as accidental anoxic crises occurring in summer, storms, or predation by oyster drills, natural mortality is generally low in the Thau lagoon. Based on a growth-monitoring network named REMORA (Fleury et al. 1999) and on the inquiries, the annual mortality rate was set at about 10% and was taken as constant.

Formulation of the growth rate

Formulation of the growth rate rests mainly on the REMORA network data and on chlorophyll *a* measurements carried out in the Thau lagoon in 1998. The French REMORA network, established in 1993, consists of the simultaneous introduction of homogeneous sets of individuals (same origin and approximately the same weight) in all the shellfish cultivated areas in order to monitor their growth rate. In 1998, the introduction took place in the beginning of March at five sites in the lagoon (Fig. 1), the average weight of the individuals being 29.6 g. Three growth measurements were made on the oysters: June, September, and December. For each, 30 individuals randomly chosen on a rope were weighed and measured.

The growth of the oysters is a direct function of the available food in the environment. Bimonthly measurements of chlorophyll *a* were carried out in the lagoon from April 28 to November 24. Water samples were taken at the five REMORA sites (Fig. 1). The growth rate is assumed to depend on the individual weight, and we used an allometric growth rate as a function of chlorophyll *a* concentration and individual weight:

$$(5) \qquad G(w,t) = aC(t)w^b$$

where $C(t)$ is the chlorophyll *a* concentration (micrograms per litre) and w is the individual weight (grams).

The growth model is represented by

Fig. 3. Mean individual growth simulated by the growth model (solid line) and compared with the observed values (squares). The chlorophyll *a* measured in 1998 is also shown for the different geographic strata (dotted line). (*a*) Stratum 1; (*b*) stratum 3; (*c*) stratum 4; (*d*) stratum 5; (*e*) stratum 6.

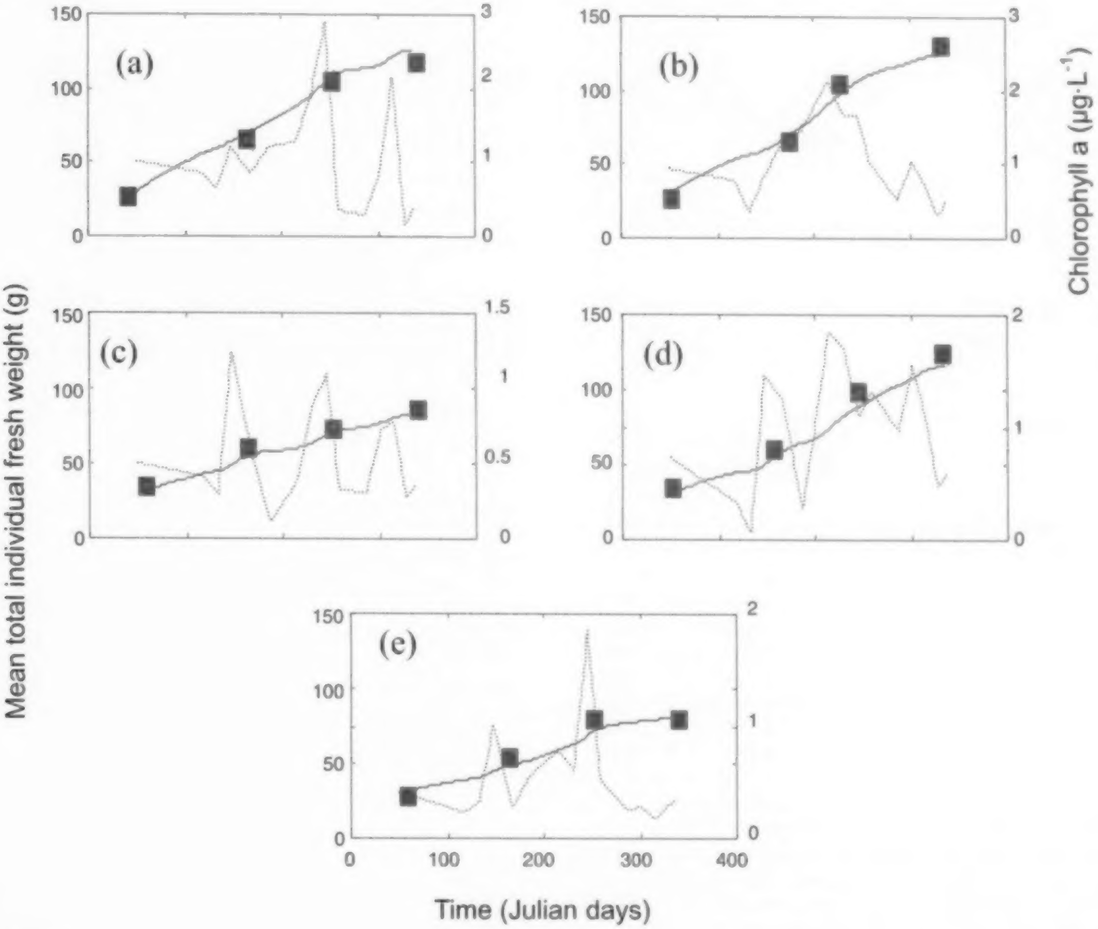

$$\frac{dw}{dt} = G. \tag{6}$$

The initial conditions were those observed for REMORA: a group of individuals with a known average weight. The numerical integration was achieved with a time step of 1 day over a 1-year simulation period. The parameters *a* and *b* were adjusted with the REMORA measurements: three observations in each of five out of six strata, spread out during the year, of the average population growth. An optimisation algorithm based on the simplex method (Press et al. 1992) yielded the *a* and *b* coefficients that gave the closest simulated weight to that observed in REMORA.

Assessment of the interindividual growth variability

The *K* coefficient was also adjusted to the measurements made during REMORA in 1998. The population model, without seeding or harvest (the REMORA conditions), simulated the average growth and gave the standard deviation of the average weight. The observed points, together with their standard deviation, were placed on the same diagram. The coefficient *K* can then be adjusted in such a manner that the individual simulated variance will fit as well as possible with the experimentally observed variance. The simulation period was 1 year, with a time step of 1 day and weight classes of 4 g.

Simulation of the stock and production

Starting from the different variables parameterised previously (seeding, growth rate, variability between individuals, harvesting and mortality rates), the population model was used to simulate the changes in the standing stock and in the production of Japanese oysters. The initial conditions were the distribution of the standing stock in April 1999 and the total number of oysters for each geographic stratum. The same initial distribution of the sample was adopted for the whole lagoon, so that all of the geographic strata presented the same initial distribution. The simulation period was 9 months (April to December 1999) and the model was integrated with a time step of 1 day and weight classes of 4 g. The weight distributions, standing stocks, and productions of the five strata were computed.

Impact assessment

Consumption of phytoplankton, excretion of dissolved organics and inorganics, and biodeposition may result in environmental im-

Fig. 4. Mean individual growth and standard deviation (thick bar) measured during the oyster growth monitoring period (REMORA network) and simulated (thin bar) by the population dynamics model applied to the REMORA initial weight distribution. (*a*) Stratum 1; (*b*) stratum 3; (*c*) stratum 4; (*d*) stratum 5; (*e*) stratum 6.

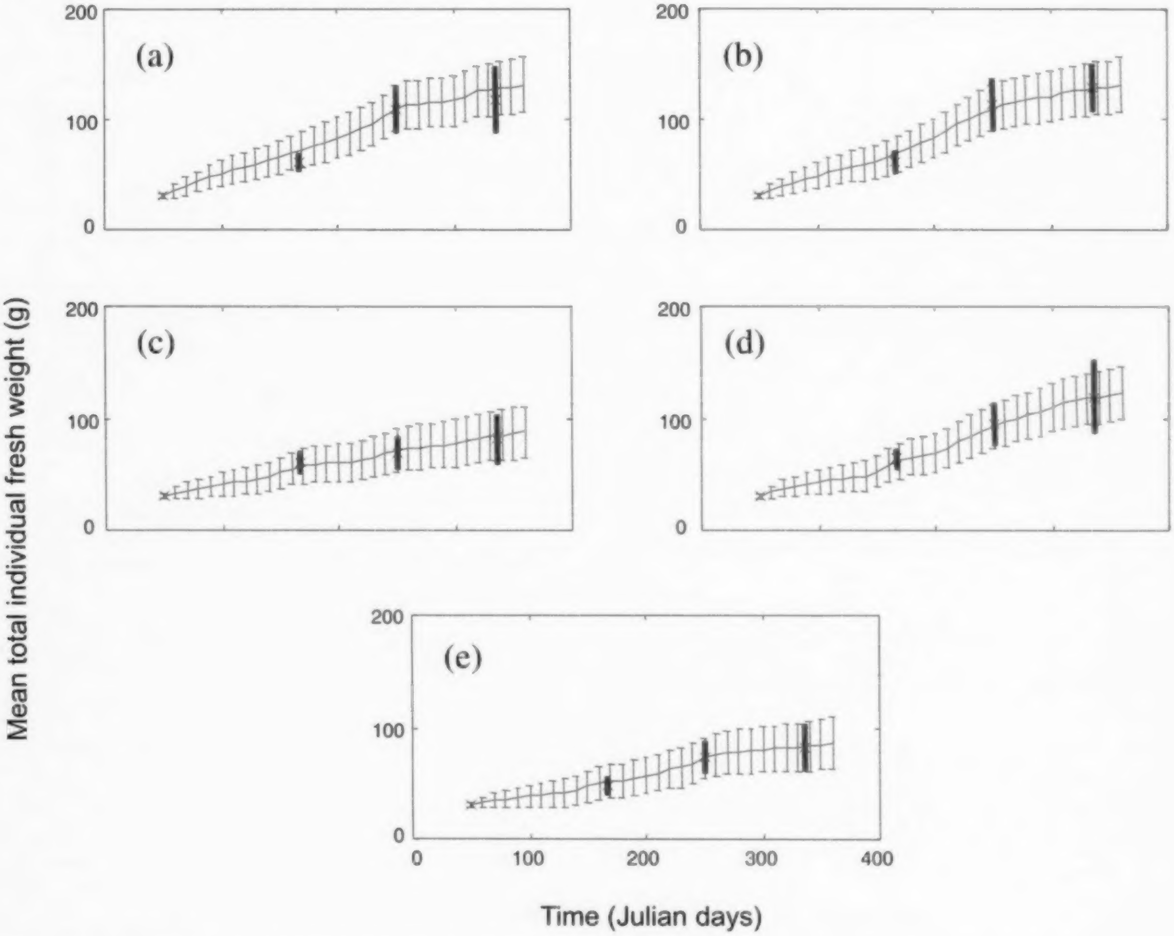

pact due to modifications to ecosystem dynamics (Dame 1993; Bacher et al. 1997). We focused here on food consumption, which was derived from the population dynamics model by adding an equation for the individual clearance rate as a function of temperature and individual weight (Bougrier et al. 1995):

$$(7) \qquad c(w,t) = [(4.83 - 0.013)(T - 18.95)^2]w^{0.44}$$

where T is the water temperature (measured series of values), w is the individual dry weight of the soma, and c is the clearance rate (cubic metres per day per individual). The REMORA data yielded a conversion factor from total fresh weight to dry meat weight equal to 0.0234. This coefficient was used to rewrite eq. 7 as a function of the total weight. The total clearance rate (cubic metres per day) was calculated as

$$(8) \qquad C(t) = \int_{w_0}^{w_{\max}} n(w,t)c(w,t)\mathrm{d}w.$$

The clearance time CT (days) is a key parameter used in the carrying capacity assessments (Dame and Prins 1998) and was written as

$$(9) \qquad \mathrm{CT}(t) = \frac{V}{C(t)}$$

where V is the volume of the lagoon. CT quantified the time needed by the population to clear the surrounding water and can be compared with the water residence time and the food production time (Dame and Prins 1998).

Results

The unknown parameters, e.g., the growth rate and the dispersion coefficients, were first determined. Their values were used in the population model to simulate the weight distribution and to derive the standing stock and production variations. Combining individual clearance rates and variation in the weight distribution allowed the computation of the clearance time by the population.

Growth parameters

The optimised coefficients were $a = 0.65$ and $b = -0.38$, and comparison between the adjusted simulation values and

Fig. 5. Weight distribution of the oyster population derived from the standing stock assessment carried out in April 1999 used as the initial condition in the population dynamics model.

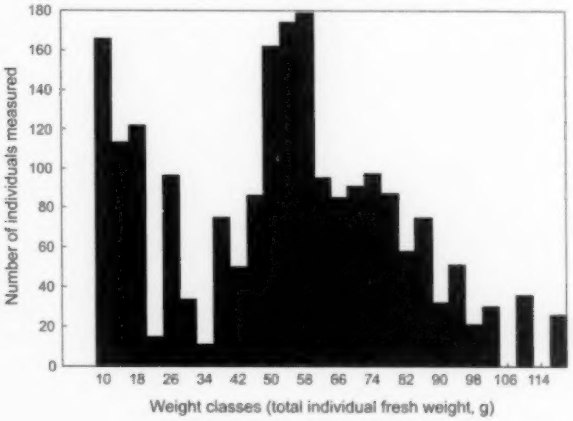

Fig. 6. Simulated stock (thick lines) and cumulative production (thin lines) between April and December 1999 for two different values of the dispersion coefficient used to represent the individual growth variability.

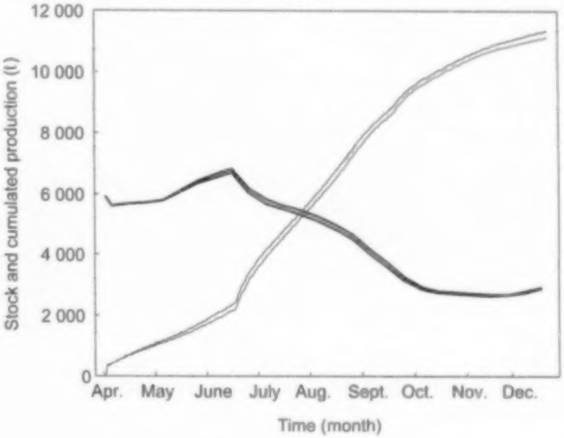

those observed with the REMORA network showed an acceptable goodness-of-fit (Fig. 3). A simple linear regression comparing the observed average weights with those simulated confirmed that the model was adequate, with a slope equal to 1 and a significant correlation ($P < 0.001$). After simulating the dynamics of the REMORA data and comparison of the simulated and observed standard deviations, the diffusion coefficient was set to 0.8. The observed and simulated standard deviations showed a reasonable agreement (Fig. 4), and the correlation between the two series was still highly significant ($P < 0.001$). However, the slope was equal to 0.57 instead of 1 and the model overestimated the lowest values and underestimated the highest values.

Variations in stock and production

The model of the population dynamics was run with the initial weight distribution in April 1999 (Fig. 5) using the above growth parameters. In April 1999, two major cohorts were identified in the sample of oysters. The first cohort contained young individuals with an average weight ranging from 10 to 20 g, whereas the second contained adults with an average weight ranging from 50 to 60 g total individual fresh weight. The population also contained many individuals having reached a commercial weight, with an individual weight ranging from 60 to 90 g. There was a deficit in the classes of 20–40 g.

The model predicted a slight decrease in the standing stock beginning in April and then an increase until mid-June, close to 1000 t, to reach a maximum of about 7000 t (Fig. 6). Starting in mid-June, the standing stock again decreased until November, reached a minimum of less than 3000 t, and then increased slightly to about 3000 t by year's end. The cumulative production showed an important harvest in the first week of the simulation period. It then grew steadily and reached a total of 11 000 t for the whole period of April to December 1999. A sensitivity analysis to the dispersion coefficient representing the individual growth variability was carried out. A second simulation with no variability ($K = 0$) was run and the comparison of the productions and standing stocks showed that the differences between the two simulations were less than 3% (Fig. 6).

Regarding the weight distribution, there was again an important cohort around an average weight of 60 g at the beginning of April, soon harvested because the individuals had reached a commercial weight (Fig. 7). The young oysters present at the start of the simulation reached a peak of 60 g in September. During the summer, the lack of seeding led to a depletion of individuals in the lower weight classes. Frequencies of the weight distribution were determined for each stratum on the last day of the simulation (Fig. 8). Since the seeding and the harvesting rates are the same for all strata, as well as the initial conditions of the simulation, the chlorophyll *a* concentration was responsible for the differences in the variations in the standing stock in the different strata. These different growth rates also yielded different harvests.

Clearance time

The individual clearance rate was computed for each weight class as a function of time using the temperature data (Fig. 9). The values lay between 40 and 160 L·day^{-1}·individual^{-1}, the highest values being obtained when the temperature reached the value corresponding to the maximum of the clearance rate in the function given by Bougrier et al. (1995). The temporal fluctuations were minor compared with the influence of the individual weight, and the clearance rate was lower during low-temperature events, e.g., at the end of the year. Combining this function with the simulation of the population dynamics yielded clearance time estimates between 3 and 8 days with low values in April when the stock was maximal (Fig. 10).

Discussion

In this study, population dynamics are represented with a continuous time- and weight-dependent equation, which includes the seeding and harvesting strategies. Ferreira et al. (1998) used a similar equation (however, without the individual variability term) coupled with an ecosystem model in

Fig. 7. Simulated standing stock as a function of weight and time.

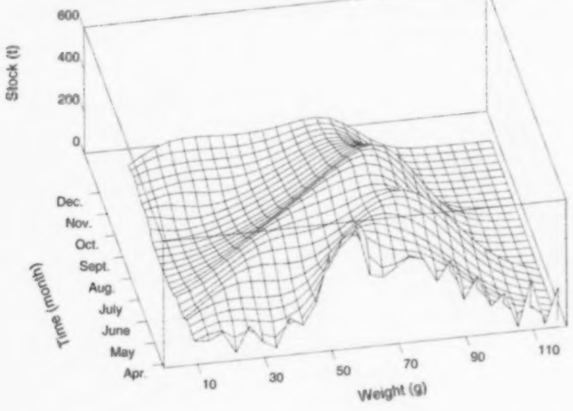

Fig. 8. Simulated final weight distribution in the different strata of the lagoon.

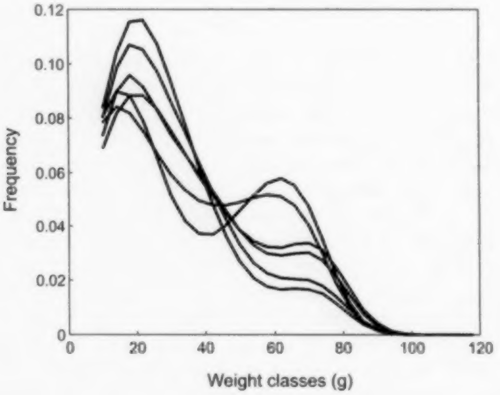

Fig. 9. Individual clearance rate for each weight class as a function of time.

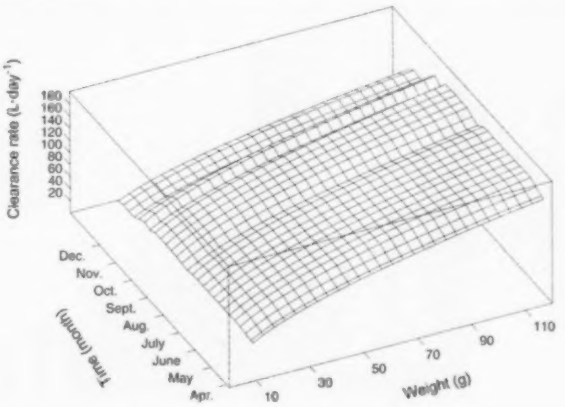

Fig. 10. Total clearance time of the simulated cultivated population by month.

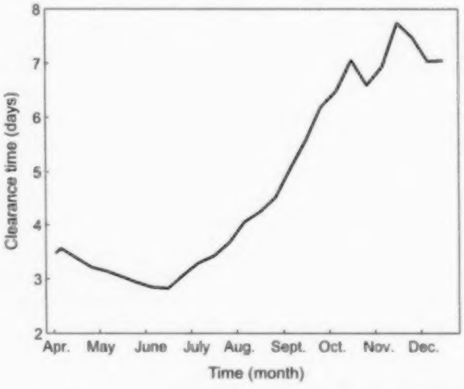

their study of the trophic capacity of Carlingford Lough (Ireland). This approach was well adapted to our first objective, which was to assess the standing stock changes and composition and the production for given trophic conditions and farming practices. As noted in the present simulation, the presence of a high weight mode observed in the initial distribution (April 1999), coupled with a rapid growth rate, explained a large production as early as the middle of the year and a steady decrease in the standing stock as the production was marketed. We found that the annual production was almost three times as high as the average standing stock, which demonstrates the high productivity of the lagoon. One must look at the events of 1998 (the sales embargo for sanitary reasons at the end of the year; Gangnery 1999) to explain the origin of this initial distribution. Other simulations (not shown in this paper) showed the sensitivity of the standing stock and production to the seeding timetable. Modifying the duration and the intensity of the seeding yields considerable change to the production and the standing stock and the weight distribution. In order to make the model operational, i.e., to predict with enough accuracy the expected production, a more complete inquiry will be carried out among the farmers.

By comparing geographic strata between and within cultivated areas, we have demonstrated the influence of different trophic conditions such as food concentrations (e.g., chlorophyll *a*) on weight distributions. Monitoring of food concentration at different sites only provides an idea of the spatial variability and remains a source of uncertainty affecting model outputs (e.g., production and weight distribution). These uncertainties could be addressed by running several simulations with different food concentrations using Monte Carlo techniques.

Differences in experimental growth between individuals could have provided another source of variability. These variations were addressed with the use of a random diffusion coefficient (Brownian motion). Although individual growth rates are, in part, related to nonrandom genetic factors, we did not consider individual trajectories in our analysis and application of this coefficient was acceptable. However, results showed that the use of such a coefficient could underestimate or overestimate the variability between individuals, even if the increase in variability with time was correctly predicted. We then used a sensitivity analysis that showed that although unexpected, growth variability did not actually change the mean growth of the population, although incorporation provided a more accurate picture of weight distribution.

As far as the oyster growth rate could be predicted by a simple function of chlorophyll *a*, which characterised the available phytoplanktonic food, a detailed description of the ecophysiology of the *C. gigas* was not required here to simulate the population dynamics as in Powell et al. (1992), Hofmann et al. (1992, 1994) for the American oyster *Crassostrea virginica*, Raillard and Ménesguen (1994), and Kobayashi et al. (1997) for *C. gigas*. In those studies, the ecophysiological responses to environmental factors such as temperature and particulate inorganic and organic matter must be quantified in order to predict the individual growth. As for environmental impact assessment, ecophysiological models may be coupled with ecosystem models to account for the effect of food consumption by the cultivated species on the nitrogen dynamics (Raillard and Ménesguen 1994; Bacher et al. 1998; Ferreira et al. 1998). In the Thau lagoon, the effect of the oyster stock on the ecosystem dynamics has been simulated by Bacher et al. (1997) and Chapelle et al. (2000). It was shown that the food consumption and biodeposition due to the oysters would modify the food concentration and the primary production. These impacts are varying in time due to several environmental factors, e.g., temperature, nutrient inputs from the watershed, and wind. In these studies, however, the standing stock was kept constant because of the lack of information on its temporal variation, and it is one of our goals to fill in this gap and provide some complementary clues on the impact. We focused here on the assessment of the clearance time variability due to the temporal variability of the standing stock. For this estimation, we assessed the volume of water within the cultivated area considered in the population dynamics model, e.g., 10% of the total area of the lagoon. The simulated standing stock represented only a fraction of the total standing stock, since we considered only one cultivation technique due to the lack of information on the individual growth rates in the other cases. The oyster density is not uniform, since the oysters are attached to ropes hanging from tables that are separated by large alleys (Mazouni et al. 1998). As a consequence, the local density is higher than the uniform density that we put in our calculation. The average figure of 5 days that we obtained should therefore be considered as a reasonable approximation of the clearance time at the scale of the cultivated area. The effect of the cultivated filter feeders on the ecosystem and the feedback on growth depend on several factors; among these, the water renewal time, the rate of primary production, the degree of nutrient recycling, the clearance time, and the biodeposition rate due to the cultivated filter feeders are the most important (Bacher et al. 1997; Dame and Prins 1998; Prins et al. 1998). In the Thau lagoon, the renewal time of the water in the cultivated areas depends on the wind, which drives the whole hydrodynamics (Millet 1989). Whatever the meteorological conditions, however, the current velocity in the lagoon is generally lower than 10 $cm \cdot s^{-1}$ and an average value of 5 $cm \cdot s^{-1}$ is realistic. We considered a typical length of 2000 m, which yielded a residence time of 0.5 day. Actually, the water residence time depends on the spatial scale and the calculation does not consider that the lagoon is almost a closed system having small exchanges with the sea. An estimation of the average primary production was given by Chapelle et al. (2000) as 60 mg $N \cdot m^{-2} \cdot day^{-1}$. Considering an average phytoplankton concentration of 1 mmol $N \cdot m^{-3}$, an average depth of 4 m yielded a turnover rate of 1 day. Again, this computation does not account for the temporal and spatial variability, which may change this value by an order of magnitude. Comparing the residence time, the turnover time, and the clearance rate shows that the standing stock would probably influence the food concentration. It is therefore likely that this impact would in turn modify the individual growth rate and the population dynamics of the cultivated mussels and oysters. To make our model operational, we have to address more thoroughly the links between the ecosystem dynamics and the feedback on the cultivated population dynamics. Our next effort will be to develop the same type of population model for the mussels and the whole oyster standing stock and to include the ecosystem dynamics described by Chapelle et al. (2000).

References

Anonymous. 1998. CEPRALMAR, bilan d'activités 1992–1997. CEPRALMAR, Montpellier, France.

Bacher, C., Millet, B., and Vaquer, A. 1997. Modélisation de l'impact des mollusques cultivés sur la biomasse phytoplanctonique de l'étang de Thau (France). C.R. Acad. Sci. Ser. III. Sci. Vie, **320**: 73–81.

Bacher, C., Duarte, P., Ferreira, J.G., Héral, M., and Raillard, O. 1998. Assessment and comparison of the Marennes–Oléron Bay (France) and Carlingford Lough (Ireland) carrying capacity with ecosystem models. Aquat. Ecol. **31**: 379–394.

Bougrier, S., Geairon, P., Deslous-Paoli, J.M., Bacher, C., and Jonquieres, G. 1995. Allometric relationships and effects of temperature on clearance and oxygen consumption rates of *Crassostrea gigas* (Thunberg). Aquaculture, **134**: 143–154.

Chapelle, A., Ménesguen, A., Deslous-Paoli, J.M., Souchu, P., Mazouni, N., Vaquer, A., and Millet, B. 2000. Modelling the nitrogen, primary production and oxygen in a Mediterranean lagoon. Impact of oysters farming and inputs from the watersheds. Ecol. Model. **127**: 161–181.

Churchhouse, R.F. (*Editor*). 1981. Numerical methods. Vol. III. Handbook of applicable mathematics. John Wiley & Sons, New York.

Dame, R.F. (*Editor*). 1993. Bivalve filter feeders in estuarine and coastal ecosystem processes. Springer-Verlag, Berlin.

Dame, R.F., and Prins, T.C. 1998. Bivalve carrying capacity in coastal ecosystems. Aquat. Ecol. **31**: 409–421.

Ferreira, J.G., Duarte, P., and Ball, B. 1998. Trophic capacity of Carlingford Lough for aquaculture — analysis by ecological modelling. Aquat. Ecol. **31**: 361–378.

Fleury, P.G., Ruelle, F., Claude, S., Palvadeau, H., Robert, S., d'Amico, F., Vercelli, C., and Chabirand, J.M. 1999. Réseau de suivi de la croissance de l'huître creuse sur les côtes françaises: REMORA; résultats des stations nationales, année 1998. La Trinité sur mer, IFREMER, France.

Gangnery, A. 1998. Estimation des stocks de bivalves en élevage et des épibiontes dans la lagune de Thau en 1998. Evolution depuis 1980. Rapp. ENSAR/IFREMER, Sète, Cedex, France.

Gangnery, A. 1999. Estimation des stocks de bivalves en élevage et des épibiontes dans la lagune de Thau et modélisation de la dynamique des populations d'huîtres creuses (*Crassostrea gigas*, Thunberg). Mémoire DEA, Université Paris VI/IFREMER, France.

Guarini, J.M. 1994. Modélisation de la dynamique de la production des moules cultivées en baie de Saint-Brieuc (Manche Ouest): quantification de la demande énergétique du cheptel et des flux de matières échangés dans l'écosystème. Mémoire DEA Université de Liège/IFREMER, France.

Gurney, W.S.C., and Nisbet, R.M. 1998. Ecological dynamics. Oxford University Press, New York.

Hamon, P.Y., and Tournier, H. 1980. Estimation de la biomasse en culture dans l'étang de Thau. Sci. Pêches Bull. Inst. Pêches Marit. **313**: 23.

Hamon, P.Y., and Tournier, H. 1984. Evolution de la biomasse de mollusques en élevage dans l'étang de Thau de 1980 à 1984. Trav. Inst. Pêches Marit. **48**: 33–44.

Hamon, P.Y., and Tournier, H. 1990. Étude des stocks de mollusques élevés dans l'étang de Thau de 1981 à 1987. Rapp. IFREMER RIDRV/RA/Sète. IFREMER, Sète, Cedex, France..

Hofmann, E.E., Powell, E.N., Klinck, J.M., and Wilson, E.A. 1992. Modeling oyster populations. III. Critical feeding periods, growth and reproduction. J. Shellfish Res. **11**: 399–416.

Hofmann, E.E., Klinck, J.M., Powell, E.N., Boyles, S., and Ellis, M. 1994. Modeling oyster populations. II. Adult size and reproductive effort. J. Shellfish Res. **13**: 165–182.

Kobayashi, M., Hofmann, E.E., Powell, E.N., Klinck, J.M., and Kusaka, K. 1997. A population dynamics model for the Japanese oyster, *Crassostrea gigas*. Aquaculture, **149**: 285–321.

Koutitas, C.G. 1988. Mathematical models in coastal engineering. Pentech Press, London, U.K.

Mazouni, N., Gaertner, J.C., and Deslous-Paoli, J.M. 1998. Influence of oyster culture on the water column characteristics in a coastal lagoon (Thau, France). Hydrobiologia, **373/374**: 149–156.

Millet, B. 1989. Fonctionnement hydrodynamique de l'étang de Thau. Validation écologique d'un modèle numérique de circulation (programme Ecothau). Oceanol. Acta, **12**: 37–46.

Powell, E.N., Hofmann, E.E., Klinck, J.M., and Ray, S.M. 1992. Modelling oyster populations. I. A commentary on filtration rate. Is faster always better? J. Shellfish Res. **11**: 387–398.

Press, W.H., Teukolsky, S.A., Vetterling, W.T., and Flannery, B.P. 1992. Numerical recipes in Fortran. The art if scientific computing. 2nd ed. Cambridge Unviversity Press, New York.

Prins, T.C., Smaal, A.C., and Dame, R.F. 1998. A review of the feedbacks between bivalve grazing and ecosystem processes. Aquat. Ecol. **31**: 349–359.

Raillard, O., and Ménesguen, A. 1994. An ecosystem box model for estimating the carrying capacity of a macrotidal shellfish system. Mar. Ecol. Prog. Ser. **115**: 117–130.

Impact of mussel (*Mytilus galloprovincialis*) raft-culture on benthic macrofauna, in situ oxygen uptake, and nutrient fluxes in Saldanha Bay, South Africa

Jeanie Stenton-Dozey, Trevor Probyn, and Alistair Busby

Abstract: Culture of the mussel *Mytilus galloprovincialis* in a South African bay created organic enrichment and anoxia in sediments. Particulate organic matter (POM) was high under rafts versus the references, especially in the first 10 cm (C = 7.5 versus 0.4%, N = 0.7 versus 0.08%). Total reducible sulphides (TRS) increased threefold downcore (from 0.04 to 0.12%). High C:N ratios (12–15) indicated accumulation of refractory POM, derived mainly from faeces and decaying mussels and foulers. Although O_2 uptake by raft sediments was the lowest, rates could not conclusively be separated from the references. Ammonium dominated N efflux, the highest and most variable rates being under mussels (825 ± 500 $\mu mol\ NH_4 \cdot m^{-2} \cdot h^{-1}$). Phosphate efflux (25–140 $\mu mol \cdot m^{-2} \cdot h^{-1}$) could not be ascribed to culture biodeposition, but there was an inconclusive trend for the molar N:P ratio to be highest in these sediments. Macrofauna biomass was reduced and trophic groups and taxa altered. Under rafts, macrofauna and organic debris were linked to O_2 uptake rates, whereas at the reference sites, macrofauna appeared to be the major O_2 consumer. It was concluded that POM and TRS in sediment as well as macrofauna biomass, and potentially molar N:P ratios, were more sensitive indicators of benthic impact from mussel culture than O_2 uptake rates or nutrient fluxes.

Résumé : La mytiliculture de la moule *Mytilus galloprovincialis* dans une baie d'Afrique du Sud cause un enrichissement organique et une désoxygénation des sédiments. La matière organique particulaire (POM) est abondante sous les radeaux par comparaison aux zones témoins, particulièrement dans les 10 cm supérieurs (carbone = 7,5 contre 0,4%, azote = 0,7 contre 0,08%). Les sulfures totaux réductibles (TRS) augmentent par un facteur de 3 en profondeur (de 0,04 à 0,12%) dans les carottes. Les rapports élevés de C:N (12–15) indiquent qu'il y a accumulation de POM réfractaire venant surtout des fèces, des moules en décomposition et des espèces qui contaminent la culture. Bien que la consommation d'O_2 soit plus faible dans les sédiments sous les radeaux, ces taux ne peuvent être clairement distingués de ceux des zones témoins. L'efflux d'azote est dominé par l'ammonium, les taux les plus élevés et les plus variables se retrouvant sous les moules (825 ± 500 $\mu mol\ NH_4 \cdot m^{-2} \cdot h^{-1}$). Les efflux de phosphate (25 à 140 $\mu mol \cdot m^{-2} \cdot h^{-1}$ ne peuvent être attribués à la biosédimentation due à la culture, mais le rapport N:P molaire tend à être plus élevé dans les zones de culture, mais de façon peu probante. Il y a une réduction de la biomasse de la macrofaune et des différences dans les groupes trophiques et les taxons. Sous les radeaux, il y a une relation entre la macrofaune et les débris organiques, d'une part, et les taux de consommation d'O_2,d'autre part, alors que dans les zones témoins, la macrofaune semble constituer le plus important consommateur d'O_2. En conclusion, la POM et les TRS, ainsi que la biomasse de la macrofaune dans les sédiments, et potentiellement les rapports N:P molaires, sont des indicateurs plus sensibles de l'impact de la mytiliculture sur la région benthique que ne le sont la consommation d'O_2 ou les flux des éléments nutritifs.

[Traduit par la Rédaction]

Introduction

The raft-culture of the mussel *Mytilus galloprovincialis* has taken place in South Africa for 15 years in Saldanha Bay (33°S, 18°E), north of Cape Town. This bay is the only natural sheltered embayment in the country and is thus seen as the major area for mariculture. In 1997, the bay was zoned to cater to mariculture expansion while defining areas for other uses such as angling, boat anchorage, marine reserves, recreation, conservation, a fishing harbour, ore loading, marina development, and net fishing (Fig. 1). At present, 80 ha is under mussel culture with an annual marketable yield of 2000–3000 t wet weight with shell. A further 1000 ha has been demarcated for mariculture, which increases the potential mussel harvest from Saldanha Bay to 30 000 t.

Environmental impacts from anthropogenic activities in the bay have been an issue since the construction of the iron ore jetty in 1977. In this year, a baseline survey of macrobenthic community structure was undertaken (Christie and Moldan 1977), and this was followed by further benthic sur-

Received February 14, 2000. Accepted January 24, 2001. Published on the NRC Research Press Web site on April 25, 2001.
J15616

J. Stenton-Dozey,[1] T. Probyn, and A. Busby. Mariculture, Marine & Coastal Management, 6th Floor Foretrust, Private Bag X2, Rogge Bay, 8012, Cape Town, South Africa.

[1]Corresponding author (e-mail: jbailey@sfri2.wcape.gov.za).

DOI: 10.1139/cjfas-58-5-1021

Fig. 1. Saldanha Bay in South Africa with the position of the present mussel farm (study area R28 (Site 1)), reference sites (RC, B10, NS), and areas demarcated for the expansion of mariculture, Site 2 (50 ha) in Small Bay and Site 3 (1000 ha) in Big Bay. RC is the original control site, B10 is a buoy that has served as a monitoring station since 1989, and NS is the new 50-ha site. The bay was zoned for different activities by the Saldanha Bay Environmental Forum in 1997.

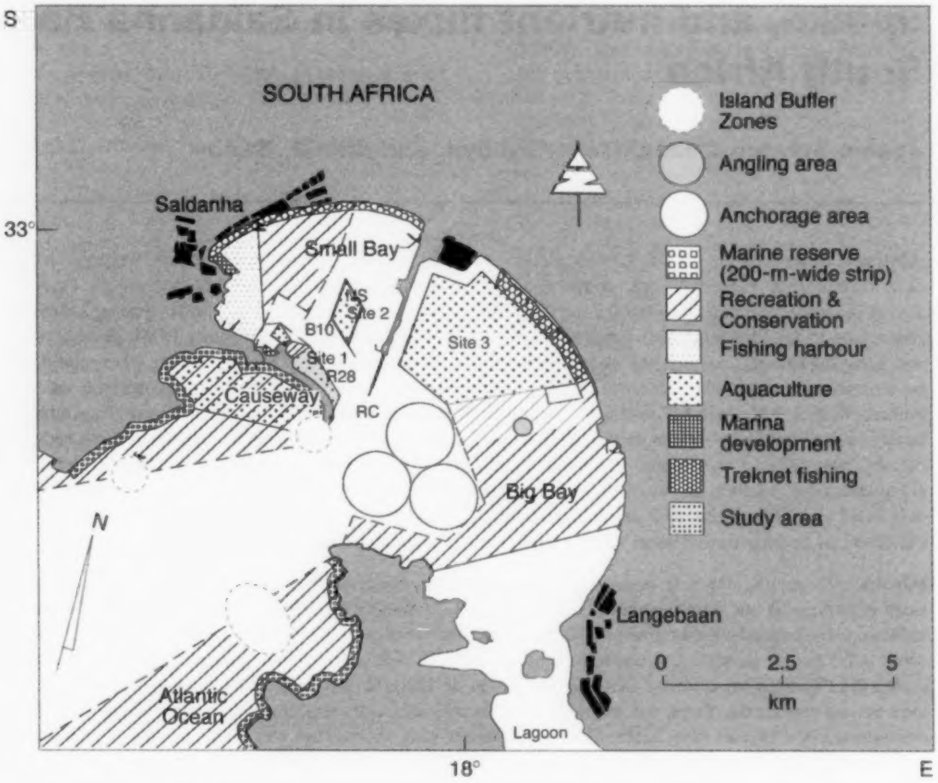

veys to assess the impact of effluents from fish factories (Moldan 1978; Jackson and McGibbon 1991). These studies indicated a shift from suspension to deposit feeders that was attributed to organic loading from fish factory effluent and the reduction in water circulation imposed by harbour construction. In response to mussel farming started in 1985, a 4-year project was initiated to assess the spatial and temporal changes in benthic macrofaunal communities under the rafts and outside the farm. Below rafts, the abundance and biomass of suspension feeders were further reduced, while those of carnivores increased (Stenton-Dozey et al. 1999). Moreover, within the farm, position rather than age of a raft correlated with the degree of community disturbance. From transect lines leading out from the farm, it was deduced that impact was localised.

Monitoring changes in macrobenthic communities has proven to be a successful signal of benthic impact from culture biodeposition (Mattsson and Lindén 1983; Gowen and Bradbury 1987; Ritz et al. 1989). However, this signal gives no indication of changes in benthic processes that could quantify the level of impact. Our focus in Saldanha Bay thus shifted toward investigating in situ net fluxes of O_2 and nutrients across the sediment–water interface in relation to the biomass of macroinfauna and sediment biogeochemistry.

The hypothesis posed in this paper is that biodeposition from mussel rafts has a significant effect on the benthic environment in Saldanha Bay leading to organic enrichment and anoxia in the sediments, altered O_2 uptake and nutrient flux rates, and impoverishment of the macrofauna. The extent of impact is assessed by comparing the raft site with three reference sites at a distance of 1–3 km from the mussel farm. Results are presented as the content of organic C, N, and S_2O_4 in sediments and in situ measures of the uptake and (or) release of O_2, ammonium (NH_4), and phosphate (PO_4). The role of benthic macrofauna in the uptake of O_2 and flux of nutrients is discussed in relation to faunal biomass and the key trophic groups, namely suspension feeders, detritivores, and carnivores.

Material and methods

Study area

The mussel farm (80 ha) is located within an area called Small Bay formed by an iron ore jetty and a causeway that shelters the rafts on the west side from the Atlantic Ocean (Fig. 1). The sediments are dominated (70%) by fine to medium sand (63–500 μm) (Stenton-Dozey et al. 1999). Currents are subject to wind and tidal forcing (Monteiro et al. 1998) as well as bay resonance at the bay scale and retardation by the rafts at the farm scale. Velocities are therefore highly variable, with an average of 7.5 cm·s^{-1} between and 1.25 cm·s^{-1} within the rafts (Boyd and Heasman 1998). The water column in Saldanha Bay varies from being strongly thermally stratified between 10 and 18°C during most of the upwelling season of summer to being well mixed between 10 and 14°C in winter (Monteiro et al. 1998).

Mussels are grown on ropes by natural seeding to a depth of 6 m, with 320 ropes per raft yielding approximately 27 t wet weight with shell (Heasman 1996). This amounts to an annual marketable yield of between 2000 and 3000 t for a total of 74 rafts with two harvests per year on average (V. Pienaar, Blue Water Aquafarms, Saldanha Bay, South Africa, personal communication).

Two field trips were undertaken, one in winter (June 1997) and another in summer (February 1998). A 10-year-old raft (R28) was selected as a study site together with three reference sites (RC, B10, and NS) similar in depth (between 12 and 15 m) and sediment granulometry but at varying distances from the farm (Fig. 1). These reference sites refer to an initial raft control site (RC), a monitoring buoy (B10), which has served as a bay monitoring site since 1989, and a new 50-ha lease site (NS), which has not yet been farmed.

Sediment C, N, and total reduced sulphides (TRS)

To assess the extent of organic debris accumulated below rafts, sediment cores were extracted by divers from beneath R28 and a reference site (RC) and analysed for the content of particulate organic C (POC) and N (PON) and TRS. The depth of cores varied between 20 and 25 cm depending on penetrability, which was often limited at the raft site by mussel shell fragments.

Of the four cores extracted per site per season, two cores were frozen and later sliced into a 1-cm section from the surface and every 2 cm thereafter, resulting in a possible maximum of 13 segments per core. Each segment was freeze-dried, ground, and analysed on a LECO CHN analyser for POC and PON after inorganic carbonates were acid leached with diluted HCl. A further two cores, segmented as above, were kept under nitrogen and frozen for later extraction into hot concentrated HCl in the presence of Chrome 11 (modified from Canfield et al. 1986). The H_2S that evolves includes acid-volatile S and S species such as iron pyrite (FeS_2), which is resistant to oxidation by gentler means. H_2S was trapped in sulphide antioxidant buffer and titrated on a Dosimat system against 0.1 M lead acetate. The endpoint was determined electrometrically using a silver/sulphide ion-selective electrode and a KCl-filled reference electrode. Data were expressed as percentages by weight of organic C and N and TRS.

In situ O_2 uptake and nutrient fluxes

A benthic data-logging respirometer with a light meter, temperature probe, and three Kent O_2 probes was deployed by divers. Two O_2 probes were inserted into benthic chambers (16 L, surface area 0.115 m^2), and one probe hung free in the water column to monitor and correct for ambient changes in O_2 levels. The chambers were flushed by a pump attached to the respirometer and then isolated to follow the decline in O_2 levels over 2 h. Water was circulated within the chambers by current-driven impellers, and O_2 levels and temperature were logged every minute. At each site, incubations were repeated on consecutive days, one of the two chambers being darkened to take account of phytobenthic activity. The sediment covered by the chambers (0.115 m^2) was sampled for macrofauna using a diver-operated suction sampler as described in Stenton-Dozey et al. (1999).

It is important to note that the sediment surface below rafts is littered with shell debris to a depth of 20 cm in some places, and above this is occasionally suspended an organic-rich nepheloid layer that varies between 10 and 30 cm in thickness, depending on benthic currents. Creamy films of chemoautotrophic sulphur bacteria, not present at reference sites, cover the bottom in patches. These conditions created difficulties for divers when placing the chambers and the respirometer. A clear, relatively smooth area devoid of shells had to be selected, and great care was necessary when positioning the chambers so as not to disturb surface sediments. Chambers were gently flushed for 0.5 h before the 2-h incubation commenced to allow the sediment surface environment to normalise.

During the 2-h incubations, 50-mL seawater samples were extracted from the benthic chambers at 0.5-h intervals, commencing at time zero. The pressure in the chambers was kept constant by active volume compensation during sampling. These were immediately filtered through GF/F filters into darkened bottles and stored on ice to be analysed ashore for NH_4, nitrites (NO_2), nitrates (NO_3), and PO_4 according to the methods of Grasshoff et al. (1983). Fluxes were defined as the slope of the regression between concentration of nutrient and incubation time.

To quantify the impact of raft mussel culture on the benthos, significant differences between raft and reference sites were assessed using univariate and multivariate analyses of variance and Tukey's honest significant difference post hoc comparative test according to Zar (1984) using Microsoft Software Statistica 5.3.

Results

Sediment carbon, nitrogen, and sulphide profiles

Sediment profiles were analysed to assess the depth of impact from biodeposition rather than to identify a seasonal trend in POC, PON, or TRS. Thus, data for the two field trips (summer and winter) were pooled, resulting in four replicates for estimates of POC, PON, and TRS for each core segment (1-cm section from the surface and 2-cm segments thereafter) for each site. Intra- and inter-site differences were analysed using one-way analysis of variance and Tukey's test for post hoc comparisons. Data without four replicates per core segment, as at depths >19 cm under the raft, were omitted from analyses.

POC was significantly greater under the raft than at reference site RC ($F_{(18,58)} = 3.53$, $p < 0.0001$), with surface POC an order of magnitude higher (7.5 versus 0.4%) (Fig. 2*a*). Downcore ≥9 cm, raft POC declined (5.8%) ($F_{(9,30)} = 7.29$, $p < 0.05$), whereas at RC, there was an increase from 0.4% subsurface to 0.9% at 19 cm ($F_{(9,30)} = 3.15$, $p < 0.05$). PON showed trends similar to those of POC (Fig. 2*b*); below mussels, the greater PON ($F_{(20,64)} = 3.28$, $p < 0.0002$) was most obvious at the surface (0.7 versus 0.08% at RC) but declined downcore ≥11 cm ($F_{(10,33)} = 5.87$, $p < 0.05$) while increasing ≥17 cm at the reference site ($F_{(10,33)} = 3.73$, $p < 0.05$). Figure 2*c* shows that organic C:N ratios were higher at R28, between 12 and 15 compared with a range of 5–7 at RC ($F_{(17,64)} = 29.76$, $p < 0.05$). Further, the ratios do not significantly vary down the sediment cores at either site (R28: $F_{(8,27)} = 1.87$, $p < 0.05$; RC: $F_{(8,27)} = 0.73$, $p < 0.05$).

Sediment below mussels was anoxic and significantly different from the reference, even at the surface (TRS = 0.04 versus 0.014% at RC) ($F_{(20,64)} = 16.94$, $p < 0.05$) (Fig. 2*d*). TRS increased threefold down to 20 cm where black colouration confirmed the reduced state of deeper raft sediments ($F_{(10,33)} = 80.60$, $p < 0.05$); this increase was the reciprocal of the downcore decline in POC (Fig. 2*a*) and PON (Fig 2*b*). At RC, TRS remained fairly constant with depth between 0.01 and 0.02% ($F_{(10,33)} = 1.04$, $p > 0.05$).

Fig. 2. Sediment core profiles (25 cm deep) at raft site R28 (squares) and reference site RC (triangles) showing the percentage by weight of (*a*) POC and (*b*) PON, (*c*) C:N ratios, and (*d*) TRS. Each data point is a mean ($n = 4$) ± 1 SE.

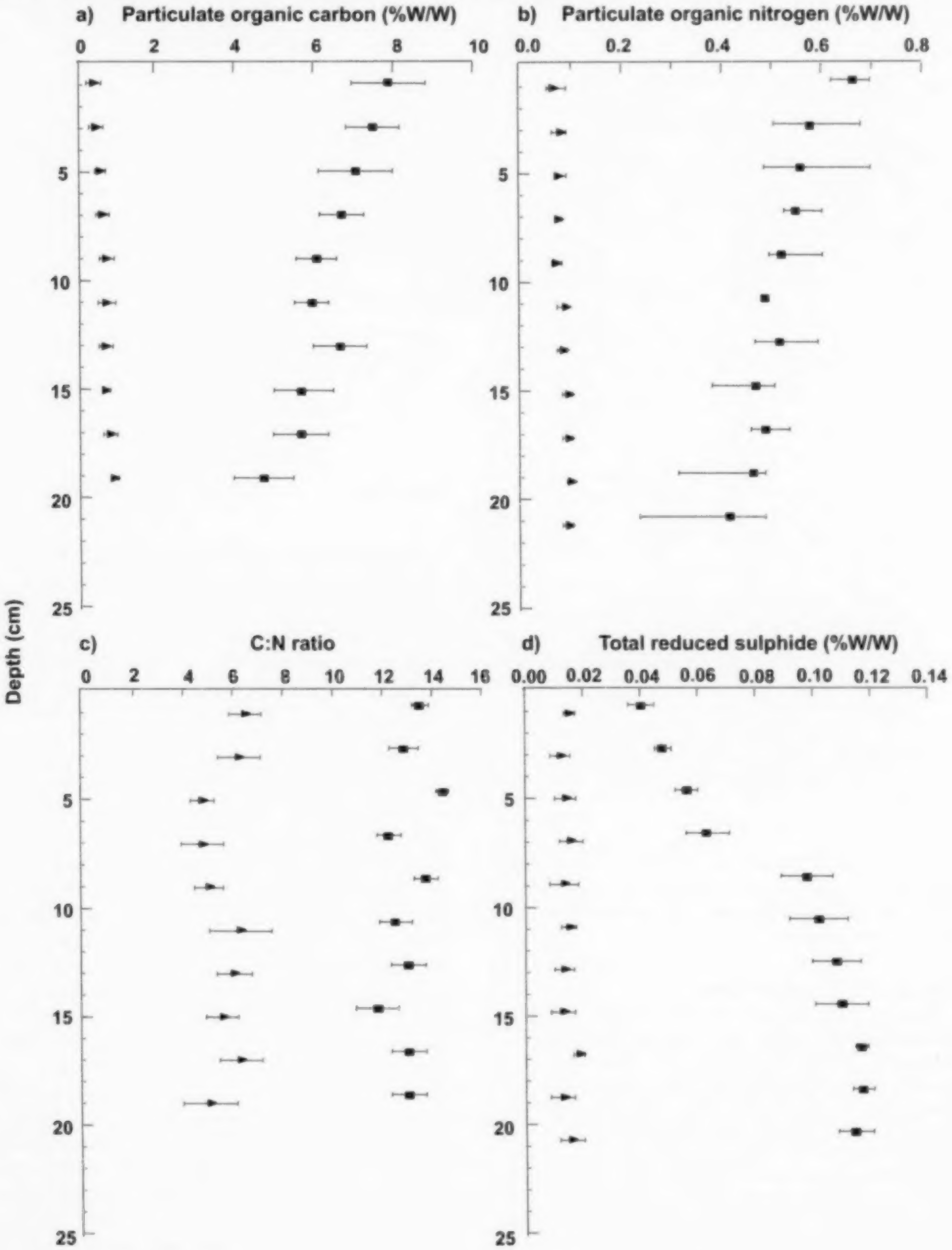

O_2 uptake and nutrient fluxes

There was little variation in measures of O_2 uptake or nutrient fluxes between light and dark chambers, so these data were combined to provide four replicates for each site. Theoretically, darkening chambers should eliminate photosynthetic production of O_2, thereby reflecting net uptake by sediments at depths of 12–15 m. These expected results were not obtained, which questions the validity of using darkened chambers during the day. Future surveys are planned to overcome this problem by incubating at night and quantifying chlorophyll production in surficial sediments.

Two-way analysis of variance (type 111 SS), followed by Tukey's test, showed that O_2 uptake by sediments was lowest under the raft ($F_{(3,24)} = 6.46$, $p < 0.002$), the principal difference being between sites ($F_{(3,24)} = 5.34$, $p < 0.006$) rather than season ($F_{(1,30)} = 1.9$, $0.05 < p < 0.178$) (Fig. 3). How-

Fig. 3. In situ fluxes of O_2 in summer (open bars) and winter (shaded bars) at raft site R28 and the three reference sites (RC, B10, NS). Each data point is a mean ($n = 4$) ± 1 SE.

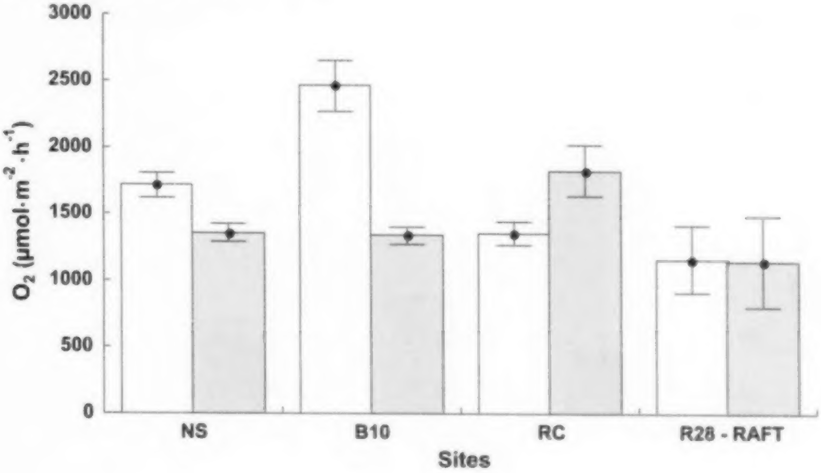

Fig. 4. In situ fluxes of NH_4 in summer (open bars) and winter (shaded bars) at raft site R28 and the three reference sites (RC, B10, NS). Each data point is a mean ($n = 4$) ± 1 SE.

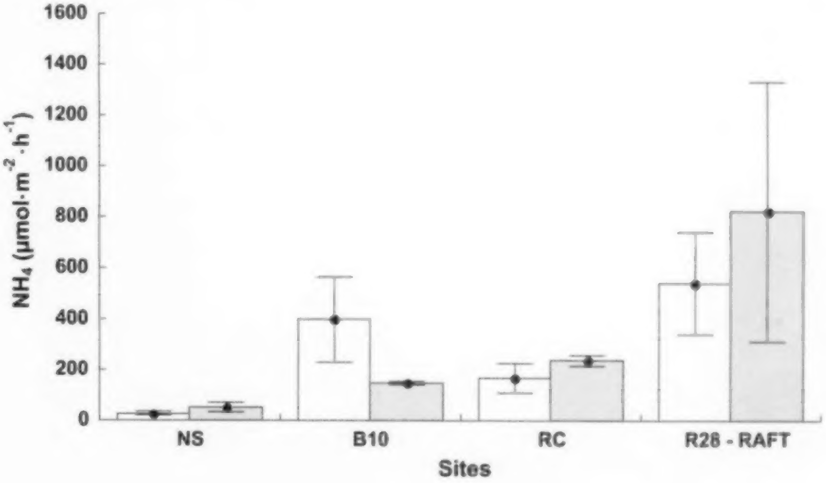

ever, these data are misleading in that intersite differences were not attributable to the low O_2 uptake rate by raft sediments (1100 $\mu mol \cdot m^{-2} \cdot h^{-1}$) but rather to a significantly high rate (2463 $\mu mol \cdot m^{-2} \cdot h^{-1}$) at one of the reference sites (B10). This site proved to be an anomalous control because of dense patches of the burrowing prawn *Upogebia capensis*. Thus, changes in the rate of O_2 uptake by sediments could not be linked to heavy biodeposition from mussel culture.

NH_4 was the main N-containing mineral component released from the sediments. Since NO_2 and NO_3 releases were consistently negligible by comparison, being two to three orders of magnitude lower (<5 $\mu mol \cdot m^{-2} \cdot h^{-1}$), these data were excluded from analyses. There was no indication of negative NH_4 fluxes, the lowest rate (40 $\mu mol \cdot m^{-2} \cdot h^{-1}$) being measured in summer at NS.

While NH_4 flux from sediments was highest under the raft (825 μmol $NH_4 \cdot m^{-2} \cdot h^{-1}$ in winter), the standard error around the mean was also the highest (±500 μmol $NH_4 \cdot m^{-2} \cdot h^{-1}$) (Fig. 4). This is indicative of within-sample variance, which negated identifying intersite differences other than between R28 and NS ($F_{(3,24)} = 3.59$, $p < 0.028$). Although not significant, reference fluxes were lower and less variable than at R28. The interaction effect of site and season was not significant ($F_{(3,24)} = 0.57$, $0.05 < p < 0.64$) and neither was season alone ($F_{(3,24)} = 0.57$, $0.05 < p < 0.83$).

PO_4 fluxes presented no conclusive result; two reference sites (B10 and RC) were atypical in having the highest rates with wide variation (Fig. 5). Rates ranged between 25 and 140 $\mu mol \cdot m^{-2} \cdot h^{-1}$ with no significant differences in a site–season interaction ($F_{(3,24)} = 0.636$, $0.05 < p < 0.56$), between sites ($F_{(3,24)} = 02.48$, $0.05 < p < 0.09$), or between seasons ($F_{(3,24)} = 3.57$, $0.05 < p < 0.07$). A ratio of mean flux rates of

Fig. 5. In situ fluxes of PO_4 in summer (open bars) and winter (shaded bars) at raft site R28 and the three reference sites (RC, B10, NS). Each data point is a mean ($n = 4$) ± 1 SE.

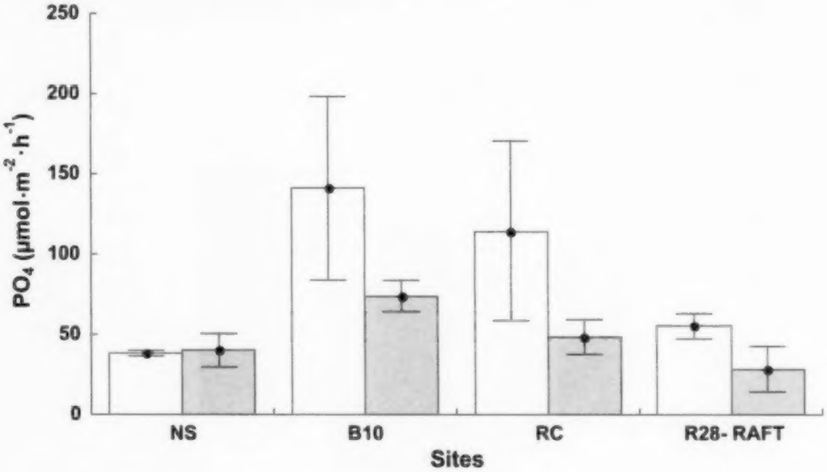

Fig. 6. Ratio of fluxes in NH_4 and PO_4 in winter 1997 (shaded bars) and summer 1998 (open bars) calculated from the means in Figs. 4 and 5 at raft site R28 and three reference sites (RC, B10, NS). Additional data from winter 1998 are included for comparison (second shaded bar for each site).

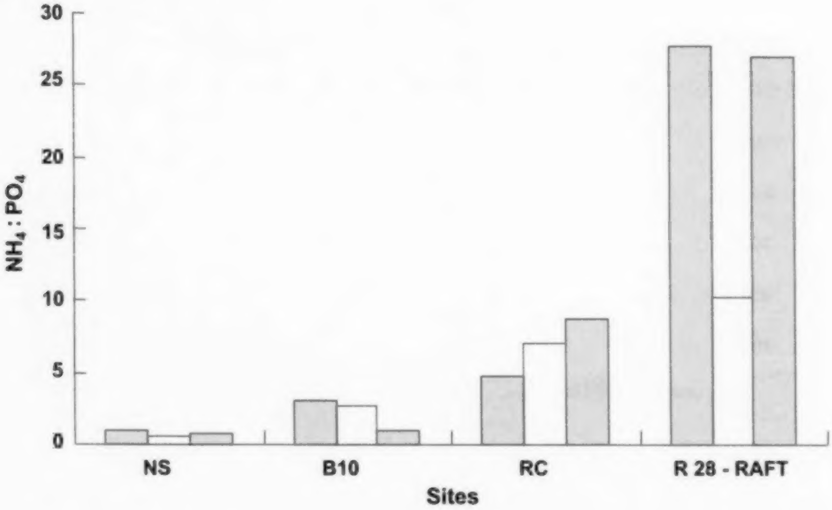

NH_4 and PO_4 provided a clearer signal of the complex interactions during decomposition, denitrification, and remineralisation in sediments (Fig. 6). With inclusion of data from the winter 1998 survey, a pattern emerged wherein NH_4:PO_4 was always highest at R28 (10:1 to 27:1), with the ratio being maximal in winter. Since neither NH_4 nor PO_4 fluxes were significantly different between reference sites, these data were combined in a multiple regression that showed a significant positive correlation between the two fluxes ($r = 0.72$, $p < 0.0001$) with a geometric mean estimate for the N:P ratio of 2.89 ± 1.8 ($n = 24$). This mean is within the range shown for reference sites in Fig. 6 (2:1 to 8:1). No such positive correlation was shown between the fluxes at R28 ($r = 0.39$, $0.05 < p < 0.07$), possibly because of the high standard errors for NH_4 flux rates (Fig. 4) and a small sample size ($n = 8$). Based on the trend in Fig. 6, however, it is likely that with more data, a significantly higher N:P ratio would be identified in relation to heavy biodeposition.

Benthic macrofauna

Macrofauna biomass (grams dry weight per square metre) was significantly different between sites ($F_{(3,24)} = 27.44$, $p < 0.0001$), seasons ($F_{(3,24)} = 11.66$, $p < 0.0023$), and in an interaction of both of these variables ($F_{(3,24)} = 10.38$, $p < 0.0001$) (Fig. 7). Biomass at R28 was diminished compared with reference sites except that for summer at RC (Tukey's test). At this reference site, low biomass could be attributed to the absence of the large burrowing prawn *U. capensis*

Fig. 7. Organic biomass of benthic macrofauna in summer (open bars) and winter (shaded bars) at raft site R28 and the three reference sites (RC, B10, NS). Each data point is a mean ($n = 4$) ± 1 SE.

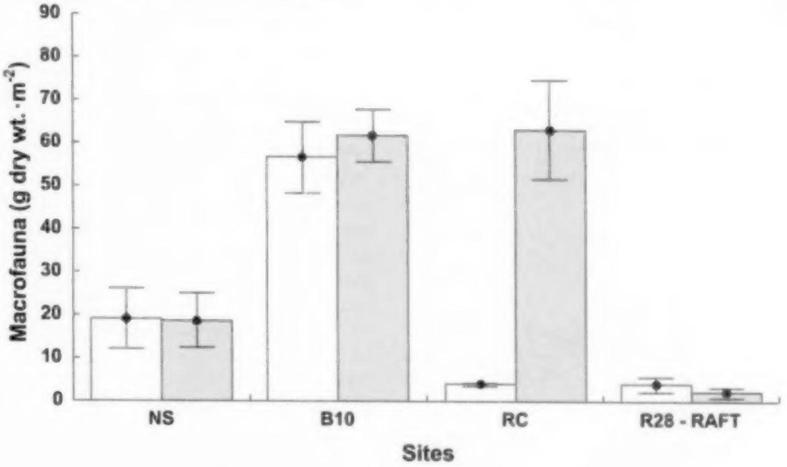

Fig. 8. Percentage of macrofauna biomass as suspension feeders (open bars), detritivores (light speckled bars), and carnivores (dark speckled bars) at raft site R28 and the three reference sites (NS, B10, RC). Summer and winter data were combined. Each data point is a mean ($n = 8$) ± 1 SE.

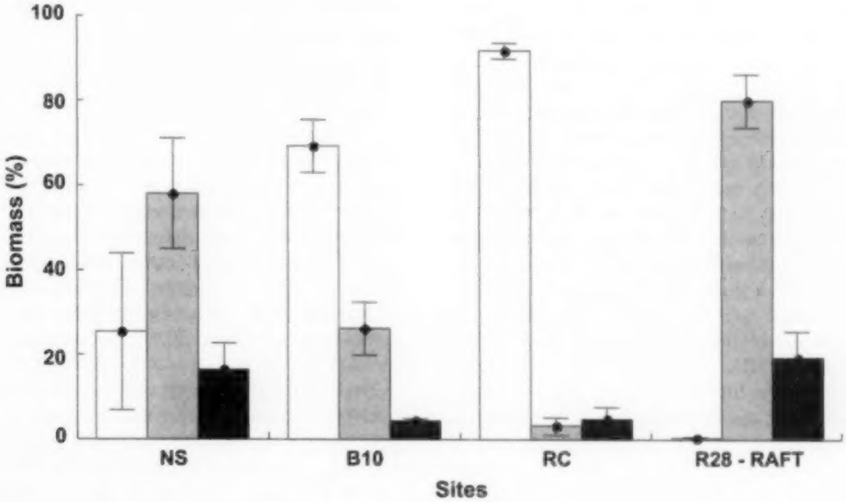

rather than to season. This species is unevenly distributed at RC and B10 and, when present in samples (e.g., winter RC), can account for up to 80% of the biomass.

When distinguishing between trophic groups, data from all seasons were used to estimate the mean percentage dominance by weight for each site ($n = 8$). At R28 detritivores (80%) and carnivores (19%) dominated and suspension feeders made up less than 1% of total biomass (Fig. 8). At B10 and RC, suspension feeders dominated (70% and 90% respectively), and at NS this group was second (25%) to detritivores (55%). The burrowing prawns *U. capensis* and *U. africana* accounted for most of the suspension feeding biomass at B10 and RC, and their dominance is reflected in Fig. 9 within the taxon Anomura. The echiuroidean *Ochaetostoma capense*, a large species like the prawns, also frequented reference sites. Under the raft, different taxa were dominant: deposit-feeding Bivalvia (*Nocula nucleous*, *Macoma crawfordi*, and *Tellina* spp.), detritivorous Polychaeta (*Polydora* spp. and *Prionospio sexuculata*), and carnivorous Gastropoda (*Nassarius speciosa* and *N. vinctus*).

O_2 and nutrient fluxes in relation to macrofauna biomass

O_2 and nutrient exchange rates across a sediment–water interface were related to the macrofauna biomass in the sediment by standardising micromoles per hour per gram dry weight for each site and season ($n = 4$) (Fig. 10). These ratios were significantly greater at the raft relative to the reference sites (O_2: $F_{(3,24)} = 11.12$, $p < 0.0001$; NH_4: $F_{(3,24)} = 3.78$, $p < 0.023$; PO_4: $F_{(3,24)} = 3.49$, $p < 0.031$), a difference that reflects the significant reduction in macrofauna biomass,

Fig. 9. Percentage of biomass of different macrofauna taxa at raft R28 and the three reference sites (NS, B10, RC). Summer and winter data were combined. Each data point is a mean ($n = 8$) ± 1 SE.

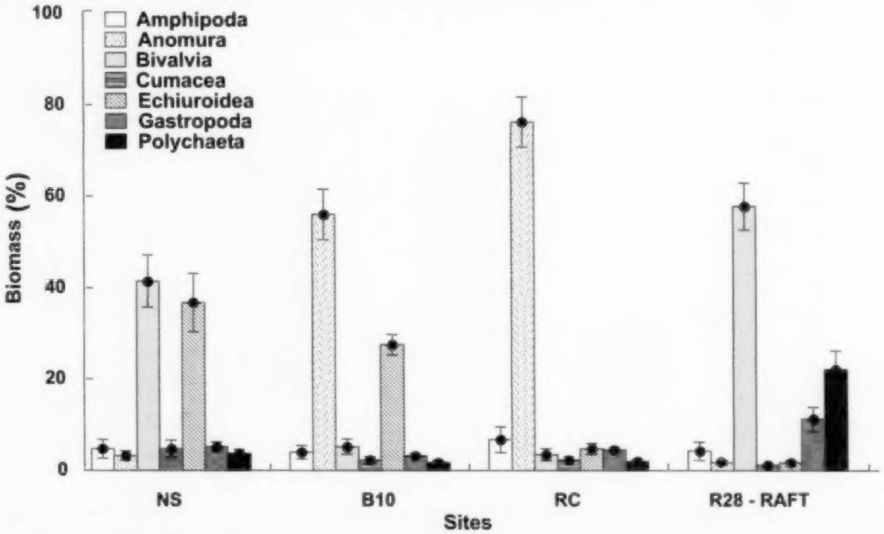

while concomitant O_2 uptake and nutrient fluxes under mussel culture could not be separated from those of the references. This discrepancy highlights the complexity of biogeochemistry in organically enriched sediments and the difficulty in interpreting the integral role of macrofauna in nutrient regeneration via metabolism and bioturbation in such sediments. Clearly, the role of macrofauna in sediment is not a simple ratio of rate against a unit of body mass.

Another way of viewing these data is to regress in situ flux rates (micromoles per square metre per hour) to in situ macrofauna biomass (grams dry weight per square metre) measured in any one chamber irrespective of season or site ($n = 32$). There was a weak positive and significant relationship between macrofauna and O_2 uptake ($r = 0.48$, $p < 0.0047$), but no such correlation existed for PO_4 flux rates ($r = 0.24$, $p < 0.18$) or NH_4 ($r = 0.15$, $p < 0.4$). Heavy biodeposition that results in high POC, TRS, and C:N ratios (Fig. 2) in sediments generates complex biogeochemical processes that cannot be decisively interpreted from the data in this study.

Discussion

Core profiles

Heavy biodeposition under rafts in Saldanha Bay created organic enrichment and anoxic conditions ≥10 cm downcore. This loading can be attributed to high biomass production of about 105 t wet weight·raft^{-1}·year^{-1}, inclusive of mussels and foulers, principally the tunicate *Ciona intestinalis* (Heasman 1996; Grant et al. 1998). Since *C. intestinalis* is a suspension feeder like *M. galloprovincialis*, ingestion and assimilation of phytoplankton would generate enormous quantities of faeces and pseudofaeces deposits, as found in other culture farms (Dahlbäck and Gunnarsson 1981). On one occasion, the biodeposition rate under R28 was measured as 845 g organic C·m^{-2}·day^{-1}; this is three times the rate measured outside the farm (P. Monteiro, Centre for Scientific and Industrial Research, Stellenbosch, South Africa, unpublished data). This value is higher than those reported for other shellfish suspended culture sites (10–508 g C·m^{-2}·day^{-1}) (Smaal and Prins 1993). Clearly, however, the quantity and rate of faecal deposition would vary with filter-feeding biomass, seston concentrations, and feeding efficiency of *M. galloprovincialis* (van Erkom Schurink and Griffiths 1992; Grant et al. 1998) and *C. intestinalis* (Kjerulf-Petersen and Riisgård 1992; Lesser et al. 1992; Grant et al. 1998) as well as food acquisition, which would be strongly dependent on the nature and magnitude of particle transportation (LaBarbera 1984) and resuspension (Prins and Smaal 1994). Besides faeces, further deposition arising from the dislodgement of mussels and foulers during harvesting and storms can amount to 20% of annual total harvest (Heasman 1996).

High POC in raft sediment also reflects an accumulation over the 10 years that the raft has been in position, the relatively high C:N ratios to reference suggesting aggregation of refractory organic C. Fabiano et al. (1994) showed that labile POC originating from the faeces of *M. galloprovincialis* was degraded by colonising bacteria and protozoans within 4 days, while the somatic tissue took longer, 42% being decomposed within 11 days. The raft sediments in Saldanha Bay thus appear to act as a sink for the less labile POC and PON that are resistant to diagenetic decomposition (Grant and Hargrave 1987). Fichez (1991), studying the biogeochemical C budget in submarine cave sediments, found that 80% of buried biodeposits (up to 15 cm) was complex structured organic matter, composed mainly of carbohydrate–protein aggregates requiring substantial energetic investment to fractionate into simple degradable organic compounds (Tenore et al. 1984).

The presence of organic C at depth in raft sediments suggests that macrofauna may be responsible for mixing sediment downcore, even under anoxic conditions as inferred from the marked increase in percent TRS downcore. Small opportunistic polychaetes, tolerant of such conditions (Ritz et al. 1989), were relatively abundant at 15 cm: species such as *Dorvillea rudolphi*, *Mediomastus capensis*, *Prionospio sexoculata*, and *Eunoe nodulosa*. It has been suggested that greater burrowing activity under mussel culture creates "microsites," tiny pockets of aerobic decomposition, which enhance nitrification despite the more reduced conditions in the sediments (Knowles 1978). With more NO_3 available for denitrification, this process could have played a role in the elevated release of NH_4 observed at the raft site. Such bioturbation would, however, also obscure the dissociation between oxic and anoxic processes, a continuum feature common to marine sediments (Thamdrup and Canfield 1996). Notwithstanding, the substantial proportion of TRS compared with the reference site indicates the importance of anaerobic metabolism in remineralisation under rafts.

O_2 uptake and nutrient fluxes

No conclusive inference could be made on the impact of biodeposition on O_2 uptake by sediments, all rates being in the range 24–62 $mmol{\cdot}m^{-2}{\cdot}day^{-1}$. These values lie within ranges measured in embayments impacted by mussel culture (Baudinet et al. 1990; Hatcher et al. 1994) but are also within the range measured in unimpacted bays (Hargrave et al. 1993). This supports the maxim that benthic O_2 fluxes may not be a sensitive indicator of higher organic input from mussel culture because of increased activity of the S cycle (as evidenced by high percent TRS in Saldanha Bay sediments) concomitant with higher rates of chemical O_2 demand and the storage of end products such as pyrite (Holmer and Kristensen 1992).

There are other factors that cloud the sensitivity of O_2 uptake as an indicator of impact. The mineralisation of organic matter and the bioturbation activity of macrofauna play a significant role in sediment O_2 demand (Hopkinson 1987), as was mentioned earlier in relation to microsites (Knowles 1978). Moreover, benthic photosynthesis can counterbalance O_2 uptake and can play a substantial role in the absorption of nutrients (Baudinet et al. 1990; Barranguet et al. 1994). Our attempt to measure net O_2 sediment uptake by eliminating photosynthetic activity in darkened incubations was unsuccessful. Later surveys in Saldanha Bay have included nighttime incubations and sediment chlorophyll analyses that will better quantify the role of phytobenthos.

From increased biodeposition of organic C and N below rafts and the concomitant increase in decomposition and denitrification (Kaspar et al. 1985; Hansen and Blackburn 1991; Hargrave et al. 1993), one may expect more NH_4 and PO_4 release (Fabiano et al. 1994; Prins and Smaal 1994) compared with unimpacted sediments. Such distinction was not consistent between the raft and reference sites or between seasons. Although NH_4 flux peaked under the raft at 19.8 mmol $NH_4{\cdot}m^{-2}{\cdot}day^{-1}$, this rate was only significantly greater than at one of the reference sites (0.48 mmol $NH_4{\cdot}m^{-2}{\cdot}day^{-1}$). In general, the range of NH_4 flux rates is comparable with that at other sites impacted by mussel culture (Kaspar et al. 1985; Grant et al. 1995; Mazouni et al. 1996).

NH_4 flux under mussel culture was widely variable in summer (SE = ±5 mmol $NH_4{\cdot}m^{-2}{\cdot}day^{-1}$) and winter (SE = ±500 mmol $NH_4{\cdot}m^{-2}{\cdot}day^{-1}$). This precluded identifying a significant impact using NH_4 flux as an indicator. Heavy biodeposition of faeces and animal tissue, accumulation of POC and PON in sediments, and the natural seasonal bloom and decay of phytoplankton (Monteiro et al. 1998; Pitcher and Calder 1998) contribute to a myriad of factors that can influence NH_4 flux. In summer, there is often a thermocline 1 m from the bottom, exposing the benthic environment to NO_3-enriched upwelled water lower in temperature and different in biogeochemical composition. This could influence the complexity of the relationship between nitrification and denitrification. Further, in winter, the water column is well mixed, possibly stimulating greater interchange and NH_4 flux across the sediment–water interface. The fact that NO_2 and NO_3 sediment flux rates were consistently low and sometimes negative (uptake by sediments) is indicative of the complexity of NH_4 production. NO_3 generated by nitrification following animal protein degradation (dislodged mus-

Fig. 10. (*a*) O_2 uptake and (*b*) NH_4 and (*c*) PO_4 fluxes ($\mu mol{\cdot}m^{-2}{\cdot}h^{-1}$) in relation to macrofauna biomass (g dry weight) in summer (open bars) and winter (shaded bars) at raft site R28 and the three reference sites. Each data point is a mean (n = 4) ± 1 SE.

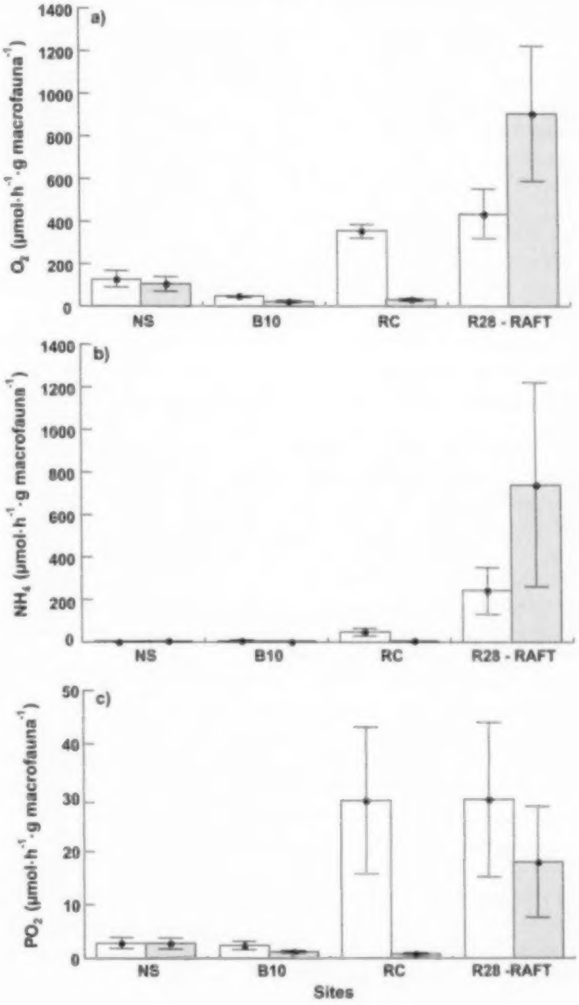

sels and foulers) and aerobic decomposition of labile organic material (faeces) would rapidly enter the denitrification loop, producing more NH_4 and PO_4.

PO_4 fluxes and molar ratios of N:P presented no conclusive results. This is unexpected, since the anoxic conditions under the raft provide a strong reducing environment that should greatly enhance PO_4 release (Balzer et al. 1983), and the decay of mussel faecal material would also be responsible for PO_4 production (Fabiano et al. 1994) relative to the references. However, this argument is counterbalanced by Sundby et al. (1992) having identified interstitial water as a trap for PO_4 due to the adsorption–desorption equilibrium of PO_4 reacting with iron oxides. Iron ore is loaded onto ships in Saldanha Bay, and based on predictive modelling of the transport and fate of trace metals (Monteiro et al. 1999), it is likely that the sediments in and around the farm are high in iron oxides.

Benthic macrofauna

Raft biodeposition had a dramatic effect on benthic macrofauna biomass, reducing it to between 5 and 15% of that at reference sites. Such an effect impacts negatively on community structure, as identified in *ABC* plots and hierarchical cluster analyses in a previous study on the mussel farm (Stenton-Dozey et al. 1999) and as found in other mariculture systems (Kaspar et al. 1985; Hatcher et al. 1994). The raft population was dominated by small *r*-strategists (e.g., polychaetes) compared with larger *K*-strategists outside the farm (e.g., prawns, tongue worms). Besides biogeochemical changes, alteration of bottom topography by debris accumulation (ropes, shells, mussels, foulers) provided a multitude of niches that were absent at the reference sites where flat sandy bottoms prevailed. In Saldanha Bay, these niches were occupied by deposit-feeding bivalves and carnivorous/scavenging gastropods that fed upon organic debris.

Macrofauna, O_2 uptake, and nutrient fluxes

A weak positive relationship existed between O_2 uptake and macrofauna biomass when these variables were paired within an individual 2-h sediment incubation, irrespective of season or site. Macrofauna represent the largest measured biological biomass in the sediments (Jackson and McGibbon 1991; Stenton-Dozey et al. 1999; J. Stenton-Dozey, personal observation), and their role in O_2 uptake must be substantial. That O_2 flux per gram of macrofauna at the raft site was up to 15 times that at reference sites can be expected, since intersite differences in O_2 uptake were minimal, while macrofauna biomass was substantially less at the raft site. This discrepancy, however, partially explains the extent to which organic debris recently deposited under rafts is responsible for uptake. Grant et al. (1995) estimated that organic deposits could account for 40% of the variance in sediment O_2 uptake below mussel lines. Within the top 10 cm of raft sediment, half the measured organic C content by weight was macrofauna and the other half was organic deposits; at the reference sites, nearly all organic weight measured was macrofauna. In effect, only 50% of the O_2 consumption under the raft could be related to macrofauna compared with nearly 100% at reference sites. The balance of raft O_2 uptake was likely attributable to increased activity of the S cycle (percent TRS) and high rates of chemical O_2 demand (Holmer and Kristensen 1992; Hargrave et al. 1993).

Application of the same approach in quantifying NH_4 release from sediments per unit organic weight is more difficult. The complex interactions between denitrification, ammonification, and decomposition merge with NH_4 excretion by fauna, the degradation of somatic tissue (Fabiano et al. 1994), and the role of bioturbation in accelerating nitrification and the exchange across the sediment–water interface. NH_4 flux could stand on its own as a sensitive indicator of impact without relating to macrofauna biomass, as found in other culture-impact research (Kaspar et al. 1985; Prins and Smaal 1994; Grant et al. 1995). However, in this study, the wide variation in raft NH_4 flux rates (up to 58% of mean) prevented such a conclusive assessment.

In overview, measures of particulate organic matter and anoxia in sediments plus independent assessment of macrofauna biomass proved the most consistent and reliable indicators of impact from mussel raft-culture. Sediments are sinks that accumulate debris and thereby reflect a compounded impact that is not subject to short-term variability as shown by nutrient fluxes. Uptake and (or) release rates of O_2 and nutrients provided no signal of seasonal or intersite differences that were rigorous enough for statistical testing. However, based on trends of the three fluxes measured, NH_4 release was the most indicative of impact and proved significantly greater than that at least one of the reference sites. Clearly, in situ measures of benthic impact from culture must be based on robust sensitivity indicators, multiple replication of measurements, and, ideally, more than one reference site to account for natural variability in faunal biomass and the dynamics of sediment–water biogeochemistry.

Acknowledgements

The authors are grateful to Geoff Bailey, Heather Sessions, and Claudia Colimo Melo for processing sediment cores and analysing nutrients and to the team for their unfailing support on land and in the water: André du Randt, Rick Harding, Liesl Arendse, Marcel van den Berg, Jon Mantel, and Niel Needham. Thanks to an anonymous referee whose comments greatly improved this manuscript. Financial support was provided in part by the National Marine Living Resources Fund.

References

Balzer, W., Grasshoff, K., Dieckmann, P., Haardt, H., and Petersohn, U. 1983. Redox-turnover at the sediment/water interface studied in a large bell jar system. Oceanol. Acta, **6**: 337–344.

Barranguet, C., Alliot, E., and Plante-Cuny, M.-R. 1994. Benthic microphytic activity at two Mediterranean shellfish cultivation sites with reference to benthic fluxes. Oceanol. Acta, **17**: 211–221.

Baudinet, D., Alliot, E., Berland, B., Grenz, C., Plante-Cuny, M.-R., Plante, R., and Salen-Picard, C. 1990. Incidence of mussel culture on biogeochemical fluxes at the sediment–water interface. Hydrobiologia, **207**: 187–196.

Boyd, A.J., and Heasman, K.G. 1998. Shellfish mariculture in the Benguela System: water flow patterns within a mussel farm in Saldanha Bay, South Africa. J. Shellfish Res. **17**: 25–32.

Canfield, D.E., Raisewell, R., Westrich, J.T., Reaves, C.M., and Berner, R.A. 1986. The use of chromium reduction in the analysis of reduced inorganic sulphur in sediments and shales. Chem. Geol. **54**: 149–155.

Christie, N.D., and Moldan, A.G.S. 1977. Effects of fish factory effluents on the benthic macrofauna of Saldanha Bay. Mar. Pollut. Bull. **8**: 41–45.

Dahlbäck, B., and Gunnarsson, L.Å.H. 1981. Sedimentation and sulphate reduction under a mussel culture. Mar. Biol. **63**: 269–275.

Fabiano, M., Danovaro, R., Olivari, E., and Misic, C. 1994. Decomposition of faecal matter and somatic tissue of *Mytilus galloprovincialis*: changes in organic matter composition and microbial succession. Mar. Biol. **119**: 375–384.

Fichez, R. 1991. Composition and fate of organic matter in submarine cave sediments; implications for the biogeochemical cycle of organic carbon. Oceanol. Acta, **14**: 369–377.

Gowen, R.J., and Bradbury, N.B. 1987. The ecological impact of salmonid farming in coastal waters: a review. Oceanogr. Mar. Biol. Annu. Rev. **25**: 563–575.

Grant, J., and Hargrave, B.T. 1987. Benthic metabolism and the quality of sediment organic carbon. Biol. Oceanogr. **4**: 243–264.

Grant, J., Hatcher, A., Scott, D.B., Pocklington, P., Schafer, C.T., and Honig, C. 1995. A multidisciplinary approach to evaluating benthic impacts of shellfish aquaculture. Estuaries, **18**: 124–144.

Grant, J., Stenton-Dozey, J.M.E., Monteiro, P., Pitcher, G., and Heasman, K. 1998. Shellfish culture in the Benguela System: a carbon budget of Saldanha Bay for raft culture of *Mytilus galloprovincialis*. J. Shellfish Res. **17**: 41–49.

Grasshoff, K., Ehrhardt, M., and Kremling, K. 1983. Methods of sea water analysis. Verlag Chemie, Weinham.

Hansen, L.S., and Blackburn, T.H. 1991. Aerobic and anaerobic mineralisation of organic material in marine sediment microcosms. Mar. Ecol. Prog. Ser. **75**: 283–291.

Hargrave, B.T., Duplisea, D.E., Pfeiffer, E., and Wildish, D. 1993. Seasonal changes in benthic fluxes of dissolved oxygen and ammonium associated with marine cultured Atlantic salmon. Mar. Ecol. Prog. Ser. **96**: 249–257.

Hatcher, A., Grant, J., and Schofield, B. 1994. Effects of suspended mussel culture (*Mytilus* spp.) on sedimentation, benthic respiration and sediment nutrient dynamics in a coastal bay. Mar. Ecol. Prog. Ser. **115**: 219–235.

Heasman, K.G. 1996. The influence of oceanographic conditions and culture methods on the dynamics of mussel farming in Saldanha Bay, South Africa. M.Sc. thesis, Rhodes University, Grahamstown, South Africa.

Holmer, M., and Kristensen, E. 1992. Impact of marine fish cage farming on metabolism and sulfate reduction of underlying sediments. Mar. Ecol. Prog. Ser. **80**: 191–201.

Hopkinson, C.S. 1987. Nutrient regeneration in shallow-water sediments of the estuarine plume region of the nearshore Georgia Bight U.S.A. Mar. Biol. **94**: 127–142.

Jackson, L.F., and McGibbon, S. 1991. Human activities and factors affecting the distribution of macrobenthic fauna in Saldanha Bay. S. Afr. J. Aquat. Sci. **17**: 89–102.

Kaspar, H.K., Gillespie, P.A., Boyer, I.C., and MacKenzie, A.L. 1985. Effects of mussel aquaculture on the nitrogen cycle and benthic communities in Kenepuru Sound, Marlborough Sounds, New Zealand. Mar. Biol. **85**: 127–136.

Kjerulf-Petersen, J., and Riisgård, H.U. 1992. Filtration capacity of the ascidian *Ciona intestinalis* and its grazing impact in a shallow fjord. Mar. Ecol. Prog. Ser. **88**: 9–17.

Knowles, R. 1978. Common intermediates of nitrification and denitrification and the metabolism of nitrous oxide. *In* Microbiology. *Edited by* D. Schlessinger. American Society for Microbiology, Washington, D.C. pp. 367–371.

LaBarbera, M. 1984. Feeding currents and particle capture mechanisms in suspension feeding animals. Am. Zool. **24**: 71–84.

Lesser, M.P., Shumway, S.E., Cucci, T., and Smith, J. 1992. Impact of fouling organisms on mussel rope culture: interspecific competition for food among suspension-feeding invertebrates. J. Exp. Mar. Biol. Ecol. **165**: 91–102.

Mattsson, J., and Lindén, O. 1983. Benthic macrofauna succession under mussels, *Mytulis edulis* L. (Bivalvia), cultured on hanging long-lines. Sarsia, **68**: 97–102.

Mazouni, N., Gaertner, J.-C., Deslous-Paoli, J.-M., Landrein, S., and Geringer d'Oedenberg, M. 1996. Nutrient and oxygen exchanges at the water–sediment interface in a shellfish farming lagoon (Thau, France). J. Exp. Mar. Biol. Ecol. **205**: 91–113.

Moldan, A.G.S. 1978. A study of the effects of dredging on the benthic macrofauna in Saldanha Bay, South Africa. S. Afr. J. Sci. **74**: 106–108.

Monteiro, P.M.S., Spolander, B., Brundit, G.B., and Nelson, G. 1998. Shellfish culture in the Benguela system: estimates of nitrogen-driven new production in Saldanha Bay using two physical models. J. Shellfish Res. **17**: 3–13.

Monteiro, P.M.S., Luger, S., Pretorius, P.J., and van Ballegooyen, R. 1999. Numerical modelling of eutrophication and particle dynamics in Saldanha Bay in order to predict the transport and fate of trace metals using the Delft3D-FLOW and -WAQ models. Proceedings Pollution 99, Lemnos, Greece. Wessex Institute of Technology Press (WIT Press), Ashurst, Southampton, U.K. pp. 1–17.

Pitcher, G.C., and Calder, D. 1998. Shellfish mariculture in the Benguela system: phytoplankton and the availability of food for commercial mussel farms in Saldanha Bay, South Africa. J. Shellfish Res. **17**: 15–24.

Prins, T.C., and Smaal, A.C. 1994. The role of the blue mussel *Mytilus edulis* in the cycling of nutrients in the Oosterschelde estuary (The Netherlands). Hydrobiologia, **282/283**: 413–429.

Ritz, D.A., Lewis, M.E., and Shen, M. 1989. Response to organic enrichment of infaunal macrobenthic communities under salmonid seacages. Mar. Biol. **103**: 211–214.

Smaal, A.C., and Prins, T.C. 1993. The uptake of organic matter and the release of inorganic nutrients by bivalve suspension feeding beds. *In* Bivalve filter feeders in estuarine and coastal ecosystems processes. *Edited by* R.F. Dame. Springer-Verlag., Berlin and Heidelberg. pp. 271–298.

Stenton-Dozey, J.M.E., Jackson, L.F., and Busby, A.J. 1999. Impact of mussel culture on macrobenthic community structure in Saldanha Bay, South Africa. Mar. Pollut. Bull. **39**: 357–366.

Sundby, B., Gobeil, C., Silberberg, N., and Mucci, A. 1992. The phosphorus cycle in coastal marine sediments. Limnol. Oceanogr. **37**: 1129–1145.

Tenore, K.R., Hanson, R., McClain, J., Maccubbin, A.E., and Hodson, R.E. 1984. Changes in composition and nutritional value to a benthic deposit feeder of decomposing detritus pools. Bull. Mar. Sci. **35**: 299–311.

Thamdrup, B., and Canfield, D.E. 1996. Pathways of carbon oxidation in continental margin sediments off central Chile. Limnol. Oceanogr. **41**: 1629–1650.

van Erkom Schurink, C., and Griffiths, C.L. 1992. Physiological energetics of four South African mussel species in relation to body size, ration and temperature. Comp. Biochem. Physiol. A, Comp. Physiol. **101**: 779–789.

Zar, J.H. 1984. Biostatistical analysis. Prentice-Hall International, Englewood Cliffs, N.J.

PERSPECTIVE

Consequences of model specification for the determination of gut evacuation rates: redefining the linear model

Alexander B. Bochdansky and Don Deibel

Abstract: The combination of gut contents and evacuation rate is an important tool to determine in situ feeding rates of many organisms. Traditionally used equations of gut evacuation models, however, have made a systematic comparison among models difficult. We changed the notation of the linear gut evacuation model to provide an algorithm compatible with the commonly used exponential model. Using examples from the literature, we demonstrate that prolonged retention of food after a true linear pattern of gut evacuation can be mistaken for an exponential pattern. In many of these examples, use of an exponential gut evacuation model causes overestimation of food consumption by approximately twofold. In situations where the entire gastrointestinal tract is examined instead of the stomach only, the time course of the gut content is best described by a plug-flow reactor for which the "input = output" rule applies. In contrast, the assumption of a "proportional release" must be met rigorously for the exponential model to be valid, which requires more complex feedback mechanisms than the simple plug-flow reactor. The new algorithm for the linear model is also consistent with the empirical observation that the gut evacuation rate is proportional to the initial gut content.

Résumé : La combinaison du contenu du tube digestif et du taux d'évacuation est une technique importante dans la détermination des taux d'alimentation in situ chez de nombreux organismes. Cependant, les équations couramment utilisées dans les modèles d'évacuation du tube digestif rendent la comparaison entre les modèles difficile. Nous avons modifié la notation du modèle linéaire d'évacuation du tube digestif de façon à produire un algorithme compatible avec le modèle exponentiel usuel. À l'aide d'exemples tirés de la littérature, nous démontrons qu'une rétention prolongée de la nourriture dans un vrai pattern linéaire d'évacuation du tube digestif peut être confondue avec un pattern exponentiel. Dans plusieurs de ces exemples, l'utilisation d'un modèle exponentiel d'évacuation du tube digestif surestime la consommation de la nourriture par un facteur d'environ 2. Dans les cas où tout le tube digestif est examiné, et non l'estomac seul, le suivi temporel du contenu intestinal se décrit de façon optimale comme le fonctionnement d'un réacteur de type blocage-écoulement dans lequel la règle que « l'entrée = la sortie » s'applique. En revanche, pour que le modèle exponentiel soit valide, il faut présumer de façon rigoureuse de l'existence d'une « évacuation proportionnelle » qui exige des mécanismes de rétroaction plus complexes que le modèle précédent. Le nouvel algorithme du modèle linéaire est aussi compatible avec l'observation empirique que le taux d'évacuation du tube digestif est proportionnel au contenu initial du tube.

[Traduit par la Rédaction]

Introduction

Despite the frequent use of gastric and gut evacuation rates in the past, fitting the appropriate model to gut evacuation continues to be arbitrary. The exponential model has been used most frequently, but others such as the linear, square root, and surface-dependent models have been applied as well (Jobling 1981; Persson 1986). The decision as to which model is most appropriate either has been based on the best least-square fit or a model was selected arbitrarily based on an apparent curvilinearity of the time series of the data set. Although all the examples in this paper are taken from the fish literature, the models are universally applicable to a variety of planktonic and benthic vertebrate and invertebrate organisms.

Although the linear model was the first model introduced for the purpose of measuring feeding rates in the field (Bajkov 1935), it only regained attention as the evacuation patterns of entire gastrointestinal tracts (i.e., guts) of many larval and juvenile fish were observed to be linear rather than curvilinear (Bromley 1987; Canino and Bailey 1995). The reluctance to apply the linear model stemmed from the

Received July 4, 2000. Accepted January 30, 2001. Published on the NRC Research Press Web site on April 25, 2001. J15848

A.B. Bochdansky.[1] Biology Department, Queen's University, Kingston, ON K7L 3N6, Canada.
D. Deibel. Ocean Sciences Centre, Memorial University of Newfoundland, St. John's, NF A1C 5S7, Canada.

[1]Corresponding author (e-mail: bochdans@biology.queensu.ca).

DOI: 10.1139/cjfas-58-5-1032

Fig. 1. (*a*) Linear and (*b*) exponential models in comparison using compatible parameter dimensions. In both cases, the evacuation rate is the slope (*E*). In the linear mode,l *E* is proportional to the initial amount of food in the gut, and in the exponential model, *E* is proportional to the food remaining in the gut (i.e., the rate changes over the time course). The cartoon represents fecal pellet size over time.

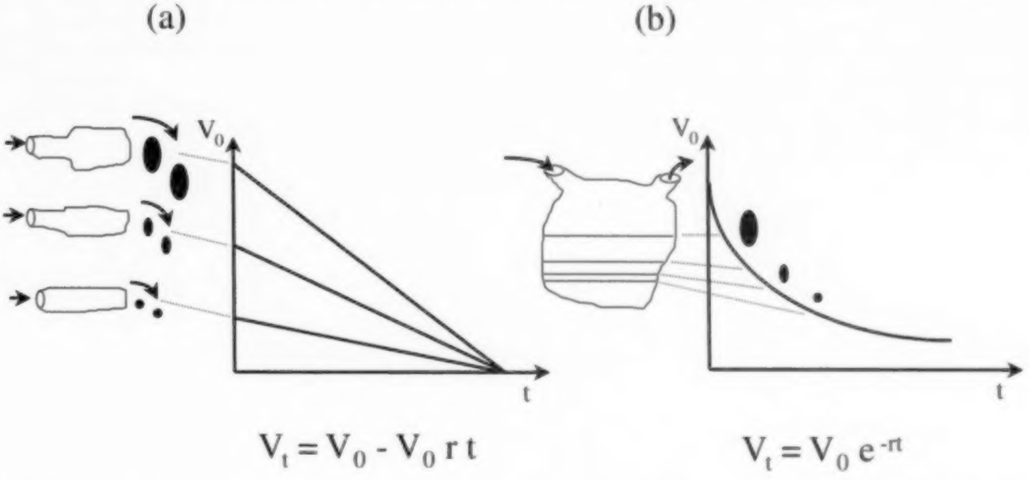

apparent curvilinearity of gut evacuation data sets and the lack of flexibility of the model with respect to gut fullness (Jobling 1981). The linear model was therefore often rejected, although the accuracy of the parameter estimates should have been used as the most important criterion for model selection. Using examples from the literature, we demonstrate for the linear model that (*i*) in many cases, it has inappropriately been rejected, (*ii*) it frequently gives the better approximation of the true feeding rates, (*iii*) it is consistent with experimental evidence from continuously feeding larvae, and (*iv*) by redefining its parameters, it can be used as flexibly and efficiently as the exponential model for calculating feeding rates over the diel cycle.

Methods

All data for this paper (i.e., gut contents versus time) were taken from previously published work, i.e., fig. 3 in Ryer and Boehlert (1983), fig. 4 in Peters and Kjelson (1975), table 2 in Talbot et al. (1984), fig. 1 in Arrhenius and Hansson (1994*a*), fig. 5 in Canino and Bailey (1995), and fig. 1 in Worischka and Mehner (1998). Data were either taken from a table (Talbot et al. 1984) or digitized from figures using Data Thief, a freeware program written by Kees Huyser and Jan van der Laan (National Institute for Nuclear Physics and High Energy Physics, Amsterdam, The Netherlands) for the Apple Macintosh. To ensure accuracy, the data were then plotted and compared by eye with the original graphs before being used in calculations.

Model specifications

The most significant hurdle for comparison of parameter estimates among models is the simplification of the various models in the form (Jobling 1981; From and Rasmussen 1984; Persson 1986)

$$(1)\qquad \mathrm{d}V_t/\mathrm{d}t = -rV_t^b$$

where V_t is the amount of food in the gut at time t, r is the gut evacuation rate constant (i.e., the instantaneous gut evacuation rate), and b is a scaling exponent that can assume values ranging from 0 to 1 (Jobling 1981; Bromley 1987). For instance, $b = 0$ in the linear model, $b = 0.5$ in the square root model, and $b = 1$ in the exponential model. With this definition, the values of r cannot be compared among models, since r has as many dimensions as there are values for the exponent b. The dimension of r_{lin} (linear model) is mass·time^{-1}, whereas for r_{exp} (exponential model), it is time^{-1}. In addition, r_{lin} is independent of the initial amount of food in the gut, which contradicts experimental evidence (Jobling 1986). We therefore propose a more realistic and practical formulation of the linear model as shown in (Fig. 1):

$$(2)\qquad V_t = V_0 - V_0rt$$

where V_0 is the initial gut content at the beginning of the evacuation period, r is the evacuation rate constant, and t is the elapsed time. The first derivative, the gut evacuation rate (E), is therefore dependent on the initial gut content:

$$(3)\qquad E = \mathrm{d}V_t/\mathrm{d}t = -V_0r.$$

In comparison, the exponential model remains as defined in Persson (1982):

$$(4)\qquad V_t = V_0e^{-rt}$$

with the first derivative (i.e., the evacuation rate E)

$$(5)\qquad E = \mathrm{d}V_t/\mathrm{d}t = -rV_0e^{-rt}.$$

The difference between the two models is that in the linear model, the slope (i.e., the gut evacuation rate E) remains constant over the individual evacuation event, while in the exponential model, E changes depending on the amount of food remaining in the gut. In the linear model, E is directly proportional to the initial gut content at the onset of the evacuation event. This can be visualized by the movement of food through a simple tube at constant gut passage times (Fig. 1). In the exponential model, a constant proportion of the food remaining in the gut is removed per unit time. In other words, r_{lin} is equivalent to the proportion of the initial amount of food removed per unit time, and r_{exp} is equivalent to the proportion of the remaining food removed per unit time. The linear and exponential models are conceptually identical to the plug-flow reactor and the continuous-flow stirred-tank reactor, respectively, as defined by Penry and Jumars (1987). The two models are compatible

Fig. 2. Time course of gut filling and gut evacuation in a hypothetical example. (*a*) The rate constants (r) for the ingestion rate (I) and the evacuation rate (E) are the same. The evacuation time course is shown for the linear model (solid circles) and the exponential model (open circles) with the same rate constant r. (*b*) If the organism retains a residual amount of food in the gut after linear gut evacuation, the resulting pattern can be mistaken as a curvilinear relationship. (*c*) With the correctly applied linear model, the resulting slope E is identical to I if only the initial portion is used in the analysis. (*d*) If the exponential model is fit to the data, the resulting slope E is much steeper than the actual feeding rates. In this example, the misinterpretation leads to an approximately twofold error. The exponential model (eq. 4) was fit using Gauss–Newton approximation.

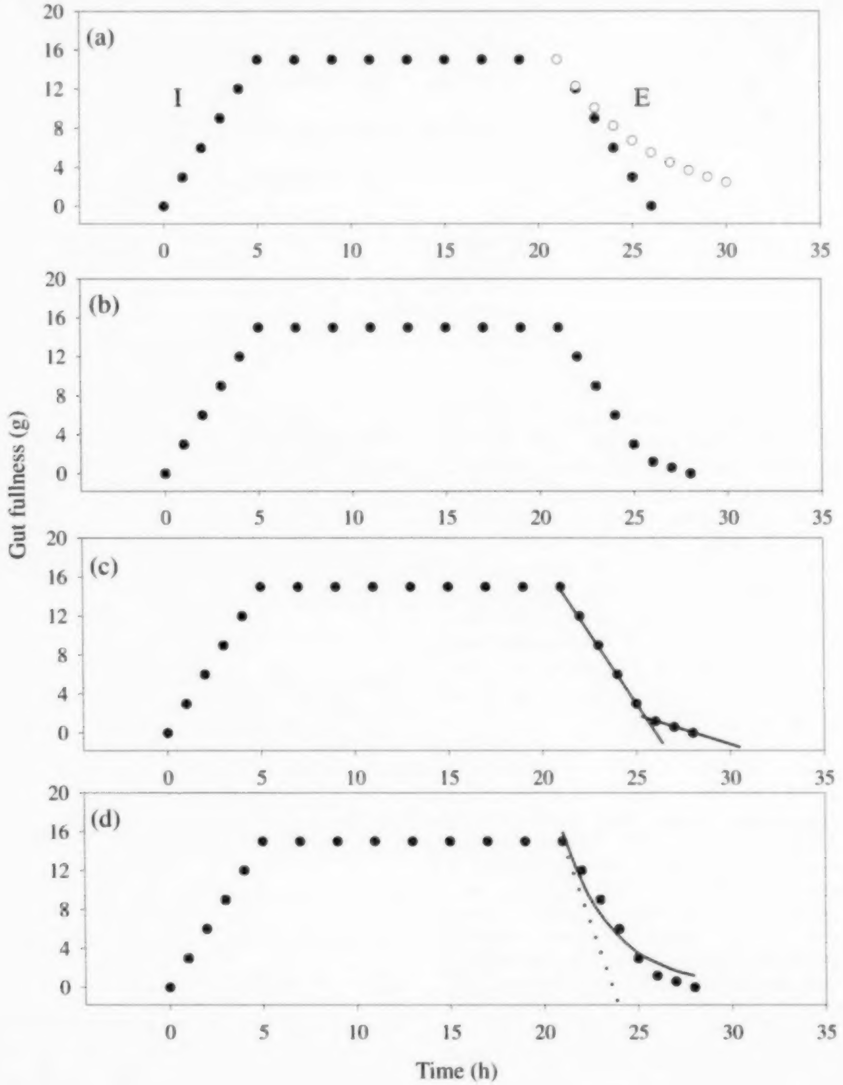

because at $t = 0$, $V_t = V_0$, and in both cases, the feeding rate (I) is calculated as $E = \mathrm{d}V_t/\mathrm{d}t = -rV_0$ assuming that $I = E$.

In the following example, we will show that this seemingly fine distinction between models has important consequences when estimating gut evacuation rates and therefore feeding rates. One central assumption in using evacuation rates to estimate feeding rates is that input = output (i.e., $I = E$) (Bromley 1987). At the beginning of a feeding interval, the amount of food in the gut increases linearly with time until a plateau is reached (Fig. 2). The slope is identical to the ingestion rate (I). When feeding stops and evacuation is initiated (usually after a lag phase), the gut content decreases with the same slope but negative sign if the linear model holds true or departs from linearity if the exponential model is correct (Fig. 2*a*). In order to obtain r_{lin}, the slope has to be divided by the initial gut content V_0 (eq. 2). The r_{exp} is derived either by natural log-transformation of the gut fullness values or, preferably, by fitting eq. 4 directly to the data by means of Gauss–Newton approximation. Zero values, which are inevitably part of a gut evacuation experiment, are not lost in the procedure when working with untransformed data. In Fig. 2*a*, r_{lin} and r_{exp} are numerically the

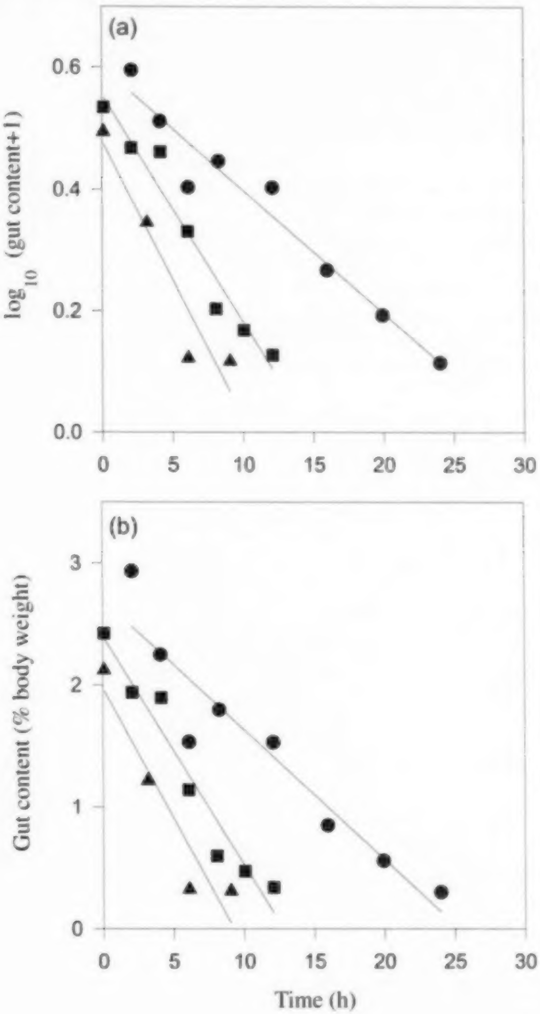

Fig. 3. Gut evacuation of the stomachless northern pipefish (*Syngnathus fuscus*) at three temperatures (*a*) as presented by Ryer and Boehlert (1983) and (*b*) using the untransformed values. There seems to be little indication that the exponential model (Fig. 3*a*) describes the process of gut evacuation more accurately than the simple linear model (Fig. 3*b*). Circles, 15°C; squares, 23°C; triangles, 27°C.

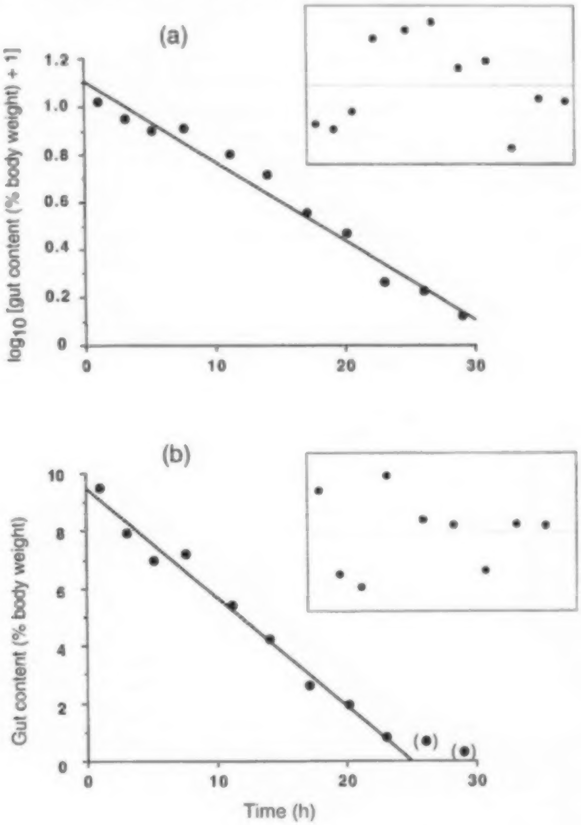

Fig. 4. Gut evacuation by pinfish (*Lagodon rhomboides*) (*a*) as shown in Peters and Kjelson (1975) and (*b*) using the untransformed data. The last two points (in parentheses) have been excluded for the calculation of the linear regression. The linear model (Fig. 4*b*) has a slightly better fit to the data than the exponential model (Fig. 4*a*) with $r^2 = 0.984$ and $r^2 = 0.968$, respectively. The residuals have a U-shaped pattern using the exponential model (inset in Fig. 4*a*) but are not associated with the model using the untransformed values and a simple linear regression (inset in Fig. 4*b*). The regression equations are $y = 1.11 - 0.033x$ ($r^2 = 0.972$, $n = 11$) for Fig. 4*a* and $y = 9.51 - 0.38x$ ($r^2 = 0.983$, $n = 9$) for Fig. 4*b*.

same, and the throughput (or gut passage) time is r^{-1} in both cases. However, the situation is complicated by the fact that fish may retain some residual food in the gut for a long period of time (Rösch 1987). For example, Pedersen (1984) found that a herring larva retained 10% of the initial amount of food for an almost infinite period of time. Let us assume that retention of food after an initial linear decrease is indeed the case (Fig. 2*b*). The correct linear model would have a slope symmetrical to the gut-filling event (Fig. 2*c*). If, however, the inflection in gut evacuation is mistaken as a curvilinear relationship, the resulting $r_{\exp}$ and consequently the estimated feeding rate is much higher (Fig. 2*d*, dotted line) than calculated from the more appropriate linear model (Fig. 2*c*). In this particular example, the difference in feeding rates ($V_0{}^*r$) is approximately twofold (3 $g \cdot h^{-1}$ for the linear model and 5.7 $g \cdot h^{-1}$ using the exponential model).

Results and discussion

There exist numerous examples in which the exponential model has been used in situations without apparent curvilinearity in the data. A particularly useful example to demonstrate problems in choosing the correct model is found in a study of the gut evacuation of adult *Syngnathus* (Ryer and Boehlert 1983). This species has a straight, stomachless gut and one would expect that the "input = output" assumption holds and that a simple, linear gut evacuation model should apply. Despite this possibility, Ryer and Boehlert (1983) chose the exponential model (Fig. 3*a*). As our plot of the un-

Table 1. Temperature dependence of the evacuation rate constants (h^{-1}) (coefficients of determination in parentheses) in the northern pipefish (*Syngnathus fuscus*).

Temperature (°C)	Exponential	Linear	Ryer and Boehlert (1983)
15	0.087 (0.92)	0.038 (0.89)	0.019 × 2.303 = 0.044
23	0.177 (0.96)	0.078 (0.95)	0.037 × 2.303 = 0.085
27	0.238 (0.90)	0.107 (0.90)	0.046 × 2.303 = 0.106

Note: The rate constants were estimated by fitting linear regressions to natural log transformed data ("exponential") and fitting a linear regression to untransformed data ("linear"). For comparison, the slope of the regression of the $\log_{10}$-transformed gut content + 1 values as given in Ryer and Boehlert (1983) multiplied by $\ln_{10}$ (2.303) are shown in the last column. Note that the Ryer and Boehlert (1983) values are similar, although not identical, to the rate constants calculated from a simple linear regression. The discrepancy between the rate constants from the exponential model and the rate constants as calculated by Ryer and Boehlert (1983) are soley due to the fact that they used gut content + 1 instead of the true gut content values.

Fig. 5. Data on Atlantic salmon (*Salmo salar*) taken from Talbot et al. (1984). (*a*) In some cases, a pattern was apparent: a lag phase, a linear phase of removal of iron particle labeled food from the gut and a prolonged retention of the marker in the gut when animals were starved (i.e., beyond 40 h). (*b* and *c*) Fish were starved before the prandium (food containing iron particles) was fed to the fish. (*d*) Fish were prefed before the prandium was provided. Circles, postprandial treatment = starvation; squares, postprandial treatment = feeding. For starving fish, only values of more than 20% of the initial values were included in our analysis, and the data were normalized by setting the initial gut content to 1 (Figs. 5*b*–5*d*). One-factor ANCOVA in pairwise comparisons revealed that the slopes were not significantly different. This means that by using the linear model, gut evacuation rates were similar to the removal of iron particles in continuously feeding fish (Figs. 5*b*–5*d*). For details on the experimental setup, see Talbot et al. (1984). One-factor ANCOVA: Fig. 5*b*: $n = 13$, $p = 0.075$; Fig. 5*c*: $n = 15$, $p = 0.434$; Fig. 5*d*: $n = 22$, $p = 0.721$.

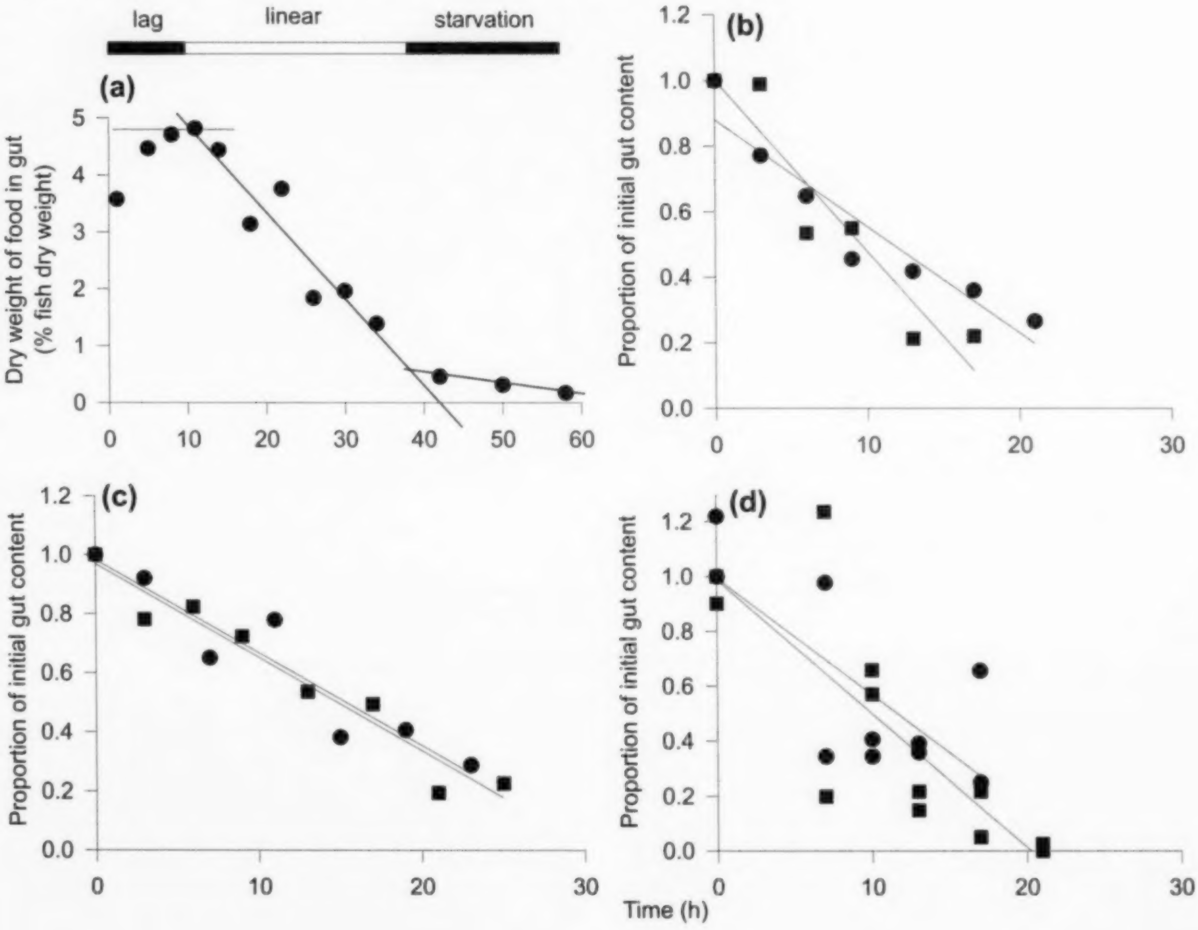

Fig. 6. Reproduction of the data taken from Arrhenius and Hansson (1994*a*). Young-of-the-year Atlantic herring (*Clupea harengus*) display a clear diel periodicity of feeding. The gut evacuation rate can be estimated by the decrease in the gut content in the nonfeeding period or by using the increase in gut content during gut filling. The asterisks indicate data that have been used by Arrhenius and Hansson (1994*a*) and in the present analysis for calculation of the evacuation rate constant using the exponential model (*k* and *r*, respectively, in Table 2). The lines show which data points we used when fitting linear regressions for both the evacuation and gut filling intervals. The horizontal bars indicate periods of darkness. The symmetry between the linear decrease and linear increase in gut content in four out of five cases strongly suggests that the linear model and not the exponential model is appropriate for estimating feeding rates. (*a*) July 15–16; (*b*) August 5–6; (*c*) August 26–27; (*d*) September 17–18; (*e*) October 27–28.

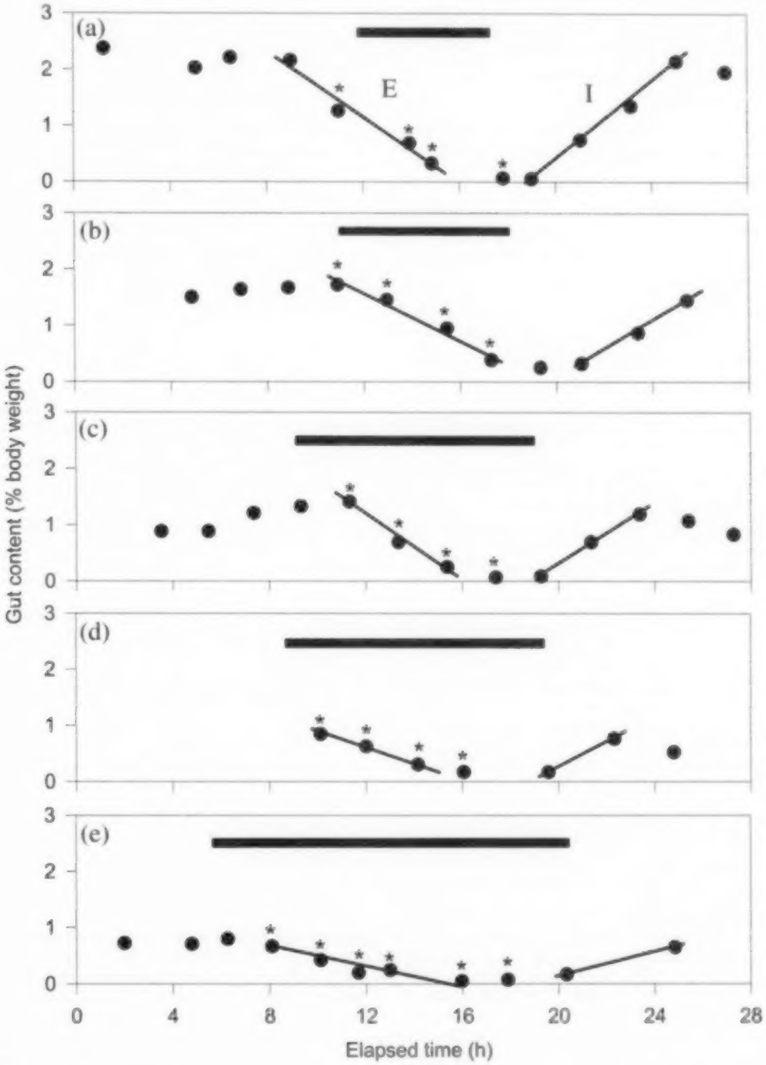

transformed values shows, there is little indication of a curvilinear relationship (Fig. 3*b*). There are more problems regarding the transformations used in this example. First, a base-10 logarithm rather than a base-e logarithm has been used. In this case, the evacuation rate constant (i.e., the slope of the linear regression drawn through the log-transformed data) has to be multiplied by 2.303 ($\ln_{10}$) in order for it to be used in the exponential model (i.e., $e^x = 10^{x/\ln_{10}}$). In addition to the obvious inconvenience, this conversion can easily be overlooked and left out of further calculations. The third major problem is the use of gut content + 1 instead of the original gut content. Although this procedure allows incorporation of zero gut values (Peters and Kjelson 1975), the parameter estimates are meaningless for calculations of evacuation or feeding rates. When applying the exponential and linear models to these data, one can see the substantial difference between the estimates of *r* (Table 1). However, as shown in Table 1, Ryer and Boehlert (1983) coincidentally (rather than by using the appropriate model) arrived at a similar result by using a series of transformations as if they

Table 2. Evacuation rate constants (r) and estimates of ingestion rates (I) based on digitized data from fig. 1 in Arrhenius and Hansson (1994*a*).

Date and model	Gut content (% body weight)	r (h^{-1})	I (% body weight·h^{-1})	k (h^{-1})
July 15–16	2.15			
Linear regression, gut emptying		0.13[a]	0.29	—
Linear regression, gut filling		0.16[a]	0.34	—
Exponential model		0.43	0.92[a]	0.35
August 5–6	1.60			
Linear regression, gut emptying		0.13[a]	0.21	—
Linear regression, gut filling		0.16[a]	0.26	—
Exponential model		0.26	0.42[a]	0.24
August 26–27	1.02			
Linear regression, gut emptying		0.29[a]	0.29	—
Linear regression, gut filling		0.27[a]	0.27	—
Exponential model		0.50	0.51[a]	0.27
September 17–18	0.64			
Linear regression, gut emptying		0.20[a]	0.13	—
Linear regression, gut filling		0.34[a]	0.22	—
Exponential model		0.28	0.18[a]	0.22
October 27–28	0.69			
Linear regression, gut emptying		0.14[a]	0.09	—
Linear regression, gut filling		0.16[a]	0.11	—
Exponential model		0.26	0.18[a]	0.20

Note: The digitized data are displayed in Fig. 6. The asterisks in Fig. 6 indicate which data points were used to determine evacuation rate constants according to Arrhenius and Hansson (1994*a*) using the exponential model. Both the decreasing gut content during the nonfeeding period and the increasing portion of the gut content during the initial feeding interval have been used to fit the linear regressions (lines in Fig. 6). We also included the estimates of the rate constants calculated by Arrhenius and Hansson (1994*a*) (k in this table and in their table 1).

[a] Calculated using the mean gut content during the light period.

Table 3. Calculations of evacuation rate constants (r) and ingestion rates (I) from digitized data taken from Canino et al. (1995, their fig. 5) on the diel feeding cycle of walleye pollock (*Theragra chalcogramma*) larvae.

Method	Gut passage time (h)	r (h^{-1})	I (no. prey·h^{-1})
Field data			
Linear regression, gut emptying	4.83	0.207	2.50
Linear regression, gut filling	4.49[a]	0.223[a]	2.26
Gut passage time (indicated in Fig. 8)	4.07	0.246[a]	2.50[a]
Exponential model	Not defined	0.57	5.81[a]
Experimental data			
Continuous feeding	4.11	0.23	—
Discontinuous feeding	28.84	0.03	—

Note: No attempt was made by the original authors to estimate the ingestion rates from the field. However, Canino and Bailey (1995) determined evacuation rate constants in separate feeding experiments and reported them as the arcsin in their table 3. We transformed the data back to the original values ("experimental data"). Note that the evacuation rate constant that we calculated from the field data using the linear model was almost identical to the rate constant calculated by Canino and Bailey (1995) for continuously feeding animals in their experiments. On the contrary, larvae, which have been starved in captivity ("discontinuous feeding"), showed extremely low evacuation rate constants.

[a] Average gut content of 10.15 prey per larva (horizontal line in Fig. 8) during the light cycle was used in the calculation.

had applied the simple linear regression on untransformed values in the first place.

The same problems can be observed in the analysis of gut evacuation data for juvenile pinfish reported by Peters and Kjelson (1975). After inverse log transformation, the linear model clearly fits the data better than the exponential model over almost the entire data set (Fig. 4). The residuals of the linear model show a random distribution, whereas the residuals of the log-transformed model show an inverted U-shaped pattern (insets in Fig. 4). An inflection was apparent, indicating retention of residual gut content after linear gut evacuation. The almost threefold difference of the calculated rate constants between the linear ($r = 0.38/9.51 = 0.040$) and exponential models ($r = 0.116$) is not trivial. This discrep-

Table 4. Comparison of the rate constants derived by using the linear model (increase and decrease) and exponential model (decrease only) for larval perch and zander (Worischka and Mehner 1998).

					Worischka and Mehner 1998	
Species	Specific gut fullness (g·g^{-1})	r_{lin} (increase) (h^{-1})	r_{lin} (decrease) (h^{-1})	r_{exp} (asterisks in Fig. 9) (h^{-1})	Linear model (h^{-1})	Exponential model (h^{-1})
Perch	0.022	0.36	0.27	0.35	0.40	0.52
Zander	0.031	0.20	0.20	0.21	0.43	0.56

Note: Both the linear and exponential models agree well in our reanalysis and using the linear increase in gut content at dawn (i.e., a true feeding rate), whereas the estimates by Worischka and Mehner (1998) were considerably higher using different methods.

Fig. 7. (*a*) *Clupea harengus* evacuation rates (*E*, circles) and ingestion rates (*I*, squares) (i.e., slopes of regressions shown in Fig. 6) in field samples from Arrhenius and Hansson (1994*a*) were significantly correlated with initial gut content. (*b*) There is no indication that the evacuation rate constant *r* changes with initial gut content. This demonstrates that gut fullness is a good indicator of feeding rates and that the evacuation processes in young-of-the-year Atlantic herring are close to the idealized representation in Fig. 1*a*.

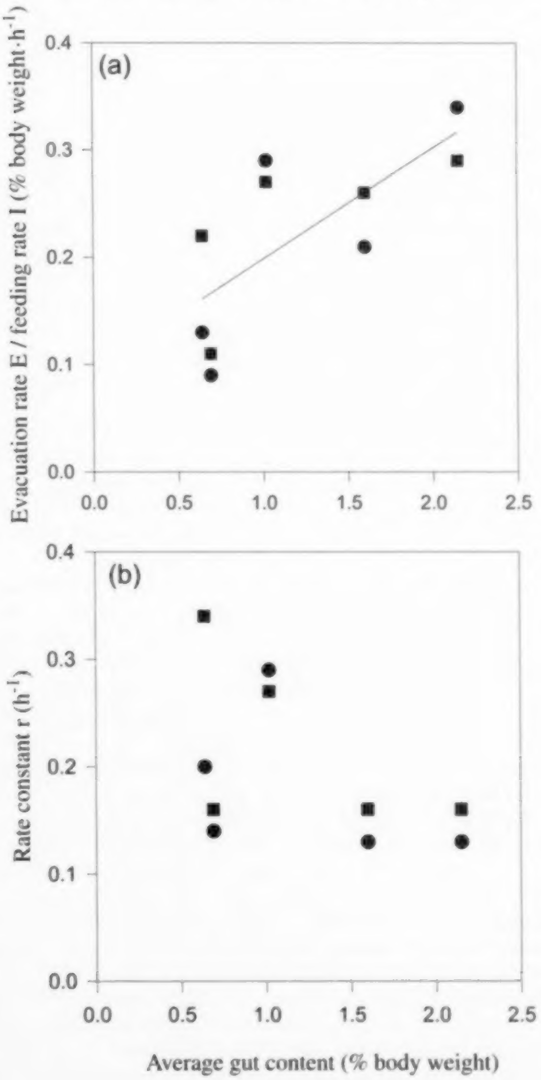

ancy shows that the choice of model is important if these values are to be used for further calculation of ingestion rates. As in the previous example, using gut content + 1 (Fig. 4*a*) gives different rate constants than using the original gut content values.

Both examples demonstrate several important problems: the exponential model has been applied without testing the linear model first, and various transforms make comparisons of parameter values between models problematic. Since no underlying conceptual models (such as the plug-flow or continuous-flow stirred-tank reactor) were used, which relate evacuation rates to actual feeding rates, it is difficult to ascribe biological meaning and to use them for calculating feeding rates.

Evidence from continuously feeding fish

Perhaps the most compelling evidence for the use of the linear model comes from reanalysis of the experimental studies by Talbot et al. (1984) on juvenile salmon. The conclusion of the authors was that the evacuation rates of tracer particles differed depending on whether the animals fed continuously or ceased feeding. One could argue that this is evidence that evacuation is inconsequential for determining ingestion and that feeding rates should be estimated in a different fashion. On the contrary, we will show that this conclusion is only justified when the wrong model is applied. We will demonstrate that the bias is introduced by prolonged retention of food in the gut during starvation. When plotting the raw data from their table II, some of the plots displayed the following pattern: first, a lag phase delayed the onset of evacuation, followed by a time interval, in which food evacuation was essentially linear (Fig. 5*a*). Finally, in cases in which the animals were starved after receiving marker particles, a period of prolonged retention of food was apparent (Fig. 5*a*). These three phases have already been identified by Rösch (1987) in experimental work on the powen, suggesting that only the linear portion be used to determine evacuation rates. The remainder of the data had either no lag phase or no discernable pattern due to high variability. In order to simplify comparisons, we set the original gut content to 1 ("normalization" according to From and Rasmussen 1984). Using Talbot et al.'s (1984) method and the square root model, one arrives at evacuation rate constants ranging over approximately fourfold (their table III). In our reanalysis using only the linear portion of the evacuation data, the rate constant ranged only from 0.032 to 0.052 (less than twofold) (Figs. 5*b*–5*d*). More importantly, when using data from the linear, initial portion of the gut evacuation time course (excluding the data below 20% of the initial gut content), the treatment (whether the fish were starved or fed continu-

Fig. 8. Diel periodicity of feeding in walleye pollock (*Theragra chalcogramma*) larvae as shown in Canino and Bailey (1995). The bars indicate the nonfeeding period during the night. We added the horizontal line, which represents the average amount of food in the gut during the daytime, and the V-shaped lines, which are linear regressions fit to the decreasing and increasing stomach content. gpt, gut passage time as determined by the regression equations.

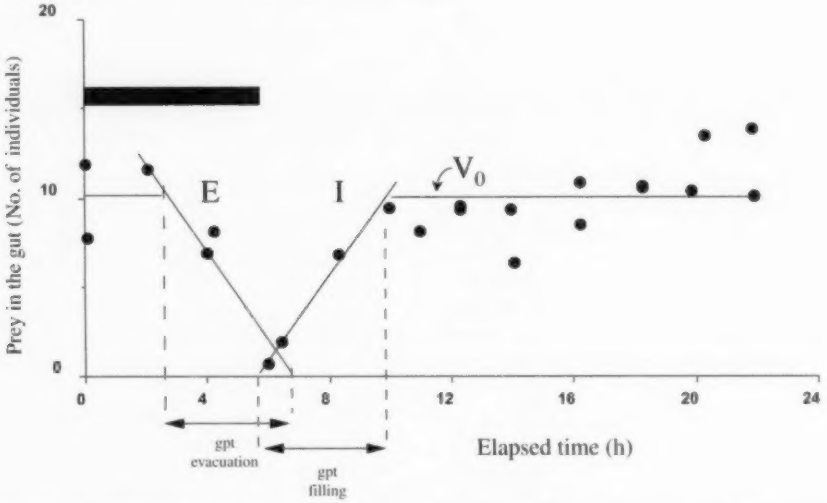

ously) had no effect on estimates of *r*, i.e., none of the slopes in Figs. 5*b* and 5*c* were significantly different in pairwise comparisons (one-factor analysis of covariance (ANCOVA); details given in the legend to Fig. 5). Thus, using the gut evacuation time course in combination with the linear model provided throughput rates (r^{-1}) identical to those measured using tracer particles in continuously feeding fish. The apparent curvilinearity was not the result of proportional release of food as requisite for using a curvilinear model, but simply prolonged retention of residual food in starving fish. In this case, the elimination of the "starvation phase" (the lower 20% of the data) produced essentially linear plots (Figs. 5*b*–5*d*). The criterion of 20% was chosen arbitrarily. Using 40% would further improve the situation, since the inflection point (changing rate) in Fig. 5*b* of the starving fish occurred at a gut content of 0.45. At least three data points are required to test for linearity.

Exploiting the diel feeding rhythm to estimate gut evacuation rates

Most fish larvae and many juvenile fish are visual predators and feeding ceases during the night. This period of starvation can serve as a natural gut evacuation experiment. Thus, conventional evacuation experiments and potential problems caused by capture trauma can be avoided. Four examples will be presented below: juvenile herring (Arrhenius and Hansson 1994*a*), walleye pollock larvae (Canino and Bailey 1995), and perch and zander larvae (Worischka and Mehner 1998). Canino and Bailey (1995) did not use the diel cycle to calculate evacuation rate, Arrhenius and Hansson (1994*a*) used the exponential model only, and Worischka and Mehner (1998) applied both the linear model in its original form (eq. 1) and the exponential model. For all the above examples, we digitized the raw data and calculated the rate constants using the exponential model and the revised linear model (eq. 2).

The points in Fig. 6 marked by asterisks were used by Arrhenius and Hansson (1994*a*) to determine the evacuation rate constant using the exponential model. For the linear model, we restricted our analysis to the linear portion of the data, indicated by lines in Fig. 6. The onset of feeding and increasing gut content are direct measures of initial ingestion rate (*I*), which can be fit with a linear model with a positive slope (Fig. 6). The rate constants (*r*) were calculated using the average gut content during the day as V_0 and dividing both of the slopes (*E* and *I*) by V_0 (eq. 2). The rate constants of the linear increase and decrease in stomach contents are much closer to one another than the rate constants derived from the exponential model on four out of five sampling dates (Table 2), the September set being the notable exception (Fig. 6*d*). The agreement between rate constants calculated using the linear decrease and the increase of gut content visually manifests itself in the symmetry between the slopes of food evacuation (*E*) and ingestion (*I*) (Fig. 6).

We also depicted the original rate constants of Arrhenius and Hansson (1994*a*) as *k* in Table 2, which in some cases differed considerably from our calculations. Even considering the erratum (Arrhenius and Hansson 1994*b*), we cannot offer an explanation for this inconsistency. The original data were unfortunately not available to us. Repeated digitization of the data resulted in internally consistent values, which led us to conclude that our method of data reproduction was not responsible for the discrepancy.

The model of linear gut evacuation displayed in Fig. 1*a* suggests that the slope (i.e., the gut evacuation rate *E*) is directly proportional to the initial amount of food in the gut (V_0) and that the evacuation rate constant remains unchanged. This assumption is at the core of the idea that gut content reflects feeding activity. The example of juvenile herring (Arrhenius and Hansson 1994*a*) is very close to this ideal situation. Figure 7 shows that the slopes of linear gut evacuation (*E*) and gut filling (*I*) are significantly correlated with gut content during the feeding period ($r^2 = 0.54$, $p = 0.015$, $n = 10$), whereas the evacuation rate constant (and con-

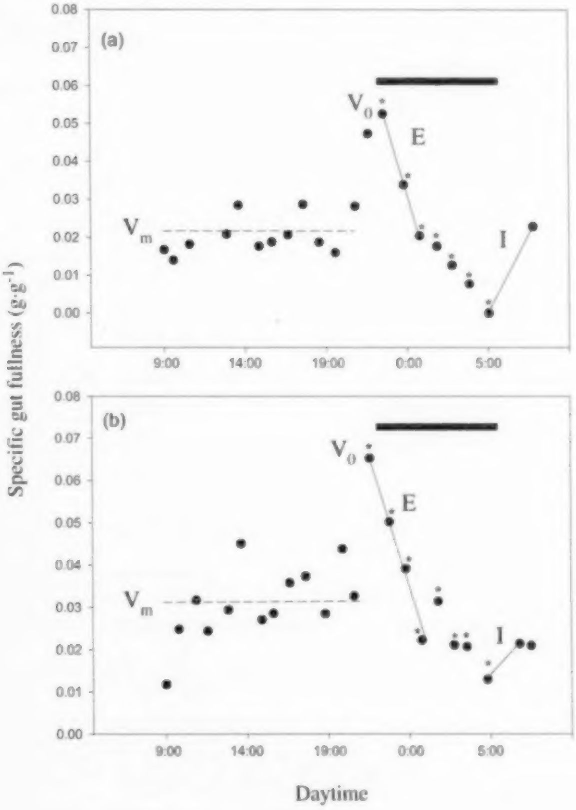

Fig. 9. Diel cycle of gut fullness in (*a*) perch and (*b*) zander larvae in a temperate reservoir in June. The black bar depicts the period of darkness. The solid lines indicate the data points used for calculating r_{lin} using the increase and decrease in gut content. The r_{exp} was calculated using the points marked by asterisks. The dashed lines depict the feeding plateaus during the day before peak feeding in the evening occurred. These values were used in the calculation of the rate constant for the linear increase in gut content in the morning. For the linear gut evacuation, r_{lin} was calculated using the intercept (V_0) of the linear evacuation regression. Note: according to the revised linear model (eq. 2), E and I are only symmetrical at equal gut filling levels ($V_0 = V_m$) such as in Fig. 6 or Fig. 8. Since the plateau in the morning is lower than the feeding peak in the evening, E is expected to be steeper than I.

sequently its inverse, the gut passage time) does not change significantly with gut content ($r^2 = 0.25$, $p = 0.14$, $n = 10$).

Symmetry of slopes between gut filling and gut evacuation can also be observed in data replotted from Canino and Bailey (1995) (Fig. 8). As in the previous example, the rate constants between linear increase and evacuation are very similar, whereas the use of the exponential model leads to substantially higher evacuation rates (Table 3). In addition, Canino and Bailey (1995) performed laboratory experiments with continuously feeding and starving larvae. The rate constant obtained for the continuously feeding larvae in their experiments was identical to the rate constant of our recalculation of their field data using the linear model (Fig. 8; Table 3). This is strong evidence for the general validity of the linear gut evacuation model.

Worischka and Mehner (1998) studied the diel cycle of gut fullness in larval perch and zander. The authors used the steepest decrease in gut content between two points to estimate gut evacuation rates. This means that a maximum value was used, which was composed of a real decrease in gut fullness plus measurement error. To obtain the rate constant of the linear model, Worischka and Mehner (1998) arbitrarily divided this maximum slope by the value of the datum point at the beginning of the steepest interval. In contrast, we followed our protocol by fitting a regression through the topmost linear part of the evacuation data after the onset of darkness (Fig. 9). The rate constant r was then calculated by dividing the slope (E) by the intercept of the regression (V_0). In addition, we fit a regression line through the increase in gut fullness at dawn (Fig. 9). An average value for the plateau in the morning hours was taken as the divisor (V_0) to calculate the rate constant r for the ingestion rate. Finally, we fit the exponential model to the data marked by asterisks (Fig. 9). The resulting r values from the linear decrease, linear increase, and exponential decrease are very similar, ranging from 0.2 to 0.36 for both species (Table 4). This translates into gut passage times from 5 to 2.8 h, respectively. However, these values depart considerably from the range of rate constants calculated by Worischka and Mehner (1998) ($r = 0.4$–0.56, gut passage time = 2.5–1.8 h, respectively). In perch, r_{exp} is closer to r_{lin} calculated from the increasing gut content, although some caution has to be applied, since the slope is based on two points. However, the rate constants calculated by Worischka and Mehner (1998) are considerably higher than those calculated from the ingestion rates at dawn, which is unrealistic, since fish larvae usually exhibit gorge feeding at the beginning of a feeding interval.

In summary, in all but two cases (i.e., Figs. 6*d* and 9*a*), the linear evacuation at dusk and linear increase at dawn were symmetrical in respect to the rate constant r. In the example of walleye pollock larvae (Canino and Bailey 1995), as well as for juvenile salmon (Talbot et al. 1984), the rate constants calculated on the basis of the linear evacuation model were nearly identical to the throughput rates of marker particles in continuously feeding fish.

Conclusion

In order to use evacuation rates to estimate feeding rates, assumptions about the relationship between feeding and evacuation must be made. The simplest assumption is that the gut performs like a simple tube and that food leaves the gut at the same rate as it is ingested. This conceptualization is known as the plug-flow reactor (Penry and Jumars 1987). An alternative model is that the rate of evacuation of food from the gut is dependent on the amount of food remaining, which requires at least one feedback mechanism. This situation is most efficiently described by means of the exponential model and the continuous-flow stirred-tank reactor (Penry and Jumars 1987). Distinguishing between these two cases is difficult solely on the basis of visual examination of the time course of gut evacuation. Fish larvae and juvenile fish tend to retain residual food in their guts over long periods of time. If there is an inflection in the gut evacuation and food is retained after a period of linear gut evacuation, the application of the exponential model may overestimate the rate constant and thereby the feeding rate. A possible solution for finding the appropriate model is to compare the evacuation rates with throughput rates of tracer particles of continuously feeding fish. Another possibility is to use the slope of increase in gut content after a period of starvation, since it represents a real feeding rate (Hofer and Uddin 1985). If the rate constant derived from the linear increase corresponds to the rate constant derived from gut evacuation, then the symmetry assumption (input = output) rule is fulfilled and the linear model applies. If the exponential model is applied to the same data instead, the rate constant is considerably higher than those estimated from the gut filling.

The intestines of many larval, juvenile, and adult fish with stomachless guts seem to be well represented by the linear model. Even stomachs of some adult fish may function as simple plug-flow reactors, since food is "stacked" in the stomach and seems to be much less homogenous than previously assumed (dos Santos and Jobling 1992). If three phases (initial lag phase, linear phase, and extended retention of the last portion of food) can be identified according to Rösch (1987), we recommend the use of only the linear portion for ingestion rate estimation. As our previous examples show, it may be sufficient to remove gut contents of less than 20% of the initial value from the analysis. We therefore conclude that the use of untransformed data in combination with the revised linear model (eq. 2) will allow a simple calculation of ingestion rate. Less pessimistic than Rösch (1987), we believe that the application of changes in stomach and gut contents is a useful tool to estimate ingestion rates of fish in the field. An important precondition is that no feeding takes place in the dark. The accuracy of the feeding estimate is greatly increased if just the indigestible components of the diet are considered (i.e., conservative markers). Whenever possible, alternative methods of measuring feeding activity (such as suggested by Talbot et al. 1984; Hofer and Uddin 1985; this paper) should be used to verify whether the calculated gut evacuation rates are representative of the actual ingestion rates. We have demonstrated that the revised linear model ($V_t = V_0 - V_0rt$) is consistent with experimental observations on continuously feeding fish and with experimental evidence that initial gut fullness is proportional to the evacuation rate. Using the new definition of the linear model, the feeding rate can easily be calculated by multiplying the gut evacuation rate constant r by the average gut fullness during the day (Eggers model) or by using r in the Elliott and Persson model (Boisclair and Leggett 1988).

Acknowledgements

We thank Drs. Pierre Pepin, Joe Brown, Jorge dos Santos, Peter Grønkjær, and Tom Johnston for their comments and critical reviews of earlier versions of this manuscript and Drs. S. Worischka and T. Mehner for supplying original data.

References

Arrhenius, F., and Hansson, S. 1994*a*. *In situ* food consumption by young-of-the-year Baltic Sea herring *Clupea harengus*: a test of predictions from a bioenergetics model. Mar. Ecol. Prog. Ser. **110**: 145–149.

Arrhenius, F., and Hansson, S. 1994*b*. Erratum. Mar. Ecol. Prog. Ser. **114**: 314.

Bajkov, A.D. 1935. How to estimate the daily food consumption of fish. Trans. Am. Fish. Soc. **65**: 288–289.

Boisclair, D., and Leggett, W.C. 1988. An *in situ* experimental evaluation of the Elliott and Persson and the Eggers models for estimating fish daily ration. Can. J. Fish. Aquat. Sci. **45**: 138–145.

Bromley, P.J. 1987. The effects of food type, meal size and body weight on digestion and gastric evacuation in turbot, *Scophthalmus maximus* L. J. Fish Biol. **30**: 501–512.

Canino, M.F., and Bailey, K.M. 1995. Gut evacuation of walleye pollock larvae in response to feeding conditions. J. Fish Biol. **46**: 389–403.

dos Santos, J., and Jobling, M. 1992. A model to describe gastric evacuation in cod (*Gadus morhua* L.) fed natural prey. ICES J. Mar. Sci. **49**: 145–154.

From, J., and Rasmussen, G. 1984. A growth model, gastric evacuation, and body composition in rainbow trout, *Salmo gairdneri* Richardson, 1836. Dana, **3**: 61–139.

Hofer, R., and Uddin, A.N. 1985. Digestive processes during the development of the roach, *Rutilus rutilus* L. J. Fish Biol. **26**: 683–689.

Jobling, M. 1981. Mathematical models of gastric emptying and the estimation of daily rates of food consumption for fish. J. Fish Biol. **19**: 245–257.

Jobling, M. 1986. Mythical models of gastric emptying and implications for food consumption studies. Environ. Biol. Fishes, **16**: 35–50.

Pedersen, B.H. 1984. The intestinal evacuation rates of larval herring (*Clupea harengus* L.) predating on wild plankton. Dana, **3**: 21–30.

Penry, D.L., and Jumars, P.A. 1987. Modeling animal guts as chemical reactors. Am. Nat. **129**: 69–96.

Persson, L. 1982. Rate of food evacuation in roach (*Rutiulus rutilus*) in relation to temperature, and the application of evacuation rate estimates for studies on the rate of food consumption. Freshwater Biol. **12**: 203–210.

Persson, L. 1986. Patterns of food evacuation in fishes: a critical review. Environ. Biol. Fishes, **16**: 51–58.

Peters, D.S., and Kjelson, M.A. 1975. Consumption and utilization of food by various postlarval and juvenile fishes of North Carolina estuaries. *In* Estuarine research. Vol. 1. *Edited by* L.E. Cronin. Academic Press, New York. pp. 448–472.

Rösch, R. 1987. Effect of experimental conditions on the stomach evacuation of *Coregonus lavaretus* L. J. Fish Biol. **30**: 521–531.

Ryer, C.H., and Boehlert, G.W. 1983. Feeding chronology, daily ration, and the effects of temperature upon gastric evacuation in the pipefish, *Syngnathus fuscus*. Environ. Biol. Fishes, **9**: 301–306.

Talbot, C., Higgins, P.J., and Shanks, A.M. 1984. Effects of pre- and post-prandial starvation on meal size and evacuation rate of juvenile Atlantic salmon, *Salmo salar* L. J. Fish Biol. **25**: 551–560.

Worischka, S., and Mehner, T. 1998. Comparison of field-based and indirect estimates of daily food consumption in larval perch and zander. J. Fish Biol. **53**: 1050–1059.

National Research Council
Canada

Conseil national de recherches
Canada

Copyright Transfer

ASSIGNMENT OF COPYRIGHT

Ms. No. ____________

To: NATIONAL RESEARCH COUNCIL OF CANADA ("NRC") Research Press

From: ____
____
____
____
(name and address of author signing this form)

This refers to the manuscript entitled: ____
____

written by myself and the following additional author(s): ____
____

for publication in: ____

1. I declare that the list of authors fairly conforms to academic conventions about who should be listed. I declare that the manuscript, or its equivalent, has not been submitted for publication elsewhere. If it is accepted for publication by the National Research Council of Canada, I will ensure that it, or its equivalent, is not submitted for publication elsewhere.

2. I declare that I am (check ONE):

☐	(a)	the sole owner of the copyright relating to the manuscript,	and →	I **assign** to NRC the entire copyright.
☐	(b)	a part owner of the copyright, in conjunction with interests held by co-authors or their employers,	and →	I **assign** to NRC my entire interest in the copyright, and I expect the co-authors to also sign a form like this one.
☐	(c)	an agent of my employer with authority to assign the copyright owned by the employer, who is: ______________________,	and →	I **assign** to NRC, on behalf of my employer, my employer's entire interest in the copyright relating to the manuscript, and I expect the co-authors to also sign a form like this one.
☐	(d)	a public servant in Canada (federal, provincial or territorial) or the United Kingdom, so that the copyright is owned by Her Majesty,	and →	I have obtained the approval of my employer, according to the terms of my employment, to grant NRC **non-exclusive permission** to publish the manuscript and administer the copyright.
☐	(e)	a public servant of the United States of America, and subject to the law that creates no U.S. copyright for the manuscript,	and →	I **assign** to NRC, on behalf of my employer, my employer's entire interest in any copyright that may exist outside the U.S., and I expect the co-authors to sign a form like this one.

3. I understand that my submission of this document does not guarantee publication, and that publication will not occur until **all authors** have provided a copyright transfer. If the manuscript is not published within 2 years after I sign this, the assignment is revoked.

Signed at ______________________________ on ______________________________
(City and Province/State) (Date)

____
(Signature)

[*Standard NRC form; alterations not acceptable.*]

Comments on Copyright Transfer
(with extracts from the *Copyright Act*, Revised Statutes of Canada 1985, chapter C-42, as amended)

The publisher is not permitted to publish the manuscript without permission or an assignment of ownership of copyright. For greatest flexibility, and to be prepared to deal with future uses of the published material, the publisher requires ownership.

The owner may assign the right, but that assignment must be in writing:

13.(4) *The owner of the copyright in any work may assign the right, either wholly or partially, and either generally or subject to territorial limitations, and either for the whole term of the copyright or for any other part thereof, and may grant any interest in the right by licence, but no assignment or grant is valid unless it is in writing signed by the owner of the right in respect of which the assignment or grant is made, or by his duly authorized agent.*

The owner may be the author, but in many cases, the owner is the author's employer:

13.(3) *Where the author of a work was in the employment of some other person under a contract of service or apprenticeship and the work was made in the course of his employment by that person, the person by whom the author was employed shall, in the absence of any agreement to the contrary, be the first owner of the copyright, but where the work is an article or other contribution to a newspaper, magazine or similar periodical, there shall, in the absence of any agreement to the contrary, be deemed to be reserved to the author a right to restrain the publication of the work, otherwise than as part of a newspaper, magazine or similar periodical.*

The only exception to taking ownership arises when the manuscript is covered by Crown copyright owned by a Canadian government.

12. *Without prejudice to any rights or privileges of the Crown, where any work is, or has been, prepared or published by or under the direction or control of Her Majesty or any government department, the copyright in the work shall, subject to any agreement with the author, belong to Her Majesty and in that case shall continue for the remainder of the calendar year of the first publication of the work and for a period of fifty years following the end of that calendar year.*

Governments, and in particular the federal government, do not have a simple mechanism for assigning ownership of this particular type of Crown asset. Therefore, when an author is a public servant so that there is Crown copyright in the manuscript, a simple permission to use is acceptable to the publisher, if it is granted by a person with appropriate authority.

Conseil national de recherches
Canada

National Research Council
Canada

Cession du droit d'auteur

CESSION DU DROIT D'AUTEUR

Document n° ________

Au : CONSEIL NATIONAL DE RECHERCHES DU CANADA (« CNRC ») Presses scientifiques
De : ______________________________
____
____
____
(nom et adresse de l'auteur qui signe le présent formulaire)

La présente cession porte sur le document intitulé : ______________________________
____

rédigé par moi, en collaboration avec l'auteur/les auteurs suivant(s) : ______________________________
____

aux fins de publication dans : ______________________________

1. Je déclare que la liste des auteurs ci-dessus respecte les pratiques usuelles de rédaction savante quant aux personnes dont le nom doit être cité. Je déclare que le document ou son équivalent n'a pas été soumis à quelque autre organisme aux fins de publication. Si le CNRC accepte de publier le document, je m'assurerai que celui-ci ou son équivalent n'est soumis à aucun autre organisme aux fins de publication sans en obtenir la permission préalable du CNRC.

2. Je déclare être (UN SEUL choix) :

☐ (a)	le seul titulaire de droit d'auteur afférent au document,	et →	je **cède** le droit d'auteur intégral au CNRC.
☐ (b)	un titulaire partite du droit d'auteur, de concert avec des coauteurs ou leurs employeurs,	et →	je **cède** ma part du droit d'auteur au CNRC et m'attends à ce que les coauteurs signent une entente comparable.
☐ (c)	un agent de mon employeur ayant l'autorité de céder le droit d'auteur appartenant à l'employeur, nommément : ______________________,	et →	je **cède** au CNRC, au nom de mon employeur, la part entière du droit d'auteur afférent au document appartenant à mon employeur, et m'attends à ce que les coauteurs signent une entente comparable.
☐ (d)	un fonctionnaire du Canada (fédéral, provincial ou territorial) ou du Royaume-Uni, donc le droit d'auteur appartient à Sa Majesté,	et →	j'ai obtenu de mon employeur, en vertu de mes conditions d'emploi, l'autorisation d'accorder au CNRC la **permission non exclusive** de publier le document et de gérer le droit d'auteur.
☐ (e)	un fonctionnaire des États-Unis d'Amérique, donc sujet à la loi qui n'associe aucun droit d'auteur américain au document,	et →	je **cède** au CNRC, au nom de mon employeur, la part entière de quelque droit d'auteur en vigueur ailleurs qu'aux É.-U. appartenant à mon employeur, et m'attends à ce que les coauteurs signent une entente comparable.

3. Je comprends que la soumission du document ne garantit aucunement sa publication et que la publication ne pourra être réalisée tant que **tous les auteurs** n'auront pas signé une cession du droit d'auteur. Si le document n'est pas publié dans les deux années suivant ma signature des présentes, la cession sera automatiquement révoquée.

Signé à ______________________________, le ______________________
(ville et province/état) (date)

____
(signature)

[*Formulaire normalisé du CNRC; aucune modification permise.*]

Commentaires sur la cession du droit d'auteur
(accompagnés d'extraits de la *Loi sur le droit d'auteur*, Lois révisées du Canada 1985, chapitre C-42 modifié)

L'éditeur ne peut publier un document sans la permission ou une cession du droit d'auteur. Pour des raisons de souplesse et en vue de l'utilisation future du document publié, l'éditeur doit devenir titulaire du droit d'auteur.

Le titulaire peut céder le droit, mais cette cession doit être faite par écrit :

13.(4) *Le titulaire du droit d'auteur sur une oeuvre peut céder ce droit, en totalité ou en partie, d'une façon générale, ou avec des restrictions territoriales, pour la durée complète ou partielle de la protection; il peut également concéder, par une licence, un intérêt quelconque dans ce droit; mais la cession ou la concession n'est valable que si elle est rédigée par écrit et signée par le titulaire du droit qui en fait l'objet, ou par son agent dûment autorisé.*

Le titulaire peut être l'auteur, mais dans plusieurs cas, le titulaire est l'employeur de l'auteur :

13.(3) *Lorsque l'auteur est employé par une autre personne en vertu d'un contrat de louage de service ou d'apprentissage, et que l'oeuvre est exécutée dans l'exercice de cet emploi, l'employeur est, à moins de stipulation contraire, le premier titulaire du droit d'auteur; mais lorsque l'oeuvre est un article ou un autre contribution, à un journal, à une revue ou à un périodique du même genre, l'auteur, en l'absence de convention contraire, est réputé posséder le droit d'interdire la publication de cette oeuvre ailleurs que dans un journal, une revue ou un périodique semblable.*

La seule exception dans la cession du droit d'auteur est lorsque le document est associé au droit d'auteur de la Couronne, qui appartient au gouvernement du Canada.

12. *Sous réserve de tous les droits ou privilèges de la Couronne, le droit d'auteur sur les oeuvres préparées ou publiées par l'entremise, sous la direction ou la surveillance de Sa Majesté ou d'un ministère du gouvernement, appartient, sauf stipulation conclue avec l'auteur, à Sa Majesté et, dans ce cas, il subsiste jusqu'à la fin de la cinquantième année suivant celle de la première publication de l'oeuvre.*

Les gouvernements, en particulier le gouvernement fédéral, ne disposent pas d'un mécanisme simple de cession de droit d'auteur pour ce genre de biens de la Couronne. C'est pourquoi lorsqu'un auteur est un fonctionnaire et que, par conséquent, le droit d'auteur appartient à la Couronne, une simple permission d'usage est suffisante pour l'éditeur, pour autant que celle-ci ait été octroyée par une personne jouissant de l'autorité nécessaire pour ce faire.

Contents (concluded) / Table des matières (suite et fin)

C.J. Cutts, C.E. Adams, and A. Campbell **961–968** Stability of physiological and behavioural determinants of performance in Arctic char (*Salvelinus alpinus*)

Michael G. Frisk, Thomas J. Miller, and Michael J. Fogarty **969–981** Estimation and analysis of biological parameters in elasmobranch fishes: a comparative life history study

Christopher Lage, Maureen Purcell, Michael Fogarty, and Irv Kornfield **982–990** Microsatellite evaluation of haddock (*Melanogrammus aeglefinus*) stocks in the northwest Atlantic Ocean

ICES: BIVALVE AQUACULTURE IN THE CONTEXT OF COASTAL MARINE ECOSYSTEMS

ICES : LA CULTURE DES BIVALVES DANS LES ÉCOSYSTÈMES MARINS CÔTIERS

Aad Smaal, Marnix van Stralen, and Egbertha Schuiling **991–1002** The interaction between shellfish culture and ecosystem processes

Jon Grant and Cedric Bacher **1003–1011** A numerical model of flow modification induced by suspended aquaculture in a Chinese bay

A. Gangnery, C. Bacher, and D. Buestel **1012–1020** Assessing the production and the impact of cultivated oysters in the Thau lagoon (Mediterranee, France) with a population dynamics model

Jeanie Stenton-Dozey, Trevor Probyn, and Alistair Busby **1021–1031** Impact of mussel (*Mytilus galloprovincialis*) raft-culture on benthic macrofauna, in situ oxygen uptake, and nutrient fluxes in Saldanha Bay, South Africa

PERSPECTIVE

PERSPECTIVE

Alexander B. Bochdansky and Don Deibel **1032–1042** Consequences of model specification for the determination of gut evacuation rates: redefining the linear model

National Research Council Canada
Ottawa, Canada
K1A 0R6

Conseil national de recherches Canada
Ottawa, Canada
K1A 0R6

Postage paid at Ottawa
Publications mail
Registration No. 1240579

Port payé à Ottawa
Poste-publication
Enregistrement n° 1240579

Canadian Journal of Fisheries and Aquatic Sciences

Journal canadien des sciences halieutiques et aquatiques

Volume 58, Number 5, May 2001

Volume 58, numéro 5, mai 2001

RAPID COMMUNICATION / COMMUNICATION RAPIDE

Philip W. Hedrick	**841–844**	Invasion of transgenes from salmon or other genetically modified organisms into natural populations

ARTICLES / ARTICLES

Emma M.C. Hatfield, Roger T. Hanlon, John W. Forsythe, and Eric P.M. Grist	**845–857**	Laboratory testing of a growth hypothesis for juvenile squid *Loligo pealeii* (Cephalopoda: Loliginidae)
L. Boegman, M.R. Loewen, P.F. Hamblin, and D.A. Culver	**858–869**	Application of a two-dimensional hydrodynamic reservoir model to Lake Erie
James L. Lake, Richard A. McKinney, Frank A. Osterman, Richard J. Pruell, John Kiddon, Stephan A. Ryba, and Alan D. Libby	**870–878**	Stable nitrogen isotopes as indicators of anthropogenic activities in small freshwater systems
William F. Kenney, Claire L. Schelske, and Andrew D. Chapman	**879–887**	Changes in polyphosphate sedimentation: a response to excessive phosphorus enrichment in a hypereutrophic lake
Karl C. Bowles, Simon C. Apte, William A. Maher, Matthew Kawei, and Ross Smith	**888–897**	Bioaccumulation and biomagnification of mercury in Lake Murray, Papua New Guinea
Yvonne C. Allen and Charles W. Ramcharan	**898–907**	*Dreissena* distribution in commercial waterways of the U.S.: using failed invasions to identify limiting factors
Tien-Shui Tsou and Jeremy S. Collie	**908–922**	Estimating predation mortality in the Georges Bank fish community
Stephen E. MacAvoy, Stephen A. Macko, and Greg C. Garman	**923–932**	Isotopic turnover in aquatic predators: quantifying the exploitation of migratory prey
John M. Dettmers, Steve Gutreuter, David H. Wahl, and Daniel A. Soluk	**933–942**	Patterns in abundance of fishes in main channels of the upper Mississippi River system
W. Nicholas Beer and James J. Anderson	**943–949**	Effect of spawning day and temperature on salmon emergence: interpretations of a growth model for Methow River chinook
U. Borgmann, W.P. Norwood, T.B. Reynoldson, and F. Rosa	**950–960**	Identifying cause in sediment assessments: bioavailability and the Sediment Quality Triad

Continued on inside back cover / Suite au verso

Canada

Printed in Canada by / Imprimé au Canada par
INTRA MEDIA INC./datamark systems
Typesetting by / Typographie par
NRC Research Press / Presses scientifiques du CNRC

0706-652X(200105)58:5;1-C